

UC-SDRL-CN-20-263-663/664

**VIBRATIONS:
EXPERIMENTAL MODAL ANALYSIS**

Dr. Randall J. Allemang, Professor
Structural Dynamics Research Laboratory
Department of Mechanical, Industrial and Nuclear Engineering
University of Cincinnati
Cincinnati, Ohio 45221-0072

March 1999

Approved for public release

Copyright © 1990-1999 UC-SDRL

PREFACE

An initial version of the following set of notes was originally prepared by Randall Allemang in 1986 for use in the dual level Mechanical Vibrations III (20-263-663/664) course at the University of Cincinnati. The Vibrations III course had a different course number (20-263-692/693) prior to 1993. The primary objective of this course is to give undergraduate and graduate students the necessary background, and their first experience, in experimental vibrations. Further clarifications and additional information has been provided by D. L. Brown, A. W. Phillips and R. W. Rost. Any comments relative to corrections or improvements will be welcomed.

PRINTING/REVISION HISTORY

In an attempt to improve and correct these notes, several revisions have been made. Please be certain that you have the latest revision.

March 1986

Revision 1: February 1992

Revision 2: April 1993

Revision 3: July 1993

Revision 4: December 1993

Revision 5: April 1994

Revision 6: February 1995

Revision 7: March 1999

Matrix Notation

$\{..\}$	braces enclose column vector expressions
$\{..\}^T$	row vector expressions
$[..]$	brackets enclose matrix expressions
$[..]^H$	complex conjugate transpose, or Hermitian transpose, of a matrix
$[..]^T$	transpose of a matrix
$[..]^{-1}$	inverse of a matrix
$[..]^+$	generalized inverse (pseudoinverse)
$[..]_{q \times p}$	size of a matrix: q rows, p columns
$\begin{bmatrix} & & \\ & & \\ & & \end{bmatrix}$	diagonal matrix

Operator Notation

A^*	complex conjugate
F	Fourier transform
F ⁻¹	inverse Fourier transform
H	Hilbert transform
H ⁻¹	inverse Hilbert transform
ln	natural logarithm
L	Laplace transform
L ⁻¹	inverse Laplace transform
Re + j Im	complex number: real part "Re", imaginary part "Im"
\dot{x}	first derivative with respect to time of dependent variable x
\ddot{x}	second derivative with respect to time of dependent variable x
\bar{y}	mean value of y
\hat{y}	estimated value of y
$\sum_{i=1}^n A_i B_i$	summation of $A_i B_i$ from i = 1 to n

$\frac{\partial}{\partial t}$	partial derivative with respect to independent variable "t"
$\det[. .]$	determinant of a matrix
$\ \cdot \ _2$	Euclidian norm

Roman Alphabet

A_{pqr}	residue for response location p, reference location q, of mode r
C	damping
COH	ordinary coherence function [†]
COH_{ik}	ordinary coherence function between any signal i and any signal k [†]
COH^n	conditioned partial coherence [†]
e	base e (2.71828...)
F	input force
F_q	spectrum of q^{th} input [†]
GFF	auto power spectrum of input [†]
GFF_{qq}	auto power spectrum of input q [†]
GFF_{ik}	cross power spectrum of input i and input k [†]
GXF	cross power spectrum of output/input [†]
GXX	auto power spectrum of output [†]
GXX_{pp}	auto power spectrum of output p [†]
$h(t)$	impulse response function [†]
$h_{pq}(t)$	impulse response function for output location p, input location q [†]
$H(s)$	transfer function [†]
$H(\omega)$	frequency response function, when no ambiguity exist, H is used instead of $H(\omega)$ [†]
$H_{pq}(\omega)$	frequency response function for output location p, input location q, when no ambiguity exist, H_{pq} is used instead of $H_{pq}(\omega)$ [†]
$H_1(\omega)$	frequency response function estimate with noise assumed on the response, when no ambiguity exist, H_1 is used instead of $H_1(\omega)$ [†]

$H_2(\omega)$	frequency response function estimate with noise assumed on the reference, when no ambiguity exist, H_2 is used instead of $H_2(\omega)^\dagger$
$H_S(\omega)$	scaled frequency response function estimate, when no ambiguity exist, H_S is used instead of $H_S(\omega)^\dagger$
$H_v(\omega)$	frequency response function estimate with noise assumed on both reference and response, when no ambiguity exist, H_v is used instead of $H_v(\omega)^\dagger$
$[I]$	identity matrix
j	$\sqrt{-1}$
K	stiffness
L	modal participation factor
M	mass
M_r	modal mass for mode r
M_{A_r}	modal A for mode r
$MCOH$	multiple coherence function [†]
N	number of modes
N_i	number of references (inputs)
N_o	number of responses (outputs)
p	output, or response point (subscript)
q	input, or reference point (subscript)
r	mode number (subscript)
R_I	residual inertia
R_F	residual flexibility
s	Laplace domain variable
t	independent variable of time (sec)
t_k	discrete value of time (sec) $t_k = k \Delta t$
T	sample period
x	displacement in physical coordinates
X	response
X_p	spectrum of p^{th} response [†]
z	Z domain variable

Greek Alphabet

$\delta(t)$	Dirac impulse function
Δf	discrete interval of frequency (Hertz or cycles/sec)
Δt	discrete interval of sample time (sec)
ε	small number
η	noise on the output
λ_r	r^{th} complex eigenvalue, or system pole $\lambda_r = \sigma_r + j\omega_r$
$[\Lambda]$	diagonal matrix of poles in Laplace domain
v	noise on the input
ω	variable of frequency (rad/sec)
ω_r	imaginary part of the system pole, or damped natural frequency, for mode r (rad/sec) $\omega_r = \Omega_r \sqrt{1 - \zeta_r^2}$
Ω_r	undamped natural frequency (rad/sec) $\Omega_r = \sqrt{\sigma_r^2 + \omega_r^2}$
ϕ_{pr}	scaled p^{th} response of normal modal vector for mode r
$\{\phi\}_r$	scaled normal modal vector for mode r
$[\Phi]$	scaled normal modal vector matrix
$\{\psi\}$	scaled eigenvector
ψ_{pr}	scaled p^{th} response of a complex modal vector for mode r
$\{\psi\}_r$	scaled complex modal vector for mode r
$[\Psi]$	scaled complex modal vector matrix
σ	variable of damping (rad/sec)
σ_r	real part of the system pole, or damping factor, for mode r
ζ	damping ratio
ζ_r	damping ratio for mode r
\dagger	vector implied by definition of function

TABLE OF CONTENTS

PREFACE	4
PRINTING/REVISION HISTORY	4
1. EXPERIMENTAL MODAL ANALYSIS	1
1.1 Introduction	1
1.2 Experimental Modal Analysis Overview	2
1.3 Degrees of Freedom	5
1.4 Basic Assumptions	9
1.5 References	11
2. MODAL ANALYSIS THEORY	1
2.1 Introduction	1
2.2 Transform Relationships	1
2.2.1 Transform Properties	2
2.3 Single Degree of Freedom Systems	3
2.3.1 Time Domain: Impulse Response Function	6
2.3.2 Frequency Domain: Frequency Response Function	8
2.3.3 Laplace Domain: Transfer Function	12
2.4 Multiple Degree of Freedom Systems	19
2.5 Damping Mechanisms	25
2.6 References	26
3. HISTORY OF EXPERIMENTAL MODAL ANALYSIS	1
3.1 Introduction	1
3.2 Data Acquisition Classification	2
3.2.1 Sinusoidal Input-Output Method	4
3.2.1.1 Forced Normal Mode Excitation Method	4
3.2.1.2 Forced Response Decomposition Method	6
3.2.2 Frequency Response Function Method	8
3.2.2.1 Theory	9
3.2.3 Damped Complex Exponential Method	11
3.2.3.1 Ibrahim Time Domain (ITD) Approach	12
3.2.3.2 Poly-Reference Time Domain (PTD) Approach	13
3.2.3.3 Eigensystem Realization Algorithm Approach	14
3.2.4 Mathematical Input-Output Model Method	16
3.2.4.1 Autoregressive Moving Average Approach	16
3.2.4.2 Reduced Structural Matrix Approach	18
3.3 References	20
4. MODAL DATA ACQUISITION	1
4.1 Introduction	1
4.2 Errors	3
4.3 Analog to Digital Conversion	

	4
4.3.1 Sampling	5
4.3.2 Quantization	9
4.3.3 ADC Implementation Issues	14
4.3.4 ADC Errors	17
4.3.4.1 Aliasing	17
4.3.4.2 Other Types of ADC Error	19
4.4 Discrete Fourier Transform	20
4.4.1 DFT/FFT Errors	24
4.4.1.1 Leakage Error	24
4.5 Increased Frequency Resolution	30
4.6 Weighting Functions	35
4.7 Averaging	39
4.7.1 General Averaging Methods	40
4.7.1.1 Linear Averaging	40
4.7.1.2 Magnitude Averaging	41
4.7.1.3 Root-Mean-Square (RMS) Averaging	42
4.7.1.4 Exponential Averaging	43
4.7.1.5 Stable Averaging	44
4.7.1.6 Peak Hold	44
4.7.2 Estimation of Frequency Response Functions	44
4.7.2.1 Asynchronous Signal Averaging	46
4.7.2.2 Synchronous Signal Averaging	46
4.7.2.3 Cyclic Signal Averaging	47
4.7.2.3.1 Theory of Cyclic Averaging	49
4.7.2.3.2 Practical Example	58
4.7.3 Special Types of Signal Averaging	65
4.7.3.1 Overlapping Time Records	65
4.8 Transducer Considerations	70
4.9 References	75
5. FREQUENCY RESPONSE FUNCTION MEASUREMENTS	1
5.1 Introduction	1
5.2 Frequency Response Function Estimation	3
5.2.1 Noise/Error Minimization	5
5.2.2 Single Input FRF Estimation	8
5.2.3 Multiple Input FRF Estimation	16
Example: H_1 Technique: Two Inputs/One Output Case	25
5.2.3.1 Multiple Input Force Analysis/Evaluation	29
5.3 Excitation	35
5.3.1 Excitation Assumptions	38
5.3.2 Terminology and Nomenclature	42
5.3.3 Classification of Excitation	45
5.3.4 Random Excitation Methods	47
Hybrid Random Excitation Methods	

	55
5.3.5	Deterministic Excitation Methods 56
5.3.6	Excitation Example - H-Frame 60
5.3.7	Impact Excitation 70
5.4	Structural Testing Conditions 74
5.5	Practical Measurement Considerations 76
5.6	References 77
6.	MODAL PARAMETER ESTIMATION 1
6.1	Introduction 1
6.2	Definition: Modal Parameters 2
6.3	Modal Identification Concepts 3
6.3.1	Concept: Data Domain 7
6.3.2	Concept: Model Order Relationships 8
6.3.3	Concept: Fundamental Measurement Models 10
6.3.4	Concept: Characteristic Space 11
6.3.5	Concept: Fundamental Modal Identification Models 18
6.3.6	Concept: Two Stage Linear Solution Procedure 24
6.3.7	Concept: Data Sieving/Filtering 29
6.3.8	Concept: Equation Condensation 29
6.3.9	Concept: Coefficient Condensation 31
6.3.10	Concept: Model Order Determination 34
6.3.10.1	Error Chart 36
6.3.10.2	Stability Diagram 37
6.3.10.3	Mode Indication Functions 39
6.3.10.3.1	Multivariate Mode Indication Function (MvMIF) 39
6.3.10.3.2	Complex Mode Indication Function (CMIF) 40
6.3.10.4	Rank Estimation 44
6.3.11	Concept: Residuals 45
6.4	SDOF Approximate Algorithms 48
6.4.1	Operating Vector Estimation 49
6.4.2	Complex Plot (Circle Fit) 53
6.4.3	Two Point Finite Difference Formulation 57
6.4.4	Least Squares (Local) SDOF Method 60
6.4.5	Least Squares (Global) SDOF Method 62
6.5	Modal Identification Algorithms 63
6.5.1	High Order Time Domain Algorithms 63
6.5.1.1	Complex Exponential Algorithm: Example 65
6.5.1.1.1	SDOF Numerical Example 67
6.5.2	First Order Time Domain Algorithms 72
6.5.3	Second Order Time Domain Algorithms 73
6.5.4	High Order Frequency Domain Algorithms 74
6.5.4.1	Rational Fraction Polynomial: Example 75
6.5.4.1.1	SDOF Numerical Example 78
6.5.4.2	Orthogonal Polynomial Concepts 81
	Chebyshev Orthogonal Polynomials

	Legendre Orthogonal Polynomials	84
6.5.5	First Order Frequency Domain Algorithms	87
6.5.6	Second Order Frequency Domain Algorithms	88
6.6	Residue Estimation	90
6.6.1	Time Domain Estimation (Single Reference)	90
6.6.2	Time Domain Estimation (Multiple References)	91
6.6.3	Frequency Domain Estimation (Single Reference)	92
6.6.4	Frequency Domain Estimation (Single Reference With Residuals)	93
6.6.5	Frequency Domain Estimation (Multiple References)	94
6.7	Summary - Future Trends	95
6.8	References	95
7.	MODAL DATA PRESENTATION/VALIDATION	1
7.1	Measurement Synthesis	1
7.2	Visual Verification	4
7.3	Finite Element Analysis	6
7.4	Modal Vector Orthogonality	6
7.5	Modal Vector Consistency	8
7.6	Modal Modification Prediction	14
7.7	Modal Complexity	14
7.8	Modal Phase Colinearity and Mean Phase Deviation	15
7.9	References	15
Appendix A:	Least Squares Method	1
A.1	Correlation Coefficient	6
A.2	Examples	7
A.2.1	Example 1	7
A.2.2	Example 2	9
A.3	References	11
Appendix B:	Singular Value Decomposition	1
B.1	References	4
Appendix C:	Bibliography	

LIST OF FIGURES

.....	1
Figure 1-1. Experimental Modal Analysis Example	4
Figure 1-2. Degrees of Freedom of a Rigid Body	6
Figure 2-1. Zoom Transform Process	3
Figure 2-2. Single Degree of Freedom System	3
Figure 2-3. Time Domain: Impulse Response Function	7
Figure 2-4. Frequency Response Function (Real/Imaginary Format)	10
Figure 2-5. Frequency Response Function (Magnitude/Phase Format)	11
Figure 2-6. Frequency Response Function (Log Magnitude/Phase Format)	11
Figure 2-7. Transfer Function (Real/Imaginary Format)	15
Figure 2-8. Transfer Function (Magnitude/Phase Format)	16
Figure 2-9. Transfer Function (Log Magnitude/Phase Format)	17
Figure 2-10. Transfer Function - LaPlace Plane Projection)	18
Figure 2-11. Multi-Degree of Freedom System)	19
Figure 4-1. Shannon Sampling Theorem	6
Figure 4-2. Basic Sampling Relationships	6
Figure 4-3. Rayleigh's Criterion	7
Figure 4-4. Quantization: 3 Bit Analog to Digital Converter	10
Figure 4-5. Quantization: ADC Input Optimization (Unwanted DC)	11
Figure 4-6. Quantization: ADC Input Optimization (Unwanted Harmonic)	11
Figure 4-7. 1.2 Hertz AC Coupling Characteristics (Magnitude and Phase)	12
Figure 4-8. Variable Sample Frequency ADC Design	14
Figure 4-9. Fixed Sample Frequency ADC Design	15
Figure 4-10. Delta-Sigma ADC Design	16
Figure 4-11. Aliasing Example	17
Figure 4-12. Aliasing Contribution (Shannon Sampling Theorem Limit)	18
Figure 4-13. Discrete Fourier Transform Concept	20
Figure 4-14. Time Domain Function: Theoretical Harmonic	26

Figure 4-15. Time Domain Function: Theoretical Window	26
Figure 4-16. Time Domain Function: Multiplication of Signals	26
Figure 4-17. Frequency Domain: Theoretical Harmonic	28
Figure 4-18. Frequency Domain: Theoretical Window	28
Figure 4-19. Frequency Domain: Convolved Signals	28
Figure 4-20. Frequency Domain: Periodic Signal	29
Figure 4-21. Frequency Domain: Nonperiodic Signal	29
Figure 4-22. Increased Frequency Resolution	31
Figure 4-23. Increased Frequency Resolution	33
Figure 4-24. Increased Frequency Resolution	33
Figure 4-25. Typical Weighting Function - Boxcar (P000) Window	35
Figure 4-26. Typical Weighting Functions - Hanning (P110) Window	37
Figure 4-27. Typical Weighting Functions - Flattop (P301) Window	37
Figure 4-28. Typical Weighting Function - Hanning (P110) Window	37
Figure 4-29. Typical Weighting Function - Flattop (P301) Window	38
Figure 4-30. Contiguous Time Records (Periodic Signal)	48
Figure 4-31. Averaged Time Records (Periodic Signal)	48
Figure 4-32. Contiguous Time Records (Non-Periodic Signal)	48
Figure 4-33. Averaged Time Records (Non-Periodic Signal)	48
Figure 4-34. Cyclic Averaging ($N_c = 4$) with Uniform Window	52
Figure 4-35. Cyclic Averaging ($N_c = 4$) with Hann Window	52
Figure 4-36. Uniform Window Characteristics	53
Figure 4-37. Cyclic Averaging ($N_c = 2$) with Uniform Window	53
Figure 4-38. Cyclic Averaging ($N_c = 4$) with Uniform Window	54
Figure 4-39. Hann Window Characteristics	54
Figure 4-40. Cyclic Averaging ($N_c = 2$) with Hann Window	55
Figure 4-41. Cyclic Averaging ($N_c = 4$) with Hann Window	55
Figure 4-42. Contiguous Time Records	56
Figure 4-43. Averaged Time Records	57
Figure 4-44. Contiguous Time Records with Hann Window	57
Figure 4-45. Averaged Time Records with Hann Window	58

Figure 4-46. Case I: Asynchronous Averaging	60
Figure 4-47. Case II: Asynchronous Averaging With Hann Window	61
Figure 4-48. Case III: Cyclic Averaging	62
Figure 4-49. Case IV: Cyclic Averaging With Hann Window	63
Figure 4-50. Overlap Processing: Zero Overlap	65
Figure 4-51. Overlap Processing: Fifty Percent Overlap	66
Figure 4-52. Random Decrement Averaging	68
Figure 4-53. Calibration Methods	73
Figure 4-54. FRF Magnitude: Calibration Errors	74
Figure 4-55. FRF Magnitude: Calibration Errors Corrected	74
Figure 5-1. Two Input, Two Output FRF Concept	5
Figure 5-2. Least Squares Concept	6
Figure 5-3. System Model: Single Input	8
Figure 5-4. FRF and Corresponding Ordinary Coherence Function	13
Figure 5-5. Ordinary Coherence Relationship - Averaging	15
Figure 5-6. System Model: Multiple Inputs	19
Figure 5-7. Two Input, One Output Model	25
Figure 5-8. AutoPower Spectrum of Input Forces	32
Figure 5-9. Principal (Virtual) Force Spectrum	33
Figure 5-10. Typical Test Configuration: Shaker	35
Figure 5-11. Typical Test Configuration: Impact Hammer	36
Figure 5-12. Input Spectrum Example	40
Figure 5-13. Total Contiguous Time Per power Spectral Average (Ensemble)	44
Figure 5-14. Signal Energy Content - Pure Random	49
Figure 5-15. Signal Energy Content - Pseudo Random	49
Figure 5-16. Signal Energy Content - Periodic Random	50
Figure 5-17. Signal Energy Content - Burst Random	51
Figure 5-18. Burst Random - Signal to Shaker	52
Figure 5-19. Burst Random - Signal from Load Cell (Voltage Feedback)	52
Figure 5-20. Burst Random - Signal from Accelerometer	53
Figure 5-21. Signal Energy Content - Burst Pseudo Random	55

Figure 5-22. Signal Energy Content - Burst Periodic Random	55
Figure 5-23. Typical Chirp Signal - Time Domain	56
Figure 5-24. Typical Chirp Signal - Frequency Domain	57
Figure 5-25. Case 1: Random Excitation with Hann Window	62
Figure 5-26. Case 2: Random Excitation with Hann Window and Cyclic Averaging	63
Figure 5-27. Case 3: Burst Random Excitation with Cyclic Averaging	63
Figure 5-28. Case 4: Pseudo Random Excitation	64
Figure 5-29. Case 5: Periodic Random Excitation	64
Figure 5-30. Case 6: Pseudo Random Excitation	65
Figure 5-31. Case 7: Periodic Random Excitation	65
Figure 5-32. Case 8: Burst Pseudo Random Excitation with Cyclic Averaging	66
Figure 5-33. Case 9: Burst Periodic Random Excitation with Cyclic Averaging	66
Figure 5-34. Case 10: Burst Random Excitation with Cyclic Averaging	67
Figure 5-35. Case 11: Random Excitation with Hann Window	67
Figure 5-36. Case 12: Random Excitation with Hann Window and Cyclic Averaging	68
Figure 5-37. Case 13: Pseudo Random Excitation with Cyclic Averaging	68
Figure 5-38. Case 14: Periodic Random Excitation with Cyclic Averaging	69
Figure 5-39. Typical Force Windows	71
Figure 5-40. Typical Response Windows	73
Figure 6-1. MDOF - SDOF Superposition (Positive Frequency Poles)	3
Figure 6-2. MDOF - SDOF Superposition (Positive Frequency Poles)	4
Figure 6-3. MDOF - SDOF Superposition (Positive - Negative Frequency Poles)	5
Figure 6-4. Conceptualization of Modal Characteristic Space	11
Figure 6-5. Characteristic Space: Column of Measurements	14
Figure 6-6. Characteristic Space: Columns of Measurements	14
Figure 6-7. Characteristic Space: Row of Measurements	15
Figure 6-8. Characteristic Space: Rows of Measurements	16
Figure 6-9. Characteristic Space: Temporal Measurements	16
Figure 6-10. Characteristic Space: Temporal Measurements	17
Figure 6-11. Underdetermined Set of Linear Equations	26
Figure 6-12. Underdetermined Set of Linear Equations	26

Figure 6-13. Determined Set of Linear Equations	27
Figure 6-14. Overdetermined Set of Linear Equations	27
Figure 6-15. Model Order Determination: Error Chart	36
Figure 6-16. Model Order Determination: Stability Diagram	38
Figure 6-17. Multivariate Mode Indication Function	40
Figure 6-18. Complex Mode Indication Function	43
Figure 6-19. Model Order Determination: Rank Estimation	44
Figure 6-20. Residual Effects From Adjacent Poles	45
Figure 6-21. Modal Vectors from the Imaginary Part of the FRF	48
Figure 6-22. Single Degree of Freedom Method - Magnitude/Phase	51
Figure 6-23. Single Degree of Freedom Method - Log Magnitude/Phase	51
Figure 6-24. Single Degree of Freedom Method - Real/Imaginary	52
Figure 6-25. Single Degree of Freedom Method - Real versus Imaginary	55
Figure 6-26. Typical Impulse Response Function	65
Figure 6-27. Case I: Impulse Response Function	69
Figure 6-28. Case II: Impulse Response Function	70
Figure 6-29. Case III: Impulse Response Function	71
Figure 6-30. Frequency Response Function, SDOF Example	79
Figure 6-31. Power Polynomials	82
Figure 6-32. Power Polynomials (Normalized Frequency)	83
Figure 6-33. Chebyshev Orthogonal Polynomials	84
Figure 6-34. Legendre Orthogonal Polynomials	87
Figure 7-1. Typical FRF Synthesis	2
Figure 7-2. Normalized Error - FRF Synthesis	3
Figure 7-3. Visual Verification of Modal Vectors	5
Figure A-1. Straight Lines Fitting the Data	1
Figure A-2. Errors in Least Squares Estimation	3
Figure A-3. Variations in Data	6
Figure A-4. Least Squares Fit of Data	8

LIST OF TABLES

Table 2-1. Modal Scaling Units	25
Table 4-2. Digitization Equations ($F_{\max} = F_{Nyq}$)	8
Table 4-3. Comparison of Averaging Methods	43
Table 4-4. Transducer Mounting Methods	71
Table 5-5. Frequency Response Function Formulations	4
Table 5-6. Summary of Frequency Response Function Estimation Models	7
Table 5-7. Excitation Characteristics	54
Table 5-8. Summary of Excitation Signals	59
Table 5-9. Test Cases - Excitation/Averaging/DSP Parameters	60
Table 6-10. Summary of Modal Parameter Estimation Algorithms	22
Table 6-11. Summary of Modal Parameter Estimation Acronyms	22
Table A-12. x and y Values for Least Squares Fit	7

1. EXPERIMENTAL MODAL ANALYSIS

1.1 Introduction

Experimental modal analysis is the process of determining the modal parameters (frequencies, damping factors, modal vectors and modal scaling) of a linear, time invariant system by way of an experimental approach. The modal parameters may be determined by analytical means, such as finite element analysis, and one of the common reasons for experimental modal analysis is the verification/correction of the results of the analytical approach (model updating). Often, though, an analytical model does not exist and the modal parameters determined experimentally serve as the model for future evaluations such as structural modifications. Predominately, experimental modal analysis is used to explain a dynamics problem, vibration or acoustic, that is not obvious from intuition, analytical models, or previous similar experience. It is important to remember that most vibration and/or acoustic problems are a function of both the forcing functions (or initial conditions) and the system characteristics described by the modal parameters. Modal analysis alone is not the answer to the whole problem but is often an important part of the process. Likewise, many vibration and/or acoustic problems fall outside of the assumptions associated with modal analysis (linear superposition, for example). For these situations, modal analysis may not be the right approach and an analysis that focuses on the specific characteristics of the problem will be more useful.

The history of experimental modal analysis began in the 1940's with work oriented toward measuring the modal parameters of aircraft so that the problem of flutter could be accurately predicted. At that time, transducers to measure dynamic force were primitive and the analog nature of the approach yielded a time consuming process that was not practical for most situations. With the advent of digital mini-computers and the Fast Fourier Transform (FFT) in the 1960's, the modern era of experimental modal analysis began. Today, experimental modal analysis represents an interdisciplinary field that brings together the signal conditioning and computer interaction of electrical engineering, the theory of mechanics, vibrations, acoustics, and control theory from mechanical engineering, and the parameter estimation approaches of applied mathematics ^[1-12].

1.2 Experimental Modal Analysis Overview

The process of determining modal parameters from experimental data involves several phases. While these phases can be, in the simplest cases, very abbreviated, experimental modal analysis depends upon the understanding of the basis for each phase. As in most experimental situations, the success of the experimental modal analysis process depends upon having very specific goals for the test situation. Such specific goals affect every phase of the process in terms of reducing the errors associated with that phase. While there are several ways of breaking down the process, one possible delineation of these phases is as follows:

- Modal Analysis Theory
- Experimental Modal Analysis Methods
- Modal Data Acquisition
- Modal Parameter Estimation
- Modal Data Presentation/Validation

Modal analysis theory refers to that portion of classical vibrations that explains, theoretically, the existence of natural frequencies, damping factors, and mode shapes for linear systems. This theory includes both lumped parameter, or discrete, models as well as continuous models. This theory also includes real normal modes as well as complex modes of vibration as possible solutions for the modal parameters. This phase of the experimental modal analysis process will not be repeated here but is summarized in *Analytical and Experimental Modal Analysis (UC-SDRL-CN-20-263-662)* as well as in other textbooks on vibration ^[1-4]. The relationships of transforms to vibration theory is very important to the comprehension of modern experimental modal analysis methods. Particularly, since discrete Fourier transforms are often involved in the modal data acquisition phase, this aspect of modal theory is critical.

Experimental modal analysis methods involve the theoretical relationship between measured quantities and the classic vibration theory often represented as matrix differential equations. All modern methods trace from the matrix differential equations but yield a final mathematical form in terms of measured data. This measured data can be raw input and output data in the time or frequency domains or some form of processed data such as impulse response or frequency response functions. Most current methods involve processed data such as frequency response

functions in the estimation of modal parameters. In summary, though, the experimental modal analysis method establishes the form of the data that must be acquired.

Modal data acquisition involves the practical aspects of acquiring the data that is required as input to the modal parameter estimation phase. Therefore, a great deal of care must be taken to assure that the data matches the requirements of the theory as well as the requirements of the numerical algorithm involved in the modal parameter estimation. This phase involves both the digital signal processing and measurement (frequency response function) formulation. The theoretical requirements involve concerns such as system linearity as well as time invariance of system parameters. It is very important, in this phase, to understand the origin of errors, both variance and bias, in the measurement process. Certain bias errors, which originate due to limitations of the fast Fourier transform (FFT) may seriously compromise the estimates of modal parameters [5-8].

Modal parameter estimation is concerned with the practical problem of estimating the modal parameters, based upon a choice of mathematical model as justified by the experimental modal analysis method, from the measured data. Problems which occur at this phase most often arise from violations of assumptions used in previous phases. Serious theoretical problems such as nonlinear considerations cause serious problems in the estimation of modal parameters and may be reason to completely invalidate the experimental modal analysis approach. Serious practical problems such as bias errors resulting from the digital signal processing will cause similar problems but are a function of data acquisition techniques which can be altered to minimize such errors. The modal parameter estimation phase is that point in the experimental modal analysis process where the errors of all previous work are accumulated [9-12].

Modal data presentation/validation is that process of providing a physical view or interpretation of the modal parameters. For example, this may simply be the numerical tabulation of the frequency, damping, and modal vectors along with the associated geometry of the measured degrees of freedom. More often, modal data presentation involves the plotting and animation of such information. This involves the additional information required to construct a three dimensional representation of the test object. Primarily, this requires a display sequence involving the order in which the degrees of freedom will be connected. Newer approaches to the plotting and animation of the modal vectors involve hidden line calculations which require surface definition as well.

Figure 1-1 is a representation of all phases of the process. First of all, a continuous beam is being evaluated for the first few modes of vibration. Modal analysis theory explains that this is a linear system and that the modal vectors of this system should be real normal modes. The experimental modal analysis method that has been used is based upon the frequency response function relationships to the matrix differential equations of motion. At each measured degree of freedom the imaginary part of the frequency response function for that measured response degree of freedom and a common input degree of freedom is superimposed perpendicular to the beam. Naturally, the modal data acquisition involved in this example involves the estimation of frequency response functions for each degree of freedom shown. Note that the frequency response functions are complex valued functions and that only the imaginary portion of each function is shown. One method of modal parameter estimation suggests that for systems with light damping and widely spaced modes, the imaginary part of the frequency response function, at the damped natural frequency, may be used as an estimate of the modal coefficient for that response degree of freedom. The damped natural frequency can be identified as the frequency of the positive and negative peaks in the imaginary part of the frequency response functions. The damping can be estimated from the sharpness of the peaks. In this very simple way, the modal parameters have been estimated. Modal data presentation for this case is shown as the lines connecting the peaks. While animation is possible, a reasonable interpretation of the modal vector can be gained in this simple case from plotting alone.

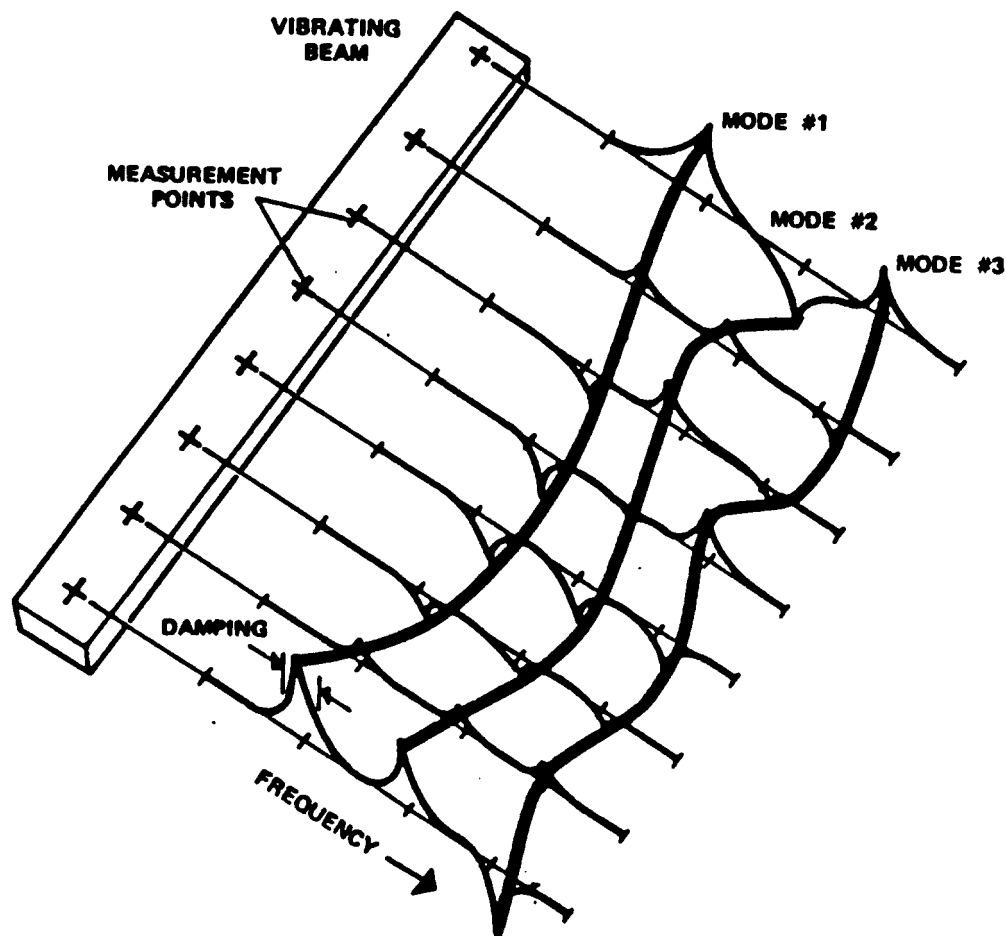


Figure 1-1. Experimental Modal Analysis Example

1.3 Degrees of Freedom

The development of any theoretical concept in the area of vibrations, including modal analysis, depends upon an understanding of the concept of the number (N) of *degrees of freedom* (DOF) of a system. This concept is extremely important to the area of modal analysis since the number of modes of vibration of a mechanical system is equal to the number of degrees of freedom. From a practical point of view, the relationship between this theoretical definition of the number of degrees of freedom and the number (N_o, N_i) of *measurement degrees of freedom* is often confusing. For this reason, the concept of degree of freedom will be reviewed as a preliminary to

the following experimental modal analysis material.

To begin with, the basic definition that is normally associated with the concept of the number of degrees of freedom involves the following statement: *The number of degrees of freedom for a mechanical system is equal to the number of independent coordinates (or minimum number of coordinates) that is required to locate and orient each mass in the mechanical system at any instant in time.* As this definition is applied to a point mass, three degrees of freedom are required since the location of the point mass involves knowing the x , y , and z translations of the center of gravity of the point mass. As this definition is applied to a rigid body mass, six degrees of freedom are required since θ_x , θ_y , and θ_z rotations are required in addition to the x , y , and z translations in order to define both the orientation and location of the rigid body mass at any instant in time. This concept is represented in Figure 1-2. As this definition is extended to any general deformable body, it should be obvious that the number of degrees of freedom can now be considered as infinite. While this is theoretically true, it is quite common, particularly with respect to finite element methods, to view the general deformable body in terms of a large number of physical points of interest with six degrees of freedom for each of the physical points. In this way, the infinite number of degrees of freedom can be reduced to a large but finite number.

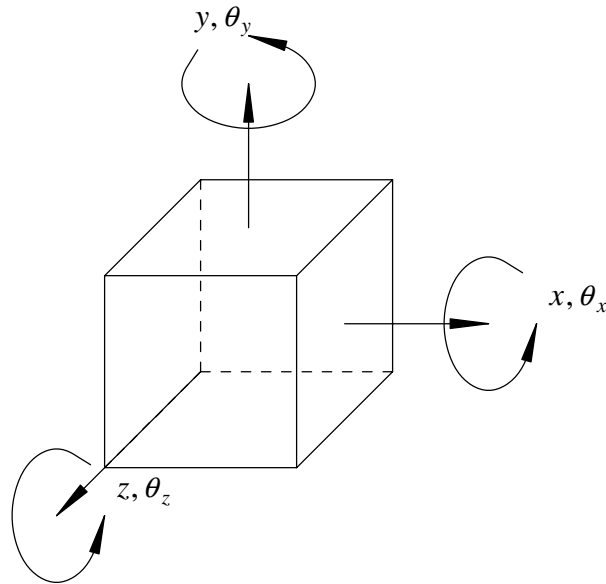


Figure 1-2. Degrees of Freedom of a Rigid Body

When measurement limitations are imposed upon this theoretical concept of the number of degrees of freedom of a mechanical system, the difference between the theoretical number (N) of degrees of freedom and the number (N_o, N_i) of measurement degrees of freedom begins to evolve. Initially, for a general deformable body, the number of degrees of freedom (N) can be considered to be infinite or equal to some large finite number if a limited set of physical points of interest is considered as discussed in the previous paragraph. The first measurement limitation that needs to be considered is that there is normally a limited frequency range that is of interest to the analysis. For example, most dominant structural modes of vibration for an automobile would be located between 0 and 100 Hertz. As this limitation is considered, the number of degrees of freedom of this system that are of interest is now reduced from infinity to a reasonable finite number. The next measurement limitation that needs to be considered involves the physical limitation of the measurement system in terms of amplitude. A common limitation of transducers, signal conditioning and data acquisition systems results in a dynamic range of 80 to 100 db (10^4 to 10^5) in the measurement. This means that the number of degrees of freedom is

reduced further due to the dynamic range limitations of the measurement instrumentation. Finally, since few rotational transducers exist at this time, the normal measurements that are made involve only translational quantities (displacement, velocity, acceleration, force) and thus do not include rotational degrees-of-freedom (RDOF). In summary, even for the general deformable body, the theoretical number of degrees of freedom that are of interest are limited to a very reasonable finite value ($N = 1 - 50$). Therefore, this number of degrees of freedom (N) is the number of modes of vibration that are of interest.

Finally, then, the number of *measurement degrees of freedom* (N_o, N_i) can be defined as the number of physical locations at which measurements are made times the number of measurements made at each physical location. For example, if x , y , and z accelerations are measured at each of 100 physical locations on a general deformable body, the number of measurement degrees of freedom would be equal to 300. It should be obvious that since the physical locations are chosen somewhat arbitrarily, and certainly without exact knowledge of the modes of vibration that are of interest, that there is no specific relationship between the number of degrees of freedom (N) and the number of measurement degrees of freedom (N_o, N_i). In general, in order to define N modes of vibration of a mechanical system, N_o, N_i must be equal to or larger than N . Even though N_o, N_i is larger than N , this is not a guarantee that N modes of vibration can be found from N_o, N_i measurement degrees of freedom. The N_o, N_i measurement degrees of freedom must include physical locations that allow a unique determination of the N modes of vibration. For example, if none of the measurement degrees of freedom are located on a portion of the mechanical system that is active in one of the N modes of vibration, portions of the modal parameters for this mode of vibration can not be found.

In the development of material in the following text, the assumption is made that a set of measurement degrees of freedom (N_o, N_i) exist that will allow for N modes of vibration to be determined. In reality, N_o, N_i is always chosen much larger than N since a prior knowledge of the modes of vibration is not available. If the set of N_o, N_i measurement degrees of freedom is large enough and if the N_o, N_i measurement degrees of freedom are distributed uniformly over the general deformable body, the N modes of vibration will normally be found.

Throughout this and many other experimental modal analysis references, the frequency response function H_{pq} notation will be used to describe the measurement of the response at measurement degree of freedom p resulting from an input applied at measurement degree of freedom q . The

single subscript p or q refers to a single sensor aligned in a specific direction ($\pm X, Y$ or Z) at a physical location on or within the structure.

1.4 Basic Assumptions

There are four basic assumptions concerning any structure that are made in order to perform an experimental modal analysis:

The first basic assumption is that the structure is assumed to be linear i.e., the response of the structure to any combination of forces, simultaneously applied, is the sum of the individual responses to each of the forces acting alone. For a wide variety of structures this is a very good assumption. When a structure is linear, its behavior can be characterized by a controlled excitation experiment in which the forces applied to the structure have a form convenient for measurement and parameter estimation rather than being similar to the forces that are actually applied to the structure in its normal environment. For many important kinds of structures, however, the assumption of linearity is not valid. Where experimental modal analysis is applied in these cases it is hoped that the linear model that is identified provides a reasonable approximation of the structure's behavior.

The second basic assumption is that the structure is time invariant i.e., the parameters that are to be determined are constants. In general, a system which is not time invariant will have components whose mass, stiffness, or damping depend on factors that are not measured or are not included in the model. For example, some components may be temperature dependent. In this case the temperature of the component is viewed as a time varying signal, and, hence, the component has time varying characteristics. Therefore, the modal parameters that would be determined by any measurement and estimation process would depend on the time (by this temperature dependence) that any measurements were made. If the structure that is tested changes with time, then measurements made at the end of the test period would determine a different set of modal parameters than measurements made at the beginning of the test period. Thus, the measurements made at the two different times will be inconsistent, violating the assumption of time invariance.

The third basic assumption is that the structure obeys Maxwell's reciprocity i.e., a force applied

at degree-of-freedom p causes a response at degree-of-freedom q that is the same as the response at degree-of-freedom p caused by the same force applied at degree-of-freedom q . With respect to frequency response function measurements, the frequency response function between points p and q determined by exciting at p and measuring the response at q is the same frequency response function as found by exciting at q and measuring the response at p ($H_{pq} = H_{qp}$).

The fourth basic assumption is that the structure is observable i.e., the input-output measurements that are made contain enough information to generate an adequate behavioral model of the structure. Structures and machines which have loose components, or more generally, which have degrees-of-freedom of motion that are not measured, are not completely observable. For example, consider the motion of a partially filled tank of liquid when complicated sloshing of the fluid occurs. Sometimes enough measurements can be made so that the system is observable under the form chosen for the model, and sometimes no realistic amount of measurements will suffice until the model is changed. This assumption is particularly relevant to the fact that the data normally describe an incomplete model of the structure. This occurs in at least two different ways. First, the data is normally limited to a minimum and maximum frequency as well as a limited frequency resolution. Secondly, no information is available relative to local rotations due to a lack of transducers available in this area.

Other assumptions can be made regarding the system being analyzed. Commonly, the modal parameters are assumed to be global. For example, this assumption means that, for a given modal frequency, the frequency and damping information is the same in every measurement. Since measurements are taken at different times and with slightly different test conditions, this is often not true with respect to the measured data. This condition is referred to as ***inconsistent*** data. Theoretical models do not attempt to recognize this problem. Another assumption is often made relative to ***repeated roots***. Repeated roots refer to the situation where one of the complex roots (modal frequency, eigenvalue, pole, etc.) occurs more than once in the characteristic equation. Each root with the same value has an independent modal vector or eigenvector. This situation can only be detected by the use of multiple inputs or references. Many modal parameter estimation algorithms involve only one measurement or one reference at a time and, therefore, cannot estimate a repeated root situation. Detection of repeated roots is critical in developing a complete modal model so that arbitrary input-output information can be synthesized. While theoretical repeated roots are of debatable significance, practical repeated root problems exist whenever two modal frequencies are very close together with respect to the

frequency resolution used in the measurements. This situation is a very real problem and is referred to as the *pseudo-repeated root* problem.

The basic assumptions are never perfectly achieved in experimental test situations involving real structural systems. Generally, the assumptions will be approximately true. The important thing to remember is that each assumption can be evaluated experimentally, either during the testing or after the testing is completed and the data analysis has been performed. It is inexcusable to perform a test without some measure of the validity of the assumptions involved.

1.5 References

- [1] Allemang, R.J., **Analytical and Experimental Modal Analysis**, UC-SDRL-CN-20-263-662, 1994, 166 pp.
- [2] Tse, F.S., Morse, I.E., Jr., Hinkle, R.T., **Mechanical Vibrations: Theory and Applications, Second Edition**, Prentice-Hall, Inc., Englewood Cliffs, New Jersey, 1978, 449 pp.
- [3] Craig, R.R., Jr., **Structural Dynamics: An Introduction to Computer Methods**, John Wiley and Sons, Inc., New York, 1981, 527 pp.
- [4] Ewins, D., **Modal Testing: Theory and Practice** John Wiley and Sons, Inc., New York, 1984, 269 pp.
- [5] Bendat, J.S.; Piersol, A.G., **Random Data: Analysis and Measurement Procedures**, John Wiley and Sons, Inc., New York, 1971, 407 pp.
- [6] Bendat, J. S., Piersol, A. G., **Engineering Applications of Correlation and Spectral Analysis**, John Wiley and Sons, Inc., New York, 1980, 302 pp.
- [7] Otnes, R.K., Enochson, L., **Digital Time Series Analysis**, John Wiley and Sons, Inc., New York, 1972, 467 pp.
- [8] Dally, J.W.; Riley, W.F.; McConnell, K.G., **Instrumentation for Engineering Measurements**, John Wiley & Sons, Inc., New York, 1984.

- [9] Strang, G., **Linear Algebra and Its Applications, Third Edition**, Harcourt Brace Jovanovich Publishers, San Diego, 1988, 505 pp.
- [10] Lawson, C.L., Hanson, R.J., **Solving Least Squares Problems**, Prentice-Hall, Inc., Englewood Cliffs, New Jersey, 1974, 340 pp.
- [11] Jolliffe, I.T., **Principal Component Analysis**, Springer-Verlag New York, Inc., 1986, 271 pp.
- [12] Ljung, Lennart, **System Identification: Theory for the User**, Prentice-Hall, Inc., Englewood Cliffs, New Jersey, 1987, 519 pp.

2. MODAL ANALYSIS THEORY

2.1 Introduction

While modal analysis theory has not changed over the last century, the application of the theory to experimentally measured data has changed significantly. The advances of recent years, with respect to measurement and analysis capabilities, have caused a reevaluation of what aspects of the theory relate to the practical world of testing. With this in mind, the aspect of transform relationships has taken on renewed importance since digital forms of the integral transforms are in constant use. The theory from the vibrations point of view involves a more thorough understanding of how the structural parameters of mass, damping, and stiffness relate to the impulse response function (time domain), the frequency response function (Fourier, or frequency domain), and the transfer function (Laplace domain) for single and multiple degree of freedom systems.

2.2 Transform Relationships

One of the keys to understanding experimental modal analysis involves the comprehension of the relationships between the different domains used to describe the dynamics of a structural system. Historically, this has involved the time, frequency (Fourier), and Laplace domains. These relationships, with respect to a structural system, are the integral transforms (Fourier and Laplace) that reflect the information contained by the governing differential equations transformed to each domain. It is important to note that these are integral relationships and that the governing differential equations represent continuous relationships in each domain. As the digital approach to the measurement of data is considered, similar relationships between time, frequency, and Z domains can be formed that reflect the information contained by the governing finite difference equations in each domain. The relationships in this discrete case are represented by discrete transforms (Discrete Fourier Transform, Z Transform). Whether the concept is approached from the continuous or discrete case, the idea of the transform relationship is of primary importance.

The concept of a transform is obviously very special. In general, there are four criteria for a mathematical process to be designated as a transform. First, the transform process must involve

a change of independent variable which represents the change from one domain to another. Second, the transformed variable must be the variable of interest. Third, the transform process must be computationally very simple but unique. Finally, there must be no loss of information in the transform process. This last criteria is often the true distinction between a transform and some form of parameter estimation. Since, with respect to modal analysis, the concepts of transforms and parameter estimation are both important, this distinction is a very important one.

2.2.1 Transform Properties

The properties of transforms must be well understood in order to process data into measurements efficiently and without error. Digital data is always truncated to a limited time period and is often multiplied by a time varying function in order to enhance certain characteristics in the data. This sort of alteration of the data in the time domain has distinctly unique but often bewildering effects in another domain if the properties of the transform are not considered.

While the complete list of transform properties for each transform can be found in numerous applied mathematics handbooks ^[1-3], several properties should be noted due to their frequent application in digital signal processing. First, scalar multiplication is commutative within and between domains. Therefore, calibration of signals using constant calibration factors can be performed without detrimental effect in any domain. Second, the multiplication of two functions in one domain is equivalent to the convolution of the transformed functions in the resulting domain. This property is essential for explaining the effects of weighting functions applied in the time domain as a possible way of minimizing the effects of the bias error that will occur due to the truncation of the data in the time domain (*leakage* error). Third, differentiation in the time domain with respect to the independent time variable is equivalent to multiplication in the transformed domain by the transformed variable. This property gives a very simple algebraic way to convert data from acceleration to velocity or displacement in the frequency or Laplace domains via multiplication. Finally, the shift theorem, which involves multiplying the time domain data by a complex function of a shift frequency [$\cos(\omega t) + j \sin(\omega t)$] is the basis for most frequency-shifted Fourier transform algorithms (Zoom) used in digital signal analyzers today. The schematic of this frequency-shifted Fourier transform process is shown in Figure 2-1 for a shift of f_c Hertz.

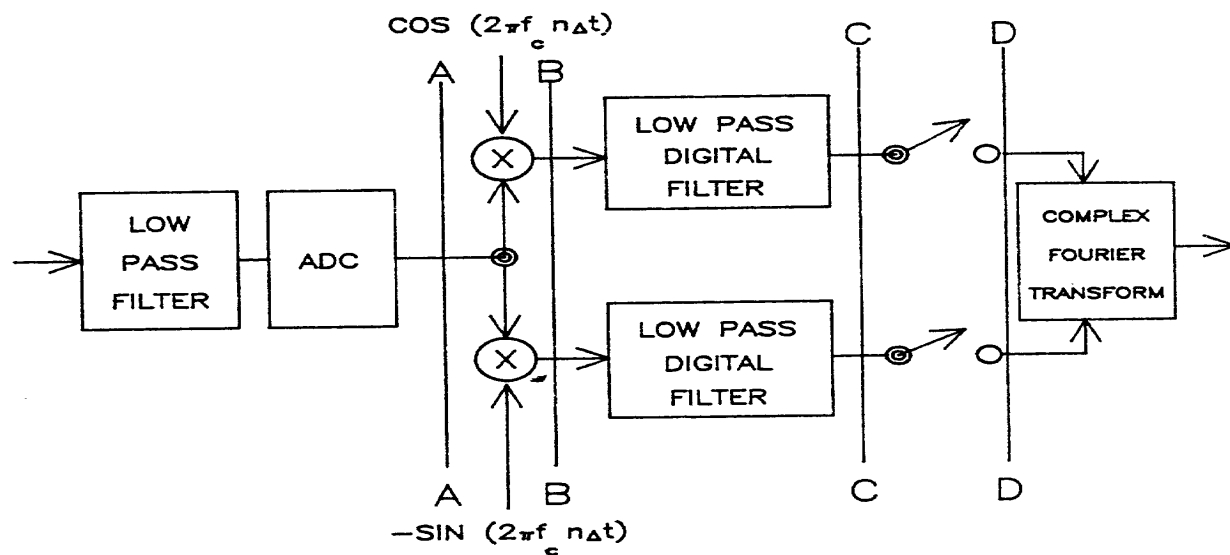


Figure 2-1. Zoom Transform Process

2.3 Single Degree of Freedom Systems

In order to understand modal analysis, the comprehension of single degree of freedom systems is necessary. In particular, the complete familiarity with single degree of freedom systems as presented and evaluated in the time, frequency (Fourier), and Laplace domains serves as the basis for many of the models that are used in modal parameter estimation. This single degree of freedom approach is obviously trivial for the modal analysis case. The true importance of this approach results from the fact that the multiple degree of freedom case can be viewed as simply a linear superposition of single degree of freedom systems.

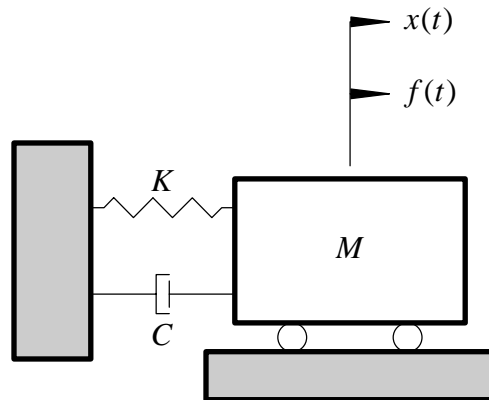


Figure 2-2. Single Degree of Freedom System

The general mathematical representation of a single degree of freedom system is expressed in Equation (2.1):

$$M \ddot{x}(t) + C \dot{x}(t) + K x(t) = f(t) \quad (2.1)$$

where:

- M = Mass constant
- C = Damping constant
- K = Stiffness constant

By setting $f(t) = 0$, the homogeneous form of Equation (2.1) can be solved.

$$M \ddot{x}(t) + C \dot{x}(t) + K x(t) = 0 \quad (2.2)$$

From differential equation theory, the solution can be assumed to be of the form $x(t) = X e^{st}$, where s is a complex constant to be determined. Taking appropriate derivatives and substituting into Equation (2.2) yields:

$$(M s^2 + C s + K) X e^{st} = 0 \quad (2.3)$$

Thus, for a non-trivial solution:

$$M s^2 + C s + K = 0 \quad (2.4)$$

where:

- s = Complex-valued frequency variable (Laplace variable)

Equation (2.4) is the characteristic equation of the system, whose roots λ_1 and λ_2 are:

$$\lambda_{1,2} = -\frac{C}{2M} \pm \left\{ \left(\frac{C}{2M} \right)^2 - \left(\frac{K}{M} \right) \right\}^{\frac{1}{2}} \quad (2.5)$$

Thus the general solution of Equation (2.2) is:

$$x(t) = A e^{\lambda_1 t} + B e^{\lambda_2 t} \quad (2.6)$$

A and B are constants determined from the initial conditions imposed on the system at time $t = 0$.

For most real structures, unless active damping systems are present, the damping ratio is rarely greater than ten percent. For this reason, all further discussion is restricted to underdamped systems ($\zeta < 1$). With reference to Eq. (2.6), this means that the two roots, $\lambda_{1,2}$, are always complex conjugates. Also, the two coefficients (A and B) are complex conjugates of one another (A and A^*). For an underdamped system, the roots of the characteristic equation can be written as:

$$\lambda_1 = \sigma_1 + j \omega_1 \quad \lambda_1^* = \sigma_1 - j \omega_1 \quad (2.7)$$

where:

- σ_1 = Damping factor
- ω_1 = Damped natural frequency

The roots of characteristic Equation (2.4) can also be written as:

$$\lambda_1, \lambda_1^* = -\zeta_1 \Omega_1 \pm j \Omega_1 \sqrt{1 - \zeta_1^2} \quad (2.8)$$

The **damping factor**, σ_1 , is defined as the real part of a root of the characteristic equation. The damping factor describes the exponential decay or growth of the oscillation. This parameter has the same units as the imaginary part of the root of the characteristic equation, typically radians per second.

With respect to the above result, critical damping and damping ratio can now be defined. **Critical damping**, C_c , is defined as being the damping which reduces the radical in the solution of the characteristic equation to zero. This form of representing the damping is a physical approach and therefore involves the appropriate units for equivalent viscous damping.

$$C_c = 2M \sqrt{\frac{K}{M}} = 2M\Omega_1 \quad (2.9)$$

The fraction of critical damping, or **damping ratio**, ζ , is the ratio of the actual system damping to the critical system damping. This approach to the description of damping is dimensionless since the units have been normalized.

$$\zeta_1 = \frac{C}{C_c} = -\sigma_1 \Omega_1 \quad (2.10)$$

2.3.1 Time Domain: Impulse Response Function

The impulse response function of the single degree of freedom system can be determined from Equation (2.6) assuming that the initial conditions are zero and that the system excitation, $f(t)$, is a unit impulse. The response of the system, $x(t)$, to such a unit impulse is known as the impulse response function, $h(t)$, of the system. Therefore:

$$h(t) = A e^{\lambda_1 t} + A^* e^{\lambda_1^* t} \quad (2.11)$$

$$h(t) = e^{\sigma_1 t} \left[A e^{(+j\omega_1 t)} + A^* e^{(-j\omega_1 t)} \right] \quad (2.12)$$

Thus, the coefficients (A and A^*) control the amplitude of the impulse response, the real part of the pole is the decay rate and the imaginary part of the pole is the frequency of oscillation. Figure 2-3 illustrates the impulse response function, for a single degree of freedom system.

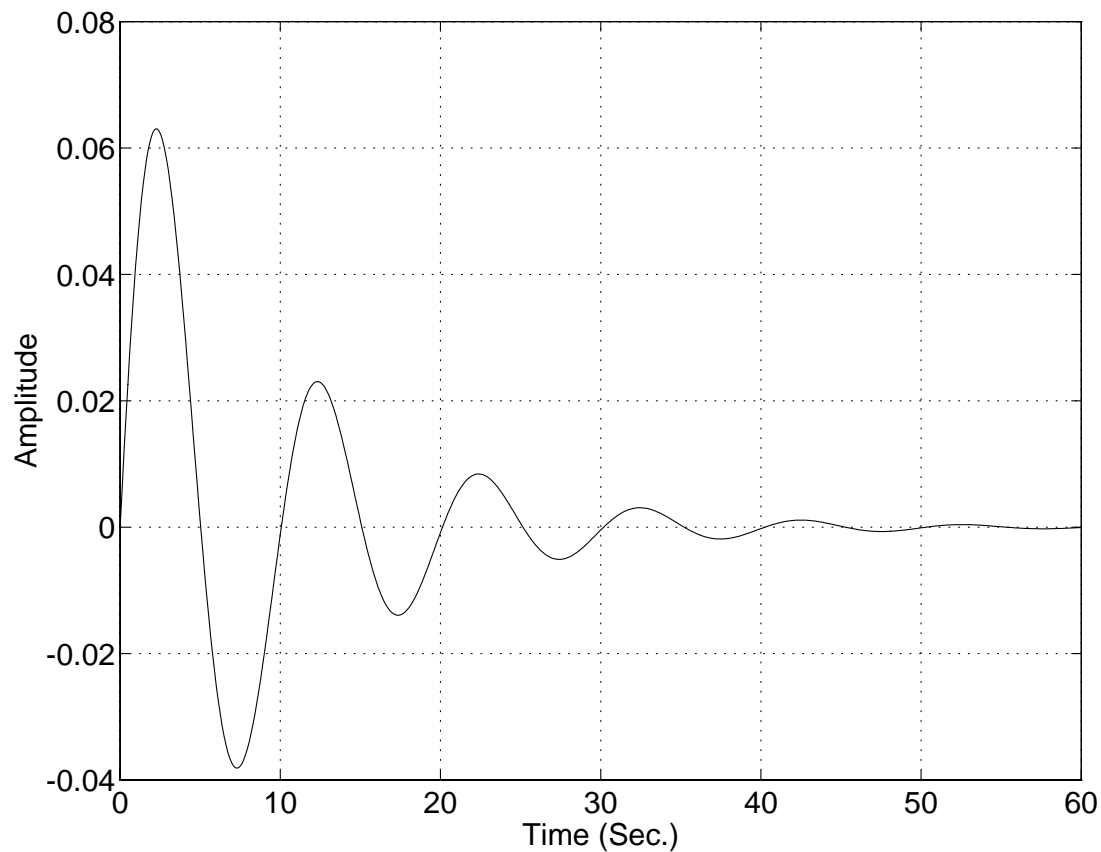


Figure 2-3. Time Domain: Impulse Response Function

2.3.2 Frequency Domain: Frequency Response Function

An equivalent equation of motion for Equation (2.1) is determined for the Fourier or frequency (ω) domain. This representation has the advantage of converting a differential equation to an algebraic equation. This is accomplished by taking the Fourier transform of Equation (2.1). Thus, Equation (2.1) becomes:

$$\left[-M \omega^2 + j C \omega + K \right] X(\omega) = F(\omega) \quad (2.13)$$

Restating the above equation:

$$B(\omega) X(\omega) = F(\omega) \quad (2.14)$$

where:

$$\bullet B(\omega) = -M \omega^2 + j C \omega + K$$

Equation (2.14) states that the system response $X(\omega)$ is directly related to the system forcing function $F(\omega)$ through the quantity $B(\omega)$, the ***impedance function***. If the system forcing function $F(\omega)$ and its response $X(\omega)$ are known, $B(\omega)$ can be calculated. That is:

$$B(\omega) = \frac{F(\omega)}{X(\omega)} \quad (2.15)$$

More frequently, the system response, $X(\omega)$, due to a known input $F(\omega)$, is of interest.

$$X(\omega) = \frac{F(\omega)}{B(\omega)} \quad (2.16)$$

Equation (2.16) becomes:

$$X(\omega) = H(\omega) F(\omega) \quad (2.17)$$

where:

$$\bullet H(\omega) = \frac{1}{-M\omega^2 + jC\omega + K}$$

The quantity $H(\omega)$ is known as the **frequency response function** of the system. The frequency response function relates the Fourier transform of the system input to the Fourier transform of the system response. From Equation (2.17), the frequency response function can be defined as:

$$H(\omega) = \frac{X(\omega)}{F(\omega)} \quad (2.18)$$

Going back to Equation (2.13), the frequency response function can be written:

$$H(\omega) = \frac{1}{-M\omega^2 + jC\omega + K} = \frac{1/M}{-\omega^2 + j\left(\frac{C}{M}\right)\omega + \left(\frac{K}{M}\right)} \quad (2.19)$$

The denominator of Equation (2.19) is known as the **characteristic equation** of the system and is of the same form as Equation (2.4). The characteristic values of this complex equation are in general complex even though the equation is a function of a real valued independent variable (ω). The **characteristic values** of this equation are known as the **complex roots** of the characteristic equation or the **complex poles** of the system. These characteristic values are also called the **modal frequencies**.

The frequency response function $H(\omega)$ can also be written as a function of the complex poles as follows:

$$H(\omega) = \frac{1/M}{(j\omega - \lambda_1)(j\omega - \lambda_1^*)} = \frac{A}{(j\omega - \lambda_1)} + \frac{A^*}{(j\omega - \lambda_1^*)} \quad (2.20)$$

where:

- λ_1 = Complex pole
- $\lambda_1 = \sigma + j\omega_1$
- $\lambda_1^* = \sigma - j\omega_1$

Since the frequency response function is a complex valued function of a real valued independent

variable (ω), the frequency response function, as shown in Figures 2-4 through 2-6 is represented by a pair of curves.

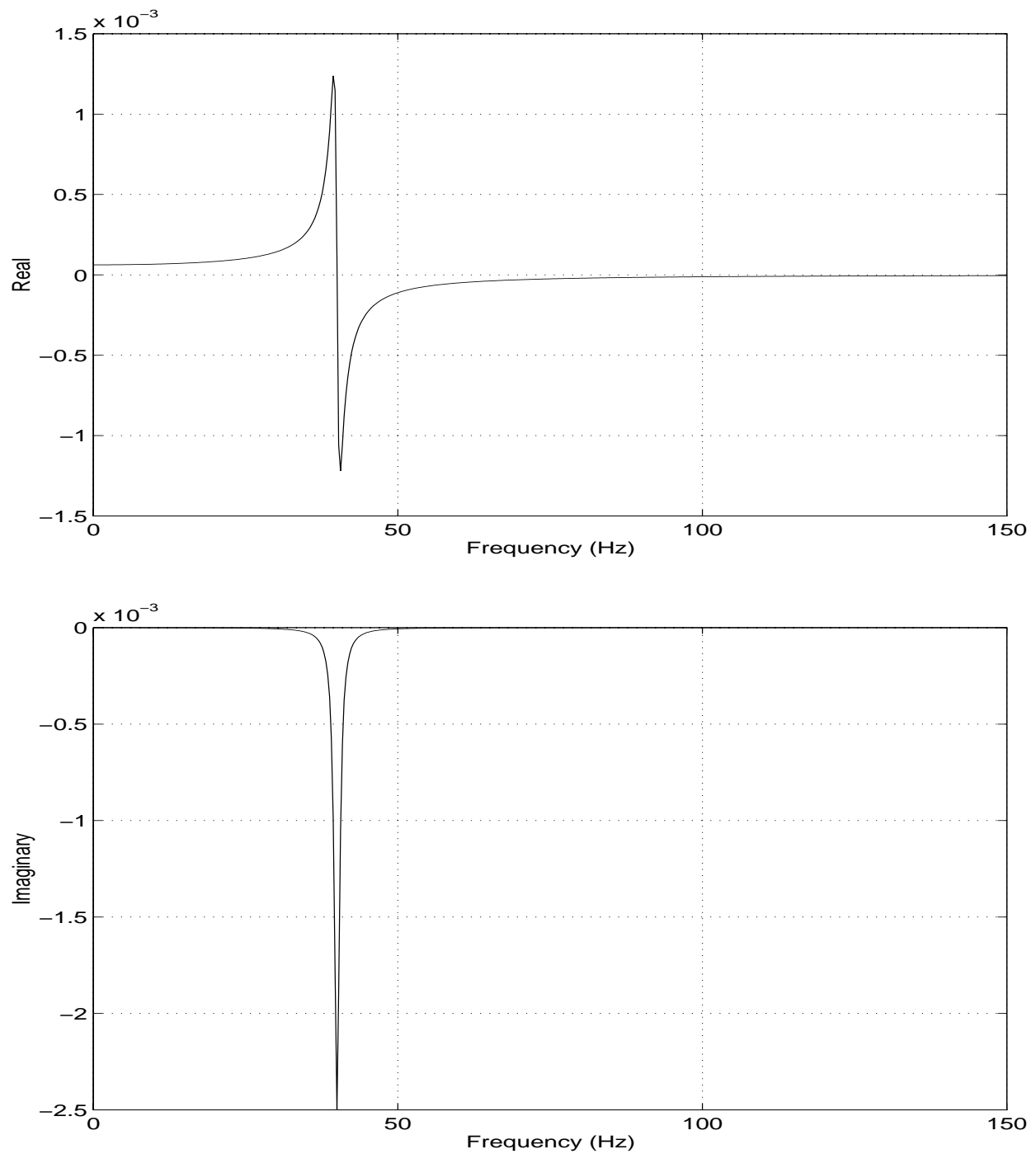
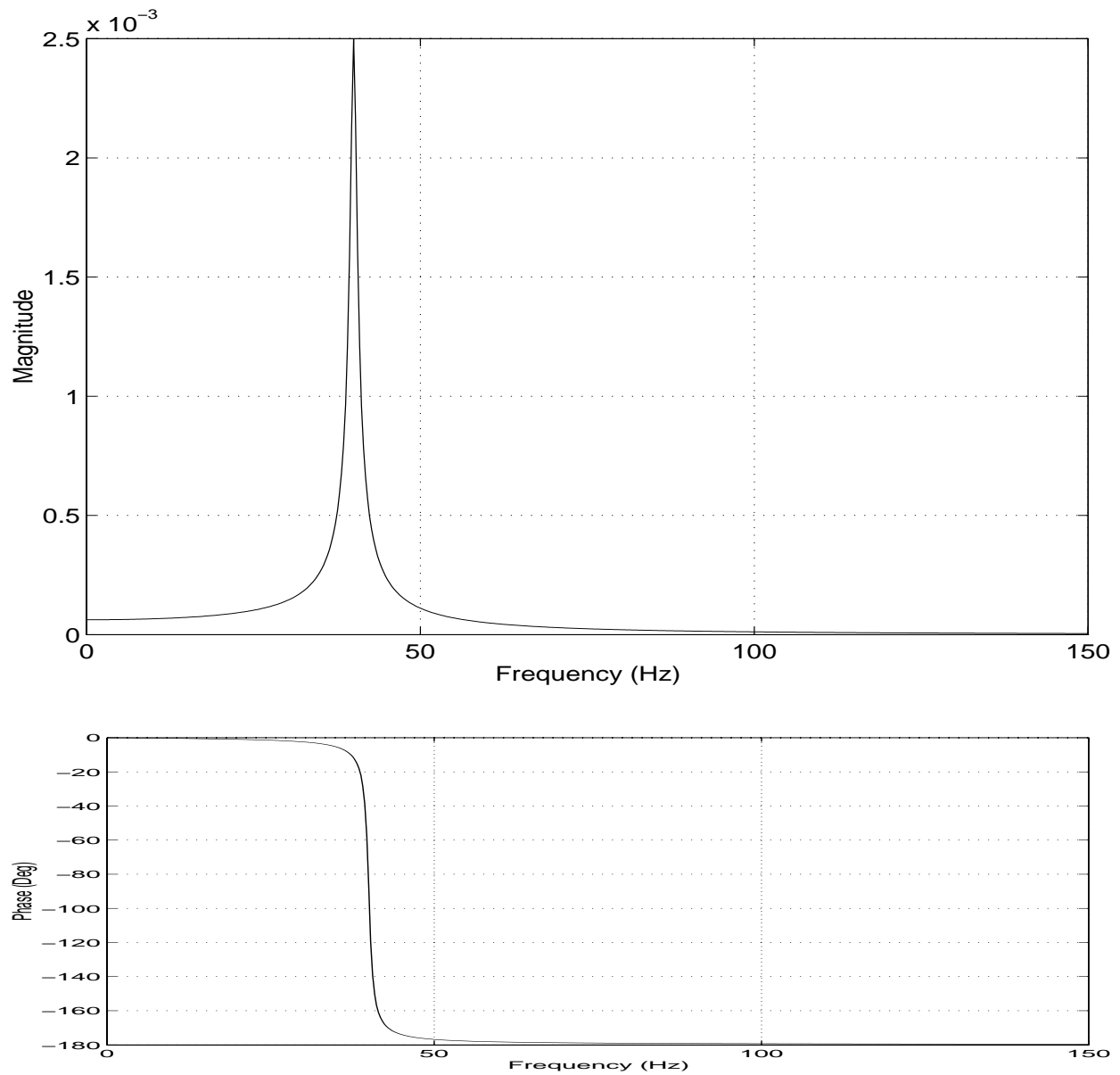


Figure 2-4. Frequency Response Function (Real/Imaginary Format)**Figure 2-5.** Frequency Response Function (Magnitude/Phase Format)

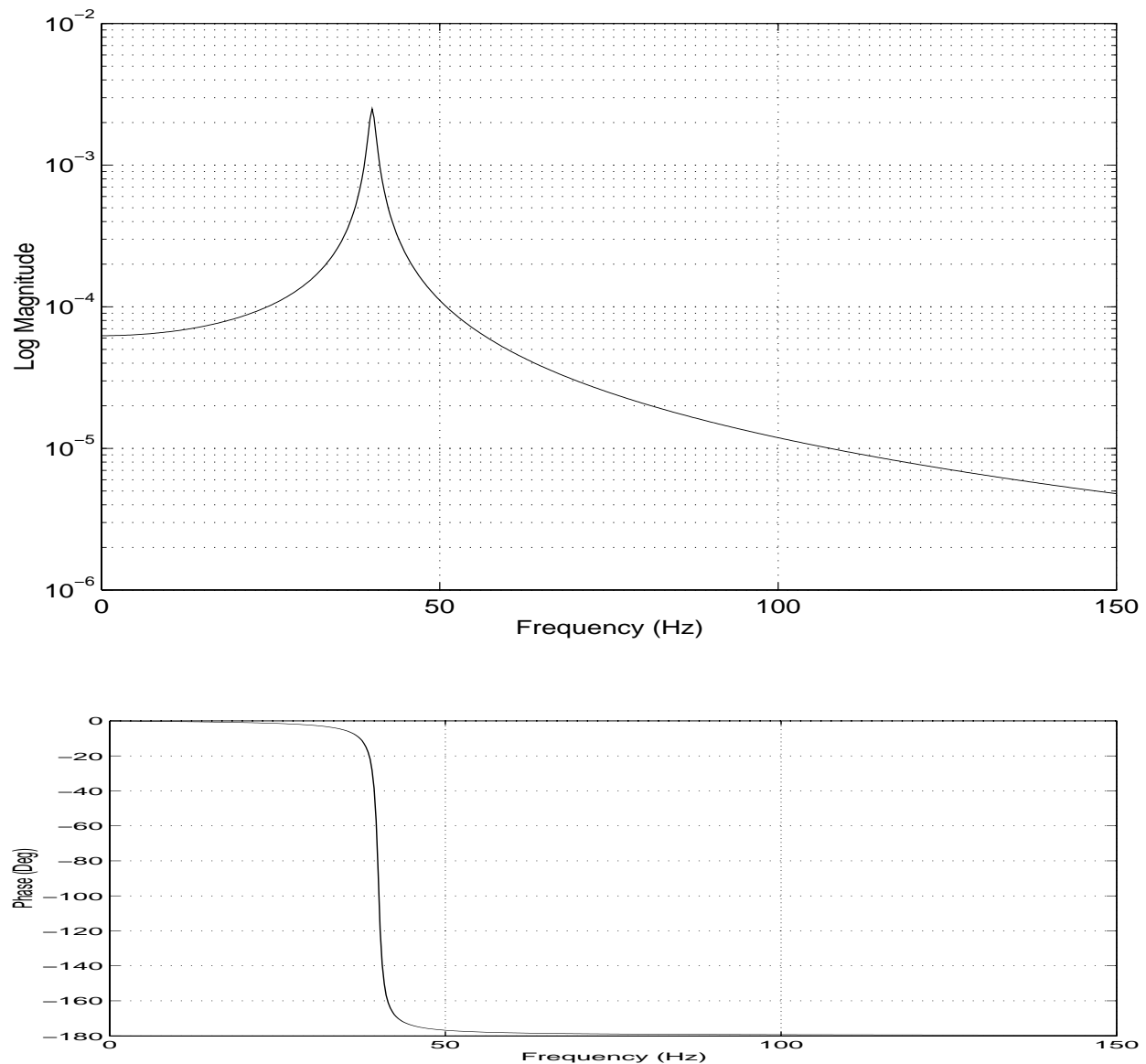


Figure 2-6. Frequency Response Function (Log Magnitude/Phase Format)

2.3.3 Laplace Domain: Transfer Function

Just as in the previous case for the frequency domain, the equivalent information can be presented in the Laplace domain by way of the Laplace transform. The only significant difference in the development concerns the fact that the Fourier transform is defined from

negative infinity to positive infinity while the Laplace transform is defined from zero to positive infinity with initial conditions. The Laplace representation, also, has the advantage of converting a differential equation to an algebraic equation. The development using Laplace transforms begins by taking the Laplace transform of Equation (2.1). Thus, Equation (2.1) becomes:

$$\left[M s^2 + C s + K \right] X(s) = F(s) + [M s + C] X(0) + M \dot{X}(0) \quad (2.21)$$

$X(0)$ and $\dot{X}(0)$ are the initial displacements and velocities at time $t = 0$.

If the initial conditions are zero, Equation (2.21) becomes:

$$\left[M s^2 + C s + K \right] X(s) = F(s) \quad (2.22)$$

Then, Equation (2.22) becomes:

$$B(s) X(s) = F(s) \quad (2.23)$$

where:

$$\bullet B(s) = M s^2 + C s + K$$

Therefore, using the same logic as in the frequency domain case, the transfer function can be defined in the same way that the frequency response function was defined previously.

$$X(s) = H(s) F(s) \quad (2.24)$$

where:

$$\bullet H(s) = \frac{1}{M s^2 + C s + K}$$

The quantity $H(s)$ is defined as the **transfer function** of the system. In other words, a transfer function relates the Laplace transform of the system input to the Laplace transform of the system response. From Equation (2.24), the transfer function can be defined as:

$$H(s) = \frac{X(s)}{F(s)} \quad (2.25)$$

Going back to Equation (2.22), the transfer function can be written:

$$H(s) = \frac{1}{M s^2 + C s + K} = \frac{1/M}{s^2 + \left(\frac{C}{M}\right)s + \left(\frac{K}{M}\right)} \quad (2.26)$$

Note that Equation (2.26) is valid under the assumption that the initial conditions are zero.

The denominator term is once again referred to as the characteristic equation of the system. As noted in the previous two cases, the roots of the characteristic equation are given in Equation (2.5).

The transfer function, $H(s)$, can now be rewritten, just as in the frequency response function case, as:

$$H(s) = \frac{1/M}{(s - \lambda_1)(s - \lambda_1^*)} = \frac{A}{(s - \lambda_1)} + \frac{A^*}{(s - \lambda_1^*)} \quad (2.27)$$

Since the transfer function is a complex valued function of a complex independent variable (s), the transfer function is represented, as shown in Figures 2-7 through 2-9, as a pair of surfaces. Remember that the variable s in Equation (2.27) is a complex variable, that is, it has a real part and an imaginary part. Therefore, it can be viewed as a function of two variables which represent a surface.

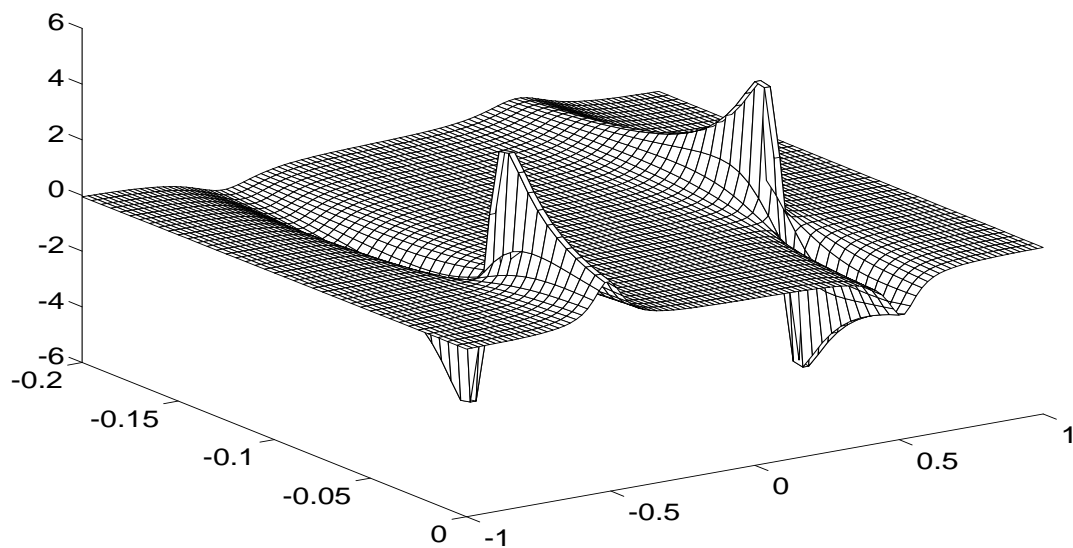
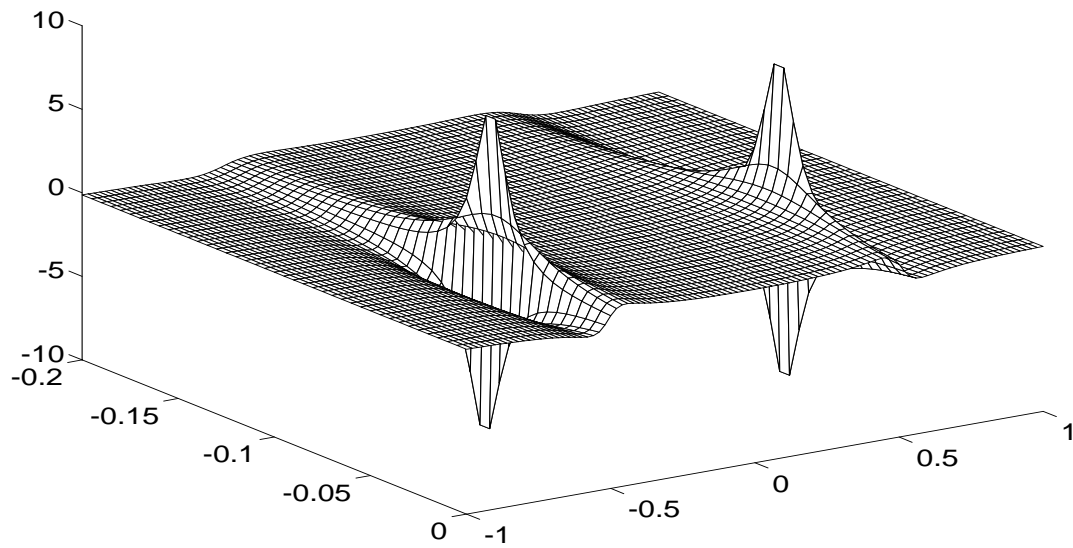


Figure 2-7. Transfer Function (Real/Imaginary Format)

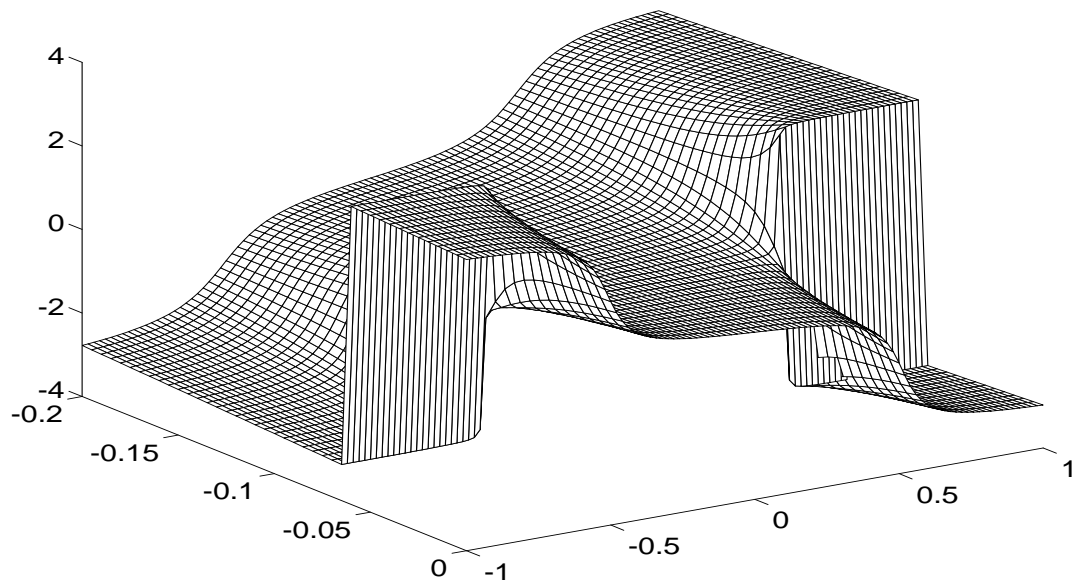
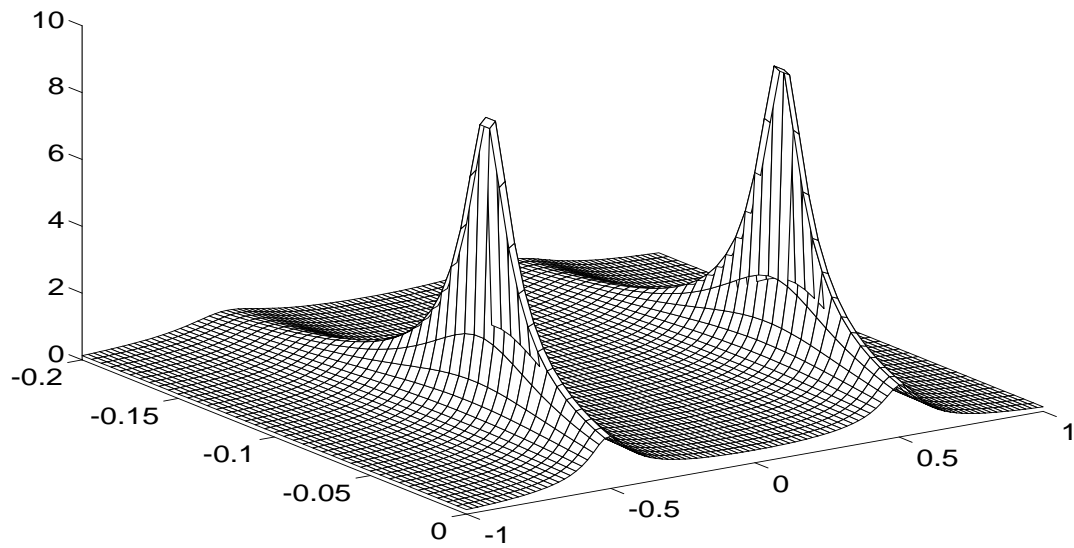


Figure 2-8. Transfer Function (Magnitude/Phase Format)

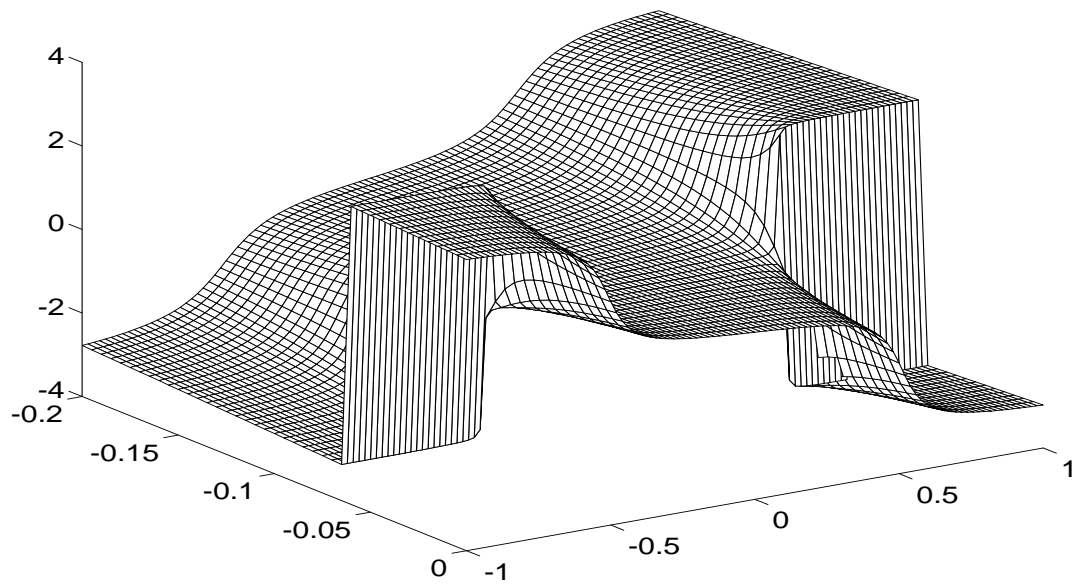
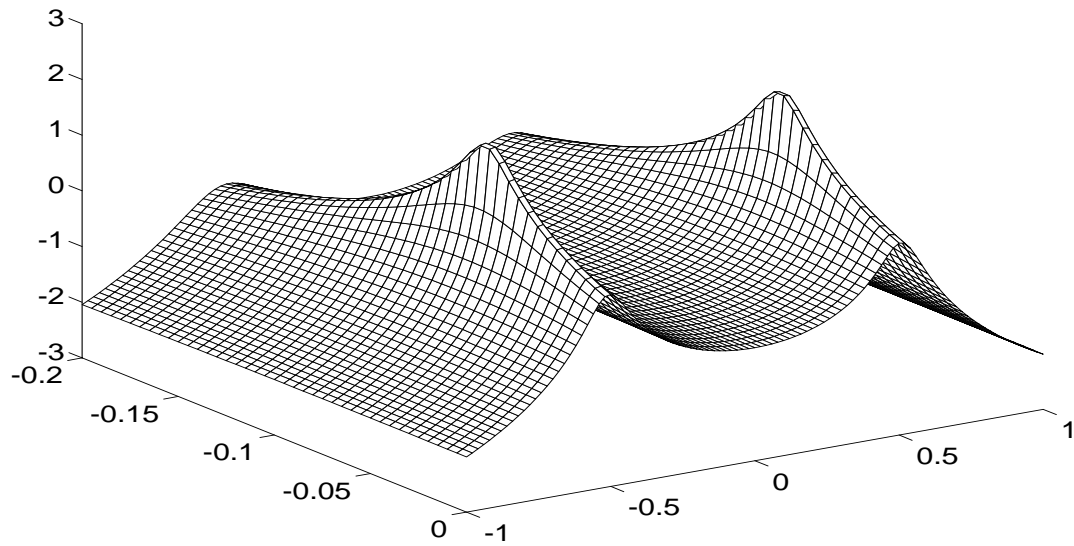


Figure 2-9. Transfer Function (Log Magnitude/Phase Format)

The definition of undamped natural frequency, damped natural frequency, damping factor, percent of critical damping, and residue are all relative to the information represented by Figures 2-6 through 2-9. The projection of this information onto the plane of zero amplitude yields the information as shown in Figure 2-10.

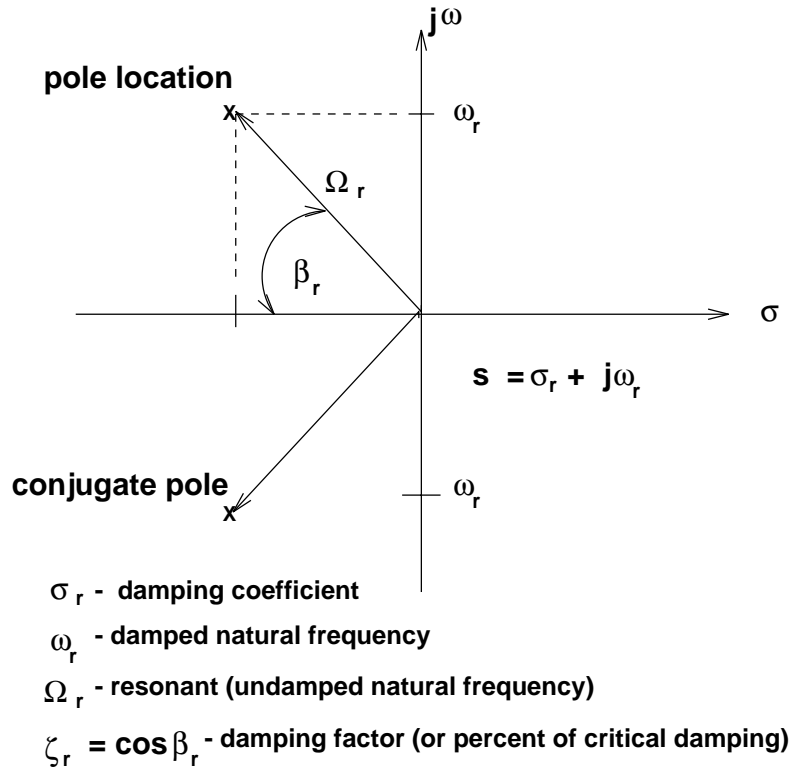


Figure 2-10. Transfer Function - LaPlace Plane Projection)

The concept of **residues** is now defined in terms of the partial fraction expansion of the transfer function equation. Equation (2.27) can be expressed in terms of partial fractions:

$$H(s) = \frac{1/M}{(s - \lambda_1)(s - \lambda_1^*)} = \frac{A}{(s - \lambda_1)} + \frac{A^*}{(s - \lambda_1^*)} \quad (2.28)$$

The **residues** of the transfer function are defined as being the constants A and A^* . The terminology and development of residues comes from the evaluation of analytic functions in

complex analysis. The residues of the transfer function are directly related to the amplitude of the impulse response function. In general, the residue A can be a complex quantity. As shown for a single degree of freedom system, A is purely imaginary.

At this point, it can be noted that the Laplace transform formulation is simply the general case of the Fourier transform development if the initial conditions are zero. The frequency response function is the part of the transfer function evaluated along the $s = j\omega$ axis.

From an experimental point of view, the transfer function is not estimated from measured input-output data. Instead, the frequency response function is actually estimated via the discrete Fourier transform.

2.4 Multiple Degree of Freedom Systems

The real application of modal analysis concepts begin when a continuous, non-homogeneous structure is described as a lumped mass, multiple degree-of-freedom system. At this point, the modal frequencies, the modal damping, and the modal vectors, or relative patterns of motion, can be found via an estimate of the mass, damping, and stiffness matrices or via the measurement of the associated frequency response functions. The two degree of freedom system, shown in Figure 2-11, is the most basic example of a multiple degree of freedom system. This example is a useful means for discussing modal analysis concepts since a theoretical solution can be formulated in terms of the mass, stiffness, and damping matrices or in terms of the frequency response functions.

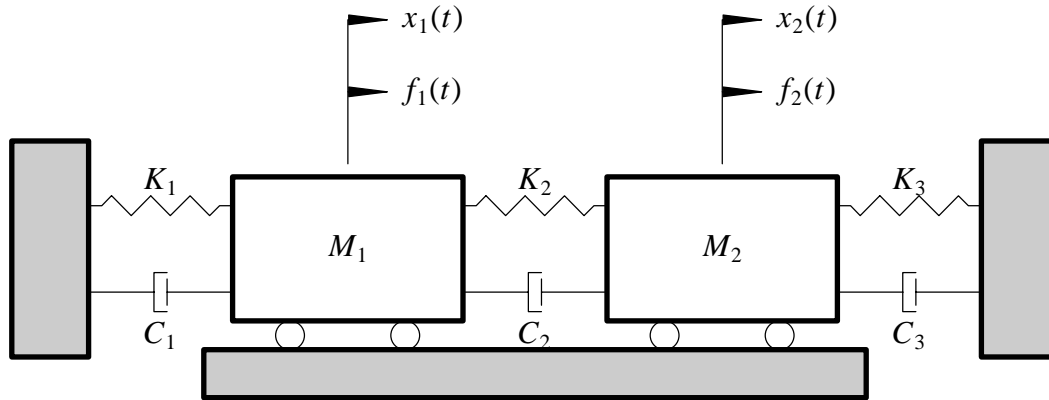


Figure 2-11. Multi-Degree of Freedom System)

The equations of motion for the system in Figure 2-11, using matrix notation, are as follows:

$$\begin{bmatrix} M_1 & 0 \\ 0 & M_2 \end{bmatrix} \begin{bmatrix} \ddot{x}_1 \\ \ddot{x}_2 \end{bmatrix} + \begin{bmatrix} (C_1 + C_2) & -C_2 \\ -C_2 & (C_2 + C_3) \end{bmatrix} \begin{bmatrix} \dot{x}_1 \\ \dot{x}_2 \end{bmatrix} + \begin{bmatrix} (K_1 + K_2) & -K_2 \\ -K_2 & (K_2 + K_3) \end{bmatrix} \begin{bmatrix} x_1 \\ x_2 \end{bmatrix} = \begin{bmatrix} f_1 \\ f_2 \end{bmatrix} \quad (2.29)$$

The process of solving Equation (2.29) when the mass, damping, and stiffness matrices are known is shown in almost every classical text concerning vibrations ^[4-6].

The development of the frequency response function solution for the multiple degree of freedom case parallels the single degree-of-freedom case. This development relates the mass, damping, and stiffness matrices to a transfer function model involving multiple degrees of freedom. Just as in the analytical case where the ultimate solution can be described in terms of one degree of freedom systems, the frequency response functions between any input and response degree of

freedom can be represented as a linear superposition of the single degree of freedom models derived previously.

As a result of the linear superposition concept, the equations for the impulse response function, the frequency response function, and the transfer function for the multiple degree of freedom system are defined as follows:

Impulse Response Function

$$[h(t)] = \sum_{r=1}^N \left[A_r \right] e^{\lambda_r t} + \left[A_r^* \right] e^{\lambda_r^* t} = \sum_{r=1}^{2N} \left[A_r \right] e^{\lambda_r t} \quad (2.30)$$

Frequency Response Function

$$[H(\omega)] = \sum_{r=1}^N \frac{\left[A_r \right]}{j\omega - \lambda_r} + \frac{\left[A_r^* \right]}{j\omega - \lambda_r^*} = \sum_{r=1}^{2N} \frac{\left[A_r \right]}{j\omega - \lambda_r} \quad (2.31)$$

Transfer Function

$$[H(s)] = \sum_{r=1}^N \frac{\left[A_r \right]}{s - \lambda_r} + \frac{\left[A_r^* \right]}{s - \lambda_r^*} = \sum_{r=1}^{2N} \frac{\left[A_r \right]}{s - \lambda_r} \quad (2.32)$$

where:

- t = Time variable
- ω = Frequency variable
- s = Laplace variable
- p = Measured degree of freedom (output)

- q = Measured degree of freedom (input)
- r = Modal vector number
- A_{pqr} = Residue
- $A_{pqr} = Q_r \psi_{pr} \psi_{qr}$
- Q_r = Modal scaling factor
- ψ_{pr} = Modal coefficient
- λ_r = System pole
- N = Number of positive modal frequencies

It is important to note that the residue, A_{pqr} , in Equations (2.30) through (2.32) is the product of the modal deformations at the input q and response p degrees of freedom and a modal scaling factor for mode r . Therefore, the product of these three terms is unique but each of the three terms by themselves is not unique. This is consistent with the arbitrary normalization of the modal vectors. **Modal scaling**, Q_r , refers to the relationship between the normalized modal vectors and the absolute scaling of the mass matrix (analytical case) and/or the absolute scaling of the residue information (experimental case). Modal scaling is normally presented as **modal mass** or **modal A**.

The driving point residue, A_{qqr} , is particularly important in deriving the modal scaling.

$$A_{qqr} = Q_r \psi_{qr} \psi_{qr} = Q_r \psi_{qr}^2 \quad (2.33)$$

For undamped and proportionally damped systems, the r -th modal mass of a multi-degree of freedom system can be defined as:

Modal Mass

$$M_r = \frac{1}{j^2 Q_r \omega_r} = \frac{\psi_{pr} \psi_{qr}}{j^2 A_{pqr} \omega_r} \quad (2.34)$$

where:

- M_r = Modal mass
- Q_r = Modal scaling constant
- ω_r = Damped natural frequency

If the largest scaled modal coefficient is equal to unity, Equation 2.34 will also compute a quantity of modal mass that has physical significance. The physical significance is that the quantity of modal mass computed under these conditions will be a number between zero and the total mass of the system. Therefore, under this scaling condition, the modal mass can be viewed as the amount of mass that is participating in each mode of vibration. Obviously, for a translational rigid body mode of vibration, the modal mass should be equal to the total mass of the system.

The **modal mass** defined in Equation 2.34 is developed in terms of displacement over force units. If measurements, and therefore residues, are developed in terms of any other units (velocity over force or acceleration over force), Equation 2.34 will have to be altered accordingly.

Once the modal mass is known, the **modal damping** and **modal stiffness** can be obtained through the following single degree of freedom equations:

Modal Damping

$$C_r = 2 \sigma_r M_r \quad (2.35)$$

Modal Stiffness

$$K_r = (\sigma_r^2 + \omega_r^2) M_r = \Omega_r^2 M_r \quad (2.36)$$

For systems with nonproportional damping, modal mass cannot be used for modal scaling. For this case, and increasingly for undamped and proportionally damped cases as well, the **modal A** scaling factor is used as the basis for the relationship between the scaled modal vectors and the residues determined from the measured frequency response functions. This relationship is as follows:

Modal A

$$M_{A_r} = \frac{\psi_{pr}\psi_{qr}}{A_{pqr}} = \frac{1}{Q_r} \quad (2.37)$$

This definition of **modal A** is also developed in terms of displacement over force units. Once **modal A** is known, **modal B** can be obtained through the following single degree of freedom equation:

Modal B

$$M_{B_r} = -\lambda_r M_{A_r} \quad (2.38)$$

For undamped and proportionally damped systems, the relationship between **modal mass** and **modal A** scaling factors can be stated.

$$M_{A_r} = \pm j2M_r\omega_r \quad (2.39)$$

In general, modal vectors are considered to be dimensionless since they represent relative patterns of motion. Therefore, the modal mass or modal A scaling terms carry the units of the respective measurement. For example, the development of the frequency response is based upon displacement over force units. The residue must therefore, have units of length over force-seconds. Since the modal A scaling coefficient is inversely related to the residue, modal A will have units of force-seconds over length. This unit combination is the same as mass over seconds. Likewise, since modal mass is related to modal A, for proportionally damped systems, through a direct relationship involving the damped natural frequency, the units on modal mass are mass units as expected.

The following table summarizes the units of modal A and modal mass for typical consistent unit applications.

Consistent Units Relationships				
Mass	Force	Length	Modal A (M_{Ar})	Modal Mass (M_r)
M	F	L	M/S	M
KG	NT	Meter	KG/S	KG
KG	KGf	g-S-S	KG/S	KG
LBm	LBf	g-S-S	LBm/S	LBm
Slug	LBf	Feet	Slug/S	Slug

Table 2-1. Modal Scaling Units

2.5 Damping Mechanisms

In order to evaluate multiple degree of freedom systems that are present in the real world, the effect of damping on the complex frequencies and modal vectors must be considered. Many physical mechanisms are needed to describe all of the possible forms of damping that may be present in a particular structure or system. Some of the classical types are: 1) Structural Damping; 2) Viscous Damping; and 3) Coulomb Damping. It is generally difficult to ascertain which type of damping is present in any particular structure. Indeed most structures exhibit damping characteristics that result from a combination of all the above, plus others that have not been described here.

Rather than consider the many, different physical mechanisms, the probable location of each mechanism, and the particular mathematical representation of the mechanism of damping that is needed to describe the dissipative energy of the system, a model will be used that is only concerned with the resultant mathematical form. This model will represent a hypothetical form of damping, that is proportional to the system mass or stiffness matrix. Therefore:

$$[C] = \alpha [M] + \beta [K] \quad (2.40)$$

Under this assumption, **proportional damping** is the case where the equivalent damping matrix is equal to a linear combination of the mass and stiffness matrices. For this mathematical form of damping, the coordinate transformation that diagonalizes the system mass and stiffness matrices, also diagonalizes the system damping matrix. **Nonproportional damping** is the case

where this linear combination does not exist.

Therefore when a system with proportional damping exists, that system of coupled equations of motion can be transformed to a system of equations that represent an uncoupled system of single degree-of-freedom systems that are easily solved. With respect to modal parameters, a system with proportional damping has real-valued modal vectors (*real or normal modes*) while a system with nonproportional damping has complex-valued modal vectors(*complex modes*) .

2.6 References

- [1] LePage, W.R., **Complex Variables and the Laplace Transform for Engineers**, Dover Publications, Inc., New York, 1961, 475 pp.
- [2] Selby, S.M., **CRC Standard Mathematical Tables, Fifteen Edition**, The Chemical Rubber Company, 1967, 664 pp.
- [3] Spiegel, M.R., **Mathematical Handbook of Formulas and Tables**, Schaum's Outline Series in Mathematics, McGraw-Hill, Inc., 1968, 271 pp.
- [4] Tse, F.S., Morse, I.E., Jr., Hinkle, R.T., **Mechanical Vibrations: Theory and Applications, Second Edition**, Prentice-Hall, Inc., Englewood Cliffs, New Jersey, 1978, 449 pp.
- [5] Craig, R.R., Jr., **Structural Dynamics: An Introduction to Computer Methods**, John Wiley and Sons, Inc., New York, 1981, 527 pp.
- [6] Ewins, D., **Modal Testing: Theory and Practice** John Wiley and Sons, Inc., New York, 1984, 269 pp.

3. HISTORY OF EXPERIMENTAL MODAL ANALYSIS

3.1 Introduction

In reviewing the literature in the area of experimental modal analysis, some sort of outline of the various techniques is helpful in categorizing the different methods that have been developed over the last fifty years. One approach is to group the methods according to whether one mode or multiple modes will be excited at one time. The terminology that is used for this is:

- Phase Resonance (One Mode Excited, All Other Modes Suppressed)
- Phase Separation (All Modes Excited Simultaneously)

At the current time, almost all experimental modal analysis would fall into the phase separation category. Phase resonance methods are used by an increasingly smaller group of aerospace testing activities.

A slightly more detailed approach, and the one that is used in the following text, is to group the methods according to the type of measured data that is acquired. When this approach is utilized, the relevant terminology is:

- Sinusoidal Input-Output Model
- Frequency Response Function Model
- Damped Complex Exponential Response Model
- General Input-Output Model

A very common concept in comparing and contrasting experimental modal analysis methodologies that is often used in the literature is based upon the type of model that will be used in the modal parameter estimation stage. The relevant nomenclature for this approach is:

- Parametric Model (Unknowns have physical significance or meaning)
 - Modal Model
 - [M], [K], [C] Model

- Non-Parametric Model (Unknowns are mathematical conveniences)
 - Polynomial Model
 - AutoRegressive Moving-Average (ARMA) Model

Finally, the different experimental modal analysis approaches may be grouped according to the domain that the modal parameter estimation model will be formulated. The relevant nomenclature for this approach is:

- Time Domain
- Frequency Domain
- Spatial Domain

Regardless of the approach used to organize or classify the different approaches to generating modal parameters from experimental data, the fundamental underlying theory is the same. The differences largely are a matter of logistics, user experience requirements, numerical or compute limitations rather than a fundamentally superior or inferior method.

3.2 Data Acquisition Classification

Over the past forty years, at least four general categories of experimental modal analysis methods, that are based upon the type of data that is acquired, can be identified as follows:

- Sinusoidal Input-Output Model
- Frequency Response Function
- Damped Complex Exponential Response
- General Input-Output Model

Historically, the modal characteristics of mechanical systems have been estimated by techniques that fall into either the first or second category. The experimental modal analysis methods that fall into the last two categories are composite approaches that utilize elaborate parameter estimation algorithms based upon structural models. This section reviews and provides references for the current work in each of these areas.

In order to evaluate and improve any approach to experimental modal analysis, the relative merits of all viable techniques must be well understood. To that goal, many articles have been written to try to compare and contrast the value of one method over another. Unfortunately, most of these comparisons have been heavily concerned with differences that are a function of specific implementations of the various techniques. These comparisons were also potentially biased by the expertise of the test engineers being restricted to only one of the areas of testing. Since each method involves very special testing awareness, this sort of analysis has limited value.

In the evaluation of experimental modal analysis methods, the differences in the theoretical approach are obviously of prime concern. Since most experimental modal analysis methods involve similar theoretical basis, the only significant areas of difference concern the concept of real versus complex modal vectors, the explicit measurement of the input and the different numerical approaches used. The debate over the need to describe complex valued modes of vibration may never end. Certainly, the concept of a complex mode, since it contains a real mode as a special case, appears to be the most general case. Likewise, some experimental modal analysis methods do not require the measurement of the input. While this can be advantageous at times where the implicit nature of the input is known or assumed, it seems prudent, where the input can be measured, to do so.

Beyond the direct theoretical differences, though, there are several key evaluation considerations which may or may not be a direct function of the theory. The availability of confidence factors, the potential for implementation, stability and precision of the solution algorithm, sensitivity to random and/or bias errors in the measured data, and the need for operator expertise may control the ability to estimate valid modal parameters. Specifically, through the knowledge of these aspects with respect to other experimental modal analysis methods, the use of each of the approaches may be enhanced due to this transfer of technology between the methods.

Generally, the methods that utilize frequency response function data, damped complex exponential response data, and/or general input-output data can all be explained using a ***Unified Matrix Polynomial Approach (UMPA)***. Most modal parameter estimation algorithms can be reformulated into this consistent mathematical formulation with a corresponding set of definitions and unifying concepts ^[1]. Particularly, this matrix polynomial approach is used to unify the presentation with respect to current algorithms such as the Least-Squares Complex Exponential (LSCE), the Polyreference Time Domain (PTD), Ibrahim Time Domain (ITD),

Eigensystem Realization Algorithm (ERA), Rational Fraction Polynomial (RFP), Polyreference Frequency Domain (PFD) and the Complex Mode Indicator Function (CMIF) Methods. The Unified Matrix Polynomial Approach provides a common formulation that encourages a discussion of the similarities and differences of the commonly used methods as well as a discussion of the numerical characteristics.

3.2.1 Sinusoidal Input-Output Method

Methods covered by this category involve excitation that consists of only one frequency during the observation period. While excitation involves only one frequency, the response will initially involve many frequencies due to the initiation of the excitation (transient). Even after this initial transient, the response may contain energy at more than one frequency due to the harmonic distortion of the excitation caused by system nonlinearities. This harmonic distortion is normally removed by filtering the response before the data is processed, leaving a single frequency of information in both the input and output signals.

The sinusoidal input/output methods require minimal data acquisition capabilities but, generally involve more sophistication in the test set-up or in the post-processing of the acquired data. Since only a single frequency is present in the input and output signals, time domain methods or at most, small blocksize Fast Fourier Transform (FFT) methods can be used to determine signal amplitudes. Depending upon the approach used, this data will yield the modal parameters somewhat directly or will require considerable post-processing. In the forced normal mode approach, the configuration of the test set-up (location and phasing of multiple exciters) yields the modal parameters somewhat directly. In the forced response decomposition approach, the test set-up is very general but, the modal parameters are found using an elaborate post-processing procedure.

3.2.1.1 Forced Normal Mode Excitation Method

The forced normal mode excitation method of experimental modal analysis is the oldest approach to the estimation of dynamic structural parameters. This approach is the first method to use the application of multiple inputs in the estimation of modal parameters. Currently, this method is still used in the aerospace industry for ground vibration testing of aircraft structures.

This method was originally outlined in an article by Lewis and Wrisley in 1950 ^[2] .and begins with the matrix form of the differential equation for the system being tested, Equation (3.1).

$$[M] \{\ddot{x}\} + [C] \{\dot{x}\} + [K] \{x\} = \{f\} \quad (3.1)$$

Very simply stated, Lewis and Wrisley found that a number of exciters, utilizing a common frequency and monophasic amplitudes, could be tuned to exactly balance the dissipative forces in a structure. This is represented by Equations (3.2) and (3.3) and occurs when the phase lag angle ϕ lags the input force by 90 ° at every response location.

$$\{f\} = \{F\} \sin(\omega t) \quad \{x\} = \{X\} \sin(\omega t - \phi) \quad (3.2)$$

$$\{f\} = [C] \{\dot{x}\} \quad (3.3)$$

When the force balance is achieved, the differential equations of motion describing the structure can be reduced to the undamped homogeneous differential equations of motion at that particular frequency. This is represented by Equation (3.4).

$$[M] \{\ddot{x}\} + [K] \{x\} = \{0\} \quad (3.4)$$

In order to more thoroughly explain this phenomena, De Veubeke published an article ^[3] which explains the theoretical basis for this testing in terms of Characteristic Phase Lag Theory. Further development of the practical application of this theory was enhanced by the concept of effective number of degrees of freedom by Trail-Nash ^[4] . This concept explains that the required number of exciters is a function of the effective number of degrees of freedom not the total number of degrees of freedom. The effective number of degrees of freedom is a function of modal density and damping. Finally, Asher utilized the determinant of the real part of the frequency response matrix to locate damped natural frequencies and determine the effective number of degrees of freedom ^[5] .

Most of the work done since 1958 has been concerned with improvements in the implementation of the method, primarily the force appropriation ^[6-7] . One of the most advanced implementations of this method involves approximately five hundred channels of data acquisition and co/quad analysis equipment controlled from a mini-computer. Extensive tuning criteria are utilized as well as real time animated displays of the modal vector as well as of the

out of phase response. This can be particularly useful for optimum exciter location as well as force appropriation. Once a modal vector is tuned using a 90° phase lag angle criteria, the excitation frequency can be varied with no change in modal vector. Theoretically, this can be used as a check to determine whether the modal vector has been adequately tuned.

In addition to this potential confidence check, the excitation can be removed from the system once a modal vector is tuned. If the modal vector contains only responses due to a single mode of vibration, the exponential decay at all response positions should contain only the excitation frequency and the envelope of exponential decay should give an accurate estimate of the system damping.

The forced normal mode excitation method works well in the presence of proportional damping but theoretically does not include the concept of complex modes of vibration nor the concept of repeated and multiple roots. (Proportional damping is a mathematical approach to the description of damping that states that the damping matrix resulting from whatever damping mechanism that is present is either proportional to the mass matrix, the stiffness matrix, or to some linear combination of the two.) Due to this theoretical limitation, the practical application of the 90° phase lag criteria is normally applied only to within plus or minus 10° . Likewise, added difficulty is encountered in evaluating the exponential decay purity as well as force appropriation. Much work has been done on automated tuning algorithms to alleviate this. These algorithms alter excitation magnitude and phase to try to achieve 90° phase lag criteria under severe impedance matching situations. Unfortunately, the location of the excitation cannot be evaluated automatically in this process.

3.2.1.2 Forced Response Decomposition Method

The forced response decomposition method uses an array of exciters (multiple input) to excite the system into a forced response at a single frequency. While the magnitude of each input and the phasing between inputs may be chosen randomly or according to some particular regime, the inputs are held constant during the observation period. Therefore, after the initial transient decays, the response is a steady-state forced response of this system. A forced response vector is created by using all output points of interest simultaneously. This is represented by Equations (3.5) through (3.7).

$$[M] \{\ddot{x}\} + [C] \{\dot{x}\} + [K] \{x\} = \{f\} \quad (3.5)$$

$$\{f\} = \{F\} \sin(\omega_k t) \quad (3.6)$$

$$\{x\} = \{X\} \sin(\omega_k t - \phi_k) \quad (3.7)$$

The forced response vector that is generated must be a linear superposition of the modal vectors of the system (expansion theorem). Since in a given frequency range of interest, N modal vectors will contribute to the response, the individual modal vectors cannot be determined from one forced response vector. If N or more independent forced response vectors can be generated, the N modal vectors can be determined. A large number of independent forced response vectors can be generated by two approaches. First of all, at a single frequency, many different input vectors can be generated with randomly chosen magnitudes and relative phasing. Each of these choices will yield a potentially independent forced response vector. Secondly, this process can be repeated for different frequencies which will, once again, yield potentially independent forced response vectors. Since the degree of independence among the forced response vectors is unknown and since the best estimate of the modal vectors is desired, many more forced response vectors, compared to the number of expected modal vectors (N), are acquired.

The post-processing of the forced response vectors involves using a singular value decomposition of the data spanned by the forced response vectors. If N_V forced response vectors are acquired (where $N_V \gg N$), the number of significant singular values in the $N_V \times N_V$ data space is an indication of the number of contributing modal vectors in the data. The singular vectors, associated with the significant singular values, provide a transformation matrix to transform the forced response vectors to modal vectors. Frequency and damping values are found in a second stage solution process. If frequency response functions or the input vectors required to force a specific normal mode are desired, these characteristics can be found at this time as well.

The forced response decomposition method, in one form or another is currently receiving much research attention ^[8-9]. While the methods have not been used commercially to this point, the methods are very attractive due to minimal data acquisition requirements (when the data acquisition has been specifically designed for this method) and due to sophisticated post-processing techniques which require minimal computational power (micro-computers or mini-computers).

3.2.2 Frequency Response Function Method

The frequency response function method of experimental modal analysis is the most commonly used approach to the estimation of modal parameters. This method originated as a testing technique as a result of the use of frequency response functions in the forced normal mode excitation method to determine natural frequencies and effective number of degrees of freedom. With the advent of the computer and mini-computer, the frequency response function method became a separate, viable technique ^[10-48].

In this method, frequency response functions are measured using excitation at single, or multiple, points. The relationships between the input ($F(\omega)$) and the response ($X(\omega)$) for both single and multiple inputs are shown in Equation (3.8) through (3.10).

Single Input Relationship

$$X_p = H_{pq} F_q \quad (3.8)$$

$$\begin{Bmatrix} X_1 \\ X_2 \\ \cdot \\ \cdot \\ X_p \end{Bmatrix} = \begin{Bmatrix} H_{1q} \\ \cdot \\ \cdot \\ \cdot \\ H_{pq} \end{Bmatrix} F_q \quad (3.9)$$

Multiple Input Relationship

$$\begin{Bmatrix} X_1 \\ X_2 \\ \cdot \\ \cdot \\ X_p \end{Bmatrix}_{N_o \times 1} = \begin{bmatrix} H_{11} & \cdot & \cdot & \cdot & \cdot & \cdot & \cdot & \cdot & H_{1q} \\ H_{21} & & & & & & & & \cdot \\ \cdot & & & & & & & & \cdot \\ \cdot & & & & & & & & \cdot \\ H_{p1} & \cdot & \cdot & \cdot & \cdot & \cdot & \cdot & \cdot & H_{pq} \end{bmatrix}_{N_o \times N_i} \begin{Bmatrix} F_1 \\ F_2 \\ \cdot \\ \cdot \\ F_q \end{Bmatrix}_{N_i \times 1} \quad (3.10)$$

The frequency response functions are used as input data to modal parameter estimation algorithms that estimate modal parameters using a frequency domain model. Through the use of the Fast Fourier Transform, the Fourier transform of the frequency response function, the impulse response function, can be calculated for use in modal parameter estimation algorithms involving time domain models [10-29] .

Most of the work over the last fifteen years has focussed on the measurement of multiple columns of the frequency response function matrix simultaneously. This work has involved establishing the numerical and excitation requirements for solving the relationship identified in Equation (3.10), developing alternate estimation algorithms and developing modal parameter estimation algorithms that are matched to this new data acquisition/estimation procedure. This work has revolutionized experimental modal analysis testing for several reasons. First of all, in order to be sure that all modal vectors have been found experimentally, a number of excitation (reference) points must be utilized, either one at a time or simultaneously. This minimizes the possibility of exciting the system at or near a node of one of the modal vectors which would provide inaccurate estimates of that modal vector. Secondly, multiple columns (or rows) of the frequency response function matrix are necessary for the detection of repeated or pseudo-repeated (close) modal frequencies. The ability to measure, detect and identify the presence of repeated or close modes was not generally possible prior to this research. Finally, the increased number of measurements per measurement cycle obtained using multiple inputs does not affect the time required to acquire frequency response function data adversely. Therefore, a more complete set of data, allowing for a more complete dynamic model of the system to be validated, is possible in the same measurement time.

3.2.2.1 Theory

If all or part of the elements of the frequency response matrix can be measured, each column will contain information which can be used to estimate modal vectors. Since the frequency response matrix is considered to be symmetric due to the Maxwell-Betti relations, each row will also contain the information needed to estimate modal vectors.

In order to obtain estimates of the modal vectors, the frequency response functions are used as input in a parameter estimation scheme based on one of the Equations (3.11) through (3.15).

Single Reference:

$$H_{pq}(\omega) = \frac{\beta_{2N-2} (j\omega)^{2N-2} + \beta_{2N-1} (j\omega)^{2N-1} + \dots + \beta_1 (j\omega)^1 + \beta_0 (j\omega)^0}{\alpha_{2N} (j\omega)^{2N} + \alpha_{2N-1} (j\omega)^{2N-1} + \dots + \alpha_1 (j\omega)^1 + \alpha_0 (j\omega)^0} \quad (3.11)$$

$$H_{pq}(\omega) = \sum_{r=1}^N \frac{A_{pqr}}{j\omega - \lambda_r} + \frac{A_{pqr}^*}{j\omega - \lambda_r^*} \quad (3.12)$$

Multiple Reference:

$$\sum_{k=0}^{2N} \left[(j\omega)^k [\alpha_k] \right] [H(\omega)] = \sum_{k=0}^{2N-2} \left[(j\omega)^k [\beta_k] \right] [I] \quad (3.13)$$

$$[H(\omega)] = \sum_{r=1}^N \frac{\begin{bmatrix} A_r \end{bmatrix}}{j\omega - \lambda_r} + \frac{\begin{bmatrix} A_r^* \end{bmatrix}}{j\omega - \lambda_r^*} = \sum_{r=1}^{2N} \frac{\begin{bmatrix} A_r \end{bmatrix}}{j\omega - \lambda_r} \quad (3.14)$$

$$[H(\omega)] = \begin{bmatrix} \psi \end{bmatrix} \begin{bmatrix} \Lambda \end{bmatrix} \begin{bmatrix} L \end{bmatrix}^T \quad (3.15)$$

where:

- $\begin{bmatrix} \Lambda \end{bmatrix} = \text{Diagonal matrix} = \begin{bmatrix} \frac{1}{j\omega - \lambda_r} \end{bmatrix}$
- $\begin{bmatrix} I \end{bmatrix} = \text{Identity Vector}$

Often Equation (3.11) through (3.15) are altered by an assumption of real modes, a specific damping mechanism, or known system poles. Under such assumptions, the estimation of the modal parameters may become simpler. Most current research and development in the area of the frequency response function method involves the modal parameter estimation algorithms that are related to the time or frequency domain models equivalent to Equation (3.11) through (3.15). Much of this work involves algorithms that utilize as much of the redundant information within multiple rows and columns of the frequency response function matrix as possible ^[31-48].

3.2.3 Damped Complex Exponential Method

The damped complex exponential response methods of experimental modal analysis are approaches that have received considerable attention. These methods are normally formulated to utilize data corresponding to the free decay of a system generated by the release of an initial condition but apply quite generally to impulse response function data as well. Since impulse response function data is scaled to include the forcing condition, use of this method on impulse response function data yields properly scaled modal parameters that can be used to calculate generalized mass and stiffness. This is not possible if free decay responses are used. Even so, the formulation of the impulse response function generally involves the computation of the frequency response function via a fast Fourier transform, potentially introducing bias errors such as leakage, which may degrade the estimation of the modal parameters.

In order to obtain estimates of the modal vectors, the damped complex exponential response functions, normally the impulse response functions, are used as input in a parameter estimation scheme based on one of the Equations (3.16) through (3.20). Note that if the true damped complex exponential response function can be measured in the time domain, such as a free decay response, bias errors such as leakage will not be a problem since the fast Fourier transform is not used.

Single Reference:

$$\sum_{k=0}^m \alpha_k h(t_{i+k}) = 0 \quad (3.16)$$

$$h_{pq}(t) = \sum_{r=1}^N A_{pqr} e^{\lambda_r t} + A_{pqr}^* e^{\lambda_r^* t} \quad (3.17)$$

Multiple Reference:

$$\sum_{k=0}^m [\alpha_k] \left\{ h_{pq}(t_i + k) \right\} = 0 \quad (3.18)$$

$$[h(t)] = \sum_{r=1}^N \left[A_r \right] e^{\lambda_r t} + \left[A_r^* \right] e^{\lambda_r^* t} = \sum_{r=1}^{2N} \left[A_r \right] e^{\lambda_r t} \quad (3.19)$$

$$[h(t)] = \left[\psi \right] \left[\Lambda \right] \left[L \right]^T \quad (3.20)$$

where:

$$\bullet \left[\Lambda \right] = \text{Diagonal matrix} = \left[e^{\lambda_r t} \right]$$

While the current implementation of methods based upon damped complex exponentials is relatively recent, the basis of much of the work was formulated in the eighteenth century by Prony ^[49]. Currently, the three approaches, that are widely used, are the Ibrahim Time Domain (ITD) approach, the Poly-Reference Time Domain (PTD) approach, and the Eigensystem Realization Algorithm (ERA) approach. These methods are discussed generally in the following sections as well as in detail in a later section on modal parameter estimation ^[50-64].

3.2.3.1 Ibrahim Time Domain (ITD) Approach

One practical implementation of the damped complex exponential method is the Ibrahim Time Domain (ITD) method ^[50-55], developed to extract the modal parameters from damped complex exponential response information. Digital free decay response data are measured at various points on the structure. If response data from all the selected measurement positions cannot be obtained simultaneously because of equipment restrictions, a common position is retained between measurement groups. A recurrence matrix is created from the free decay data, and the eigenvalues of this matrix are exponential functions of the poles of the system, from which the poles are easily computed. The eigenvectors of the recurrence matrix are response residues, from which the mode shapes are determined. The Ibrahim Time Domain method generates a matrix polynomial characteristic equation with matrix dimension equal to the number of response

sensors (N_o) and low model order.

The damped complex exponential response method is rather straight forward in application if the necessary data acquisition hardware, computer facilities and software are available. This approach computes the poles and residues based upon a specific initial vibration condition of the structure. A number of different initial conditions can be established, analogous to the practice of using several exciter positions in ordinary single input modal surveys, until all the important modes have been excited. All the modes cannot be established from one exciter position, and likewise all the modes cannot be determined from one initial condition.

Although this technique is based upon free decay data, the ITD method can also be used with operating inputs if the free decay is computed from the operating inputs by using ***random-decrement*** averaging or from measured auto and cross correlation functions. Again, it should be emphasized that this can only be done if there are no poles or zeros in the input spectrum in the frequency range of interest.

An additional development with respect to this technique is the concept of ***modal confidence factor*** ^[50]. The modal confidence factor is a complex number calculated for each identified mode of the structure, while undergoing an exponential decay form of vibration test. The modal confidence factor is based upon the modal deflection at a particular measurement point being related to the modal deflection at that same measurement point at any time earlier or later in the free decay response. Therefore, if modal vectors are estimated from exponential decay data and two separate estimates are calculated from sets of data taken some fixed time Δt apart, the relationship between the measured second estimate of the modal vector and the calculated estimate of the modal vector based upon the measured first estimate of the modal vector is defined as the modal confidence factor. The purpose of the modal confidence factor is to provide an indicator for determining whether an estimated modal vector is real or computational.

3.2.3.2 Poly-Reference Time Domain (PTD) Approach

A more recent implementation of the damped complex exponential approach to experimental modal analysis is the Poly-Reference Time Domain (PTD) approach developed by Vold ^[56-58]. Most of the comments relative to the ITD approach can also be repeated with respect to the PTD

approach. Of particular importance, once again, is the desirability of acquiring all response data simultaneously to reduce time invariance problems.

In contrast to the ITD approach, the Poly-Reference Time Domain approach utilizes all measured damped complex exponential information, from all references or initial conditions, simultaneously in the estimation of modal frequencies. Since multiple initial conditions or reference data is accounted for in the algorithm, the Poly-Reference Time Domain method is the first algorithm to be able to solve for closely-spaced or repeated roots. Additionally, the PTD approach broke new ground in the estimation of a single modal coefficient for each measurement degree of freedom in the presence of multiple initial conditions or references. This characteristic is shared by the frequency response function method when the Poly-Reference Frequency Domain (PFD) approach is used as the parameter estimation algorithm and with some of the approaches within the mathematical input-output model methods. The formulation of the algorithm such that constraints are included to account for redundant information is an advantage but requires that the total data set be acquired so as to match this assumption. The data acquisition best matches the analysis procedure when all of the data can be acquired simultaneously. The Poly-Reference Time Domain method generates a matrix polynomial characteristic equation with matrix dimension equal to the number of reference sensors (N_i for a multi-shaker test and N_o for a roving impact hammer test) and high model order.

While much of the work utilizing the Poly Reference approach is quite recent, the evaluation of the method based upon comparisons between experimentally measured and synthesized frequency response functions is quite impressive when compared to other modal parameter estimation approaches.

3.2.3.3 Eigensystem Realization Algorithm Approach

The Eigensystem Realization Algorithm (ERA) approach is a recent technique that is basically an extended version of the Ho-Kalman system realization algorithm ^[59-64]. The ERA algorithm was developed at NASA-Langley Research Center under an interdisciplinary effort involving structural dynamics and controls. This method is similar to the other damped complex exponential methods in that all involve solutions of a matrix eigenvalue problem. Since the ERA approach utilizes multiple reference data, the ERA approach is similar to the Polyreference Time

Domain approach. This means that repeated roots can be identified with this approach as well as the Polyreference Time Domain approach. Other significant attributes of this approach include the extensive use of accuracy indicators to assess effects of noise and nonlinearities as well as rank information provided by singular value decomposition techniques.

The ERA approach is based upon well-established realization (state-space) theory using the concepts of controllability and observability. The approach determines a complete state-space model based upon the important principles of minimal realization theory attributed to Ho and Kalman. The Ho-Kalman procedure uses a sequence of real matrices known as Markov parameters (impulse response functions) to construct a state-space representation of a linear system. The ERA approach begins with a block data matrix formulated from damped complex exponential functions, such as free decay responses. This block data matrix is similar to a general Hankel matrix and includes information from several initial conditions and a weighted set of damped complex exponential functions. The weighted set of functions means that points of interest or points with large response can be emphasized without loss of capability of the method. The state-space matrices are found from the block data matrix by factorization of the block data matrix using singular value decomposition. Based upon the rank evaluation of the block data matrix in this factorization procedure, a state-space set of matrices can be formulated based on the reduced order. Eigenvalues and eigenvectors of this reduced order, state-space model are then found. Accuracy indicators such as the rank of the block data matrix, modal amplitude coherence, modal phase collinearity, and data reconstruction are used to identify the final set of modal parameters. The Eigensystem Realization Algorithm (ERA) generates a matrix polynomial characteristic equation with matrix dimension equal to the number of response sensors (N_o) and low model order.

The ERA approach is a recent method that demonstrates extensive use of accuracy indicators. Several studies comparing multiple reference algorithms indicate good agreement between all methods but the identification of non-realistic modal parameters is still a significant problem. The ERA approach, through the extensive development and use of accuracy indicators, attempts to deal with this part of the identification problem more completely than most other approaches. The accuracy indicators utilized in the ERA approach are already being applied to several other approaches with similar success. The primary limitation of this and other low order methods is the amount of computer memory required to solve the problem for cases with a large number of response sensors.

3.2.4 Mathematical Input-Output Model Method

The experimental modal analysis methods that are included within the category of mathematical input-output model methods are those approaches that generally involve input and response data independently without the need for creating auto and cross moment functions. There is no other restriction with regard to time or frequency domain models, effective number of degrees of freedom, etc. On this basis, two approaches are currently in use that can be described in this fashion. First of all, the autoregressive moving average approach is a time domain formulation that utilizes a pole-zero model as the basis for the description of the system characteristics. While this model is appropriate, the model cannot be easily constrained to account for known system information. Additionally, although the current application of this technique does not involve multiple inputs, the theoretical background for the multiple input case is well developed.

The other approach currently in use involves a reduced structural matrix model for the basis of the description of the system characteristics. This model involves the reduced mass, stiffness, and damping matrices with regard to the measured degrees of freedom. This model easily accounts for constraints such as known elements in the mass, stiffness, and damping matrices or known characteristics of the distribution within the matrices such as symmetric or banded characteristics. This method also incorporates the multiple input case routinely as known terms in the forcing vector of the matrix differential equation that serves as the mathematical model. These two approaches to experimental modal analysis will be briefly described in the following paragraphs.

3.2.4.1 Autoregressive Moving Average Approach

One approach to estimating the modal characteristics from time domain input-output data is the *autoregressive moving-average (ARMA)* procedure. This method has been applied to the determination of structural parameters by Gersch ^[65-70] and Pandit ^[71-72]. With this technique the response data is assumed to be caused by a white random noise input to the structure. The technique computes the best statistical model of the system in terms of its poles (from the autoregressive part), and zeros (from the moving-average part), as well as statistical confidence factors on the parameters. It has been primarily used to estimate the characteristics of buildings being excited by wind forces. The data used in the computational process are the autocorrelation

functions of the responses measured at various points on the structure. Since in the general case the inputs are not measured, the modal vectors are determined by referencing each response function to a single response to provide relative magnitude and phase information.

Single Reference:

$$\sum_{i=0}^m a_i x(t - i\Delta t) = \sum_{i=0}^n b_i f(t - i\Delta t) \quad (3.21)$$

Multiple Reference:

$$\sum_{i=0}^m \begin{bmatrix} a_i \end{bmatrix} \{ x(t - i\Delta t) \} = \sum_{i=0}^n \begin{bmatrix} b_i \end{bmatrix} \{ f(t - i\Delta t) \} \quad (3.22)$$

The solution for the autoregressive moving average coefficients proceeds in a two stage least squares fashion in the Gersch solution. In the first stage a *long* auto regressive model is solved linearly by using the Yule-Walker equations. This process uses output covariance functions to determine the auto regressive coefficients based upon a determination of the order of the auto regressive model. The second stage involves setting up an equivalent moving average model for the output involving convolution of the impulse response function and the input function. This procedure also involves computations using covariance functions and results in the least squares computation of the moving average coefficients. Since the solution for the autoregressive moving average coefficients, and thus the structural parameter estimates, are statistically based, statistical confidence factors, called coefficients of variation, for the natural frequencies and damping can be easily calculated. These coefficients represent the ratio of standard deviation of each parameter with respect to the actual parameter.

Note that if the response function $x(t)$ is replaced by the impulse response function $h(t)$ and the forcing function $f(t)$ is replaced by an impulsive force (unity at time 0, zero after time 0), the ARMA approach is essentially the same approach as the damped complex exponential response methods (PTD, ITD, ERA) ^[1].

3.2.4.2 Reduced Structural Matrix Approach

Over the last fifteen years, there has been increasing interest in being able to estimate reduced structural (mass, stiffness, and damping) matrices from experimental data. Most of these methods are based upon an indirect approach utilizing the estimated modal parameters to synthesize the reduced matrices [74-82]. This approach has not generated the anticipated results due to a number of reasons. First of all, regardless of the approach used, the solution for the reduced matrices is not unique. There are many combinations of matrix relationships that can be generated from the given set of estimated modal parameters. Second, the reduced frequency range of the modal parameter estimates means that the matrices will be weighted to represent an incomplete model. Third, the limitation of the precision of the modal parameter estimates as a result of commonly accepted experimental error tends to desensitize the process of estimating the reduced matrices. Finally, the problem of invalid modal parameter estimates will obviously result in invalid estimates of reduced matrices.

Time Domain:

$$[M] \{\ddot{x}\} + [C] \{\dot{x}\} + [K] \{x\} = \{f\} \quad (3.23)$$

Frequency Domain:

$$-\omega^2[M] \{X\} + j\omega[C] \{X\} + [K] \{X\} = \{F\} \quad (3.24)$$

Time Domain:

$$\begin{bmatrix} \alpha_2 \end{bmatrix} \{\ddot{x}\} + \begin{bmatrix} \alpha_1 \end{bmatrix} \{\dot{x}\} + \begin{bmatrix} \alpha_0 \end{bmatrix} \{x\} = \begin{bmatrix} \beta_0 \end{bmatrix} \{f\} \quad (3.25)$$

Frequency Domain:

$$(j\omega)^2 \begin{bmatrix} \alpha_2 \end{bmatrix} \{X\} + j\omega \begin{bmatrix} \alpha_1 \end{bmatrix} \{X\} + \begin{bmatrix} \alpha_0 \end{bmatrix} \{X\} = \begin{bmatrix} \beta_0 \end{bmatrix} \{F\} \quad (3.26)$$

An algorithm has been developed in Germany by Link and Vollan ^[77] which attempts to use frequency domain input and response data to directly estimate the reduced matrices. This method has been designated Identification of Structural System Parameters (ISSPA). Leuridan used this formulation as a starting point and has published results ^[78-82] using the same general approach for the estimation of modal parameters referred to as the Direct System Parameter Identification (DSPI) method. Since modal parameters are found as a result of the solution of the eigenvalue problem using the reduced matrix estimations, the process of estimating the reduced matrices may represent the ultimate goal in experimental modal analysis. If this process could be correlated with a purely theoretical finite element approach, the engineering design cycle would be complete.

Since there are many more known pieces of information (input and output information at different times) than unknowns that must be estimated the solution, then, is a function of the pseudo-inverse procedure chosen. Leuridan and Vold have evaluated pseudo-inverse numerical procedures utilizing the normal equations, least squares approach and the Householder reflections approach. Since the system matrix that results is often ill-conditioned, the Householder reflections approach yields more numerical precision for a given computational word size but at a sacrifice in speed.

Link and Vollan formulate the pseudo inverse based upon a singular value decomposition procedure under the restriction that the rank of the data dependent matrices are equal to the effective number of degrees of freedom. This effective number of degrees of freedom is dependent upon the number of theoretical system poles in the frequency range of interest, the accuracy of the measured data, and the computational precision of the computer with respect to the solution algorithm utilized.

Once the unknown elements of the mass, stiffness, and damping matrices are found, the modal parameters are estimated from the $[M]$, $[C]$, and $[K]$ matrices by way of a complex eigenvalue-eigenvector solution algorithm such as the QR algorithm.

A confidence or validity check of the frequencies, damping factors, and modal vectors can be performed using a back substitution procedure. The dynamic response is calculated and compared to the original measured response. The agreement between these responses is regarded as a measure of the accuracy of the estimated modal parameters.

Note that if the response function $X(\omega)$ is replaced by the frequency response function $H(\omega)$ and the forcing function $F(\omega)$ is replaced by an impulsive force (unity at all frequencies), the frequency domain, reduced structural matrix approach is essentially the same approach as the low order frequency response function methods (PFD). Also, if the response function $x(t)$ is replaced by the impulse response function $h(t)$ and the forcing function $f(t)$ is replaced by an impulsive force (unity at time 0, zero after time 0), the time domain, reduced structural matrix approach is essentially the same approach as the low order complex exponential response methods (ITD, ERA) ^[1].

3.3 References

- [1] Allemang, R.J., Brown, D.L., Fladung, W., "Modal Parameter Estimation: A Unified Matrix Polynomial Approach", *Proceedings, International Modal Analysis Conference*, 1994, pp. 501-514.
- [2] Lewis, R.C.; Wrisley, D.L., "A System for the Excitation of Pure Natural Modes of Complex Structures", *Journal of Aeronautical Sciences*, Volume 17, Number 11, 1950, pp. 705-722.
- [3] De Veubeke, B.F., "A Variational Approach to Pure Mode Excitation Based on Characteristic Phase Lag Theory", AGARD, Report 39, 1956, 35 pp.
- [4] Trail-Nash, R.W., "On the Excitation of Pure Natural Modes in Aircraft Resonance Testing", *Journal of Aeronautical Sciences*, Volume 25, Number 12, 1958, pp. 775-778.
- [5] Asher, G. W., "A Method of Normal Mode Excitation Utilizing Admittance Measurements", *Dynamics of Aeroelasticity*, Proceedings, Institute of the Aeronautical Sciences, 1958, pp. 69-76.
- [6] Stahle, C. V.; Forlifer, W. R., "Ground Vibration Testing of Complex Structures", *Flight Flutter Testing Symposium*, NASA-SP-385, 1958, pp. 83-90.
- [7] Stahle, C. V., Jr., "Phase Separation Technique for Ground Vibration Testing", *Aerospace Engineering*, July 1962, 1962, 8 pp.
- [8] DeBlauwe, F., "Investigation of a Parameter Estimation Algorithm for Spatial Sine Testing", *Doctoral Dissertation*, University of Cincinnati, 1991, 117 pp.
- [9] Deblauwe, F., Shih, C.Y., Rost, R., Brown, D.L., "Survey of Parameter Estimation Algorithms Applicable to Spatial Domain Sine Testing", *Proceedings, Twelfth International Seminar on Modal Analysis*, Katholieke Universiteit te Leuven, 1987, 15 pp.

- [10] Pendered, J. W.; Bishop, R. E. D., "A Critical Introduction to Some Industrial Resonance Testing Techniques", *Journal of Mechanical Engineering Science*, Volume 5, Number 4, 1963, pp. 368-378.
- [11] Pendered, J. W. Bishop, R. E. D., "Extraction of Data for a Sub-System From Resonance Test Results", *Journal of Mechanical Engineering Science*, Volume 5, Number 4, 1963, pp. 368-378.
- [12] Pendered, J. W.; Bishop, R. E. D., "The Determination of Modal Shapes in Resonance Testing", *Journal of Mechanical Engineering Science*, Volume 5, Number 4, 1963, pp. 379-385.
- [13] Bishop, R. E. D.; Gladwell, G. M. L., "An Investigation into the Theory of Resonance Testing", *Philosophical Transactions, Royal Society of London, Series A*, Volume 225, A-1055, 1963, pp. 241-280.
- [14] Klosterman, A., "On the Experimental Determination and Use of Modal Representations of Dynamic Characteristics", Doctor of Philosophy Dissertation, University of Cincinnati, Mechanical Engineering Department, 1971, 184 pp.
- [15] Van Loon, Patrick, "Modal Parameters of Mechanical Structures", Doctoral Dissertation, University of Lieven, Belgium, 1974, 183 pp.
- [16] Potter, R. W., "A General Theory of Modal Analysis for Linear Systems", *Shock and Vibration Digest*, Volume 7, Number 11, 1975, 8 pp.
- [17] Richardson, M., Potter, R., "Viscous vs. Structural Damping in Modal Analysis", *Proceedings, 46th Shock and Vibration Symposium*, 1975, 8 pp.
- [18] Sloane, E.; McKeever, B., "Modal Survey Techniques and Theory", SAE Paper Number 751067, 1975, 27 pp.
- [19] Wada, B. K., "Modal Test - Measurement and Analysis Requirements", SAE Paper Number 751066, 1975, 17 pp.
- [20] Ramsey, K., "Effective Measurements for Structural Dynamics Testing: Part I", *Sound and Vibration*, November, 1975.
- [21] Ramsey, K., "Effective Measurements for Structural Dynamics Testing: Part II", *Sound and Vibration*, April, 1976.
- [22] Brown, D.L., Carbon, G., Zimmerman, R.D., "Survey of Excitation Techniques Applicable to the Testing of Automotive Structures", SAE Paper No. 770029, 1977, 10 pp.
- [23] Halvorsen, W.G., Brown, D.L., "Impulse Technique for Structural Frequency Response Testing", *Sound and Vibration Magazine*, November, 1977, pp. 8-21.
- [24] Allemang, R. J., "Investigation of Some Multiple Input/Output Frequency Response Function Experimental Modal Analysis Techniques", Doctor of Philosophy Dissertation, University of Cincinnati, Mechanical Engineering Department, 1980, 358 pp.
- [25] Allemang, R.J., Rost, R.W., Brown, D.L., "Dual Input Estimation of Frequency Response Functions for Experimental Modal Analysis of Aircraft Structures", *Proceedings, International Modal Analysis Conference*, pp.333-340, 1982.
- [26] Carbon, G.D., Brown, D.L., Allemang, R.J., "Application of Dual Input Excitation Techniques to the Modal Testing of Commercial Aircraft", *Proceedings, International Modal Analysis Conference*, pp.559-565, 1982.
- [27] Allemang, R.J., Brown, D.L., Rost, R.W., "Dual Input Estimation of Frequency Response Functions for Experimental Modal Analysis of Automotive Structures", SAE Paper Number 820193.
- [28] Allemang, R.J., Rost, R.W., Brown, D.L., "Multiple Input Estimation of Frequency Response Functions: Excitation Considerations", ASME Paper Number 83-DET-73, 1983, 11 pp.

- [29] Allemang, R.J., Brown, D.L., Rost, R.W., "Multiple Input Estimation of Frequency Response Functions for Experimental Modal Analysis", U.S. Air Force Report Number AFATL-TR-84-15, 1984, 185 pp.
- [30] Richardson, M., Formenti, D.L., "Parameter Estimation from Frequency Response Measurements Using Rational Fraction Polynomials," *Proceedings, International Modal Analysis Conference*, 1982, pp. 167-182.
- [31] Vold, H., "Orthogonal Polynomials in the Polyreference Method," *Proceedings, International Seminar on Modal Analysis*, Katholieke University of Leuven, Belgium, 1986.
- [32] Van der Auweraer, H., Leuridan, J., "Multiple Input Orthogonal Polynomial Parameter Estimation", *Mechanical Systems and Signal Processing*, Vol. 1, No. 3, 1987, pp. 259-272.
- [33] Allemang, R.J., Brown, D.L., "Modal Parameter Estimation", Experimental Modal Analysis and Dynamic Component Synthesis, USAF Technical Report, Contract No. F33615-83-C-3218, AFWAL-TR-87-3069, Vol. 3, 1987, 130 pp.
- [34] Zhang, L., Kanda, H., Brown, D.L., Allemang, R.J. "A Polyreference Frequency Domain Method for Modal Parameter Identification," ASME Paper No. 85-DET-106 1985, 8 pp.
- [35] Lembregts, F., Leuridan, J., Zhang, L., Kanda, H., "Multiple Input Modal Analysis of Frequency Response Functions based on Direct Parameter Identification," *Proceedings, International Modal Analysis Conference*, 1986, pp. 589-598.
- [36] Lembregts, F., "Frequency Domain Identification Techniques for Experimental Multiple Input Modal Analysis", Doctoral Dissertation, Katholieke University of Leuven, Belgium, 1988, 213 pp.
- [37] Lembregts, F., Leuridan, J.L., Van Brussel, H., "Frequency Domain Direct Parameter Identification for Modal Analysis: State Space Formulation", *Mechanical Systems and Signal Processing*, Vol. 4, No. 1, 1989, pp. 65-76.
- [38] Lembregts, F., Snoeys, R., Leuridan, J., "Application and Evaluation of Multiple Input Modal Parameter Estimation", *Journal of Analytical and Experimental Modal Analysis*, Vol. 2, No. 1, 1987, pp. 19-31.
- [39] Lembregts, F., Leuridan, J.L., Van Brussel, H., "Frequency Domain Direct Parameter Identification for Modal Analysis: State Space Formulation", *Mechanical Systems and Signal Processing*, Vol. 4, No. 1, 1989, pp. 65-76.
- [40] Ebersbach, P., Irretier, H., "On the Application of Modal Parameter Estimation Using Frequency Domain Algorithms", *Journal of Analytical and Experimental Modal Analysis*, Vol. 4, No. 4, 1989, pp. 109-116.
- [41] Yam, Y., Bayard, D.S., Hadaegh, F.Y., Mettler, E., Milman, M.H., Scheid, R.E., "Autonomous Frequency Domain Identification: Theory and Experiment", NASA/JPL Publication 89-8, 1989, 204 pp.
- [42] Coppolino, R.N., "A Simultaneous Frequency Domain Technique for Estimation of Modal Parameters from Measured Data," SAE Paper No. 811046, 1981, 12 pp.
- [43] Craig, R.R., Kurdila, A.J., Kim, H.M., "State-Space Formulation of Multi-Shaker Modal Analysis", *Journal of Analytical and Experimental Modal Analysis*, Vol. 5, No. 3, 1990, pp. 169-183.
- [44] Shih, C.Y., "Investigation of the Numerical Conditioning of Frequency Domain Modal Parameter Estimation Methods", Doctoral Dissertation, University of Cincinnati, 1989, 188 pp.
- [45] Shih, C.Y., Tsuei, Y.G., Allemang, R.J., Brown, D.L., "A Frequency Domain Global Parameter Estimation Method for Multiple Reference Frequency Response Measurements", *Mechanical System and Signal Processing*, Vol. 2, No. 4, 1988, pp. 349-365.
- [46] Shih, C.Y., Tsuei, Y.G., Allemang, R.J., Brown, D.L., "Complex Mode Indication Function and Its Application to Spatial Domain Parameter Estimation", *Mechanical System and Signal Processing*, Vol. 2, No. 4, 1988, pp. 367-377.

- [47] Shih, C.Y., Tsuei, Y.G., Allemang, R.J., Brown, D.L., "Extension of a Parameter Estimation Method to Multiple Reference Frequency Response Measurements", Workshop, Eleventh International Seminar on Modal Analysis, Katholieke University of Leuven, Belgium, 1986.
- [48] Vold, H., Shih, C.Y., "On the Numerical Conditioning of Some Modal Parameter Estimation Methods", Proceedings, Thirteenth International Seminar on Modal Analysis, Katholieke University of Leuven, Belgium, 1988.
- [49] Prony, R., "Essai Experimental et Analytique sur les Lois de la Dilatabilite des Fluides Elastiques et sur Celles de la Force Expansive de la Vapeur de l'eau et de la Vapeur de l'Alcool, a Differentes Temperatures", *Journal de l' Ecole Polytechnique (Paris)*, Volume 1, Cahier 2, Floreal et Prairial, An. III, 1795, pp. 24-76.
- [50] Ibrahim, S. R., "Modal Confidence Factor in Vibration Testing", *Shock and Vibration Bulletin*, Volume 48, Part 1, 1978, pp. 65-75.
- [51] Ibrahim, S. R.; Mikulcik, E. C., "A Method for the Direct Identification of Vibration Parameters from the Free Response", *Shock and Vibration Bulletin*, Volume 47, Part 4, 1977, pp. 183-198.
- [52] Pappa, R.S., Ibrahim, S.R. , "A Parametric Study of the "ITD" Modal Identification Algorithm", *Shock and Vibration Bulletin*, Volume Number 51, Part 3, 1981, pp. 43-72.
- [53] Pappa, R.S., "Some Statistical Performance Characteristics of the "ITD" Modal Identification Algorithm", AIAA Paper No. 82-0768, 1982, 19 pp.
- [54] Pappa, R.S., "Close-Mode Identification Performance of the ITD Algorithm", AIAA Paper Number 83-0878, 1983, 13 pp.
- [55] Fukuzono, K., "Investigation of Multiple-Reference Ibrahim Time Domain Modal Parameter Estimation Technique," M. S. Thesis, Dept. of Mechanical and Industrial Engineering, University of Cincinnati, 1986, 220 pp.
- [56] Brown, D.L., Zimmerman, R.D., Allemang, R.J., Mergeay, M., "Parameter Estimation Techniques for Modal Analysis", SAE Paper Number 790221, SAE Transactions, Volume 88, pp. 828-846, 1979.
- [57] Vold, H., Kundrat, J., Rocklin, T., Russell, R., "A Multi-Input Modal Estimation Algorithm for Mini-Computers", SAE Paper Number 820194, 1982, 10 pp.
- [58] Vold, H., Rocklin, T., "The Numerical Implementation of a Multi-Input Modal Estimation Algorithm for Mini- Computers", Proceedings, International Modal Analysis Conference, pp. 542-548, 1982.
- [59] Pappa, R. S., Juang, J. N., "Galileo Spacecraft Modal Identification Using an Eigensystem Realization Algorithm", AIAA Paper Number 84-1070-CP, 1984, 18 pp.
- [60] Pappa, R. S., Juang, J. N., "An Eigensystem Realization Algorithm (ERA) for Modal Parameter Identification", NASA-JPL Workshop, Identification and Control of Flexible Space Structures, June, 1984 (Pasadena, CA.) 20 pp.
- [61] Juang, J.N., Pappa, R.S., "Effects of Noise on ERA-Identified Modal Parameters", AAS Paper Number AAS-85-422, August, 1985 (Vail, CO.) 23 pp.
- [62] Juang, Jer-Nan, Pappa, Richard S., "An Eigensystem Realization Algorithm for Modal Parameter Identification and Model Reduction", *AIAA Journal of Guidance, Control, and Dynamics*, Vol. 8, No. 4, 1985, pp. 620-627.
- [63] Juang, J.N., "Mathematical Correlation of Modal Parameter Identification Methods Via System Realization Theory", *Journal of Analytical and Experimental Modal Analysis*, Vol. 2, No. 1, 1987, pp. 1-18.
- [64] Longman, Richard W., Juang, Jer-Nan, "Recursive Form of the Eigensystem Realization Algorithm for System Identification", *AIAA, Journal of Guidance, Control, and Dynamics*, Vol. 12, No. 5, 1989, pp. 647-652.

- [65] Gersch, W., "On the Achievable Accuracy of Structural System Parameter Estimates", *Journal of Sound and Vibration*, Volume 34, Number 1, 1974, pp. 63-79.
- [66] Gersch, W.; Nielsen, N. N.; Akaike, H., "Maximum Likelihood Estimation of Structural Parameters from Random Vibration Data", *Journal of Sound and Vibration*, Volume 31, Number 3, 1973, pp. 295-308.
- [67] Gersch, W.; Luo, S., "Discrete Time Series Synthesis of Randomly Excited Structural System Responses", *Journal of the Acoustical Society of America*, Volume 51, Number 1, 1972, pp. 402-408.
- [68] Gersch, W., "Estimation of the Auto Regressive Parameters of a Mixed Autoregressive Moving-Average Time Series", *IEEE Transactions on Automatic Control*, Volume AC-15, October 1970, pp. 583-588.
- [69] Gersch, W.; Sharpe, D. R., "Estimation of Power Spectra with Finite-Order Autoregressive Models", *IEEE Transactions on Automatic Control*, Volume AC-18, August 1973, pp. 367-369.
- [70] Gersch, W.; Fouth, D. A., "Least Squares Estimates of Structural System Parameters Using Covariance Function Data", *IEEE Transactions on Automatic Control*, Volume AC-19, Number 6, December 1974, pp. 898-903.
- [71] Pandit, S. M.; Suzuki, H., "Application of Data Dependent Systems to Diagnostic Vibration Analysis", *ASME Paper Number 79-DET-7*, September, 1979, 9 pp.
- [72] Pandit, S. M., "Analysis of Vibration Records by Data Dependent Systems", *Shock and Vibration Bulletin*, Number 47, September, 1977, pp. 161-174.
- [73] Hollkamp, J.J., Batill, S.M., "A Recursive Algorithm for Discrete Time Domain Parameter Identification", *AIAA Paper No. AIAA-90-1221*, 1990, 10 pp.
- [74] Ross, R. G., Jr., "Synthesis of Stiffness and Mass Matrices from Experimental Vibration Modes", *SAE Paper Number 710787*, 1971, 9 pp.
- [75] Thoren, A. R., "Derivation of Mass and Stiffness Matrices from Dynamic Test Data", *AIAA Paper Number 72-346*, 1972, 9 pp.
- [76] Potter, R. W.; Richardson, M., "Mass, Stiffness, and Damping Matrices from Measured Modal Properties", *Instrument Society of America, ISA-74-630*, 1974, 5 pp.
- [77] Link, M.; Vollan, A., "Identification of Structural System Parameters from Dynamic Response Data", *Zeitschrift Fur Flugwissenschaften*, Volume 2, Number 3, 1978, pp. 165-174.
- [78] Leuridan, J., "Direct System Parameter Identification of Mechanical Structures with Application to Modal Analysis", *Master of Science Thesis, University of Cincinnati*, 1981, 200 pp.
- [79] Leuridan, J., "Some Direct Parameter Model Identification Methods Applicable for Multiple Input Modal Analysis," *Doctoral Dissertation, University of Cincinnati*, 1984, 384 pp.
- [80] Vold, H., Leuridan, J., "A Generalized Frequency Domain Matrix Estimation Method for Structural Parameter Identification", *Proceedings, 7th. International Seminar on Modal Analysis, Katholieke Universiteit te Leuven, Belgium*, 1982.
- [81] Leuridan, J., Kundrat, J., "Advanced Matrix Methods for Experimental Modal Analysis - A Multi-Matrix Method for Direct Parameter Extraction", *Proceedings, International Modal Analysis Conference*, 1982, pp. 192-200.
- [82] Leuridan, J., Brown, D., Allemang, R., "Direct System Parameter Identification of Mechanical Structures with Application to Modal Analysis", *AIAA Paper Number 82-0767, Proceedings, 23rd. Structures, Structural Dynamics and Materials Conference, Part 2*, 1982, pp. 548-556.

4. MODAL DATA ACQUISITION

4.1 Introduction

Acquisition of data that will be used in the estimation of a modal model involves many important technical concerns. The primary concern is the digital signal processing or the converting of analog signals into a corresponding sequence of digital values that accurately describe the time varying characteristics of the inputs to, and responses from, a system. Once the data is available in digital form, the most common approach is to transform the data from the time domain to the frequency domain by use of a discrete Fourier transform algorithm. Since this algorithm involves discrete data over a limited time period, there are significant potential problems with this approach that must be well understood. Modal data acquisition also includes the typical digital signal processing that is performed on the digital data to minimize common errors that are random or deterministic (bias) in nature. This includes many forms of averaging as well as windowing.

In order to determine modal parameters, the measured input (excitation) and response data must be processed and put into a form that is compatible with the test and modal parameter estimation methods. As a result, digital signal processing of the data is a very important step in structural testing. This is one of the technology areas where a clear understanding of the time-frequency domain relationships are important. The conversion of the data from the time domain into the frequency domain is important in both the measurement process and subsequently in the parameter estimation process.

Digital signal processing of the measured input and response data is used for the following reasons:

- Condensation - In general, the amount of measured data tremendously exceeds the information present in the desired measurements (frequency response, unit impulse response, coherence function, etc). Therefore, digital signal processing is used to condense the data.

- Measurements - Estimation of the measurements which will be used subsequently in the modal parameter estimation process. Since there are many excitation, measurement and modal parameter estimation procedures, there is likewise a large number of digital signal processing options which can be used.
- Noise Reduction -- Signal processing is used to reduce the influences of noise in the measurement process. The types of noise have been classified for convenience as follows:
 - Non-Coherent Noise - The noise is due to electrical noise on the transducer signals, noise due to unmeasured excitation sources, etc. which are non-coherent with respect to the measured input signals or to some other signal which is used in the averaging process. Zero mean non-coherent noise can be eliminated by averaging with respect to a reference signal. This reference signal could be the input signal in terms of a spectrum averaging process or could be a synchronization or trigger signal in terms of cyclic averaging or random decrement process.
 - Signal Processing Noise - The signal processing itself may generate noise. For example, "leakage" is a classic source of noise when using Fast Fourier Transforms (FFT) for computing frequency domain measurements. This type of noise is reduced or eliminated by using completely observed time signals (periodic or transient); by using various types of windows; or by increasing the frequency resolution.
 - Nonlinear Noise - If the system is nonlinear then, free decay, frequency response or unit impulse function measurements may be distorted which consequentially causes problems when estimating modal parameters. Nonlinear distortion noise can be eliminated by linearizing the test structure before testing or by randomizing the input signals to the structure. This will cause the nonlinear distortion noise to become non-coherent with respect to the input signal. The nonlinear noise can then be averaged from the data in the same manner as ordinary non-coherent noise.

Historically, frequency response function or unit impulse response function have been the most important measurements estimated. There has been a great deal of research in the area of signal processing for determining these measurements ^[1-5]. Much of the research work conducted over the last fifteen years in this area has been involved in understanding the digital signal processing implications on the ultimate estimate of measurement characteristics. Future work will involve establishing the statistical error bounds on the ultimate estimates of the modal

parameters that are derived from the measurements. In this way, importance can be properly given to the relative errors in the different phases of the measurement process (calibration, instrumentation, data acquisition, estimation algorithm, etc.).

4.2 Errors

The accurate measurement of frequency response functions depends heavily upon minimizing the errors involved with the digital signal processing. In order to take full advantage of experimental data in the evaluation of experimental procedures and verification of theoretical approaches, the errors in measurement, generally designated noise, must be reduced to acceptable levels. With the increasing use of personal computer (PC) instrumentation, great care must be taken by the user to be certain that errors are minimized.

With respect to the frequency response function measurement, the errors in the estimate are generally grouped into two categories: variance and bias. The *variance* portion of the error is due to random deviations of each sample function from the mean. Statistically, then, if sufficient sample functions are evaluated (averages), the averaged estimate will closely approximate the expected (true) function with a high degree of confidence. The *bias* portion of the error, on the other hand, does not necessarily reduce as a result of many samples (averages). The bias error is due to a system characteristic or measurement procedure consistently resulting in an incorrect estimate. Therefore, the averaged value is not equal to the expected (true) value. Examples of this are system nonlinearities or digitization errors such as aliasing or leakage. With this type of error, knowledge of the form and origin of the error is vital in reducing the resultant effect in the frequency response function measurement.

Specifically, two general categories of problems exist which may cause significant error even when great care has been taken to deal with inaccurate system assumptions and obvious measurement mistakes. The first category is concerned with the limitations of using finite information. Any measurement instrument is limited in time resolution, or frequency bandwidth. However, sampling a signal at discrete times also introduces a form of amplitude error (*aliasing*) that converts high frequency energy to lower frequencies. This source of error would be classified as a bias. Thus, the time resolution and frequency bandwidth parameters are generally dictated by an anti-aliasing filter in front of the sampler. The shape of this filter influences the in-

band accuracy and the stop-band rejection characteristics of the instrument. Obviously, filters are not perfect, and there is no such thing as absolute rejection. Strong signals with potential aliasing are often present to some extent. Another form of amplitude error is involved in the quantization of the analog signal to a digital signal. Since only discrete amplitude levels are possible, the amplitude will often be in error. This source of error is normally Gaussian distributed and therefore is part of the variance portion of the total error.

Analogous to time resolution limits, there is always a limit on frequency resolution. This is ultimately determined by the total effective time (observation window) over which coherent data is collected. The effect of this finite collection time is the introduction of another type of non-linear error (*leakage*), which converts energy at each frequency into energy within a relatively narrow band nearby. This type of error is controlled to some extent by weighting (or windowing) the original time domain data. However, this type of error will always cause a considerable bias in any portion of a measurement that is sufficiently close to a strong signal. In the situation of excitation of lightly damped structures, this leakage error, compared to all other sources of error, is usually the largest bias error and often will be much greater than the variance error.

4.3 Analog to Digital Conversion

The process of representing an analog signal as a series of digital values is a basic requirement of modern digital signal processing analyzers. In practice, the goal of the analog to digital conversion (ADC) process is to obtain the conversion while maintaining sufficient accuracy in terms of frequency, magnitude, and phase. When dealing strictly with analog devices, this concern was satisfied by the performance characteristics of each individual analog device. With the advent of digital signal processing, the performance characteristics of the analog device is only the first criteria of consideration. The characteristics of the analog to digital conversion has now become of prime importance.

This process of analog to digital conversion involves two separate concepts, each of which are related to the dynamic performance of a digital signal processing analyzer. *Sampling* is the part of the process related to the timing between individual digital pieces of the time history. *Quantization* is the part of the process related to describing an analog amplitude as a digital value. Primarily, sampling considerations alone affect the frequency accuracy while both

sampling and quantization considerations affect magnitude and phase accuracy.

4.3.1 Sampling

Sampling is the process of recording the independent variable of an analog process. This can be done in an absolute sense where the independent variable is in terms of time. Quite often, particular advantage can be gained if the sampling process proceeds in a relative sense where this independent variable is in terms of some event. This relative approach is the basis of the processing of data related to rotating equipment where the event is a revolution of a shaft and the sampling involves an integer number of samples per revolution (rather than samples per second). In either case, the same theories apply to the sampling process. In the relative approach, there is simply a change of variable associated with the independent axis (time versus event).

The process of sampling arises from the need to describe analog time histories in a digital fashion. This can be done, in general, by recording a digitized amplitude and a reference time of measurement or in the more common method of recording amplitudes at uniform increments of time (Δt). Since all analog to digital converters sample at constant sampling increments during each sample period, all further discussion will be restricted to this case.

Sampling Theory:

Two theories or principles apply to the process of digitizing analog signals and recovering valid frequency information. *Shannon's Sampling Theorem* states, very simply, the following:

$$F_{\text{samp}} = \frac{1}{\Delta t} = F_{\text{Nyq}} \times 2.0 \quad (4.1)$$

$$F_{\text{Nyq}} \geq F_{\text{max}} \quad (4.2)$$

Obviously, this theorem has to do with the maximum frequency which can be described accurately. The *Nyquist frequency* (F_{Nyq}) is the theoretical limit for the maximum frequency and is defined according to Equation (4-1) to be one half of the sampling frequency. This means that there will be at least two samples per period for any frequency below the Nyquist frequency.

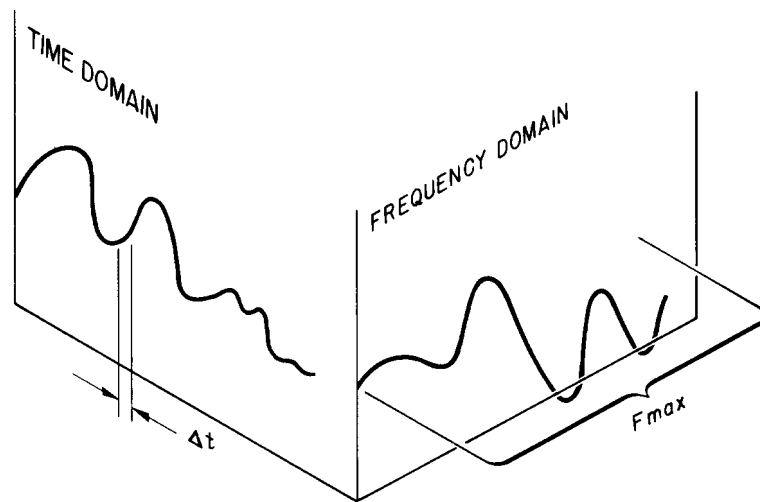


Figure 4-1. Shannon Sampling Theorem

In order to be certain that Equations (4-1) and (4-2) are always met, an analog, low pass filter (LPF) with a cutoff frequency below the Nyquist frequency is always used when acquiring data. Generally, this filter will be built into the digital signal analyzer. For reasons involving the practical limitation of the analog filters used prior to any digitization, the sampling frequency is normally chosen to be greater than two times the maximum frequency of interest (typically 2.56). In this case, Equation (4.2) still applies as stated by the inequality. Note that in this situation the resulting maximum frequency (F_{max}) is less than the Nyquist frequency. This may lead to some confusion when the data is recorded and/or displayed. Figure 4-2 shows the common frequency relationship between the maximum frequency, the analog, low pass filter cutoff frequency and the Nyquist frequency.

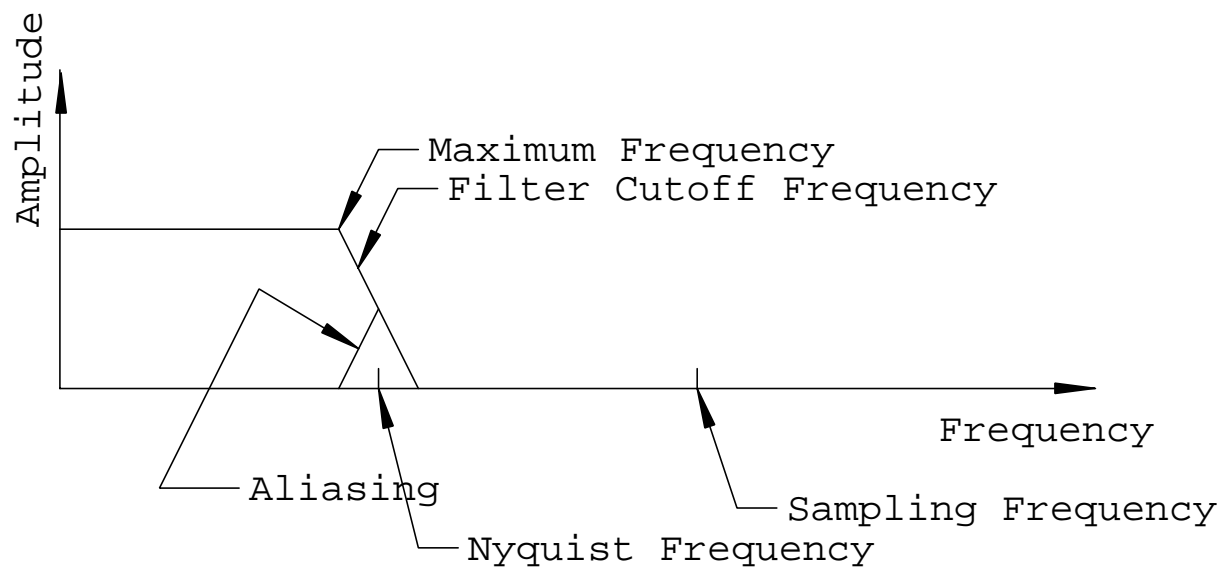


Figure 4-2. Basic Sampling Relationships

Rayleigh's criterion was first formulated in the field of optics and has to do with being able to resolve two closely related spaced frequency components. For a time record of T seconds, the lowest frequency component measurable is:

$$\Delta f = \frac{1.0}{T} \quad (4.3)$$

It should be emphasized that Equation (4.3) is always true regardless of the absolute frequencies of interest.

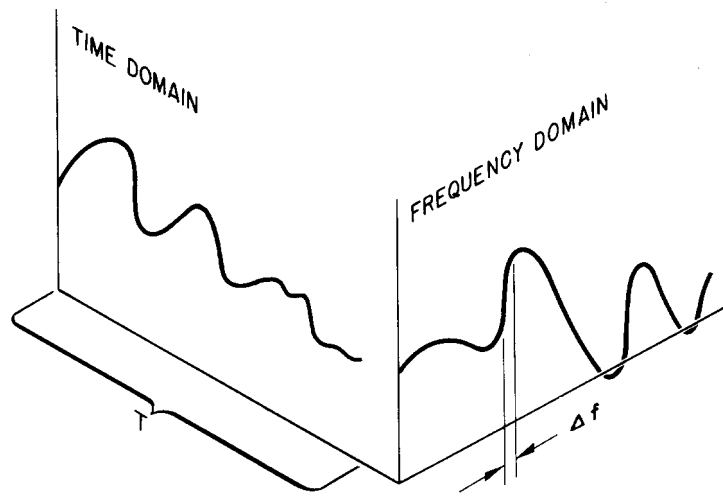


Figure 4-3. Rayleigh's Criterion

With these two principles in mind, the selection of sampling parameters can be summarized as shown in Table (4-1). Note that for this case, the equality in Equation (4.2) has been used.

Sampling Relationships		
Sampling Parameter	Automatically Determines	Blocksize Determines
Δt	$F_{\max} = \frac{1}{2\Delta t}$	$T = N\Delta t$ $\Delta f = \frac{1}{N\Delta t}$
F_{\max}	$\Delta t = \frac{1}{2F_{\max}}$	$T = N\Delta t$ $\Delta f = \frac{1}{N\Delta t}$
Δf	$T = \frac{1}{\Delta f}$	$\Delta t = \frac{T}{N}$ $F_{\max} = \frac{N}{2} \Delta f$
T	$\Delta f = \frac{1}{T}$	$\Delta t = \frac{T}{N}$ $F_{\max} = \frac{N}{2} \Delta f$

TABLE 4-1. Digitization Equations ($F_{\max} = F_{Nyq}$)

4.3.2 Quantization

Quantization is the conversion of a specific analog value of amplitude to the nearest discrete value available in the analog to digital converter. This process involves representing a range of voltage by a fixed number of integer steps. Normally, the range of voltage is chosen to be between positive and negative limits for a given voltage limit. The number of discrete levels is a function of the number of bits in the analog to digital conversion. An ADC with an "M-BIT" converter is able to determine signal amplitude within one part in 2 raised to the M power. Fourteen and sixteen bit converters are very common. An example of a three bit converter is

shown in Figure 4-4.

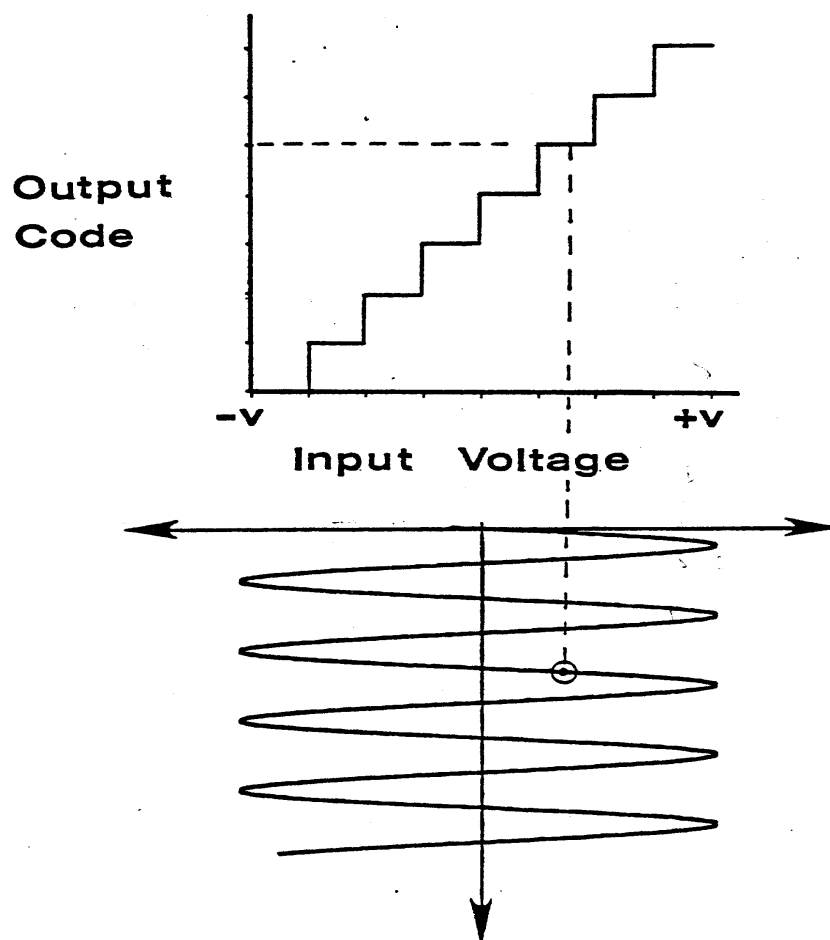


Figure 4-4. Quantization: 3 Bit Analog to Digital Converter

The most important consideration with respect to optimum quantization depends upon the concept of **actual** word size versus **effective** word size. The actual word size is the number of bits available in each word in the ADC or computer. The effective word size is the number of bits used in each word in any operation in the ADC or computer. The first consideration is that of **dynamic range**. Dynamic range refers to the amplitude range, minimum to maximum, that can be recorded as an input to the ADC in the digitization process. Since the actual word size of the ADC is fixed, the dynamic range of the ADC (84 dB for 14 bits, 96 dB for 16 bits, etc.) is only meaningful if the quantization of an input signal of interest involves all of the bits of the

actual word. Two situations may exist where this is not true. First, if the input ranges for the ADC are not automatically or manually set to the optimum position, some loss of dynamic range will occur. This means that the maximum level of the data should not be less than one half of the input voltage range. Secondly, if the signal has more dominant information content outside the band of interest, a significant portion of the dynamic range will be used to describe the unwanted characteristic. This will reduce the potential dynamic range available to the portion of the signal in which there is interest. Some common examples of this are a large mean value offset or large harmonic component (such as 60 Hertz) as shown in Figure 4-5 and 4-6. Both of these situations cause the effective word size of the ADC to be smaller than the actual word size of the ADC with respect to the information of interest.

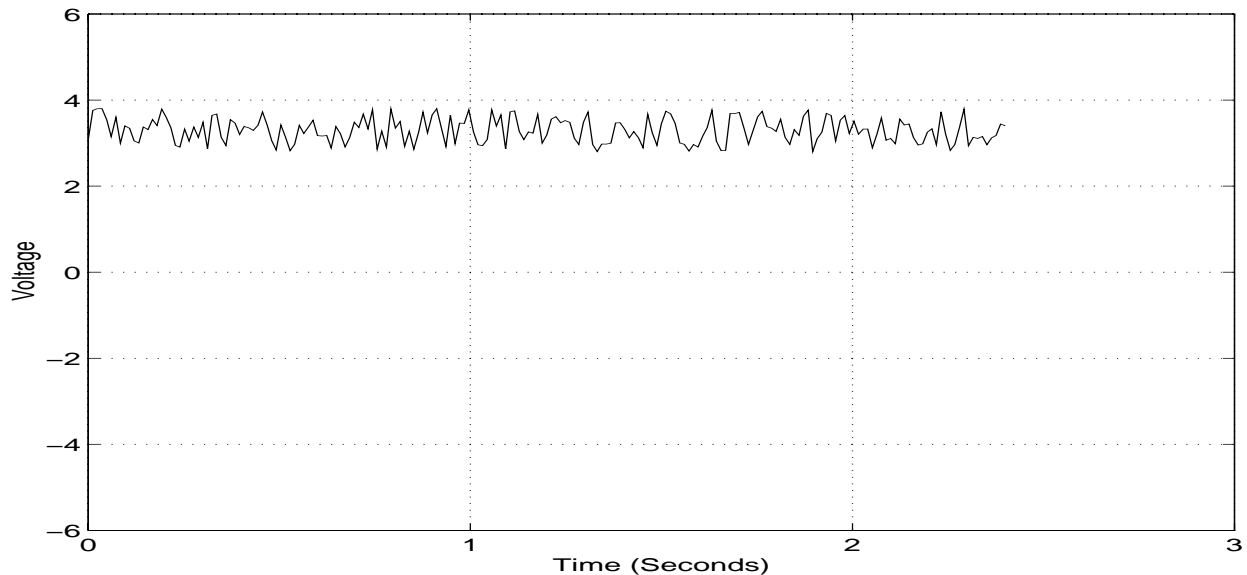


Figure 4-5. Quantization: ADC Input Optimization (Unwanted DC)

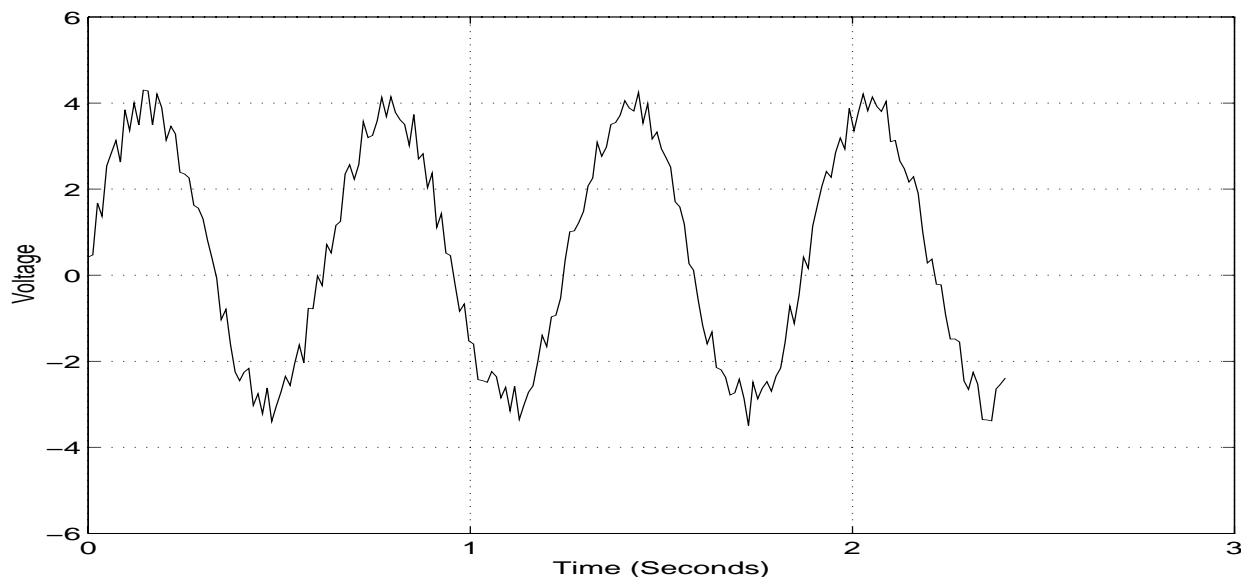


Figure 4-6. Quantization: ADC Input Optimization (Unwanted Harmonic)

The quantization problem associated with Figure 4-5 is often solved by using an AC coupling circuit to remove the DC component. This will not cause a problem as long as the frequencies of interest are above 5-10 Hertz. Figure 4-7 shows the characteristics of a 1.2 Hertz AC coupling network. These plots clearly indicate that the AC coupling network is simply a first order system (RC circuit) designed to pass frequency information above 1.2 Hertz. It is important to note that filter specifications denote the cut-off frequency of the filter (in this case the high pass frequency of the AC coupling network) at the frequency where the amplitude is attenuated by 3 db. This means that the amplitude is 0.707 of the original signal at this frequency. If important dynamic information exists in frequency range from 1-5 Hertz, it is clear that this data will be corrupted by the AC coupling network. When this is the case, DC coupling should be used. The DC signal can be removed by using a summing amplifier that adds in the appropriate DC voltage (isolated) to give the data signal a zero mean characteristic. While this is generally the preferred approach, this method is not always available and is more expensive to implement.

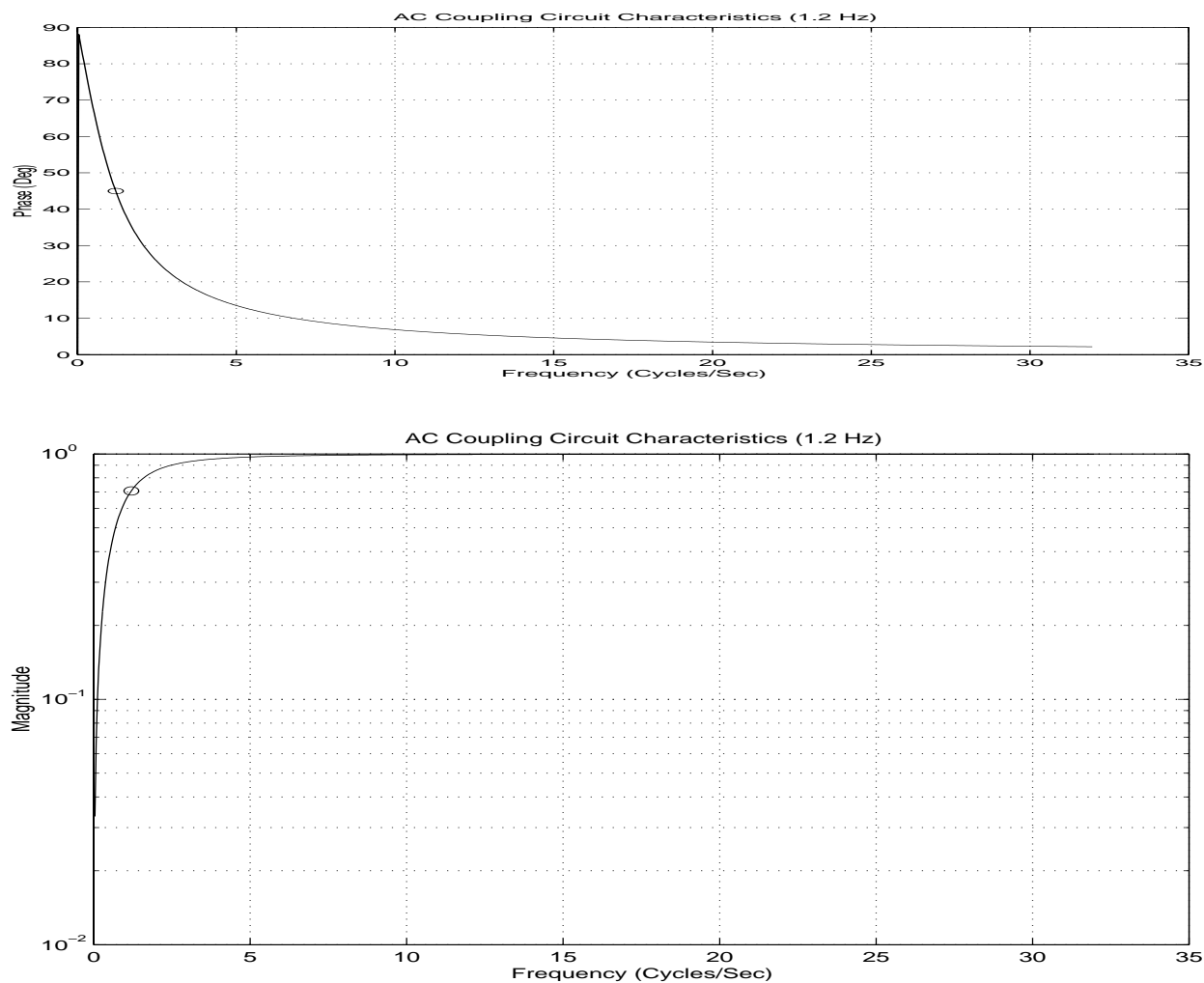


Figure 4-7. 1.2 Hertz AC Coupling Characteristics (Magnitude and Phase)

This dynamic range consideration with respect to quantization is particularly important when a multiplexer is used to obtain a large number of channels of data in parallel. Since a multiplexer configuration often involves only one ADC channel for a number of multiplexer channels, the dynamic range of all the channels must be similar or the effective word size for many of the channels will be much less than the actual word size. In this situation, the signals must be amplified prior to digitization so that each channel has approximately the same dynamic range. Naturally, this amplification factor must be taken into account in the final calibration of the data.

4.3.3 ADC Implementation Issues

While the discussion concerning sampling and quantization is theoretically correct, the hardware implementation of an ADC has changed considerably since 1970. Originally, the ADC was implemented in hardware as a direct implementation of the theory. This means that each ADC channel contained an accurate sampling clock (crystal based) that could be set to a number of desired sampling frequencies and the actual ADC involved a non-integrating or integrating (successive approximation, dual-slope, etc.) design. In order to achieve stable, low noise, and linear characteristics as well as higher bit count in these ADCs, the cost per channel is significant. The maximum frequency was set to approximately 70-75 percent of the Nyquist frequency with an analog low pass filter (LPF) set at approximately 75-80 percent of the Nyquist frequency to be certain that Equation (4-1) will be satisfied. This approach works well but the high cost per channel (general analog LPF filter plus ADC), and the need for every channel to be magnitude and phase matched, meant that multichannel data acquisition beyond 2-4 channels was not practical for most users. This ADC design approach referred to as a variable sample frequency ADC design and is shown schematically in Figure 4-8.

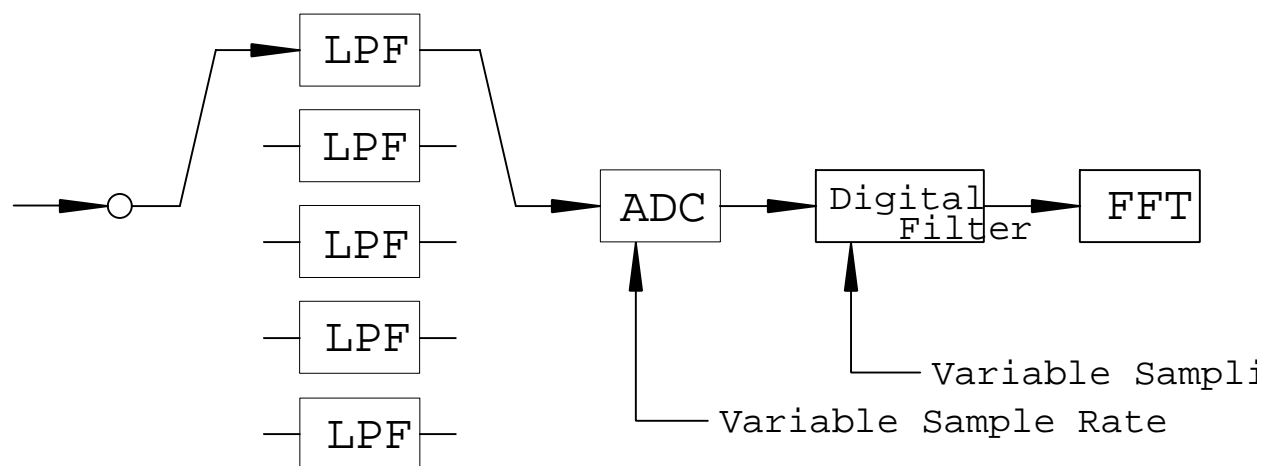


Figure 4-8. Variable Sample Frequency ADC Design

Once digital computers became more powerful and were routinely included as a part of the data acquisition system, digital filtering was added to the variable sample rate ADC design in order to implement the band selectable Fourier (zoom) transform.

The addition of the digital filter led to another ADC design approach that was more cost effective and, therefore, permitted a multichannel data acquisition system. These data acquisition systems use essentially the same initial analog filter ADC design but limit the number of sampling frequencies to one or two. This means that there will be only one analog low pass filter (LPF) for each sampling frequency rather than multiple filters and multiple sampling rates in the ADC. The final frequency content of the data is then achieved by digitally filtering the sampled data into the lower, required frequency range of interest. This ADC design approach is much cheaper than the previous approach but still is limited by the cost of increasingly more accurate ADCs (14-16 bit). For example, the maximum frequency of interest for most structural and acoustic measurement situations is below 25 kHz. Therefore, 25 kHz can be used as the maximum frequency (f_{\max}). For this case, the sampling frequency (f_{samp}) is normally chosen to be 64 kHz. While this choice of sampling frequency is higher than the minimum identified by Shannon's Sampling Theorem, this choice of sampling frequency obeys the inequality of Shannon's Sampling Theorem and provides for a conservative sampling situation. With this sampling criteria, the low-pass analog filter (with 80-100 db/octave rolloff) can be set at 25 kHz in order to eliminate aliasing effects. Note that, since the sampling frequency is chosen higher than necessary (2.56X compared to 2X), this provides a guard band of frequency before any aliasing effects could contaminate the digitized data below the maximum frequency. Since most structural and acoustic measurement situations do not require information from 0 Hz to 25 kHz, further reduction of the digitized information into an appropriate frequency band of interest can be achieved through the use of digital filtering and decimation of the resulting time data. This ADC design approach referred to as a fixed sample rate ADC design and is shown schematically in Figure 4-9.

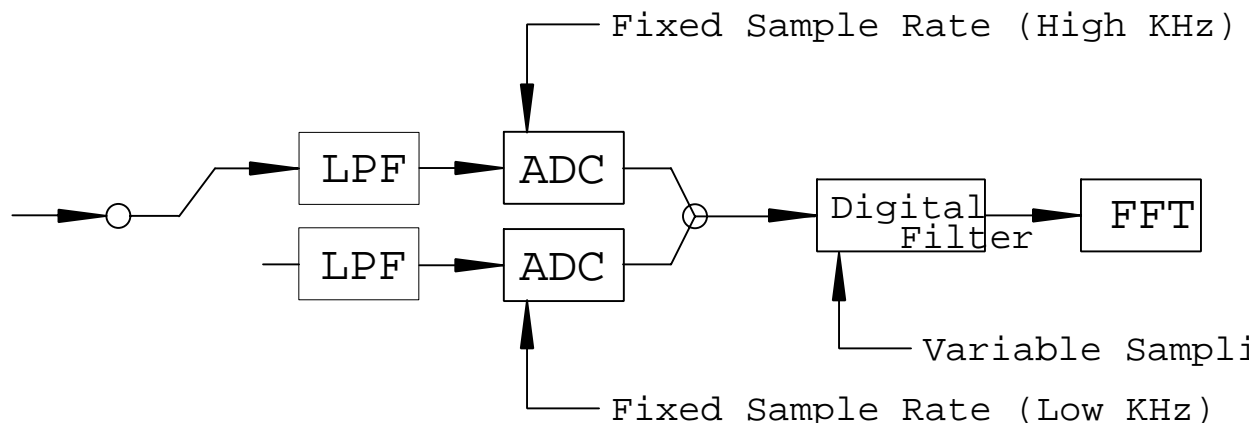


Figure 4-9. Fixed Sample Frequency ADC Design

Most modern ADC designs now take advantage of delta-sigma (also referred to as sigma-delta) ADC design approaches. This delta-sigma ADC design approach utilizes an oversampling approach that involves a much higher sampling frequency (MHz) but only a one bit ADC. The one bit ADC means that the cost of the ADC is quite low and only a single, low pass analog filter, set above the highest frequency of interest, with minimal roll-off characteristics is required per channel. The effective bit size of the ADC is a function of the ratio of this high sampling frequency to the sampling frequency required for the highest frequency of interest and the characteristics of the digital filter that is used to achieve the final desired frequency range. The sampling rate for a delta-sigma ADC is actually much lower than a simple oversampling ADC due to the use of the digital filter that will be used in post-processing the data coming out of the oversampling, one bit ADC. Currently, delta-sigma ADCs achieve 16 bit characteristics at effective sample rates up to 50 kHz using oversampling frequencies in the 5-10 MHz range. This delta-sigma ADC design approach is shown schematically in Figure 4-10.

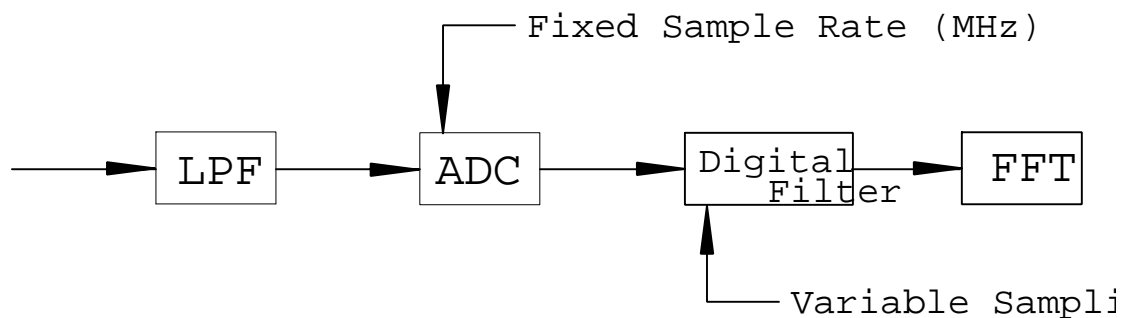


Figure 4-10. Delta-Sigma ADC Design

4.3.4 ADC Errors

Most modern data acquisition systems minimize errors associated with the analog to digital conversion of data to the extent that the average user does not need to be concerned with the residual error(s). However, specialized data acquisition, use of PC data acquisition, use of older data acquisition equipment, etc. can necessitate the need for the advanced user to be aware of the potential problems. The primary ADC errors are aliasing and quantization errors.

4.3.4.1 Aliasing

If frequency components larger than one half the sampling frequency occur in the analog time history, amplitude and frequency errors will result. These errors are a result of the inability of the Fourier transform to decide which frequencies are within the analysis band and which frequencies are outside the analysis band. This problem is explained graphically in Figure 4-11 from a time domain point of view.

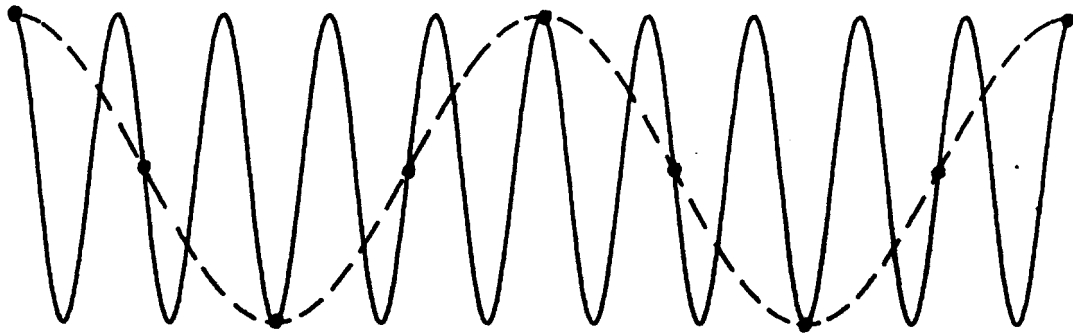


Figure 4-11. Aliasing Example

A summary of what happens to signals above the F_{Nyq} defined by the equality in Equation (4.1) is shown graphically in Figure 4-12 from a frequency domain point of view. This demonstrates that a signal above F_{Nyq} will appear after being digitized as a frequency below F_{Nyq} . This serious error is controlled by using analog filters prior to digitization to low pass only the information below F_{Nyq} . Naturally, since filters have a limited out of band rejection, the positioning of the cutoff frequency of the filters must be made with respect to the F_{Nyq} , the desired maximum frequency F_{max} and the rolloff characteristic of the filter.

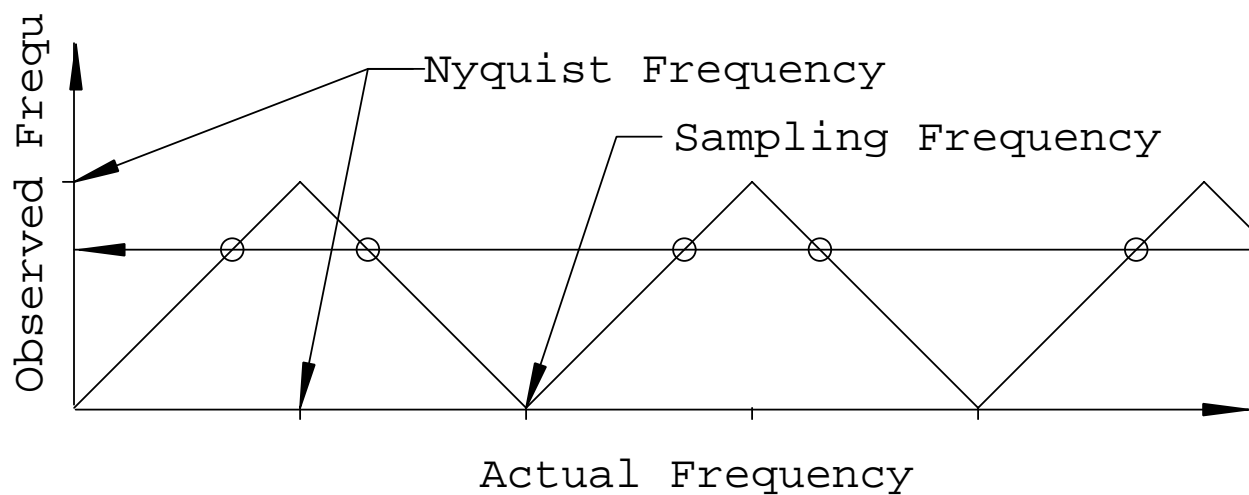


Figure 4-12. Aliasing Contribution (Shannon Sampling Theorem Limit)

4.3.4.2 Other Types of ADC Error

A number of other errors must be discussed in order to understand that the possibility for error originates at every step in the measurement process. While all of the following errors are possible, many of the errors are a function of the way in which the ADC hardware operates or often malfunctions. Many of these errors can be evaluated by performing a histogram on a signal with known characteristics.

Quantization Error: The difference between the actual analog signal and the measured digitized value. Normally this is plus or minus one half of one part in 2 raised to the M power. Since this error is a random event, averaging will minimize the effect on the resulting measurements. Note that, when measuring transient events that cannot be averaged, this error limits the magnitude accuracy that is achievable.

Differential Nonlinearity: If the roundoff that occurs to cause quantization error is not regular (some of the spacing between counts varies) this type of error results. This causes the "noise" from quantization error to be biased.

Bit Dropout : One bit in the ADC may never be set. Obviously, any sample requiring this bit in the ADC word to be set will be in error and the error will be biased. A similar problem exists if one bit of the ADC word is always set.

Reference Voltage: The reference voltage used by the ADC may drift within or between sample periods. Since this drift is not known or measured, this error will cause a bias in any resulting estimate of the dependent variable.

Overload and Overload Recovery: When the ADC is overloaded, it may take several sampling increments to recover. This is normally only a problem under severe overloads but if it occurs the result will be a bias in the estimate of the amplitude.

Aperture Error - Clock Jitter: The value of the amplitude recorded does not correspond to the assumed instant in time, t . This type of error will result in a bias in the estimate of time and frequency parameters.

Digitizer Noise: The random setting of plus or minus one bit when the input is zero is referred to as digitizer noise. This error may become dominant in transient excitation since a large part of the observed histories may be very small or actually zero as in the case of impact testing. This

error can be controlled to some extent by averaging and the use of special window functions.

4.4 Discrete Fourier Transform

The Fourier series concept explains that any physically realizable signal (signal that satisfies the Dirichlet conditions) can be uniquely separated into a summation of sine and cosine terms at appropriate frequencies. This will generate a unique set of sine and cosine terms due to the orthogonal nature of sine functions at different frequencies, the orthogonal nature of cosine functions at different frequencies and the orthogonal nature of sine functions compared to cosine functions. If the choice of frequencies is limited to a discrete set of frequencies, the discrete Fourier transform will describe the amount of each sine and cosine term at each discrete frequency. The real part of the discrete Fourier transform describes the amount of each cosine term; the imaginary part of the discrete Fourier transform describes the amount of each sine term. Figure 4-13 is a graphical representation of this concept for a signal that can be represented by a summation of sinusoids.

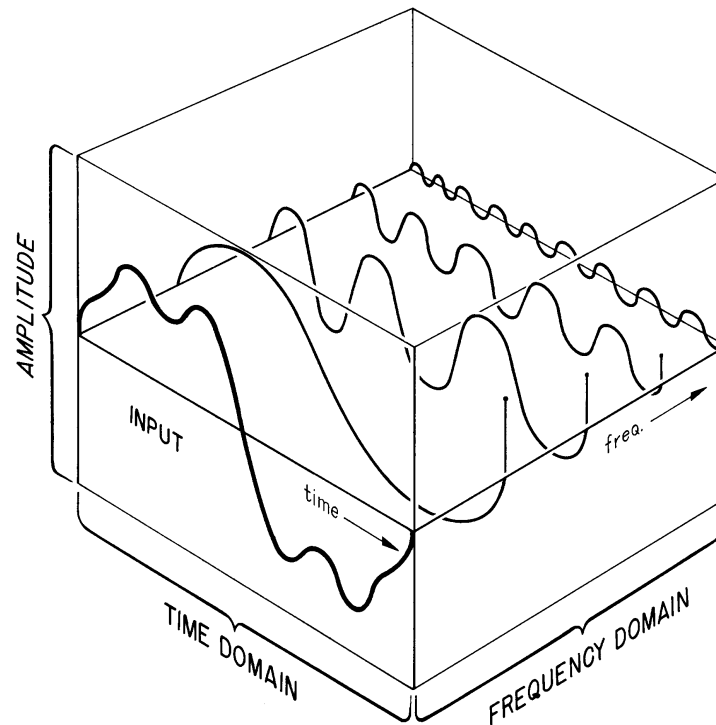


Figure 4-13. Discrete Fourier Transform Concept

The discrete Fourier transform algorithm is the basis for the formulation of any frequency domain function in modern data acquisition systems. In terms of an integral Fourier transform, the function must exist for all time in a continuous sense in order to be evaluated. For the realistic measurement situation, data is available in a discrete sense over a limited time period. The discrete Fourier transform, therefore, is based upon a set of assumptions concerning this discrete sequence of values. The assumptions can be reduced to two situations that must be met by every signal processed by the discrete Fourier transform algorithm. The first assumption is that the signal must be a ***totally observed transient*** with respect to the time period of observation. If this is not true, then the signal must be composed only of ***harmonics of the time period of observation***. If one of these two assumptions is not met by any discrete history processed by the discrete Fourier transform algorithm, then the resulting spectrum will contain bias errors accordingly. Much of the data processing that is considered with respect to acquisition of data with respect to the formulation of a modal model revolves around an attempt to assure that the input and response histories match one of these two assumptions. For a more complete

understanding of the discrete Fourier transform algorithm and the associated problems, there are a number of good references which explain all of the pertinent details ^[1-12].

Integral Fourier Transform (Forward)

$$X(f) = \int_{-\infty}^{\infty} x(t) e^{-j2\pi f t} dt \quad (4.4)$$

$$X(f) = \int_{-\infty}^{\infty} x(t) [\cos(2\pi f t) - j \sin(2\pi f t)] dt \quad (4.5)$$

$$X(f) = \int_{-\infty}^{\infty} x(t) \cos(2\pi f t) dt - j \int_{-\infty}^{\infty} x(t) \sin(2\pi f t) dt \quad (4.6)$$

Integral Fourier Transform (Reverse)

$$x(t) = \int_{-\infty}^{\infty} X(f) e^{j2\pi f t} df \quad (4.7)$$

Discrete Fourier Transform (Forward)

$$X (f_k) = \Delta t \sum_{n=0}^{N-1} x (t_n) e^{-j2\pi f_k t_n} \quad (4.8)$$

where:

- $N = \text{Blocksize (Power of 2 Typical But Not Required)}$
- $\Delta t = \text{Time spacing}$
- $\Delta f = \text{Frequency spacing}$
- $n = 0, 1, 2, \dots, (N - 1)$
- $k = 0, \pm 1, \pm 2, \dots, \pm(N - 1)$
- $\Delta f = \frac{1}{T}$
- $f_k = k \Delta f$
- $T = N \Delta t$
- $t_n = n\Delta t$

$$X (f_k) = \Delta t \sum_{n=0}^{N-1} x (t_n) e^{-j2\pi(k\Delta f) n\Delta t} \quad (4.9)$$

$$X (f_k) = \Delta t \sum_{n=0}^{N-1} x (t_n) e^{-j2\pi(\frac{k}{T}) n\Delta t} \quad (4.10)$$

$$X (f_k) = \Delta t \sum_{n=0}^{N-1} x (t_n) e^{-j2\pi(\frac{k}{N\Delta t}) n\Delta t} \quad (4.11)$$

$$X (f_k) = \Delta t \sum_{n=0}^{N-1} x (t_n) e^{-j2\pi(\frac{kn}{N})} \quad (4.12)$$

Discrete Fourier Transform (Reverse)

$$x(t_n) = \sum_{k=0}^{N-1} X(f_k) e^{j2\pi(\frac{kn}{N})} \quad (4.13)$$

4.4.1 DFT/FFT Errors

The primary digital signal processing error involved with making measurements is an error associated with the discrete or fast Fourier transform that is used to transform the digital time data to digital frequency data. This error is a bias error that is known as leakage or truncation error. In some respects, it is not really an error but is limitation of discrete and/or fast Fourier transform. Note that this error does not imply that the accuracy of the digitized time domain data has been compromised in some way. This is not the case. Likewise, the accuracy of the FFT algorithm is not the issue either. Typical FFT algorithms are accurate within 1 part in 10^{15} after a series of forward and reverse FFTs [12]. The problem is that the user expects the discrete and/or fast Fourier transform to give the same answer as the integral Fourier transform. This will be true only when certain conditions are met concerning the time domain data.

4.4.1.1 Leakage Error

This error is basically due to a violation of an assumption of the fast Fourier transform algorithm. This assumption is that the true signal is periodic within the sample period used to observe the sample function. In the cases where both input and output are totally observable (transient input with completely observed decay output within the sample period) or are harmonic functions of the time period of observation (T), there will be no contribution to the bias error, due to the truncation that occurs in the time domain (T), which is referred to as leakage.

Leakage is probably the most common and, therefore, the most serious digital signal processing error. Unlike aliasing and many other errors, the effects of leakage can only be reduced, not completely eliminated. The leakage error can be reduced by any of the following methods:

- Cyclic averaging
- Periodic Excitation
- Increase in Frequency Resolution
- Frequency Response Function Estimation Algorithm
- Windowing or Weighting Functions

In order to understand how each of these methods reduce the leakage error, the origin of leakage must be well understood.

The fast Fourier transform algorithm assumes that the data to be transformed is periodic with respect to the frequency resolution of the sampling period. Since, in general, the real world does not operate on the basis of multiples of some arbitrary frequency resolution, this introduces an error known as leakage.

The following is one approach (there are many other equivalent presentations) used to explain leakage in terms of convolution.

The concept of multiplication and convolution represents a transform pair with respect to Fourier and LaPlace transforms. More specifically, if two functions are multiplied in one domain, the result is the convolution of the two transformed functions in the other domain. Conversely, if two functions are convolved in one domain, the result is the multiplication of the two transformed functions in the other domain. When a signal is observed in the time domain with respect to a limited observation period, T , the signal that is observed can be viewed as the multiplication of two infinite time functions as shown in Figure 4-14 and 4-15. The resulting time domain function is, in the limit, the signal that is processed by the Fourier transform which is shown in Figure 4-16. Therefore, by this act of multiplication, the corresponding frequency domain functions of Figure 4-14 and 4-15 will be convolved to give the result equivalent to the Fourier transform of Figure 4-16. In this way, the difference between the infinite and the truncated signal can be evaluated theoretically.

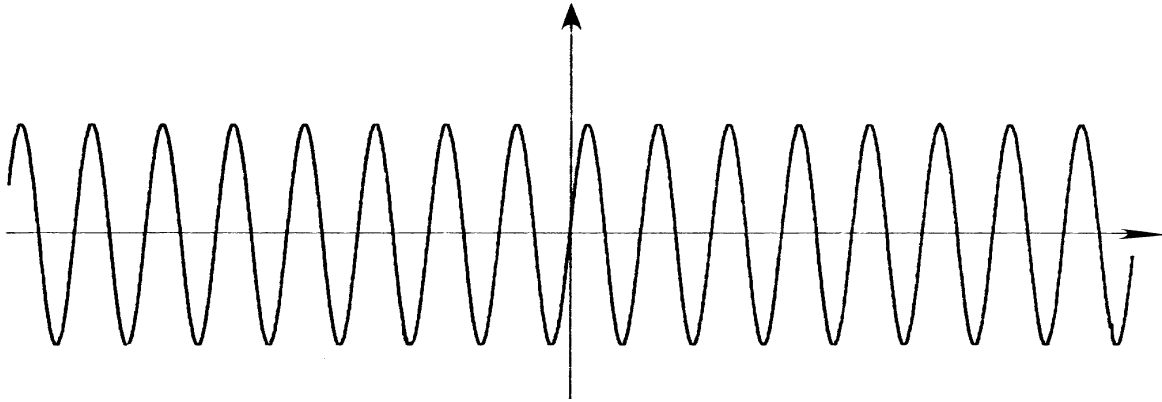


Figure 4-14. Time Domain Function: Theoretical Harmonic

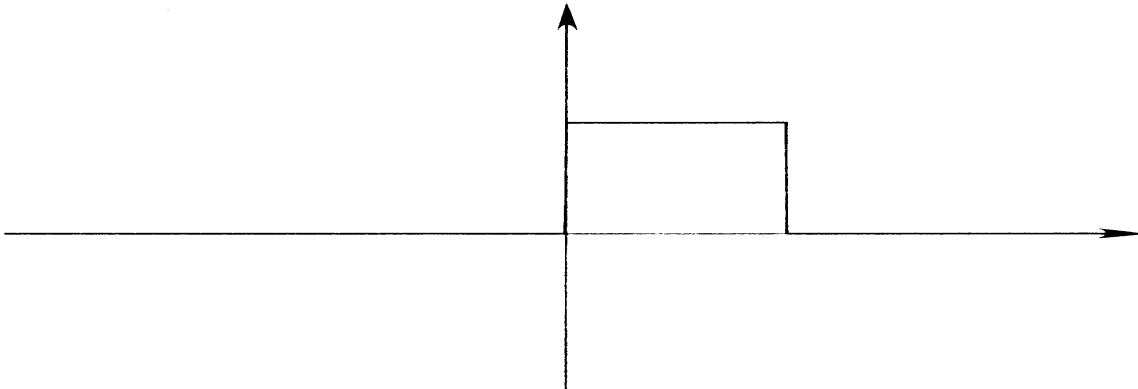


Figure 4-15. Time Domain Function: Theoretical Window

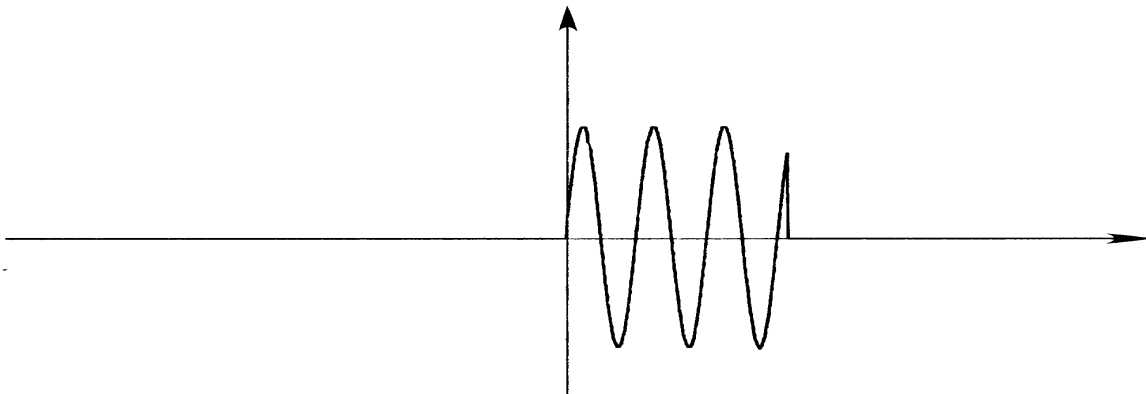


Figure 4-16. Time Domain Function: Multiplication of Signals

In order to evaluate the frequency domain result, the concept of convolution must now be understood. First of all, the integral equation representing the convolution of two time domain signals $x(t)$ and $y(t)$ can be given by Equation (4.14).

$$Z(\phi) = \int_{-\infty}^{\infty} X(\omega) Y(\phi - \omega) d\omega \quad (4.14)$$

Therefore, the evaluation of the convolution of two functions is a function as well. The value of the new function can be viewed as the integration (or summation) over all frequencies of the product of the two frequency domain functions, where one function has been shifted in frequency. This result is shown in Figure 4-19. Note that only the amplitude results are shown for simplicity. For a complete understanding of any errors, a discussion of the phase effects is also needed. Figure 4-17 is the Fourier transform of Figure 4-14. Figure 4-18 is the Fourier transform of Figure 4-15. Figure 4-19 is the convolution of Figure 4-17 and Figure 4-18.

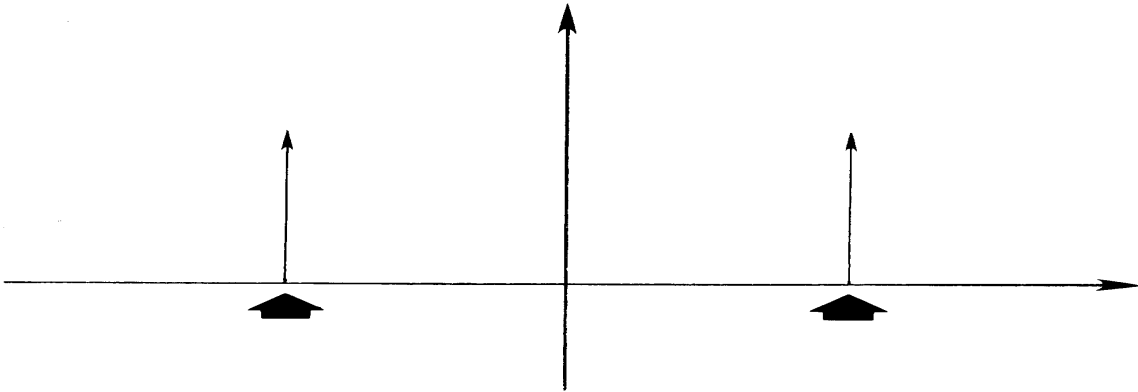


Figure 4-17. Frequency Domain: Theoretical Harmonic

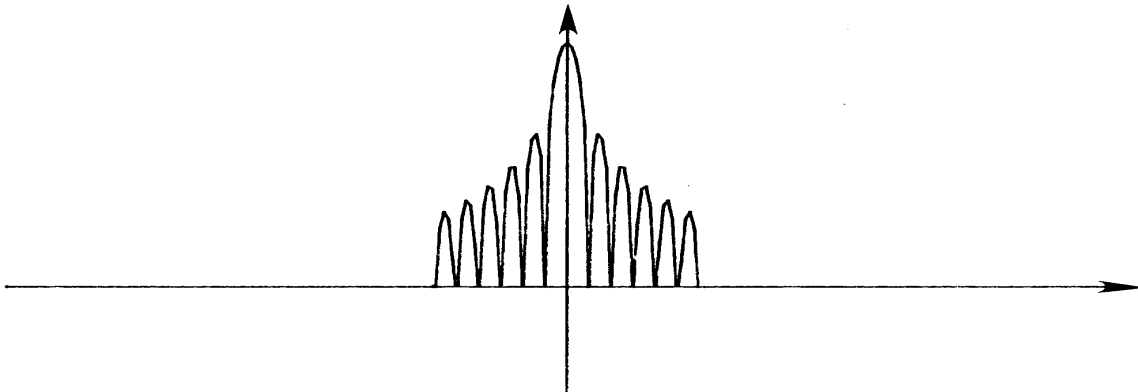


Figure 4-18. Frequency Domain: Theoretical Window

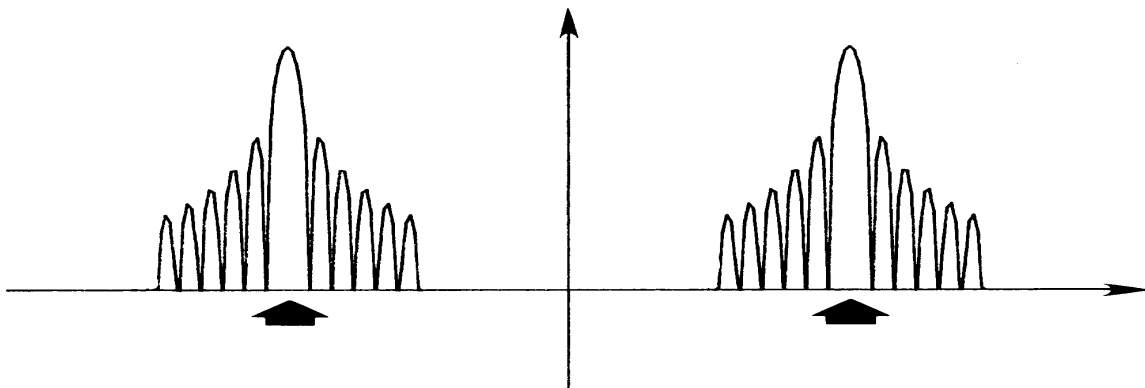


Figure 4-19. Frequency Domain: Convolved Signals

For the practical case, the resulting functions shown in Figure 4-16 and Figure 4-19 are not continuous but occur in a digital sense. For this case, Equation (4.14) can be formulated accordingly as shown in Equation (4.15).

$$Z(\phi) = \sum_{i=-N}^{+N} X(i \Delta \omega) Y(\phi - i \Delta \omega) \quad (4.15)$$

where:

- $\phi = k \Delta \omega$
- $k = -N \longleftrightarrow +N$

With this in mind, two cases must be evaluated with respect to whether the theoretical harmonic chosen for the example is periodic or not with respect to the window period, T . These cases are shown in Figure 4-20 and Figure 4-21. Note that an harmonic signal was chosen for this example since any other signal can be thought to be simply a linear sum of such harmonics. Since the Fourier transform is also linear in this sense, the result shown is valid for any theoretical signal satisfying the Dirichlet conditions.

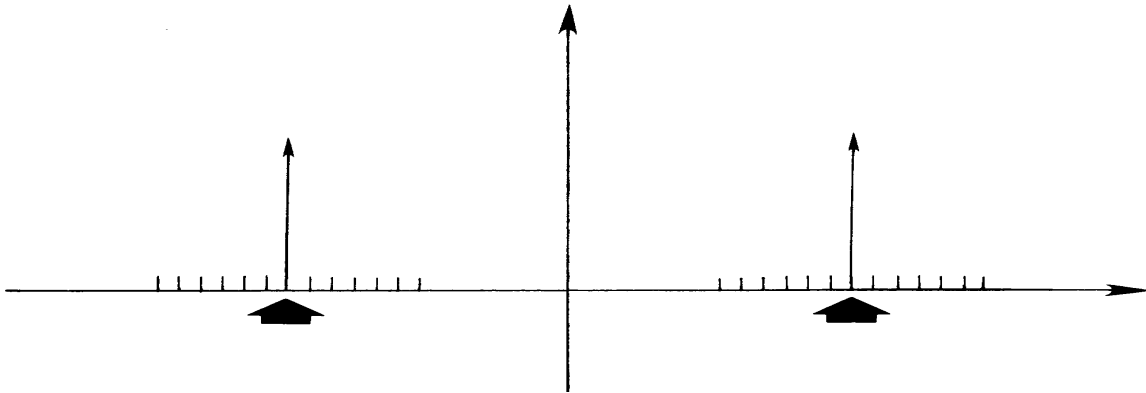


Figure 4-20. Frequency Domain: Periodic Signal

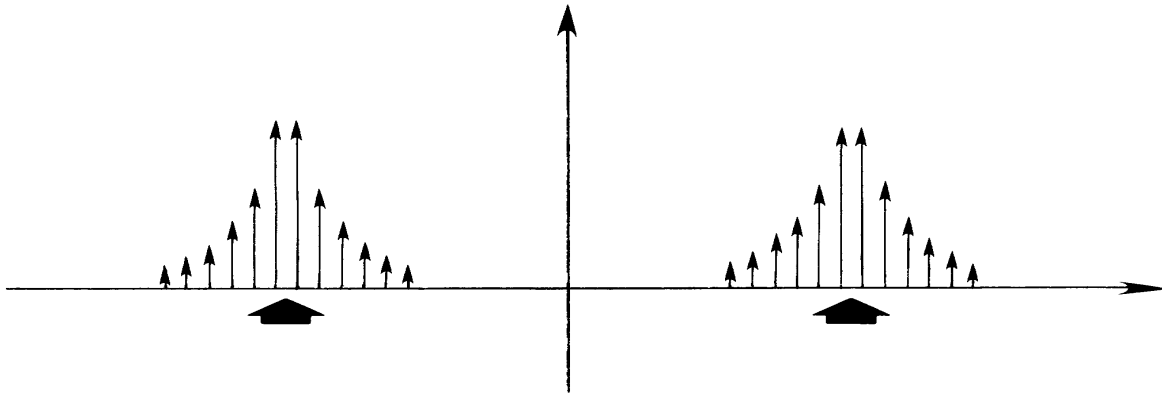


Figure 4-21. Frequency Domain: Nonperiodic Signal

Therefore, when an analog signal is digitized in a Fourier analyzer, the analog signal has been multiplied by a function of unity (for a period of time T) in the time domain. This results in a convolution of the two signals in the frequency domain. This process of multiplying an analog signal by some sort of weighting function is loosely referred to as "windowing". Whenever a time function is sampled, the transform relationship between multiplication and convolution must be considered. Likewise, whenever an additional weighting function such as a Hanning window is utilized, the effects of such a window can be evaluated in the same fashion.

4.5 Increased Frequency Resolution

An increase in the frequency resolution of a frequency response function effects measurement errors in several ways. Obviously, finer frequency resolution allows more exact determination of the damped natural frequency of each modal vector. The increased frequency resolution means that the level of a broadband signal is reduced. The most important benefit of increased frequency resolution, though, is a reduction of the leakage error. Since the distortion of the frequency response function due to leakage is a function of frequency spacing, not frequency, the increase in frequency resolution will reduce the true bandwidth of the leakage error centered at each damped natural frequency. In order to increase the frequency resolution, the total time per history must be increased in direct proportion. The longer data acquisition time will increase the variance error problem when transient signals are utilized for input as well as emphasizing any nonstationary problem with the data. The increase of frequency resolution will often require

multiple acquisition and/or processing of the histories in order to obtain an equivalent frequency range. This will increase the data storage and documentation overhead as well as extending the total test time.

There are two approaches for increasing the frequency resolution of a frequency response function. The first approach involves increasing the number of spectral lines in a baseband measurement. The advantage of this approach, is that no additional hardware or software is required. Often, FFT analyzers do not have the capability to alter the number of spectral lines used in the measurement. The second approach involves the reduction of the bandwidth of the measurement while holding the number of spectral lines constant. If the lower frequency limit of the bandwidth is always zero, no additional hardware or software is required. Ideally, though, for an arbitrary bandwidth, hardware and/or software to perform a frequency shifted, or digitally filtered, FFT will be required. The concept of a frequency shifted FFT is presented in the following figure.

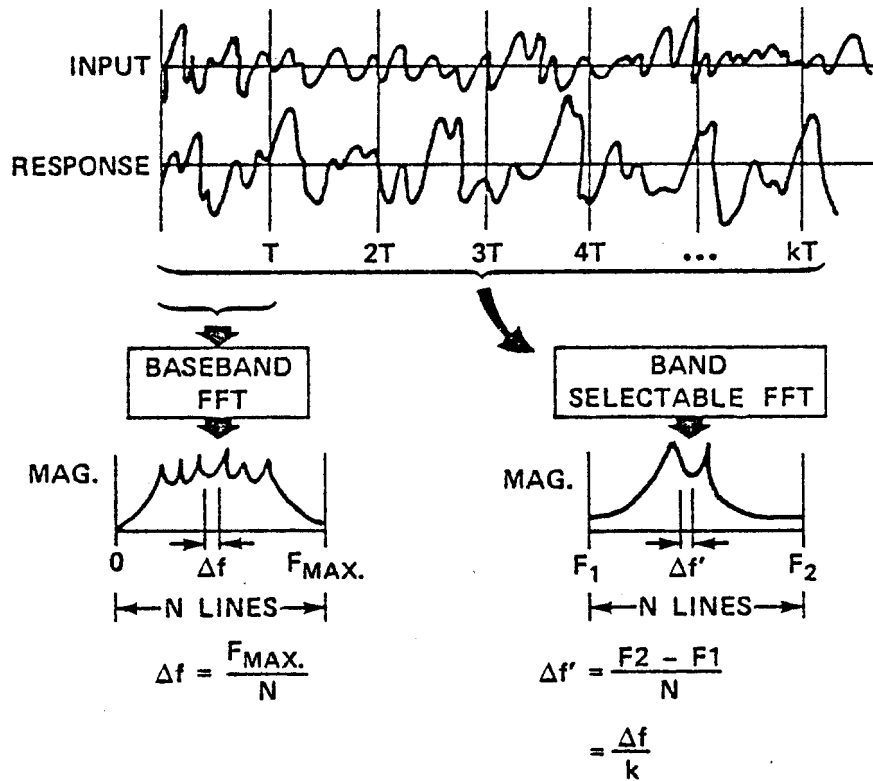


Figure 4-22. Increased Frequency Resolution

The frequency shifted FFT process for computing the frequency response function has additional characteristics pertinent to the reduction of errors. Primarily, more accurate information can be obtained on weak spectral components if the bandwidth is chosen to avoid strong spectral components. The out-of-band rejection of the frequency shifted FFT is better than most analog filters that could be used in a measurement procedure to attempt to achieve the same results. Additionally, the precision of the resulting frequency response function will be improved due to processor gain inherent in the frequency shifted FFT calculation procedure.

The Fourier transform shift theorem is:

$$X(f - f_s) = \int_{-\infty}^{\infty} (x(t) e^{-j2\pi f_s t}) e^{-j2\pi f t} dt \quad (4.16)$$

Once the digitized time domain data is multiplied by the shift frequency term ($e^{-j2\pi f_s t} = \cos(2\pi f_s t) - j \sin(2\pi f_s t)$), the digitized time domain data will be complex valued. This data must be filtered and decimated before the Fourier transform is applied. This is schematically shown in the following figure.

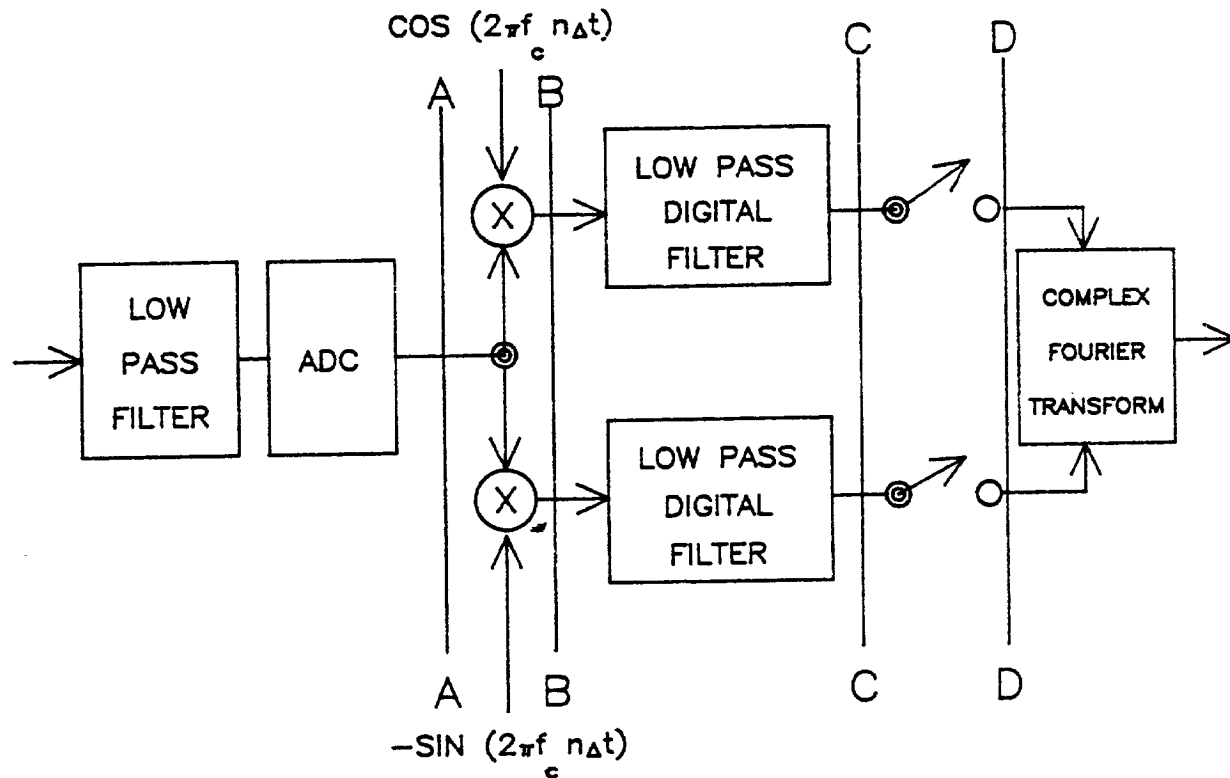


Figure 4-23. Increased Frequency Resolution

An example of the improvement of the frequency response function using a frequency shifted FFT can be seen in Figure 4-24.

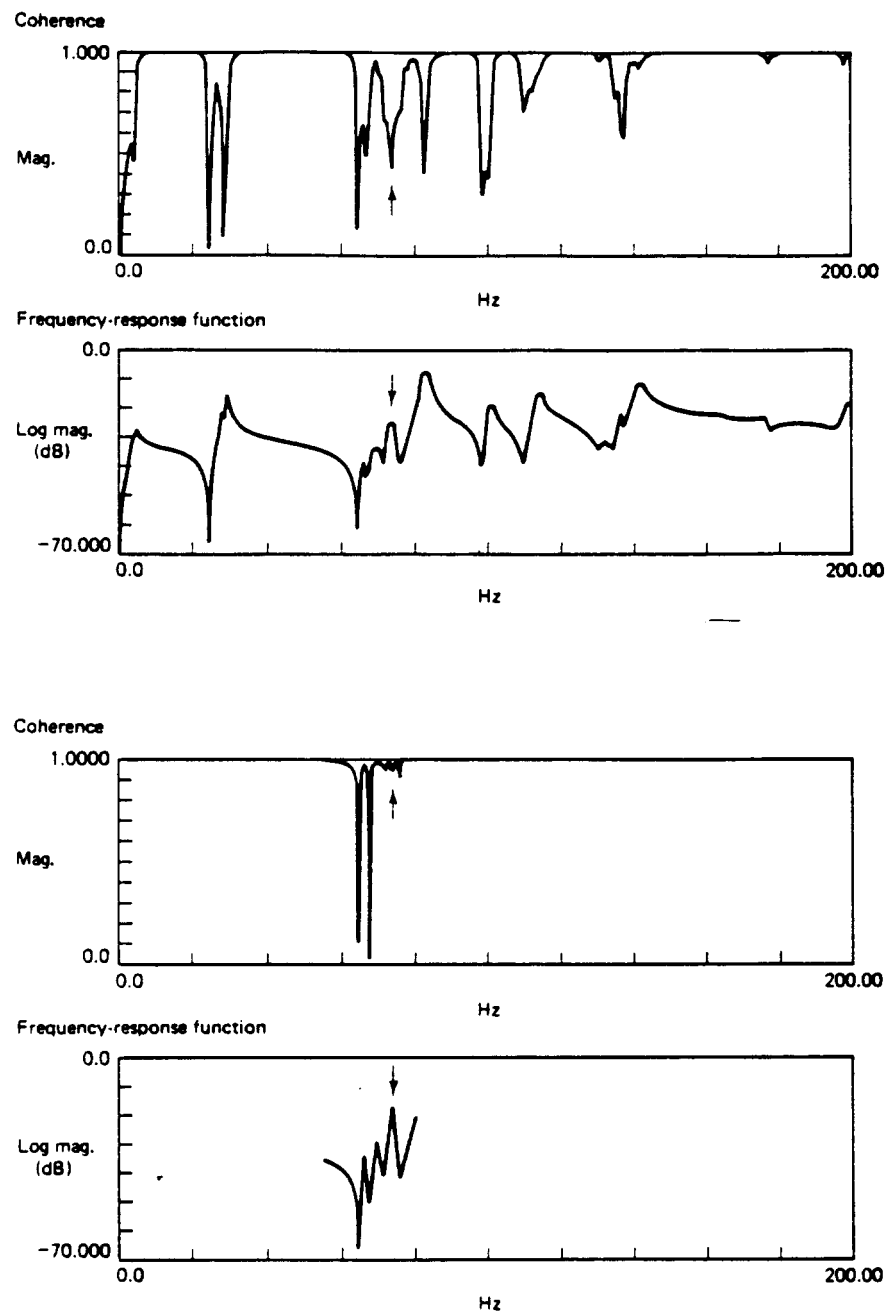


Figure 4-24. Increased Frequency Resolution

4.6 Weighting Functions

Weighting functions, or data windows, are probably the most common approach to the reduction of the leakage error in the frequency response function. While weighting functions are sometimes desirable and necessary to modify the frequency domain effects of truncating a signal in the time domain, weighting functions are too often utilized when one of the other approaches to error reduction would give superior results. Averaging, selective excitation, and increasing the frequency resolution all act to reduce the leakage error by the elimination of the cause of the error. Weighting functions, on the other hand, attempt to compensate for the leakage error after the fact.

Figure 4-25 shows the frequency domain, magnitude characteristic of the basic boxcar, or rectangular, window that was represented in Figure 4-18. It is important to note that Figure 4-25 shows the magnitude distortion, which is called leakage, as a function of Δf , not absolute frequency. This error will be associated with any signal that is truncated in the time domain and Fourier transformed to the frequency domain. The effective impact of this magnitude distortion on the frequency domain data is the same as a narrow, analog, bandpass filter, with a filter bandwidth described by this characteristic. A narrow, bandpass filter with this frequency domain characteristic is effectively applied to the data at each discrete frequency of the discrete Fourier transform. This is another very useful analogy for understanding leakage and the similarity between analog and digital data acquisition. In this analogy, it is easy to understand that the value of the spectra may be a function of information several Δf frequencies away rather than just the immediate Δf frequency bandwidth. Note that frequency information that occurs at integer multiples of the Δf does not contribute to this error.

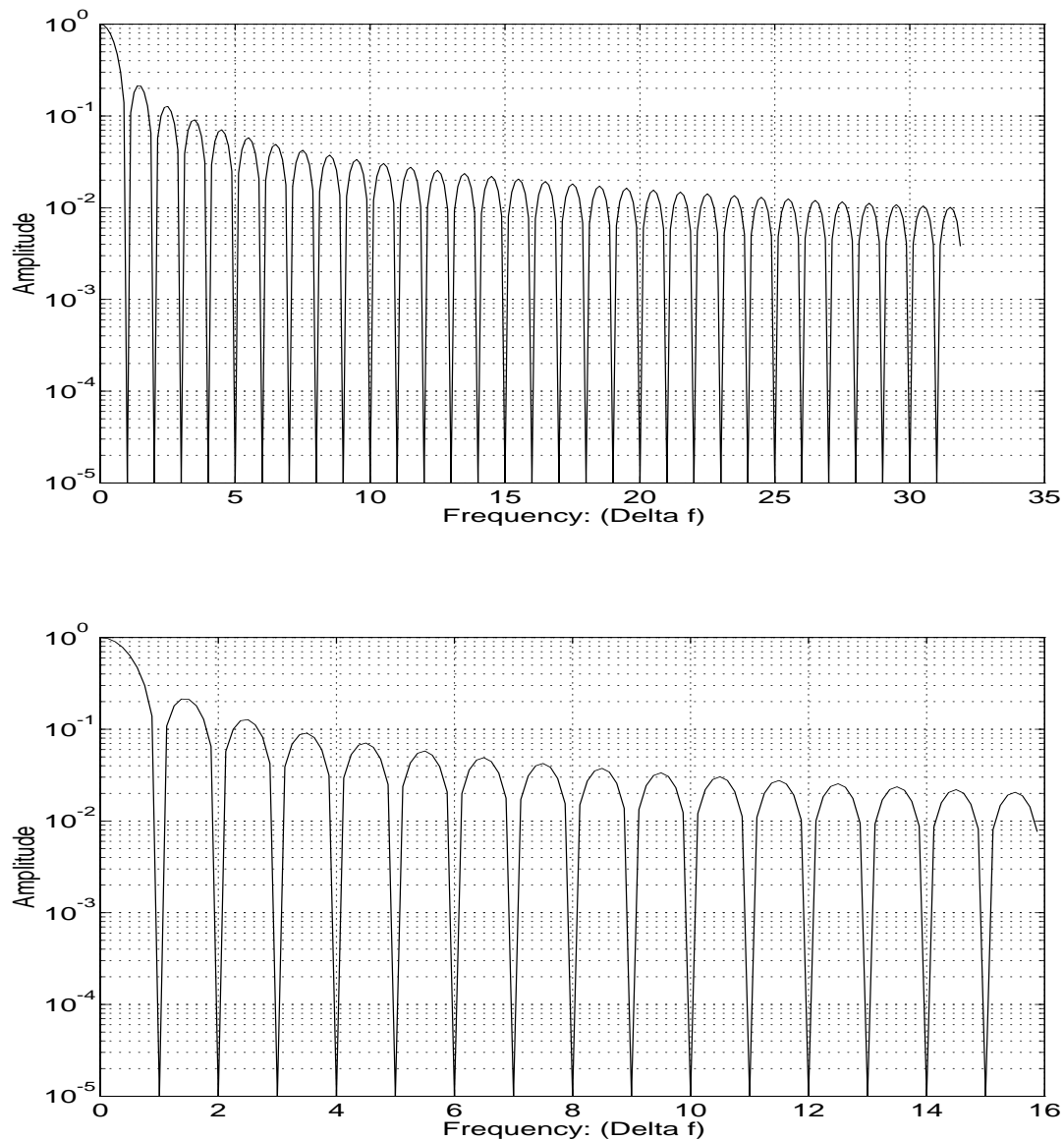


Figure 4-25. Typical Weighting Function - Boxcar (P000) Window

Windows alter, or compensate for, the frequency domain characteristic associated with the truncation of data in the time domain. Essentially, again using the narrow bandpass filter analogy, windows alter the characteristics of the bandpass filters that are applied to the data. This compensation for the leakage error causes an attendant distortion of the frequency and phase information of the frequency response function, particularly in the case of closely spaced,

lightly damped system poles. This distortion is a direct function of the width of the main lobe and the size of the side lobes of the spectrum of the weighting function. Examples of some common weighting functions are given in the following figures (Time domain: Figure 4-26 and 4-27, Frequency domain: Figure 4-28 and 4-29). Complete details concerning these and many other weighting functions are available from many sources [1-4,25-26].

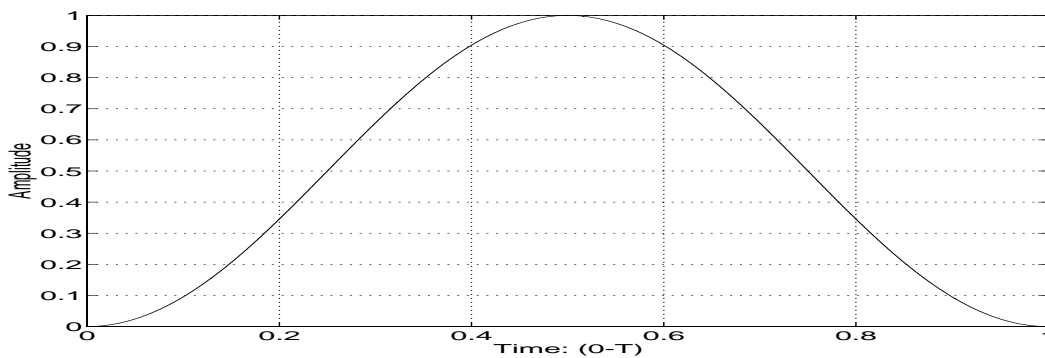


Figure 4-26. Typical Weighting Functions - Hanning (P110) Window

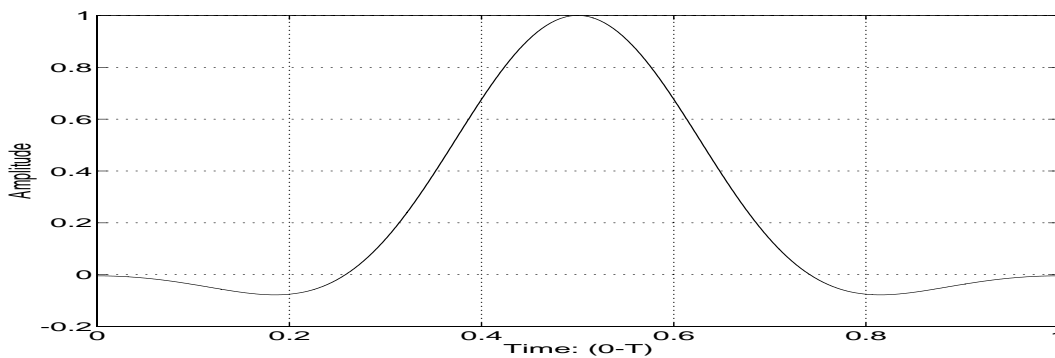


Figure 4-27. Typical Weighting Functions - Flattop (P301) Window

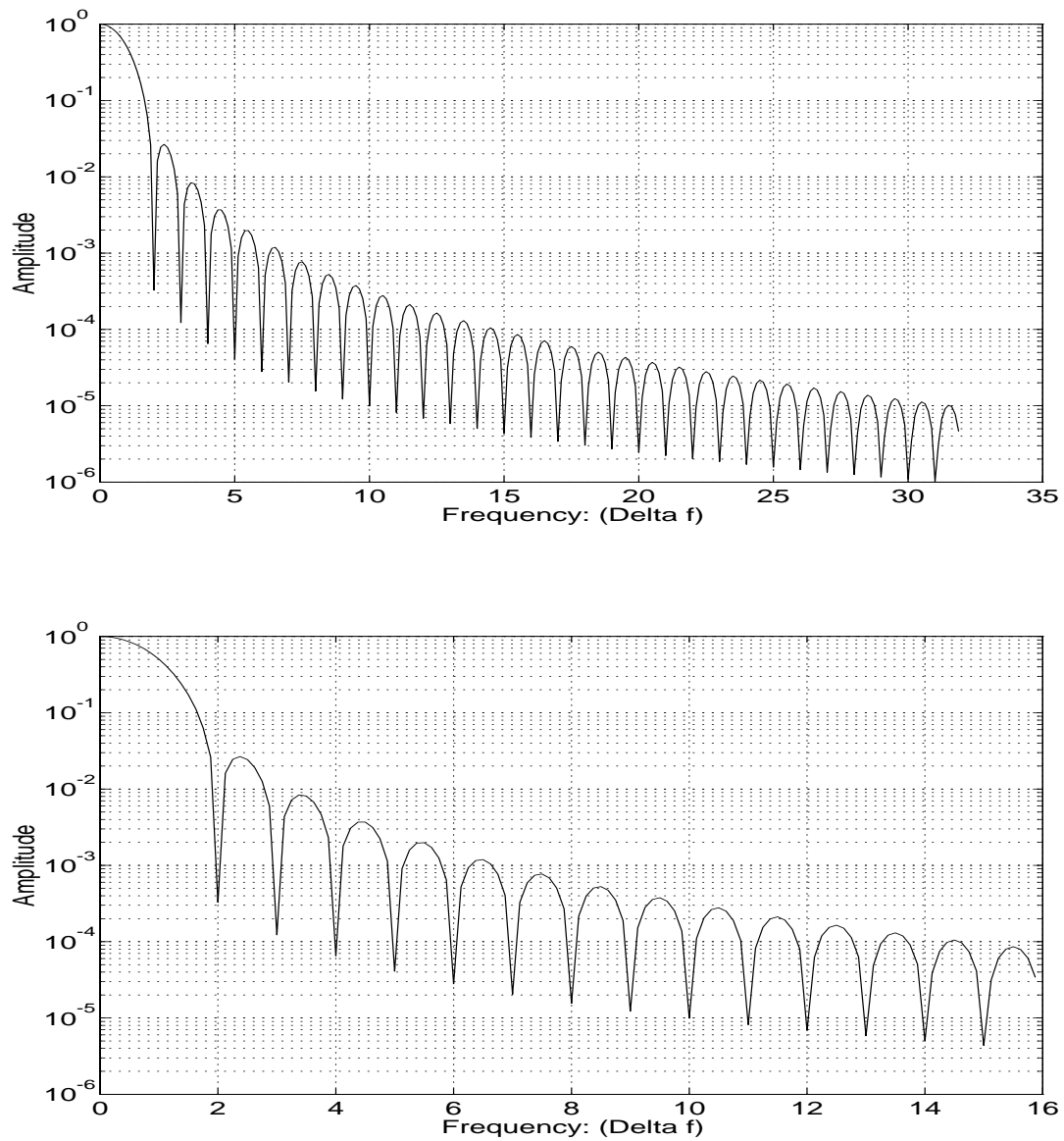


Figure 4-28. Typical Weighting Function - Hanning (P110) Window

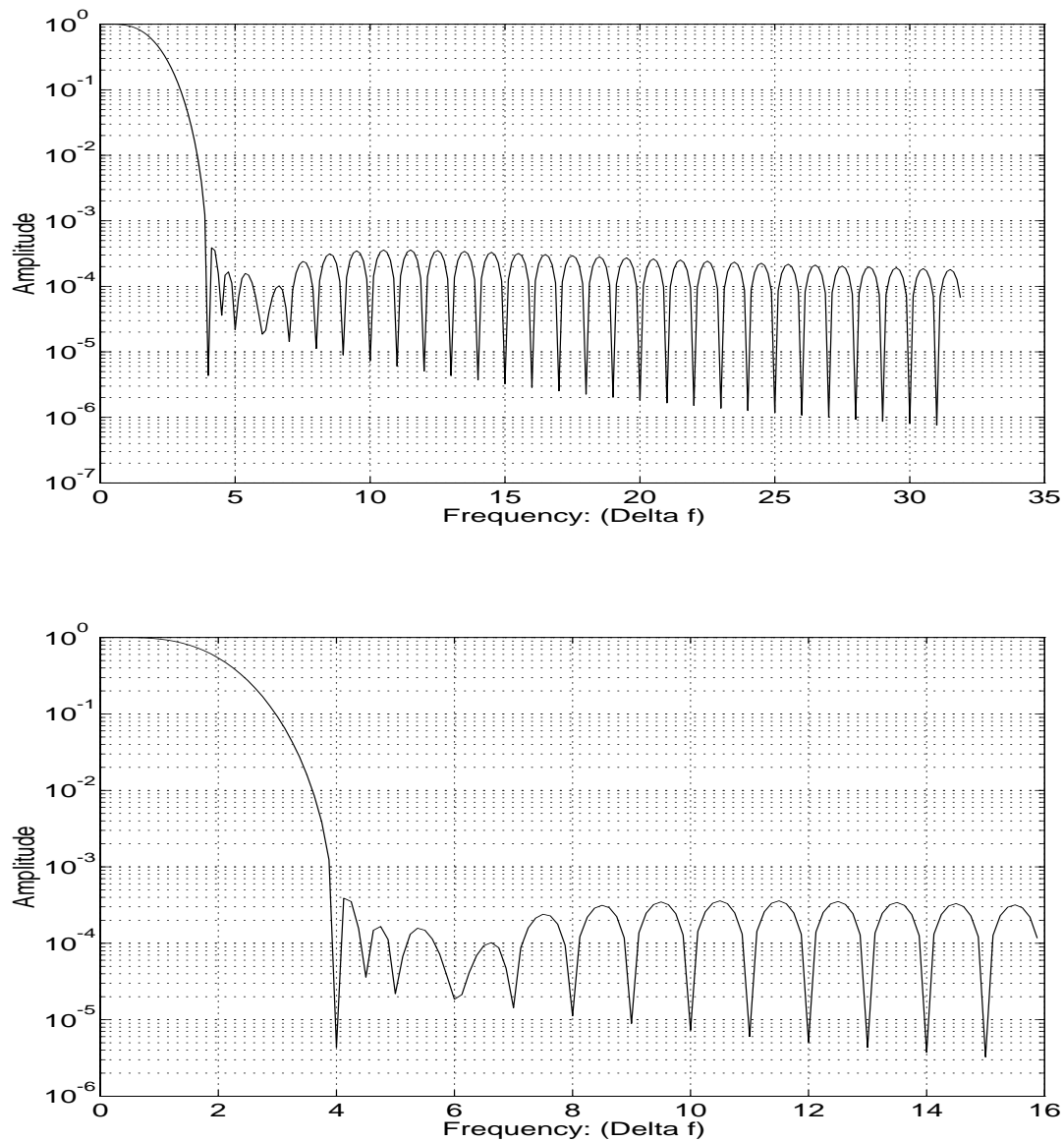


Figure 4-29. Typical Weighting Function - Flattop (P301) Window

4.7 Averaging

The averaging of signals is normally viewed as a summation or weighted summation process where each sample function has a common abscissa. Normally, the designation of *history* is given to sample functions with the abscissa of absolute time and the designation of *spectra* is

given to sample functions with the abscissa of absolute frequency. The spectra are normally generated by Fourier transforming the corresponding history. In order to generalize and consolidate the concept of signal averaging as much as possible, the case of relative time can also be considered. In this way *relative history* can be discussed with units of the appropriate event rather than seconds and a *relative spectrum* will be the corresponding Fourier transform with units of cycles per event. This concept of signal averaging is used widely in structural signature analysis where the event is a revolution. This kind of approach simplifies the application of many other concepts of signal relationships such as Shannon's sampling theorem and Rayleigh's criterion of frequency resolution.

4.7.1 General Averaging Methods

When comparing data taken with different equipment, care must be taken to be certain that the averaging is being performed the same way. The terminology with regard to averaging is not always the same so some sort of evaluation may be required using test cases to be certain that the same form of averaging is being used.

4.7.1.1 Linear Averaging

Linear averaging is the simplest form of averaging and is what most people think of as averaging. Essentially, linear averaging is simply trying to find the mean value in a set of numbers. Since measurements deal with information at different times or frequencies, linear averaging refers to finding the mean value at each time or frequency over a number of ensembles or averages. Linear averaging is fundamentally calculated with the following formulae:

$$\bar{X}(\omega)_{N_{avg}} = \frac{\sum_{i=1}^{N_{avg}} X(\omega)_i}{N_{avg}} \quad (4.17)$$

$$\bar{x}(t)_{N_{avg}} = \frac{\sum_{i=1}^{N_{avg}} x(t)_i}{N_{avg}} \quad (4.18)$$

Linear averaging is useful primarily when some form of initial trigger is available in order for information that is synchronized with the trigger to be emphasized. Note that if no trigger is available and the averages are collected in a free-run data acquisition mode, the phasing of any dynamic signals will be random from ensemble to ensemble. With a large number of averages, only the DC signal content will be preserved.

If some sort of initializing trigger is available, the averaged data reduce the noise and enhance the signal giving an improved signal to noise ratio (SNR). The variance is reduced as a function of $\frac{1}{\sqrt{N_{avg}}}$. This means that to reduce the variance to 10 percent of the variance on a single average, 100 averages must be taken.

The terminology ***time averaging*** refers to a special case of linear averaging when the trigger of each average is synchronized with a specific position of a rotating shaft (for example, top dead center). In this case, each ensemble will have a fixed number of rotations in the time history and each data point in the time history will be collected when the rotating system is in the same position as long as the speed of rotation is constant. If the data is sampled at fixed intervals during the rotation (for example, by utilizing an encoder to give 32 samples per revolution), the fixed speed is not required. The processing of data for this situation requires further consideration and will not be presented here.

4.7.1.2 Magnitude Averaging

Magnitude, or amplitude, averaging involves finding the mean value of the absolute values of the data at each time or frequency. While this form of averaging is not very common, it has been used in some older digital signal analyzers. This form of averaging has generally been replaced by RMS averaging in most current digital signal analyzers. Magnitude averaging and RMS averaging will give nearly identical results if there is little dynamic range in the data being averaged. Since the absolute value is formed, the phasing provided by an initial trigger, is not required for magnitude averaging. However, magnitude averaging does not improve the signal to noise ratio (SNR) since the noise magnitude accumulates in the same way as the signal magnitude. Therefore, magnitude averaging does not reduce the variance in the data with averages in the same way as linear averaging. Magnitude averaging is fundamentally calculated

with the following formula:

$$\bar{X}(\omega)_{N_{avg}} = \frac{\sum_{i=1}^{N_{avg}} \sqrt{X(\omega)_i \times X(\omega)_i^*}}{N_{avg}} \quad (4.19)$$

$$\bar{x}(t)_{N_{avg}} = \frac{\sum_{i=1}^{N_{avg}} \sqrt{x(t)_i \times x(t)_i}}{N_{avg}} \quad (4.20)$$

Magnitude averaging is generally not a concern unless historical data or data acquisition procedures are involved. This can be a concern if data or data acquisition procedures are specified, particularly in patents or other historical documents.

4.7.1.3 Root-Mean-Square (RMS) Averaging

Root-Mean-Square (RMS) averaging is commonly used in many digital signal analyzers and is the basis for estimating frequency response and coherence functions from auto and cross power spectra. RMS averaging refers to the computational procedure involving the mean squared value of the data at each time or frequency. This is useful for determining the power, or energy, in the data which may contain positive and negative values and/or real and complex values. Since the squared value is formed, the phasing provided by an initial trigger, is not required for RMS averaging. However, RMS averaging does not improve the signal to noise ratio (SNR) since the noise power accumulates in the same way as the signal power. Therefore, RMS averaging does not reduce the variance in the data with averages in the same way as linear averaging. In the estimation of the frequency response function, the variance error is reduced by choosing the FRF estimation algorithm based upon the location of the noise in the inputs and outputs. Magnitude averaging and RMS averaging will give nearly identical results if there is little dynamic range in the data being averaged. RMS averaging is fundamentally calculated with the following formula:

$$\bar{x}(t)_{N_{avg}} = \sqrt{\frac{\sum_{i=1}^{N_{avg}} x(t)_i \times x(t)_i}{N_{avg}}} \quad (4.21)$$

$$\bar{X}(\omega)_{N_{avg}} = \sqrt{\frac{\sum_{i=1}^{N_{avg}} X(\omega)_i \times X(\omega)_i^*}{N_{avg}}} \quad (4.22)$$

Note that in the above equations, the units on the averaged data are the same as the units of each average. Frequently, digital signal analyzers show the resulting averaged data with units squared. This is simply indicating that the averaged data is being displayed without the square root. This is simply a display issue and the user can choose between units and units squared.

As a simple example of the difference between linear, magnitude and RMS averaging, Table 4-2 indicates the problem.

Ensemble	Linear	Magnitude	RMS
1	2	2	4
2	3	3	9
3	4	4	16
4	-2	2	4
5	-3	3	9
6	-4	4	16
Total	0	18	58
Average	0	3.000	3.109

TABLE 4-2. Comparison of Averaging Methods

4.7.1.4 Exponential Averaging

Exponential averaging weights new data differently (typically more heavily) than old data. This is useful for tracking time varying characteristics in the data (not used in data used for experimental modal analysis). The weighting is generally dependent on the number of averages chosen for the exponential averaging (typically a power of 2, either 4 or 8). Once the exponential averaging is started, the averaging continues until it is stopped (it does not stop after the number of averages selected, the number of averages determines the weighting or "forgetting" factor).

For the first few averages, linear and exponential averaging is nearly the same. Exponential averaging is fundamentally calculated with the following formula:

$$\bar{X}(\omega)_{N_{avg}} = (1 - 2^{-N_{avg}}) \bar{X}(\omega)_{N_{avg}-1} + 2^{-N_{avg}} X(\omega)_i \quad (4.23)$$

4.7.1.5 Stable Averaging

Stable averaging is not really a separate form of averaging but refers to a display characteristic. If the averaging process is stopped before N_{avg} are reached, stable averaging always shows the display information with the appropriate correction for the number of averages. Stable averaging means that the above equations are reformulated in a recursive form so that the displayed can be updated, average by average, so that the amplitude of the data is correct regardless of when the average is stopped. The recursive form of the averaging equations weights old and new data records appropriately to yield the appropriate arithmetic mean for the current number of averages.

4.7.1.6 Peak Hold

Peak hold data collection is often included in the averaging selection of a digital signal analyzer. Peak hold, as the name indicates, is not really a form of averaging since only the peak value is retained at each time or frequency and no arithmetic mean (in the common understanding of the term) is formed. Normally, the peak magnitude or peak RMS information is retained over a number of ensembles. This data collection approach is very useful for identifying the maxima that occur during transients or general time varying events.

4.7.2 Estimation of Frequency Response Functions

The process of signal averaging as it applies to frequency response function estimation involves linear averaging of auto and cross power spectra. This is a bit confusing since the general averaging concepts always are explained in terms of a single data signal. With frequency response function estimation, there are a number of input and output signals that are all initiated (triggered) at the same start time for each average and are all sampled at the same time. The

reduction of noise on the frequency response function estimates depends upon the noise model that is used to describe where the noise enters the measurements, on the inputs, on the outputs or both. Based upon the noise model, the FRF estimation algorithm will reduce the random noise according to a least squared error procedure. Note that, since the least squared error procedure minimizes the squared error by eliminating the phase information, these procedures will affect the magnitude but not the phase.

It is important to realize that, while the frequency response function is assumed to be unique, the auto and cross power spectra used to estimate the FRF are not unique unless the input is stationary and a sufficiently large number of averages is taken. Generally, this is never the case. This is not a concern, however, since the desired information is the frequency response function not auto and cross power spectra. After a reasonable number of averages (5-100), the auto and cross power spectra may still appear to be noisy. Some of the 'noise' is due to random or bias errors in the data and some of the noise is simply due to the uneven excitation that occurs with transient or random input(s) to the system being tested. The uneven excitation in the auto and cross spectra is consistent between the input and output power spectra (related by the FRF) and will cancel when the frequency response function is estimated. The random portion of the noise will be minimized due to the least squared error estimation of the frequency response function. The bias portion of the noise will not generally be eliminated. Therefore, it is critical that bias errors, such as leakage, be eliminated if possible.

The triggering issues relative to averaging of auto and cross power spectra that will be used to estimate FRFs required some additional terminology in order to clarify the measurement procedure. One of two forms of linear averaging, asynchronous and synchronous averaging, are always used to estimate FRFs depending upon the type of excitation. Additionally, cyclic averaging, a special case of time domain, linear averaging, may be used when leakage is a serious problem in conjunction with traditional averaging methods (asynchronous or synchronous averaging). Cyclic averaging reduces the leakage bias error by digitally filtering the data to eliminate the frequency information that cannot be described by the FFT (only integer multiples of Δf are retained) prior to the application of the FFT. Cyclic averaging can always be used, together with asynchronous or synchronous averaging, to reduce both the leakage error as well as the random errors.

Since the Fourier transform is a linear function, there is no theoretical difference between the use

of time or frequency domain data when averaging. Practically, though, synchronous and asynchronous averaging is normally performed in the frequency domain and cyclic averaging is normally performed in the time domain. Therefore, these three classifications primarily refer to the initial trigger and sampling relationships between averages or ensembles while collecting the the auto and cross power spectra used to estimate frequency response functions. This will be explained further in the following sections.

4.7.2.1 Asynchronous Signal Averaging

The asynchronous classification of linear signal averaging of the auto and cross power spectra represents the case where no known relationship exists each average. The FRF is correctly estimated solely on the basis of the uniqueness of the frequency response function. In this case, the auto and cross power spectra (least squares) approach to the estimate of frequency response must be used since no other way of preserving phase and improving the estimate is available. In this situation, the trigger to initiate each average takes place in a random fashion dependent only upon the data acquisition equipment timing. The triggering is said to be in a free-run mode.

4.7.2.2 Synchronous Signal Averaging

The synchronous classification of linear signal averaging adds the additional constraint that each average must be initiated with respect to a specific trigger condition (often the magnitude and slope of the excitation). This means that the frequency response function could be formed as $X(\omega)_{Navg}$ divided by $F(\omega)_{Navg}$ since phase is preserved. Even so, linear averaging of the auto and cross power spectra is still the preferred FRF estimation method due to the reduction of variance and the ability to estimate the ordinary coherence function. The ability to synchronize the initiation of digitization for each average allows for use of non-stationary or deterministic inputs with a resulting increased signal to noise ratio.

The synchronization takes place as a function of a trigger signal occurring in the input (internally) or in some event related to the input (externally). An example of an internal trigger would be the case where an impulsive input is used to estimate the frequency response. Each average would be initiated when the input reached a certain amplitude and slope. A similar example of an external trigger would be the case where the impulsive excitation to a speaker is

used to trigger the estimate of frequency response between two microphones in the sound field. Again, each average would be initiated when the trigger signal reached a certain amplitude and slope.

4.7.2.3 Cyclic Signal Averaging

The cyclic classification of signal averaging involves a special case of linear averaging with the added constraint that the digitization is coherent between averages. This means that the exact time between each average is used to enhance the signal averaging process. Rather than trying to keep track of elapsed time between averages, the normal procedure is to allow no time to elapse between successive averages. This simple averaging procedure results in a digital comb filter in the frequency domain, with the teeth (passbands) of the comb at frequency increments that are integer multiples of the $\Delta f = 1/T$ relationship. The result is an attenuation of the spectrum between the teeth not possible with other forms of averaging. Cyclic signal averaging is generally performed in the time domain and is coupled with asynchronous or synchronous averaging procedures in the frequency domain.

This form of signal averaging is very useful for filtering periodic components from a noisy signal since the teeth of the filter are positioned at harmonics of the frequency of the sampling reference signal. This is of particular importance in applications where it is desirable to extract signals connected with various rotating members. This same form of signal averaging is particularly useful for reducing leakage during frequency response measurements.

A very common application of cyclic signal averaging is in the area of analysis of rotating structures. In such an application, the peaks of the comb filter are positioned to match the fundamental and harmonic frequencies of a particular rotating shaft or component. This is particularly powerful, since in one measurement it is possible to enhance all of the possible frequencies generated by the rotating member from a given data signal. With a zoom Fourier transform type of approach, one shaft frequency at a time can be examined depending upon the zoom power necessary to extract the shaft frequencies from the surrounding noise.

The application of cyclic averaging to the estimation of frequency response functions can be easily observed by noting the effects of cyclic averaging on a single frequency sinusoid. Figures

4-30 and 4-31 represent the cyclic averaging of a sinusoid that is periodic with respect to the observation time period T . Figures 4-32 and 4-33 represent the cyclic averaging of a sinusoid that is aperiodic with respect to the observation time period T . By comparing Figure 4-31 to Figure 4-33, the attenuation of the nonperiodic signal can be clearly observed.

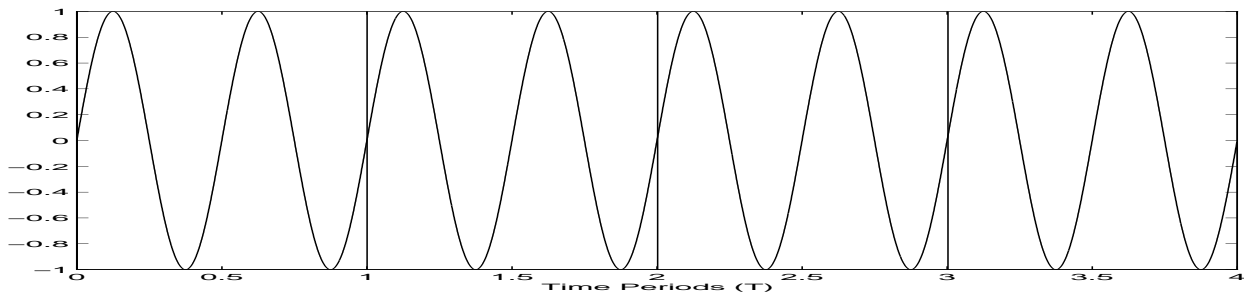


Figure 4-30. Contiguous Time Records (Periodic Signal)

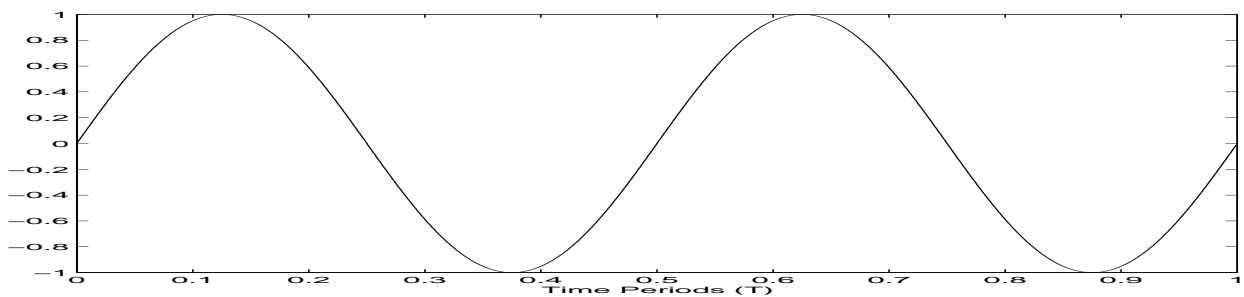


Figure 4-31. Averaged Time Records (Periodic Signal)

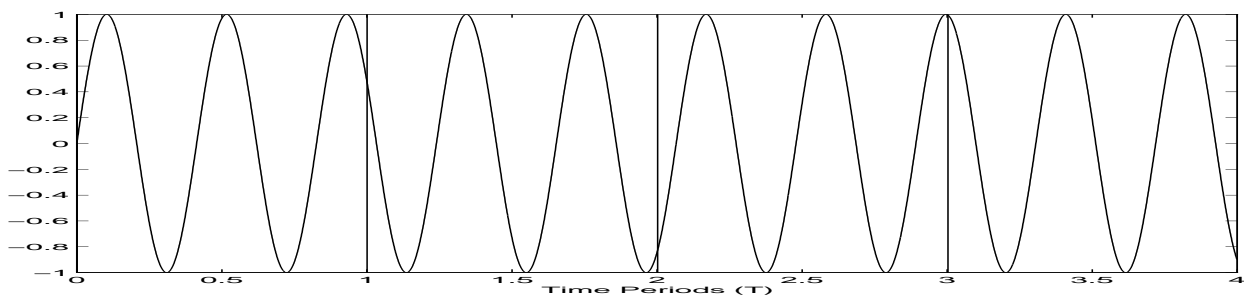


Figure 4-32. Contiguous Time Records (Non-Periodic Signal)

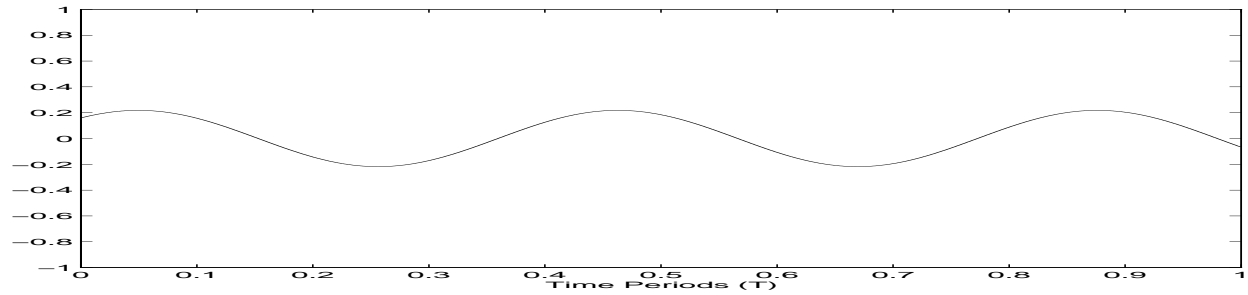


Figure 4-33. Averaged Time Records (Non-Periodic Signal)

4.7.2.3.1 Theory of Cyclic Averaging

In the application of cyclic averaging to frequency response function estimates, the corresponding fundamental and harmonic frequencies that are enhanced are the frequencies that occur at the integer multiples of Δf . In this case, the spectra between each Δf is reduced with an associated reduction of the bias error called *leakage*.

The first observation to be noted is the relationship between the Fourier transform of a history and the Fourier transform of a time shifted history. In the averaging case, each history will be of some finite time length T which is the observation period of the data. Note that this time period of observation T determines the fundamental frequency resolution Δf of the spectra via the Rayleigh Criteria ($\Delta f = \frac{1}{T}$).

The Fourier transform of a history is given by:

$$X(\omega) = \int_{-\infty}^{+\infty} x(t) e^{-j\omega t} dt \quad (4.24)$$

Using the time shift theorem of the Fourier transform, the Fourier transform of the same history that has been shifted in time by an amount t_0 is ^[5]:

$$X(\omega) e^{-j\omega t_0} = \int_{-\infty}^{+\infty} x(t + t_0) e^{-j\omega t} dt \quad (4.25)$$

For the case of a discrete Fourier transform, each frequency in the spectra is assumed to be an integer multiple of the fundamental frequency $\Delta f = \frac{1}{T}$. Making this substitution in Equation (4-25) ($\omega = k \frac{2\pi}{T}$ with k as an integer) yields:

$$X(\omega) e^{-j n \frac{2\pi}{T} t_0} = \int_{-\infty}^{+\infty} x(t + t_0) e^{-j\omega t} dt \quad (4.26)$$

Note that in Equation (4-26), the correction for the cases where $t_0 = N T$ with N is an integer will be a unit magnitude with zero phase. Therefore, if each history that is cyclic averaged occurs at a time shift, with respect to the initial average, that is an integer multiple of the observation period T , then the correction due to the time shift does not effect the frequency domain characteristics of the averaged result. All further discussion will assume that the time shift t_0 will be an integer multiple of the basic observation period T .

The signal averaging algorithm for histories averaged with a boxcar or uniform window is:

$$\bar{x}(t) = \frac{1}{N_c} \sum_{i=0}^{N_c-1} x_i(t) \quad (4.27)$$

where:

- N_a Number of asynchronous averages
- N_c Number of cyclic averages

For the case where $x(t)$ is continuous over the time period $N_c T$, the complex Fourier coefficients of the cyclic averaged time history become:

$$C_k = \frac{1}{T} \int_0^T \bar{x}(t) e^{-j\omega_k t} dt \quad (4.28)$$

$$C_k = \frac{1}{T} \int_0^T \frac{1}{N_c} \sum_{i=0}^{N_c-1} x_i(t) e^{-j\omega_k t} dt \quad (4.29)$$

Finally:

$$C_k = \frac{1}{N_c T} \int_0^T \sum_{i=0}^{N_c-1} x_i(t) e^{-j\omega_k t} dt \quad (4.30)$$

Since $x(t)$ is a continuous function, the sum of the integrals can be replaced with an integral evaluated from 0 to $N_c T$ over the original function $x(t)$. Therefore:

$$C_k = \frac{1}{N_c T} \int_0^{N_c T} x(t) e^{-j\omega_k t} dt \quad (4.31)$$

The above equation indicates that the Fourier coefficients of the cyclic averaged history (which are spaced at $\Delta f = \frac{1}{T}$) are the same Fourier coefficients from the original history (which are spaced at $\Delta f = N_c T$). Note that the number of Fourier coefficients for the cyclic averaged history will be $\frac{1}{N_c}$ the number of coefficients of the original history since the number and size of the frequency spacing changes by this factor. Also note that Parseval's Theorem, concerning the energy representation of each Fourier coefficient, is not preserved by the cyclic averaging process since the frequency information not related to the harmonics of $\Delta f = \frac{1}{T}$ is removed [5].

The approach used to understand the frequency domain effects of windows on digital data can be used to understand the effect of cyclic averaging [34-35]. Since cyclic averaging yields the Fourier coefficients of an effectively larger observation time ($N_c T$ compared to T), the effect of cyclic averaging results in an effective frequency domain window characteristic that is a result of this longer observation time. However, the Δf axis needs to be adjusted to account for the actual frequencies that occur in the cyclic averaged spectra.

Figure 4-34 shows the two-sided frequency domain characteristic of the cyclic averaged ($N_c = 4$) case with a uniform window. Likewise, Figure 4-35 shows the two-sided frequency domain characteristic of the cyclic averaged ($N_c = 4$) case with a Hann window. Further detail of these characteristics is given in Figures 4-36 through 4-41. Figures 4-36 through 4-38 show the cyclic averaging effect in the frequency domain for the cases of 1, 2 and 4 averages with a uniform window applied to the data. Figure 4-36 essentially represents no cyclic averaging and is the

familiar characteristic of a uniform window [34-35]. Figures 4-37 and 4-38 show how cyclic averaging effects this window characteristic with respect to the $\Delta f = \frac{1}{T}$ frequency spacing. Figures 4-39 through 4-41 show the cyclic averaging effect in the frequency domain for the cases of 1, 2 and 4 averages with a Hann window applied to the original contiguous data. Figure 4-39 essentially represents no cyclic averaging and is the familiar characteristic of a Hann window [34-35]. Figures 4-40 and 4-41 show how cyclic averaging effects this window characteristic with respect to the $\Delta f = \frac{1}{T}$ frequency spacing.

These figures demonstrate the effectiveness of cyclic averaging in rejecting nonharmonic frequencies. Practically, these figures also demonstrate that, based upon effectiveness or the limitations of the dynamic range of the measured data, a maximum of 16 to 32 averages is recommended. Realistically, 4 to 8 cyclic averages together with a Hann window provides a dramatic improvement in the FRF estimate.

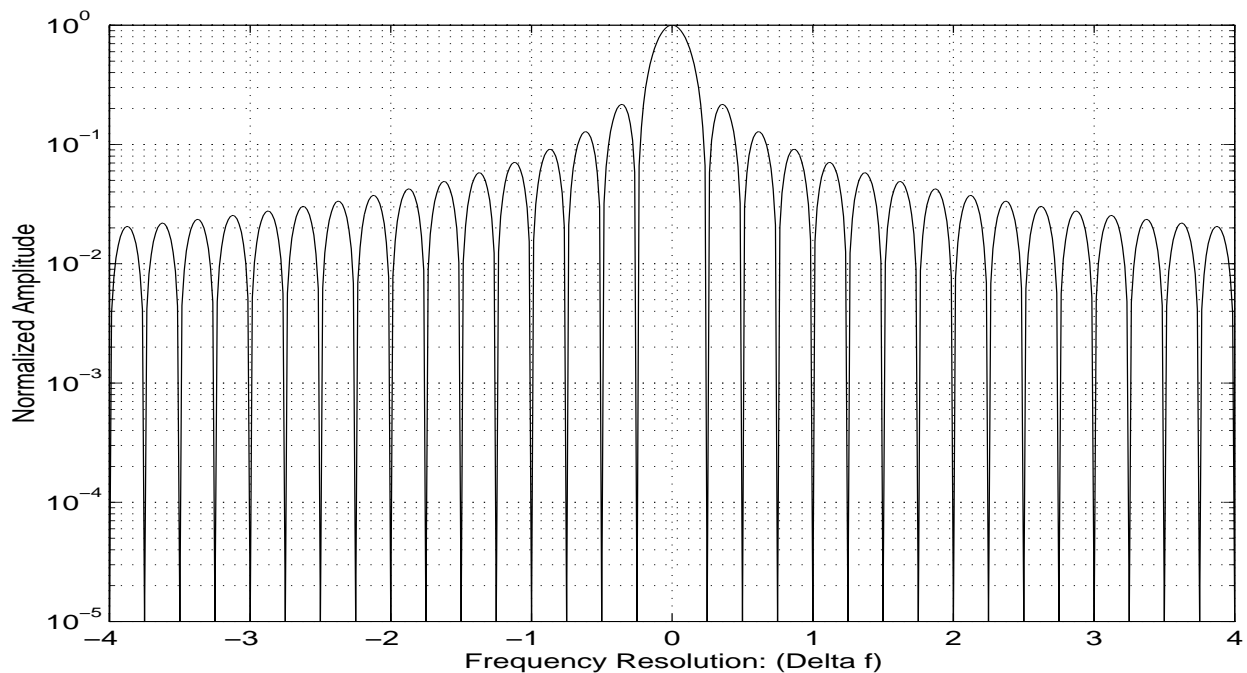


Figure 4-34. Cyclic Averaging ($N_c = 4$) with Uniform Window

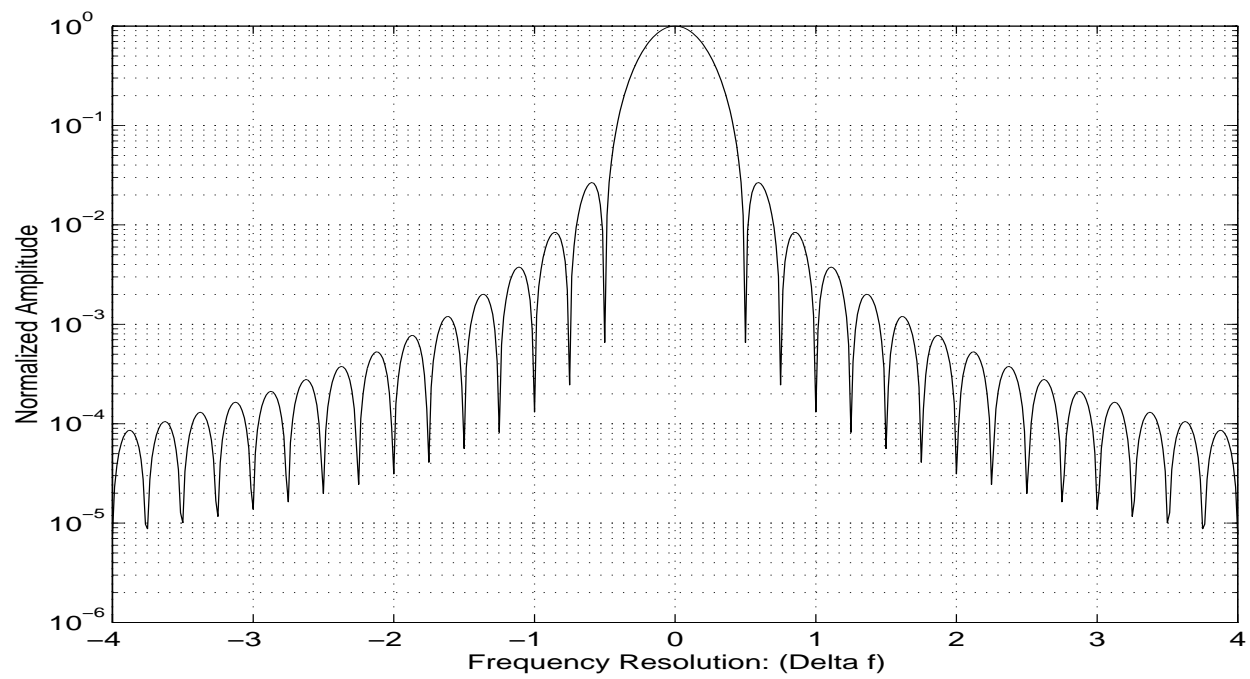


Figure 4-35. Cyclic Averaging ($N_c = 4$) with Hann Window

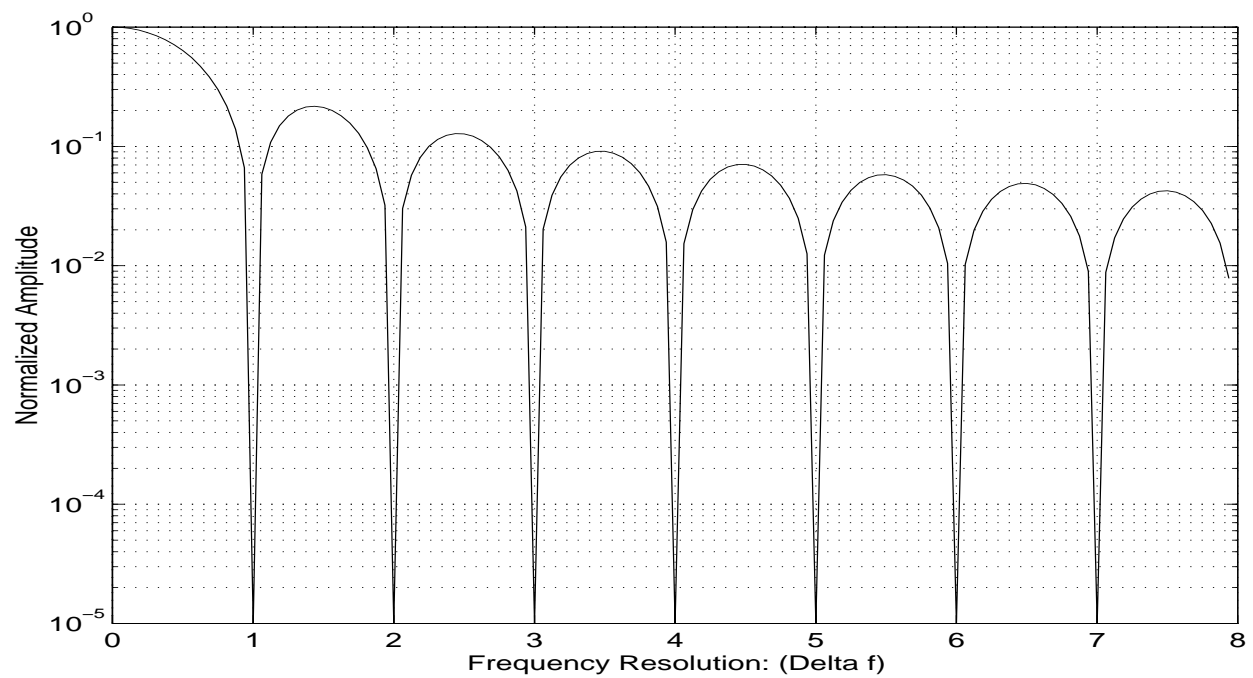


Figure 4-36. Uniform Window Characteristics

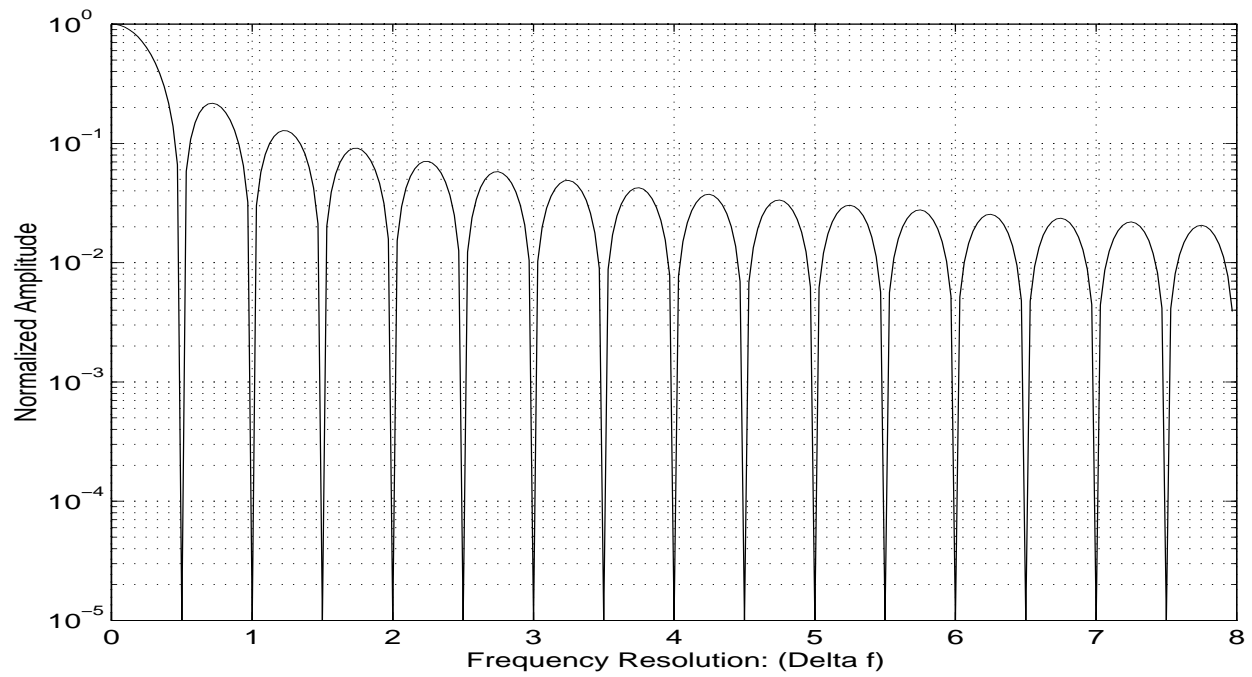


Figure 4-37. Cyclic Averaging ($N_c = 2$) with Uniform Window

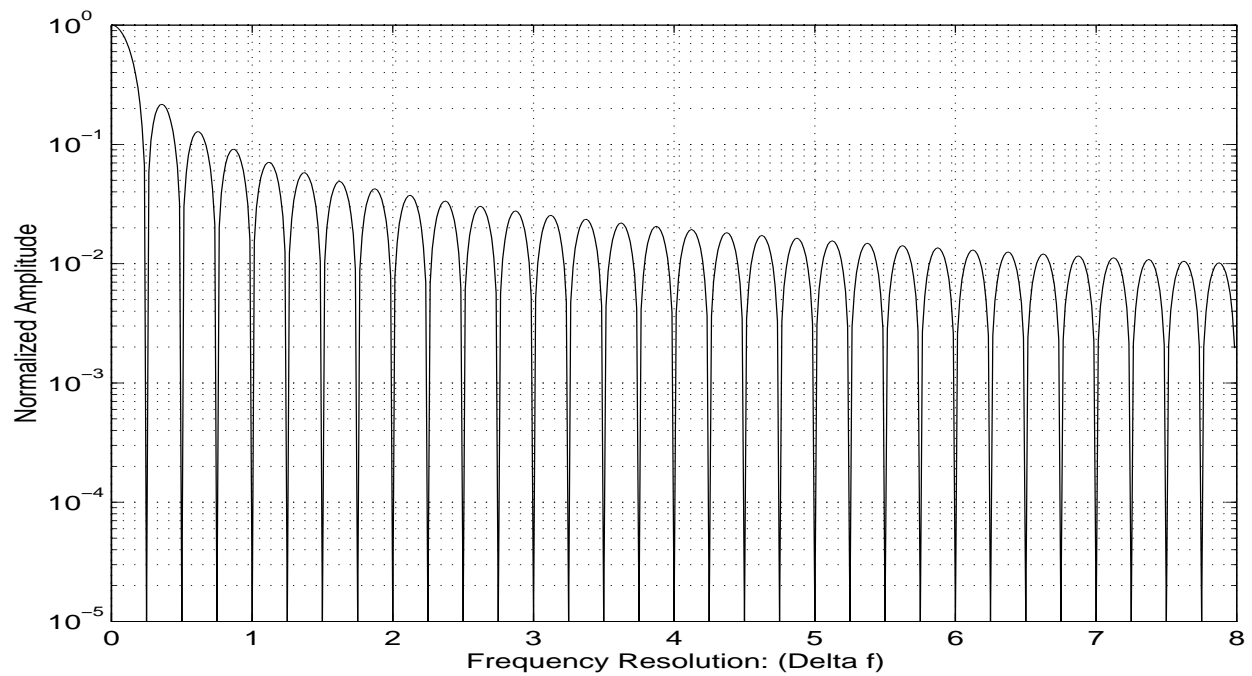
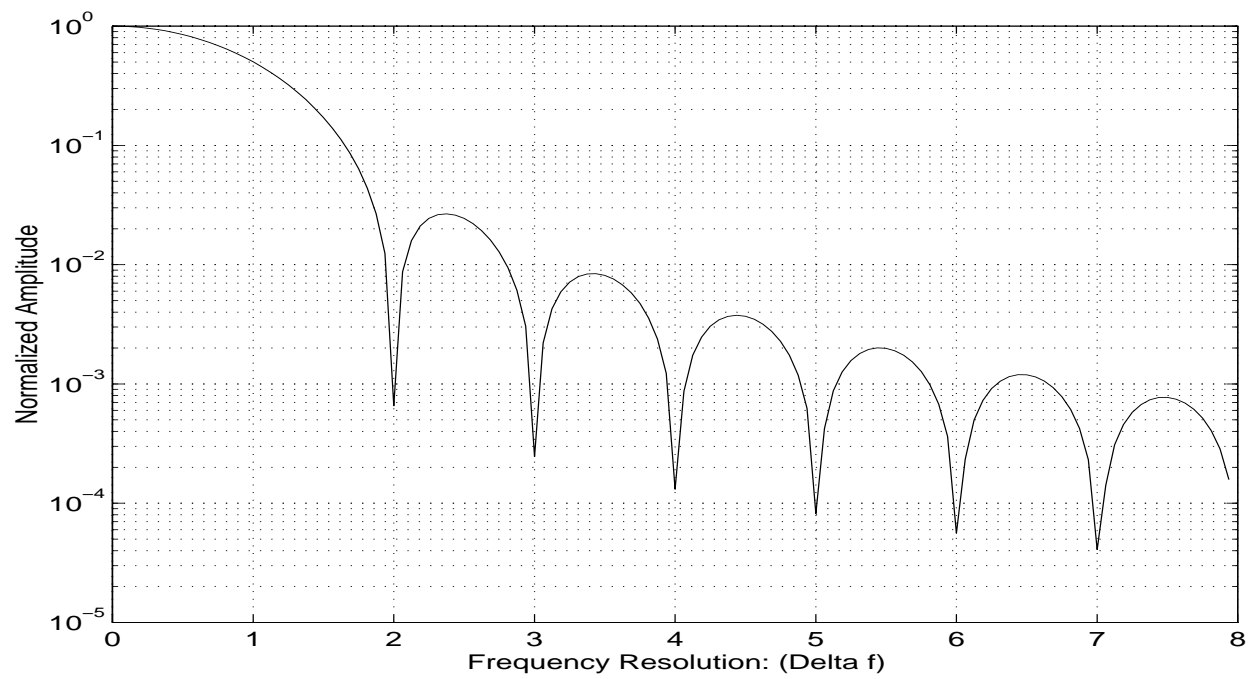
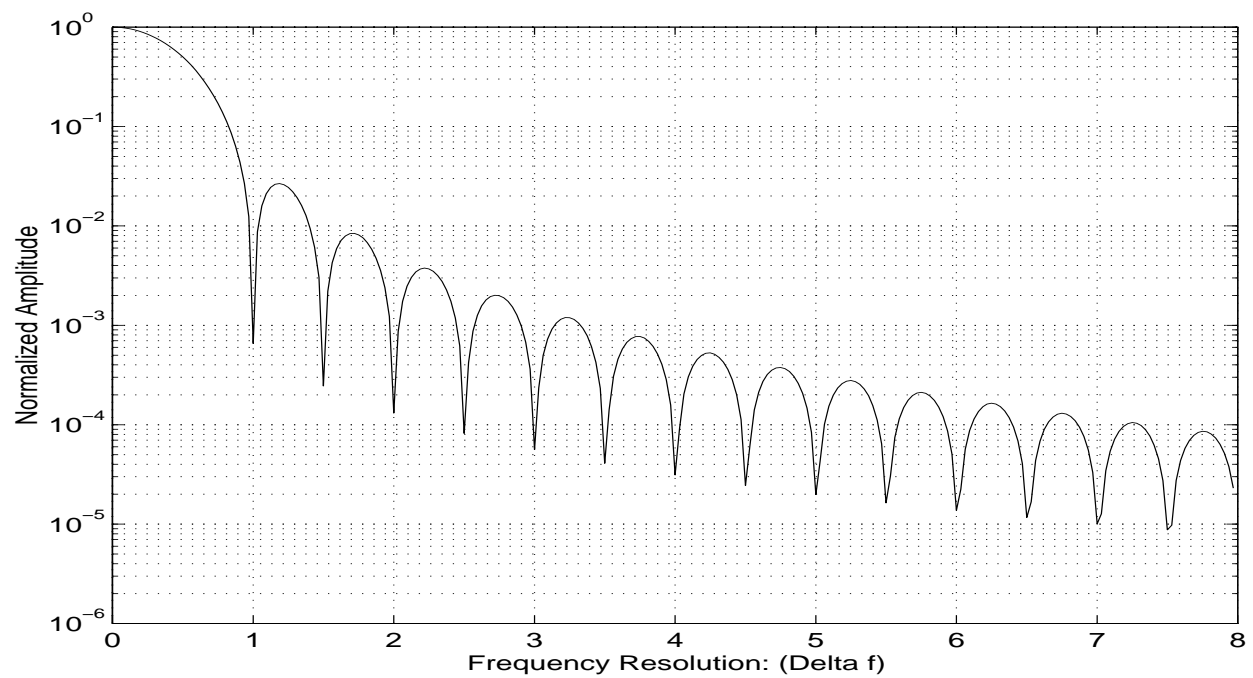


Figure 4-38. Cyclic Averaging ($N_c = 4$) with Uniform Window

**Figure 4-39.** Hann Window Characteristics**Figure 4-40.** Cyclic Averaging ($N_c = 2$) with Hann Window

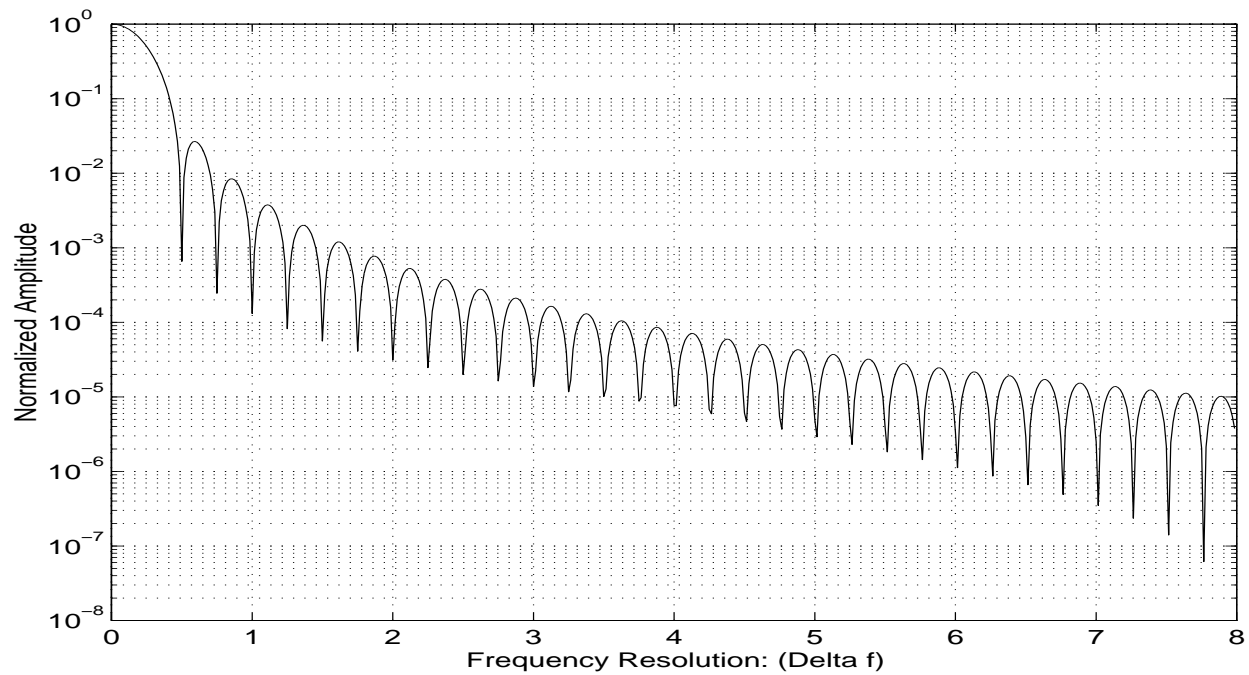


Figure 4-41. Cyclic Averaging ($N_c = 4$) with Hann Window

The results of cyclic averaging of a general random signal with the application of a uniform window are shown in Figures 4-42 and 4-43. Likewise, the results of cyclic averaging of a general random signal with the application of a Hann window are shown in Figures 4-44 and 4-45.

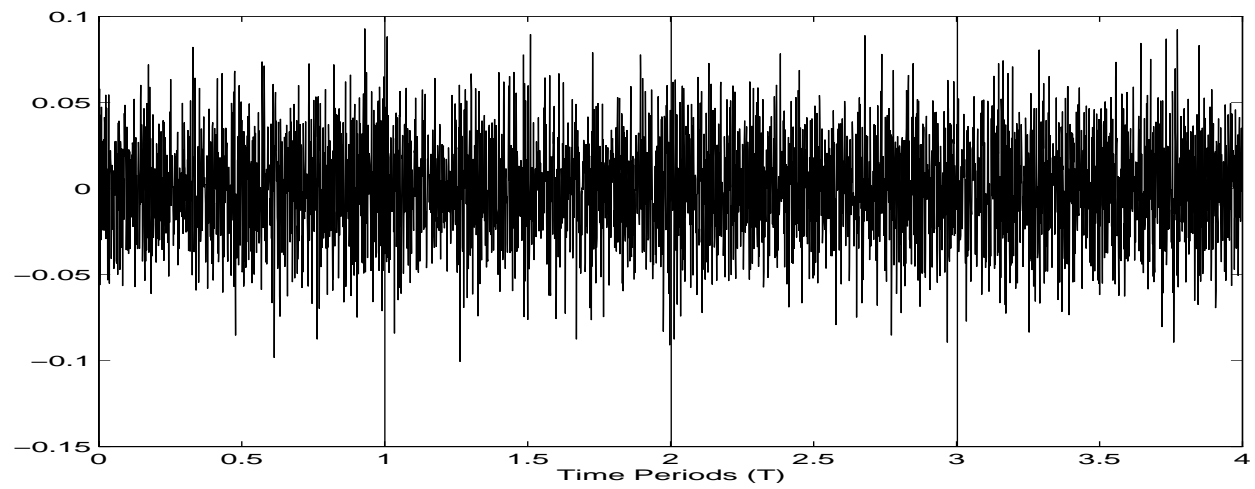


Figure 4-42. Contiguous Time Records

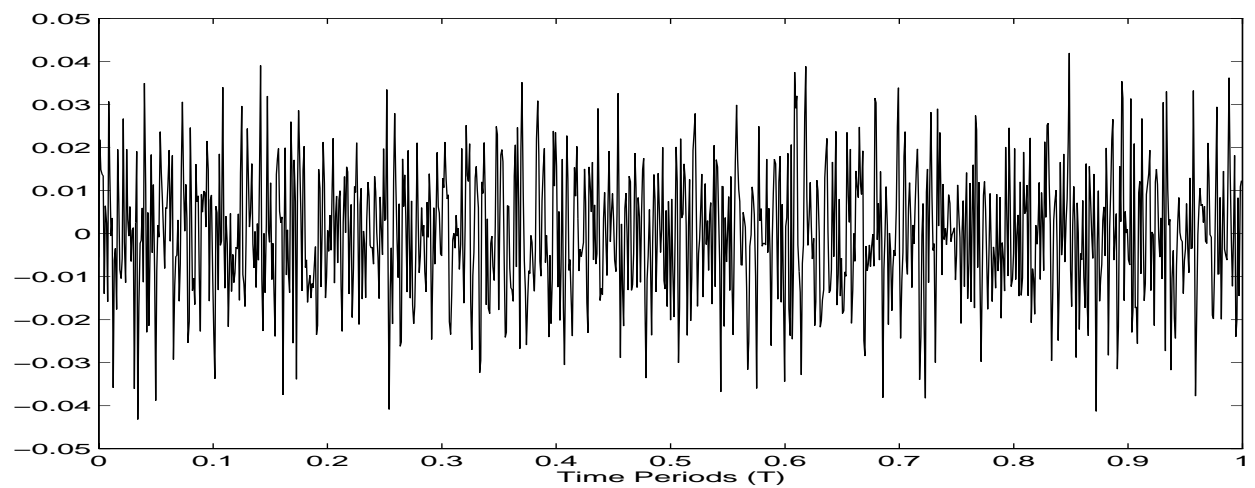


Figure 4-43. Averaged Time Records

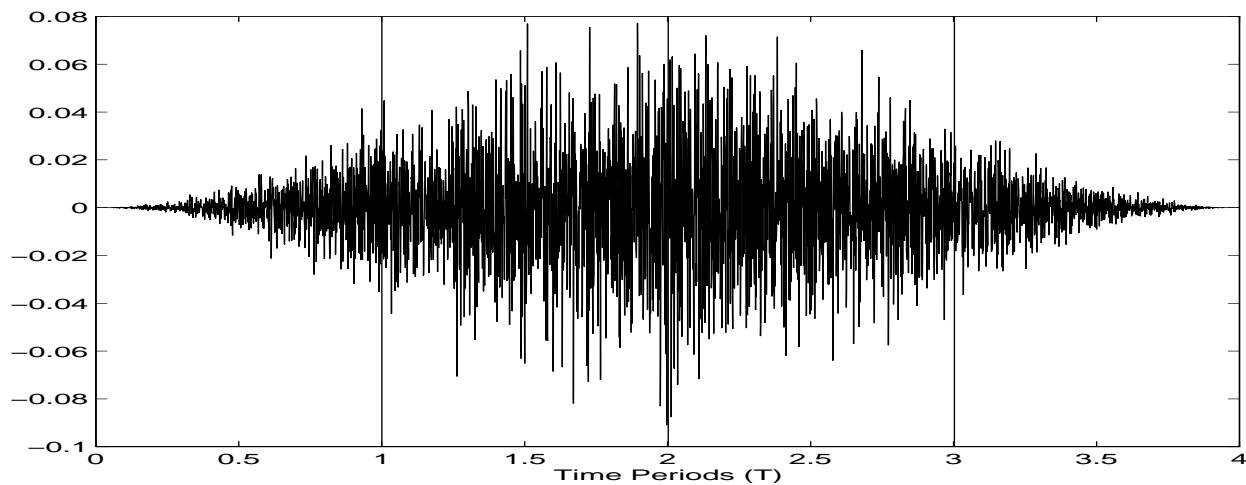


Figure 4-44. Contiguous Time Records with Hann Window

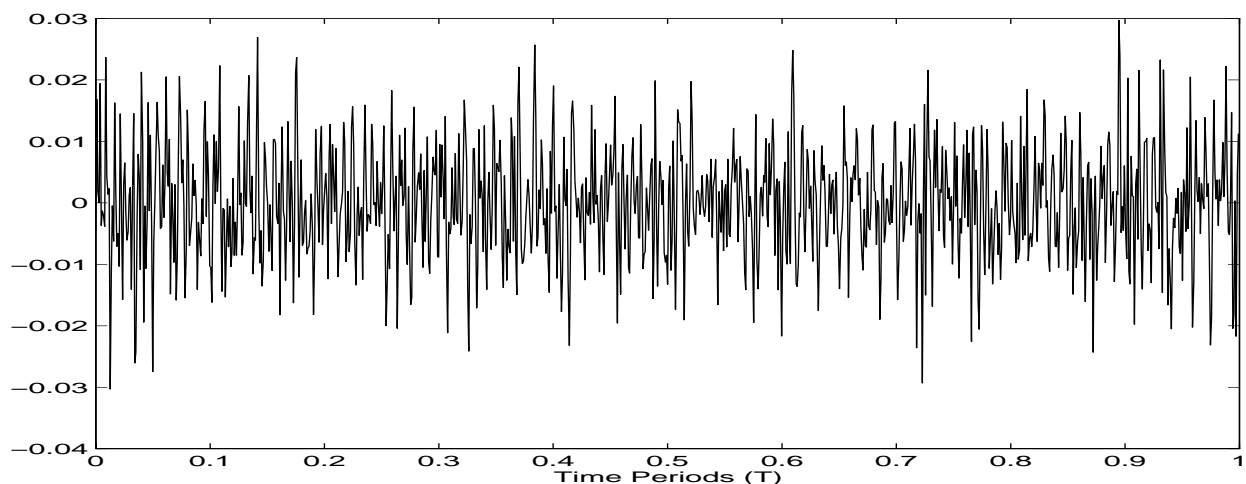


Figure 4-45. Averaged Time Records with Hann Window

4.7.2.3.2 Practical Example

The implementation of cyclic signal averaging to frequency response function (FRF) estimation is not easily applicable to many existing discrete Fourier transform analyzers. The reason for this is that the user is not given control of the time data acquisition such that the cyclic averaging requirements can be met. However, many users currently are acquiring data with personal computer (PC) data acquisition boards or the VXI based data acquisition boards where control of

the time data acquisition is more available to the user. In this environment, cyclic averaging is simple to implement by acquiring long data records and breaking the long data record into N_c contiguous time records which can be cyclic averaged.

The cyclic averaged inputs and outputs are normally computed by simply summing successive time records. The important requirement of the successive time records is that no data is lost. Therefore, these successive time records could be laid end to end to create the original longer time data record ($N_c T$). The cyclic averaged records are then created by simply adding each time record of length T together in a block mode.

While the basic approach to cyclic averaging involves using the data weighted uniformly over the total sample time $N_c T$, the benefits that can be gained by using weighting functions can also be applied. The application of a Hanning window to the successive time records before the summation occurs yields an even greater reduction of the bias error. Therefore, for frequency response function measurements, Hanning weighted signal averaging should drastically reduce the leakage errors which can exist when using broadband random excitation techniques to measure frequency response.

In Figure 4-46 through Figure 4-49, four different measurement cases are documented for the same FRF measurement. This data was acquired as typical data from a lightly damped, cantilever beam. Each figure shows the amplitude of an FRF with the associated ordinary coherence function shown as a measurement quality indicator. In each case, the H_1 FRF estimation algorithm was used; only the windowing and the number of asynchronous (N_a) and the number of cyclic (N_c) averages were changed. The four cases are as follows:

- Case I: The FRF is computed from 64 asynchronous averages ($N_a = 64$). A uniform window (no additional window) is applied to the data. This is an unacceptable measurement and represents poor measurement procedure.
- Case II: The FRF is computed from 64 asynchronous averages ($N_a = 64$). A Hann window is applied to the data. This is a marginally acceptable measurement and represents a common measurement procedure.
- Case III: The FRF is computed from 16 cyclic averages ($N_c = 4$) and 16 asynchronous averages ($N_a = 16$). A uniform window (no additional window) is applied to the data. This is a marginally acceptable measurement and compares reasonably to Case II.

- Case IV: The FRF is computed from 16 cyclic averages ($N_c = 4$) and 16 asynchronous averages ($N_a = 16$). A Hann window is applied to the data. This is a good measurement. Note particularly the increase in the FRF amplitude at the peak frequency locations compared to the three previous cases.

The value of N_c indicates the number of cyclic time records averaged together and N_a is the number of asynchronous auto and cross spectrum averages: a total of $N_c N_a$ time records were sampled. This is done so that, statistically, the same amount of independent information is available in each averaging case. *Note that in this example, the data for these cases was acquired only once. Each case results from processing the original time data differently.*

Clearly, the measurement using cyclic averaging with the Hann window (Figure 4-49) shows a significant reduction of the bias error. An interesting point is that the data near the antiresonance is also drastically improved due to the sharp roll off of the line shape of the Hanning weighted averaging.

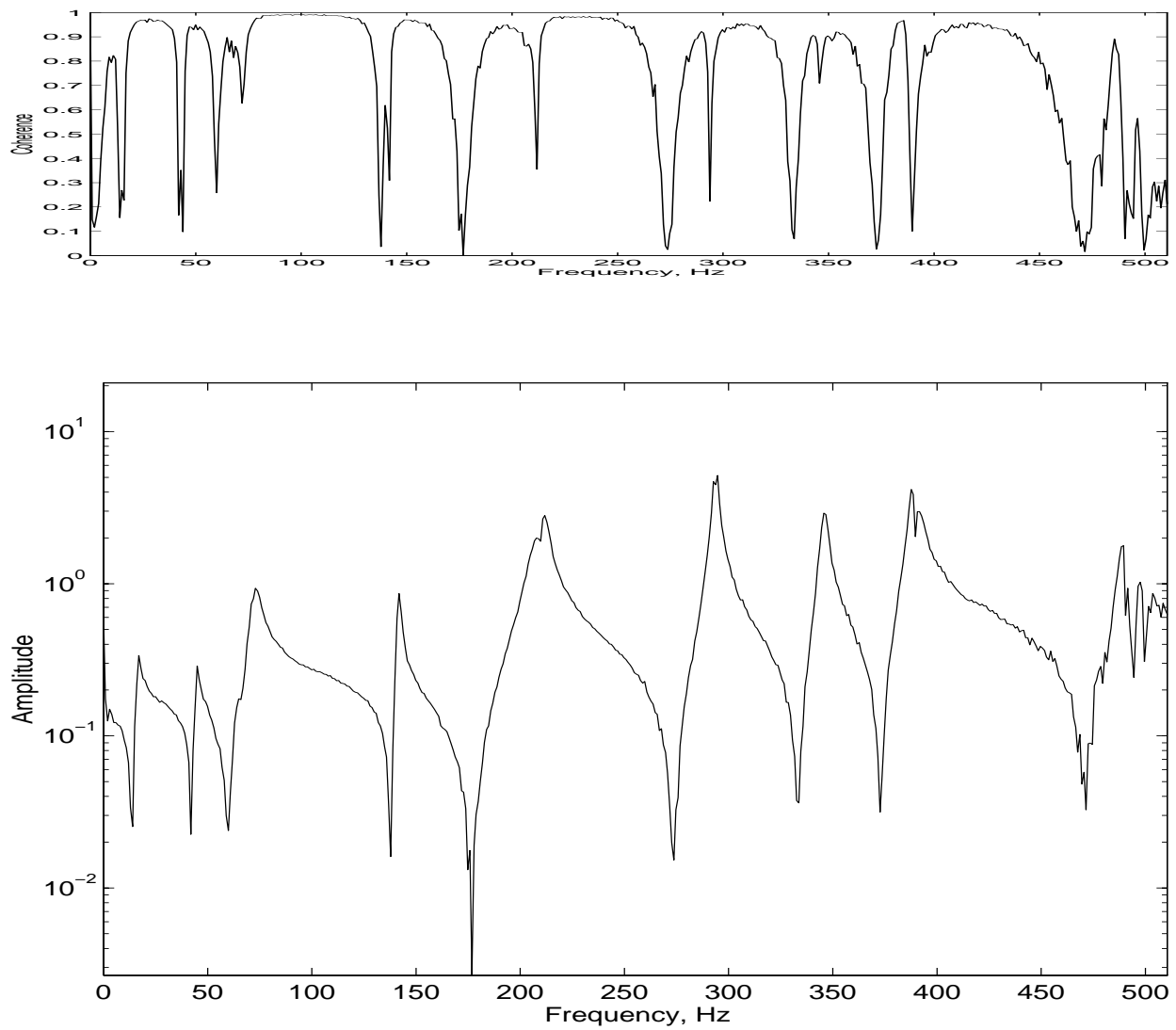


Figure 4-46. Case I: Asynchronous Averaging

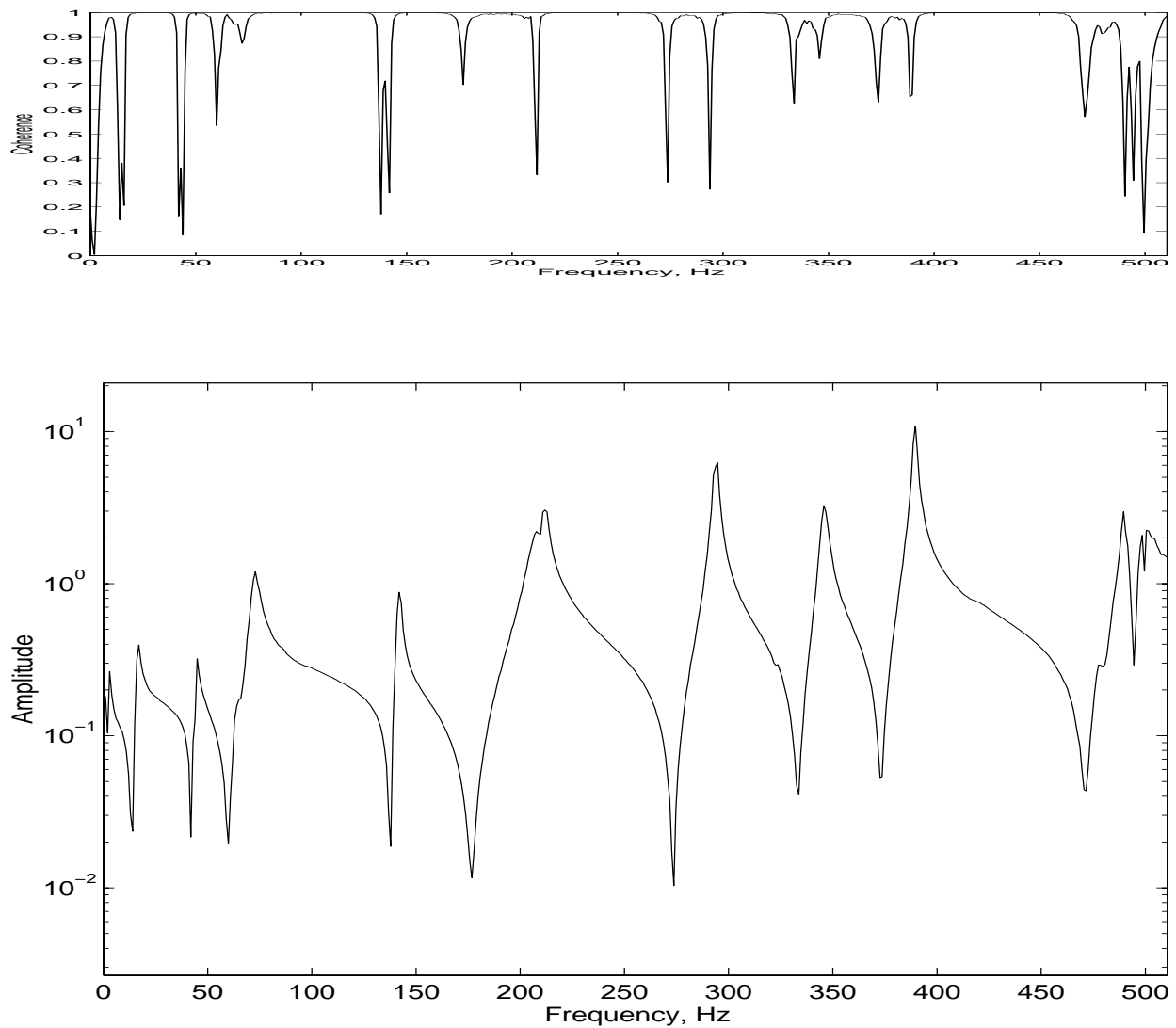


Figure 4-47. Case II: Asynchronous Averaging With Hann Window

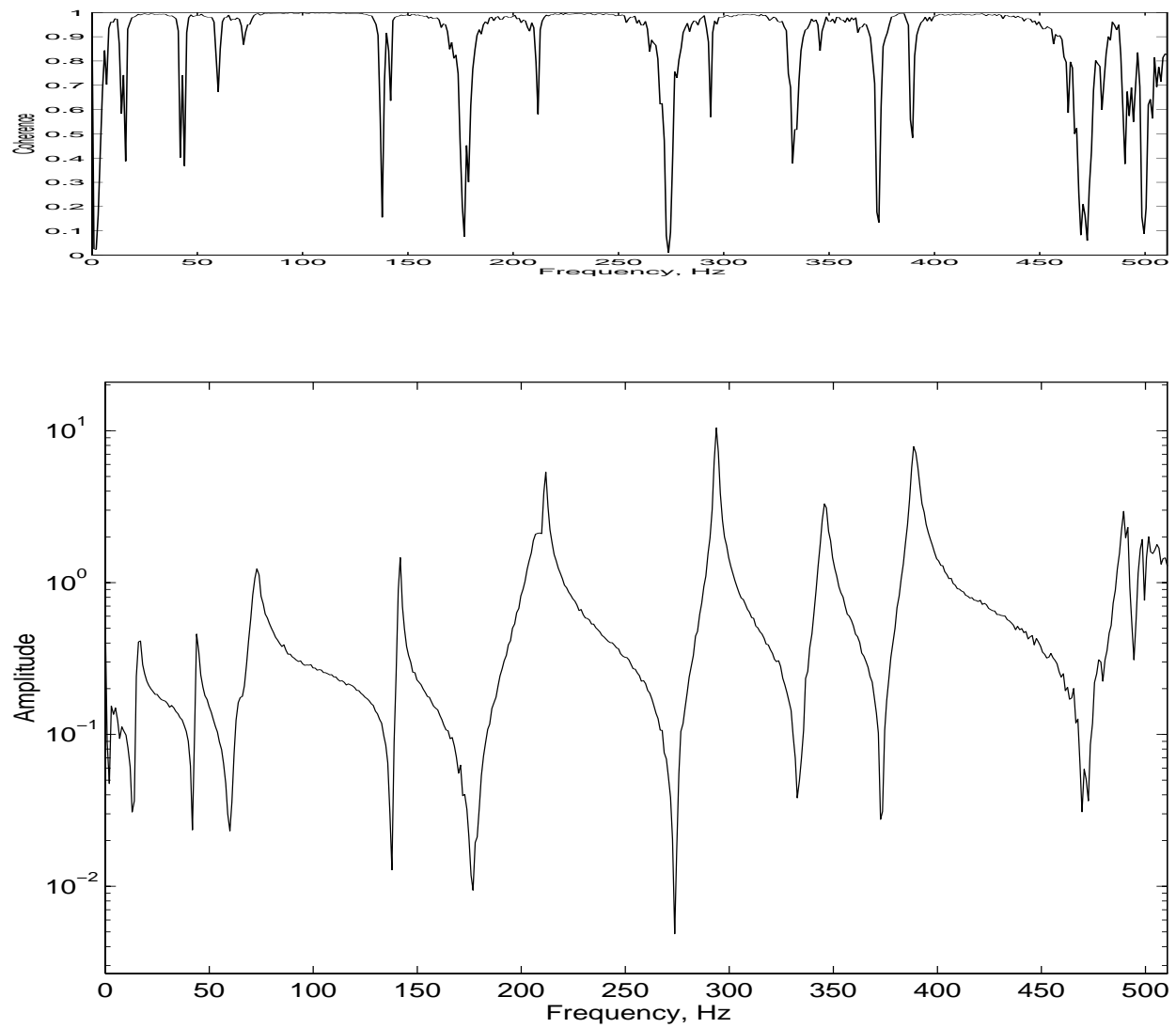


Figure 4-48. Case III: Cyclic Averaging

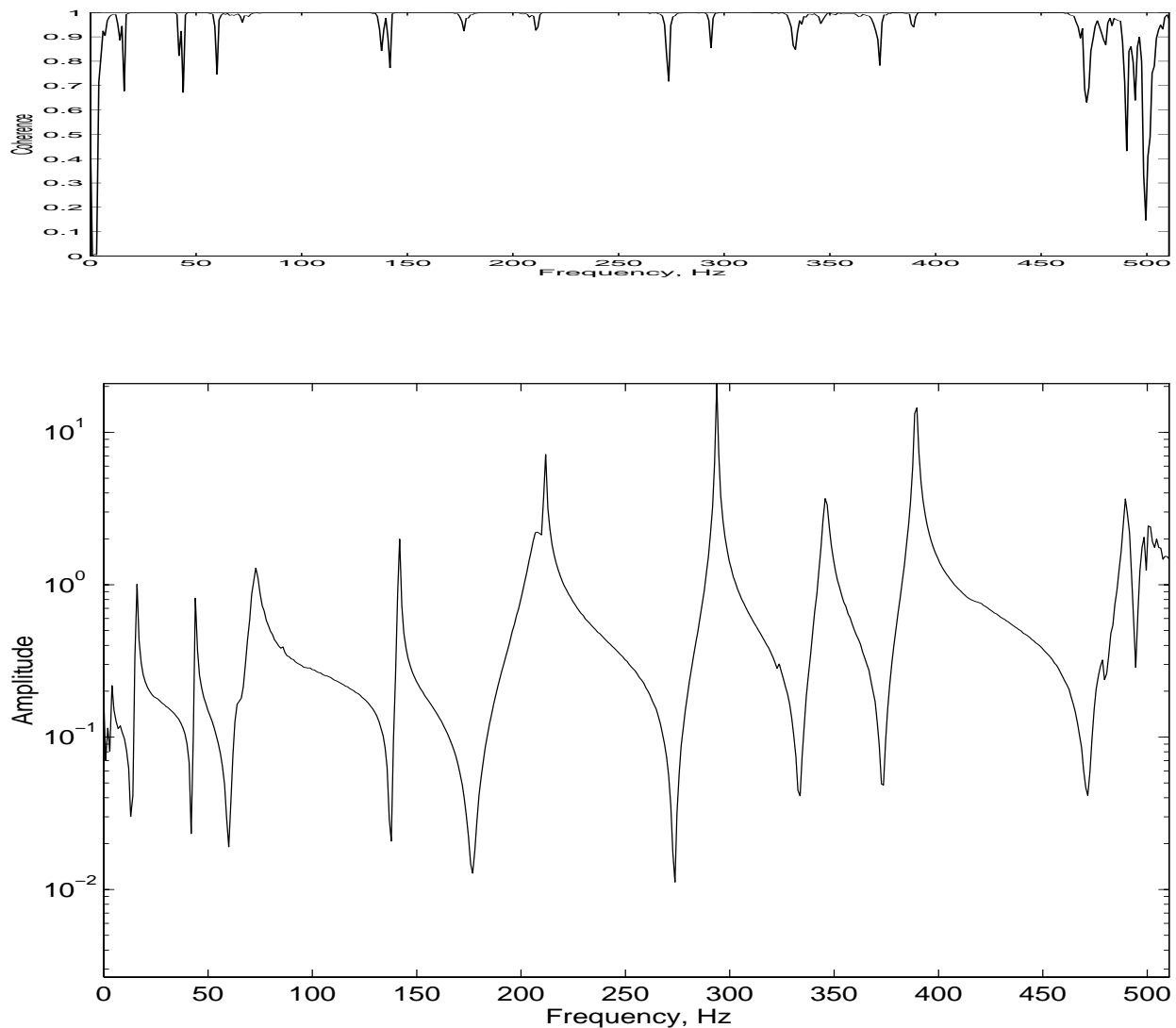


Figure 4-49. Case IV: Cyclic Averaging With Hann Window

Cyclic averaging is a powerful digital signal processing tool that minimizes the leakage error when FRF measurements are being estimated. While existing discrete Fourier analyzers may not be able to include cyclic averaging for the FRF estimation case, computer-based data acquisition common to personal computer or workstation systems generally permit the user to apply cyclic averaging together with asynchronous or synchronous averaging to effectively minimize both random errors and the leakage bias error.

4.7.3 Special Types of Signal Averaging

4.7.3.1 Overlapping Time Records

There are at least two common averaging techniques that use histories which may or may not overlap. In both cases, the averaging techniques involve processing random data histories in order to enhance the data. The first case is that of overlap processing. Overlap processing involves using individual sample histories which are not totally independent from one another. The dependence that occurs results from each successive history starting before the previous history ends. For the general case where the time data is not weighted in any fashion, it should be obvious that this averaging procedure does not involve any new data and, therefore, statistically does not improve the estimation process. In the special case where weighting functions are involved, this technique can utilize data that is otherwise ignored. Figure 4-50 is an example of a data record that has been weighted to reduce the leakage error using a Hanning weighting function. The data prior to twenty percent of each sample period and after eighty percent of each sample period is nearly eliminated by the Hanning window used. Using an overlap factor of at least twenty to thirty percent as in Figure 4-51 involves this data once again in the averaging process.

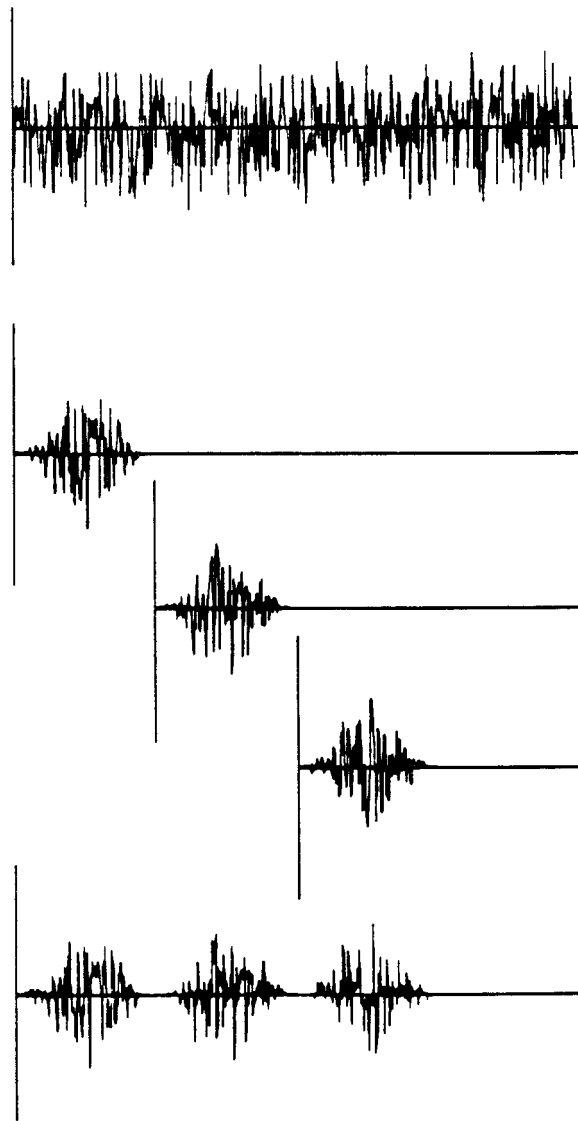


Figure 4-50. Overlap Processing: Zero Overlap

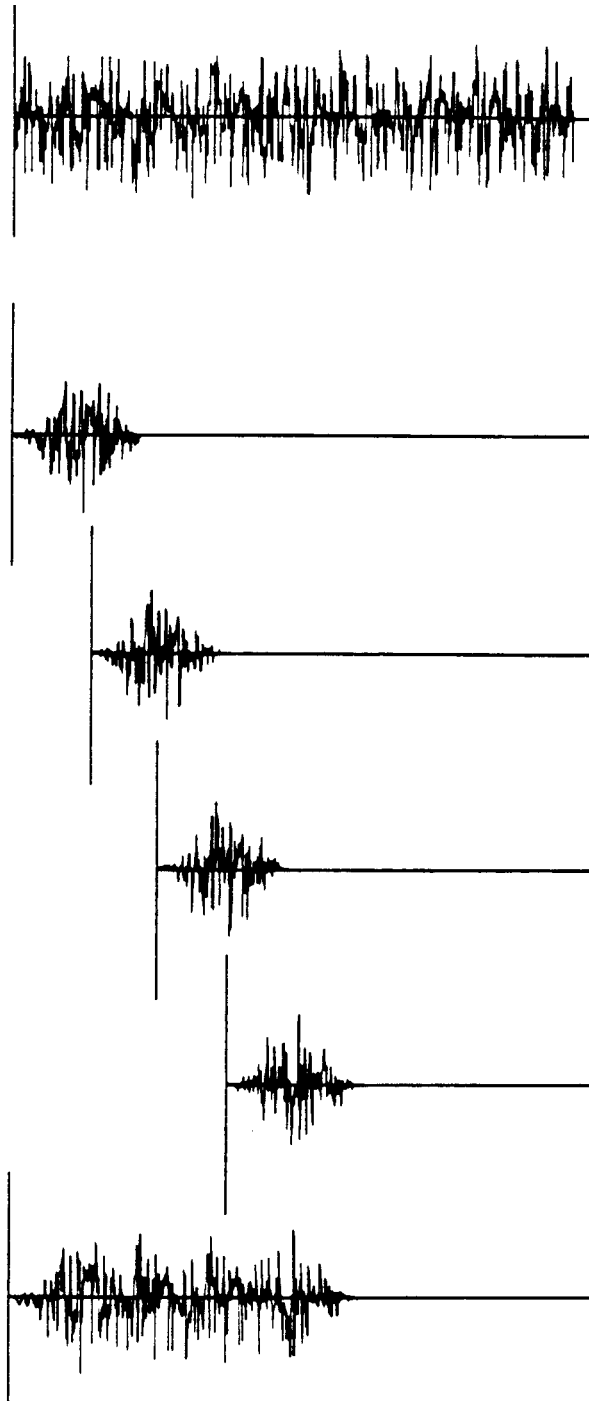


Figure 4-51. Overlap Processing: Fifty Percent Overlap

The second case involving overlapping histories is that of random decrement analysis [27-31] .

This process involves the overlapping of histories in order to enhance the deterministic portion of the random record. In general, the random response data can be considered to be made up of two parts: a deterministic part and a random part. Averaging in the time domain, the random part can be reduced if a trigger signal with respect to the information of interest exists. In the previous discussions, this trigger signal has been a function of the input (asynchronous or synchronous averaging) or of the sampling frequency (cyclic averaging). More generally, though, the trigger function can be any function with characteristics related to the response history. Specifically, then, the random decrement technique utilizes the assumption that the deterministic part of the random response signal itself contains free decay step and impulse response functions and can be used as the trigger function. Therefore, by starting each history at a specific value and slope of the random response function, characteristics related to the deterministic portion of the history will be enhanced.

There are three specific cases of random decrement averaging that represent the limiting results of its use. The first case occurs when each starting value is chosen when the random response history reaches a specific constant level with alternating slopes for each successive starting value. The random decrement history for this case becomes the free decay step response function. An example of this case for the first few averages is shown in Figure 4-52.

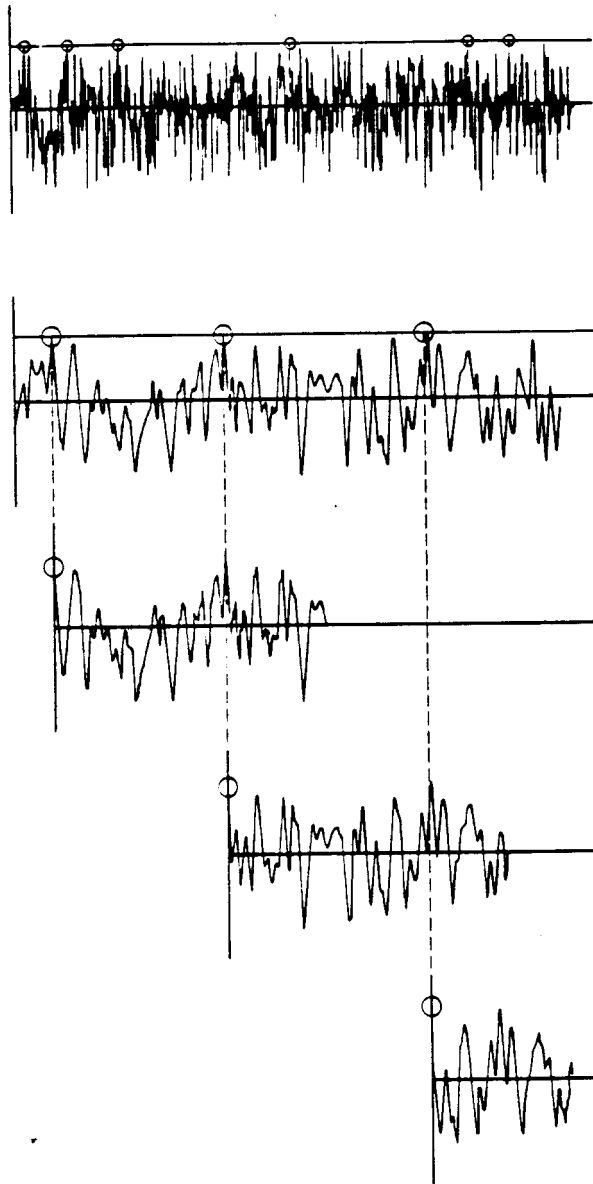


Figure 4-52. Random Decrement Averaging

The second case occurs when each starting value is chosen when the random response history crosses the zero axis with positive slope. The random decrement history for this case becomes the free decay positive impulse response function.

The third case occurs when each starting value is chosen when the random response history

crosses zero with negative slope. The random decrement history for this case becomes the free decay negative impulse response function.

Therefore, in each of these cases, the random decrement technique acts like a notched digital filter with pass bands at the poles of the trigger function. This tends to eliminate spectral components not coherent with the trigger function.

If a secondary function is utilized as the trigger function, only the history related to the poles of the secondary function will be enhanced by this technique. If the trigger function is sinusoidal, the random decrement history will contain information related only to that sinusoid. Likewise, if the trigger function is white noise, the random decrement history will be a unit impulse function at time zero. One useful example of this concept was investigated for conditioning random response histories so that information unrelated to the theoretical input history is removed. In this situation, the theoretical input history serves as the trigger function. The random decrement history formed on the basis of this trigger function represents the random response function that would be formed if the theoretical input history were truly the system input. In reality, the measured input history may vary due to noise, impedance mismatch, etc.

4.8 Transducer Considerations

The transducer considerations are often the most overlooked aspect of the experimental modal analysis process. Considerations involving the actual type and specifications of the transducers, mounting of the transducers, and calibration of the transducers will often be some of the largest sources of error.

Transducer specifications are concerned with the magnitude and frequency limitations that the transducer is designed to meet. This involves the measured calibration at the time that the transducer was manufactured, the frequency range over which this calibration is valid, and the magnitude and phase distortion of the transducer, compared to the calibration constant over the range of interest. The specifications of any transducer signal conditioning must be included in this evaluation.

Transducer mounting involves evaluation of the mounting system to ascertain whether the

mounting system has compromised any of the transducers specifications. This normally involves the possibility of relative motion between the structure under test and the transducer. Very often, the mounting systems which are convenient to use and allow ease of alignment with orthogonal reference axes are subject to mounting resonances which result in substantial relative motion between the transducer and the structure under test in the frequency range of interest. Therefore, the mounting system which should be used depends heavily upon the frequency range of interest and upon the test conditions. Test conditions are factors such as temperature, roving or fixed transducers, and surface irregularity. A brief review of many common transducer mounting methods is shown in Table 4-3.

Transducer Mounting Methods			
Method	Frequency Range (Hertz)	Main Advantages	Main Disadvantages
Hand-held	20-1000	Quick look	Poor measurement quality for long sample periods
Putty	0-200	Good axis alignment, ease of mounting	Low frequency range, creep problems during measurement
Wax	0-2000	Ease of application	Temperature limitations, frequency range limited by wax thickness, axis alignment limitations
Hot glue	0-2000	Quick setting time, good axis alignment	Temperature sensitive transducers (during cure)
Magnet	0-2000	Quick setup	Requires magnetic material, axis alignment limitations, bounce problem with impact excitation, surface preparation
Adhesive film	0-2000	Quick Setup	Axis alignment limitations, requires flat surface
Epoxy cement	0-5000	Mount on irregular surface, good axis alignment	Long curing time
Dental cement	0-5000	Mount on irregular surface, good axis alignment	Medium curing time, brittle
Stud mount	0-10,000	Accurate alignment if carefully machined	Difficult setup, requires drill and tap

Note: Applicable frequency ranges are approximate - actual frequency ranges depend on transducer mass and contact conditions.

TABLE 4-3. Transducer Mounting Methods

Transducer calibration refers to the actual engineering unit per volt output of the transducer and

signal conditioning system. Calibration of the complete measurement system is needed to verify that the performance of the transducer and signal conditioning system is proper. Obviously, if the measured calibration differs widely from the manufacturers specifications, the use of that particular transducer and signal conditioning path should be questioned. Also, certain applications, such as impact testing, involve slight changes in the transducer system (such as adding mass to the tip of an instrumented hammer) that affect the associated calibration of the transducer.

Ideally, on-site calibration should be performed both before and after every test to verify that the transducer and signal conditioning system is operating as expected. The calibration can be performed using the same signal processing and data analysis equipment that will be used in the data acquisition. There are a number of calibration methods which can be used to calibrate the transducer and signal conditioning. Some of these methods yield a calibration curve, with magnitude and phase, as a function of frequency while other methods simply estimate a calibration constant. Most of the current calibration methods are reviewed in Figure 4-53. Note that some of the methods are more suited for field calibration while other methods are more suited for permanent installations in calibration laboratories.


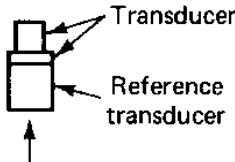
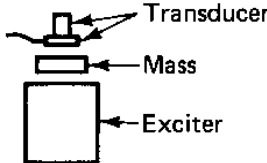
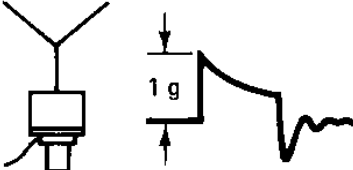
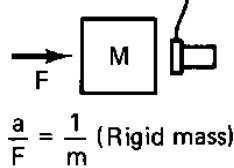
Method	Calibration methods			Remarks
Inversion test		Constant		Can only be used with transducer that has stable dc output; calibration against local earth's gravity
Comparison method		Frequency response		Calibration against reference transducer
Reciprocity method		Constant and/or frequency response		Calibration against mass-loaded shaker
Drop method		Constant		Calibration against local earth and gravity; used for ac-coupled transducers
Ratio method		Frequency-response ratio		Calibration against known a/F for a rigid mass

Figure 4-53. Calibration Methods

In many cases, somewhat obvious but important errors are made with respect to calibration. Generally, the calibration information must be entered into the data acquisition equipment so that the data can be scaled accordingly. It is very important to check the units requested by data acquisition equipment (engineering units per volt versus volts per engineering unit). An example of this common error is shown in Figure 4-54 for the case of six different teams testing the same circular plate structure. Figure 4-54 shows the six frequency response functions (magnitude

only) for this situation.

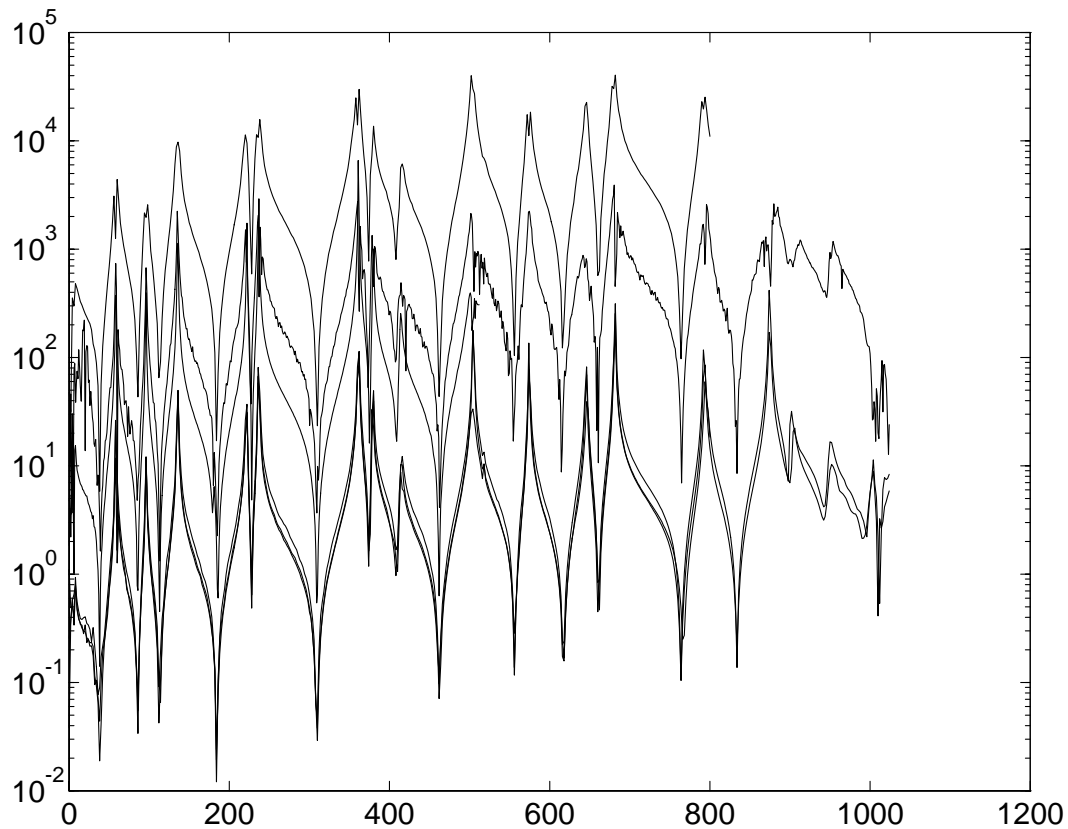


Figure 4-54. FRF Magnitude: Calibration Errors

Once the assorted calibration errors were identified and corrected, Figure 4-55 shows the result. Note that there is still some small differences between each measurement due to different testing methods, numbers of averages, types of excitation signal and other errors. These results are very similar to the results from a test structure that was sent to several testing laboratories in order to compare and contrast results [32].

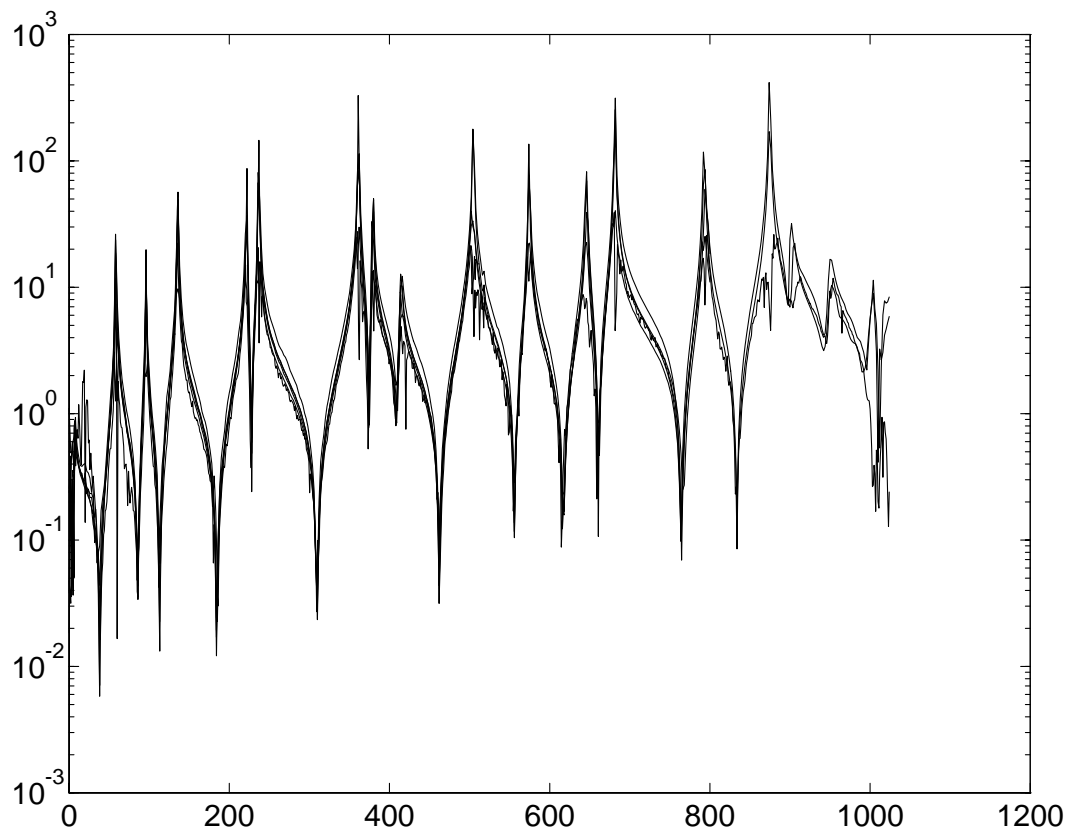


Figure 4-55. FRF Magnitude: Calibration Errors Corrected

4.9 References

- [1] Bendat, J.S.; Piersol, A.G., **Random Data: Analysis and Measurement Procedures**, John Wiley and Sons, Inc., New York, 1971, 407 pp.
- [2] Bendat, J. S., Piersol, A. G., **Engineering Applications of Correlation and Spectral Analysis**, John Wiley and Sons, Inc., New York, 1980, 302 pp.
- [3] Otnes, R.K., Enochson, L., **Digital Time Series Analysis**, John Wiley and Sons, Inc., New York, 1972, 467 pp.
- [4] Oppenheim, Alan V., Schaffer, Ronald W., "Digital Signal Processing", Prentice-Hall, 1975.
- [5] Hsu, H.P., **Fourier Analysis**, Simon and Schuster, 1970, 274 pp.

- [6] Bracewell, Ronald N., "The Fourier Transform and its Applications", Mc-Graw Hill, Second Edition, 1978.
- [7] Brigham, E. Oran, "The Fast Fourier Transform" Prentice-Hall, 1974.
- [8] Cooley, J.W., Tukey, J.W., "An Algorithm for the Machine Calculation of Complex Fourier Series", Mathematics of Computation, Vol. 19, No. 90, pp. 297, April 1965.
- [9] Gentleman, W.M., Sande, G., "Fast Fourier Transforms-for Fun and Profit", Proceedings, 1966 Fall Joint Computer Conference, AFIPS Conference Proceedings, Vol. 29, pp. 563-578, Spartan Books, Washington, D.C., 1966.
- [10] Kaneko, T., Liu, B., "Accumulation of Roundoff Error in Fast Fourier Transforms", Journal Assoc. Comput. Mach., Vol. 17, No. 4, pp. 637-654, October, 1970.
- [11] Weinstein, C.J., "Roundoff Noise in Floating Point Fast Fourier Transform Computation", IEEE Transactions, Audio Electroacoustics, Vol. AU-17, pp. 209-215, September, 1969.
- [12] IEEE Digital Signal Processing Committee, "Programs for Digital Signal Processing", IEEE Press, John Wiley and Sons, Inc. 1979, 300 pp.
- [13] Dally, J.W.; Riley, W.F.; McConnell, K.G., **Instrumentation for Engineering Measurements**, John Wiley & Sons, Inc., New York, 1984.
- [14] "The Fundamentals of Signal Analysis", Application Note 243, The Hewlett Packard Company, 1985, 57 pp., (Revised) 1994, 66 pp.
- [15] "Specifying A/D and D/A Converters", Application Note AN-156, National Semiconductor Corporation, 1976, 6 pp.
- [16] Sauerwald, M., "Effects of Aperture Time and Jitter in a Sampled Data System", Application Note AD-03, National Semiconductor Corporation, 1994, 4 pp.
- [17] "Effective Machinery Measurements Using Dynamic Signal Analyzers", Application Note 243-1, The Hewlett Packard Company, 1994, 85 pp.
- [18] Jarman, D., "A Brief Introduction to Sigma Delta Conversion", Application Note AN9504, Harris Semiconductor, 1995, 8 pp.
- [19] Melkonian, L.G., "Dynamic Specifications for Sampling A/D Converters", Application Note AN-769, National Semiconductor Corporation, 1991, 8 pp.
- [20] Tweed, D., "Digital Processing in an Analog World - Basic Issues (Part 1 of 3)", **Circuit Cellar INK**, Issue 99 (October), 1998, pp. 68-75.
- [21] Tweed, D., "Digital Processing in an Analog World - Technology Choices (Part 2 of 3)", **Circuit Cellar INK**, Issue 100 (November), 1998, pp. 64-71.
- [22] Tweed, D., "Digital Processing in an Analog World - Dithering Your Conversion (Part 3 of 3)", **Circuit Cellar INK**, Issue 101 (December), 1998, pp. 68-73.
- [23] Kester, W., Bryant, J. Buxton, J., "High Resolution Signal Conditioning ADCs", **Systems Application Guide**, Section 3, Analog Devices, Inc, 1993, 40 pp.
- [24] Kester, W., "Undersampling Applications", **Systems Application Guide**, Section 5, Analog Devices, Inc, 1993, 20 pp.
- [25] Potter, R.W., "Compilation of Time Windows and Line Shapes for Fourier Analysis", Hewlett-Packard Company, 1972, 26 pp.
- [26] Durrani, T.S.; Nightingale, J.M., "Data Windows for Digital Spectral Analysis", Institution of Electrical Engineers Proceedings, Volume 119, 1972, pp. 343-352.

- [27] "Using Cyclic Averaging with Impact Testing", William A. Fladung, Andrew T. Zucker, Allyn W. Phillips, Randall J. Allemang Proceedings, International Modal Analysis Conference, 7 pp., 1999.
- [28] "Frequency Resolution Effects on FRF Estimation: Cyclic Averaging vs. Large Block Size", Allyn W. Phillips, Andrew T. Zucker, Randall J. Allemang Proceedings, International Modal Analysis Conference, 4 pp., 1999.
- [29] "An Overview of MIMO-FRF Excitation/Averaging Techniques", Phillips, A.W., Allemang, R.J., Zucker, A.T., Proceedings, International Conference on Noise and Vibration Engineering, Volume 1, Katholieke Universiteit Leuven, Belgium, 12 pp., 1998.
- [30] "A new Excitation Method: Combining Burst Random Excitation with Cyclic Averaging", Phillips, A.W., Allemang, R.J., Proceedings, International Modal Analysis Conference, 10 pp., 1998.
- [31] "Cyclic Averaging for Frequency Response Function Estimation", Allemang, R.J., Phillips, A.W., Proceedings, International Modal Analysis Conference, pp. 415-422, 1996.
- [32] "Investigation of Some Multiple Input/Output Frequency Response Function Experimental Modal Analysis Techniques", R.J. Allemang, Doctor of Philosophy Dissertation, University of Cincinnati, Mechanical Engineering Department, 1980, 358 pp.
- [33] Cole, H.A., Jr., "On-the-Line Analysis of Random Vibrations", AIAA Paper Number 68-288, April, 1968.
- [34] Cole, H.A., Jr., "Failure Detection of a Space Shuttle Wing Flutter Model by Random Decrement", NASA TM X-62, 041, May, 1971.
- [35] Cole, H.A., Jr., "On-Line Failure Detection and Damping Measurement of Aerospace Structures by Random Decrement Signatures", NASA CR-2205, March, 1973.
- [36] Hammond, C.E., Doggett, R.V., Jr., "Determination of Subcritical Damping by Moving-Block/ Randomdec Applications", Flutter Testing Techniques, NASA-SP-415, October, 1975, pp. 59-76.
- [37] Reed, R.E., "Analytical Aspects of Randomdec Analysis", AIAA Paper Number 79-0828, 1979, pp. 404-409.
- [38] Ewins, D.J., Griffin, J., "A State-of-the-Art Assessment of Mobility Measurement Techniques - Results for the Mid-Range Structures", Journal of Sound and Vibration, Volume 78, Number 2, 1981, pp. 197-222.
- [39] "The Fundamentals of Modal Testing", Application Note 243-1, The Hewlett Packard Company, 1994, 85 pp.

5. FREQUENCY RESPONSE FUNCTION MEASUREMENTS

5.1 Introduction

For current approaches to experimental modal analysis, the frequency response function is the most important measurement to be made. When estimating frequency response functions, a measurement model is needed that will allow the frequency response function to be estimated from measured input and output data in the presence of noise (errors). Some of the errors are:

- Digital Signal Processing Errors (Leakage, Aliasing)
- Noise
 - Equipment problem (Power supply noise)
 - Cabling problems (RFI,EMI)
 - Rattles, cable motion
- Calibration (operator error)
 - Complete system calibration
 - Transducer calibration

Since the frequency response function can be expressed in terms of system properties of mass, stiffness, and damping, it is reasonable to conclude that in most realistic structures, the frequency response functions are considered to be constants just like mass, stiffness, and damping. This concept means that when formulating the frequency response function using H_1 , H_2 , or H_v algorithms, the estimate of frequency response is intrinsically unique, as long as the system is linear and the noise can be minimized or eliminated. The estimate of frequency response is valid whether the input is stationary, non-stationary, or deterministic. Therefore, several important points to remember before estimating frequency response functions are:

- The system (with the boundary conditions for that test) determines the frequency response functions for the given input/output locations.
- It is important to eliminate or at least minimize all errors (aliasing, leakage, noise, calibration, etc.) when collecting data.

- If all noise terms are identically zero, the assumption concerning the source/location of the noise does not matter ($H_1 = H_2 = H_v = H_s = H$). Therefore, concentrate on eliminating the source of the noise.
- Since modal parameters are computed from estimated frequency response functions, the modal parameters are only as accurate as the estimated frequency response functions.

There are at least four different testing configurations that can be compared. These different testing conditions are largely a function of the number of acquisition channels or excitation sources that are available to the test engineer. In general, the best testing situation is the multiple input/multiple output configuration (MIMO) since the data is collected in the shortest possible time with the fewest changes in the test conditions.

- Single input/single output. (SISO)
 - Only option if 2 channel data acquisition system.
 - Longest testing time. Roving inputs. Roving outputs.
 - Time invariance problems between measurements.
- Single input/multiple output. (SIMO)
 - Multiple channel system (3 or more). (One ADC channel for each response signal to be measured plus one ADC channel for an input signal.)
 - Shorter testing time than SISO. Transducers not necessarily moved.
 - Consistent frequency and damping for data acquired simultaneously.
 - Time invariance problems between measurements from different inputs.
- Multiple input/single output. (MISO)
 - Multiple channel system required (3 or more.). (One ADC channel for each input signal to be measured plus one ADC channel for a response signal.)
 - Long testing time. Roving response transducer.
 - More than one input location per measurement cycle.
 - Detects repeated roots. Maxwell reciprocity checks are possible.

- Time invariance problems between measurements from different responses.
- Multiple input/multiple output. (MIMO)
 - Multiple channel system (up to 512 channels). Increased set-up time. Large amount of data to be stored and organized.
 - Shortest testing time.
 - Consistent frequency and damping for all data acquired simultaneously.
 - Detects repeated roots. Maxwell reciprocity checks are possible.
 - Best overall testing scheme.

5.2 Frequency Response Function Estimation

Frequency response functions are normally used to describe the input-output (force-response) relationships of any system. Most often, the system is assumed to be linear and time invariant although this is not necessary. In the cases where assumptions of linearity and time invariance are not valid, the measurement of frequency response functions are also dependent upon the independent variables of time and input. In this way, a conditional frequency response function is measured as a function of other independent variables in addition to frequency. Note that the different possible formulations listed in Table 5-1 can all be considered frequency response functions since each of these formulations can be numerically manipulated (synthetic differentiation, integration, etc.) into the equivalent displacement over force relationship. This assumes that initial conditions can be ignored.

Receptance	$\frac{Acceleration}{Force}$
Effective Mass	$\frac{Force}{Acceleration}$
Mobility	$\frac{Velocity}{Force}$
Impedance	$\frac{Force}{Velocity}$
Dynamic Compliance	$\frac{Displacement}{Force}$
Dynamic Stiffness	$\frac{Force}{Displacement}$

TABLE 5-1. Frequency Response Function Formulations

The estimation of the frequency response function depends upon the transformation of data from the time to frequency domain. The Fourier transform is used for this computation. Unfortunately, though, the integral Fourier transform definition requires time histories from negative infinity to positive infinity. Since this is not possible experimentally, the computation is performed digitally using a ***fast Fourier transform (FFT)*** algorithm which is based upon only a limited time history. In this way the theoretical advantages of the Fourier transform can be implemented in a digital computation scheme. The frequency response function(s) satisfy the following single and multiple input relationships:

Single Input Relationship

$$X_p = H_{pq} F_q \quad (5.1)$$

Multiple Input Relationship

$$\begin{bmatrix} X_1 \\ X_2 \\ \vdots \\ X_p \end{bmatrix}_{N_o \times 1} = \begin{bmatrix} H_{11} & \cdot & \cdot & \cdot & \cdot & \cdot & \cdot & \cdot & H_{1q} \\ H_{21} & & & & & & & & \cdot \\ \cdot & & & & & & & & \cdot \\ \cdot & & & & & & & & \cdot \\ H_{p1} & \cdot & \cdot & \cdot & \cdot & \cdot & \cdot & \cdot & H_{pq} \end{bmatrix}_{N_o \times N_i} \begin{bmatrix} F_1 \\ F_2 \\ \cdot \\ \cdot \\ F_q \end{bmatrix}_{N_i \times 1} \quad (5.2)$$

An example of a two input, two output case for Equation (5.2) is shown in Equation (5.3) and Figure 5-1.

$$\begin{bmatrix} X_1 \\ X_2 \end{bmatrix} = \begin{bmatrix} H_{11} & H_{12} \\ H_{21} & H_{22} \end{bmatrix} \begin{bmatrix} F_1 \\ F_2 \end{bmatrix} \quad (5.3)$$

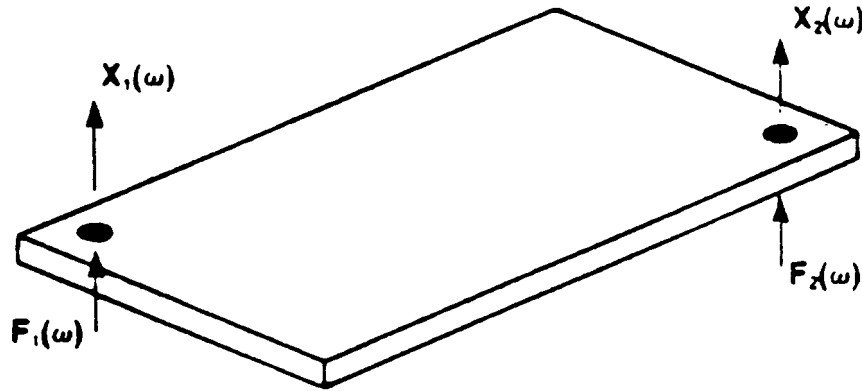


Figure 5-1. Two Input, Two Output FRF Concept

5.2.1 Noise/Error Minimization

The most reasonable, and most common, approach to the estimation of frequency response functions is by use of *least squares* (LS) or *total least squares* (TLS) techniques ^[1-3,6-7]. This is a standard technique for estimating parameters in the presence of noise. Least squares methods minimize the square of the magnitude error and, thus, compute the *best* estimate of the

magnitude of the frequency response function but have little effect on the phase of the frequency response function. The primary difference in the algorithms used to estimate frequency response functions is in the assumption of where the noise enters the measurement problem. The different assumptions of the source of the error is noted graphically in Figure 5-2.

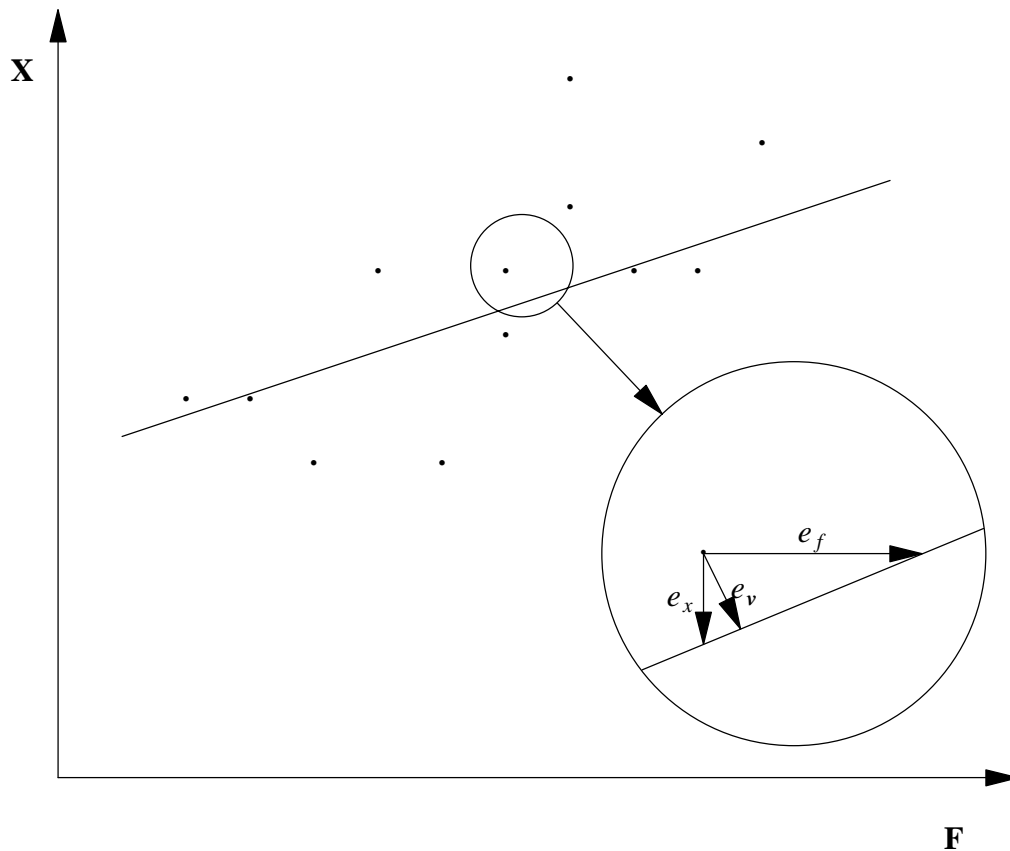


Figure 5-2. Least Squares Concept

Three algorithms, referred to as the H_1 , H_2 , and H_v algorithms, are commonly available for estimating frequency response functions. Table 5-2 summarizes this characteristic for the three methods that are widely used.

Frequency Response Function Models			
Technique	Solution	Assumed Location of Noise	
	Method	Force Inputs	Response
H_1	LS	no noise	noise
H_2	LS	noise	no noise
H_v	TLS	noise	noise

TABLE 5-2. Summary of Frequency Response Function Estimation Models

Consider the case of N_i inputs and N_o outputs measured during a modal test. Based upon the assumed location of the noise entering the estimation process, Eqs. (5.4) through (5.6) represent the corresponding model for the H_1 , H_2 , and H_v estimation procedures.

 H_1 Technique

$$[H]_{N_o \times N_i} \{F\}_{N_i \times 1} = \{X\}_{N_o \times 1} - \{\eta\}_{N_o \times 1} \quad (5.4)$$

 H_2 Technique

$$[H]_{N_o \times N_i} \{ \{F\}_{N_i \times 1} - \{v\}_{N_i \times 1} \} = \{X\}_{N_o \times 1} \quad (5.5)$$

 H_v Technique

$$[H]_{N_o \times N_i} \{ \{F\}_{N_i \times 1} - \{v\}_{N_i \times 1} \} = \{X\}_{N_o \times 1} - \{\eta\}_{N_o \times 1} \quad (5.6)$$

Note that in all methods, the inversion of a matrix is involved. Therefore, the inputs (references) that are used must not be fully correlated so that the inverse will exist. Extensive evaluation tools (using eigenvalue decomposition) have been developed in order to detect and avoid this condition [8].

5.2.2 Single Input FRF Estimation

Figure 5.3 represents the model of the measurement situation for a single input, single output frequency response function measurement.

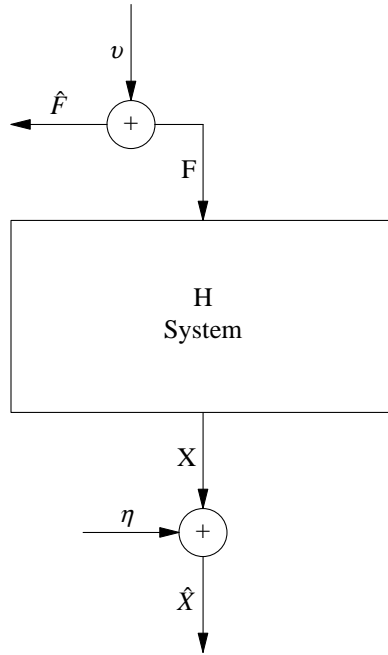


Figure 5-3. System Model: Single Input

With reference to Figure 5.3 for a case involving only one input and one output (input location q and response location p), the equation that is used to represent the input-output relationship is:

$$\hat{X}_p - \eta_p = H_{pq}(\hat{F}_q - v_q) \quad (5.7)$$

where:

- $F = \hat{F} - v = \text{Actual input}$
- $X = \hat{X} - \eta = \text{Actual output}$

- \hat{X} = Spectrum of the p – th output, measured
- \hat{F} = Spectrum of the q – th input, measured
- H = Frequency response function
- v = Spectrum of the noise part of the input
- η = Spectrum of the noise part of the output
- X = Spectrum of the p – th output, theoretical
- F = Spectrum of the q – th input, theoretical

If $v = \eta = 0$, the theoretical (expected) frequency response function of the system is estimated. If $\eta \neq 0$ and/or $v \neq 0$, a least squares method is used to estimate a *best* frequency response function, in the presence of noise.

In order to develop an estimation of the frequency response function, a number of averages N_{avg} is used to minimize the random errors (variance). This can be easily accomplished through use of intermediate measurement of the auto and cross power spectrums. The estimate of the auto and cross power spectrums for the model in Figure 5.3 can be defined as follows. Note that each function is a function of frequency.

Cross Power Spectra

$$GXF_{pq} = \sum_1^{N_{avg}} X_p F_q^* \quad (5.8)$$

$$GFX_{qp} = \sum_1^{N_{avg}} F_q X_p^* \quad (5.9)$$

Auto Power Spectra

$$GFF_{qq} = \sum_1^{N_{avg}} F_q F_q^* \quad (5.10)$$

$$GXX_{pp} = \sum_1^{N_{avg}} X_p X_p^* \quad (5.11)$$

where:

- F^* = Complex conjugate of $F(\omega)$
- X^* = Complex conjugate of $X(\omega)$

H₁ Algorithm: Minimize Noise on Output (η)

The most common formulation of the frequency response function, often referred to as the H_1 algorithm, tends to minimize the noise on the output. This formulation is shown in Eq. (5.12).

$$H_{pq} = \frac{GXF_{pq}}{GFF_{qq}} \quad (5.12)$$

H₂ Algorithm: Minimize Noise on Input (v)

Another formulation of the frequency response function, often referred to as the H_2 algorithm, tends to minimize the noise on the input. This formulation is shown in Eq. (5.13).

$$H_{pq} = \frac{GXX_{pp}}{GFX_{qp}} \quad (5.13)$$

In the H_2 formulation, an auto power spectrum is divided by a cross power spectrum. This can be a problem since the cross power spectrum can theoretically be zero at one or more frequencies. In both formulations, the phase information is preserved in the cross-power spectrum term.

H_v Algorithm: Minimize Noise on Input and Output (η and v)

The solution for H_{pq} using the H_v algorithm is found by the eigenvalue decomposition of a matrix of power spectrums. For the single input case, the following matrix involving the auto and cross power spectrums can be defined:

$$[GFFX_p] = \begin{bmatrix} GFF_{qq} & GXF_{pq} \\ GXF_{pq}^H & GXX_{pp} \end{bmatrix}_{2 \times 2} \quad (5.14)$$

The solution for H_{pq} is found by the eigenvalue decomposition of the $[GFFX]$ matrix as follows:

$$[GFFX_p] = [V] \begin{bmatrix} \Lambda \end{bmatrix} [V]^H \quad (5.15)$$

where:

- $\begin{bmatrix} \Lambda \end{bmatrix} = \text{diagonal matrix of eigenvalues}$

Solution for the H_{pq} matrix is found from the eigenvector associated with the smallest (minimum) eigenvalue (λ_1). The size of the eigenvalue problem is second order resulting in finding the roots of a quadratic equation. This eigenvalue solution must be repeated for each frequency and that the complete solution process must be repeated for each response point X_p .

Alternately, the solution for H_{pq} is found by the eigenvalue decomposition of the following matrix of auto and cross power spectrums:

$$[GXFF_p] = \begin{bmatrix} GXX_{pp} & GXF_{pq}^H \\ GXF_{pq} & GFF_{qq} \end{bmatrix}_{2 \times 2} \quad (5.16)$$

$$[GXFF_p] = [V] \begin{bmatrix} \Lambda \end{bmatrix} [V]^H \quad (5.17)$$

where:

- $\begin{bmatrix} \Lambda \end{bmatrix} = \text{diagonal matrix of eigenvalues}$

The solution for H_{pq} is again found from the eigenvector associated with the smallest (minimum)

eigenvalue (λ_1).

The frequency response function is found from the normalized eigenvector associated with the smallest eigenvalue. If $[GFFX_p]$ is used, the eigenvector associated with the smallest eigenvalue must be normalized as follows:

$$\{V\}_{\lambda_{\min}} = \begin{Bmatrix} H_{pq} \\ -1 \end{Bmatrix} \quad (5.18)$$

If $[GXFF_p]$ is used, the eigenvector associated with the smallest eigenvalue must be normalized as follows:

$$\{V\}_{\lambda_{\min}} = \begin{Bmatrix} -1 \\ H_{pq} \end{Bmatrix} \quad (5.19)$$

One important consideration of the three formulations for frequency response function estimation is the behavior of each formulation in the presence of a bias error such as leakage. In all cases, the estimate differs from the expected value particularly in the region of a resonance (magnitude maxima) or anti-resonance (magnitude minima). For example, H_1 tends to underestimate the value at resonance while H_2 tends to overestimate the value at resonance. The H_v algorithm gives an answer that is always bounded by the H_1 and H_2 values. The different approaches are based upon minimizing the magnitude of the error but have no effect on the phase characteristics.

In addition to the attractiveness of H_1 , H_2 and H_v in terms of the minimization of the error, the availability of auto and cross power spectra allows the determination of other important functions. The quantity γ_{pq}^2 is called the scalar or **ordinary coherence function** and is a frequency dependent, real value between zero and one. The ordinary coherence function indicates the degree of causality in a frequency response function. If the coherence is equal to one at any specific frequency, the system is said to have perfect causality at that frequency. In other words, the measured response power is caused totally by the measured input power (or by sources which are coherent with the measured input power). A coherence value less than unity at any frequency indicates that the measured response power is greater than that due to the measured input. This is due to some extraneous noise also contributing to the output power. It

should be emphasized, however, that low coherence does not necessarily imply poor estimates of the frequency response function, but simply means that more averaging is needed for a reliable result. The ordinary coherence function is computed as follows:

$$COH_{pq} = \gamma_{pq}^2 = \frac{|GXF_{pq}|^2}{GFF_{qq} GXX_{pp}} = \frac{GXF_{pq} GFX_{qp}}{GFF_{qq} GXX_{pp}} \quad (5.20)$$

When the coherence is zero, the output is caused totally by sources other than the measured input. In general, then, the coherence can be a measure of the degree of noise contamination in a measurement. Thus, with more averaging, the estimate of coherence may contain less variance, therefore giving a better estimate of the noise energy in a measured signal. This is not the case, though, if the low coherence is due to bias errors such as nonlinearities, multiple inputs or leakage. A typical ordinary coherence function is shown in Fig. 5.4 together with the corresponding frequency response function magnitude. In Fig. 5.4, the frequencies where the coherence is lowest is often the same frequencies where the frequency response function is at a maxima in magnitude or at a minima in magnitude. This is often an indication of leakage since the frequency response function is most sensitive to the leakage error at the lightly damped peaks corresponding to the maxima. At the minima, where there is little response from the system, the leakage error, even though it is small, may still be significant.

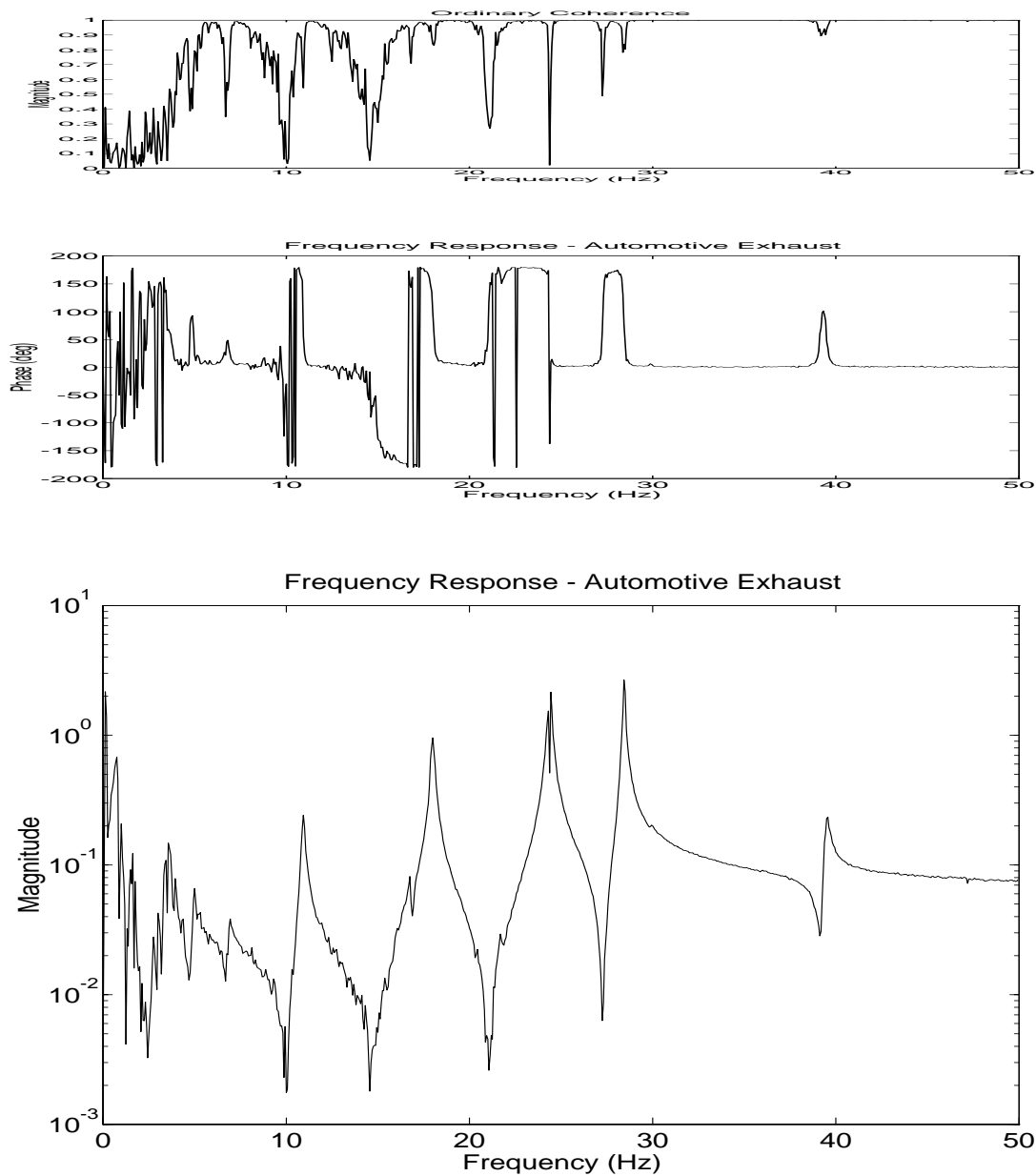


Figure 5-4. FRF and Corresponding Ordinary Coherence Function

In all of these cases, the estimated coherence function will approach, in the limit, the expected value of coherence at each frequency, dependent upon the type of noise present in the structure and measurement system. Note that, with more averaging, the estimated value of coherence will

not increase; the estimated value of coherence always approaches the expected value from the upper side. This is described in Figure 5-4. Note that a high value of coherence (0.9) after 16 averages has approximately the same possible variance of the frequency response function as a low value of coherence (0.1) after 256 averages.

90% confidence limits on the measurement of the amplitude $|H|$ and phase ϕ of transfer functions, as a function of the measured value of coherence and the number of averages.

Measured value of coherence function	Number of Averages				
	16	32	64	128	256
0.2	+ 5.2	+ 3.8	+ 2.8	+ 2.1	+ 1.5
	- 14.6	- 7.1	- 4.2	- 2.7	- 1.8
	(± 54)	(± 34)	(± 23)	(± 16)	(± 11)
0.3	+ 4.2	+ 3.1	+ 2.2	+ 1.6	+ 1.2
	- 8.4	- 4.8	- 3.0	- 2.0	- 1.4
	(± 38)	(± 25)	(± 17)	(± 12)	(± 8)
0.4	+ 3.5	+ 2.6	+ 1.8	+ 1.3	+ 1.0
	- 6.0	- 3.6	- 2.3	- 1.6	- 1.1
	(± 30)	(± 20)	(± 14)	(± 10)	(± 7)
0.5	+ 3.0	+ 2.1	+ 1.5	+ 1.1	+ 0.8
	- 4.5	- 2.8	- 1.9	- 1.3	- 0.9
	(± 24)	(± 16)	(± 11)	(± 8)	(± 5)
0.6	+ 2.5	+ 1.8	+ 1.3	+ 0.9	+ 0.7
	- 3.5	- 2.2	- 1.5	- 1.0	- 0.7
	(± 19)	(± 13)	(± 9)	(± 6)	(± 4)
0.7	+ 2.1	+ 1.5	+ 1.0	+ 0.7	+ 0.5
	- 2.7	- 1.7	- 1.2	- 0.8	- 0.6
	(± 15)	(± 10)	(± 7)	(± 5)	(± 4)
0.8	+ 1.6	+ 1.1	+ 0.8	+ 0.6	+ 0.4
	- 2.0	- 1.3	- 0.9	- 0.6	- 0.4
	(± 12)	(± 8)	(± 6)	(± 4)	(± 3)
0.9	+ 1.1	+ 0.8	+ 0.5	+ 0.4	+ 0.3
	- 1.3	- 0.8	- 0.6	- 0.4	- 0.3
	(± 8)	(± 5)	(± 4)	(± 3)	(± 2)

For each entry, the first two digits are the upper and lower bounds on $|H|$, in dB.
 Digits in parentheses are the bounds on ϕ , in degrees.

Figure 5-5. Ordinary Coherence Relationship - Averaging

Two special cases of low coherence are worth particular mention. The first situation occurs when a *leakage error* occurs in one or both of the input and output measurements. This causes the coherence in the area of the peaks of the frequency response to be less than unity. This error can

be reduced by the use of weighting functions or by cyclic averaging. The second situation occurs when a significant *propagation time delay* occurs between the input and output as may be the case with acoustic measurements. If a propagation delay of length t is compared to a sample function length of T , a low estimate of coherence will be estimated as a function of the ratio t/T . This propagation delay causes a bias error in the frequency response and should be removed prior to computation if possible.

5.2.3 Multiple Input FRF Estimation

Multiple input estimation of frequency response functions is desirable for several reasons. The principal advantage is the increase in the accuracy of estimates of the frequency response functions. During single input excitation of a system, there may exist large differences in the amplitudes of vibratory motion at various locations because of the dissipation of the excitation power within the structure. This is especially true when the structure has heavy damping. Small nonlinearities in the structure will consequently cause errors in the measurement of the response. With multiple input excitation, the vibratory amplitudes across the structure typically will be more uniform, with a consequent decrease in the effect of nonlinearities.

A second reason for improved accuracy is the increase in consistency of the frequency response functions compared to the single input method. When a number of exciter systems are used, the elements from columns of the frequency response function matrix corresponding to those exciter locations are being determined simultaneously. With the single input method, each column is determined independently, and it is possible for small errors of measurement due to nonlinearities and time dependent system characteristics to cause a change in resonance frequencies, damping, or mode shapes among the measurements in the several columns. This is particularly important for the polyreference modal parameter estimation algorithms that use frequency response functions from multiple columns or rows of the frequency response function matrix simultaneously.

An additional, significant advantage of the multiple input excitation is a reduction of the test time. In general, using multiple input estimation of frequency response functions, frequency response functions are obtained for all input locations in approximately the same time as required for acquiring a set of frequency response functions for one of the input locations, using a single

input estimation method.

Another potential advantage of the simultaneous measurement of a number of columns or rows of the frequency response function matrix is the ability to use a linear combination of frequency response functions in the same row of the matrix in order to enhance specific modes of the system. This technique is analogous to the forced normal mode excitation experimental modal analysis in which a structure is excited by a forcing vector which is proportional to the modal vector of interest. For this analysis, the coefficients of a preliminary experimental modal analysis are used to weight the frequency response functions, so that the sum emphasizes the modal vector that is sought. The revised set of conditioned frequency response functions is analyzed to improve the accuracy of the modal vector. A simple example of this approach for a structure with approximate geometrical symmetry would be to excite at two symmetric locations. The sum of the two frequency response functions at a specific response location should enhance the symmetric modes. Likewise, the difference of the two functions should enhance the antisymmetric modes.

Multiple Input versus Single Input***Advantages***

- Better energy distribution reduces nonlinearities at input location.
- Better energy distribution excites the structure more evenly.
- Data collected simultaneously has consistent frequency and damping information which is consistent with parameter estimation algorithms.
- Advances in hardware/software has kept data collection time the same for single input/multiple output.
More measurements per measurement cycle.
- Multiple input data permits the detection of repeated or closely spaced roots.

Disadvantages:

- Inputs must not be correlated.
- More equipment required.

The theoretical basis of multiple-input frequency response function analysis is well documented in a number of sources ^[1-3,18-27]. While much had been written about multiple input theory, the application of multiple input theory to experimental modal analysis apparently had not been seriously investigated prior to 1980 ^[18-27]. It also needs to be noted that this application of multiple input-output theory represents a very special case of multiple-input, multiple-output data analysis. For this case, everything about the inputs is known or can be controlled. The number of inputs, the location of the inputs, and the characteristics of the inputs are controlled by the test procedure. For the general case, none of these characteristics may be known.

Consider the case of N_i inputs and N_o outputs measured during a modal test on a dynamic

system as shown in Figure 5-6. The model assumed for the dynamics is:

$$\hat{X}_p - \eta_p = \sum_{q=1}^{N_i} H_{pq} * (\hat{F}_q - v_q) \quad (5.21)$$

where:

- $F = \hat{F} - v$ = Actual input
- $X = \hat{X} - \eta$ = Actual output
- \hat{X}_p = Spectrum of the p – th output, measured
- \hat{F}_q = Spectrum of the q – th input, measured
- H_{pq} = Frequency response function of output p with respect to input q
- v_q = Spectrum of the noise part of the input
- η_p = Spectrum of the noise part of the output
- X_p = Spectrum of the p – th output, theoretical
- F_q = Spectrum of the q – th input, theoretical

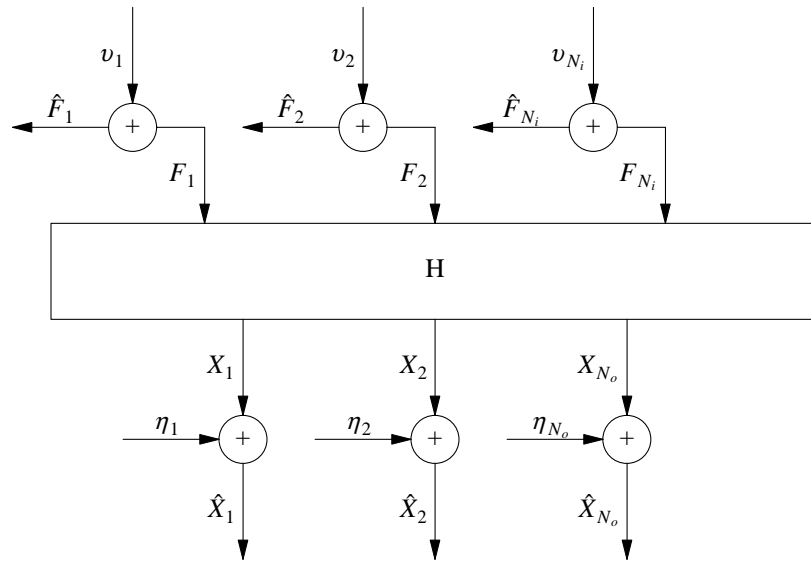


Figure 5-6. System Model: Multiple Inputs

In order to develop an estimation of the frequency response function for the multiple input case, a number of averages N_{avg} will be used to minimize the random errors (variance). This can be easily accomplished through use of intermediate measurement of the auto and cross power spectrums as defined in Equations (5.8) through (5.11). Additional matrices, constructed from the auto and cross power spectrums need to be defined as follows. Note that each function and, therefore, each resulting matrix is a function of frequency.

Input/Output Cross Spectra Matrix

$$[GXF] = \{X\}\{F\}^H = \begin{Bmatrix} X_1 \\ X_2 \\ \vdots \\ X_{N_o} \end{Bmatrix} [F_1^* \ F_2^* \ \dots \ F_{N_i}^*] = \begin{bmatrix} GFX_{11} & \cdot & \cdot & \cdot & GFX_{1N_i} \\ \cdot & \cdot & & & \cdot \\ \cdot & \cdot & & & \cdot \\ GFX_{N_o1} & \cdot & \cdot & \cdot & GFX_{N_oN_i} \end{bmatrix} \quad (5.22)$$

Input Cross Spectra Matrix

$$[GFF] = \{F\}\{F\}^H = \begin{Bmatrix} F_1 \\ F_2 \\ \vdots \\ F_{N_i} \end{Bmatrix} [F_1^* \ F_2^* \ \dots \ F_{N_i}^*] = \begin{bmatrix} GFF_{11} & \cdot & \cdot & \cdot & GFF_{1N_i} \\ \cdot & \cdot & & & \cdot \\ \cdot & \cdot & & & \cdot \\ GFF_{N_i1} & \cdot & \cdot & \cdot & GFF_{N_iN_i} \end{bmatrix} \quad (5.23)$$

The frequency response functions can now be estimated for the three algorithms as follows:

H₁ Algorithm: Minimize Noise on Output (η)

$$[H]_{N_o \times N_i} \{F\}_{N_i \times 1} = \{X\}_{N_o \times 1} - \{\eta\}_{N_o \times 1} \quad (5.24)$$

$$[H] \{F\} \{F\}^H = \{X\} \{F\}^H - \{\eta\} \{F\}^H \quad (5.25)$$

$$[H]_{N_o \times N_i} \{F\}_{N_i \times 1} \{F\}_{1 \times N_i}^H = \{X\}_{N_o \times 1} \{F\}_{1 \times N_i}^H \quad (5.26)$$

The above relationship can be concisely stated as:

$$[H][GFF] = [GXF] \quad (5.27)$$

$$[H] = [GXF][GFF]^{-1} \quad (5.28)$$

where:

- $[]^H$ = Complex conjugate transpose (Hermitian Matrix)

In the experimental procedure, the input and response signals are measured, and the averaged cross spectra and auto spectra necessary to create the $[GXF]$ and $[GFF]$ matrices are computed. If the computation of ordinary, multiple, or partial coherence functions will be required, then the diagonal elements of the output cross spectrum matrix $[GXX]$ must be computed also.

Equation (5.27) is valid regardless of whether the various inputs are correlated. Unfortunately, there are a number of situations where the input cross spectrum matrix $[GFF]$ may be singular for specific frequencies or frequency intervals. When this happens, the inverse of $[GFF]$ will not exist and Equation (5.28) cannot be used to solve for the frequency response function at those frequencies or in those frequency intervals. A computational procedure that solves Equation (5.28) for $[H]$ should therefore monitor the rank the matrix $[GFF]$ that is to be inverted, and desirably provide direction on how to alter the input signals or use the available data when a problem exists. The current approach for evaluating whether the inputs are sufficiently uncorrelated at each frequency involves determining the principal/virtual forces using principal component analysis ^[8]. This will be covered in a later section.

H₂ Algorithm: Minimize Noise on Input (v)

$$[H]_{N_o \times N_i} \{ \{F\}_{N_i \times 1} - \{v\}_{N_i \times 1} \} = \{X\}_{N_o \times 1} \quad (5.29)$$

$$[H] \{ \{F\} - \{v\} \} \{X\}^H = \{X\} \{X\}^H \quad (5.30)$$

$$[H]_{N_o \times N_i} \{F\}_{N_i \times 1} \{X\}_{1 \times N_o}^H = \{X\}_{N_o \times 1} \{X\}_{1 \times N_o}^H \quad (5.31)$$

One problem with using the H_2 algorithm is that the solution for $[H]$ can only be found directly using an inverse when the number of inputs N_i and number of outputs N_o are equal. Then:

$$[H] [GFX] = [GXX] \quad (5.32)$$

$$[H] = [GXX] [GFX]^{-1} \quad (5.33)$$

H_v Algorithm: Minimize Noise on Input and Output (v and η)

$$[H]_{N_o \times N_i} \{ \{F\}_{N_i \times 1} - \{v\}_{N_i \times 1} \} = \{X\}_{N_o \times 1} - \{\eta\}_{N_o \times 1} \quad (5.34)$$

$$[H] \{ \{F\} - \{v\} \} = \{X\} - \{\eta\} \quad (5.35)$$

The solution for $[H]$ is found by the eigenvalue decomposition of one of the following two matrices:

$$[GFFX_p] = \begin{bmatrix} [GFF] & [GXF_p] \\ [GXF_p]^H & [GXX_p] \end{bmatrix}_{(N_i+1) \times (N_i+1)} \quad (5.36)$$

$$[GXFF_p] = \begin{bmatrix} [GXX_p] & [GXF_p]^H \\ [GXF_p] & [GFF] \end{bmatrix}_{(N_i+1) \times (N_i+1)} \quad (5.37)$$

Therefore, the eigenvalue decomposition would be:

$$[GFFX_p] = [V] \begin{bmatrix} \Lambda \end{bmatrix} [V]^H \quad (5.38)$$

Or:

$$[GXFF_p] = [V] \begin{bmatrix} \Lambda \end{bmatrix} [V]^H \quad (5.39)$$

where:

- $\begin{bmatrix} \Lambda \end{bmatrix} = \text{diagonal matrix of eigenvalues}$

Solution for the $p - th$ row of the $[H]$ matrix is found from the eigenvector associated with the smallest (minimum) eigenvalue. Note that the size of the eigenvalue problem is $N_i + 1$ and that the eigenvalue solution must be repeated for each frequency. Note also that the complete solution process must be repeated for each response point X_p .

The frequency response functions associated with a single output p and all inputs is found by normalizing the eigenvector associated with the smallest eigenvalue. If $[GFFX_p]$ is used, the eigenvector associated with the smallest eigenvalue must be normalized as follows:

$$\{V\}_{\lambda_{\min}} = \begin{bmatrix} H_{p1} \\ H_{p2} \\ \cdot \\ \cdot \\ H_{pN_i} \\ -1 \end{bmatrix} \quad (5.40)$$

If $[GXFF_p]$ is used, the eigenvector associated with the smallest eigenvalue must be normalized as follows:

$$\{V\}_{\lambda_{\min}} = \begin{bmatrix} -1 \\ H_{p1} \\ H_{p2} \\ \cdot \\ \cdot \\ H_{pN_i} \end{bmatrix} \quad (5.41)$$

The concept of the coherence function, as defined for single-input measurement, needs to be expanded to include the variety of relationships that are possible for multiple inputs. **Ordinary coherence** is defined in this general sense as the correlation coefficient describing the linear relationship between any two spectra. This is consistent with the ordinary coherence function that is defined for single input, single output measurements. Great care must be taken in the interpretation of ordinary coherence when more than one input is present. The ordinary coherence of an output with respect to an input can be much less than unity even though the

linear relationship between inputs and outputs is valid, because of the influence of the other inputs.

The ordinary coherence function can be formulated in terms of the elements of the matrices defined previously. The ordinary coherence function between the p^{th} output and the q^{th} input can be computed from the following formula:

Ordinary Coherence Function

$$COH_{pq} = \gamma_{pq}^2 = \frac{|GXF_{pq}|^2}{GFF_{qq} GXX_{pp}} \quad (5.42)$$

where:

- GXX_{pp} = Auto power spectrum of the output p
- GFF_{qq} = Auto power spectrum of the input q
- GXF_{pq} = Cross power spectrum between output p and input q

Partial coherence is defined as the ordinary coherence between a conditioned output and another conditioned output, between a conditioned input and another conditioned input, or between a conditioned input and a conditioned output. The output and input are conditioned by removing contributions from other input(s). The removal of the effects of the other input(s) is formulated on a linear least squares basis. The order of removal of the inputs during "conditioning" has a definite effect upon the partial coherence if some of the input(s) are mutually correlated. There will be a partial coherence function for every input/output, input/input and output/output combination for all permutations of conditioning. The usefulness of partial coherence, especially between inputs, for experimental modal analysis is of limited value.

Multiple coherence is defined as the correlation coefficient describing the linear relationship between an output and all known inputs. There is a multiple coherence function for every output. Multiple coherence can be used to evaluate the importance of unknown contributions to each output. These unknown contributions can be measurement noise, nonlinearities, or unknown inputs. Particularly, as in the evaluation of ordinary coherence, a low value of multiple

coherence near a resonance will often mean that the "leakage" error is present in the frequency response function. Unlike the ordinary coherence function, a low value of multiple coherence is not expected at antiresonances. The antiresonances for different response locations occur at the same frequency. Though one response signal may have a poor signal-to-noise ratio at its antiresonance, other inputs will not at the same frequency.

The formulation of the equations for the multiple coherence functions can be simplified from the normal computational approach to the following equation.

Multiple Coherence Function

$$MCOH_p = \sum_{q=1}^{N_i} \sum_{t=1}^{N_i} \frac{H_{pq} GFF_{qt} H_{pt}^*}{GXX_{pp}} \quad (5.43)$$

where:

- H_{pq} = Frequency response function for output p and input q
- H_{pt} = Frequency response function for output p and input t
- GFF_{qt} = Cross power spectrum between output q and output t
- GXX_{pp} = Auto power spectrum of output p

If the multiple coherence of the p – th output is near unity, then the p – th output is well predicted from the set of inputs using the least squares frequency response functions.

Example: H_1 Technique: Two Inputs/One Output Case

To begin to understand the size of the problem involved, start with the two input, one output case.

$$\hat{X}_p - \eta_p = H_{p1} F_1 + H_{p2} F_2 \quad (5.44)$$

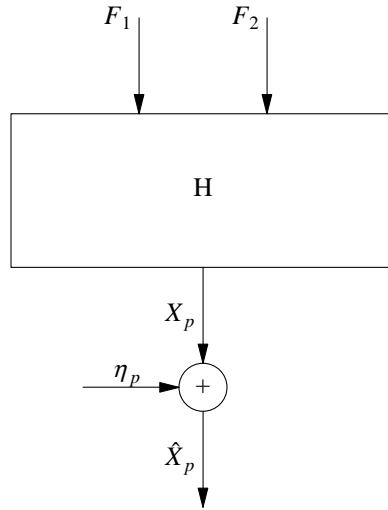


Figure 5-7. Two Input, One Output Model

If more than one output is measured, the equations become:

$$\{X_p\} [F_1^* \ F_2^*] = [H_{p1} \ H_{p2}] \begin{Bmatrix} F_1 \\ F_2 \end{Bmatrix} [F_1^* \ F_2^*] \quad (5.45)$$

Therefore, for input locations 1 and 2, each output is used with the two inputs to compute two frequency response functions. Therefore, there will be $2 \times N_o$ frequency response functions to be computed.

$$\begin{bmatrix} H_{11} & H_{12} \\ H_{21} & H_{22} \\ H_{31} & H_{32} \\ \vdots & \vdots \\ \vdots & \vdots \\ H_{N_o1} & H_{N_o2} \end{bmatrix} = \begin{bmatrix} GXF_{11} & GXF_{12} \\ GXF_{21} & GXF_{22} \\ GXF_{31} & GXF_{32} \\ \vdots & \vdots \\ \vdots & \vdots \\ GXF_{N_o1} & GXF_{N_o2} \end{bmatrix} \begin{bmatrix} GFF_{11} & GFF_{12} \\ GFF_{21} & GFF_{22} \end{bmatrix}^{-1} \quad (5.46)$$

For each output location, one formulation of the equations to be solved can be developed by replacing the inverse of the $[GFF]$ matrix with the equivalent adjoint of the $[GFF]$ matrix divided by the determinant of the $[GFF]$ matrix. In this way, it is clear that the frequency response functions can be found as long as the determinant of the $[GFF]$ matrix is not zero.

$$H_{p1} = \frac{GXF_{p1} GFF_{22} - GXF_{p2} GFF_{21}}{\det[GFF]} \quad (5.47)$$

$$H_{p2} = \frac{GXF_{p2} GFF_{11} - GXF_{p1} GFF_{12}}{\det[GFF]} \quad (5.48)$$

where:

- $\det[GFF]$ = Determinant of $[GFF]$ matrix
- $\det[GFF] = GFF_{11} GFF_{22} - GFF_{21} GFF_{12}$

For the two input, one output case several possible coherence functions can be formulated. While the ordinary coherence between the output and each input can be formulated, these coherence functions may not provide useful information due to the possible interaction between the two forces.

Ordinary Coherence (Output p and Input 1)

$$COH_{p1} = \frac{|GXF_{p1}|^2}{GFF_{11} GXX_{pp}} \quad (5.49)$$

Ordinary Coherence (Output p and Input 2)

$$COH_{p2} = \frac{|GXF_{p2}|^2}{GFF_{22} GXX_{pp}} \quad (5.50)$$

The ordinary coherence between the two inputs is a useful function since this is a measure of whether the forces are correlated. If the forces are perfectly correlated at a frequency, the inverse of the $[GFF]$ matrix will not exist and the frequency response functions cannot be estimated at that frequency. In this case, the ordinary coherence between the two forces cannot be unity, although values from 0.0 to 0.99 are theoretically acceptable. The limit is determined by the accuracy of the measured data and the numerical precision of the computation.

Ordinary Coherence (Input 1 and Input 2)

$$COH_{12} = \frac{|GFF_{12}|^2}{GFF_{11} GFF_{22}} \quad (5.51)$$

Multiple coherence is always a good measure of whether the output response is caused by the combination of the measured inputs. Multiple coherence is used in multiple input situations in the same way that ordinary coherence is used in the single input situations.

Multiple Coherence

$$MCOH_p = \sum_{q=1}^2 \sum_{t=1}^2 \frac{H_{pq} GFF_{qt} H_{pt}^*}{GXX_{pp}} \quad (5.52)$$

Summary of Methods***H₁ Technique:***

- Underestimates amplitude at resonances. Causes damping to be overestimated.
- Underestimates amplitude at anti-resonances.

H₂ Technique:

- Overestimates amplitude at resonances. Causes damping to be underestimated.
- Overestimates amplitude at anti-resonances.

H_v Technique:

- Best estimate of amplitude at resonances. Causes damping to be estimated best.
- Best estimate of amplitude at anti-resonances.
- Phase characteristics not altered.

5.2.3.1 Multiple Input Force Analysis/Evaluation

Of the variety of situations that can cause difficulties in the computation of the frequency response functions, the highest potential for trouble is the case of coherent inputs. If two of the inputs are fully coherent at one of the analysis frequencies, then there are no unique frequency response functions associated with those inputs at that analysis frequency. Unfortunately, there

are a number of situations where the input cross spectrum matrix $[GFF]$ may be singular at specific frequencies or frequency intervals. When this happens, the inverse of $[GFF]$ will not exist and Equation (5.28) cannot be used to solve for the frequency response function at those frequencies or in those frequency intervals. First, one of the input autospectra may be zero in amplitude over some frequency interval. When this occurs, then all of the cross spectra in the same row and column in the input cross spectrum matrix $[GFF]$ will also be zero over that frequency interval. Consequently, the input cross spectrum matrix $[GFF]$ will be singular over that frequency interval. Second, two or more of the input signals may be fully coherent over some frequency interval. Although the signals used as inputs to the exciter systems must be uncorrelated random inputs, the response of the structure at resonance, combined with the inability to completely isolate the exciter systems from this response results in the ordinary or conditioned partial coherence functions with values other than zero, particularly, at the system poles. For example, for the two input case, as long as the coherence function between the inputs is not unity at these frequencies, Equation (5.28) can be solved uniquely for the frequency response functions. Note that the auto and cross spectra involved in the calculation of the multiple input case for the estimation of frequency response functions should be computed from analog time data that has been digitized *simultaneously*. If data is not processed in this manner, many more averages are required to reduce the variance on each individual auto and cross spectrum and the efficiency of the multiple input approach to the estimation of frequency response functions will not be as attractive. Finally, numerical problems, which cause the computation of the inverse to be inexact, may be present. This can happen when an autospectrum is near zero in amplitude, when the cross spectra have large dynamic range with respect to the precision of the computer, or when the matrix is ill-conditioned because of nearly redundant input signals.

Due to the form of the equations that must be solved to compute frequency response functions in the presence of multiple inputs, special care must be taken to assure that the input spectrum matrix is not singular. Therefore, techniques have been investigated to evaluate the form of the input spectrum matrix before taking any data. Singular, in this case, implies that:

- Input forces may not be coherent at any frequency.
- Independent, uncorrelated noise sources must be used. (Random, Random Transient, Periodic Random)

- The impedance of the structure at the input locations may tend to correlate the inputs at resonance.
- There are no zero's in the input spectrum matrix.

Ordinary and Partial Coherence Functions

The historical approach that was used to try to evaluate the correlation between the forces utilized ordinary and partial coherence functions. The ordinary coherence function measures the degree of linear dependence (or correlation) between the spectra of two signals. The partial coherence function measures the degree of linear dependence between the spectra of two signals, after eliminating in a least squares sense, the contribution of some other signals. Both functions can be used in systematic procedure to verify that the forces are not correlated or that the input cross spectra matrix $[GFF]$ is not singular. For cases involving more than two inputs, this approach is very difficult and requires considerable judgement. In reality, only the ordinary coherence function, for the case of two inputs, is still used.

$$COH_{ik} = \frac{|GFF_{ik}|^2}{GFF_{ii} GFF_{kk}} \quad (5.53)$$

where:

- GFF_{ik} = Cross power spectrum between inputs i and k
- GFF_{ii} = Auto power spectrum of input i
- GFF_{kk} = Auto power spectrum of input k

Principal/Virtual Input Forces (Virtual Forces)

The current approach used to determine correlated inputs involves utilizing principal component analysis to determine the number of contributing forces to the $[GFF]$ matrix. In this approach, the matrix that must be evaluated is:

$$[GFF] = \begin{bmatrix} GFF_{11} & \cdot & \cdot & \cdot & GFF_{1N_i} \\ \cdot & & & & \cdot \\ \cdot & & & & \cdot \\ \cdot & & & & \cdot \\ GFF_{N_i1} & \cdot & \cdot & \cdot & GFF_{N_iN_i} \end{bmatrix} \quad (5.54)$$

where:

- $GFF_{ik} = GFF_{ki}^*$ (Hermitian Matrix)
- $GFF_{ik} = \sum F_i F_k^*$
- GFF is the power spectrum of a given input.

Principal component analysis involves an eigenvalue decomposition of the $[GFF]$ matrix [8]. Since the eigenvectors of such a decomposition are unitary, the eigenvalues should all be of approximately the same size if each of the inputs is contributing. If one of the eigenvalues is much smaller at a particular frequency, one of the inputs is not present or one of the inputs is correlated with the other input(s).

$$[GFF] = [V][\Lambda][V]^H \quad (5.55)$$

Since the eigenvectors of such a decomposition are unitary, the eigenvalues should all be of approximately the same size if each of the inputs is contributing. If one of the eigenvalues is much smaller at a particular frequency, one of the inputs is not present or one of the inputs is correlated with the other input(s). $[\Lambda]$ represents the eigenvalues of the $[GFF]$ matrix. If any of the eigenvalues of the $[GFF]$ matrix are zero or insignificant, then the $[GFF]$ matrix is singular. Therefore, for a three input test, the $[GFF]$ matrix should have three eigenvalues. (The number of eigenvalues is the number of uncorrelated inputs). This concept is shown graphically in Figure 5-8 for the auto power spectra for a three input case. It is difficult to determine if the inputs are mutually correlated from these plots. Figure 5-9 shows the principal force plots for the same case. At the frequencies where the third principal/virtual force drops (lowest curve), this indicates that the inputs are mutually correlated at those frequencies. This is not apparent from Figure 5-8.

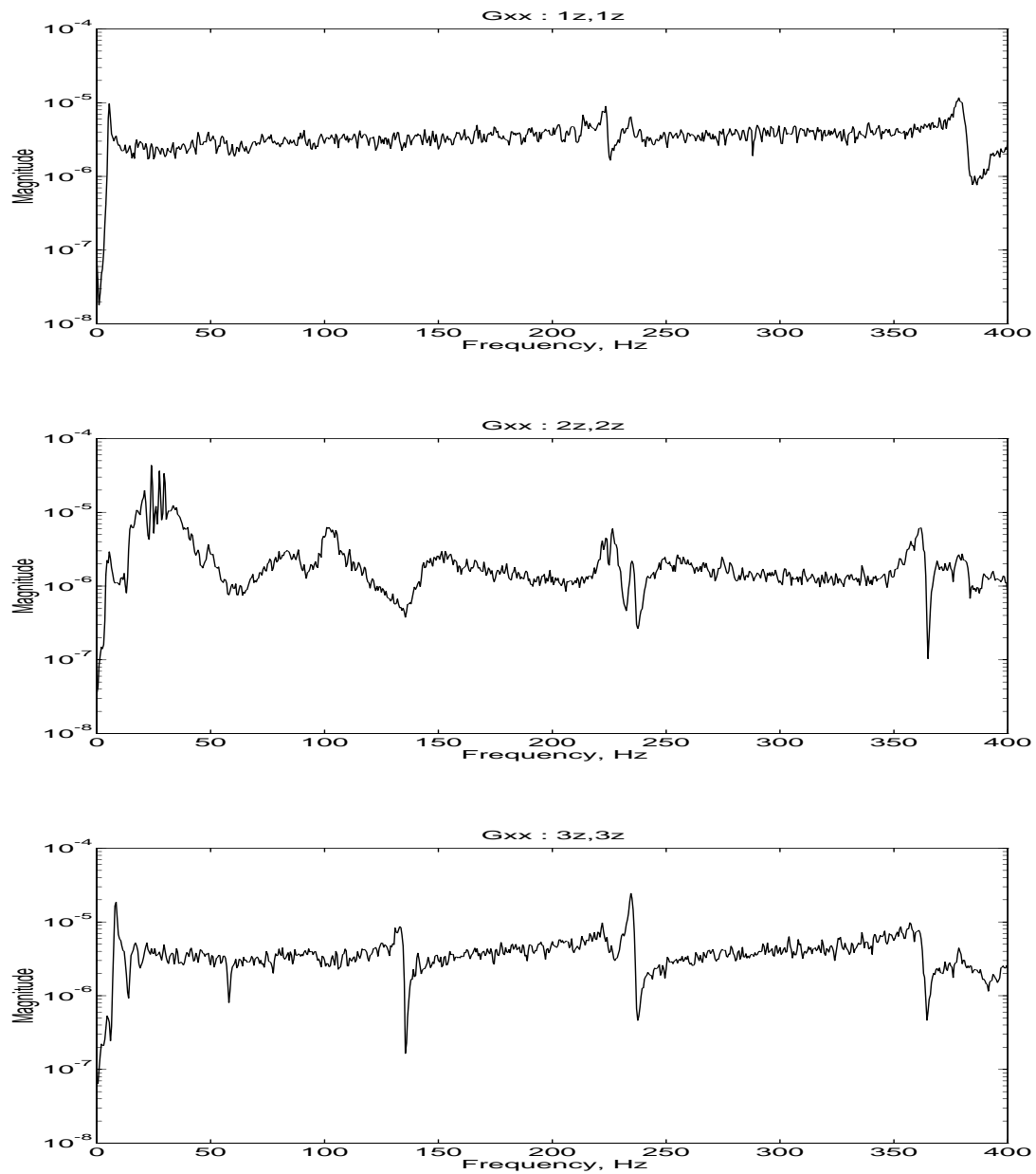


Figure 5-8. AutoPower Spectrum of Input Forces

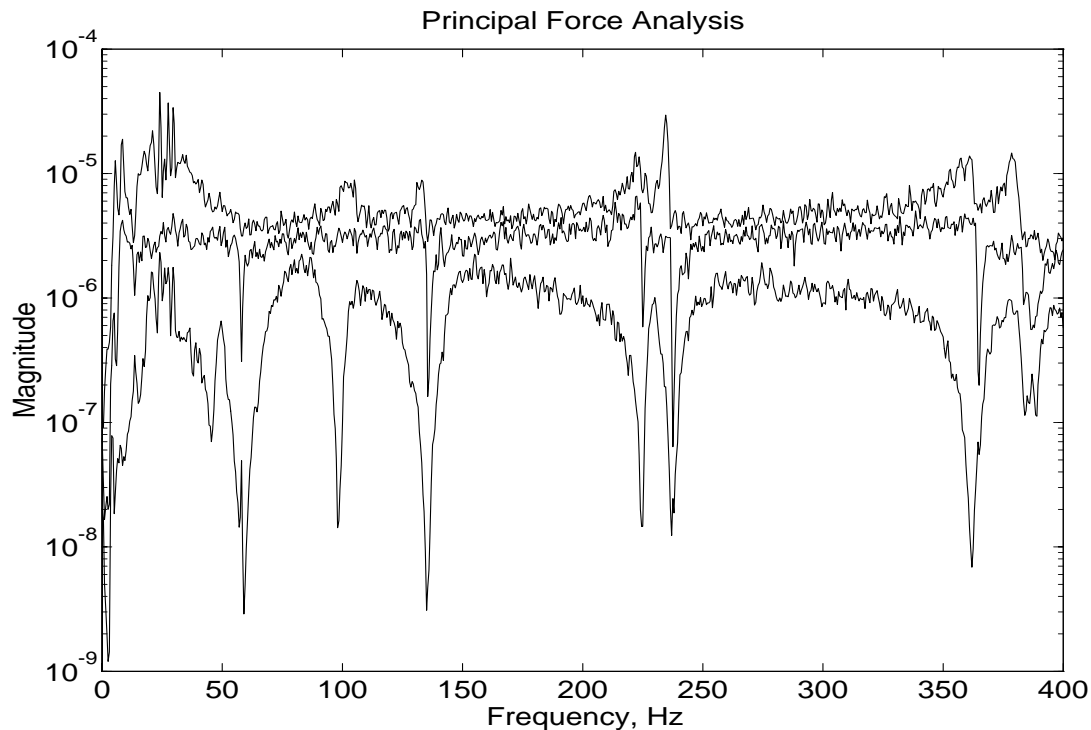


Figure 5-9. Principal (Virtual) Force Spectrum

Optimum Number Of Inputs

The location and number of inputs has a direct effect on the quality of frequency response functions that are estimated. This is an area that has not been researched completely and is still being reviewed. It is clear that beyond some number of inputs, the return from the investment of more equipment, in the form of inputs, is not warranted. Some considerations are:

- Two at symmetric locations. Frequency response functions can be added or subtracted to enhance in phase or out of phase modes.
- To excite as many modes as possible in one test configuration.

- Two vertical and one horizontal on a car.
- One on each wing and one on each horizontal stabilizer, all symmetric, on an aircraft structure.
- To excite "operating" conditions.

5.3 Excitation

Excitation includes any form of input that is used to create a response in a mechanical system. This can include environmental or operational inputs as well as the controlled force input(s) that are used in a vibration or modal analysis test. In general, the following discussion will be limited to the force inputs that can be measured and/or controlled in some rigorous way. With respect to frequency response function measurements to be used in experimental modal analysis, the excitation normally is applied using shakers or with impact devices (hammers). For those excitation signals that require the use of a shaker, Figure 5-10 shows a typical test configuration; Figure 5-11 shows a typical test configuration when an impact form of excitation is to be used.

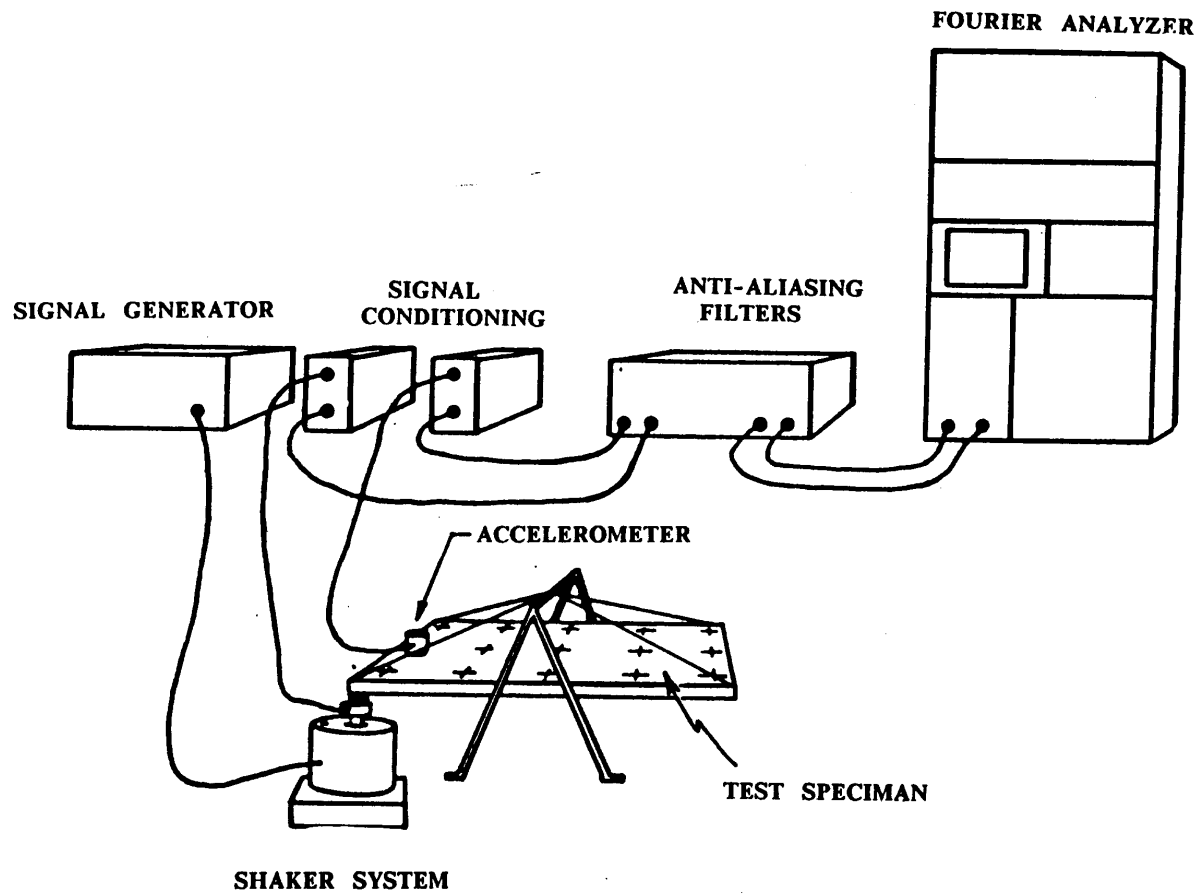


Figure 5-10. Typical Test Configuration: Shaker

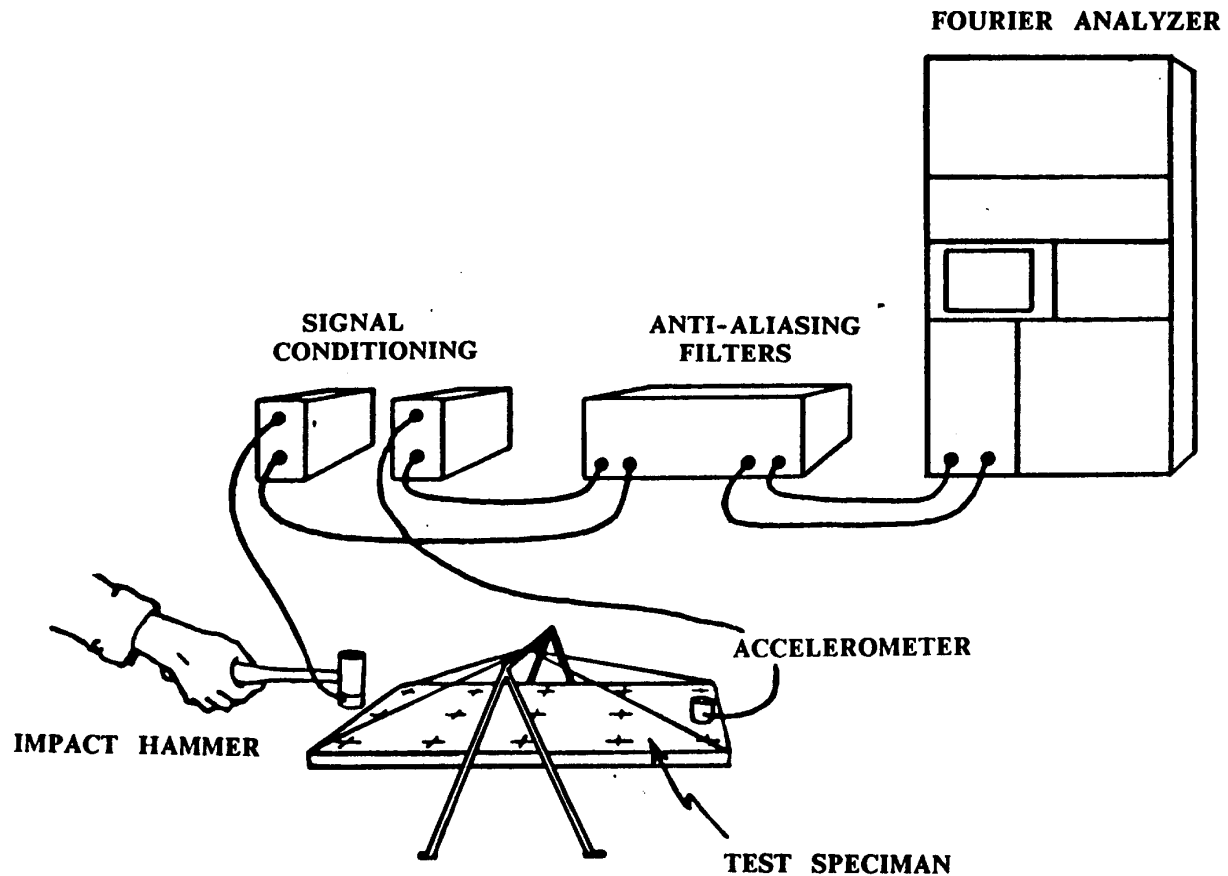


Figure 5-11. Typical Test Configuration: Impact Hammer

Single and multiple input estimation of frequency response functions (FRFs) via shaker excitation has become the mainstay of most mechanical structure measurements, particularly in the automotive and aircraft industries. While there are appropriate occasions for the use of deterministic excitation signals (sinusoids), the majority of these measurements are made using broadband (random) excitation signals. These signals work well for moderate to heavily damped mechanical structures which exhibit linear characteristics. When the mechanical structures are very lightly damped, care must be taken to minimize the leakage error so that accurate frequency response function (FRF) data can be estimated in the vicinity of the modal frequencies of the system. Frequently, when random excitation methods are compared to deterministic methods (sinusoids), the comparisons are questionable since proper procedures for eliminating the leakage error have not been followed.

Historically, a number of random excitation signals have been utilized, together with appropriate

digital signal processing techniques [1-5], to obtain accurate FRF data. The most common random signal that is used in this situation is the pure random signal together with a Hann window. This signal is normally generated by the data acquisition system utilizing built-in random signal generator(s) or via external random signal generator(s). While this approach does not eliminate the source of leakage and the effect of applying the Hann window must be considered, this approach is normally considered as a baseline random excitation method for estimating FRF measurements since this method is available with almost any data acquisition system.

Other forms of random signals (pseudo random, periodic random, burst random, etc.) utilize more control or frequency shaping of the excitation signal(s) and generally require digital-to-analog (DAC) converter(s). For this reason, some of these alternate methods are infrequently available and therefore not used. This is unfortunate since these methods often yield a superior FRF measurement in less total testing time.

When FRFs are measured on lightly damped systems, great care must be taken to eliminate the leakage error. Regardless of the type of excitation signal hardware involved (random signal generator or DAC), there are random excitation methods that can nearly eliminate the leakage error. In some cases, one approach will be superior on the basis of minimizing the total test time but on the basis of accurate, leakage-free FRFs, one of the methods will always work if test time can be sacrificed. Note that these alternate forms of random excitation focus on eliminating the source of leakage by customizing the random signal to match the requirements of fast Fourier transform (FFT) that is used in converting from the time to frequency domain. The FFT requires that the time domain signal must either be totally observed in the observation period (T) or be periodic in the observation period (T). For leakage free FRF measurements, all of the input and output signals must match one of these two requirements. Burst random excitation is an attempt to match the first requirement; pseudo and periodic random excitations are attempts to match the second requirement.

5.3.1 Excitation Assumptions

The primary assumption concerning the excitation of a linear structure is that the excitation is observable. Whenever the excitation is measured, this assumption simply implies that the measured characteristic properly describes the actual input characteristics. For the case of multiple inputs, the different inputs must often be uncorrelated for the computational procedures

to yield a solution. In most cases this means only that the multiple inputs must not be perfectly correlated at any frequency. As long as the excitation is measured, the validity of these limited assumptions can be evaluated.

Currently, there are a number of techniques that can be used to estimate modal characteristics from response measurements with no measurement of the excitation. If this approach is used, the excitation assumptions are much more imposing. Obviously, if the excitation is not measured, estimates of modal scaling (modal mass, modal A, residues, etc.) cannot be generated. Even under the assumption that the estimation of these parameters is not required, all of these techniques have one further restriction: an assumption has to be made concerning the characteristics of the excitation of the system. Usually, one assumes that the autospectrum of the excitation signal is sufficiently smooth over the frequency interval of interest.

In particular, the following assumptions about the excitation signal can be used:

- The excitation is impulsive. The autospectrum of a short pulse (time duration much smaller than the period of the greatest frequency of interest) is nearly uniform, or constant in amplitude, and largely independent of the shape of the pulse.
- The excitation is white noise. White noise has an autospectrum that is uniform over the bandwidth of the signal.
- The excitation signal is a step. A step signal has an autospectrum that decreases in amplitude in proportion to the reciprocal of frequency. The step signal can be viewed as the integral of an impulsive signal.
- There is no excitation. This is called the free response or free decay situation. The structure is excited to a condition of nonzero displacement, or nonzero velocity, or both. Then the excitation is removed, and the response is measured during free decay. This kind of response can be modeled as the response of the structure to an excitation signal that is a linear combination of impulsive and step signals.

When the excitation autospectrum is uniform, the autospectrum of the response signal is proportional to the square of the modulus of the frequency response function. Using the notation of a pole-zero model, the poles of the response spectrum are the poles of the frequency response, which are the parameters of the system resonances. If the autospectrum is not uniform, then the

excitation spectrum can be modeled as an analytic function, to a precision comparable to typical experimental error in the measurement of spectra. In this model, the excitation spectrum has poles that account for the nonuniformity of the spectrum amplitude. The response signal, therefore, can be modeled by a spectrum that contains zeros at the zeros of the excitation and the zeros of the frequency response, and contains poles at the poles of the excitation and at the poles of the frequency response. It is obviously important that the force spectrum should have no poles or zeros which coincide with poles of the frequency response.

For transient inputs, such as an impact or step relaxation, the assumption of smooth excitation spectra is generally true, but for operating inputs or inputs generated by an exciter system, care must be taken to insure the input force spectrum is smooth. This is especially true for tests performed using a hydraulic or an electro-mechanical exciter, because the system being analyzed may "load" the exciter system (the structure's impedance is so low that the desired force level cannot be achieved within the constraint of small motion), and this causes a nonuniformity in the input force spectrum.

To determine the characteristics of the system from the response, it is necessary that the response have the same poles as the frequency response, or that the analysis process corrects for the zeros and poles of the excitation. If the force input spectrum has a zero in the frequency range of interest, the pole location measured from the response spectrum will not match that of the frequency response. This potential problem is demonstrated in Figure 5-12 for the typical case of shaker excitation. The top figure is the magnitude of the frequency response function. The middle figure is the auto power spectrum of the input and the lower figure is the auto power spectrum of the response. Note that the estimates of modal parameters that would be derived from the auto power spectrum of the response would be quite different from those derived from the frequency response function.

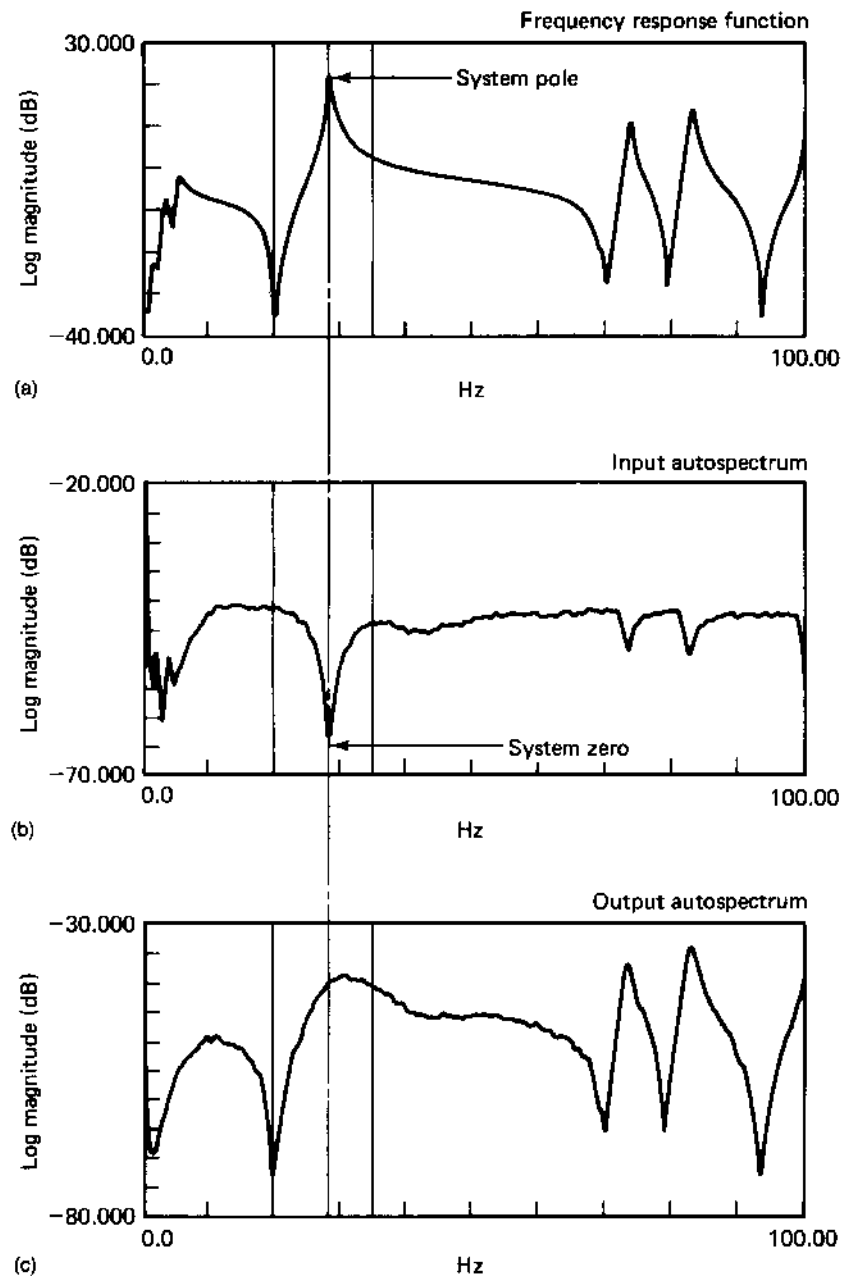


Figure 5-12. Input Spectrum Example

Presently, there is a great deal of interest in determining modal parameters from measured response data taken on operating systems (for example: turbulent flow over an airfoil, road inputs to automobiles, and environmental inputs to proposed large space structures). For these cases,

care must be taken not to confuse poles that are system resonances with those that exist in the output spectrum due to inputs.

In general, the poles of the response include those of the frequency response and of the input spectrum. Therefore, if the force is not measured, it is not possible without some prior knowledge about the input to determine if the poles of the response are truly system characteristics. If no poles or zeros exist in the force spectrum in the frequency range of interest, then any poles in the response in this range must be a result of the system characteristics. Obviously, when the excitation can be measured, it is prudent to do so.

5.3.2 Terminology and Nomenclature

Historically, a number of terminology and nomenclature issues have not been rigorously defined when excitation methods have been described.

The following terminology is important to the explanation of different excitation methods together with the associated digital signal processing requirements.

Signal Type - Signal type refers to the basic form of the signal, such as random, impact, sinusoidal or chirp.

Frequency Shaping - Frequency shaping refers to any frequency domain constraint or characteristic that is applied to the specific signal type. With respect to random excitation, a common frequency shaping is pseudo random. Other frequency shaping is commonly applied to sinusoids and chirps via the rate at which the change of frequency and/or amplitude occurs. Impact excitation is commonly frequency shaped by controlling the tip characteristic of the hammer.

Delay Blocks - The number of contiguous blocks of excitation that take place without the associated input and output data being acquired are referred to as the delay blocks (N_d). This is normally associated with a excitation technique that is periodic in nature. The delay blocks are needed in order to give the transient response to any start or change in the periodic excitation to decay out of the response signal(s) so that both the input(s) and output(s) are periodic with respect to any observation period (T). It is this requirement that makes swept sinusoidal excitation methods (analog swept or digitally stepped) so time consuming, particularly on lightly

damped systems. Each delay block is equal in length to the observation period (T) and the number of delay blocks is normally chosen as an integer. The number of delay blocks does not have to be an integer for all excitation methods but, for the purposes of this paper and in common usage, is normally chosen as an integer. The delay blocks are not recorded and are not used in the estimation of the FRFs.

Capture Blocks - The number of capture blocks refers to the number of contiguous blocks of time data (excitation (input) and response (output)) that are recorded or captured for each average (N_c). The number of capture blocks is also the number of cyclic averages that will be used to reduce the leakage error. Each group of contiguous capture blocks (N_c) is used as the time domain data contributing to one power spectral average that contributes to the estimate of the FRF measurements.

Window Function - The window function refers to the digital signal processing, time domain window that is applied to the capture blocks. The application of the window function to the capture blocks is on the basis of the group of contiguous capture blocks not on each capture block individually.

Average (Ensemble) - The average or ensemble refers to the total collection of contiguous time blocks that contribute to each power spectral average. The total time of each average is equal to the sum of the number of delay blocks (N_d) plus the number of capture blocks (N_c) times the observation period (T) which is the same for all delay and capture blocks. The number of averages (N_{avg}) refers to the number of these contiguous collections of time blocks and is, therefore, the same as the number of power spectral averages. The number of capture blocks can also be thought of as the number of cyclic averages (N_c). Cyclic signal averaging is often used with excitation characteristics in order to better match the time domain input and output signals to the requirements of the FFT prior to the application of the FFT. Cyclic signal averaging essentially digitally comb filters the time domain data to reduce the amount of information in the data that is not periodic with the observation period (T). This type of averaging reduces the effects of the leakage error. As long as the N_c successive blocks of data are contiguous, the blocks of time domain data can be averaged together, with or without windows, to achieve the benefit of leakage reduction [9-10].

Periodic - If the excitation signal is repeated for each delay and capture block, the signal is referred to as periodic. This classification is consistent with the definition of a periodic function and includes typical examples of sinusoids and chirps as well as a random signal that is repeated on the basis of the observation period (T). The periodic classification does not define whether

the same signal is repeated for each successive group of contiguous delay and capture blocks.

Burst Length - Burst length is the percentage (0 to 100%) of the average or ensemble time that the excitation signal is present. Burst length is normally adjusted in order to achieve a signal that is a totally observed transient. The decay of the signal is a function of the system damping and the characteristics of the excitation hardware. Burst length can be defined as the percentage of the total number of contiguous delay and capture blocks or of a percentage of just the capture blocks. For the purpose of this paper, the burst length refers to the percentage of the total number of contiguous delay and capture blocks.

Power Spectral Averages - The number of power spectral averages (N_{avg} or N_a) is the number of auto and cross spectra that are averaged together to estimate the FRF measurements. The actual amount of test time contributing to each power spectral average is a function of the number of contiguous delay and capture blocks. The purpose of power spectral averages is to eliminate the noise that is random with respect to the averaging procedure in order to reduce the variance on the resulting FRF estimate. This type of averaging does not reduce the effects of bias errors like the leakage error.

In order to clarify the preceding terminology, Figure 5-13 is a schematic representation of the number of contiguous blocks of time domain data contributing to one power spectral average. In this example, the two blocks marked "D" represent delay blocks and the four blocks marked "C" represent capture blocks. The total time for each power spectral average is, therefore, six contiguous blocks of time data ($6 \times T$ seconds of data).

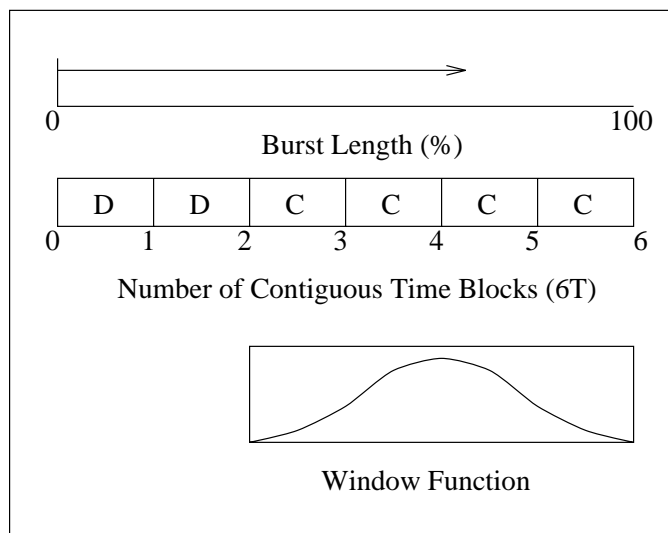


Figure 5-13. Total Contiguous Time Per power Spectral Average (Ensemble)

5.3.3 Classification of Excitation

Inputs which can be used to excite a system in order to determine frequency response functions belong to one of two classifications. The first classification is that of a random signal. Signals of this form can only be defined by their statistical properties over some time period. Any subset of the total time period is unique and no explicit mathematical relationship can be formulated to describe the signal. Random signals can be further classified as stationary or non-stationary. Stationary random signals are a special case where the statistical properties of the random signals do not vary with respect to translations with time. Finally, stationary random signals can be classified as ergodic or non-ergodic. A stationary random signal is ergodic when a time average on any particular subset of the signal is the same for any arbitrary subset of the random signal. All random signals which are commonly used as input signals fall into the category of ergodic, stationary random signals.

The second classification of inputs which can be used to excite a system in order to determine frequency response functions is that of a deterministic signal. Signals of this form can be represented in an explicit mathematical relationship. Deterministic signals are further divided into periodic and non-periodic classifications. The most common inputs in the periodic deterministic signal designation are sinusoidal in nature while the most common inputs in the

non-periodic deterministic designation are transient in form.

The choice of input to be used to excite a system in order to determine frequency response functions depends upon the characteristics of the system, upon the characteristics of the parameter estimation, and upon the expected utilization of the data. The characterization of the system is primarily concerned with the linearity of the system. As long as the system is linear, all input forms should give the same expected value. Naturally, though, all real systems have some degree of nonlinearity. Deterministic input signals result in frequency response functions that are dependent upon the signal level and type. A set of frequency response functions for different signal levels can be used to document the nonlinear characteristics of the system. Random input signals, in the presence of nonlinearities, result in a frequency response function that represents the best linear representation of the nonlinear characteristics for a given level of random signal input. For small nonlinearities, use of a random input will not differ greatly from the use of a deterministic input.

The characterization of the parameter estimation is primarily concerned with the type of mathematical model being used to represent the frequency response function. Generally, the model is a linear summation based upon the modal parameters of the system. Unless the mathematical representation of all nonlinearities is known, the parameter estimation process cannot properly weight the frequency response function data to include nonlinear effects. For this reason, random input signals are prevalently used to obtain the best linear estimate of the frequency response function when a parameter estimation process using a linear model is to be utilized.

The expected utilization of the data is concerned with the degree of detailed information required by any post-processing task. For experimental modal analysis, this can range from implicit modal vectors needed for trouble-shooting to explicit modal vectors used in an orthogonality check. As more detail is required, input signals, both random and deterministic, will need to match the system characteristics and parameter estimation characteristics more closely. In all possible uses of frequency response function data, the conflicting requirements of the need for accuracy, equipment availability, testing time, and testing cost will normally reduce the possible choices of input signal.

With respect to the reduction of the variance and bias errors of the frequency response function,

random or deterministic signals can be utilized most effectively if the signals are periodic with respect to the sample period or totally observable with respect to the sample period. If either of these criteria are satisfied, regardless of signal type, the predominant bias error, leakage, will be eliminated. If these criteria are not satisfied, the leakage error may become significant. In either case, the variance error will be a function of the signal-to-noise ratio and the amount of averaging.

5.3.4 Random Excitation Methods

Inputs which can be used to excite a system in order to determine frequency response functions (FRFs) belong to one of two classifications, random or deterministic ^[6-8]. Random signals are widely utilized for general single-input and multiple-input shaker testing when evaluating structures that are essentially linear. Signals of this form can only be defined by their statistical properties over some time period. Any subset of the total time period is unique and no explicit mathematical relationship can be formulated to describe the signal. Random signals can be further classified as stationary or non-stationary. Stationary random signals are a special case where the statistical properties of the random signals do not vary with respect to translations with time. Finally, stationary random signals can be classified as ergodic or non-ergodic. A stationary random signal is ergodic when a time average on any particular subset of the signal is the same for any arbitrary subset of the random signal. All random signals which are commonly used as input signals fall into the category of ergodic, stationary random signals. Deterministic signals can be characterized directly by mathematical formula and the characteristic of the excitation signal can be computed for any instance in time. While this is true for the theoretical signal sent to the exciter, it is only approximately true for the actual excitation signal due to the amplifier/shaker/structure interaction that is a function of the impedances of these electro-mechanical systems. Deterministic signals can, nevertheless, be controlled more precisely and are frequently utilized in the characterization of nonlinear systems for this reason. The random classification of excitation signals is the only signal type discussed in this paper.

The choice of input to be used to excite a system in order to determine frequency response functions depends upon the characteristics of the system, upon the characteristics of the modal parameter estimation, and upon the expected utilization of the data. The characterization of the system is primarily concerned with the linearity of the system. As long as the system is linear, all input forms should give the same expected value. Naturally, though, all real systems have some degree of nonlinearity. Deterministic input signals result in frequency response functions

that are dependent upon the signal level and type. A set of frequency response functions for different signal levels can be used to document the nonlinear characteristics of the system. Random input signals, in the presence of nonlinearities, result in a frequency response function that represents the best linear representation of the nonlinear characteristics for a given RMS level of random signal input. For systems with small nonlinearities, use of a random input will not differ greatly from the use of a deterministic input.

The characterization of the modal parameter estimation is primarily concerned with the type of mathematical model being used to represent the frequency response function. Generally, the model is a linear summation based upon the modal parameters of the system. Unless the mathematical representation of all nonlinearities is known, the parameter estimation process cannot properly weight the frequency response function data to include nonlinear effects. For this reason, random input signals are prevalently used to obtain the best linear estimate of the frequency response function when a parameter estimation process using a linear model is to be utilized.

The expected utilization of the data is concerned with the degree of detailed information required by any post-processing task. For experimental modal analysis, this can range from implicit modal vectors needed for trouble-shooting to explicit modal vectors used in an orthogonality check. As more detail is required, input signals, both random and deterministic, will need to match the system characteristics and parameter estimation characteristics more closely. In all possible uses of frequency response function data, the conflicting requirements of the need for accuracy, equipment availability, testing time, and testing cost will normally reduce the possible choices of input signal.

With respect to the reduction of the variance and bias errors of the frequency response function, random or deterministic signals can be utilized most effectively if the signals are periodic with respect to the sample period or totally observable with respect to the sample period. If either of these criteria are satisfied, regardless of signal type, the predominant bias error, leakage, will be minimized. If these criteria are not satisfied, the leakage error may become significant. In either case, the variance error will be a function of the signal-to-noise ratio and the amount of averaging.

Many signals are appropriate for use in experimental modal analysis. Some of the most commonly used random signals, used with single and multiple input shaker testing, are described in the following sections.

Pure Random - The pure random signal is an ergodic, stationary random signal which has a Gaussian probability distribution. In general, the frequency content of the signal contains energy at all frequencies (not just integer multiples of the FFT frequency increment ($\Delta f = 1/T$)). This characteristic is shown in Figure 5-14. This is undesirable since the frequency information between the FFT frequencies is the cause of the leakage error. The pure random signal may be filtered (F_{\min} to F_{\max}) to include only information in a frequency band of interest. The measured input spectrum of the pure random signal, as with all random signals, will be altered by any impedance mismatch between the system and the exciter. The number of power spectral averages used in the pure random excitation approach is a function of the reduction of the variance error and the need to have a significant number of averages to be certain that all frequencies have been adequately excited.

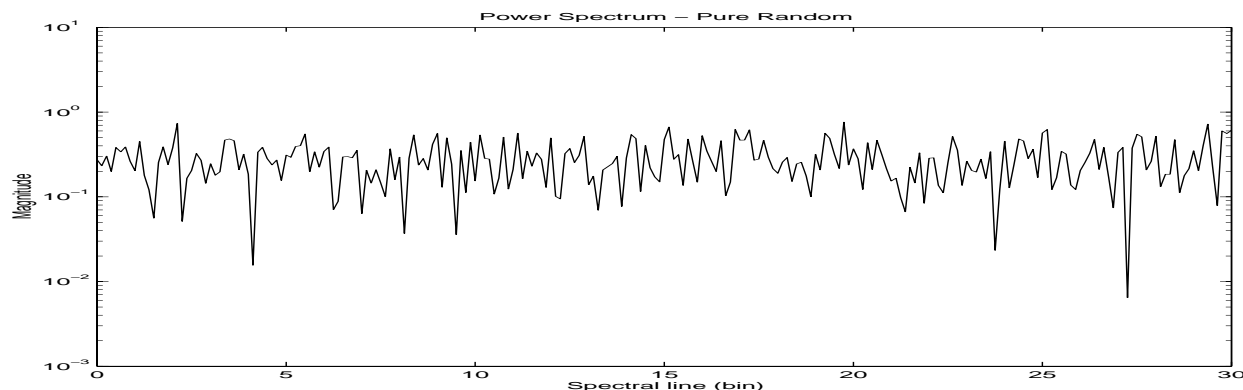


Figure 5-14. Signal Energy Content - Pure Random

Pseudo Random - The pseudo random signal is an ergodic, stationary random signal consisting of energy content only at integer multiples of the FFT frequency increment (Δf). The frequency spectrum of this signal is shaped to have a constant amplitude with random phase. This characteristic is shown in Figure 5-15. If sufficient delay time is allowed in the measurement procedure for any transient response to the initiation of the signal to decay (number of delay blocks), the resultant input and output histories are periodic with respect to the sample period. The number of power spectral averages used in the pseudo random excitation approach is a function of the reduction of the variance error. In a noise free environment, only one average (per input) may be necessary.

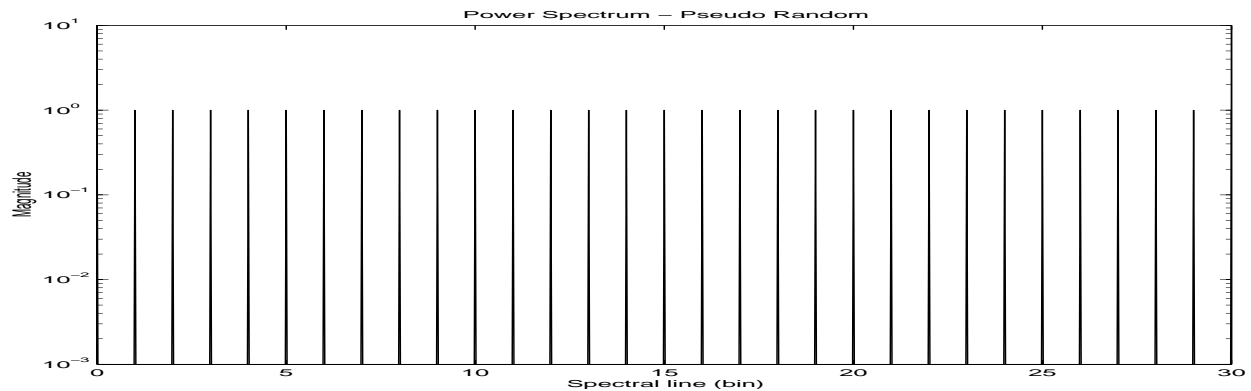


Figure 5-15. Signal Energy Content - Pseudo Random

Periodic Random - The periodic random signal is an ergodic, stationary random signal consisting only of integer multiples of the FFT frequency increment. The frequency spectrum of this signal has random amplitude and random phase distribution. This characteristic is shown in Figure 5-16. For each average, input signal(s) are created with random amplitude and random phase. The system is excited with these input(s) in a repetitive cycle until the transient response to the change in excitation signal decays (number of delay blocks). The input and response histories should then be periodic with respect to the observation time (T) and are recorded as one power spectral average in the total process. With each new average, a new history, random with respect to previous input signals, is generated so that the resulting measurement will be completely randomized. The number of power spectral averages used in the periodic random excitation approach is a function of the reduction of the variance error and the need to have a significant number of averages to be certain that all frequencies have been adequately excited.

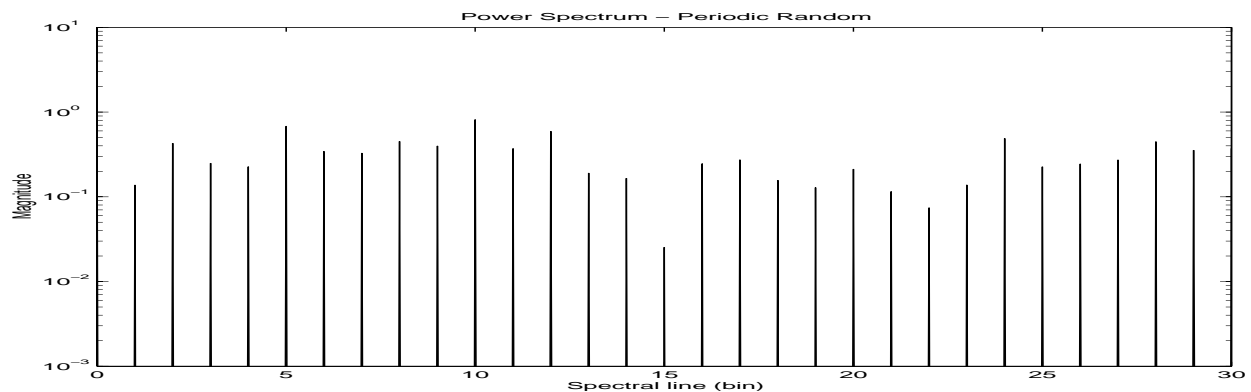


Figure 5-16. Signal Energy Content - Periodic Random

Burst Random (Random Transient) - The burst random signal is neither a completely transient deterministic signal nor a completely ergodic, stationary random signal but contains properties of both signal types. The frequency spectrum of this signal has random amplitude and random phase distribution and contains energy throughout the frequency spectrum. This characteristic is shown in Figure 5-17. The difference between this signal and the random signal is that the random transient history is truncated to zero after some percentage of the observation time (T). Normally, an acceptable percentage is fifty to eighty percent. The measurement procedure duplicates the random procedure but without the need to utilize a window to reduce the leakage problem as long as both the input and output decays to zero in the observation time (T).

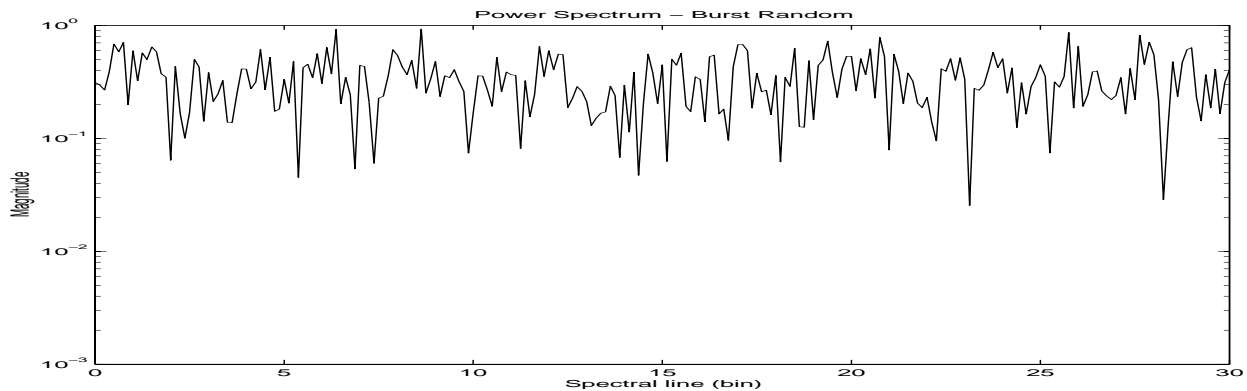


Figure 5-17. Signal Energy Content - Burst Random

The burst length (0-100%) is chosen so that the response history decays to zero within the observation time (T). For moderate to heavily damped systems, the response history will decay to zero very quickly due to the damping provided by the system being tested. These systems do not cause a leakage error in the first place.

For lightly damped cases, burst random will force the response to decay to zero in the observation time (T) primarily due to the exciter system characteristics. Exciter systems, particularly electromagnetic, attempt to match the excitation signal to some physical characteristic of the exciter. Typically, this means that the displacement, velocity or acceleration of the armature of the shaker will attempt to match the excitation signal. (Note that this is normally an open loop control process; no attempt is made to exactly match the excitation signal.) Electromagnetic shaker systems work either in a voltage or current feedback configuration in order to control the shaker according to the desired input signal. **Voltage feedback** refers to the type of amplifier in the exciter system that attempt to match the voltage

supplied to the shaker to the excitation signal. This effectively means that the displacement of the armature will follow the excitation signal. Therefore, if a zero voltage signal is sent to the exciter system, the exciter will attempt to prevent the armature from moving. This damping force, provided by the exciter/amplifier system, is often overlooked in the analysis of the characteristics of this signal type. Since this measured input, although not part of the generated signal, includes the variation of the input during the decay of the response history, the input and response histories are totally observable within the sample period and the system damping that will be computed from the measured FRF data is unaffected.

Current feedback refers to the type of amplifier in the exciter system that attempt to match the current supplied to the shaker to the excitation signal. This effectively means that the acceleration of the armature will follow the excitation signal. Therefore, if a zero voltage signal is sent to the exciter system, the exciter will allow the armature to move, preventing any force to be applied by the exciter system. The characteristic of a voltage feedback exciter system for a burst random excitation is shown in the following figures. Note the difference between the desired burst random signal and the actual force measured.

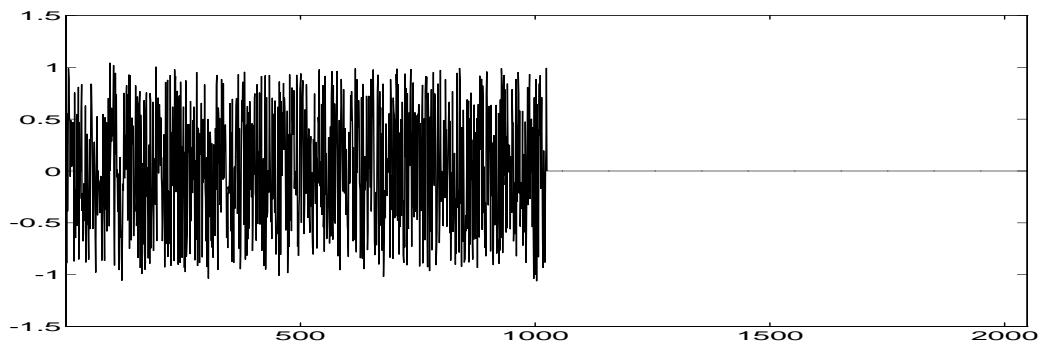


Figure 5-18. Burst Random - Signal to Shaker

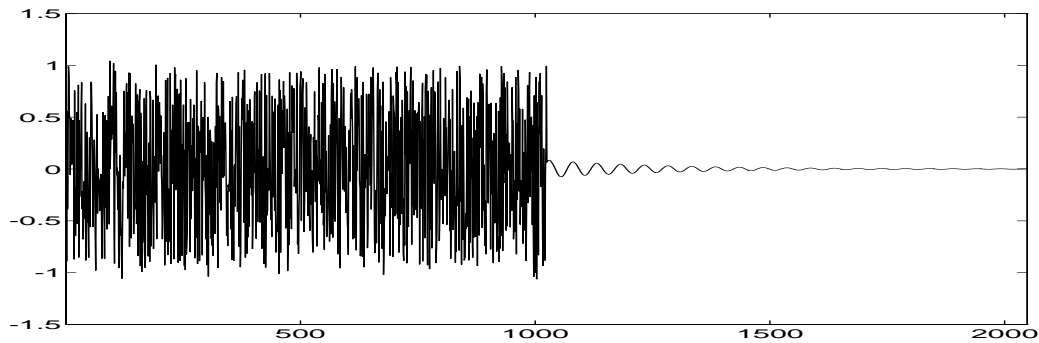


Figure 5-19. Burst Random - Signal from Load Cell (Voltage Feedback)

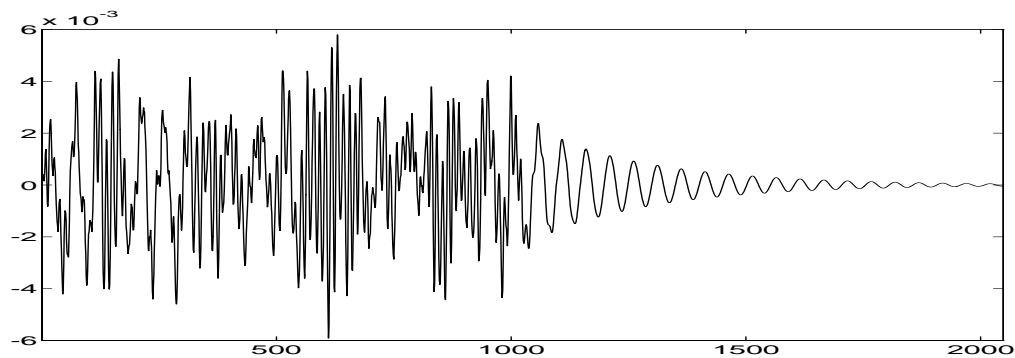


Figure 5-20. Burst Random - Signal from Accelerometer

For very lightly damped systems, the burst length may have to be shortened below 20 percent. This may yield an unacceptable signal to noise ratio (SNR). The number of power spectral averages used in the burst random excitation approach is a function of the reduction of the variance error and the need to have a significant number of averages to be certain that all frequencies have been adequately excited. plus the exciter/amplifier system trying to maintain the input at zero (voltage feedback amplifier in the excitation system).

Slow Random - The slow random signal is an ergodic, stationary random signal consisting only of integer multiples of the FFT frequency increment. This signal behaves just like the pseudo random signal but without the frequency shaping of the amplitude. The slow random signal is generated by cyclic averaging a random signal in order to produce digitally comb filtered excitation signal(s) with the proper characteristics.

MOOZ Random - The MOOZ random signal is an ergodic, stationary random signal consisting only of integer multiples of the FFT frequency increment frequency band limited to the frequency band of a ZOOM fast Fourier transform (FFT) (F_{\min} to F_{\max}). The MOOZ (ZOOM spelled backwards) random signal requires synchronization between the data acquisition and the digital-to-analog converter (DAC). The MOOZ random signal is essentially a slow random excitation signal adjusted to accommodate the frequencies of a ZOOM FFT.

The relationship between delay blocks and averages for some of the most commonly used random excitation methods are summarized in Table 5-3.

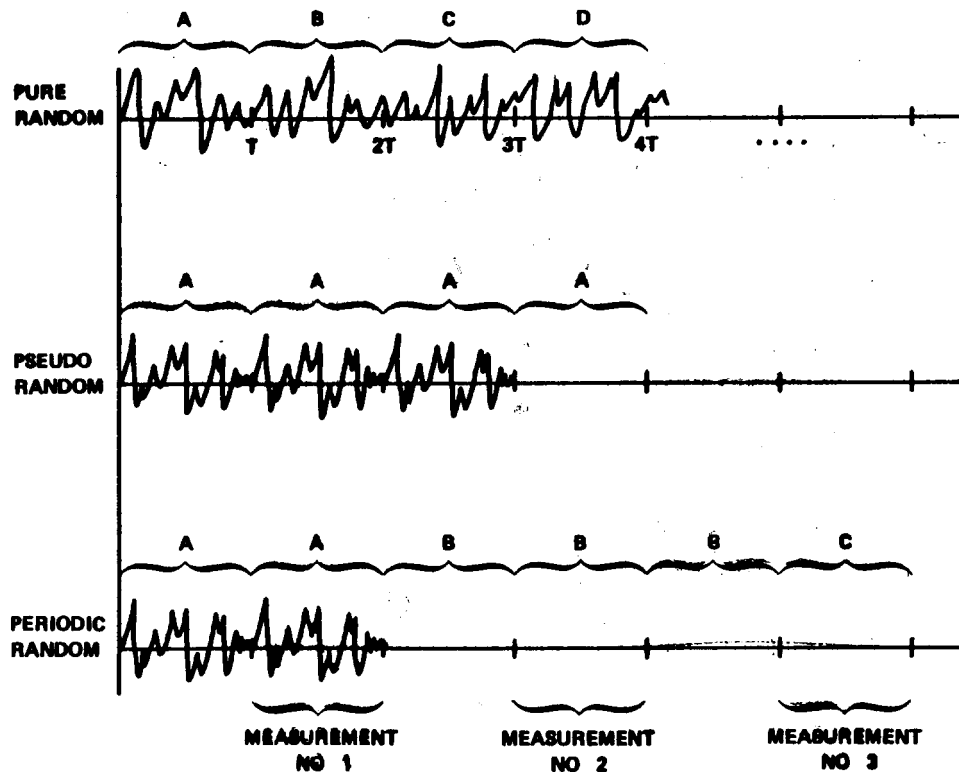


TABLE 5-3. Excitation Characteristics

Hybrid Random Excitation Methods

Several random excitation methods have recently been demonstrated that are hybrid methods involving combinations of burst random and pseudo random, burst random and periodic random together with cyclic averaging.

Burst Pseudo Random - Figure 5-21 shows the energy content of a hybrid excitation method that combines pseudo random with burst random. This excitation signal would be combined with cyclic averaging.

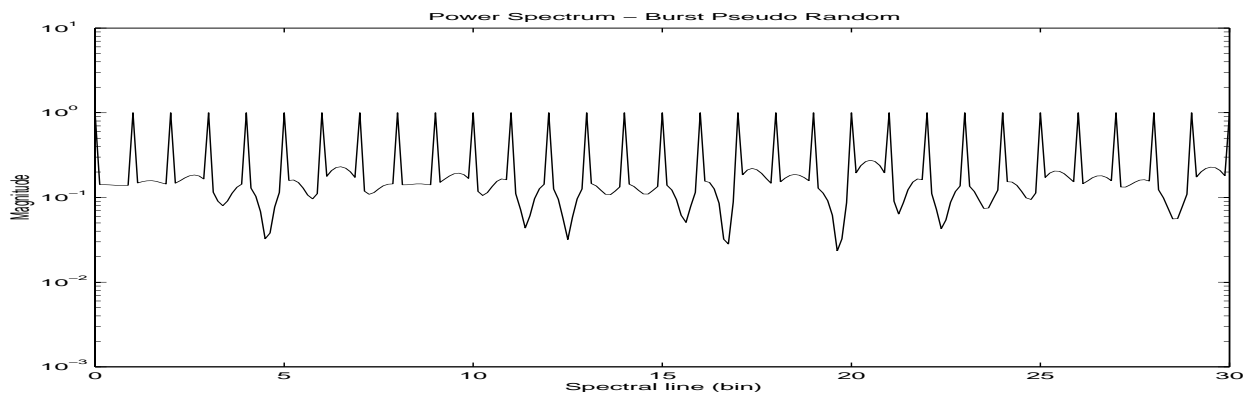


Figure 5-21. Signal Energy Content - Burst Pseudo Random

Burst Periodic Random - Figure 5-22 shows the energy content of a hybrid excitation method that combines periodic random with burst random. This excitation signal would be combined with cyclic averaging.

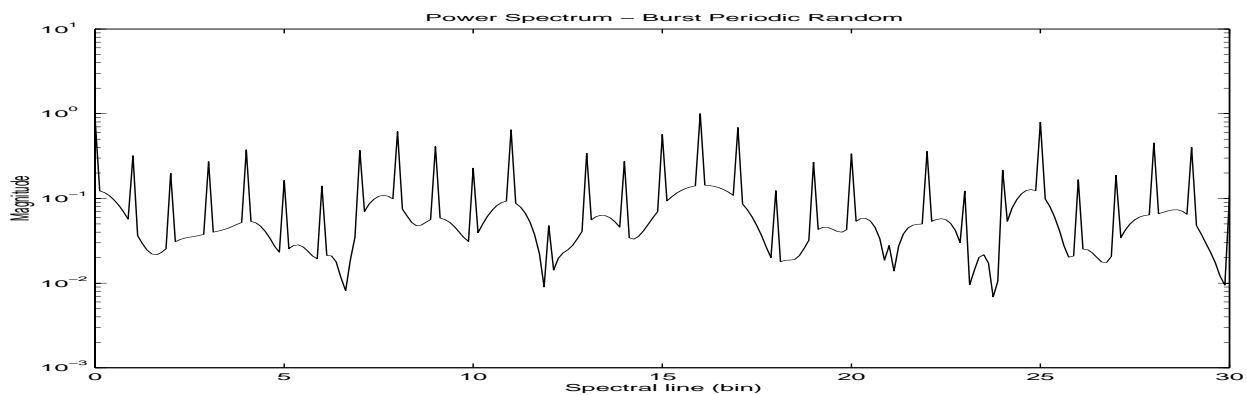


Figure 5-22. Signal Energy Content - Burst Periodic Random

5.3.5 Deterministic Excitation Methods

Slow Swept Sine - The slow swept sine signal is a periodic deterministic signal with a frequency that is an integer multiple of the FFT frequency increment. Sufficient time is allowed in the measurement procedure for any transient response to the changes in frequency to decay so that the resultant input and response histories will be periodic with respect to the sample period. Therefore, the total time needed to compute an entire frequency response function will be a function of the number of frequency increments required and the system damping.

Periodic Chirp - The periodic chirp is a deterministic signal where a sinusoid is rapidly swept from F_{\min} to F_{\max} within a single observation period (T). This signal is then repeated in a periodic fashion. While this signal is not random in characteristic, it is often included in discussions of random excitation since it has similar properties as pseudo random.

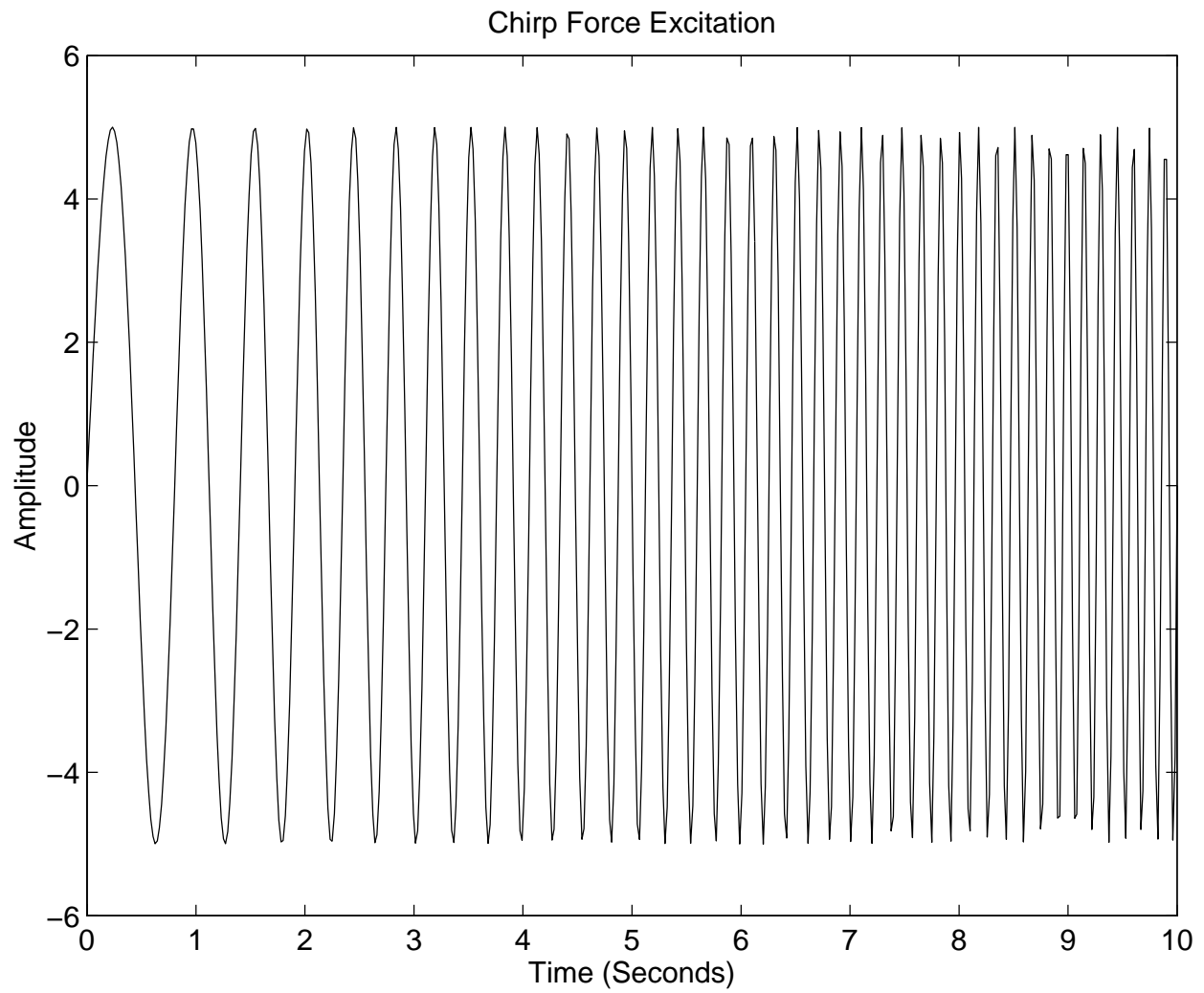


Figure 5-23. Typical Chirp Signal - Time Domain

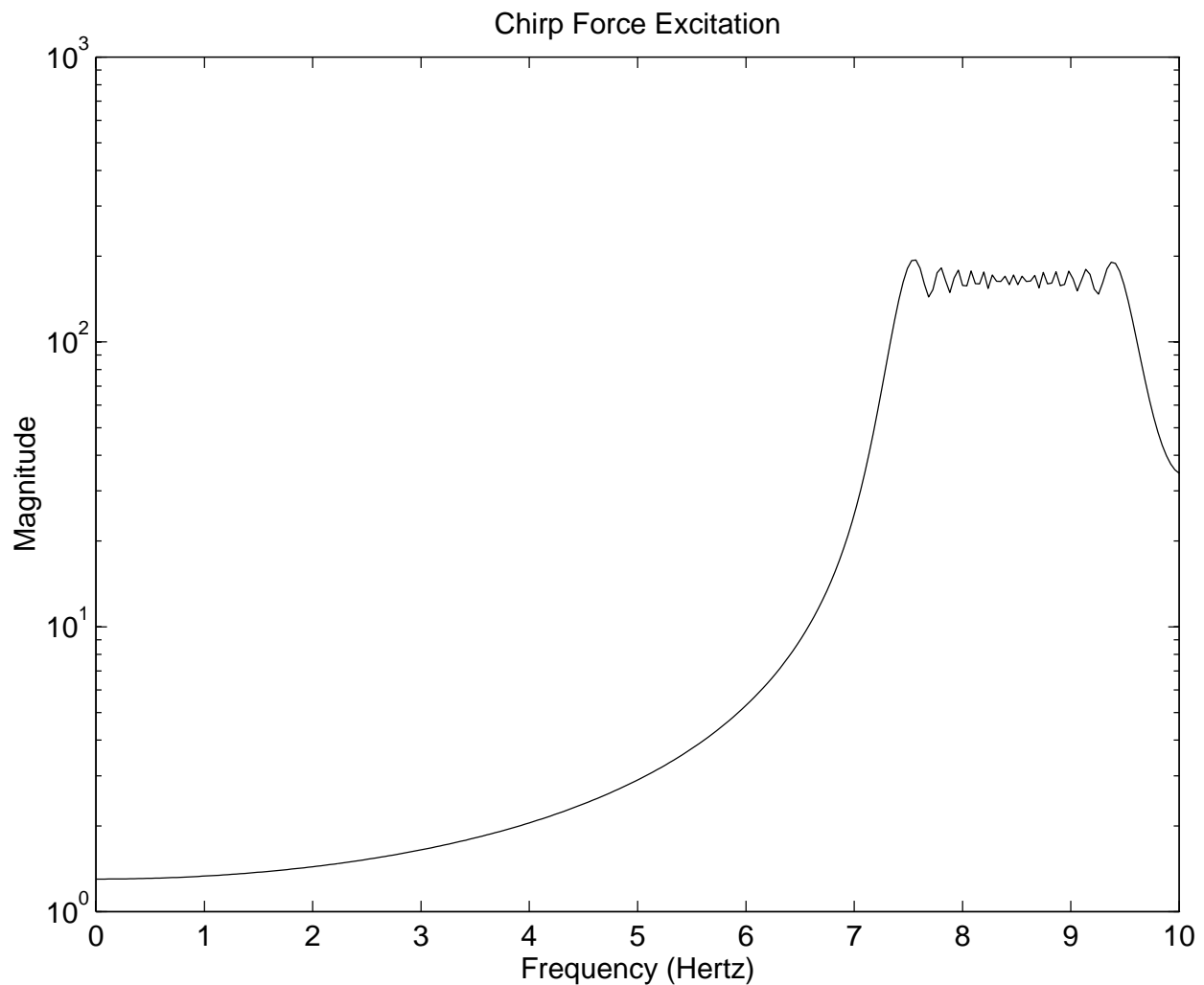


Figure 5-24. Typical Chirp Signal - Frequency Domain

Impact (Impulse) - The impact signal is a transient deterministic signal which is formed by applying an input pulse to a system lasting only a very small part of the sample period. The width, height, and shape of this pulse will determine the usable spectrum of the impact. Briefly, the width of the pulse will determine the frequency spectrum while the height and shape of the pulse will control the level of the spectrum. Impact signals have proven to be quite popular due to the freedom of applying the input with some form of an instrumented hammer. While the concept is straight forward, the effective utilization of an impact signal is very involved [33,34,37].

Step Relaxation - The step relaxation signal is a transient deterministic signal which is formed by releasing a previously applied static input. The sample period begins at the instant that the release occurs. This signal is normally generated by the application of a static force through a cable. The cable is then cut or allowed to release through a shear pin arrangement ^[39].

Table 5-4 summarizes the advantages and disadvantages for the most commonly used excitation signals.

Excitation Signal Characteristics								
	Steady State Sine	Pure Random	Pseudo Random	Periodic Random	Fast Sine	Impact	Burst Sine	Burst Random
Minimize Leakage	No	No	Yes	Yes	Yes	Yes	Yes	Yes
Signal-to-Noise Ratio	Very High	Fair	Fair	Fair	High	Low	High	Fair
RMS-to-Peak Ratio	High	Fair	Fair	Fair	High	Low	High	Fair
Test Measurement Time	Very Long	Good	Very Short	Fair	Fair	Very Short	Very Short	Very Short
Controlled Frequency Content	Yes	Yes *	Yes *	Yes *	Yes *	No	Yes *	Yes *
Controlled Amplitude Content	Yes	No	Yes *	No	Yes *	No	Yes *	No
Removes Distortion	No	Yes	No	Yes	No	No	No	Yes
Characterize Nonlinearity	Yes	No	No	No	Yes	No	Yes	No

* Special Hardware Required

TABLE 5-4. Summary of Excitation Signals

5.3.6 Excitation Example - H-Frame

The following example presents a single FRF measurement on an H-frame test structure in a test lab environment as a representative example. The configuration of the test involved two shaker locations (inputs) and eight response accelerometers (outputs). The test results are representative of all data taken on the H-frame structure. This H-frame test structure is very lightly damped and has been the subject of many previous studies.

For all FRF measurement cases, the same test configuration was used. Sensors were installed and left in place; no additions or changes were made to the test configuration other than altering the excitation, averaging and digital signal processing parameters. Therefore, any changes in the FRF measurements are assumed to be due to the change in measurement technique and not due to a test set-up variation. The test results were repeated to be certain that the results are representative.

All FRF measurements are estimated using the H_1 estimation algorithm using 1024 spectral (frequency) lines of information. The frequency bandwidth is from 0 to 250 Hertz for the 1024 spectral lines; only the first 80 % of the spectral lines (0 to 200 Hertz) are displayed in order to exclude the data affected by the anti-aliasing filters.

The FRF data is plotted with phase above log magnitude. The log magnitude portion of the plot also contains the relevant multiple coherence plotted on a linear scale in the background. The log magnitude scaling is annotated on the left side of the plot and the multiple coherence scaling is annotated on the right side of the plot.

Fourteen representative cases were measured on this structure. The relevant excitation and digital signal processing characteristics of each case are shown in Table 5-5.

Case	Signal Type	Frequency Shaping	Periodic Function	Burst Length	Window Function	N_d	N_c	N_{avg}	Total Blocks
Case 1	Random	No	No	No	Hann	0	1	20	20
Case 2	Random	No	No	No	Hann	0	5	4	20
Case 3	Random	No	No	Yes (75%)	Uniform	0	5	4	20
Case 4	Random	Pseudo	No	No	Uniform	4	1	4	20
Case 5	Random	No	Yes	No	Uniform	4	1	4	20
Case 6	Random	Pseudo	No	No	Uniform	3	1	5	20
Case 7	Random	No	Yes	No	Uniform	3	1	5	20
Case 8	Random	Pseudo	No	Yes (75%)	Uniform	0	5	4	20
Case 9	Random	No	Yes	Yes (75%)	Uniform	0	5	4	20
Case 10	Random	No	No	Yes (75%)	Uniform	0	8	12	20
Case 11	Random	No	No	No	Hann	0	1	96	96
Case 12	Random	No	No	No	Hann	0	8	12	96
Case 13	Random	Pseudo	No	No	Uniform	3	2	4	20
Case 14	Random	No	Yes	No	Uniform	3	2	4	20

TABLE 5-5. Test Cases - Excitation/Averaging/DSP Parameters

Case 1 (Figure 5-25) is considered a baseline case since this a very popular method for making a FRF measurement and it can be easily made on all data acquisition equipment. However, it is clear that in this measurement situation, there is a significant drop in the multiple coherence function at frequencies consistent with the peaks in the FRF measurement. This characteristic drop in multiple (or ordinary) coherence is often an indication of a leakage problem. This can be confirmed if a leakage reduction method reduces or eliminates the problem when the measurement is repeated. In all subsequent cases, the test configuration was not altered in any way - data was acquired simply using different excitation, averaging and digital signal processing combinations.

Case 2 (Figure 5-26) demonstrates an improvement over Case 1 when the same total measurement time is used but cyclic averaging is used to reduce the leakage error. Case 3 (Figure 5-27) further demonstrates that burst random with cyclic averaging improves the measurement further. Again the total measurement time remains the same.

Cases 4 through 7 (Figures 5-28 through 5-31) demonstrate the quality of FRF measurements

that can be achieved with pseudo and periodic random excitation methods with very few power spectral averages.

Cases 8 and 9 (Figures 5-32 through 5-33) are hybrid techniques involving the combination of burst random with pseudo and periodic random excitation together with cyclic averaging.

Case 10 (Figure 5-34) demonstrates that Case 3 can be marginally improved with more averages, both cyclic and power spectral averages. However, Case 11 (Figure 5-35) demonstrates that Case 1 (Random with Hann Window) cannot be improved by adding power spectral averages. This is a popular misconception that adding power spectral averages will improve the FRF estimate. This is clearly not true for this case.

Case 12 (Figure 36) demonstrates that additional cyclic averages, together with power spectral averages, is an improvement over Case 2 but the improvement is not significant considering the additional measurement time.

Finally, Cases 13 and 14 (Figures 5-37 through 5-38) demonstrate that, when pseudo and periodic random excitation is coupled with cyclic averaging, a nearly perfect FRF measurement results. Note also that in almost every case where high quality FRF measurements have been achieved, window functions are not required so correction for the window characteristics is unnecessary.

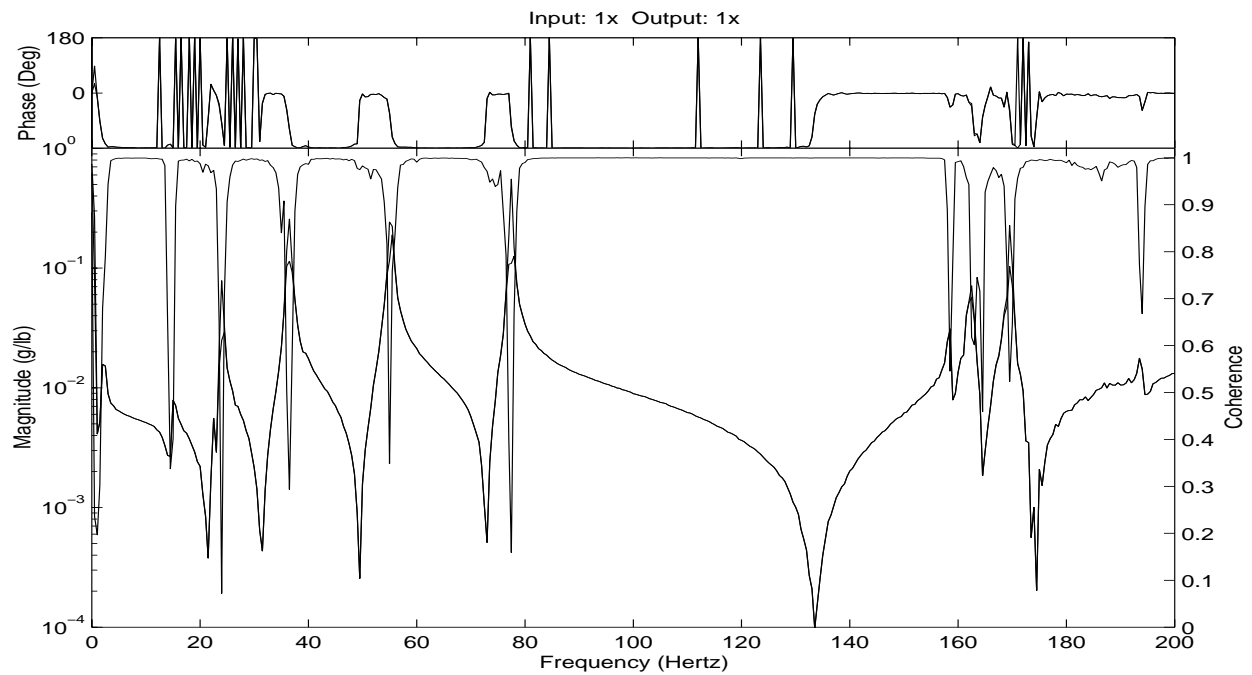


Figure 5-25. Case 1: Random Excitation with Hann Window

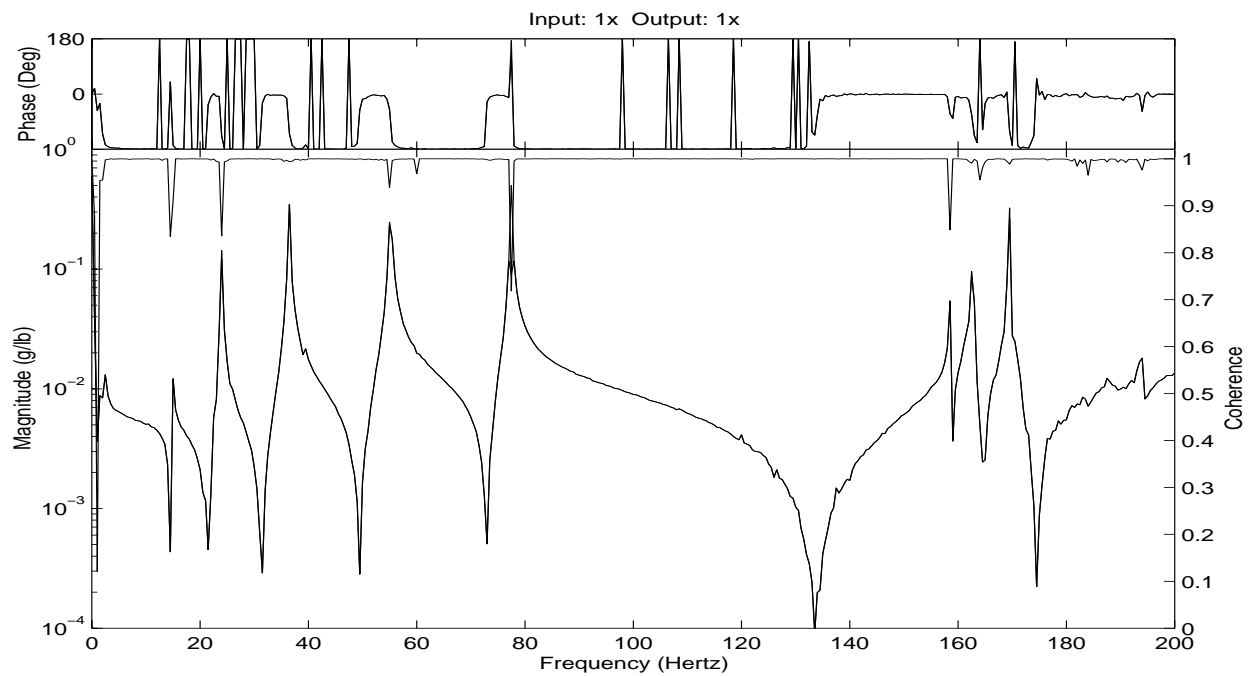


Figure 5-26. Case 2: Random Excitation with Hann Window and Cyclic Averaging

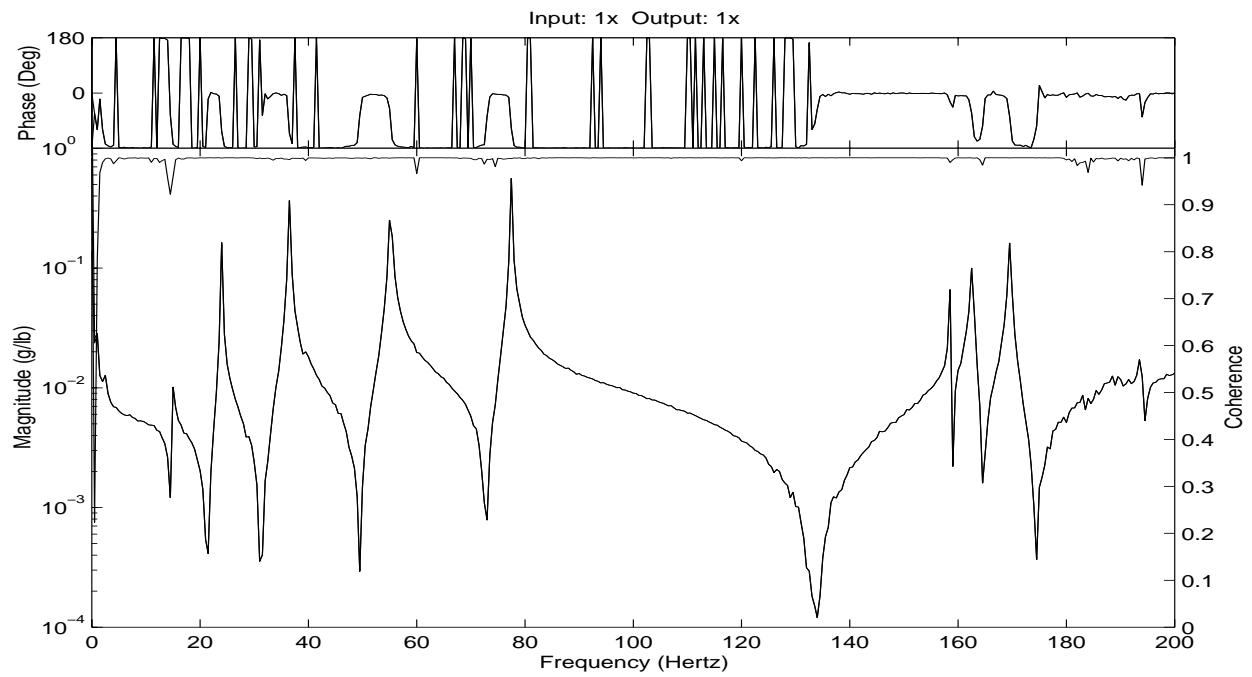


Figure 5-27. Case 3: Burst Random Excitation with Cyclic Averaging

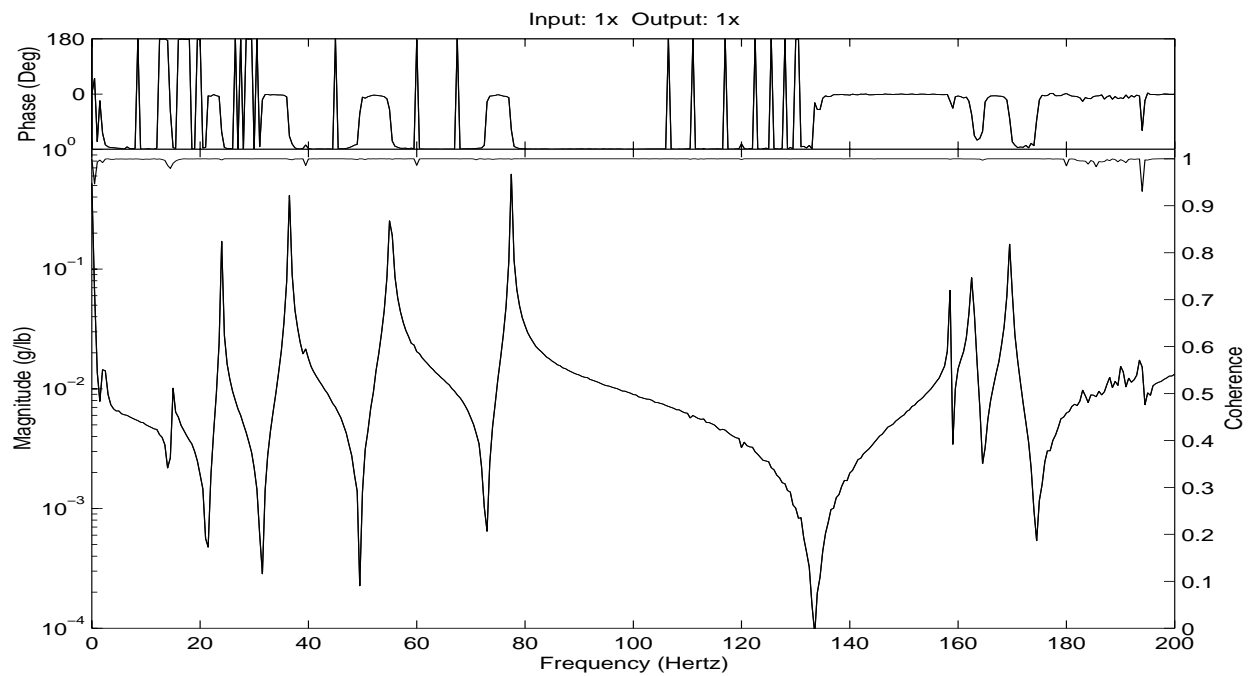


Figure 5-28. Case 4: Pseudo Random Excitation

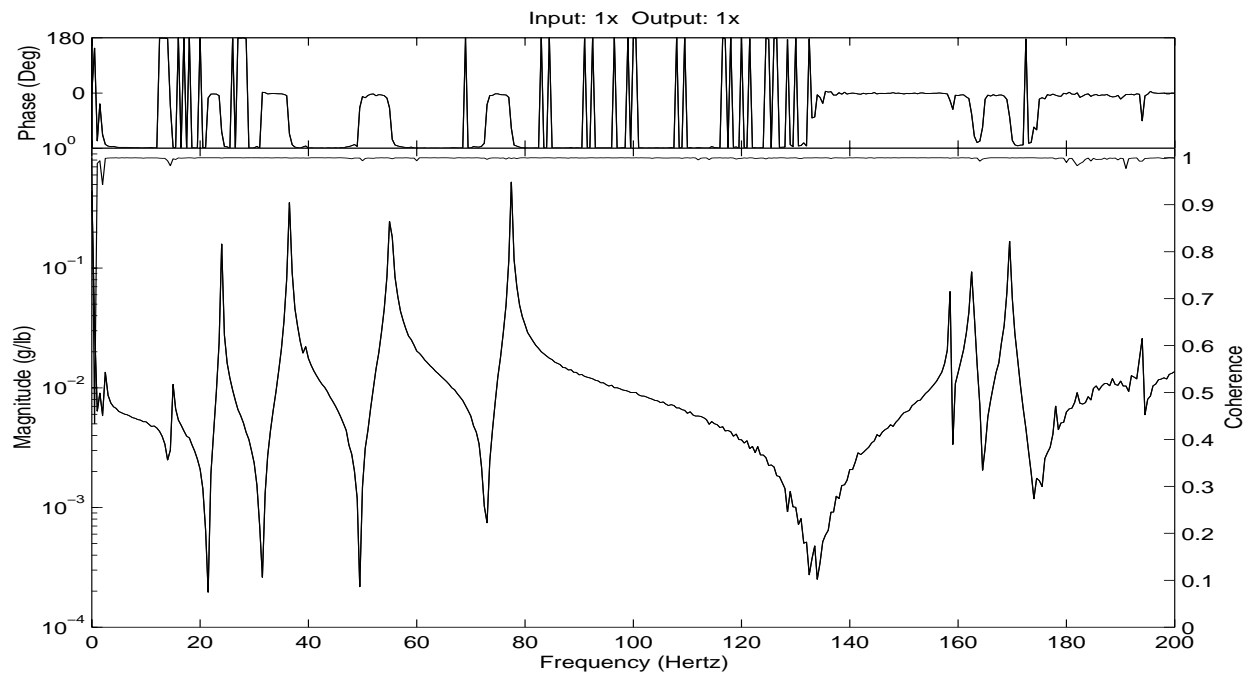


Figure 5-29. Case 5: Periodic Random Excitation

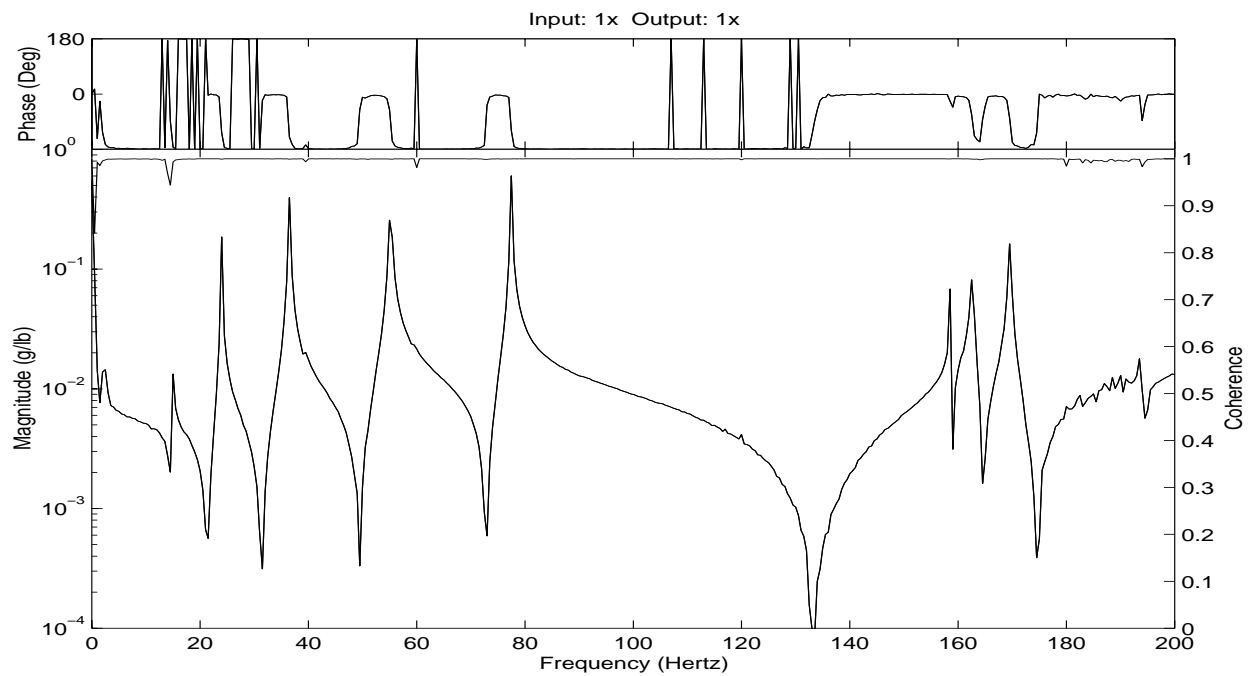


Figure 5-30. Case 6: Pseudo Random Excitation

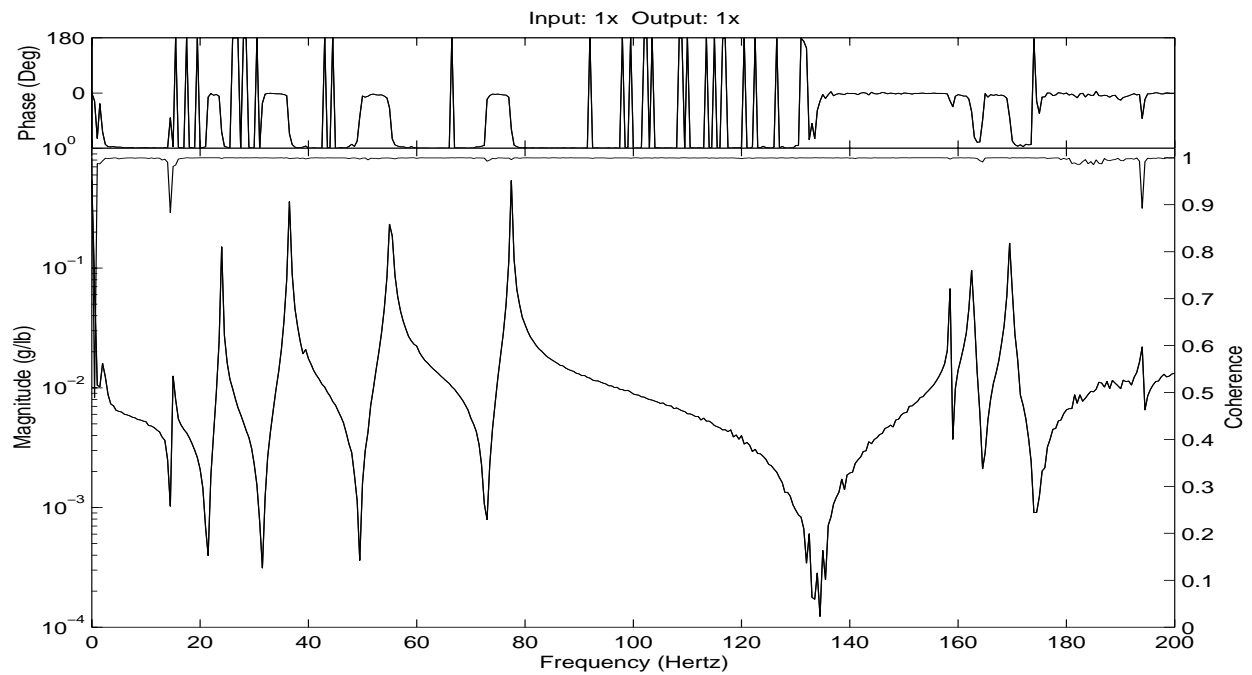


Figure 5-31. Case 7: Periodic Random Excitation

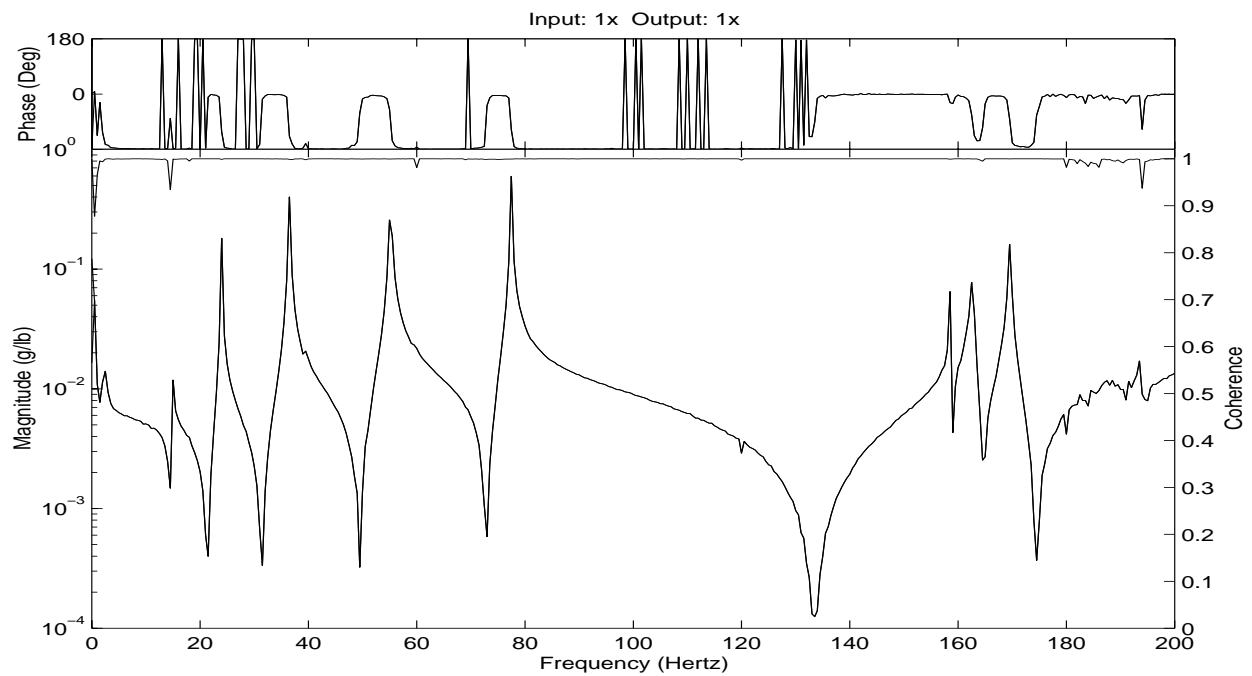


Figure 5-32. Case 8: Burst Pseudo Random Excitation with Cyclic Averaging

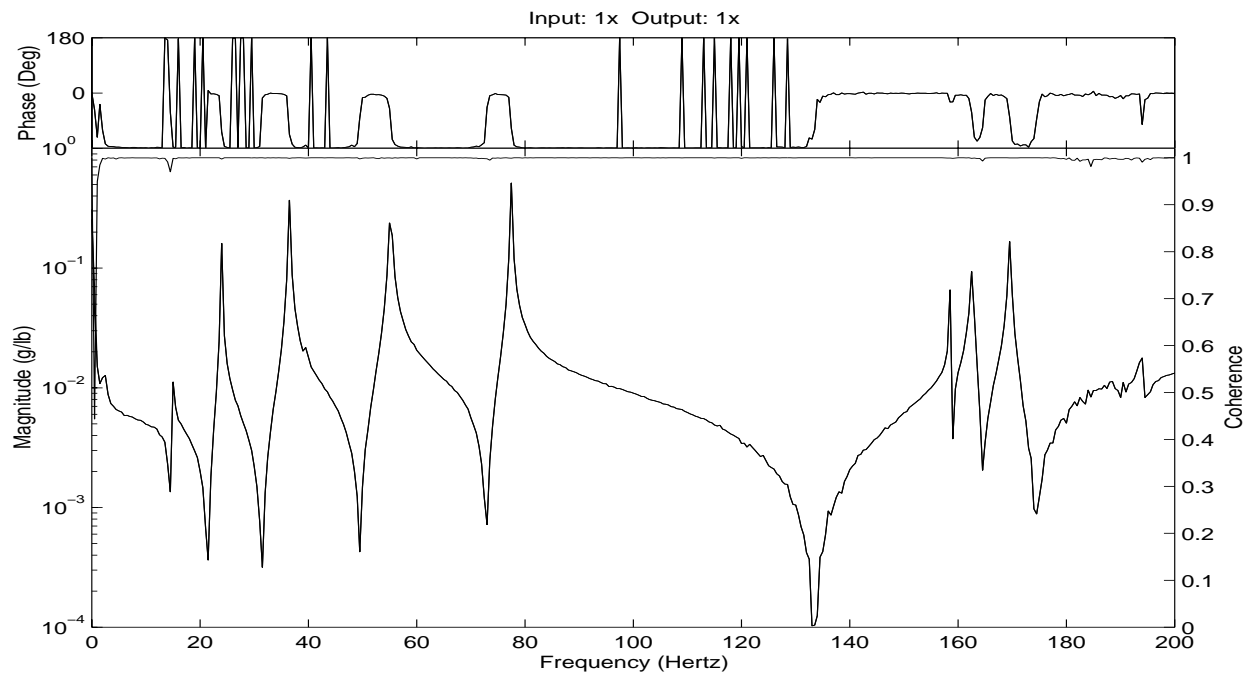


Figure 5-33. Case 9: Burst Periodic Random Excitation with Cyclic Averaging

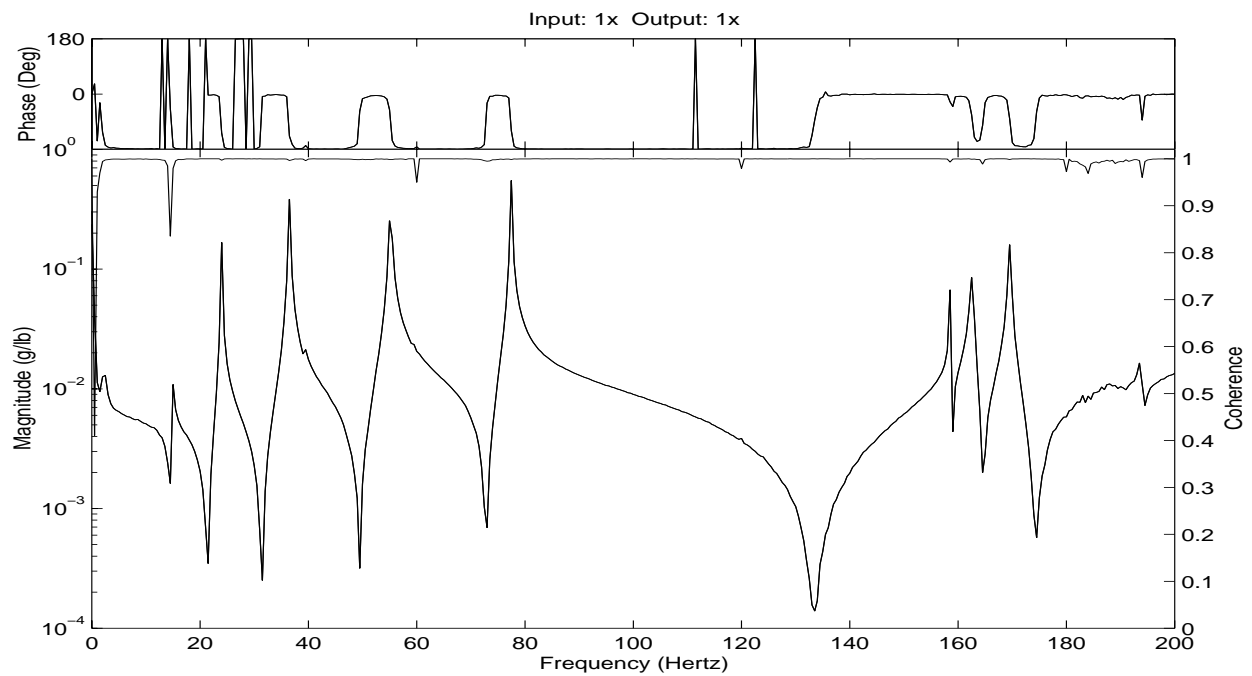


Figure 5-34. Case 10: Burst Random Excitation with Cyclic Averaging

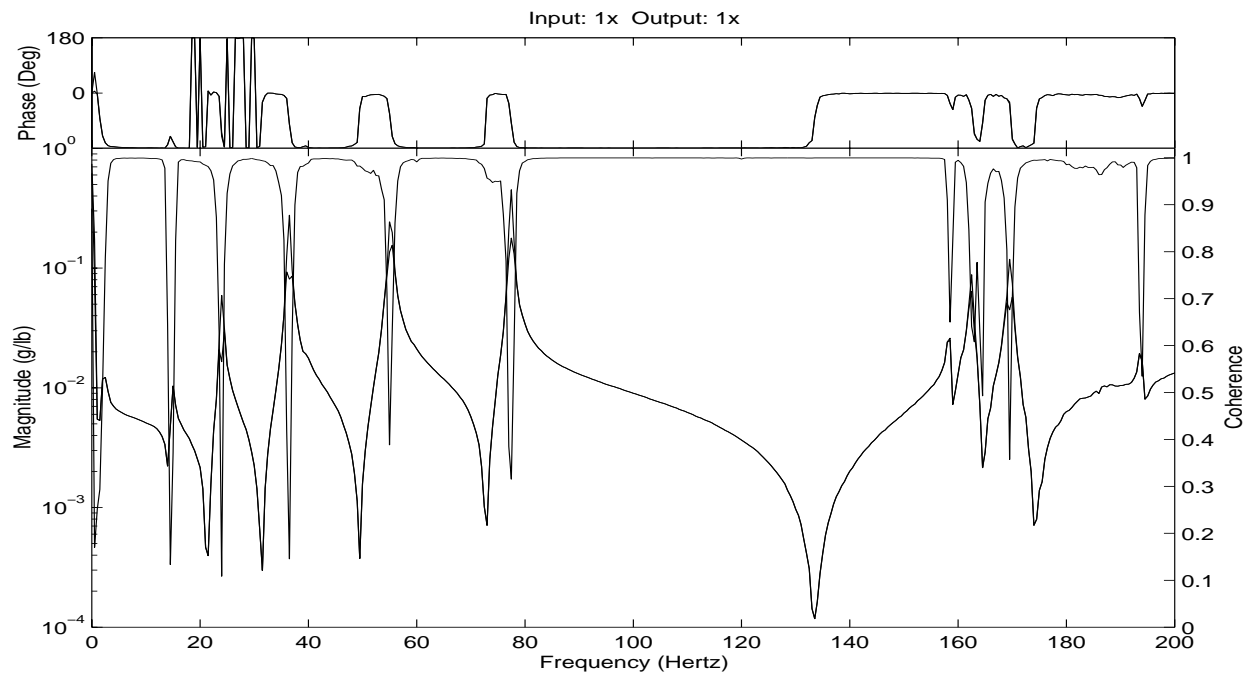


Figure 5-35. Case 11: Random Excitation with Hann Window

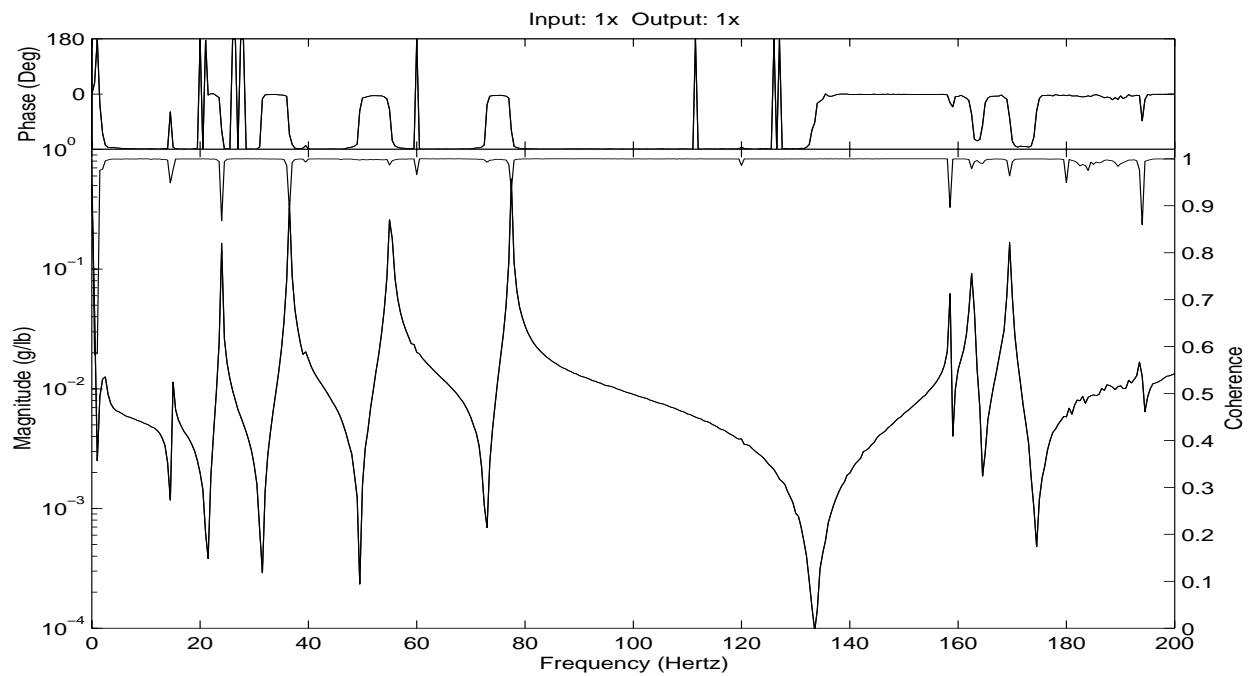


Figure 5-36. Case 12: Random Excitation with Hann Window and Cyclic Averaging

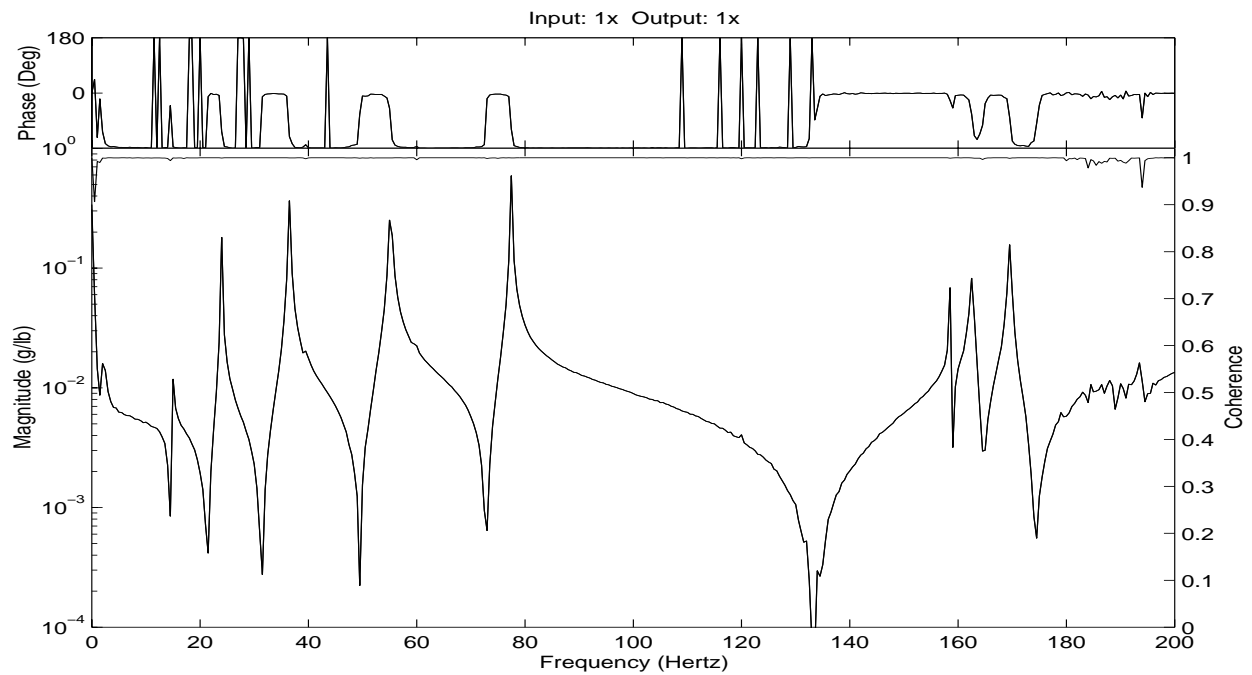


Figure 5-37. Case 13: Pseudo Random Excitation with Cyclic Averaging

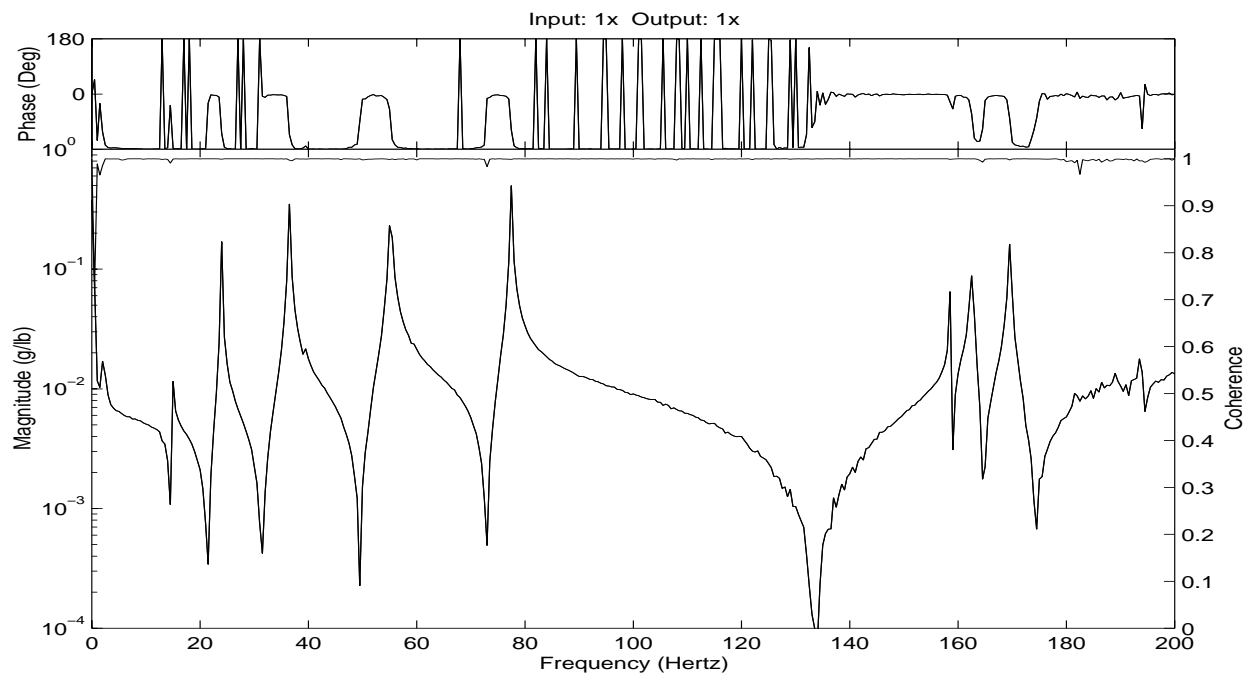


Figure 5-38. Case 14: Periodic Random Excitation with Cyclic Averaging

It is clear that in many of the measurement cases, the multiple coherence can be improved dramatically using simple excitation, averaging and digital signal processing methods. Note that, as the multiple coherence improves, dramatic changes in the FRF magnitude accompany the improvement (factors of 2 to more than 10). When estimating modal parameters, the frequency and mode shape would probably be estimated reasonably in all cases. However, the damping and modal scaling would be distorted (over estimating damping and under estimating modal scaling). Using these results for model prediction or FE correction would bias the predicted results.

The most important conclusion that can be drawn from the results of this measurement exercise on a lightly damped mechanical system is that accurate data is an indirect function of measurement time or number of averages but is a direct function of measurement technique. The leakage problem associated with utilizing fast Fourier transform (FFT) methodology to estimate frequency response functions on a mechanical system with light damping is a serious problem that can be managed with proper measurement techniques, like periodic and pseudo random excitation or cyclic averaging with burst random excitation. Hybrid techniques demonstrated in this paper clearly show that a number of measurement techniques are acceptable but some commonly used techniques are clearly unacceptable.

It is also important to note that while ordinary/multiple coherence can indicate a variety of input/output problems, a drop in the ordinary/multiple coherence function, at the same frequency as a lightly damped peak in the frequency response function, is often a direct indicator of a leakage problem. Frequently, comparisons are made between results obtained with narrowband (sinusoid) excitation and broadband (random) excitation when the ordinary/multiple coherence function clearly indicates a potential leakage problem. It is important that good measurement technique be an integral part of such comparisons.

5.3.7 Impact Excitation

Impact testing is an attempt to match the input and output data to the requirement of the discrete or fast Fourier transform that the data be a totally observed transient in the observation time (T). While the impact is almost always totally observable, the response for lightly damped systems may not be. Special windows are often used for impact testing that accommodate the characteristics of the transient input and the response of the system to a transient input.

Impact excitation is widely used due to the minimal equipment required, portability and low cost of the impact devices and broad applicability to both small, medium and large size structures. However, impact testing also suffers from limitations imposed by the human control of the impact. Repeatability and consistency of the impact (force and direction) cannot be guaranteed, particularly as the test becomes long and repetitious. Care must be taken to ensure that the impact and response is not too small, not too large (overload) and that there is only one impact per observation period.

When impact testing is used, windows are generally required on both the force and response data in order to minimize different errors. The force window is used to eliminate the signal coming from the impact device after the short duration impact is over. This eliminates electrical noise and spurious output from the hammer during data acquisition that is caused by motion of the impact device that does not put force into the system. The response (exponential) window is used to force the response closer to zero by the end of the observation period (T) and should be used carefully. If the response is already near zero at time T , no response window should be added. To be theoretically correct and to allow for the effects of this response window to be accounted for, the decay rate of the exponential must be recorded and the same window should also be applied to the input data, in addition to the force window.

Force Window

Force windows are used to improve the signal-to-noise problem caused by the noise on the input channel measured after the impact is completed. Note that the exponential window used on the response should also be applied to the input in addition to the force window.

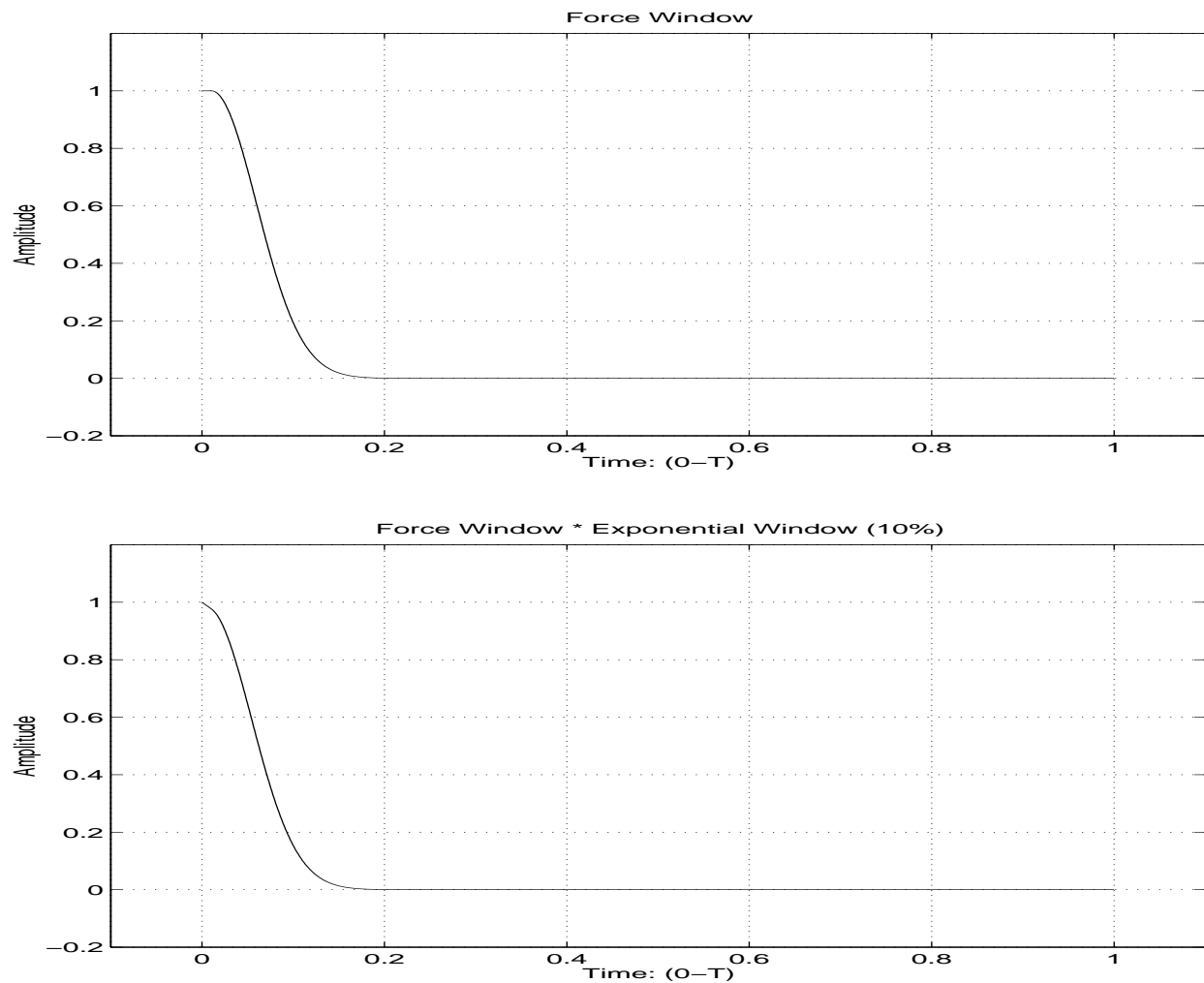
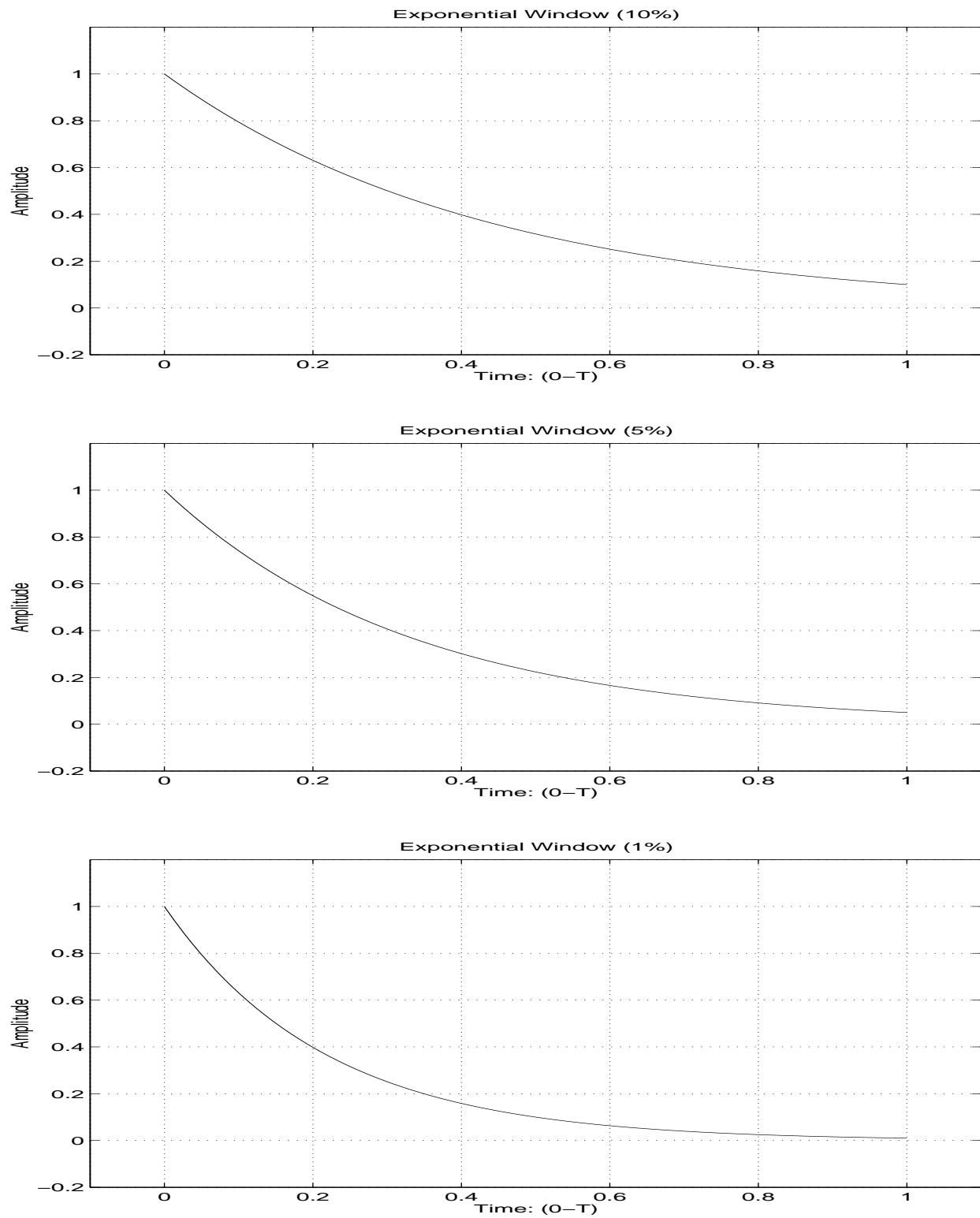


Figure 5-39. Typical Force Windows

Response (Exponential) Windows

Response (exponential) windows are used to minimize the leakage error for lightly damped systems by attenuating the response so that it decays to zero within the observation period. Normally, for lightly damped systems, a window that attenuates to 1-5 percent at the end of the response is appropriate. For heavily damped systems, a window that is similar to the decay of the system will attenuate any noise.

**Figure 5-40. Typical Response Windows**

Response (Exponential) Windows Correction

The windows that are added to the force and response signals must be corrected. Primarily, the response (exponential) window may add significant damping to the resultant frequency response function. This can only be corrected after the modal damping for each mode is found.

- $h_{pq}(t) = \sum_{r=1}^{2N} A_{pqr} e^{\lambda_r t}$
- $e^{\beta t} h_{pq}(t) = e^{\beta t} \sum_{r=1}^{2N} A_{pqr} e^{\lambda_r t}$
- $e^{\beta t} h_{pq}(t) = \sum_{r=1}^{2N} A_{pqr} e^{\beta t} e^{\lambda_r t}$
- $e^{\beta t} h_{pq}(t) = \sum_{r=1}^{2N} A_{pqr} e^{(\lambda_r + \beta)t} = \sum_{r=1}^{2N} A_{pqr} e^{\hat{\lambda}_r t}$
- $\hat{\lambda}_r = \hat{\sigma}_r + j \hat{\omega}_r = (\sigma_r + \beta) + j \omega_r$
- $\hat{\sigma}_r = \sigma_r + \beta$
- $\sigma_r = \hat{\sigma}_r - \beta$
- $\omega_r = \hat{\omega}_r$

5.4 Structural Testing Conditions

The test condition for any modal analysis test involves several environmental factors as well as appropriate boundary conditions. First of all, the temperature, humidity, vacuum, and gravity effects must be properly considered to match with previous analysis models or to allow the experimentally determined model to properly reflect the system.

In addition to the environmental concerns, the boundary conditions of the system under test are very important. Traditionally, modal analysis tests have been performed under the assumption that the test boundary conditions can be made to conform to one of four conditions:

- Free-free boundary conditions (Impedance is zero).
- Fixed boundary conditions (Impedance is infinite)
- Operating boundary conditions (Impedance is correct).
- Arbitrary boundary conditions (Impedance is known).

It should be obvious that, except in very special situations, none of these boundary conditions can be practically achieved. Instead, practical guidelines are normally used to evaluate the appropriateness of the chosen boundary conditions. For example, if a free-free boundary is chosen, the desired frequency of the highest rigid body mode should be a factor of ten below the first deformation mode of the system under test. Likewise, for the fixed boundary test, the desired interface stiffness should be a factor of ten greater than the local stiffness of the system under test. While either of these practical guidelines can be achieved for small test objects, a large class of flight vehicle systems can not be acceptably tested in either configuration. Arguments have been made that the impedance of a support system can be defined (via test and/or analysis) and the effects of such a support system can be eliminated from the measured data. This technique is theoretically sound but, due to significant dynamics in the support system and limited measurement dynamics, this approach has not been uniformly applicable.

In response to this problem, many alternate structural testing concepts have been proposed and are under current evaluation. Active, or combinations of active and passive, suspension systems are being evaluated, particularly for application to very flexible space structures. Active inert gas suspension systems have been used in the past for the testing of smaller commercial and military aircraft and, in general, such approaches are formulated to better match the requirements of a free-free boundary condition.

Another alternate test procedure is to define a series of relatively conventional tests with various boundary conditions. The various boundary conditions are chosen in such a way that each perturbed boundary condition can be accurately modeled (for example, the addition of a large mass at interface boundaries). Therefore, as the experimental model is acquired for each configuration and used to validate and correct the associated analytical model, the underlying model will be validated and corrected accordingly. This procedure has the added benefit of adding the influence of modes of vibration that would normally occur above the maximum frequency of the test into the validation of the model. For example, the inertial effect of the

addition of a mass at an interface will cause a downward shift in frequency of any mode that is active at the interface (modes that are not affected by the interface dynamics will not be shifted). Since this shift is measured and the analytical model can accurately define the dynamics of the added mass, any inaccuracy in the analytical prediction of the frequency shifts as well as the corresponding effects on the modal vectors will be due to the lack of fidelity of the underlying analytical model.

Recently, other researchers have proposed multiple configurations of test conditions as a methodology of utilizing practical test configurations in the testing of flight vehicle systems. In a related research area, work is progressing on using constrained testing together with direct parameter estimation methods to define the characteristics of the unconstrained structure. In this test procedure, the excitation forces and the constraint forces are measured together with appropriate response information. The direct parameter estimation method produces a general matrix model that describes the unconstrained (free-free) structural system. All of these newer methods will increase the cost (time, financial, technical) of performing structural tests with the attendant incremental increase in the accuracy of the test results.

5.5 Practical Measurement Considerations

There are several factors that contribute to the quality of actual measured frequency response function estimates. Some of the most common sources of error are due to measurement mistakes. With a proper measurement approach, most of this type of error, such as overloading the input, extraneous signal pick-up via ground loops or strong electric or magnetic fields nearby, etc., can be avoided. Violation of test assumptions are often the source of another inaccuracy and can be viewed as a measurement mistake. For example, frequency response and coherence functions have been defined as parameters of a linear system. Nonlinearities will generally shift energy from one frequency to many new frequencies, in a way which may be difficult to recognize. The result will be a distortion in the estimates of the system parameters, which may not be apparent unless the excitation is changed. One way to reduce the effect of nonlinearities is to randomize these contributions by choosing a randomly different input signal for each of the n measurements. Subsequent averaging will reduce these contributions in the same manner that random noise is reduced. Another example involves control of the system input. One of the most obvious requirements is to excite the system with energy at all frequencies for which

measurements are expected. It is important to be sure that the input signal spectrum does not have "holes" where little energy exist. Otherwise, coherence will be very low, and the variance on the frequency response function will be large.

Assuming that the system is linear, the excitation is proper, and obvious measurement mistakes are avoided, some amount of error (noise) will be present in the measurement process. Five different approaches can be used to reduce the error involved in frequency response function measurements in current fast Fourier transform (FFT) analyzers. First of all, the use of *different frequency response function estimation algorithms* (H_v compared to H_1) will reduce the effect of the leakage error on the estimation of the frequency response function computation. The use of *averaging* can significantly reduce errors of both variance and bias and is probably the most general technique in the reduction of errors in frequency response function measurement. *Selective excitation* is often used to verify nonlinearities or randomize characteristics. In this way, bias errors due to system sources can be reduced or controlled. The *increase of frequency resolution* through the zoom fast Fourier transform can improve the frequency response function estimate primarily by reduction of the leakage bias error due to the use of a longer time sample. The zoom fast Fourier transform by itself is a linear process and does not involve any specific error reduction characteristics compared to a baseband fast Fourier transform(FFT). Finally, the *use of weighting functions(windows)* is widespread and much has been written about their value ^[1-3,40-41]. Primarily, weighting functions compensate for the bias error (leakage) caused by the analysis procedure.

5.6 References

- [1] Bendat, J.S.; Piersol, A.G., **Random Data: Analysis and Measurement Procedures**, John Wiley and Sons, Inc., New York, 1971, 407 pp.
- [2] Bendat, J. S., Piersol, A. G., **Engineering Applications of Correlation and Spectral Analysis**, John Wiley and Sons, Inc., New York, 1980, 302 pp.
- [3] Otnes, R.K., Enochson, L., **Digital Time Series Analysis**, John Wiley and Sons, Inc., New York, 1972, 467 pp.
- [4] Hsu, H.P., **Fourier Analysis**, Simon and Schuster, 1970, 274 pp.
- [5] Dally, J.W.; Riley, W.F.; McConnell, K.G., **Instrumentation for Engineering Measurements**, John Wiley & Sons, Inc., New York, 1984.

- [6] Strang, G., **Linear Algebra and Its Applications, Third Edition**, Harcourt Brace Jovanovich Publishers, San Diego, 1988, 505 pp.
- [7] Lawson, C.L., Hanson, R.J., **Solving Least Squares Problems**, Prentice-Hall, Inc., Englewood Cliffs, New Jersey, 1974, 340 pp.
- [8] Jolliffe, I.T., **Principal Component Analysis** Springer-Verlag New York, Inc., 1986, 271 pp.
- [9] Akaike, H., "On the Statistic Estimation of the Frequency Response Function of a System Having Multiple Inputs", *Annals of the Institute of Statistical Mathematics*, Volume 17, Number 2, 1965.
- [10] Carter, G.C.; Knapp, C.H.; Nuttall, A.H., "Estimation of the Magnitude-Squared Coherence Function Via Overlapped Fast Fourier Transform Processing", *IEEE Transactions on Audio and Electroacoustics*, August 1973, pp. 337-344.
- [11] Wada, B. K., "Modal Test - Measurement and Analysis Requirements", SAE Paper Number 751066, 1975, 17 pp.
- [12] Ramsey, K. A.; Richardson, M., "Making Effective Transfer Function Measurements for Modal Analysis", Hewlett-Packard Co., 1975.
- [13] Ramsey, K., "Effective Measurements for Structural Dynamics Testing: Part I", *Sound and Vibration*, November, 1975.
- [14] Ramsey, K., "Effective Measurements for Structural Dynamics Testing: Part II", *Sound and Vibration*, April, 1976.
- [15] Potter, R. W., "Matrix Formulation of Multiple and Partial Coherence", *Journal of the Acoustic Society of America*, Volume 66, Number 3, March 1977, pp. 776-781.
- [16] Dodds, C.J., Robson, J.D., "Partial Coherence in Multivariate Random Processing", *Journal of Sound and Vibration*, Volume 42, Number 2, 1975, pp. 243-249.
- [17] Ewins, D.J., Griffin, J., "A State-of-the-Art Assessment of Mobility Measurement Techniques - Results for the Mid-Range Structures", *Journal of Sound and Vibration*, Volume 78, Number 2, 1981, pp. 197-222.
- [18] Allemang, R. J., "Investigation of Some Multiple Input/Output Frequency Response Function Experimental Modal Analysis Techniques", Doctor of Philosophy Dissertation, University of Cincinnati, Mechanical Engineering Department, 1980, 358 pp.
- [19] Allemang, R.J., Rost, R.W., Brown, D.L., "Dual Input Estimation of Frequency Response Functions for Experimental Modal Analysis of Aircraft Structures", *Proceedings, International Modal Analysis Conference*, pp.333-340, 1982.
- [20] Carbon, G.D., Brown, D.L., Allemang, R.J., "Application of Dual Input Excitation Techniques to the Modal Testing of Commercial Aircraft", *Proceedings, International Modal Analysis Conference*, pp.559-565, 1982.
- [21] Allemang, R.J., Brown, D.L., Rost, R.W., "Dual Input Estimation of Frequency Response Functions for Experimental Modal Analysis of Automotive Structures", SAE Paper No. 820193.
- [22] Allemang, R.J., Rost, R.W., Brown, D.L., "Dual Input Estimation of Frequency Response Functions for Experimental Modal Analysis of Aircraft Structures", *Proceedings, International Modal Analysis Conference*, pp.333-340, 1982.
- [23] Allemang, R.J., Brown, D.L., Rost, R.W., "Multiple Input Estimation of Frequency Response Functions for Experimental Modal Analysis", U.S. Air Force Report Number AFATL-TR-84-15, 1984, 185 pp.
- [24] Allemang, R.J., Brown, D.L., Rost, R.W., "Measurement Techniques for Experimental Modal Analysis", *Experimental Modal Analysis and Dynamic Component Synthesis*, USAF Technical Report, Contract Number F33615-83-C-3218, AFWAL-TR-87-3069, Volume 2, 1987.

- [25] Cobb, R.E., Mitchell, L.D., "A Method for the Unbiased Estimate of System FRFs in the presence of Multiple-Correlated Inputs", *Journal of Analytical and Experimental Modal Analysis*, Volume 3, Number 4, 1988, pp. 123-128.
- [26] Mitchell, L.D., Cobb, R.E., Deel, J.C., Luk, Y.W., "An Unbiased Frequency Response Function Estimator", *Journal of Analytical and Experimental Modal Analysis*, Volume 3, Number 1, 1988, pp. 12-19.
- [27] Vold, H., Crowley, J., Rocklin, G. "A Comparison of H_1 , H_2 , H_v , Frequency Response Functions," Proceedings, International Modal Analysis Conference, 1985, pp.272-278.
- [28] Brown, D.L., Carbon, G., Zimmerman, R.D., "Survey of Excitation Techniques Applicable to the Testing of Automotive Structures", SAE Paper No. 770029, 1977.
- [29] Allemang, R.J., Phillips, A.W., "A New Excitation Method: Combining Burst Random Excitation with Cyclic Averaging", Proceedings, International Modal Analysis Conference, pp. 891-899, 1998.
- [30] "Using Cyclic Averaging with Impact Testing", William A. Fladung, Andrew T. Zucker, Allyn W. Phillips, Randall J. Allemang Proceedings, International Modal Analysis Conference, 7 pp., 1999.
- [31] "Frequency Resolution Effects on FRF Estimation: Cyclic Averaging vs. Large Block Size", Allyn W. Phillips, Andrew T. Zucker, Randall J. Allemang Proceedings, International Modal Analysis Conference, 4 pp., 1999.
- [32] "A Comparison of MIMO-FRF Excitation/Averaging Techniques on Heavily and Lightly Damped Structures", Phillips, A.W., Zucker, A.T., Allemang, R.J., Proceedings, International Modal Analysis Conference, 10 pp., 1999.
- [33] "An Overview of MIMO-FRF Excitation/Averaging Techniques", Phillips, A.W., Allemang, R.J., Zucker, A.T., Proceedings, International Conference on Noise and Vibration Engineering, Volume 1, Katholieke Universiteit Leuven, Belgium, 12 pp., 1998.
- [34] Halvorsen, W.G., Brown, D.L., "Impulse Technique for Structural Frequency Response Testing", Sound and Vibration Magazine, November, 1977, pp. 8-21.
- [35] Imes, R.S., Jennings, W.P., Olsen, N.L., "The Use of Transient Testing Techniques in Boeing YC-14 Flutter Clearance Program", AIAA Paper Number 78-0505, 1978.
- [36] Allemang, R.J., Rost, R.W., Brown, D.L., "Multiple Input Estimation of Frequency Response Functions: Excitation Considerations", ASME Paper Number 83-DET-73, 1983, 11 pp.
- [37] Van Karsen, C., "A Survey of Excitation Techniques for Frequency Response Function Measurement", Master of Science Thesis, University of Cincinnati, 1987, 81 pp.
- [38] Mitchell, L.K.; Elliott, K.B., "How to Design Stingers for Vibration Testing of Structures", Sound and Vibration Magazine, April 1984, pp. 14-18.
- [39] Stenger, G., "Step Relaxation Method for Structural Dynamic Excitation", Master of Science Thesis, Department of Mechanical Engineering, University of Cincinnati, 1979, 54 pp.
- [40] Coleman, A.D., Driskill, T.C., Anderson, J.B., Brown, D.L., "A Mass Additive Technique for Modal Testing as Applied to the Space Shuttle ASTRO-1 Payload", Proceedings, International Modal Analysis Conference, 1988, pp. 154-159.
- [41] Kuo, Chin-Po, Wada, B.K., "Multiple Boundary Condition Test (MBCT): Identification With Mode Shapes", NASA JPL Report, NPO-17574, 1989.

6. MODAL PARAMETER ESTIMATION

6.1 Introduction

Modal parameter estimation is a special case of system identification where the *a priori* model of the system is known to be in the form of modal parameters. Therefore, regardless of the form of measured input-output data, the form of the model used to represent the experimental data can be stated in a modal model using temporal (time or frequency) and spatial (input DOF and output DOF) information. Research into modal parameter estimation represents the largest body of work impacting the area of structural testing over the last ten years. This research effort has yielded many algorithms that are being used privately or being sold as a part of commercial software. While most of these individual algorithms are well understood, the comparison of one algorithm to another has become one of the current thrusts of this research effort. This recent work attempts to characterize different classes of modal parameter estimation techniques in terms of similarities and differences rather than performance. Since the modal parameter estimation process involves a greatly over-determined problem, the estimates of modal parameters resulting from different algorithms will not be the same due to differences in the modal model and model domain, differences in how the algorithms use the data, differences in the way the data is weighted, or condensed, and differences in the user expertise.

Nevertheless, the solution to many difficult problems in the modal parameter estimation area have been advanced over the last ten years and much is now known on how to compare and contrast different modal parameter estimation algorithms. The repeated and multiple (weakly coupled) root problem is now a well understood and solvable problem. This solution also explains much of the difficulty that users encountered during the 1970s and early 1980s when applying single reference, multiple degree of freedom modal parameter estimation algorithms. Insufficient spatial data was available to resolve repeated or pseudo-repeated modal frequencies with those early algorithms. Detection and identification of repeated and multiple roots is critical in the development of a complete modal model so that arbitrary input-output information can be synthesized. While great strides have been made in this area, further work is needed to adequately describe the multiple root problem.

Much of the recent work has focused on the development of a conceptual understanding of

modal parameter estimation technology. This understanding involves the ability to conceptualize the data and data domain, the evaluation of the order of the problem, the condensation of the data, and a common parameter estimation theory that can serve as the basis for developing any of the algorithms in use today. The following sections will review these concepts as applied to the current modal parameter estimation methodology.

6.2 Definition: Modal Parameters

Modal identification involves estimating the modal parameters of a structural system from measured input-output data. Most current modal parameter estimation is based upon the measured data being the frequency response function or the equivalent impulse response function, typically found by inverse Fourier transforming the frequency response function. **Modal parameters** include the complex-valued **modal frequencies** (λ_r), **modal vectors** ($\{\psi_r\}$) and **modal scaling** (modal mass or modal A). Additionally, most current algorithms estimate modal participation vectors ($\{L_r\}$) and residue vectors ($\{A_r\}$) as part of the overall process.

Modal participation vectors are a result of multiple reference modal parameter estimation algorithms and relate how well each modal vector is excited from each of the reference locations included in the measured data. The combination of the modal participation vector ($\{L_r\}$) and the modal vector ($\{\psi_r\}$) for a given mode give the residues ($A_{pqr} = L_{qr}\psi_{pr}$) for that mode. In general, these two vectors represent portions of the right and left eigenvectors associated with the structural system for that specific mode of vibration. Normally, the system can be assumed to be reciprocal and the right and left eigenvectors, and therefore the modal participation vector and the modal vector, will be proportional to one another. Under this assumption, the modal participation vector can be used in a weighted least squares error solution procedure to estimate the modal vectors in the presence of multiple references. Theoretically, for reciprocal systems, these modal participation factors should be in proportion to the modal coefficients of the reference degrees of freedom for each modal vector. Most multiple reference, modal parameter estimation methods estimate modal participation factors as part of the first stage estimation together with the global, complex-valued modal frequencies.

In general, modal parameters are considered to be global properties of the system. The concept of global modal parameters simply means that there is only one answer for each modal parameter

and that the modal parameter estimation solution procedure enforces this constraint. Every frequency response or impulse response function measurement theoretically contains the information that is represented by the characteristic equation, the modal frequencies and damping. If individual measurements are treated in the solution procedure independent of one another, there is nothing to guarantee that a single set of modal frequencies and damping will be generated. In likewise manner, if more than one reference is measured in the data set, redundant estimates of the modal vectors can be estimated unless the solution procedure utilizes all references in the estimation process simultaneously. Most of the current modal parameter estimation algorithms estimate the modal frequencies and damping in a global sense but very few estimate the modal vectors in a global sense.

6.3 Modal Identification Concepts

The current approach in modal identification involves using numerical techniques to separate the contributions of individual modes of vibration in measurements such as frequency response functions. The concept involves estimating the individual single degree of freedom (SDOF) contributions to the multiple degree of freedom (MDOF) measurement.

$$[H(\omega)]_{N_o \times N_i} = \sum_{r=1}^N \frac{[A_r]_{N_o \times N_i}}{j\omega - \lambda_r} + \frac{[A_r^*]_{N_o \times N_i}}{j\omega - \lambda_r^*} \quad (6.1)$$

This concept is mathematically represented in Equation (6.1) and graphically represented in Figures 6-1 through 6-3.

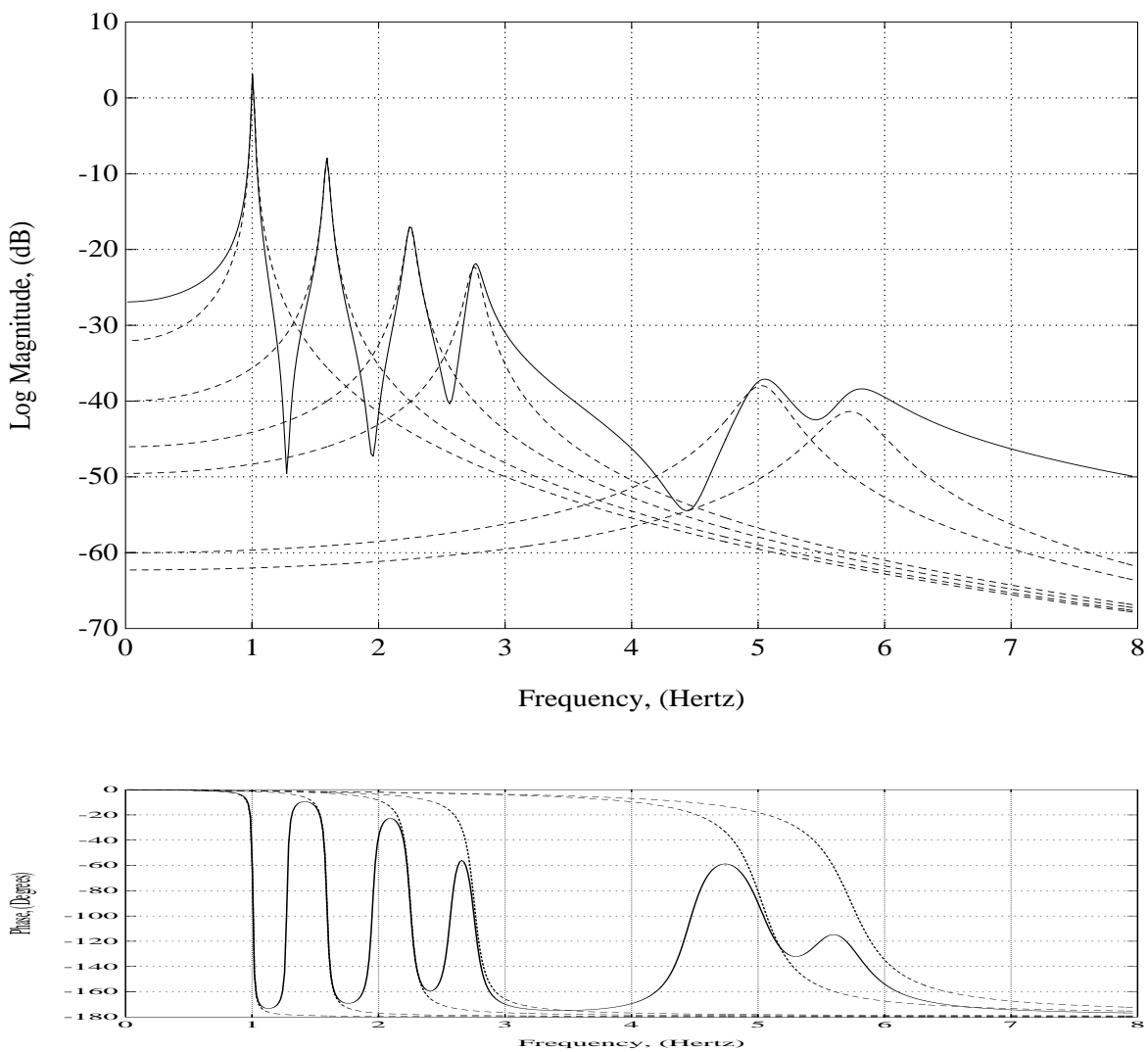


Figure 6-1. MDOF - SDOF Superposition (Positive Frequency Poles)

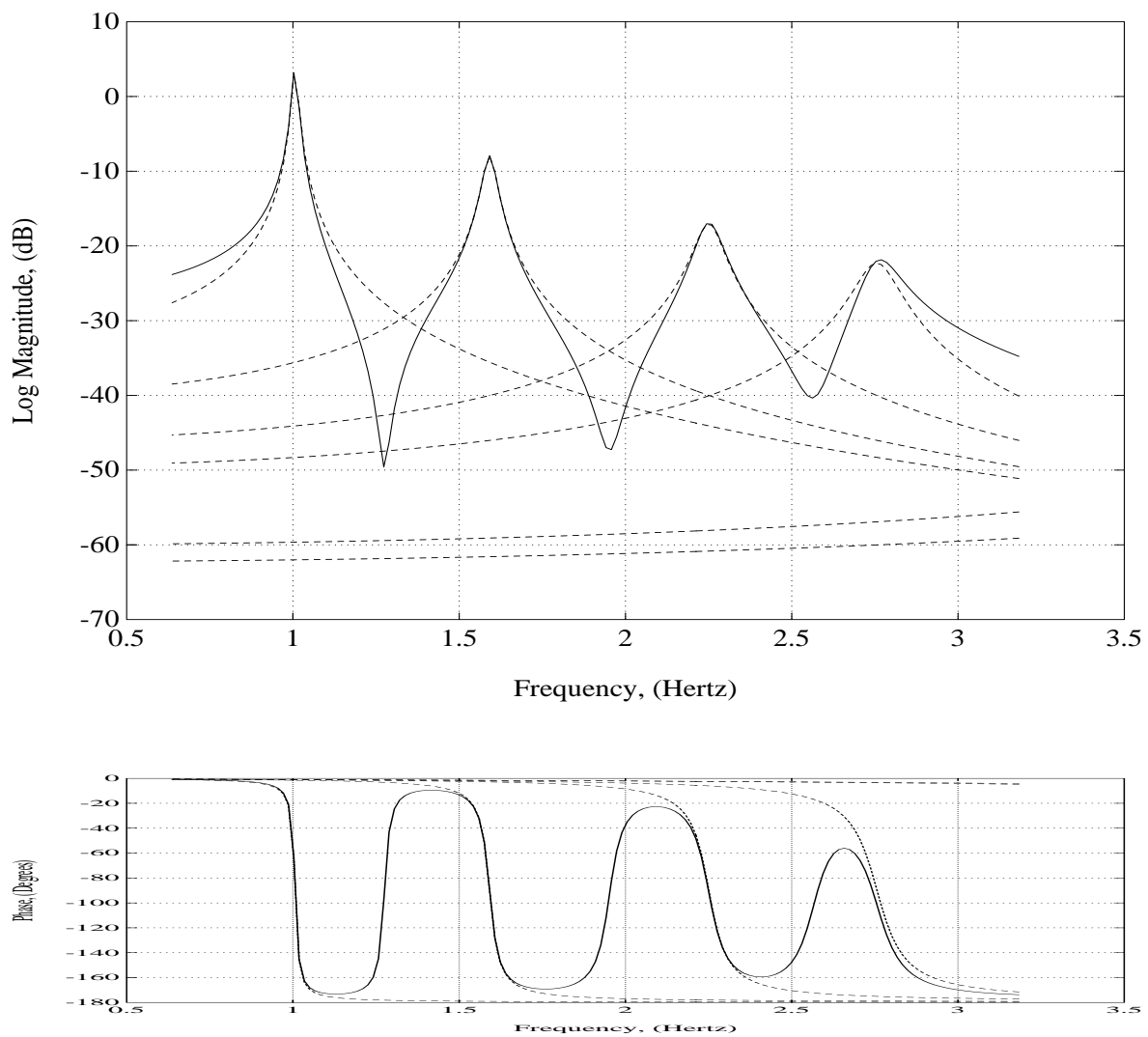


Figure 6-2. MDOF - SDOF Superposition (Positive Frequency Poles)

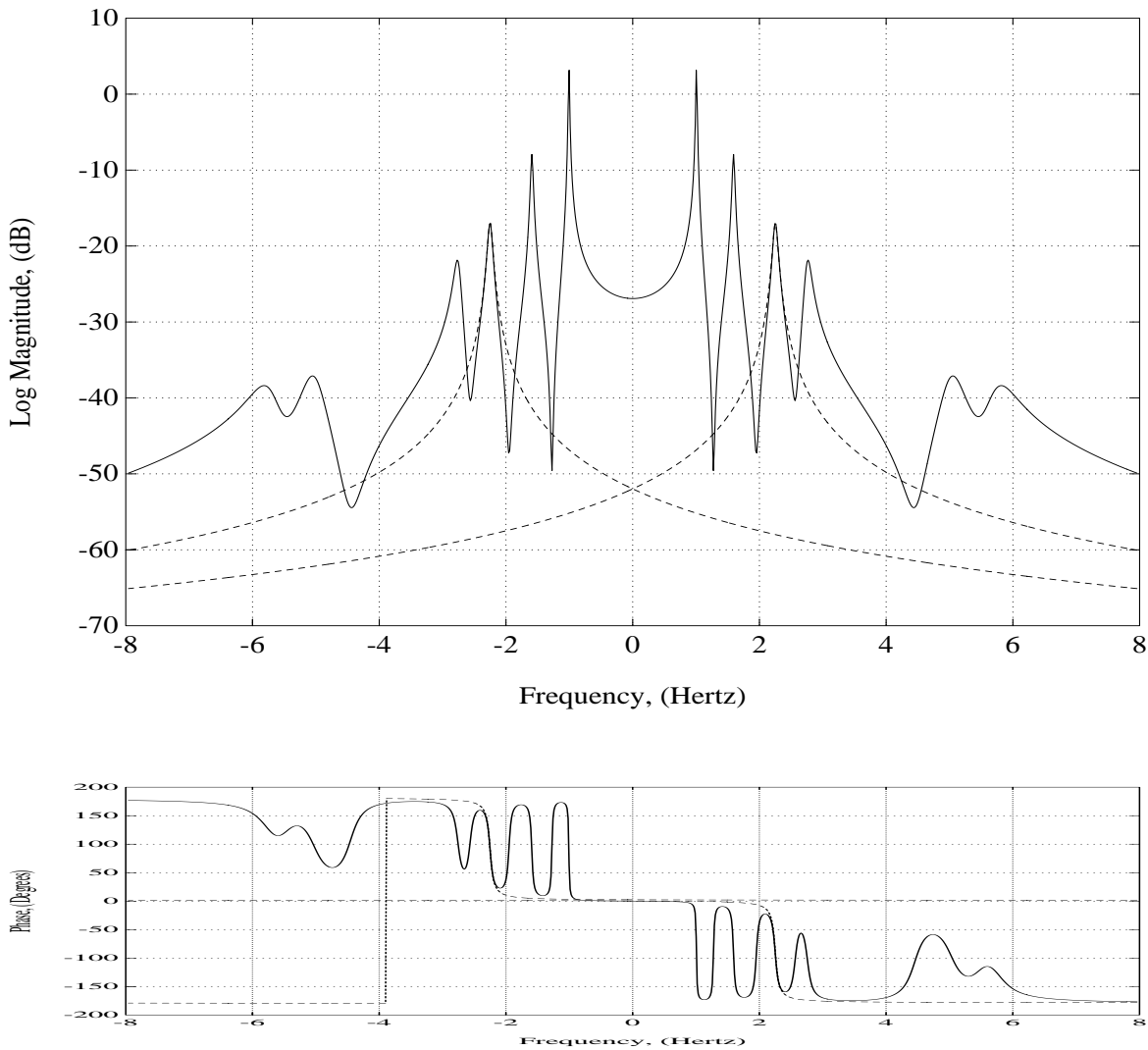


Figure 6-3. MDOF - SDOF Superposition (Positive - Negative Frequency Poles)

Equation (6.1) is often formulated in terms of modal vectors ($\{\psi_r\}$) and modal participation vectors ($\{L_r\}$) instead of residue matrices ($[A_r]$). Equation (6.1) represents a mathematical problem that, at first observation, is nonlinear in terms of the unknown modal parameters. Rather than use a nonlinear solution approach, the numerical process generally is separated into several linear stages. Typically, the modal frequencies and modal participation vectors are found in a first stage and residues, modal vectors and modal scaling are determined in a second stage. One important current trend is a reformulation of modal parameter estimation algorithms into a

single, consistent mathematical formulation with a corresponding set of definitions and unifying concepts [6]. Particularly, this approach recognizes that most modal parameter estimation methods manipulate the measured data into a matrix polynomial characteristic equation. This concept is used to unify the presentation with respect to current algorithms such as the Least-Squares Complex Exponential (LSCE), the Polyreference Time Domain (PTD), Ibrahim Time Domain (ITD), Eigensystem Realization Algorithm (ERA), Rational Fraction Polynomial (RFP), Polyreference Frequency Domain (PFD) and the Complex Mode Indicator Function (CMIF) Methods. Using this unified matrix polynomial approach (UMPA) encourages a discussion of the similarities and differences of the commonly used methods as well as a discussion of the numerical characteristics. Some of the different numerical methods that are used in different methods are the Least Squares (LS), Total Least Squares (TLS), Double Least Squares (DLS) and Singular Value Decomposition (SVD) methods (to take advantage of redundant measurement data) and the Eigenvalue and Singular Value Decomposition transformation methods (to reduce the effective size of the resulting eigenvalue-eigenvector problem) [2-5].

6.3.1 Concept: Data Domain

Modal parameters can be estimated from a variety of different measurements that exist as discrete data in different data domains (time and/or frequency). These measurements can include free-decays, forced responses, frequency responses and unit impulse responses. These measurements can be processed one at a time or in partial or complete sets simultaneously. The measurements can be generated with no measured inputs, a single measured input, or multiple measured inputs. The data can be measured individually or simultaneously. In other words, there is a tremendous variation in the types of measurements and in the types of constraints that can be placed upon the testing procedures used to acquire this data. For most measurement situations, frequency response functions are utilized in the frequency domain and impulse response function are utilized in the time domain.

Another important concept in experimental modal analysis, and particularly modal parameter estimation, involves understanding the relationships between the temporal (time and/or frequency) information and the spatial (input DOF and output DOF) information. Input-output data measured on a structural system can always be represented as a superposition of the underlying temporal characteristics (modal frequencies) together with the superposition of the

underlying spatial characteristics (modal vectors).

6.3.2 Concept: Model Order Relationships

The estimation of an appropriate model order is the most important problem encountered in modal parameter estimation. This problem is complicated due to the formulation of the parameter estimation model in the time or frequency domain, due to a single or multiple reference formulation of the modal parameter estimation model, and the effects of random and bias errors on the modal parameter estimation model. The basis of the formulation of the correct model order can be seen by expanding the second order matrix ($N \times N$) equation of motion to a higher order model ($2N$). This is a necessary process required to handle the case where the spatial information is truncated to a size smaller than the number of eigenvalues in the measured data. There are several ways that this concept can be developed. One method is to start with the homogeneous matrix equation of motion and, for example, Laplace transform this equation to determine the characteristic equation in matrix form.

$$\left[[M] s^2 + [C] s + [K] \right] \{X(s)\} = \{0\} \quad (6.2)$$

The above matrix equation yields a matrix characteristic equation in the following form:

$$\left| [M] s^2 + [C] s + [K] \right| = 0 \quad (6.3)$$

This characteristic equation is a matrix polynomial of second order which can be partitioned as follows:

$$\begin{aligned}
& \left[\begin{array}{cccccccc} [M_{11}] & . & . & . & . & . & . & [M_{1n}] \\ [M_{21}] & & & & & & & [M_{2n}] \\ . & & & & & & & . \\ . & & & & & & & . \\ [M_{n1}] & . & . & . & . & . & . & [M_{nn}] \end{array} \right] s^2 + \\
& \left[\begin{array}{cccccccc} [C_{11}] & . & . & . & . & . & . & [C_{1n}] \\ [C_{21}] & & & & & & & [C_{2n}] \\ . & & & & & & & . \\ . & & & & & & & . \\ [C_{n1}] & . & . & . & . & . & . & [C_{nn}] \end{array} \right] s + \\
& \left[\begin{array}{cccccccc} [K_{11}] & . & . & . & . & . & . & [K_{1n}] \\ [K_{21}] & & & & & & & [K_{2n}] \\ . & & & & & & & . \\ . & & & & & & & . \\ [K_{n1}] & . & . & . & . & . & . & [K_{nn}] \end{array} \right] = 0 \quad (6.4)
\end{aligned}$$

This partitioned equation can be expanded to a higher order matrix polynomial and put in a generic form as follows:

$$\left[[\Upsilon_{2n}] s^{2n} + [\Upsilon_{2n-1}] s^{2n-1} + [\Upsilon_{2n-2}] s^{2n-2} + \dots + [\Upsilon_0] \right] = 0 \quad (6.5)$$

Note that the size of the matrices $[\Upsilon]$ is the same as the size of the partitioned submatrices in the previous equation. Also note that each $[\Upsilon]$ matrix involves a matrix product and summation of several $[M_{kl}]$, $[C_{kl}]$, and $[K_{kl}]$ submatrices. The roots of this matrix characteristic equation are the same as the original second order matrix polynomial equation.

The limit of this process would be to reduce the size of the matrices to a single order or to a scalar equation.

$$\alpha_{2N} s^{2N} + \alpha_{2N-1} s^{2N-1} + \alpha_{2N-2} s^{2N-2} + \dots + \alpha_0 = 0 \quad (6.6)$$

Likewise, the roots of this scalar characteristic equation are the same as the original second order

matrix polynomial equation.

Therefore, the number of characteristic values (number of modal frequencies, number of roots, number of poles, etc.) that can be determined depends upon the size of the matrix coefficients involved in the model and the order of the highest polynomial term in the model. There are a significant number of procedures that have been formulated particularly for aiding in these decisions and selecting the appropriate estimation model. Procedures for estimating the appropriate matrix size and model order are another of the differences between various estimation procedures.

6.3.3 Concept: Fundamental Measurement Models

Most current modal parameter estimation algorithms utilize frequency or impulse response functions as the data, or known information, to solve for modal parameters. The general equation that can be used to represent the relationship between the measured frequency response function matrix and the modal parameters is shown in Equations (6.7) and (6.8). Note that these equations are essentially Equation (6.1) with the residue matrix $[A_r]$ split into two matrices $[\psi]$ and $[L]$ to allow the summation to be eliminated and to reflect that the spatial information involves two components, the input and output measurement degrees of freedom.

$$[H(\omega)]_{N_o \times N_i} = [\psi]_{N_o \times 2N} \left[\frac{1}{j\omega - \lambda_r} \right]_{2N \times 2N} [L]^T_{2N \times N_i} \quad (6.7)$$

$$[H(\omega)]^T_{N_i \times N_o} = [L]_{N_i \times 2N} \left[\frac{1}{j\omega - \lambda_r} \right]_{2N \times 2N} [\psi]^T_{2N \times N_o} \quad (6.8)$$

Impulse response functions are rarely directly measured but are calculated from associated frequency response functions via the inverse FFT algorithm. The general equation that can be used to represent the relationship between the impulse response function matrix and the modal parameters is shown in Equations (6.9) and (6.10).

$$[h(t)]_{N_o \times N_i} = [\psi]_{N_o \times 2N} \left[e^{\lambda_r t} \right]_{2N \times 2N} [L]^T_{2N \times N_i} \quad (6.9)$$

$$[h(t)]_{N_i \times N_o}^T = [L]_{N_i \times 2N} \begin{bmatrix} e^{\lambda_r t} \end{bmatrix}_{2N \times 2N} \begin{bmatrix} \psi \end{bmatrix}_{2N \times N_o}^T \quad (6.10)$$

Many modal parameter estimation algorithms have been originally formulated from Equations (6.7) through (6.10). However, a more general development for all algorithms is based upon relating the above equations to a general matrix polynomial approach.

6.3.4 Concept: Characteristic Space

From a conceptual viewpoint, the measurement space of a modal identification problem can be visualized as occupying a volume with the coordinate axes defined in terms of the three sets of characteristics. Two axes of the conceptual volume correspond to spatial information and the third axis to temporal information. The spatial coordinates are in terms of the input and output degrees of freedom (DOF) of the system. The temporal axis is either time or frequency depending upon the domain of the measurements. These three axes define a 3-D volume which is referred to as the *Characteristic Space* as noted in Figure 6-4.

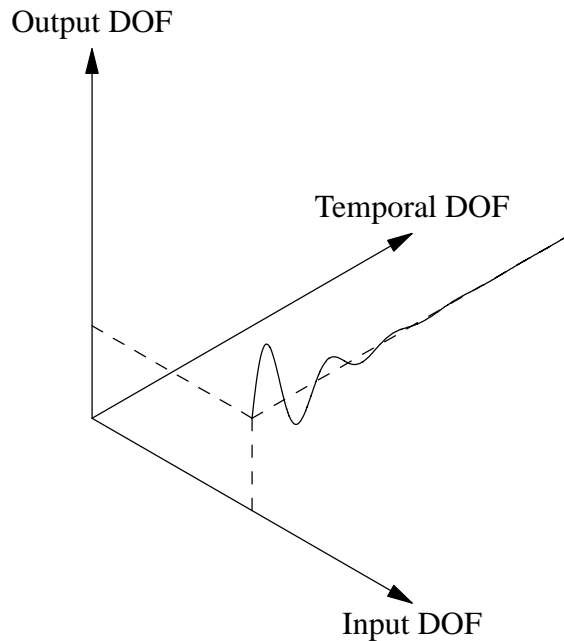


Figure 6-4. Conceptualization of Modal Characteristic Space

This space or volume represents all possible measurement data as expressed by Equations (6.7) through (6.10). This conceptual representation is very useful in understanding what data subspace has been measured. Also, this conceptual representation is very useful in recognizing how the data is organized and utilized with respect to different modal parameter estimation algorithms. Information parallel to one of the axes consists of a solution composed of the superposition of the characteristics defined by that axis. The other two characteristics determine the scaling of each term in the superposition.

Historically, data collection concentrated on measuring the temporal aspect (time/frequency) at a sufficient resolution in order to determine the modal parameters. In this approach, the accuracy of the modal parameters, particularly frequency and damping, is essentially limited by Shannon's Sampling Theorem and Rayleigh's Criteria. This focus on the temporal information ignores the added information, and accuracy, that use of the spatial information brings to the estimation of modal parameters. Recognizing the characteristic space aspects of the measurement space and using these characteristics (modal vector/participation vector) concepts in the solution procedure leads to the remarkable conclusion that the spatial information can compensate for the limitations of temporal information. In other words, there is a trade-off between temporal and spatial information for a given requirement of accuracy. This is particularly notable in the case of repeated roots. No amount of temporal resolution (accuracy) can theoretically solve repeated roots but the addition of spatial information in the form of multiple inputs and/or outputs resolves this problem.

Any structural testing procedure measures a subspace of the total possible data available. Modal parameter estimation algorithms may then use all of this subspace or may choose to further limit the data to a more restrictive subspace. This is not a problem since it is theoretically possible to estimate the characteristics of the total space by measuring a subspace which samples all three characteristics. Experimentally, any point in this space can be measured. The particular subspace which is measured and the weighting of the data within the subspace in an algorithm are the main differences between the various modal identification procedures which have been developed.

In general, the amount of information in a measured subspace greatly exceeds that which is necessary to solve for the unknown modal characteristics. Another major difference between the various modal parameter estimation procedures is the type of condensation algorithms that are

used to reduce the data to match the number of unknowns (for example, *least squares* (LS), *singular value decomposition* (SVD), etc). This will be discussed in a later section. As is the case with any over-specified solution procedure, there is no unique answer. The answer that is obtained depends upon the data that is selected, the weighting of the data and the unique algorithm used in the solution process. As a result, the answer is the *best* answer depending upon the objective functions associated with the algorithm being used. Historically, this point has created some confusion since many users expect different methods to give exactly the same answer.

As mentioned previously, various modal identification algorithms use a different subspace. As might be expected, the selection of the subspace has a significant influence on the results. In order to estimate all of the modal parameters, the subspace must encompass a region which includes contributions of all three characteristics. A classic example is the necessity to use multiple reference (inputs and outputs) data in order to estimate *repeated roots*.

In the past, many modal techniques used information (subspace) where only one or two characteristics were varied. For example, in the early 1970's, the modal parameter estimation methods of that era only fit one unit impulse function or one frequency response at a time. With reference to the characteristic space of the problem, this is represented by Figure 6-4. In this case, only the temporal characteristic is used and as might be expected only temporal characteristics (modal frequencies) can be estimated from the single measurement. In practice, multiple measurements were taken and the spatial information was extracted from the multiple measurements by successive estimation of the residues for each mode from each measurement.

As the sophistication of data acquisition equipment and modal parameter estimation algorithms evolved, later techniques fit the data in a plane of the characteristic space. For example, this corresponds to the data taken at a number of response points but from a single excitation point or reference. This representation of a column of measurements is shown in Figure 6-5. For this case, representing a single input (reference), it is not possible to compute repeated roots and it is difficult to separate closely coupled modes due to the lack of spatial data.

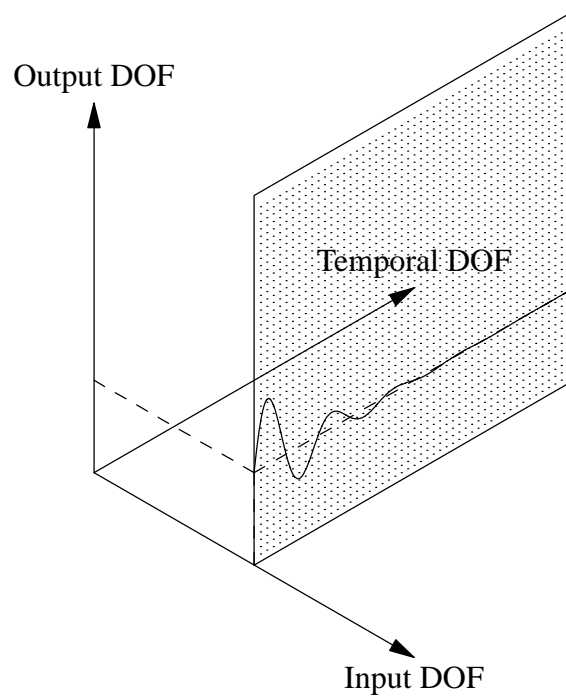


Figure 6-5. Characteristic Space: Column of Measurements

Many modal identification algorithms utilize data taken at a large number of output DOFs due to excitation at a small number of input DOFs. Data taken in this manner is consistent with a multi-exciter type of test. The conceptual representation of several columns of the potential measurement matrix is shown in Figure 6-6.

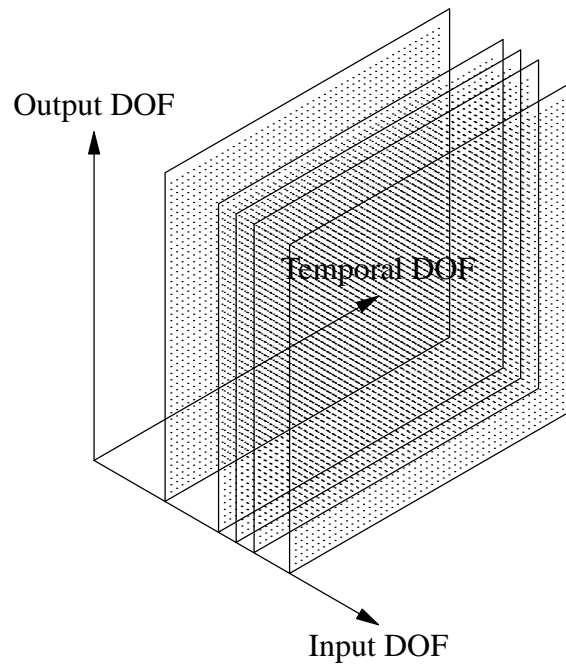


Figure 6-6. Characteristic Space: Columns of Measurements

Some modal identification algorithms utilize data taken at a large number of input DOFs and a small number of output DOFs. Data taken in this manner is consistent with a roving hammer type of excitation with several fixed output sensors. This data can also be generated by transposing the data matrix acquired using a multi-exciter test. The conceptual representation of several rows of the potential measurement matrix is shown in Figure 6-7 and 6-8.

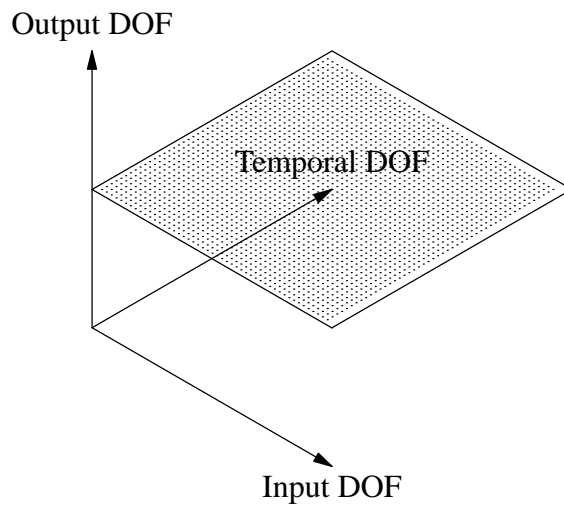


Figure 6-7. Characteristic Space: Row of Measurements

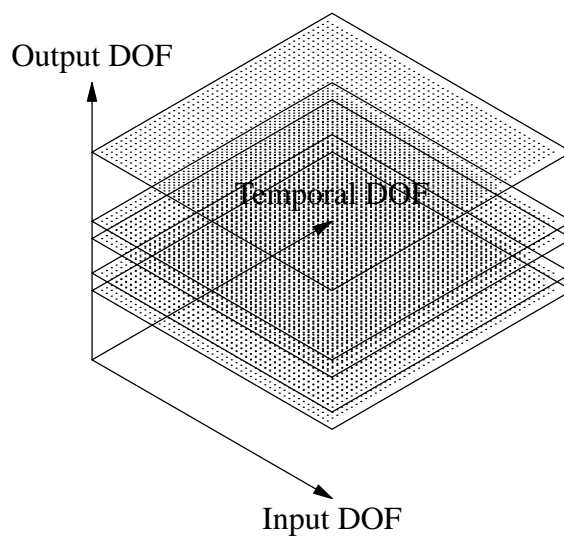


Figure 6-8. Characteristic Space: Rows of Measurements

A small number of modal identification algorithms utilize data taken at a large number of output DOFs and input DOFs for a limited number of times or frequencies (temporal DOFs). The conceptual representation of several columns of the potential measurement matrix is shown in Figure 6-9 and 6-10.

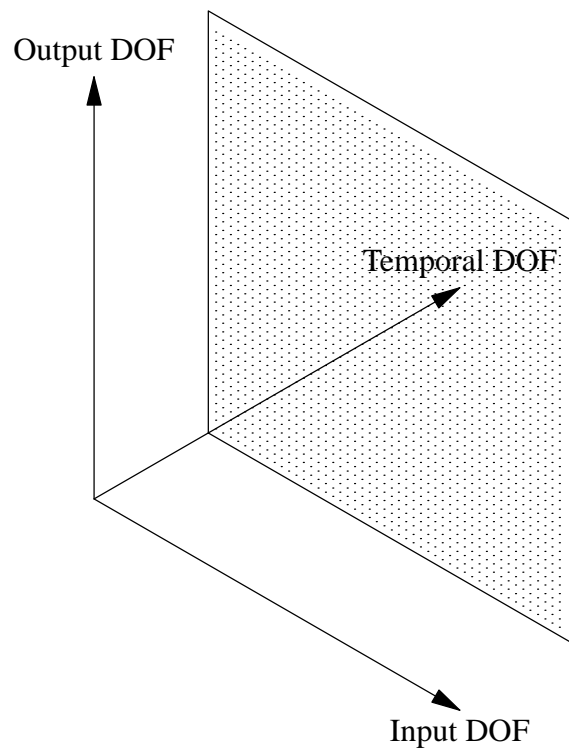


Figure 6-9. Characteristic Space: Temporal Measurements

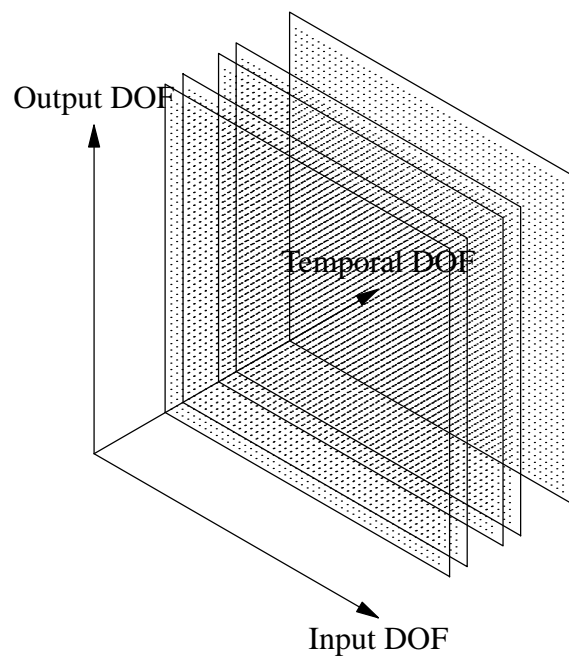


Figure 6-10. Characteristic Space: Temporal Measurements

Measurement data spaces involving many planes of measured data are the best possible modal identification situations since the data subspace includes contributions from temporal and spatial characteristics. This allows the best possibility of estimating all the important modal parameters.

It should be obvious that the data which defines the subspace needs to be acquired in a consistent measurement process in order for the algorithms to estimate accurate modal parameters. This fact has triggered the need to measure all of the data simultaneously and has led to recent advancements in data acquisition, digital signal processing and instrumentation designed to facilitate this measurement problem.

6.3.5 Concept: Fundamental Modal Identification Models

Rather than using a physically based mathematical model, the common characteristics of different modal parameter estimation algorithms can be more readily identified by using a matrix polynomial model. One way of understanding the basis of this model can be developed from the polynomial model used historically for the frequency response function.

$$H_{pq}(\omega) = \frac{X_p(\omega)}{F_q(\omega)} = \frac{\beta_n (j\omega)^n + \beta_{n-1} (j\omega)^{n-1} + \cdots + \beta_1 (j\omega)^1 + \beta_0 (j\omega)^0}{\alpha_m (j\omega)^m + \alpha_{m-1} (j\omega)^{m-1} + \cdots + \alpha_1 (j\omega)^1 + \alpha_0 (j\omega)^0} \quad (6.11)$$

This can be rewritten:

$$H_{pq}(\omega) = \frac{X_p(\omega)}{F_q(\omega)} = \frac{\sum_{k=0}^n \beta_k (j\omega)^k}{\sum_{k=0}^m \alpha_k (j\omega)^k} \quad (6.12)$$

Further rearranging yields the following equation that is linear in the unknown α and β terms:

$$\sum_{k=0}^m \alpha_k (j\omega)^k X_p(\omega) = \sum_{k=0}^n \beta_k (j\omega)^k F_q(\omega) \quad (6.13)$$

Noting that the response function X_p can be replaced by the frequency response function H_{pq} if

the force function F_q is assumed to be unity, the above equation can be restated:

$$\sum_{k=0}^m \alpha_k (j\omega)^k H_{pq}(\omega) = \sum_{k=0}^n \beta_k (j\omega)^k \quad (6.14)$$

The above formulation is essentially a linear equation in terms of the unknown coefficients α_k and β_k . The equation is valid at each frequency of the measured frequency response function. Since, in the worst case, the number of unknowns is $m + n + 2$, the unknown coefficients can theoretically be determined if the frequency response function has $m + n + 2$ or more discrete frequencies. Practically, this will always be the case. Note that the total number of unknown coefficients (or coefficient matrices) is actually $m + n + 1$ since one coefficient (or coefficient matrix) can be assumed to be one (or the identity matrix). This occurs since the equation can be divided, or normalized, by one of the unknown coefficients (or coefficient matrices). Note that numerical problems can result if the equation is normalized by a coefficient (or coefficient matrix) that is close to zero. Normally, the coefficient α_0 (or coefficient matrix $[\alpha_0]$) is chosen as unity (or the identity matrix).

The previous models can be generalized to represent the general multiple input, multiple output case as follows:

$$\sum_{k=0}^m [\alpha_k] (j\omega)^k \{X(\omega)\} = \sum_{k=0}^n [\beta_k] (j\omega)^k \{F(\omega)\} \quad (6.15)$$

Note that the size of the coefficient matrix $[\alpha_k]$ will normally be $N_i \times N_i$ or $N_o \times N_o$ when the equations are developed from experimental data. The size of the coefficient matrix $[\beta_k]$ will normally be $N_i \times N_o$ or $N_o \times N_i$ when the equations are developed from experimental data.

Rather than developing the basic model in terms of force and response information, the models can be stated in terms of power spectra or frequency response information. First, post multiply both sides of the equation by $\{F\}^H$:

$$\sum_{k=0}^m [\alpha_k] (j\omega)^k \{X(\omega)\} \{F(\omega)\}^H = \sum_{k=0}^n [\beta_k] (j\omega)^k \{F(\omega)\} \{F(\omega)\}^H \quad (6.16)$$

Now recognize that the product of $\{X(\omega)\} \{F(\omega)\}^H$ is the output-input cross spectra matrix

$([G_{xf}(\omega)])$ for one ensemble and $\{F(\omega)\} \{F(\omega)\}^H$ is the input-input cross spectra matrix $([G_{ff}(\omega)])$ for one ensemble. With a number of ensembles (averages), these matrices are the common matrices used to estimate the FRFs in a MIMO case. This yields the following cross spectra model:

$$\sum_{k=0}^m [\alpha_k] (j\omega)^k [G_{xf}(\omega)] = \sum_{k=0}^n [\beta_k] (j\omega)^k [G_{ff}(\omega)] \quad (6.17)$$

The previous cross spectra model can be reformulated to utilize frequency response function (FRF) data by post multiplying both sides of the equation by $[G_{ff}(\omega)]^{-1}$:

$$\sum_{k=0}^m [\alpha_k] (j\omega)^k [G_{xf}(\omega)] [G_{ff}(\omega)]^{-1} = \sum_{k=0}^n [\beta_k] (j\omega)^k [G_{ff}(\omega)] [G_{ff}(\omega)]^{-1} \quad (6.18)$$

Therefore, the multiple input - multiple output FRF model is:

$$\sum_{k=0}^m [\alpha_k] (j\omega)^k [H(\omega)] = \sum_{k=0}^n [\beta_k] (j\omega)^k [I] \quad (6.19)$$

The unknowns in the above linear equation are the matrix alpha and beta coefficients. Note that the size of the coefficient matrix $[\alpha_k]$ will normally be $N_o \times N_o$ and the coefficient matrix $[\beta_k]$ will normally be $N_o \times N_i$ when the equations are developed from experimental data.

Since the FRF matrix is normally considered to be reciprocal ($H_{pq} = H_{qp}$), the previous formulation can be developed from the transposed FRF matrix. This means that the size of the coefficient matrix $[\alpha_k]$ will be $N_i \times N_i$ and the coefficient matrix $[\beta_k]$ will normally be $N_i \times N_o$ for this case.

The above model, in the frequency domain, corresponds to an ***AutoRegressive-Moving-Average*** (ARMA) model that is developed from a set of finite difference equations in the time domain ^[5]. The general characteristic matrix polynomial model concept recognizes that both the time and frequency domain models generate essentially the same matrix polynomial models. For that reason, the ***Unified Matrix Polynomial Approach*** (UMPA) terminology is used to describe both domains since the ARMA terminology has been connected primarily with the time domain.

Paralleling the development of Equation (6.13), a time domain model representing the relationship between a single response degree of freedom and a single input degree of freedom can be stated as follows:

$$\sum_{k=0}^m \alpha_k x(t_{i+k}) = \sum_{k=0}^n \beta_k f(t_{i+k}) \quad (6.20)$$

In the time domain, this model is commonly known as the AutoRegressive Moving-Average (ARMA(m,n)) model. For the general multiple input, multiple output case:

$$\sum_{k=0}^m [\alpha_k] \{x(t_{i+k})\} = \sum_{k=0}^n [\beta_k] \{f(t_{i+k})\} \quad (6.21)$$

If the discussion is limited to the use of free decay or impulse response function data, the previous time domain equations can be greatly simplified by noting that the forcing function can be assumed to be zero for all time greater than zero. If this is the case, the $[\beta_k]$ coefficients can be eliminated from the equations.

$$\sum_{k=0}^m [\alpha_k] \left\{ h_{pq}(t_{i+k}) \right\} = 0 \quad (6.22)$$

In light of the above discussion, it is now apparent that most of the modal parameter estimation processes available can be developed by starting from a general matrix polynomial formulation that is justifiable based upon the underlying matrix differential equation. The general matrix polynomial formulation yields essentially the same characteristic matrix polynomial equation, for both time and frequency domain data. For the frequency domain data case, this yields:

$$\left| [\alpha_m] s^m + [\alpha_{m-1}] s^{m-1} + [\alpha_{m-2}] s^{m-2} + \dots + [\alpha_0] \right| = 0 \quad (6.23)$$

For the time domain data case, this yields:

$$\left| [\alpha_m] z^m + [\alpha_{m-1}] z^{m-1} + [\alpha_{m-2}] z^{m-2} + \dots + [\alpha_0] \right| = 0 \quad (6.24)$$

With respect to the previous discussion of **model order**, the characteristic matrix polynomial

equation, Equation (6.23) or Equation (6.24) has a model order of m and the number of modal frequencies or roots that will be found from this characteristic matrix polynomial equation will be m times the size of the coefficient matrices $[\alpha]$. In terms of sampled data, the time domain matrix polynomial results from a set of finite difference equations and the frequency domain matrix polynomial results from a set of linear equations where each equation is formulated at one of the frequencies of the measured data. This distinction is important to note since the roots of the matrix characteristic equation formulated in the time domain are in the ***z-domain*** (z_r) and must be converted to the frequency domain (λ_r) while the roots of the matrix characteristic equation formulated in the frequency domain (λ_r) are already in the desired domain [5-6]. The roots that are estimated in the time domain are limited to maximum values determined by the Shannon's Sampling Theorem relationship (discrete time steps).

$$z_r = e^{\lambda_r \Delta t} \quad \lambda_r = \sigma_r + j \omega_r$$

$$\sigma_r = \text{Re} \left[\frac{\ln z_r}{\Delta t} \right] \quad \omega_r = \text{Im} \left[\frac{\ln z_r}{\Delta t} \right]$$

Algorithm	Domain		Matrix Polynomial Order			Coefficients	
	Time	Freq	Zero	Low	High	Scalar	Matrix
CEA	•				•	•	
LSCE	•				•	•	
PTD	•				•		$N_i \times N_i$
ITD	•			•			$N_o \times N_o$
MRITD	•			•			$N_o \times N_o$
ERA	•			•			$N_o \times N_o$
PFD		•		•			$N_o \times N_o$
SFD		•		•			$N_o \times N_o$
MRFD		•		•			$N_o \times N_o$
RFP		•			•	•	Both
OP		•			•	•	Both
CMIF		•	•				$N_o \times N_i$

TABLE 6-1. Summary of Modal Parameter Estimation Algorithms

Algorithm	Acronym
Complex Exponential Algorithm ^[7-8]	CEA
Least Squares Complex Exponential ^[7,9]	LSCE
Polyreference Time Domain ^[10-12]	PTD
Ibrahim Time Domain ^[13-16]	ITD
Multi-Reference Ibrahim Time Domain ^[16]	MRITD
Eigensystem Realization Algorithm ^[17-20]	ERA
Polyreference Frequency Domain ^[21-24]	PFD
Simultaneous Frequency Domain ^[25]	SFD
Multi-Reference Frequency Domain ^[26]	MRFD
Rational Fraction Polynomial ^[27-28]	RFP
Orthogonal Polynomial ^[27,29-34]	OP
Complex Mode Indicator Function ^[35-36]	CMIF

TABLE 6-2. Summary of Modal Parameter Estimation Acronyms

Using this general formulation, the most commonly used modal identification methods can be summarized as shown previously in Tables 6-1 and 6-2.

The high order model is typically used for those cases where the system is undersampled in the spatial domain. For example, the limiting case is when only one measurement is made on the structure. For this case, the left hand side of the general linear equation corresponds to a scalar polynomial equation with the order equal to or greater than the number of desired modal frequencies. This type of high order model may yield significant numerical problems for the frequency domain case.

The low order model is used for those cases where the spatial information is complete. In other words, the number of independent physical coordinates is greater than the number of desired modal frequencies. For this case, the order of the lefthand side of the general linear equation, Equation (6.19) or (6.22), is equal to one or two.

The zero order model corresponds to a case where the temporal information is neglected and only the spatial information is used. These methods directly estimate the eigenvectors as a first

step. In general, these methods are programmed to process data at a single temporal condition or variable. In this case, the method is essentially equivalent to the single-degree-of-freedom (SDOF) methods which have been used with frequency response functions. In others words, the zeroth order matrix polynomial model compared to the higher order matrix polynomial models is similar to the comparison between the SDOF and MDOF methods used historically in modal parameter estimation.

6.3.6 Concept: Two Stage Linear Solution Procedure

Almost all modal parameter estimation algorithms in use at this time involve a two stage linear solution approach. For example, with respect to Equations (6.7) through (6.10), if all modal frequencies and modal participation vectors can be found, the estimation of the complex residues can proceed in a linear fashion. This procedure of separating the nonlinear problem into a multi-stage linear problem is a common technique for most estimation methods today. For the case of structural dynamics, the common technique is to estimate modal frequencies and modal participation vectors in a first stage and then to estimate the modal coefficients plus any residuals in a second stage.

Therefore, based upon Equations (6.7) through (6.10), most modern modal identification algorithms can be outlined as follows:

First Stage of Modal Parameter Estimation

- Load Measured Data into Linear Equation Form (Equation (6.19) or (6.22)).
- Find Scalar or Matrix Autoregressive Coefficients ($[\alpha_k]$).
 - Normalize Frequency Range (Frequency Domain Only)
 - Utilize Orthogonal Polynomials (Frequency Domain Only)
- Solve Matrix Polynomial for Modal Frequencies.
 - Formulate Companion Matrix.
 - Obtain Eigenvalues of Companion Matrix. (λ_r or z_r).
 - Convert Eigenvalues from z_r to λ_r (Time Domain Only).
 - Obtain Modal Participation Vectors L_{qr} or Modal Vectors $\{\psi\}_r$ from Eigenvectors of the Companion Matrix.

Second Stage of Modal Parameter Estimation

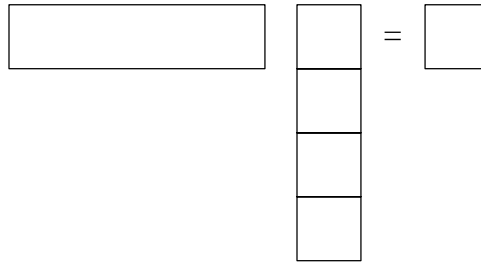
- Find Modal Vectors and Modal Scaling from Equations (6.7) through (6.10).

Equation (6.19) or (6.22) is used to formulate a single, block coefficient linear equation as shown in the graphical analogy of Case 1a of Figure 6-11. As an example, Figure 6-11 is the graphical analogy of the single input, single output form of the time domain equation (Equation 6.22) as follows:

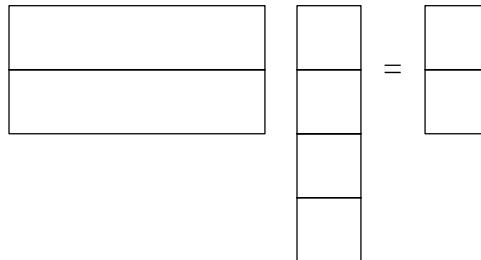
$$\left[h_{pq}(t_{i+0}) \ h_{pq}(t_{i+1}) \ \cdots \ h_{pq}(t_{i+2N-1}) \right] \left\{ \begin{array}{c} \alpha_0 \\ \alpha_1 \\ \dots \\ \alpha_{2N-1} \end{array} \right\} = -h_{pq}(t_{i+2N})$$

In order to estimate complex conjugate pairs of roots, at least two equations must be used from each piece or block of data in the data space. This situation is shown in Case 1b of Figure 6-12.

Case 1a:

**Figure 6-11.** Underdetermined Set of Linear Equations

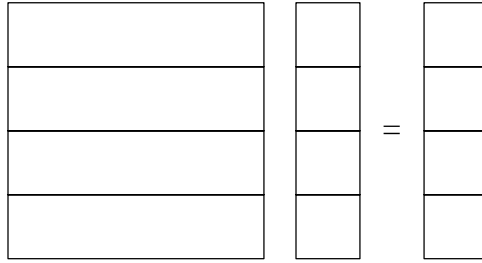
Case 1b:

**Figure 6-12.** Underdetermined Set of Linear Equations

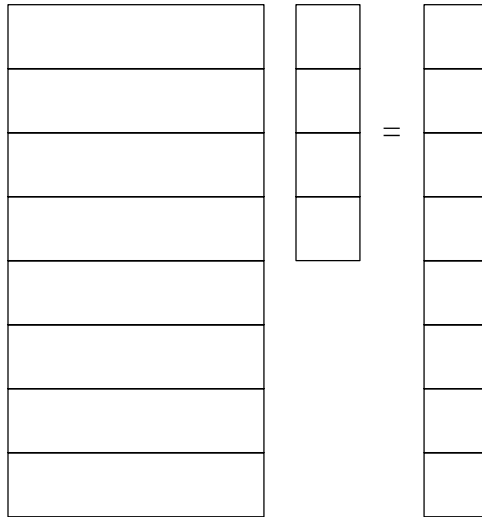
In order to develop enough equations to solve for the unknown matrix coefficients, further information is taken from the same block of data or from other blocks of data in the data space until the number of equations equals (Case 2) or exceeds (Case 3) the number of unknown as shown in Figure 6-13 and 6-14. In the frequency domain, this is accomplished by utilizing a different frequency, from within each measurement, for each equation. In the time domain, this is accomplished by utilizing a different starting time or time shift, from within each measurement, for each equation. The exact form and requirements for Equation (6.16) or (6.19) for many of the commonly used modal identification algorithms is given in later sections. As before, these graphical analogies are representative of the following time domain equation:

$$\begin{bmatrix} h_{pq}(t_0) & h_{pq}(t_1) & h_{pq}(t_2) & \cdots & h_{pq}(t_{2N-1}) \\ h_{pq}(t_1) & h_{pq}(t_2) & h_{pq}(t_3) & \cdots & h_{pq}(t_{2N}) \\ h_{pq}(t_2) & h_{pq}(t_3) & h_{pq}(t_4) & \cdots & h_{pq}(t_{2N+1}) \\ \cdots & \cdots & \cdots & \cdots & \cdots \\ h_{pq}(t_{2N-1}) & h_{pq}(t_{2N}) & h_{pq}(t_{2N+1}) & \cdots & h_{pq}(t_{4N-2}) \end{bmatrix} \begin{Bmatrix} \alpha_0 \\ \alpha_1 \\ \alpha_2 \\ \cdots \\ \alpha_{2N-1} \end{Bmatrix} = \begin{Bmatrix} h_{pq}(t_{2N}) \\ h_{pq}(t_{2N+1}) \\ h_{pq}(t_{2N+2}) \\ \cdots \\ h_{pq}(t_{4N-1}) \end{Bmatrix}$$

Case 2:

**Figure 6-13.** Determined Set of Linear Equations

Case 3:

**Figure 6-14.** Overdetermined Set of Linear Equations

Once the matrix coefficients ($[\alpha]$) have been found, the modal frequencies (λ_r or z_r) can be

found using a number of numerical techniques. While in certain numerical situations, other numerical approaches may be more robust, a companion matrix approach yields a consistent concept for understanding the process. Therefore, the roots of the matrix characteristic equation can be found as the eigenvalues of the associated companion matrix. The companion matrix can be formulated in one of several ways. The most common formulation is as follows:

$$[C] = \begin{bmatrix} -[\alpha]_{m-1} & -[\alpha]_{m-2} & \cdots & \cdots & \cdots & -[\alpha]_1 & -[\alpha]_0 \\ [I] & [0] & \cdots & \cdots & \cdots & [0] & [0] \\ [0] & [I] & \cdots & \cdots & \cdots & [0] & [0] \\ [0] & [0] & \cdots & \cdots & \cdots & [0] & [0] \\ \cdots & \cdots & \cdots & \cdots & \cdots & \cdots & \cdots \\ \cdots & \cdots & \cdots & \cdots & \cdots & \cdots & \cdots \\ \cdots & \cdots & \cdots & \cdots & \cdots & \cdots & \cdots \\ [0] & [0] & \cdots & \cdots & \cdots & [0] & [0] \\ [0] & [0] & \cdots & \cdots & \cdots & [0] & [0] \\ [0] & [0] & \cdots & \cdots & \cdots & [I] & [0] \end{bmatrix} \quad (6.25)$$

Note again that the numerical characteristics of the eigenvalue solution of the companion matrix will be different for low order cases compared to high order cases for a given data set. The companion matrix can be used in the following eigenvalue formulation to determine the modal frequencies for the original matrix coefficient equation:

$$[C]\{X\} = \lambda [I]\{X\} \quad (6.26)$$

The eigenvectors that can be found from the eigenvalue-eigenvector solution utilizing the companion matrix may, or may not, be useful in terms of modal parameters. The eigenvector that is found, associated with each eigenvalue, is of length model order times matrix coefficient size. In fact, the unique (meaningful) portion of the eigenvector is of length equal to the size of the coefficient matrices and is repeated in the eigenvector a model order number of times. Each time the unique portion of the eigenvector is repeated, the unique portion is multiplied by a scalar multiple of the associated modal frequency. Therefore, the eigenvectors of the companion matrix have the following form:

$$\{\phi\}_r = \begin{Bmatrix} \lambda_r^m \{\psi\}_r \\ \cdot \\ \cdot \\ \cdot \\ \lambda_r^2 \{\psi\}_r \\ \cdot \\ \lambda_r^1 \{\psi\}_r \\ \lambda_r^0 \{\psi\}_r \end{Bmatrix}_r \quad (6.27)$$

Note that, unless the size of the coefficient matrices is at least as large as the number of measurement degrees of freedom, only a partial set of modal coefficients, the modal participation coefficients (L_{qr}) will be found. For the case involving scalar coefficients, no meaningful modal coefficients will be found.

If the size of the coefficient matrices, and therefore the modal participation vector, is less than the largest spatial dimension of the problem, then the modal vectors are typically found in a second stage solution process using one of Equations (6.7) or (6.10). Even if the complete modal vector ($\{\psi\}$) of the system is found from the eigenvectors of the companion matrix approach, the modal scaling and modal participation vectors for each modal frequency are normally found in this second stage formulation.

6.3.7 Concept: Data Sieving/Filtering

For almost all cases of modal identification, a large amount of redundancy or overdetermination exists. This means that for Case 3 defined in Figure 6-14, the number of equations available compared to the number required for the determined Case 2, defined as the overdetermination factor, will be quite large. Beyond some value of overdetermination factor, the additional equations contribute little to the result but may add significantly to the solution time. For this reason, the data space is often *filtered* (limited in the temporal sense) or *sieved* (limited in the input DOF or output DOF sense) in order to obtain a reasonable result in the minimum time. For frequency domain data, the filtering process normally involves limiting the data set to a range of frequencies or a different frequency resolution according to the desired frequency range of interest. For time domain data, the filtering process normally involves limiting the starting time value as well as the number of sets of time data taken from each measurement. Data sieving involves limiting the data set to certain degrees of freedom that are of primary interest. This normally involves restricting the data to specific directions (X, Y and/or Z directions) or specific locations or groups of degrees of freedom, such as components of a large structural system.

6.3.8 Concept: Equation Condensation

Several important concepts should be delineated in the area of equation condensation methods. Equation condensation methods are used to reduce the number of equations based upon

measured data to more closely match the number of unknowns in the modal parameter estimation algorithms. There are a large number of condensation algorithms available. Based upon the modal parameter estimation algorithms in use today, the three types of algorithms most often used are:

- **Least Squares:** Least squares (LS), weighted least squares (WLS), total least squares (TLS) or double least squares (DLS) methods are used to minimize the squared error between the measured data and the estimation model. Historically, this is one of the most popular procedures for finding a pseudo-inverse solution to an over specified system. The main advantage of this method is computational speed and ease of implementation while the major disadvantage is numerical precision.
- **Transformations:** There are a large number of transformation that can be used to reduce the data. In the transformation methods, the measured data is reduced by approximating the data by the superposition of a set of significant vectors. The number of significant vectors is equal to the amount of independent measured data. This set of vectors is used to approximate the measured data and used as input to the parameter estimation procedures.
- **Singular Value Decomposition:** Singular Value Decomposition (SVD) is an example of one of the more popular transformation methods. The major advantage of these methods is numerical precision and the disadvantage is computational speed and memory requirements.
- **Coherent Averaging:** Coherent averaging is another popular method for reducing the data. In the coherent averaging method, the data is weighted by performing a dot product between the data and a weighting vector (spatial filter). Information in the data which is not coherent with the weighting vectors is averaged out of the data. The method is often referred to as a spatial filtering procedure. This method has both speed and precision but, in order to achieve precision, requires a good set of weighting vectors. In general, the optimum weighting vectors are connected with the solution which is unknown. It should be noted that least squares is an example of a non-coherent averaging process.

The least squares and the transformation procedures tend to weight those modes of vibration which are well excited. This can be a problem when trying to extract modes which are not well excited. The solution is to use a weighting function for condensation which tends to enhance the mode of interest. This can be accomplished in a number of ways:

- In the time domain, a spatial filter or a coherent averaging process can be used to filter the response to enhance a particular mode or set of modes. For example, by averaging the data from two symmetric exciter locations the symmetric modes of vibration can be enhanced. A second example would be using only the data in a local area of the system to enhance local modes. The third method is using estimates of the modes shapes as weighting functions to enhance particular modes.
- In the frequency domain, the data can be enhanced in the same manner as the time domain plus the data can be additionally enhanced by weighting the data in a frequency band near the natural frequency of the mode of interest.

Obviously, the type of equation condensation method that is utilized in a modal identification algorithm has a significant influence on the results of the parameter estimation process.

6.3.9 Concept: Coefficient Condensation

For the low order modal identification algorithms, the number of physical coordinates (typically N_o) is often much larger than the number of desired modal frequencies ($2N$). For this situation, the numerical solution procedure is constrained to solve for N_o or $2N_o$ modal frequencies. This can be very time consuming and is unnecessary. The number of physical coordinates (N_o) can be reduced to a more reasonable size ($N_e \approx N_o$ or $N_e \approx 2N_o$) by using a decomposition transformation from physical coordinates (N_o) to the approximate number of effective modal frequencies (N_e). Currently, singular value decompositions (SVD) or eigenvalue decompositions (ED) are used to preserve the principal modal information prior to formulating the linear equation solution for unknown matrix coefficients [23,37-38]. In most cases, even when the spatial information must be condensed, it is necessary to use a model order greater than two to compensate for distortion errors or noise in the data and to compensate for the case where the location of the transducers is not sufficient to totally define the structure.

$$[H'] = [T] [H] \quad (6.28)$$

where:

- $[H']$ is the transformed (condensed) frequency response function matrix .
- $[T]$ is the transformation matrix.
- $[H]$ is the original FRF matrix.

The difference between the two techniques lies in the method of finding the transformation matrix, $[T]$. Once $[H]$ has been condensed, however, the parameter estimation procedure is the same as for the full data set. Because the data eliminated from the parameter estimation process ideally corresponds to the noise in the data, the poles of the condensed data are the same as the poles of the full data set. However, the participation factors calculated from the condensed data may need to be expanded back into the full space.

$$[\Psi] = [T]^T [\Psi'] \quad (6.29)$$

where:

- $[\Psi]$ is the full-space participation matrix.
- $[\Psi']$ is the condensed-space participation matrix.

Eigenvalue Decomposition

In the eigenvalue decomposition method (sometimes referred to as *Principal Component Analysis* ^[4]), the $[T]$ matrix is composed of the eigenvectors corresponding to the N_e largest eigenvalues of the power spectrum of the FRF matrix as follows:

$$[H(\omega)]_{N_o \times N_i N_s} [H(\omega)]_{N_i N_s \times N_o}^H = [V] [\Lambda] [V]^H \quad (6.30)$$

The eigenvalues and eigenvectors are then found, and the $[T]$ matrix is constructed from the eigenvectors corresponding to the N_e largest eigenvalues:

$$[T]_{N_e \times N_o} = \left[\left[\begin{matrix} \left\{ v_1 \right\} \\ \left\{ v_2 \right\} \end{matrix} \right] \cdots \left[\begin{matrix} \left\{ v_k \right\} \\ \left\{ v_{N_e} \right\} \end{matrix} \right] \right]^T \quad (6.31)$$

where:

- $\{v_k\}$ is the $N_o \times 1$ eigenvector corresponding to the $k - th$ eigenvalue.

This technique may be adapted for condensing on the input space, as well. The power spectrum matrix is again found, but the FRF matrix must be reshaped (transposed) so that it is an $N_i \times N_o$ matrix for each spectral line:

$$[H(\omega)]_{N_i \times N_o N_s} [H(\omega)]_{N_o N_s \times N_i}^H = [V] [\Lambda] [V]^H \quad (6.32)$$

The eigenvalues and eigenvectors are again found as before, and the transformation matrix $[T]$ becomes:

$$[T]_{N_e \times N_i} = \left[\left[\begin{matrix} \left\{ v_1 \right\} \\ \left\{ v_2 \right\} \end{matrix} \right] \cdots \left[\begin{matrix} \left\{ v_k \right\} \\ \left\{ v_{N_e} \right\} \end{matrix} \right] \right]^T \quad (6.33)$$

where:

- $\{v_k\}$ is the $N_i \times 1$ eigenvector corresponding to the $k - th$ eigenvalue.

Singular Value Decomposition

The singular value decomposition condensation technique is similar to the eigenvalue-based technique, but operates on the FRF matrix directly instead of the power spectrum of the FRF matrix. The basis for this technique is the singular value decomposition [2-5], by which the matrix $[H]$ is broken down into three component parts, $[U]$, $[\Sigma]$, and $[V]$:

$$[H]_{N_o \times N_i N_s} = [U]_{N_o \times N_o} [\Sigma]_{N_o \times N_i N_s} [V]_{N_i N_s \times N_i N_s}^H \quad (6.34)$$

The left-singular vectors corresponding to the N_e largest singular values are the first N_e columns of $[U]$. These become the transformation matrix $[T]$:

$$[T]_{N_e \times N_o} = \left[\left[\begin{matrix} \left\{ u_1 \right\} \\ \left\{ u_2 \right\} \end{matrix} \right] \cdots \left[\begin{matrix} \left\{ u_k \right\} \\ \left\{ u_{N_e} \right\} \end{matrix} \right] \right]^T \quad (6.35)$$

where:

- $\{u_k\}$ is the $k - th$ column of $[U]$, which corresponds to the $k - th$ singular value.

This technique may also be adapted for condensing the input space, as long as the FRF matrix $[H]$ is reshaped (transposed) to an $N_i \times N_o$ matrix at each spectral line. The SVD operation then becomes

$$[H]_{N_i \times N_o N_s} = [U]_{N_i \times N_i} [\Sigma]_{N_i \times N_o N_s} [V]_{N_o N_s \times N_o N_s}^H \quad (6.36)$$

The transformation matrix $[T]$ is still composed of the left singular vectors corresponding to the N_e largest singular values,

$$[T]_{N_e \times N_i} = \left[\left[\begin{matrix} \left\{ u_1 \right\} \\ \left\{ u_2 \right\} \end{matrix} \right] \cdots \left[\begin{matrix} \left\{ u_k \right\} \\ \left\{ u_{N_e} \right\} \end{matrix} \right] \right]^T \quad (6.37)$$

where:

- $\{u_k\}$ is again the $k - th$ column of $[U]$, which corresponds to the $k - th$ singular value.

6.3.10 Concept: Model Order Determination

Much of the work concerned with modal parameter estimation since 1975 has involved methodology for determining the correct model order for the modal parameter model. Technically, model order refers to the highest power in the matrix polynomial equation. The number of modal frequencies found will be equal to the model order times the size of the matrix coefficients, normally N_o or N_i . For a given algorithm, the size of the matrix coefficients is normally fixed; therefore, determining the model order is directly linked to estimating N , the number of modal frequencies that are of interest in the measured data. As has always been the case, an estimate for the minimum number of modal frequencies can be easily found by counting

the number of peaks in the frequency response function in the frequency band of analysis. This is a minimum estimate of N since the frequency response function measurement may be at a node of one or more modes of the system, repeated roots may exist and/or the frequency resolution of the measurement may be too coarse to observe modes that are closely spaced in frequency. Several measurements can be observed and a tabulation of peaks existing in any or all measurements can be used as a more accurate minimum estimate of N . A more automated procedure for including the peaks that are present in several frequency response functions is to observe the summation of frequency response function power. This function represents the auto power or auto moment of the frequency response functions summed over a number of response measurements and is normally formulated as follows:

$$H_{power}(\omega) = \sum_{p=1}^{N_o} \sum_{q=1}^{N_i} H_{pq}(\omega) H_{pq}^*(\omega) \quad (6.38)$$

These simple techniques are extremely useful but do not provide an accurate estimate of model order when repeated roots exist or when modes are closely spaced in frequency. For these reasons, an appropriate estimate of the order of the model is of prime concern and is the single most important problem in modal parameter estimation.

In order to determine a reasonable estimate of the model order for a set of representative data, a number of techniques have been developed as guides or aids to the user. Much of the user interaction involved in modal parameter estimation involves the use of these tools. Most of the techniques that have been developed allow the user to establish a maximum model order to be evaluated (in many cases, this is set by the memory limits of the computer algorithm). Data is acquired based upon an assumption that the model order is equal to this maximum. In a sequential fashion, this data is evaluated to determine if a model order less than the maximum will describe the data sufficiently. This is the point that the user's judgement and the use of various evaluation aids becomes important. Some of the commonly used techniques are:

- Measurement Synthesis and Comparison (Curve-Fit).
- Error Chart.
- Stability Diagram.

- Mode Indication Functions.
- Rank Estimation.

One of the simplest techniques is to synthesize an impulse response function or a frequency response function and compare it to the measured function to see if modes have obviously been missed. This curve-fitting procedure is also used as a measure of the overall success of the modal parameter estimation procedure. The difference between the two functions can be quantified and normalized to give an indicator of the degree of fit. Obviously, a poor comparison can be due to many reasons, an incorrect model order simply being one of the possibilities.

6.3.10.1 Error Chart

Another method that has been used to more directly indicate the correct model order is the error chart. Essentially, the error chart is a plot of the error in the model as a function of increasing model order. The error in the model is a normalized quantity that represents the ability of the model to predict data that was not involved in the estimate of the model parameters. For example, when using measured data in the form of an impulse response function, only a small percentage of the total number of data values are involved in the estimate of modal parameters. If the model is estimated based upon 10 modes, only 4 times 10 data points are required, at a minimum, to estimate the modal parameters if no additional spatial information is used. The error in the model can then be estimated by the ability of the model to predict the next several data points in the impulse response function compared to the measured data points. For the case of 10 modes and 40 data points, the error in the model would be calculated from the predicted and measured data points 41 through 50. When the model order is insufficient, this model error will be large but when the model error reaches the "correct" value, further increase in the model order will not result in a further decrease in the error. Figure 6-15 is an example of an error chart.

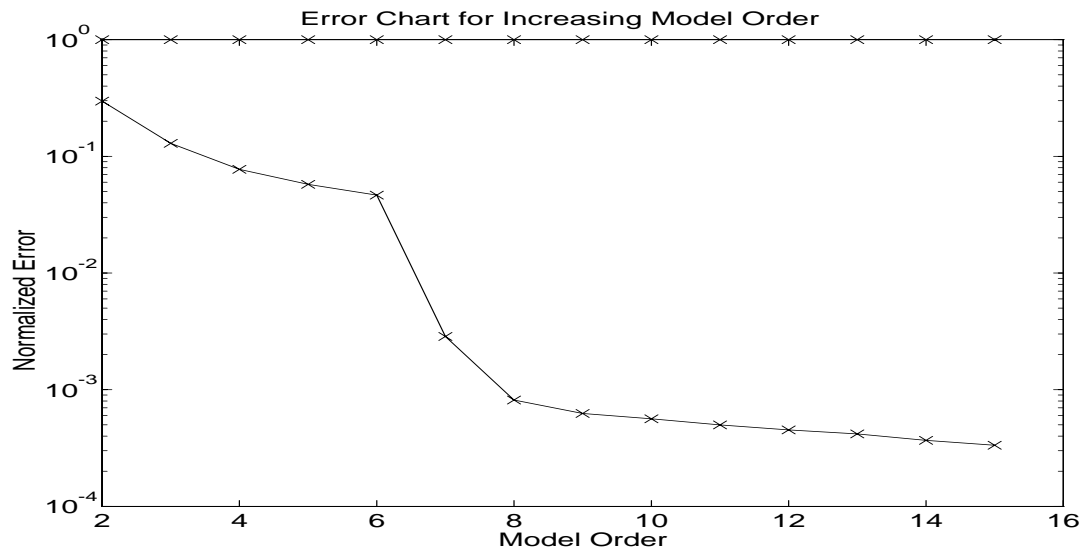


Figure 6-15. Model Order Determination: Error Chart

6.3.10.2 Stability Diagram

A further enhancement of the error chart is the stability diagram. The stability diagram is developed in the same fashion as the error chart and involves tracking the estimates of frequency, damping, and possibly modal participation factors as a function of model order. As the model order is increased, more and more modal frequencies are estimated but, hopefully, the estimates of the physical modal parameters will stabilize as the correct model order is found. For modes that are very active in the measured data, the modal parameters will stabilize at a very low model order. For modes that were poorly excited in the measured data, the modal parameters may not stabilize until a very high model order is chosen. Nevertheless, the nonphysical (computational) modes will not stabilize at all during this process and can be sorted out of the modal parameter data set more easily. Note that inconsistencies (frequency shifts, leakage errors, etc.) in the measured data set will obscure the stability and render the stability diagram difficult to use. Normally, a tolerance, in percentage, is given for the stability of each of the modal parameters that are being evaluated. Figure 6-16 is an example of a stability diagram. In Figure 6-16, a summation of the frequency response function power is plotted on the stability diagram for reference. Other mode indication functions can be plotted against the stability diagram for reference.

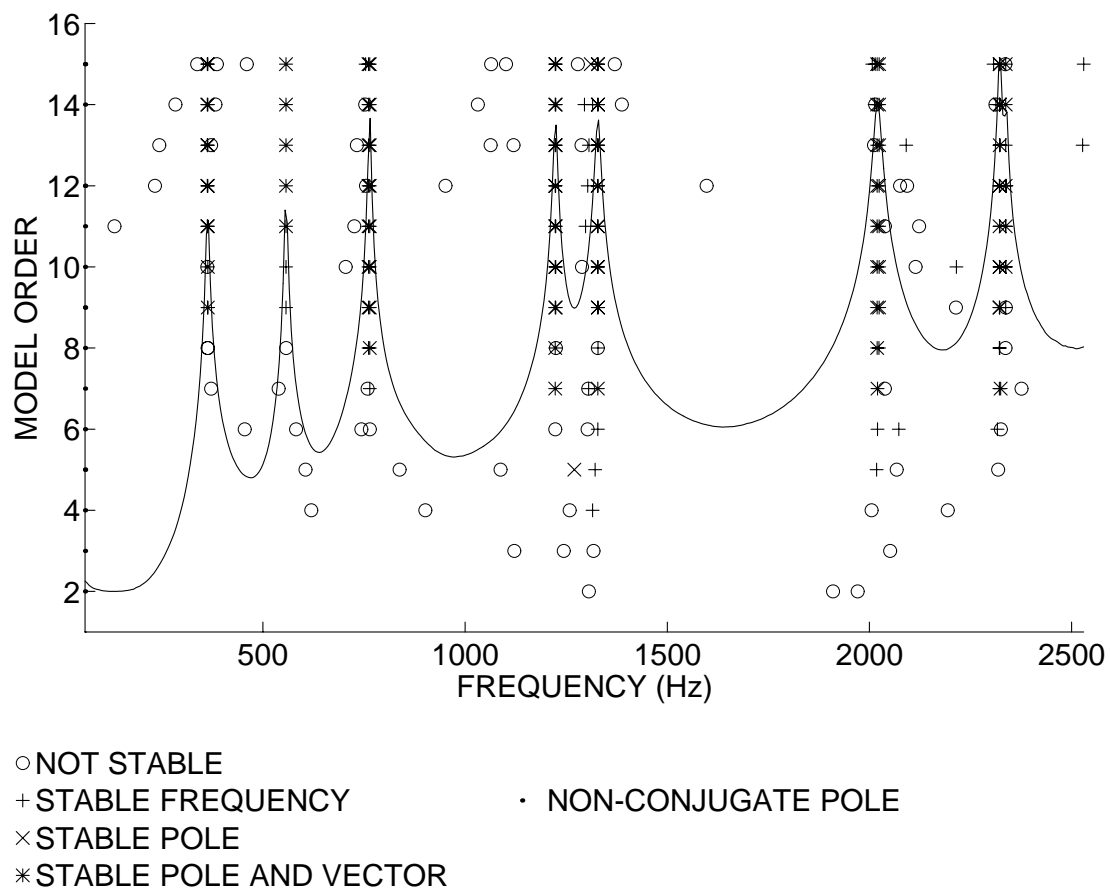


Figure 6-16. Model Order Determination: Stability Diagram

Stability diagrams have traditionally only been used for the high order model cases, such as the LSCE or the PTD. If the concept of stability is broadened to include consistency, a stability/consistency diagram can be constructed for almost any modal parameter estimation method where the vertical axis is a function of a change in model order, a change in the data subset used to estimate the modal frequencies or even a change in modal parameter estimation method.

6.3.10.3 Mode Indication Functions

Mode indication functions (MIF) are normally real-valued, frequency domain functions that exhibit local minima or maxima at the natural frequencies of real normal modes. One mode indication function can be plotted for each reference available in the measured data. The primary mode indication function will exhibit a local minimum or maximum at each of the natural frequencies of the system under test. The secondary mode indication function will exhibit a local minimum or maximum at repeated or pseudo-repeated roots of order two or more. Further mode indication functions yield local minima or maxima for successively higher orders of repeated or pseudo-repeated roots of the system under test.

6.3.10.3.1 Multivariate Mode Indication Function (MvMIF)

The *multivariate mode indication function* is based upon finding a force vector $\{F\}$ that will excite a normal mode at each frequency in the frequency range of interest ^[39]. If a normal mode can be excited at a particular frequency, the response to such a force vector will exhibit the 90 ° phase lag characteristic. Therefore, the real part of the response will be as small as possible particularly when compared to the imaginary part or the total response. In order to evaluate this possibility, a minimization problem can be formulated as follows:

$$\min_{\|F\|=1} \frac{\{F\}^T [H_{Real}]^T [H_{Real}] \{F\}}{\{F\}^T \left([H_{Real}]^T [H_{Real}] + [H_{Imag}]^T [H_{Imag}] \right) \{F\}} = \lambda \quad (6.39)$$

This minimization problem is similar to a Rayleigh quotient and it can be shown that the solution to the problem is found by finding the smallest eigenvalue λ_{min} and the corresponding eigenvector $\{F\}_{min}$ of the following problem:

$$[H_{Real}]^T [H_{Real}] \{F\} = \lambda \left([H_{Real}]^T [H_{Real}] + [H_{Imag}]^T [H_{Imag}] \right) \{F\} \quad (6.40)$$

The above eigenvalue problem is formulated at each frequency in the frequency range of interest. Note that the result of the matrix product $[H_{Real}]^T [H_{Real}]$ and $[H_{Imag}]^T [H_{Imag}]$ in each case is a square, real-valued matrix of size equal to the number of references in the measured data

$N_i \times N_i$. The resulting plot of a mode indication function for a seven reference case can be seen in Figure 6-17.

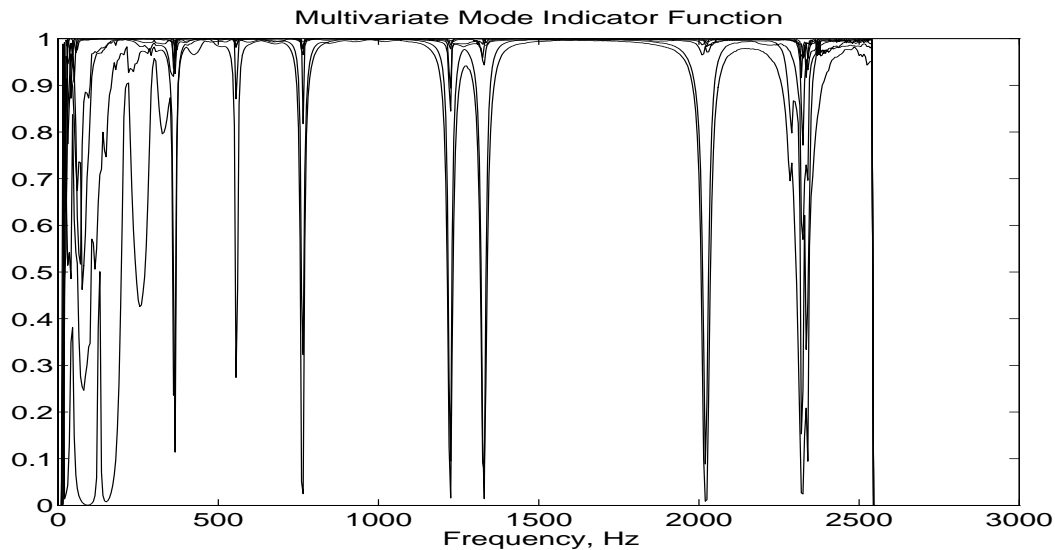


Figure 6-17. Multivariate Mode Indication Function

6.3.10.3.2 Complex Mode Indication Function (CMIF)

An algorithm based on singular value decomposition (SVD) methods applied to multiple reference FRF measurements, identified as the **Complex Mode Indication Function** (CMIF), was first developed for traditional FRF data in order to identify the proper number of modal frequencies, particularly when there are closely spaced or repeated modal frequencies [29,35]. Unlike the Multivariate Mode Indication Function (MvMIF), which indicates the existence of real normal modes, CMIF indicates the existence of real normal or complex modes and the relative magnitude of each mode. Furthermore, MvMIF yields a set of force patterns that can best excite the real normal mode, while CMIF yields the corresponding mode shape and modal participation vector.

The CMIF was originally defined as the eigenvalues, solved from the normal matrix formed from FRF matrix, at each spectral line. The normal matrix is obtained by premultiplying the FRF

matrix by its Hermitian matrix as $[H(\omega)]^H [H(\omega)]$. The CMIF is the plot of these eigenvalues on a log magnitude scale as a function of frequency. The peaks detected in the CMIF plot indicate the existence of modes, and the corresponding frequencies of these peaks give the damped natural frequencies for each mode. In the application of CMIF to traditional modal parameter estimation algorithms, the number of modes detected in CMIF determines the minimum number of degrees-of-freedom of the system equation for the algorithm. A number of additional degrees-of-freedom may be needed to take care of residual effects and noise contamination.

$$[H(\omega)]^H [H(\omega)] = [V(\omega)] [\Lambda(\omega)] [V(\omega)]^H \quad (6.41)$$

By taking the singular value decomposition of the FRF matrix at each spectral line, a similar expression to Equation (6.41) is obtained.

$$[H(\omega)] = [U(\omega)] [\Sigma(\omega)] [V(\omega)]^H \quad (6.42)$$

where:

- N_e is the number of effective modes. The effective modes are the modes that contribute to the response of the structure at this particular frequency ω .
- $[U(\omega)]$ is the left singular matrix of size $N_o \times N_e$, which is an unitary matrix.
- $[\Lambda(\omega)]$ is the eigenvalue matrix of size $N_d \times N_e$, which is a diagonal matrix.
- $[\Sigma(\omega)]$ is the singular value matrix of size $N_e \times N_e$, which is a diagonal matrix.
- $[V(\omega)]$ is the right singular matrix of size $N_d \times N_i$, which is also an unitary matrix.

Most often, the number of input points (reference points), N_i , is less than the number of response points, N_o . In Equation (6.42), if the number of effective modes is less than or equal to the smaller dimension of the FRF matrix, ie. $N_e \leq N_i$, the singular value decomposition leads to approximate mode shapes (left singular vectors) and approximate modal participation factors (right singular vectors). The singular value is then equivalent to the the scaling factor Q_r divided by the difference between the discrete frequency and the modal frequency $j\omega - \lambda_r$. For a given mode, since the scaling factor is a constant, the closer the modal frequency is to the discrete frequency, the larger the singular value will be. Therefore, the damped natural frequency is the frequency at which the maximum magnitude of the singular value occurs. If different modes are

compared, the stronger the mode contribution (larger residue value), the larger the singular value will be.

$$CMIF_k(\omega) \equiv \Lambda_k(\omega) = \Sigma_k(\omega)^2 \quad k = 1, 2, \dots, N_e \quad (6.43)$$

where:

- $CMIF_k(\omega)$ is the k – *th* CMIF as a function of frequency ω .
- $\Lambda_k(\omega)$ is the k – *th* eigenvalue of the normal matrix of FRF matrix as a function of frequency ω .
- $\Sigma_k(\omega)$ is the k – *th* singular value of the FRF matrix as a function of frequency ω .

In practical calculations, the normal matrix formed from the FRF matrix, $[H(\omega)]^H [H(\omega)]$, is calculated at each spectral line. The eigenvalues of this matrix are obtained. The CMIF plot is the plot of these eigenvalues on a log magnitude scale as a function of frequency. An automatic peak detector based on preset criteria is used to identify the existence of modes. The eigenvector corresponding to the peak detected is equivalent to the modal participation factor.

The peak in the CMIF indicates the location on the frequency axis that is nearest to the pole. The frequency is the estimated damped natural frequency, to within the accuracy of the frequency resolution. The magnitude of the eigenvalue indicates the relative magnitude of the modes, residue over damping factor. Figure 6-18 represents a typical CMIF for a multiple reference set a data. It must be noted that not all peaks in CMIF indicate modes. Errors such as noise, leakage, nonlinearity and a ***cross eigenvalue effect*** can also make a peak. The cross eigenvalue effect is due to the way the CMIF is plotted. In a CMIF plot, the eigenvalue curves are plotted as a function of magnitude - the largest eigenvalue is plotted first at each frequency followed by subsequently smaller eigenvalues. Since the contributions from different modes vary along the frequency axis, at a specific frequency, the contribution of two modes can be approximately equal. At this frequency, these two eigenvalue curves cross each other. Because of the limited frequency resolution and the way that the CMIF is plotted, the lower eigenvalue curve appears to peak, while the higher eigenvalue curve appears to dip. Therefore, the peak in this case is not due to a system pole but is caused by an equal contribution from two modes. In Figure 6-18, the cross-eigenvalue effect can be noticed in both the third and fourth curves around 1300 Hertz.

This characteristic is identifiable since the peak occurs in the lower eigenvalue curve at the same frequency as a dip in the higher eigenvalue curve. This effect is referred to as the cross eigenvalue effect. Another way of identifying the cross eigenvalue effect is to check the corresponding eigenvectors $[V(\omega)]$ associated with each eigenvalue curves, ie. the modal participation vectors. The peaks that occur due to this cross eigenvalue effect can easily be identified by checking eigenvectors of adjacent spectral lines. If the eigenvectors of adjacent spectral lines do not represent the same shape as the eigenvector at the peak, this peak is not a system pole but is caused by the cross eigenvalue effect.

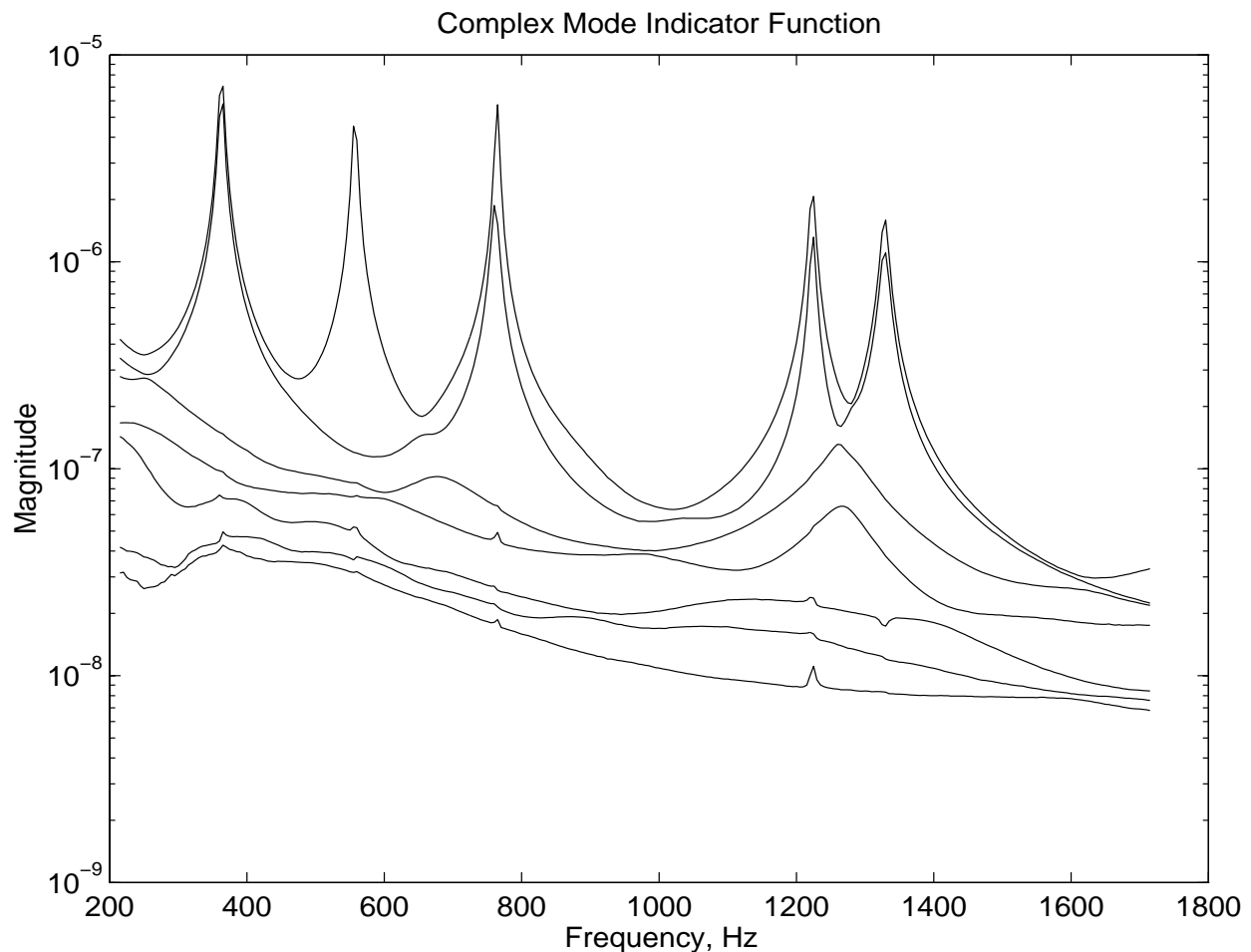


Figure 6-18. Complex Mode Indication Function

Since the mode shapes that contribute to each peak do not change much around each peak,

several adjacent spectral lines from the FRF matrix can be used simultaneously for a better estimation of mode shapes. By including several spectral lines of data in the singular value decomposition calculation, the effect of the leakage error can be minimized. If only the quadrature part of the FRF matrix is used in CMIF, the mode shape obtained turns out to be the same as in the Multi-MAC method ^[36].

6.3.10.4 Rank Estimation

A more recent model order evaluation technique involves the estimate of the rank of the matrix of measured data. An estimate of the rank of the matrix of measured data gives a good estimate of the model order of the system. Essentially, the rank is an indicator of the number of independent characteristics contributing to the data. While the rank cannot be calculated in an absolute sense, the rank can be estimated from the singular value decomposition (SVD) of the matrix of measured data. For each mode of the system, one singular value should be found by the SVD procedure. The SVD procedure finds the largest singular value first and then successively finds the next largest. The magnitude of the singular values are used in one of two different procedures to estimate the rank. The concept that is used is that the singular values should go to zero when the rank of the matrix is exceeded. For theoretical data, this will happen exactly. For measured data, due to random errors and small inconsistencies in the data, the singular values will not become zero but will be very small. Therefore, the rate of change of the singular values is used as an indicator rather than the absolute values. In one approach, each singular value is divided by the first (largest) to form a normalized ratio. This normalized ratio is treated much like the error chart and the appropriate rank (model order) is chosen when the normalized ratio approaches an asymptote. In another similar approach, each singular value is divided by the previous singular value forming a normalized ratio that will be approximately equal to one if the successive singular values are not changing magnitude. When a rapid decrease in the magnitude of the singular value occurs, the ratio of successive singular values drops (or peaks if the inverse of the ratio is plotted) as an indicator of rank (model order) of the system. Figure 6-19 shows examples of these rank estimate procedures.

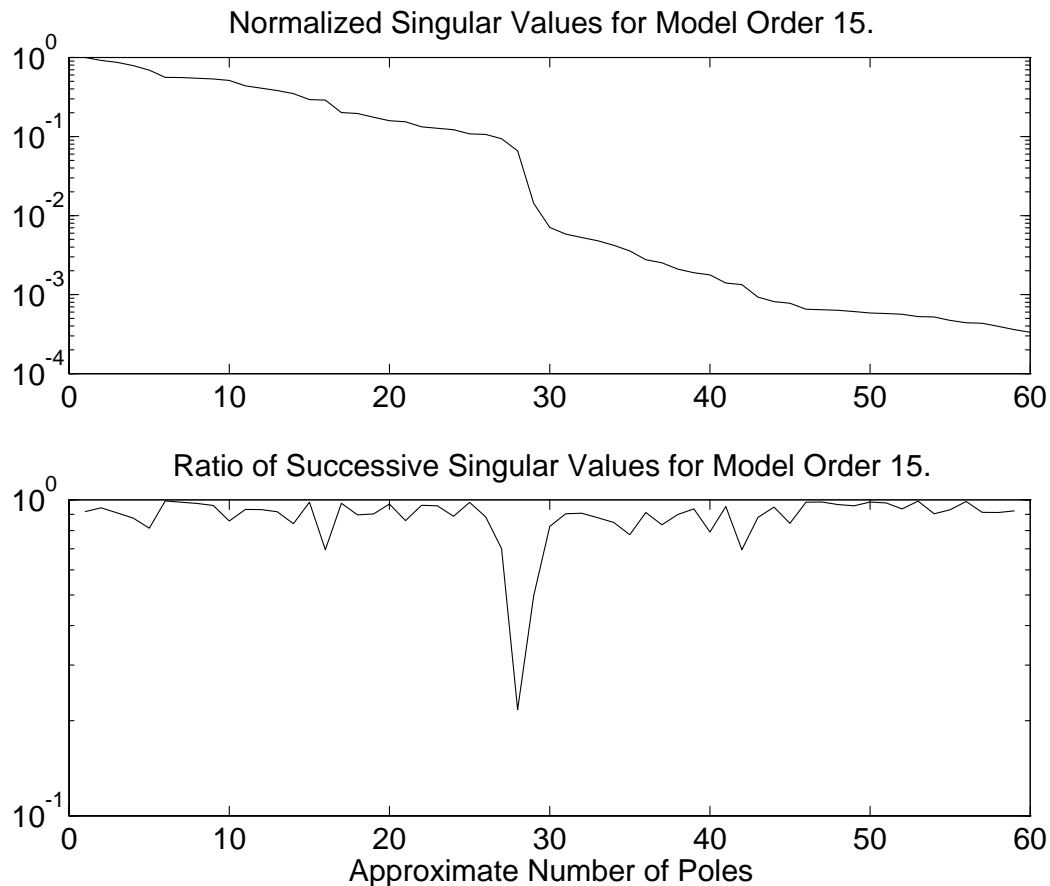


Figure 6-19. Model Order Determination: Rank Estimation

6.3.11 Concept: Residuals

Continuous systems have an infinite number of degrees of freedom but, in general, only a finite number of modes can be used to describe the dynamic behavior of a system. The theoretical number of degrees of freedom can be reduced by using a finite frequency range. Therefore, for example, the frequency response can be broken up into three partial sums, each covering the modal contribution corresponding to modes located in the frequency ranges. Note how the mode at 2.2 Hertz affects the modes below and above in the frequency range plotted in Figure 6-20.

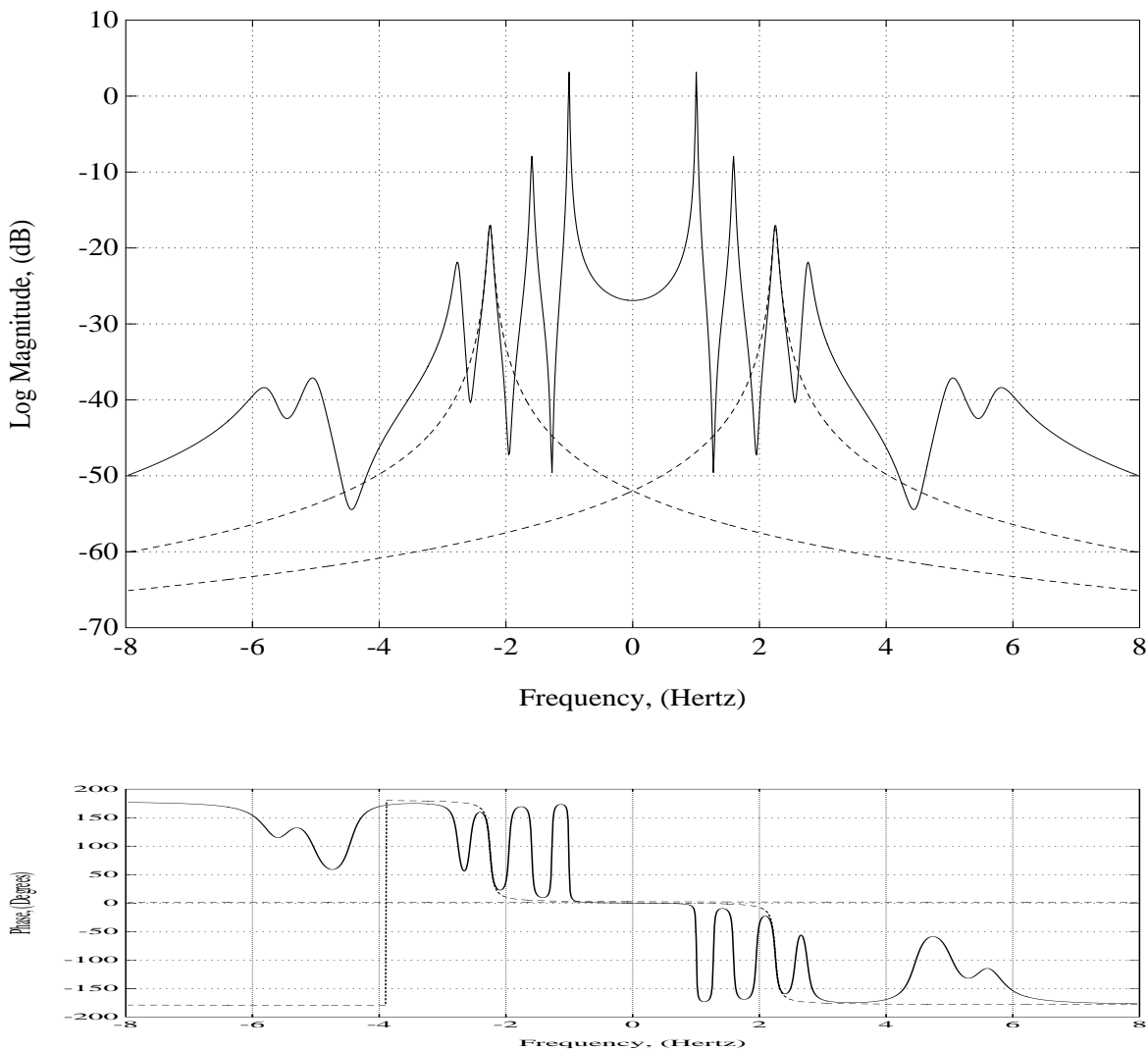


Figure 6-20. Residual Effects From Adjacent Poles

In the frequency range of interest, the modal parameters can be estimated to be consistent with Equation (6.1). In the lower and higher frequency ranges, residual terms can be included to account for modes in these ranges. In this case, Equation (6.1) can be rewritten for a single frequency response function as:

$$H_{pq}(\omega) = R_{F_{pq}} + \sum_{r=1}^N \frac{A_{pqr}}{j\omega - \lambda_r} + \frac{A_{pqr}^*}{j\omega - \lambda_r^*} + R_{I_{pq}}(\omega) \quad (6.44)$$

where:

- $R_{F_{pq}}$ = Residual Flexibility
- $R_{I_{pq}}(s)$ = Residual Inertia

In many cases the lower residual term is called the *inertia restraint*, or *residual inertia*, and the upper residual term is called the *residual flexibility*. These residuals are a function of each frequency response function measurement and are not global properties of the frequency response function matrix. Therefore, residuals cannot be estimated unless the frequency response function has been measured. Note that in this common formulation of residuals, both terms are real valued quantities. Also note that in general this is a simplification: the residual effects of modes below and/or above the frequency range of interest cannot be completely represented by such simple relationships. The lower residual is a term reflecting the inertia or mass of the lower modes and is an inverse function of the frequency squared. The upper residual is a term reflecting the flexibility of the upper modes and is constant with frequency.

In this case, the form of the residual is based upon a physical concept of how the system poles below and above the frequency range of interest will affect the data in the range of interest. As the system poles below and above the range of interest are located in the proximity of the boundaries, these effects are not the simple real valued quantities noted in Equation (6.44). In these cases, residual modes may be included in the model to partially account for these effects. When this is done, the modal parameters that are associated with these residual poles have no physical significance but may be required in order to compensate for strong dynamic influences from outside the frequency range of interest. Using the same argument, the lower and upper residuals can take on any mathematical form that is convenient as long as the lack of physical significance is understood. Mathematically, power functions of frequency (zero, first, and second order) are commonly used within such a limitation. In general, the use of residuals is confined to frequency response function models. This is primarily due to the difficulty of formulating a reasonable mathematical model and solution procedure in the time domain for the general case that includes residuals.

6.4 SDOF Approximate Algorithms

For any real system, the use of single degree of freedom algorithms to estimate modal parameters is always an approximation since any realistic structural system will have many degrees of freedom. Nevertheless, in cases where the modes are not close in frequency and do not affect one another significantly, single degree of freedom algorithms are very effective. Specifically, single degree of freedom algorithms are quick, rarely involving much mathematical manipulation of the data, and give sufficiently accurate results for most modal parameter requirements. Naturally, most multiple degree of freedom algorithm can be constrained to estimate only a single degree of freedom at a time if further mathematical accuracy is desired. The most commonly used single degree of freedom algorithms involve using the information at a single frequency as an estimate of the modal vector. Figure 6-21 is an example of using the information at the peak frequency location (positive or negative peak in the imaginary part of the X/F frequency response functions) as an estimate of the modal vectors of a simple beam.

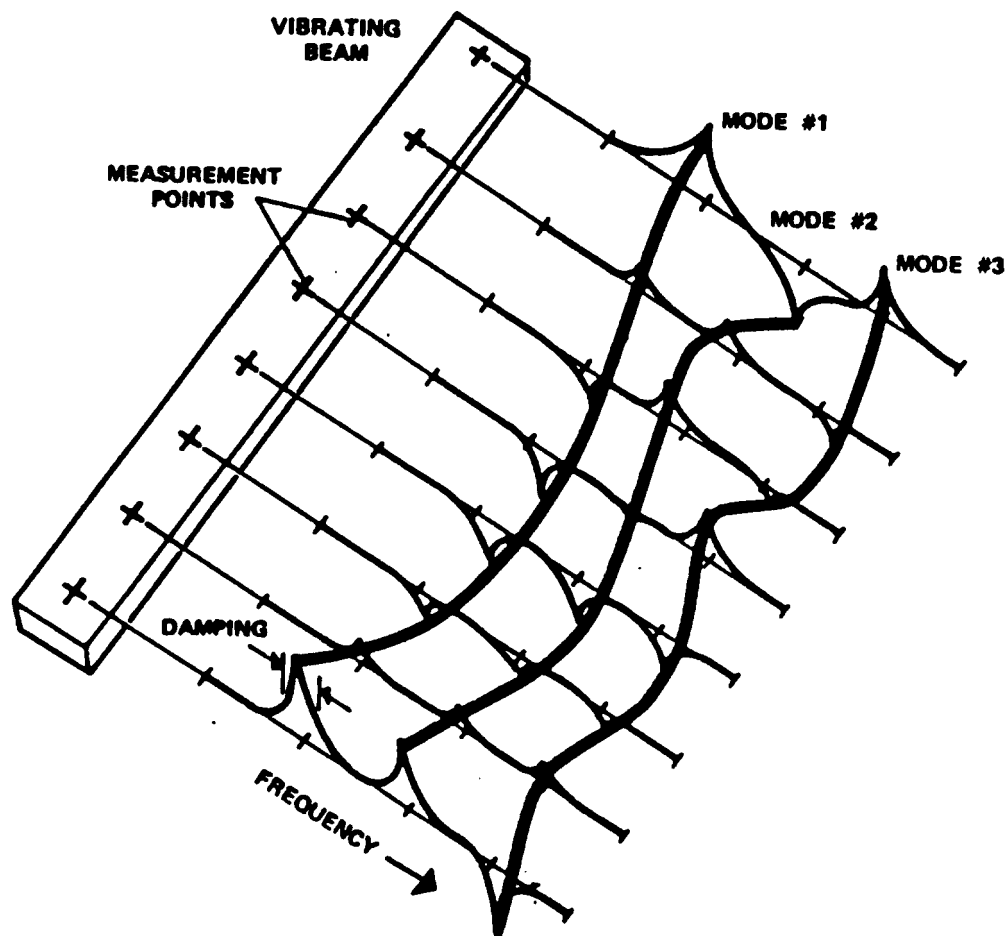


Figure 6-21. Modal Vectors from the Imaginary Part of the FRF

6.4.1 Operating Vector Estimation

Technically, when many single degree of freedom approaches are used to estimate modal parameters, sufficient simplifying assumptions are made such that the results are not actually modal parameters. In these cases, the results are often referred to as *operating vectors* rather than modal vectors. This term refers to the fact that if the structural system is excited at this frequency, the resulting motion will be a linear combination of the modal vectors rather than a single modal vector. If one mode is dominant, then the operating vector will be approximately equal to the mode vector.

Summary

- Methods are Simple, Approximate Methods
- Modal Frequency
 - Peak in Imaginary Part of FRF
 - Zero Crossing in Real Part of FRF
 - Peak in Magnitude or Log Magnitude of FRF
- Modal Damping: Half Power Method
- Residue: SDOF Equation
 - Complex Amplitude of FRF
 - Imaginary Part of FRF - X/F or A/F
 - Real Part of FRF - V/F
 - Magnitude of FRF (+/- sign depending on phase angle)
- Separation of Close Modes is Generally Not Possible
- No Residuals

The approximate relationships that are used in these cases are represented in the following two equations.

$$H_{pq}(\omega_r) \approx \frac{A_{pqr}}{j\omega_r - \lambda_r} + \frac{A_{pqr}^*}{j\omega_r - \lambda_r^*} \quad (6.45)$$

$$H_{pq}(\omega_r) \approx \frac{A_{pqr}}{-\sigma_r} \quad (6.46)$$

For these less complicated methods, the damped natural frequencies (ω_r) are estimated by observing the maxima in the frequency response functions. The damping factors (σ_r) are estimated using half-power methods ^[1]. The residues (A_{pqr}) are then estimated from Equation (6.45) or (6.46) using the frequency response function data at the damped natural frequency.

Figures 6-22 through 24 show frequency response function measurements in different formats to

emphasize that the data can be determined in several ways. Note the characteristics of the FRF data, in each format, in the frequency range around the damped natural frequency (ω_r).

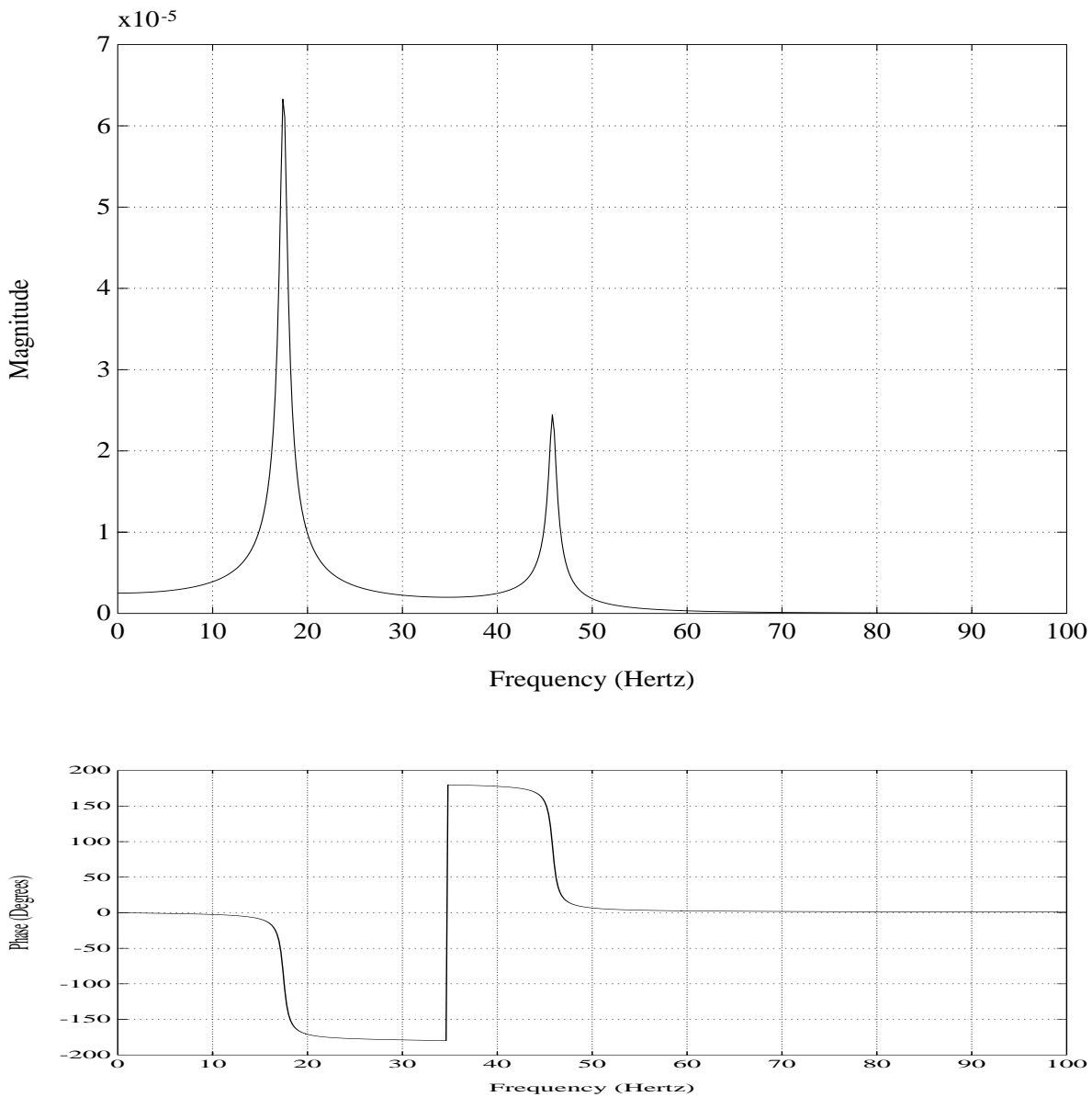


Figure 6-22. Single Degree of Freedom Method - Magnitude/Phase

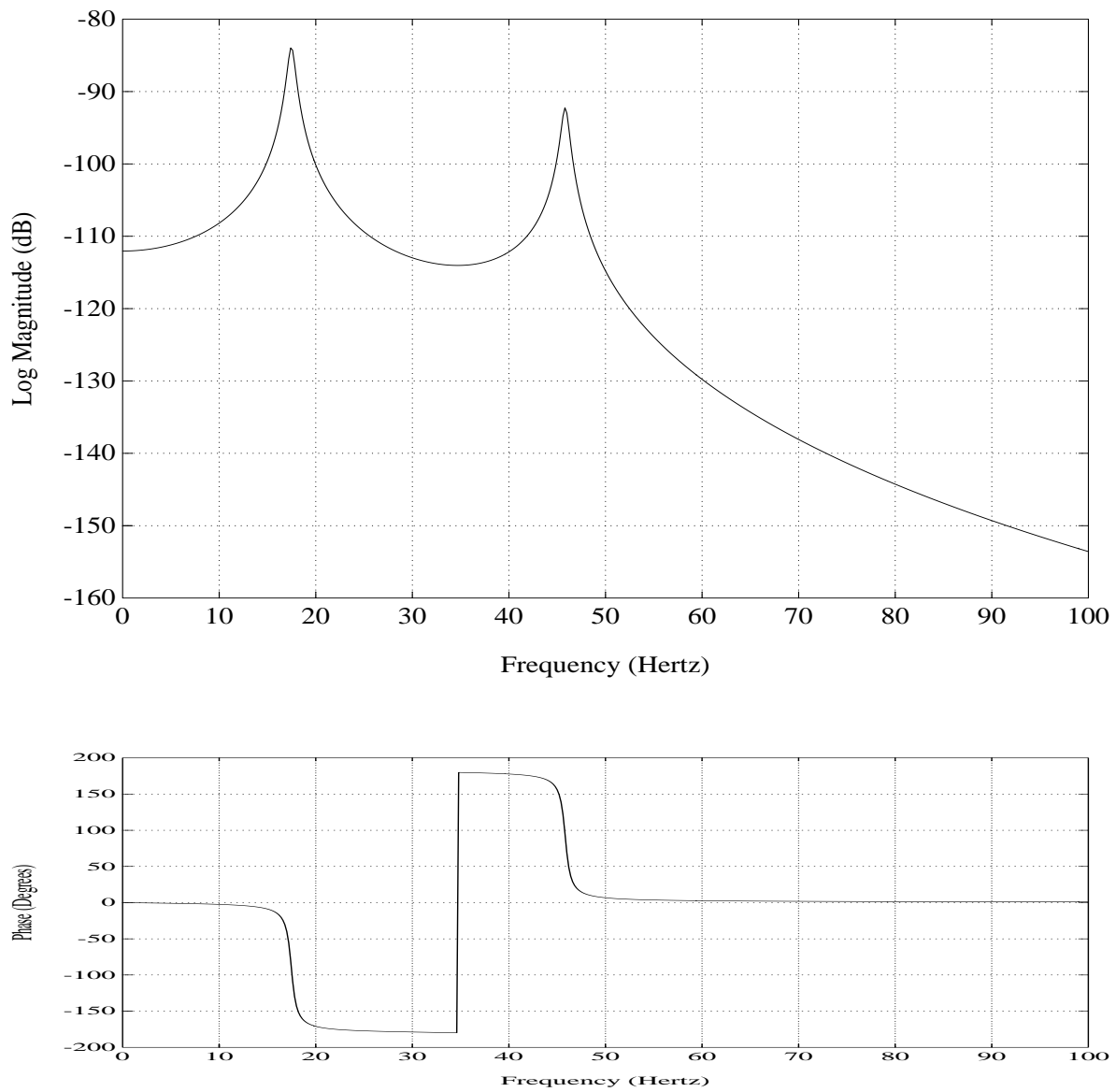


Figure 6-23. Single Degree of Freedom Method - Log Magnitude/Phase

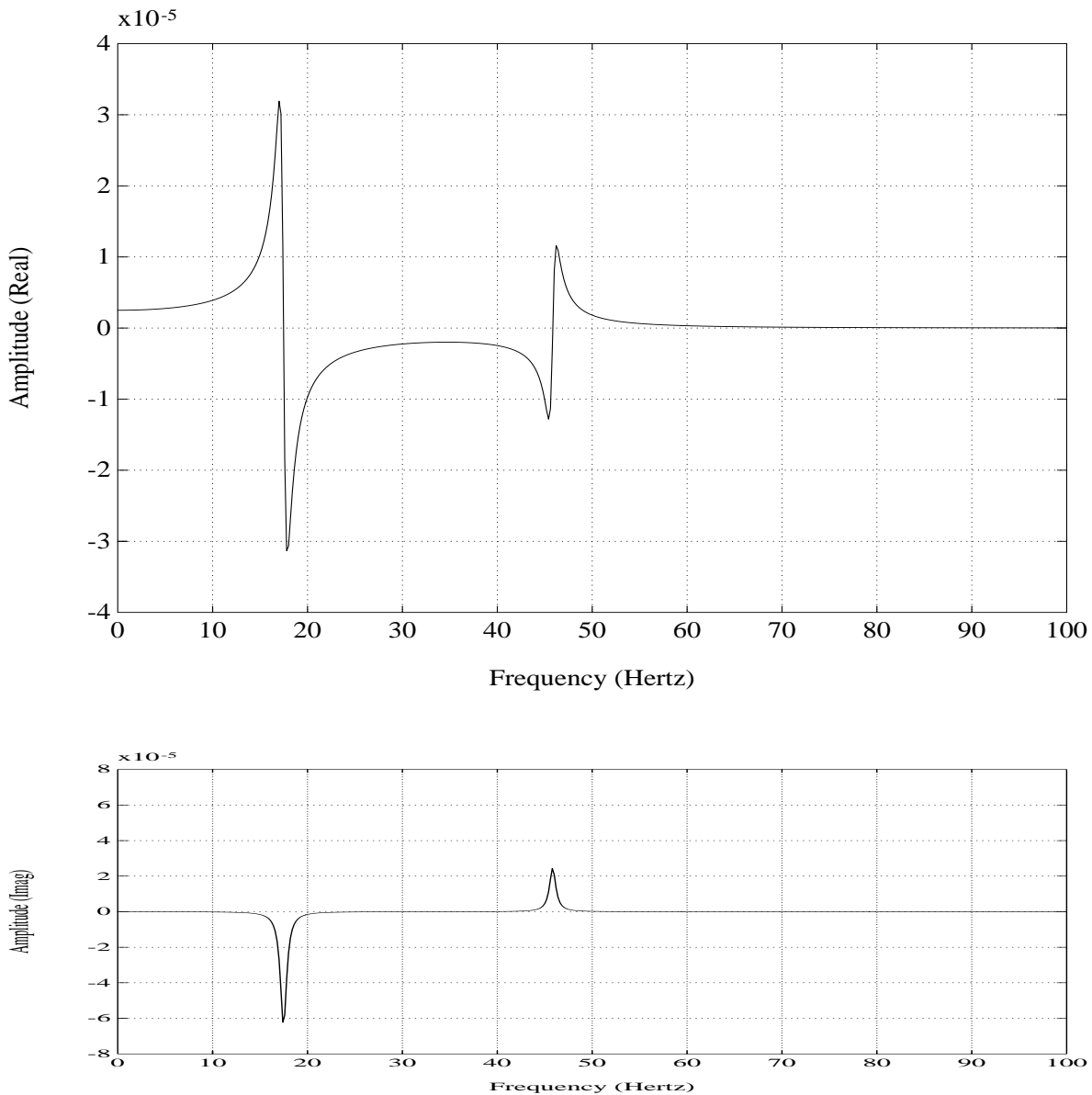


Figure 6-24. Single Degree of Freedom Method - Real/Imaginary

6.4.2 Complex Plot (Circle Fit)

The Circle Fit method is based upon a technique first reported by Kennedy and Pancu in 1947 [40]. This method utilizes the concept that the data curve in the vicinity of a modal frequency looks circular. In fact, the diameter of the circle is used to estimate the residue once the damping

factor is estimated. More importantly, though, Kennedy and Pancu noted that the distance along the curve between data points at equidistant frequency maximized in the neighborhood of the modal frequency. In this way, the circle fit method was the first method to detect closely spaced modes.

This method can give erroneous answers when the modal coefficient is near zero. This occurs essentially because when the mode does not exist in a particular frequency response function (either the input or response degree of freedom is at a node of the mode), the remaining data in the frequency range of the mode will be strongly affected by the next higher or lower mode. Therefore, the diameter of the circle that will be estimated will be a function of the modal coefficient for the next higher or lower mode. This can be detected visually but is somewhat difficult to detect automatically.

Summary

- Simple Historical Method (Kennedy and Pancu, 1947)
- Modal Frequency: Frequency Where Largest Spacing Between Data Points Occurs (Frequency at Bottom or Top of Complex Plot)
- Modal Damping: Half Power Method
- Residue: SDOF Equation
 - Diameter of the circle $\approx \frac{A_{pqr}}{-\sigma_r}$
- Separation of Close Modes Possible
- Residuals Possible
 - Center of the circle not on axis
- Complex Modal Coefficients
- Problem: Error when modal coefficient should be zero.

The approximate relationship that is used in this case is represented in the following equation.

$$H_{pq}(\omega_r) \approx R_{pq} + \frac{A_{pqr}}{j\omega_r - \lambda_r} + \frac{A_{pqr}^*}{j\omega_r - \lambda_r^*} \quad (6.47)$$

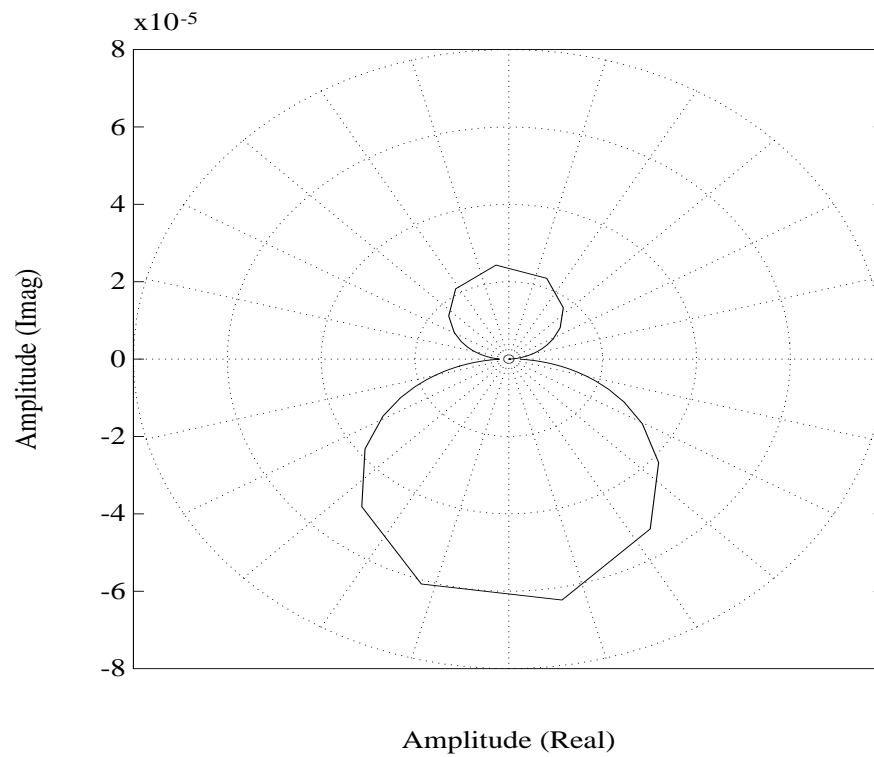


Figure 6-25. Single Degree of Freedom Method - Real versus Imaginary

General Equation of a Circle

$$x^2 + y^2 + a x + b y + c = 0$$

$$a x + b y + c = -x^2 - y^2$$

Center of Circle:

$$x_c = -\frac{a}{2} \quad y_c = -\frac{b}{2}$$

Radius of Circle:

$$Radius = \left(\left(\frac{a}{2} \right)^2 + \left(\frac{b}{2} \right)^2 - c \right)^{0.5}$$

Data Points for Circle:

$$x_i = Real(H_{pq}(\omega_i)) \quad y_i = Imag(H_{pq}(\omega_i))$$

Direct Solution (Three data points):

$$\begin{aligned} a x_1 + b y_1 + c &= -x_1^2 - y_1^2 \\ a x_2 + b y_2 + c &= -x_2^2 - y_2^2 \\ a x_3 + b y_3 + c &= -x_3^2 - y_3^2 \end{aligned}$$

$$\begin{bmatrix} x_1 & y_1 & 1 \\ x_2 & y_2 & 1 \\ x_3 & y_3 & 1 \end{bmatrix} \begin{Bmatrix} a \\ b \\ c \end{Bmatrix} = \begin{Bmatrix} -x_1^2 - y_1^2 \\ -x_2^2 - y_2^2 \\ -x_3^2 - y_3^2 \end{Bmatrix} \quad or \quad [T] \begin{Bmatrix} a \\ b \\ c \end{Bmatrix} = \{S\}$$

$$\begin{Bmatrix} a \\ b \\ c \end{Bmatrix} = [T]^{-1} \{S\}$$

Least Squares Solution (More than three data points):

$$\begin{bmatrix} x_1 & y_1 & 1 \\ x_2 & y_2 & 1 \\ x_3 & y_3 & 1 \\ x_4 & y_4 & 1 \\ \dots & \dots & \dots \\ x_n & y_n & 1 \end{bmatrix} \begin{Bmatrix} a \\ b \\ c \end{Bmatrix} = \begin{Bmatrix} -x_1^2 - y_1^2 \\ -x_2^2 - y_2^2 \\ -x_3^2 - y_3^2 \\ -x_4^2 - y_4^2 \\ \dots \\ -x_n^2 - y_n^2 \end{Bmatrix} \quad or \quad [T] \begin{Bmatrix} a \\ b \\ c \end{Bmatrix} = \{S\}$$

$$[T]^T [T] \begin{Bmatrix} a \\ b \\ c \end{Bmatrix} = [T]^T \{S\}$$

$$\begin{Bmatrix} a \\ b \\ c \end{Bmatrix} = \left[[T]^T [T] \right]^{-1} [T]^T \{S\}$$

6.4.3 Two Point Finite Difference Formulation

The difference method formulations are simple methods that are based upon comparing adjacent frequency information in the vicinity of a resonance frequency. When a ratio of this information, together with information from the derivative of the frequency response function at the same frequencies, is formed, a reasonable estimation of the modal frequency and residue for each mode can be determined under the assumption that modes are not too close together. This method can give erroneous answers when the modal coefficient is near zero. This problem can be detected by comparing the predicted modal frequency to the frequency range of the data used in the finite difference algorithm. As long as the predicted modal frequency lies within the frequency band, the estimate of the residue (modal coefficient) should be valid.

Summary

- Common method implemented on many two channel digital signal processing analyzers.
- Solves for both modal frequency (λ_r) and residue (A_{pqr}).
- Uses the frequency response function information at two frequencies in the vicinity of a single mode.
- Several combinations of two frequencies can be used and the results averaged.
- Approximate method (ignores complex conjugate contribution).
- No Residuals.
- Problem: Error when modal coefficient should be zero.

The approximate relationships that are used in this case is represented in the following three equations. The frequencies noted in these relationships are as follows: ω_1 is a frequency near the damped natural frequency ω_r and ω_p is the peak frequency close to the damped natural frequency ω_r .

$$H_{pq}(\omega_1) \approx \frac{A_{pqr}}{j\omega_1 - \lambda_r} \quad (6.48)$$

$$H_{pq}(\omega_p) \approx \frac{A_{pqr}}{j\omega_p - \lambda_r} \quad (6.49)$$

The finite difference relationships are formulated as follows:

$$\Delta_1 = H_{pq}(\omega_p) - H_{pq}(\omega_1) \approx \frac{A_{pqr}(j\omega_1 - j\omega_p)}{(j\omega_1 - \lambda_r)(j\omega_p - \lambda_r)} \quad (6.50)$$

$$\Delta_2 = j\omega_p H_{pq}(\omega_p) - j\omega_1 H_{pq}(\omega_1) \approx \frac{A_{pqr}(j\omega_1 - j\omega_p)\lambda_r}{(j\omega_1 - \lambda_r)(j\omega_p - \lambda_r)} \quad (6.51)$$

$$\Delta_3 = j(\omega_1 - \omega_p) H_{pq}(\omega_1) H_{pq}(\omega_p) \approx \frac{j(\omega_1 - \omega_p) A_{pqr} A_{pqr}}{(j\omega_1 - \lambda_r)(j\omega_p - \lambda_r)} \quad (6.52)$$

Modal Frequency (λ_r)

$$\lambda_r \approx \frac{\Delta_2}{\Delta_1} = \frac{j\omega_p H_{pq}(\omega_p) - j\omega_1 H_{pq}(\omega_1)}{H_{pq}(\omega_p) - H_{pq}(\omega_1)} \quad (6.53)$$

Residue (A_{pqr})

$$A_{pqr} \approx \frac{\Delta_3}{\Delta_1} = \frac{j(\omega_1 - \omega_p) H_{pq}(\omega_1) H_{pq}(\omega_p)}{H_{pq}(\omega_p) - H_{pq}(\omega_1)} \quad (6.54)$$

Least Squares Solution

Since both of the equations that are used to estimate modal frequency λ_r and residue A_{pqr} are linear equations, a least squares solution can be formed by using other frequency response function data in the vicinity of the resonance. For this case, additional equations can be developed using $H_{pq}(\omega_2)$ or $H_{pq}(\omega_3)$ in the above equations instead of $H_{pq}(\omega_1)$. Starting with Equation (6.53) and (6.54) for any frequency (ω_1) in the vicinity of the peak frequency (ω_p) (rearranging the equations slightly):

$$(H_{pq}(\omega_p) - H_{pq}(\omega_1)) \lambda_r = j\omega_p H_{pq}(\omega_p) - j\omega_1 H_{pq}(\omega_1) \quad (6.55)$$

$$(H_{pq}(\omega_p) - H_{pq}(\omega_1)) A_{pqr} = j(\omega_1 - \omega_p) H_{pq}(\omega_1) H_{pq}(\omega_p) \quad (6.56)$$

Two more equations, involving the same two unknowns, can now be written for any other frequency in the vicinity of the peak frequency (ω_p). Putting these equations into matrix form yields:

$$\begin{bmatrix} H_{pq}(\omega_p) - H_{pq}(\omega_1) \\ H_{pq}(\omega_p) - H_{pq}(\omega_2) \\ H_{pq}(\omega_p) - H_{pq}(\omega_3) \\ H_{pq}(\omega_p) - H_{pq}(\omega_p) \\ \dots \\ H_{pq}(\omega_p) - H_{pq}(\omega_s) \end{bmatrix}_{N_s \times 1} \{ \lambda_r \}_{1 \times 1} = \begin{bmatrix} j\omega_p H_{pq}(\omega_p) - j\omega_1 H_{pq}(\omega_1) \\ j\omega_p H_{pq}(\omega_p) - j\omega_2 H_{pq}(\omega_2) \\ j\omega_p H_{pq}(\omega_p) - j\omega_3 H_{pq}(\omega_3) \\ j\omega_p H_{pq}(\omega_p) - j\omega_p H_{pq}(\omega_p) \\ \dots \\ j\omega_p H_{pq}(\omega_p) - j\omega_s H_{pq}(\omega_s) \end{bmatrix}_{N_s \times 1} \quad (6.57)$$

$$\begin{bmatrix} H_{pq}(\omega_p) - H_{pq}(\omega_1) \\ H_{pq}(\omega_p) - H_{pq}(\omega_2) \\ H_{pq}(\omega_p) - H_{pq}(\omega_3) \\ H_{pq}(\omega_p) - H_{pq}(\omega_p) \\ \dots \\ H_{pq}(\omega_p) - H_{pq}(\omega_s) \end{bmatrix}_{N_s \times 1} \left\{ A_{pqr} \right\}_{1 \times 1} = \begin{bmatrix} j(\omega_1 - \omega_p) H_{pq}(\omega_1) H_{pq}(\omega_p) \\ j(\omega_2 - \omega_p) H_{pq}(\omega_2) H_{pq}(\omega_p) \\ j(\omega_3 - \omega_p) H_{pq}(\omega_3) H_{pq}(\omega_p) \\ j(\omega_p - \omega_p) H_{pq}(\omega_p) H_{pq}(\omega_p) \\ \dots \\ j(\omega_s - \omega_p) H_{pq}(\omega_s) H_{pq}(\omega_p) \end{bmatrix}_{N_s \times 1} \quad (6.58)$$

The above equations represent overdetermined sets of linear equations that can be solved using any psuedo-inverse or normal equations approach.

6.4.4 Least Squares (Local) SDOF Method

The least squares, local SDOF formulations are simple methods that are based upon using a SDOF model in the vicinity of a resonance frequency. A reasonable estimation of the modal frequency and residue for each mode can be determined under the assumption that modes are not too close together. This method can give erroneous answers when the modal coefficient is near zero. This problem can be detected by comparing the predicted modal frequency to the frequency range of the data used in the algorithm. As long as the predicted modal frequency lies within the frequency band, the estimate of the residue (modal coefficient) should be valid.

Summary

- Common method implemented on many two channel digital signal processing analyzers.
- Solves for both modal frequency (λ_r) and residue (A_{pqr}).
- Uses the frequency response function information in the vicinity of a single mode.
- Approximate method (ignores complex conjugate contribution).
- No Residuals.
- Problem: Error when modal coefficient should be zero.

The approximate relationship that is used in this case is represented in the following equation. The frequency ω_1 is a frequency near the damped natural frequency ω_r .

$$H_{pq}(\omega_1) \approx \frac{A_{pqr}}{j\omega_1 - \lambda_r} \quad (6.59)$$

$$H_{pq}(\omega_1) (j\omega_1 - \lambda_r) = A_{pqr} \quad (6.60)$$

$$H_{pq}(\omega_1) \lambda_r + A_{pqr} = (j\omega_1) H_{pq}(\omega_1) \quad (6.61)$$

Repeating the above equation for several frequencies in the vicinity of the peak frequency:

$$\begin{bmatrix} H_{pq}(\omega_1) & 1 \\ H_{pq}(\omega_2) & 1 \\ H_{pq}(\omega_3) & 1 \\ H_{pq}(\omega_p) & 1 \\ \dots & \dots \\ H_{pq}(\omega_s) & 1 \end{bmatrix}_{N_s \times 2} \begin{Bmatrix} \lambda_r \\ A_{pqr} \end{Bmatrix}_{2 \times 1} = \begin{Bmatrix} (j\omega_1) H_{pq}(\omega_1) \\ (j\omega_2) H_{pq}(\omega_2) \\ (j\omega_3) H_{pq}(\omega_3) \\ (j\omega_p) H_{pq}(\omega_p) \\ \dots \\ (j\omega_s) H_{pq}(\omega_s) \end{Bmatrix}_{N_s \times 1} \quad (6.62)$$

The above equation again represents an overdetermined set of linear equations that can be solved using any psuedo-inverse or normal equations approach.

6.4.5 Least Squares (Global) SDOF Method

The least squares, global SDOF formulations are simple methods that are based upon using a SDOF model in the vicinity of a resonance frequency for all measurements in a row or column of the FRF matrix. A reasonable estimation of the modal frequency and residue for each mode can be determined under the assumption that modes are not too close together. This method can give erroneous results for a specific residue when the modal coefficient is near zero.

Summary

- Solves for both modal frequency (λ_r) and residue (A_{pqr}).
- Uses the frequency response function information in the vicinity of a single mode.
- Approximate method (ignores complex conjugate contribution).
- No Residuals.
- Problem: Error when modal coefficient should be zero.

The approximate relationship that is used in this case begins with the result of the least squares, local SDOF method.

$$\begin{bmatrix} H_{pq}(\omega_1) & 1 \\ H_{pq}(\omega_2) & 1 \\ H_{pq}(\omega_3) & 1 \\ H_{pq}(\omega_p) & 1 \\ \dots & \dots \\ H_{pq}(\omega_s) & 1 \end{bmatrix}_{N_s \times 2} \begin{Bmatrix} \lambda_r \\ A_{pqr} \end{Bmatrix}_{2 \times 1} = \begin{Bmatrix} (j\omega_1) H_{pq}(\omega_1) \\ (j\omega_2) H_{pq}(\omega_2) \\ (j\omega_3) H_{pq}(\omega_3) \\ (j\omega_p) H_{pq}(\omega_p) \\ \dots \\ (j\omega_s) H_{pq}(\omega_s) \end{Bmatrix}_{N_s \times 1} \quad (6.63)$$

Note that the above equation can be written for each measurement in a column or row of the frequency response function matrix. When this is done, the modal frequency (λ_r) is the same for each measurement while the residue (A_{pqr}) changes with each measurement. This is described by the matrix version of the above equation:

$$\begin{bmatrix} \left\{ H_{pq}(\omega_1) \right\} & [I] \\ \left\{ H_{pq}(\omega_2) \right\} & [I] \\ \left\{ H_{pq}(\omega_3) \right\} & [I] \\ \left\{ H_{pq}(\omega_4) \right\} & [I] \\ \dots & \dots \\ \left\{ H_{pq}(\omega_s) \right\} & [I] \end{bmatrix}_{N_o N_s \times N_o + 1} \begin{Bmatrix} \lambda_r \\ \{A_{pqr}\} \end{Bmatrix}_{N_o + 1 \times 1} = \begin{bmatrix} (j\omega_1) \left\{ H_{pq}(\omega_1) \right\} \\ (j\omega_2) \left\{ H_{pq}(\omega_2) \right\} \\ (j\omega_3) \left\{ H_{pq}(\omega_3) \right\} \\ (j\omega_4) \left\{ H_{pq}(\omega_4) \right\} \\ \dots \\ (j\omega_s) \left\{ H_{pq}(\omega_s) \right\} \end{bmatrix}_{N_o N_s \times 1} \quad (6.64)$$

In the above equation, the size of the frequency response function column ($\{H_{pq}(\omega_1)\}$) determines the number of residues that will be estimated as well as the size of the identity matrix. The above equation again represents an overdetermined set of linear equations that can be solved using any psuedo-inverse or normal equations approach.

6.5 Modal Identification Algorithms

All multiple degree of freedom equations can be represented in a unified matrix polynomial approach that has been explained earlier. The methods that will be summarized in the following sections are listed Table 6-1.

6.5.1 High Order Time Domain Algorithms

The algorithms that fall into the category of high order time domain algorithms include the most successful algorithms used to determine modal parameters historically. The Complex Exponential (CE) algorithms was adapted from the area of sonar signal processing by the University of Cincinnati, Structural Dynamics Research Lab (UC-SDRL) in 1974. One of the first algorithms to utilize more than one frequency response function, in the form of impulse response functions, at a time in the solution for modal frequency was the high order time domain

algorithm, the Least Squares Complex Exponential (LSCE) algorithm. This algorithm was developed jointly by the UC-SDRL and the University of Leuven, Belgium in 1977. The Polyreference Time Domain (PTD) algorithm is an extension to the LSCE algorithm that allows multiple references to be included in a meaningful way so that the ability to resolve close modal frequencies is enhanced. This algorithm was developed by Vold at SDRC in 1982. Since both the LSCE and PTD algorithms have good numerical characteristics, these algorithms are still the most commonly used algorithms today. The only limitations for these algorithms are the cases involving high damping. Note that as a high order algorithm, more time domain information is required compared to the low order algorithms.

Summary

- Typical Algorithms
 - Complex Exponential (CE)
 - Least Squares Complex Exponential (LSCE)
 - Polyreference Time Domain (PTD)
- General Linear Equation Formulation
 - High Order ($m \geq 2N/N_i$)
 - Matrix Coefficients ($N_i \times N_i$)

Basic Equation:

$$\begin{bmatrix} [h(t_{i+0})] & [h(t_{i+1})] & \cdots & [h(t_{i+m-1})] \end{bmatrix}_{N_o \times N_i m} \begin{bmatrix} [\alpha_0] \\ [\alpha_1] \\ \vdots \\ [\alpha_{m-1}] \end{bmatrix}_{N_i m \times N_i} = - [h(t_{i+m})]_{N_o \times N_i} \quad (6.65)$$

6.5.1.1 Complex Exponential Algorithm: Example

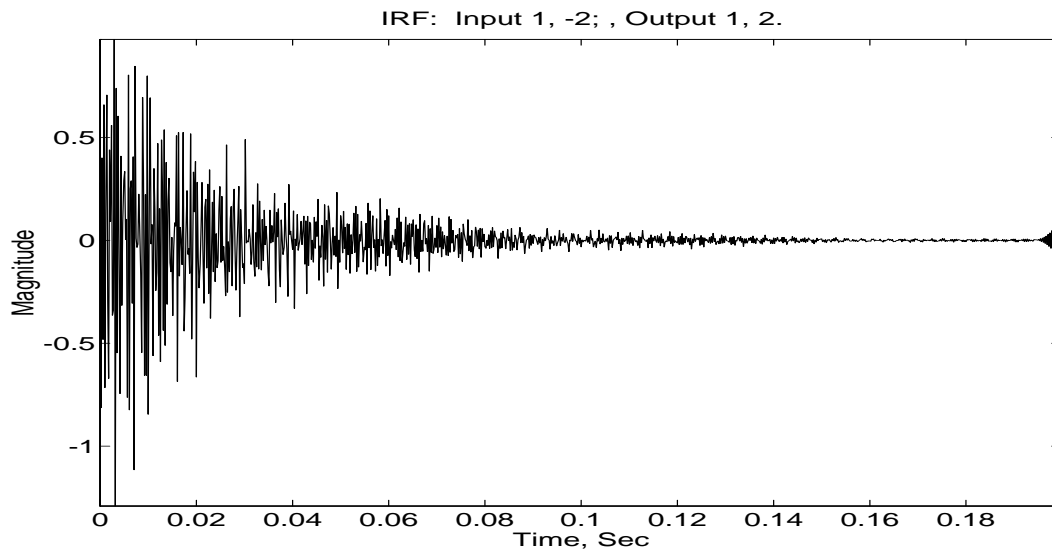


Figure 6-26. Typical Impulse Response Function

Starting with Equation (6.53) for the high order, time domain algorithm, the equation can be simplified by assuming that single input/output data will be used ($N_i = 1$ and $N_o = 1$) and that the model order will be chosen so that $2N$ modal frequencies will be found:

$$\left[h_{pq}(t_{i+0}) \ h_{pq}(t_{i+1}) \ \cdots \ h_{pq}(t_{i+2N-1}) \right] \left\{ \begin{array}{c} \alpha_0 \\ \alpha_1 \\ \vdots \\ \alpha_{2N-1} \end{array} \right\} = -h_{pq}(t_{i+2N})$$

where:

- α_k is the k - th denominator coefficient.
- $h_{pq}(t_{i+k})$ is the $i+k$ time value of the impulse response of the system.
- i is the index for starting time sample (t_i).
- $2N$ is the order of the model.

Since the i -th starting point is arbitrary, $2N$ equations can now be formulated (with $i = 0$).

$$[T]_{2N \times 2N} \{\alpha\}_{2N \times 1} = -\{S\}_{2N \times 1}$$

where:

$$[T] = \begin{bmatrix} h_{pq}(t_0) & h_{pq}(t_1) & h_{pq}(t_2) & \cdots & h_{pq}(t_{2N-1}) \\ h_{pq}(t_1) & h_{pq}(t_2) & h_{pq}(t_3) & \cdots & h_{pq}(t_{2N}) \\ h_{pq}(t_2) & h_{pq}(t_3) & h_{pq}(t_4) & \cdots & h_{pq}(t_{2N+1}) \\ \vdots & \vdots & \vdots & \ddots & \vdots \\ h_{pq}(t_{2N-1}) & h_{pq}(t_{2N}) & h_{pq}(t_{2N+1}) & \cdots & h_{pq}(t_{4N-2}) \end{bmatrix}$$

$$\{\alpha\} = \left\{ \begin{array}{c} \alpha_0 \\ \alpha_1 \\ \alpha_2 \\ \vdots \\ \alpha_{2N-1} \end{array} \right\} \quad \{S\} = \left\{ \begin{array}{c} h_{pq}(t_{2N}) \\ h_{pq}(t_{2N+1}) \\ h_{pq}(t_{2N+2}) \\ \vdots \\ h_{pq}(t_{4N-1}) \end{array} \right\}$$

Companion Matrix Solution:

$$[C] = \begin{bmatrix} -\alpha_{2N-1} & -\alpha_{2N-2} & -\alpha_{2N-3} & \cdots & \cdots & -\alpha_2 & -\alpha_1 & -\alpha_0 \\ 1 & 0 & 0 & \cdots & \cdots & 0 & 0 & 0 \\ 0 & 1 & 0 & \cdots & \cdots & 0 & 0 & 0 \\ 0 & 0 & 1 & \cdots & \cdots & 0 & 0 & 0 \\ \cdots & \cdots & \cdots & \cdots & \cdots & \cdots & \cdots & \cdots \\ \cdots & \cdots & \cdots & \cdots & \cdots & \cdots & \cdots & \cdots \\ \cdots & \cdots & \cdots & \cdots & \cdots & \cdots & \cdots & \cdots \\ 0 & 0 & 0 & \cdots & \cdots & 0 & 0 & 0 \\ 0 & 0 & 0 & \cdots & \cdots & 1 & 0 & 0 \\ 0 & 0 & 0 & \cdots & \cdots & 0 & 1 & 0 \end{bmatrix}$$

$$[C]\{X\} = \lambda \{X\}$$

$$[C]\{X\} = \lambda [I] \{X\}$$

Convert z_r to λ_r :

$$z_k = e^{\lambda_k \Delta t} \quad \lambda_k = \sigma_k + j \omega_k$$

$$\sigma_k = \operatorname{Re} \left[\frac{\ln z_k}{\Delta t} \right] \quad \omega_k = \operatorname{Im} \left[\frac{\ln z_k}{\Delta t} \right]$$

6.5.1.1.1 SDOF Numerical Example

Theoretical Values:

$$M = 10, C = 10, K = 16000$$

System Pole:

$$\lambda_1 = -0.500 + j 39.997 \text{ rad/sec}$$

Residue:

$$A_{pq1} = -j 0.00125$$

Applicable Equations:

$$\begin{bmatrix} h_{pq}(t_0) & h_{pq}(t_1) \\ h_{pq}(t_1) & h_{pq}(t_2) \end{bmatrix} \begin{bmatrix} \alpha_0 \\ \alpha_1 \end{bmatrix} = - \begin{bmatrix} h_{pq}(t_2) \\ h_{pq}(t_3) \end{bmatrix}$$

$$\alpha_2 z^2 + \alpha_1 z + \alpha_0 = 0$$

$$z_k = e^{\lambda_k \Delta t}$$

$$\lambda_k = \sigma_k + j \omega_k = \frac{\ln z_k}{\Delta t} = \operatorname{Re} \left[\frac{\ln z_k}{\Delta t} \right] + j \operatorname{Im} \left[\frac{\ln z_k}{\Delta t} \right]$$

Case I ($\Delta t = 0.025$)

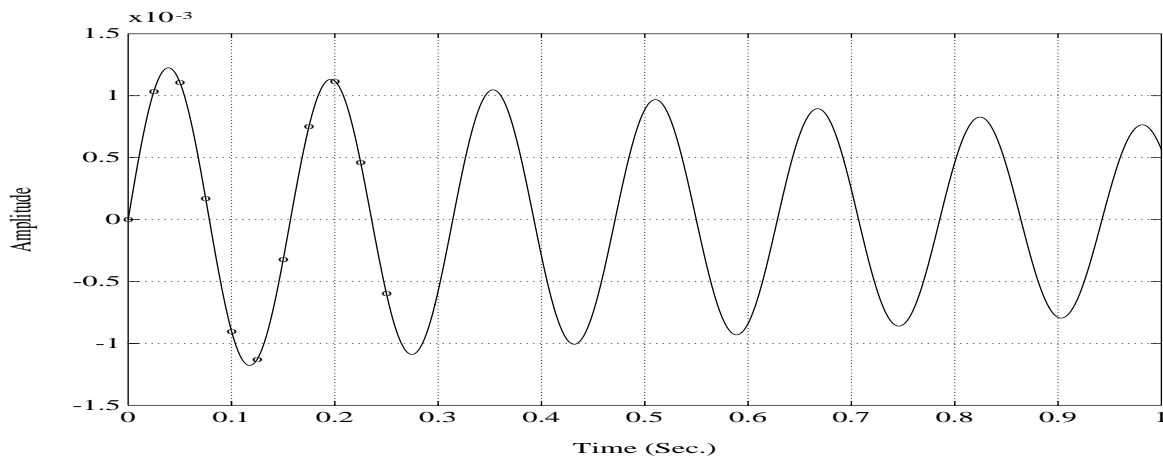


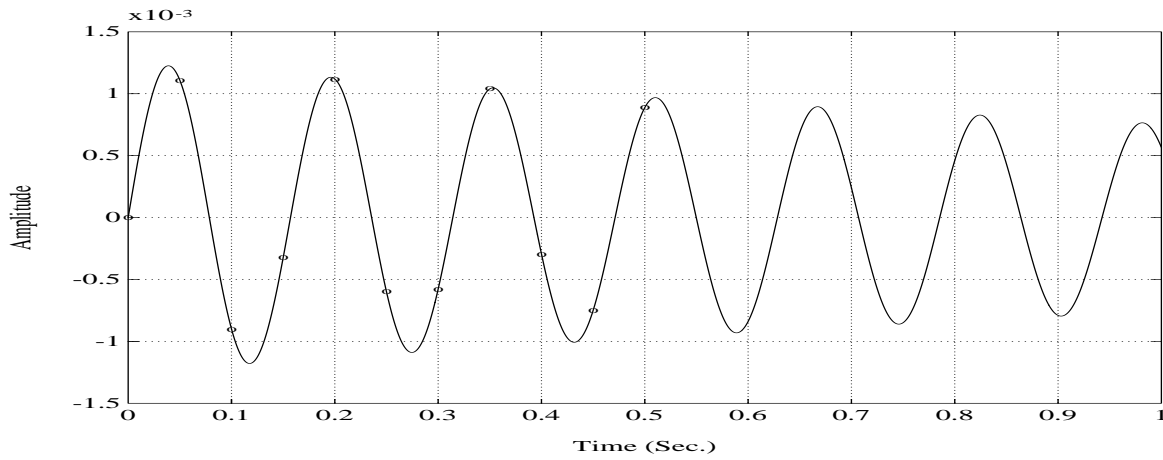
Figure 6-27. Case I: Impulse Response Function

Case I	
Time	Amplitude
0.000	0.0000e+000
0.025	10.3880e-004
0.050	11.0872e-004
0.075	1.7020e-004
0.100	-8.9969e-004
0.125	-11.2625e-004
0.150	-3.2458e-004
0.175	7.5202e-004
0.200	11.1920e-004
0.225	4.6109e-004
0.250	-5.9944e-004

$$\begin{bmatrix} 0.0000e+000 & 10.3880e-004 \\ 10.3880e-004 & 11.0872e-004 \end{bmatrix} \begin{Bmatrix} \alpha_0 \\ \alpha_1 \end{Bmatrix} = - \begin{Bmatrix} 11.0872e-004 \\ 1.7020e-004 \end{Bmatrix}$$

$$\alpha_2 = 1.0 \quad \alpha_1 = -1.06731 \quad \alpha_0 = 0.97530$$

$$z_1 = 0.533654 + j 0.8309739 \quad \lambda_1 = -0.5000 + j 39.9969$$

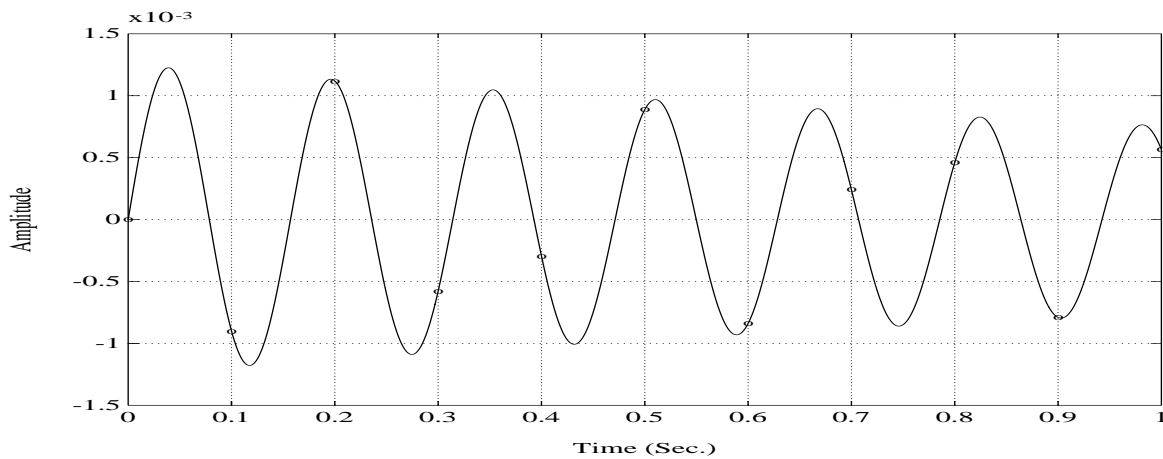
Case II ($\Delta t = 0.050$)**Figure 6-28.** Case II: Impulse Response Function

Case II	
Time	Amplitude
0.000	0.0000e+000
0.050	11.0872e-004
0.100	-8.9969e-004
0.150	-3.2458e-004
0.200	11.1920e-004
0.250	-5.9944e-004
0.300	-5.7819e-004
0.350	10.3940e-004
0.400	-2.9344e-004
0.450	-7.5058e-004
0.500	8.8820e-004

$$\begin{bmatrix} 0.0000e+000 & 11.0870e-004 \\ 11.0870e-004 & -8.9969e-004 \end{bmatrix} \begin{bmatrix} \alpha_0 \\ \alpha_1 \end{bmatrix} = - \begin{bmatrix} -8.9969e-004 \\ -3.2458e-004 \end{bmatrix}$$

$$\alpha_2 = 1.0 \quad \alpha_1 = 0.81148 \quad \alpha_0 = 0.95126$$

$$z_1 = -0.405741 + j 0.8869241 \quad \lambda_1 = -0.4997 + j 39.9969$$

Case III ($\Delta t = 0.100$)**Figure 6-29.** Case III: Impulse Response Function

Case III	
Time	Amplitude
0.000	0.0000e+000
0.100	-8.9969e-004
0.200	11.1920e-004
0.300	-5.7819e-004
0.400	-2.9344e-004
0.500	8.8820e-004
0.600	-8.3939e-004
0.700	2.4050e-004
0.800	4.6033e-004
0.900	-7.9026e-004
1.000	5.6654e-004

$$\begin{bmatrix} 0.0000e+000 & -8.9969e-004 \\ -8.9969e-004 & 11.1920e-004 \end{bmatrix} \begin{bmatrix} \alpha_0 \\ \alpha_1 \end{bmatrix} = - \begin{bmatrix} 11.1920e-004 \\ -5.7819e-004 \end{bmatrix}$$

$$\alpha_2 = 1.0 \quad \alpha_1 = 1.24398 \quad \alpha_0 = 0.90484$$

$$z_1 = -0.621991 + j 0.7196996 \quad \lambda_1 = -0.4999 + j 22.83498$$

Note that Cases I and II give acceptable answers for the modal frequencies but Case III does not. Case III represents the case where the data has been undersampled and an aliasing condition results. This can happen if data points are skipped when loading the data into the matrices. As long as all off the measured data is used, this will not occur.

6.5.2 First Order Time Domain Algorithms

The first order time domain algorithms include several well-known algorithms such as the Ibrahim Time Domain (ITD) algorithm and the Eigensystem Realization Algorithm (ERA). These algorithms are essentially a state-space formulation with respect to the second order time domain algorithms. Note that the historical development of these algorithms is quite different than that presented here but the resulting solution of linear equations is the same regardless of development. There is a great body of published work on both the ITD and ERA algorithms, much of which discusses the various approaches for condensing the overdetermined set of equations that results from the data (least squares, double least squares, singular value decomposition). Note that the low order time domain algorithms require very few time points in order to generate a solution due to the increased use of spatial information.

Summary

- Typical Algorithms
 - Ibrahim Time Domain (ITD)
 - Multiple Reference Time Domain (MRITD)
 - Eigensystem Realization Algorithm (ERA)
- General Linear Equation Formulation
 - Matrix Coefficients ($2N_o \times 2N_o$)

Basic Equation:

$$\begin{bmatrix} [h(t_{i+0})] & [h(t_{i+1})] \end{bmatrix}_{N_i \times 2N_o} \begin{bmatrix} [\alpha_0] \end{bmatrix}_{2N_o \times 2N_o} = - \begin{bmatrix} [h(t_{i+1})] & [h(t_{i+2})] \end{bmatrix}_{N_i \times 2N_o} \quad (6.66)$$

6.5.3 Second Order Time Domain Algorithms

The second order time domain algorithm has not been reported in the literature previously but is simply modeled after the second order matrix differential equation with matrix dimension N_o . Since an impulse response function can be thought to be a linear summation of a number of complementary solutions to such a matrix differential equation, the general second order matrix form is a natural model that can be used to determine the modal parameters. It is interesting to note that this method was developed by noting that it would be the time domain equivalent to a frequency domain algorithm known as the Polyreference Frequency Domain (PFD) algorithm. Note that the low order time domain algorithms require very few time points in order to generate a solution due to the increased use of spatial information.

Summary

- Typical Algorithms
 - Time Domain Equivalent to Polyreference Frequency Domain
- General Linear Equation Formulation
 - Matrix Coefficients ($N_o \times N_o$)

Basic Equation:

$$\begin{bmatrix} [h(t_{i+0})] & [h(t_{i+1})] \end{bmatrix}_{N_i \times 2N_o} \begin{bmatrix} [\alpha_0] \\ [\alpha_1] \end{bmatrix}_{2N_o \times N_o} = - \begin{bmatrix} h(t_{i+2}) \end{bmatrix}_{N_i \times N_o} \quad (6.67)$$

6.5.4 High Order Frequency Domain Algorithms

The high order frequency domain algorithms, in the form of scalar coefficients, were the first multiple degree of freedom algorithms utilized to estimate modal parameters once discrete data was available. These algorithms work well for narrow frequency bands and limited numbers of modes but have poor numerical characteristics otherwise. While the use of multiple references reduces the numerical conditioning problem, the problem is still significant and not easily handled. In order to circumvent the poor numerical characteristics, many approaches have been used (frequency normalization, orthogonal polynomials) but the use of low order frequency domain models has proven more effective.

Summary

- Typical Algorithms
 - Rational Fraction Polynomial (RFP)
 - Orthogonal Polynomial (OP)
- General Linear Equation Formulation
 - High Order ($m \geq 2N/N_i$)
 - Matrix Coefficients ($N_i \times N_i$)

Basic Equation:

$$\begin{bmatrix} [\hat{H}] & [\hat{R}] \end{bmatrix}_{1 \times (m+n+1)N_i} \begin{bmatrix} [\alpha_0] \\ [\alpha_1] \\ \dots \\ [\alpha_{m-1}] \\ [\beta_0] \\ [\beta_1] \\ \dots \\ [\beta_n] \end{bmatrix}_{(m+n+1)N_i \times N_i} = - (j\omega_0)^m [H(\omega_0)]_{1 \times N_i} \quad (6.68)$$

where:

$$[\hat{H}] = \begin{bmatrix} [H(\omega_0)] & (j\omega_0)^1 [H(\omega_0)] & (j\omega_0)^2 [H(\omega_0)] & \dots & (j\omega_0)^{m-1} [H(\omega_0)] \end{bmatrix}_{1 \times mN_i}$$

$$[\hat{R}] = \begin{bmatrix} -[R] - (j\omega_0)^1 [R] - (j\omega_0)^2 [R] \dots - (j\omega_0)^n [R] \end{bmatrix}_{1 \times (n+1)N_i}$$

$$[H(\omega_k)]_{1 \times N_i} = \begin{bmatrix} H_{p1}(\omega_k) & H_{p2}(\omega_k) & \dots & H_{pp}(\omega_k) & \dots & H_{pq}(\omega_k) \end{bmatrix}$$

$$[R]_{1 \times N_i} = [0 \quad 0 \quad \dots \quad 1 \quad \dots \quad 0]$$

6.5.4.1 Rational Fraction Polynomial: Example

The basic approach to the rational fraction polynomial case for a single measurement begins with Equation (6.16).

$$\sum_{k=0}^m [\alpha_k] H_{pq}(s) = \sum_{k=0}^n [\beta_k]$$

One equation can be developed for each frequency of the transfer function:

$$\sum_{k=0}^m (s_i)^k \alpha_k H_{pq}(s_i) = \sum_{k=0}^n (s_i)^k \beta_k$$

$$\sum_{k=0}^m (s_i)^k \alpha_k H_{pq}(s_i) - \sum_{k=0}^n (s_i)^k \beta_k = 0$$

Since this represents a homogeneous equation, one of the unknown coefficients can be chosen arbitrarily. Letting $\alpha_m = 1.0$, the basic equation is now in final form and conforms to the presentation of Equation (6.54):

$$\sum_{k=0}^{m-1} (s_i)^k \alpha_k H_{pq}(s_i) - \sum_{k=0}^n (s_i)^k \beta_k = -(s_i)^m H_{pq}(s_i)$$

Assuming that the number of poles is known $m = 2N$, the model can be restated as follows:

$$\sum_{k=0}^{2N-1} (s_i)^k \alpha_k H_{pq}(s_i) - \sum_{k=0}^{2N-2} (s_i)^k \beta_k = -(s_i)^{2N} H_{pq}(s_i)$$

where:

- α_k is the k-th denominator coefficient.
- β_k is the k-th numerator coefficient.
- $H_{pq}(s_i)$ is the i – th frequency value of a frequency response function of the system.
- i is the index for frequency ($s_i = j\omega_i$).
- $2N$ is the order of the model.
- $\alpha_{2N} = 1.0$.

The previous equation can be rewritten in vector form:

$$[[T]:[R]] \left\{ \begin{array}{c} \alpha_0 \\ \alpha_1 \\ \dots \\ \alpha_{2N-1} \\ \beta_0 \\ \beta_1 \\ \dots \\ \beta_{2N-2} \end{array} \right\} = -(s_i)^{2N} H_{pq}(s_i)$$

(6-76)

$$[T] = \begin{bmatrix} (s_i)^0 H_{pq}(s_i) & (s_i)^1 H_{pq}(s_i) & \cdots & (s_i)^{2N-1} H_{pq}(s_i) \end{bmatrix}$$

$$[R] = \begin{bmatrix} (s_i)^0 & (s_i)^1 & \cdots & (s_i)^{2N-2} \end{bmatrix}$$

This equation is linear in the unknown coefficients α_m and β_n . There are a total of $m + n + 1$ unknown coefficients ($2N + 2N - 1$). If the same number, or more, equations can be found equal to the number of unknowns, a solution for the unknown coefficients can be found. Therefore, $2N + 2N - 1$, or more, equations can now be formulated by using additional frequency information. Note that in order to estimate both the positive and negative poles (complex conjugates), positive ($s_i = +j\omega_i$) and negative ($s_i = -j\omega_i$) frequency information must be included.

Therefore, the general form of the linear equation solution is as follows:

$$[T : R] \begin{Bmatrix} \alpha_0 \\ \alpha_1 \\ \alpha_2 \\ \vdots \\ \alpha_{2N-1} \\ \beta_0 \\ \beta_1 \\ \beta_2 \\ \vdots \\ \beta_{2N-2} \end{Bmatrix} = - \begin{Bmatrix} (s_1)^{2N} H_{pq}(s_1) \\ (s_2)^{2N} H_{pq}(s_2) \\ (s_3)^{2N} H_{pq}(s_3) \\ \vdots \\ (s_i)^{2N} H_{pq}(s_i) \end{Bmatrix}$$

$$[T] = \begin{bmatrix} (s_1)^0 H_{pq}(s_1) & (s_1)^1 H_{pq}(s_1) & (s_1)^2 H_{pq}(s_1) & \cdots & (s_1)^{2N-1} H_{pq}(s_1) \\ (s_2)^0 H_{pq}(s_2) & (s_2)^1 H_{pq}(s_2) & (s_2)^2 H_{pq}(s_2) & \cdots & (s_2)^{2N-1} H_{pq}(s_2) \\ (s_3)^0 H_{pq}(s_3) & (s_3)^1 H_{pq}(s_3) & (s_3)^2 H_{pq}(s_3) & \cdots & (s_3)^{2N-1} H_{pq}(s_3) \\ \vdots & \vdots & \vdots & \vdots & \vdots \\ (s_i)^0 H_{pq}(s_i) & (s_i)^1 H_{pq}(s_i) & (s_i)^2 H_{pq}(s_i) & \cdots & (s_i)^{2N-1} H_{pq}(s_i) \end{bmatrix}$$

$$[R] = \begin{bmatrix} -(s_1)^0 & -(s_1)^1 & -(s_1)^2 & \cdots & -(s_1)^{2N-2} \\ -(s_2)^0 & -(s_2)^1 & -(s_2)^2 & \cdots & -(s_2)^{2N-2} \\ -(s_3)^0 & -(s_3)^1 & -(s_3)^2 & \cdots & -(s_3)^{2N-2} \\ \vdots & \vdots & \vdots & \vdots & \vdots \\ -(s_i)^0 & -(s_i)^1 & -(s_i)^2 & \cdots & -(s_i)^{2N-2} \end{bmatrix}$$

6.5.4.1.1 SDOF Numerical Example

Theoretical Values:

$$M = 10, C = 10, K = 16000$$

System Pole:

$$\lambda_1 = -0.500 + j 39.997 \text{ rad/sec}$$

Residue:

$$A_{pq1} = -j 0.00125$$

Applicable Equations:

$$[T]_{3 \times 3} \{\alpha\}_{3 \times 1} = -\{S\}_{3 \times 1}$$

$$\begin{bmatrix} (j\omega_1)^0 H_{pq}(\omega_1) & (j\omega_1)^1 H_{pq}(\omega_1) & -1 \\ (j\omega_2)^0 H_{pq}(\omega_2) & (j\omega_2)^1 H_{pq}(\omega_2) & -1 \\ (j\omega_3)^0 H_{pq}(\omega_3) & (j\omega_3)^1 H_{pq}(\omega_3) & -1 \end{bmatrix} \begin{Bmatrix} \alpha_0 \\ \alpha_1 \\ \beta_0 \end{Bmatrix} = - \begin{Bmatrix} -(j\omega_1)^2 H_{pq}(\omega_1) \\ -(j\omega_2)^2 H_{pq}(\omega_2) \\ -(j\omega_3)^2 H_{pq}(\omega_3) \end{Bmatrix}$$

$$\alpha_2 s^2 + \alpha_1 s + \alpha_0 = 0$$

$$1.0 s^2 + \alpha_1 s + \alpha_0 = 0$$

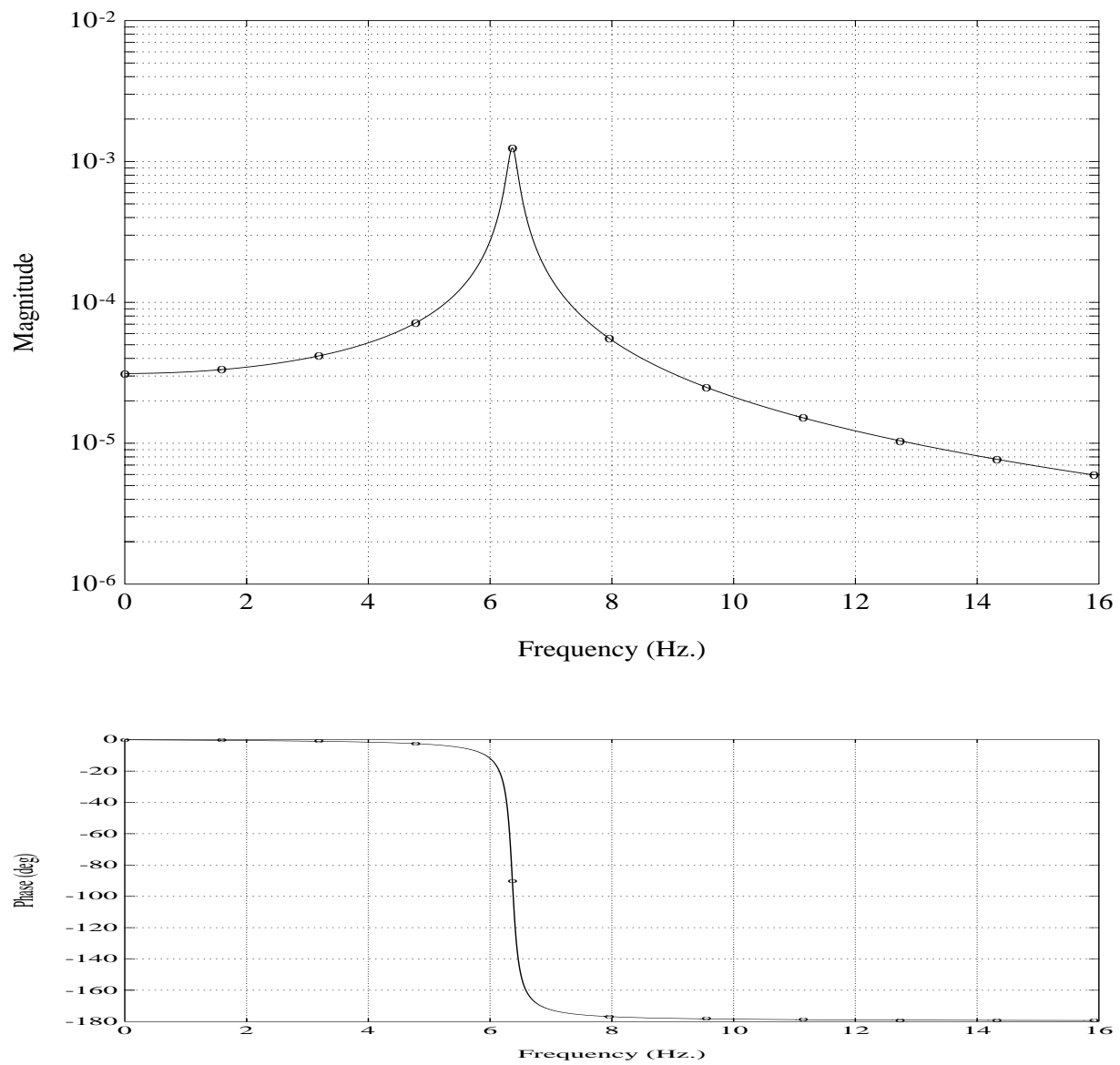


Figure 6-30. Frequency Response Function, SDOF Example

Frequency		Frequency Response Function Data			
(Hz)	(rad/sec)	Real	Imag	Mag	Phase
0	0	3.1250e-05	0.0	3.1250e-05	0.0
1.59	10	3.3332e-05	-2.2221e-07	3.3333e-05	-0.4
3.18	20	4.1655e-05	-6.9425e-07	4.1661e-05	-1.0
4.77	30	7.1298e-05	-3.0556e-06	7.1363e-05	-2.4
6.37	40	-1.9109e-18	-1.2500e-03	1.2500e-03	-90.0
7.96	50	-5.5385e-05	-3.0769e-06	5.5470e-05	-176.8
9.55	60	-2.4978e-05	-7.4933e-07	2.4989e-05	-178.3
11.14	70	-1.5145e-05	-3.2125e-07	1.5148e-05	-178.8
12.73	80	-1.0414e-05	-1.7356e-07	1.0415e-05	-179.1
14.32	90	-7.6908e-06	-1.0649e-07	7.6916e-06	-179.2
15.91	100	-5.9515e-06	-7.0852e-08	5.9520e-06	-179.3

$$\begin{bmatrix} (+7.1298e-05 - j3.0556e-06) & (j30)(+7.1298e-05 - j3.0556e-06) & -1 \\ (-1.9109e-18 - j1.2500e-03) & (j40)(-1.9109e-18 - j1.2500e-03) & -1 \\ (-5.5385e-05 - j3.0769e-06) & (j50)(-5.5385e-05 - j3.0769e-06) & -1 \end{bmatrix} \begin{Bmatrix} \alpha_0 \\ \alpha_1 \\ \beta_0 \end{Bmatrix}$$

$$= - \begin{Bmatrix} -(j30)^2(+7.1298e-05 - j3.0556e-06) \\ -(j40)^2(-1.9109e-18 - j1.2500e-03) \\ -(j50)^2(-5.5385e-05 - j3.0769e-06) \end{Bmatrix}$$

$$\alpha_0 = 1.6000e+03 - j2.2845e-02$$

$$\alpha_1 = 1.0006e+00 + j4.6897e-04$$

$$\beta_0 = 5.0001e-02 - j3.7646e-07$$

$$1.0 s^2 + \alpha_1 s + \alpha_0 = 0$$

$$\lambda_1 = -0.50000 + j39.997 \text{ rad/sec}$$

$$\lambda_2 = -0.50058 - j39.997 \text{ rad/sec}$$

6.5.4.2 Orthogonal Polynomial Concepts

The fundamental problem with using a rational fraction polynomial (power polynomial) method can be highlighted by looking at the characteristics of the data matrix $[T]$ and $[R]$. These matrices involve power polynomials that are functions of increasing powers of $s = j\omega$. These matrices are of the Vandermonde form and are known to be ill-conditioned for cases involving wide frequency ranges and high ordered models.

Vandermonde Matrix Form:

$$\begin{bmatrix} (s_1)^0 & (s_1)^1 & (s_1)^2 & \cdots & (s_1)^{2N-1} \\ (s_2)^0 & (s_2)^1 & (s_2)^2 & \cdots & (s_2)^{2N-1} \\ (s_3)^0 & (s_3)^1 & (s_3)^2 & \cdots & (s_3)^{2N-1} \\ \cdots & \cdots & \cdots & \cdots & \cdots \\ (s_i)^0 & (s_i)^1 & (s_i)^2 & \cdots & (s_i)^{2N-1} \end{bmatrix} \quad (6.69)$$

Ill-conditioning, in this case, means that the accuracy of the solution for the matrix coefficients α_m is limited by the numerical precision of the available arithmetic of the computer. Since the matrix coefficients α_m are used to determine the complex valued modal frequencies, this presents a serious limitation for the high order frequency domain algorithms. The ill-conditioning problem can be best understood by evaluating the condition number of the Vandermonde matrix. The ***condition number*** measures the sensitivity of the solution of linear equations to errors, or small amounts of noise, in the data. The condition number gives an indication of the accuracy of the results from matrix inversion and/or linear equation solution. The condition number for a matrix is computed by taking the ratio of the largest singular value to the smallest singular value. A good condition number is a small number close to unity; a bad condition number is a large number. For the theoretical case of a singular matrix, the condition number is infinite.

The ill-conditioned characteristic of matrices that are of the Vandermonde form can be reduced, but not eliminated, by the following:

- Minimizing the frequency range of the data.
- Minimizing the order of the model.
- Normalizing the frequency range of the data (0,1) or (-1,1).
- Use of orthogonal polynomials.

For example, for the case of a Vandermode matrix, made up of power polynomials for the first ten polynomials, evaluated for frequency information from plus to minus 10 rad/sec, the condition number is $4.1114\text{e}+08$. This means that if this matrix is utilized in the solution of a set of linear equations, as it is with the high order frequency domain methods, the number of significant digits in the measured data must exceed 8 in order to have any significance in the result. This is not likely in the case of measured data. The first several power polynomial coefficients are plotted in the following figure.

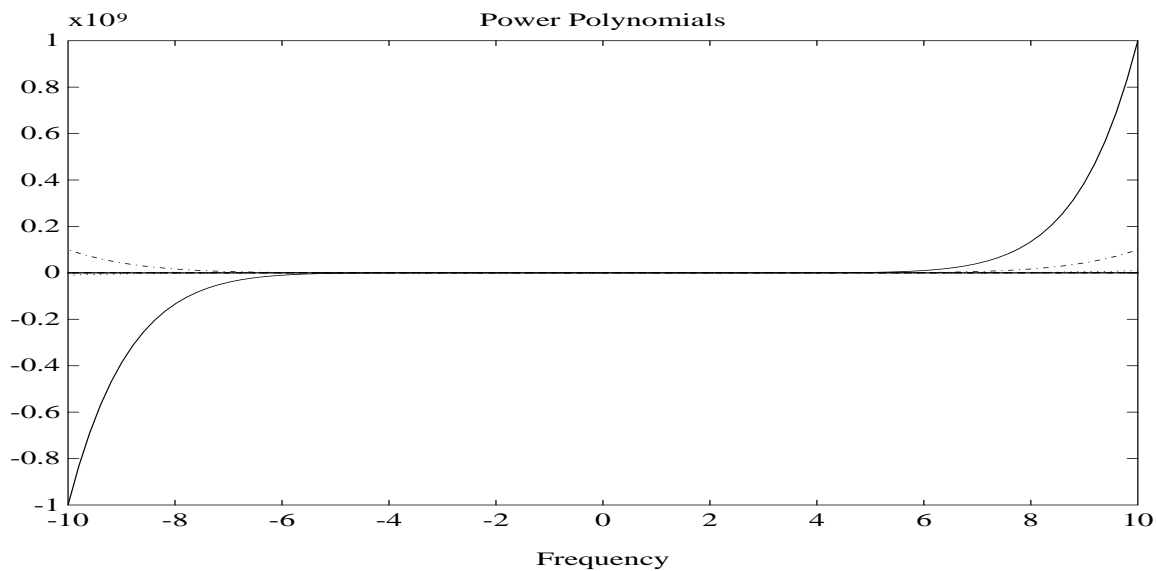


Figure 6-31. Power Polynomials

For the previous case, if the frequency information is scaled from plus to minus 1 rad/sec, the condition number improves to $1.1622\text{e}+03$. When the final modal frequencies are computed using this normalized frequency approach, the modal frequencies must be corrected by rescaling to the original frequency range. This rescaling is a simple multiplication and does not negatively effect the accuracy of the result. The first several power polynomial coefficients, for this

normalized frequency case, are plotted in the following figure.

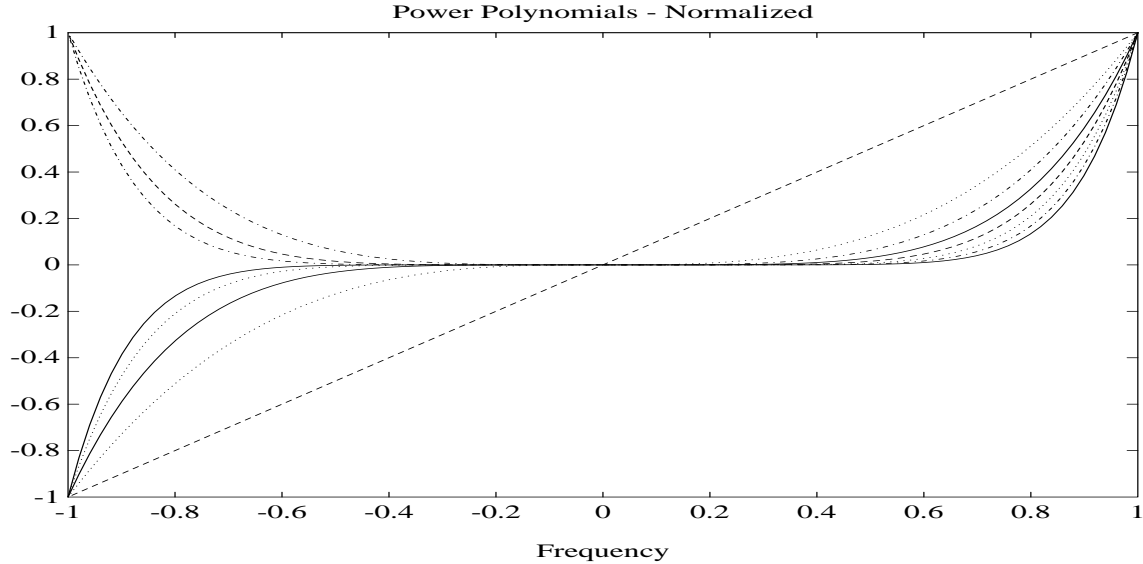


Figure 6-32. Power Polynomials (Normalized Frequency)

Any power polynomial series can be represented by an equivalent number of terms in an orthogonal polynomial series. This is represented by the following relationship.

$$\sum_{k=0}^m (s)^k \alpha_k = \sum_{k=0}^m T_k(s) \gamma_k \quad (6.70)$$

Several orthogonal polynomials have been applied to the frequency domain modal parameter estimation problem, such as:

- Forsythe Polynomials (Richardson)
- Chebyshev Polynomials (Vold, Shih)
- Legendre Polynomials
- Laguerre Polynomials

Chebyshev Orthogonal Polynomials

When Chebyshev orthogonal polynomials are used to replace the power polynomials over the normalized frequency range from plus to minus 1 rad/sec, the condition number improves to 2.8130e+00. The first several Chebyshev polynomial coefficients, for this normalized frequency case, are plotted in the following figure.

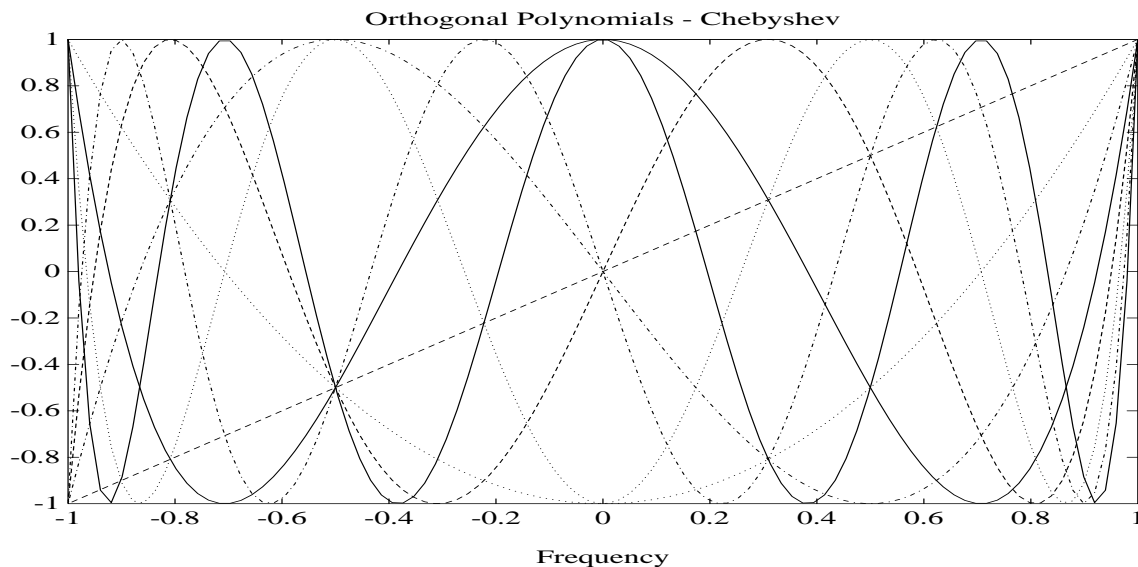


Figure 6-33. Chebyshev Orthogonal Polynomials

The computation of the Chebyshev orthogonal polynomial coefficients is quite simple and is based upon the general relationship shown in Equation (6.55). The problem that remains is that in order to solve for the modal frequencies, the solution of the linear equation must be transformed from orthogonal polynomial back to power polynomials. This transformation matrix is not a simple multiplication but involves a matrix that has the same condition number as the original power polynomial matrix. Recent research has involved solving for the modal frequencies directly from the orthogonal polynomials in order to avoid this numerical conditioning problem.

Chebyshev Polynomial Coefficients*Power Polynomials to Orthogonal Polynomials*

- $T_0(s) = 1$
- $T_1(s) = s$
- $T_2(s) = 2 s^2 - 1$
- $T_3(s) = 4 s^3 - 3 s$
- $T_4(s) = 8 s^4 - 8 s^2 + 1$
- $T_{i+1}(s) = 2 s T_i(s) - T_{i-1}(s)$

While orthogonal polynomials improve the condition number of the data matrix compared to power polynomials, in order to solve for the poles of the system the coefficients of the orthogonal polynomials must be transformed back to the coefficients of the orthogonal polynomials. Unfortunately, this transformation matrix is ill-conditioned.

Power Polynomial Coefficients

Orthogonal Polynomials to Power Polynomials

- $1 = T_0(s)$
- $s = T_1(s)$
- $s^2 = \frac{T_0(s) + T_2(s)}{2}$
- $s^3 = \frac{3 T_1(s) + T_3(s)}{4}$
- $s^4 = \frac{3 T_0(s) + 4 T_2(s) + T_4(s)}{8}$
- $s^5 = \frac{10 T_1(s) + 5 T_3(s) + T_5(s)}{16}$

Legendre Orthogonal Polynomials

As another representative example, the use of Legendre orthogonal polynomials results in a slightly different result with a condition number of 3.1132e+00. Essentially, though, the result from a numerical point of view is the same as before.

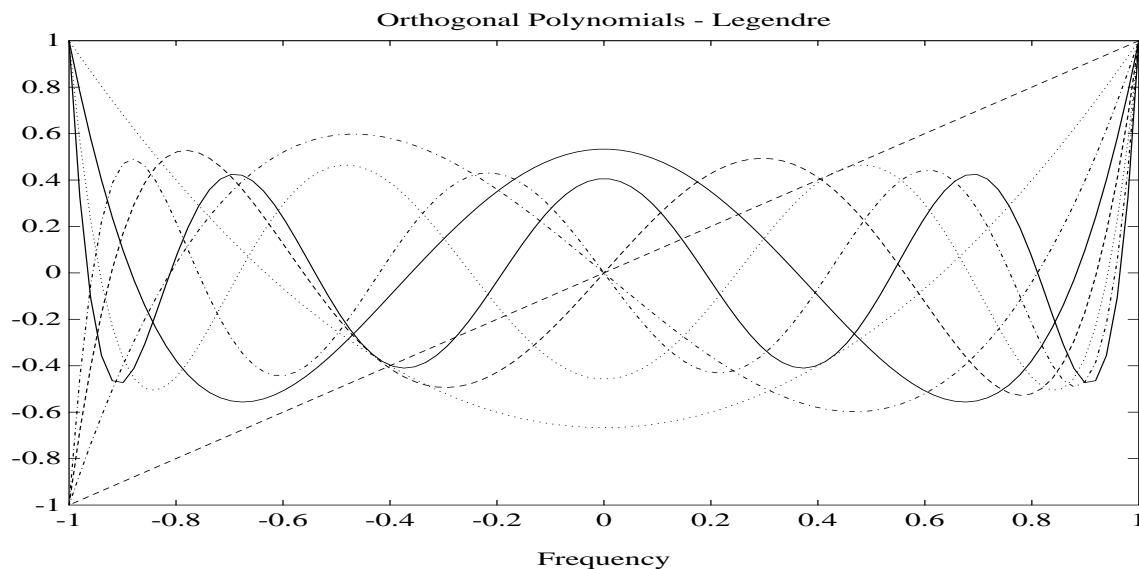


Figure 6-34. Legendre Orthogonal Polynomials

6.5.5 First Order Frequency Domain Algorithms

Several algorithms have been developed that fall into the category of first order frequency domain algorithms, including the Simultaneous Frequency Domain (SFD) algorithm first reported by Coppolino and the Multiple Reference Simultaneous Frequency Domain algorithm reported by Craig. These algorithms are essentially frequency domain equivalents to the ITD and ERA algorithms and effectively involve a state-space formulation when compared to the second order frequency domain algorithms. The state-space formulation utilizes the derivatives of the frequency response functions as well as the frequency response function in the solution. These algorithms have superior numerical characteristics compared to the high order frequency domain algorithms. Unlike the low order time domain algorithms, though, sufficient data from across the complete frequency range of interest must be included in order to obtain a satisfactory solution.

Summary

- Typical Algorithms
 - Simultaneous Frequency Domain (SFD)
 - Multiple Reference Simultaneous Frequency Domain (MRSFD)
 - Frequency Domain Equivalent to ITD, MRITD, ERA
- General Linear Equation Formulation
 - Low Order ($m = 1$ and $2N_o \geq 2N$)
 - Matrix Coefficients ($2N_o \times 2N_o$)

Basic Equation:

$$\begin{aligned}
 & \left[\begin{array}{ccc} [H(\omega_0)] & (j\omega_0)^1 [H(\omega_0)] & -[R] \\ -[R] & -(j\omega_0)[R] & \end{array} \right]_{1 \times 4N_o} \left[\begin{array}{c} [\alpha_0] \\ [\beta_0] \end{array} \right]_{4N_o \times 2N_o} \\
 & = - \left[\begin{array}{cc} (j\omega_0)^1 [H(\omega_0)] & (j\omega_0)^2 [H(\omega_0)] \end{array} \right]_{1 \times 2N_o} \quad (6.71)
 \end{aligned}$$

where:

$$\begin{aligned}
 [H(\omega_k)]_{1 \times N_o} &= \left[\begin{array}{cccccc} H_{1q}(\omega_k) & H_{2q}(\omega_k) & \cdots & H_{qq}(\omega_k) & \cdots & H_{pq}(\omega_k) \end{array} \right] \\
 [R]_{1 \times N_o} &= [\begin{array}{cccccc} 0 & 0 & \cdots & 1 & \cdots & 0 \end{array}]
 \end{aligned}$$

6.5.6 Second Order Frequency Domain Algorithms

The second order frequency domain algorithms include the Polyreference Frequency Domain (PFD) algorithms that were developed at the University of Leuven, Belgium and the University

of Cincinnati, Structural Dynamics Research Lab (UC-SDRL) in slightly different forms. These algorithms have superior numerical characteristics compared to the high order frequency domain algorithms. Unlike the low order time domain algorithms, though, sufficient data from across the complete frequency range of interest must be included in order to obtain a satisfactory solution.

Summary

- Typical Algorithms
 - Polyreference Frequency Domain (PFD)
- General Linear Equation Formulation
 - Matrix Coefficients ($N_o \times N_o$)

Basic Equation:

$$\begin{aligned}
 & \left[\begin{array}{c} [H(\omega_0)] \quad (j\omega_0)^1 [H(\omega_0)] \quad -[R] \quad -(j\omega_0)[R] \end{array} \right]_{1 \times 4N_o} \begin{bmatrix} [\alpha_0] \\ [\alpha_1] \\ [\beta_0] \\ [\beta_1] \end{bmatrix}_{4N_o \times N_o} \\
 & = -(j\omega_0)^2 [H(\omega_0)]_{1 \times N_o} \quad (6.72)
 \end{aligned}$$

where:

$$\begin{aligned}
 [H(\omega_k)]_{1 \times N_o} &= \left[H_{1q}(\omega_k) \quad H_{2q}(\omega_k) \quad \cdots \quad H_{qq}(\omega_k) \quad \cdots \quad H_{pq}(\omega_k) \right] \\
 [R]_{1 \times N_o} &= [0 \quad 0 \quad \cdots \quad 1 \quad \cdots \quad 0]
 \end{aligned}$$

6.6 Residue Estimation

Once the modal frequencies and modal participation vectors have been estimated, the associated modal vectors and modal scaling (residues) can be found with standard least squares methods in either the time or frequency domain. The most common approach is to estimate residues in the frequency domain utilizing residuals if appropriate. These methods are summarized in the following sections.

6.6.1 Time Domain Estimation (Single Reference)

$$\{h_{pq}(t)\}_{N_t \times 1} = \begin{bmatrix} e^{\lambda t} \end{bmatrix}_{N_t \times 2N} \{A_{pqr}\}_{2N \times 1} \quad (6.73)$$

where:

- N_t = Number of Time Points
- $N_t \geq 2N$

$$\begin{bmatrix} e^{\lambda t} \end{bmatrix} = \begin{bmatrix} e^{\lambda_1 t_1} & e^{\lambda_2 t_1} & e^{\lambda_3 t_1} & \dots & e^{\lambda_{2N} t_1} \\ e^{\lambda_1 t_2} & e^{\lambda_2 t_2} & e^{\lambda_3 t_2} & \dots & e^{\lambda_{2N} t_2} \\ e^{\lambda_1 t_3} & e^{\lambda_2 t_3} & e^{\lambda_3 t_3} & \dots & e^{\lambda_{2N} t_3} \\ \dots & \dots & \dots & \dots & \dots \\ e^{\lambda_1 t_{N_t}} & e^{\lambda_2 t_{N_t}} & e^{\lambda_3 t_{N_t}} & \dots & e^{\lambda_{2N} t_{N_t}} \end{bmatrix}$$

$$\{A_{pqr}\} = \begin{Bmatrix} A_{pq1} \\ A_{pq2} \\ A_{pq3} \\ \dots \\ A_{pq2N} \end{Bmatrix} \quad \{h_{pq}(t)\} = \begin{Bmatrix} h_{pq}(t_1) \\ h_{pq}(t_2) \\ h_{pq}(t_3) \\ \dots \\ h_{pq}(t_{N_t}) \end{Bmatrix}$$

6.6.2 Time Domain Estimation (Multiple References)

$$\{h(t_i)\}_{N_i \times 1}^T = [L]_{N_i \times 2N} \begin{bmatrix} e^{\lambda_r t_i} \end{bmatrix}_{2N \times 2N} \{\psi\}_{2N \times 1}^T \quad (6.74)$$

where:

- N_t = Number of Time Points
- $N_t \geq 2N$
- Above equation is repeated N_t times

$$\left\{ h_{pq}(t_i) \right\} = \begin{bmatrix} h_{p1}(t_i) \\ h_{p2}(t_i) \\ h_{p3}(t_i) \\ \dots \\ h_{pq}(t_i) \end{bmatrix} \quad \left[e^{\lambda t_i} \right] = \begin{bmatrix} e^{\lambda_1 t_i} & 0 & 0 & \dots & 0 \\ 0 & e^{\lambda_2 t_i} & 0 & \dots & 0 \\ 0 & 0 & e^{\lambda_3 t_i} & \dots & 0 \\ \dots & \dots & \dots & \dots & \dots \\ 0 & 0 & 0 & \dots & e^{\lambda_{2N} t_i} \end{bmatrix}$$

The residues are calculated from the modal participation vectors L and the modal coefficients ψ ($A_{pqr} = L_{qr} \psi_{pr}$). Note that if one column q of the modal participation matrix L is normalized to unity, the modal coefficients that are found will be equal to the residues for that reference A_{pqr} .

$$\left[\psi_{pr} \right] = \begin{bmatrix} \psi_{p1} \\ \psi_{p2} \\ \psi_{p3} \\ \dots \\ \psi_{p2N} \end{bmatrix} \quad \left[L_{rq} \right] = \begin{bmatrix} L_{11} & L_{12} & L_{13} & \dots & L_{12N} \\ L_{21} & L_{22} & L_{23} & \dots & L_{22N} \\ L_{31} & L_{32} & L_{33} & \dots & L_{32N} \\ \dots & \dots & \dots & \dots & \dots \\ L_{N_i 1} & L_{N_i 2} & L_{N_i 3} & \dots & L_{N_i 2N} \end{bmatrix}$$

6.6.3 Frequency Domain Estimation (Single Reference)

$$\{H_{pq}(\omega)\}_{N_s \times 1} = \left[\frac{1}{j\omega - \lambda_r} \right]_{N_s \times 2N} \{A_{pqr}\}_{2N \times 1} \quad (6.75)$$

where:

- N_s = Number of Spectral Lines
- $N_s \geq 2N$

$$\left[\frac{1}{j\omega - \lambda_r} \right] = \begin{bmatrix} \frac{1}{j\omega_1 - \lambda_1} & \frac{1}{j\omega_1 - \lambda_2} & \frac{1}{j\omega_1 - \lambda_3} & \cdots & \frac{1}{j\omega_1 - \lambda_{2N}} \\ \frac{1}{j\omega_2 - \lambda_1} & \frac{1}{j\omega_2 - \lambda_2} & \frac{1}{j\omega_2 - \lambda_3} & \cdots & \frac{1}{j\omega_2 - \lambda_{2N}} \\ \frac{1}{j\omega_3 - \lambda_1} & \frac{1}{j\omega_3 - \lambda_2} & \frac{1}{j\omega_3 - \lambda_3} & \cdots & \frac{1}{j\omega_3 - \lambda_{2N}} \\ \cdots & \cdots & \cdots & \cdots & \cdots \\ \frac{1}{j\omega_{N_s} - \lambda_1} & \frac{1}{j\omega_{N_s} - \lambda_2} & \frac{1}{j\omega_{N_s} - \lambda_3} & \cdots & \frac{1}{j\omega_{N_s} - \lambda_{2N}} \end{bmatrix}$$

$$\{A_{pqr}\} = \begin{bmatrix} A_{pq1} \\ A_{pq2} \\ A_{pq3} \\ \cdots \\ A_{pq2N} \end{bmatrix} \quad \{H_{pq}(\omega)\} = \begin{bmatrix} H_{pq}(\omega_1) \\ H_{pq}(\omega_2) \\ H_{pq}(\omega_3) \\ \cdots \\ H_{pq}(\omega_{N_s}) \end{bmatrix}$$

6.6.4 Frequency Domain Estimation (Single Reference With Residuals)

$$\{H_{pq}(\omega)\}_{N_s \times 1} = \left[\frac{1}{j\omega - \lambda_r} \right]_{N_s \times (2N+2)} \{A_{pqr}\}_{(2N+2) \times 1} \quad (6.76)$$

where:

- N_s = Number of Spectral Lines
- $N_s \geq 2N + 2$

$$\left[\frac{1}{j\omega - \lambda_r} \right] = \begin{bmatrix} \frac{1}{j\omega_1 - \lambda_1} & \frac{1}{j\omega_1 - \lambda_2} & \frac{1}{j\omega_1 - \lambda_3} & \cdots & \frac{1}{j\omega_1 - \lambda_{2N}} & \frac{-1}{\omega_1^2} & 1 \\ \frac{1}{j\omega_2 - \lambda_1} & \frac{1}{j\omega_2 - \lambda_2} & \frac{1}{j\omega_2 - \lambda_3} & \cdots & \frac{1}{j\omega_2 - \lambda_{2N}} & \frac{-1}{\omega_2^2} & 1 \\ \frac{1}{j\omega_3 - \lambda_1} & \frac{1}{j\omega_3 - \lambda_2} & \frac{1}{j\omega_3 - \lambda_3} & \cdots & \frac{1}{j\omega_3 - \lambda_{2N}} & \frac{-1}{\omega_3^2} & 1 \\ \cdots & \cdots & \cdots & \cdots & \cdots & \cdots & \cdots \\ \frac{1}{j\omega_{N_s} - \lambda_1} & \frac{1}{j\omega_{N_s} - \lambda_2} & \frac{1}{j\omega_{N_s} - \lambda_3} & \cdots & \frac{1}{j\omega_{N_s} - \lambda_{2N}} & \frac{-1}{\omega_{N_s}^2} & 1 \end{bmatrix}$$

$$\{A_{pqr}\} = \begin{bmatrix} A_{pq1} \\ A_{pq2} \\ A_{pq3} \\ \cdots \\ A_{pq2N} \\ R_{I_{pq}} \\ R_{F_{pq}} \end{bmatrix} \quad \{H_{pq}(\omega)\} = \begin{bmatrix} H_{pq}(\omega_1) \\ H_{pq}(\omega_2) \\ H_{pq}(\omega_3) \\ \cdots \\ H_{pq}(\omega_{N_s}) \end{bmatrix}$$

6.6.5 Frequency Domain Estimation (Multiple References)

$$\{H(\omega_i)\}_{N_i \times 1}^T = [L]_{N_i \times 2N} \left[\frac{1}{j\omega_i - \lambda_r} \right]_{2N \times 2N} \{\psi\}_{2N \times 1}^T \quad (6.77)$$

where:

- N_s = Number of Spectral Lines
- $N_s \geq 2N$
- Above equation is repeated N_s times

$$\left\{ H_{pq}(\omega_i) \right\} = \begin{Bmatrix} H_{p1}(\omega_i) \\ H_{p2}(\omega_i) \\ H_{p3}(\omega_i) \\ \dots \\ H_{pq}(\omega_i) \end{Bmatrix}$$

$$\left[\frac{1}{j\omega_i - \lambda_r} \right] = \begin{bmatrix} \frac{1}{j\omega_i - \lambda_1} & 0 & 0 & \dots & 0 \\ 0 & \frac{1}{j\omega_i - \lambda_2} & 0 & \dots & 0 \\ 0 & 0 & \frac{1}{j\omega_i - \lambda_3} & \dots & 0 \\ \dots & \dots & \dots & \dots & \dots \\ 0 & 0 & 0 & \dots & \frac{1}{j\omega_i - \lambda_{2N}} \end{bmatrix}$$

The residues are calculated from the modal participation vectors L and the modal coefficients ψ ($A_{pqr} = L_{qr}\psi_{pr}$). Note that if one column q of the modal participation matrix L is normalized to unity, the modal coefficients that are found will be equal to the residues for that reference A_{pqr} .

$$\left[\psi_{pr} \right] = \begin{Bmatrix} \psi_{p1} \\ \psi_{p2} \\ \psi_{p3} \\ \dots \\ \psi_{p2N} \end{Bmatrix} \quad \left[L_{rq} \right] = \begin{bmatrix} L_{11} & L_{12} & L_{13} & \dots & L_{12N} \\ L_{21} & L_{22} & L_{23} & \dots & L_{22N} \\ L_{31} & L_{32} & L_{33} & \dots & L_{32N} \\ \dots & \dots & \dots & \dots & \dots \\ L_{N_i1} & L_{N_i2} & L_{N_i3} & \dots & L_{N_i2N} \end{bmatrix}$$

6.7 Summary - Future Trends

Modal parameter estimation is probably one of the most misunderstood aspects of the total experimental modal analysis process. It should be obvious that the modal identification algorithm cannot compensate for basic errors made in the measurement of the data used in the estimation process. Since most modal parameter estimation methods are mathematically intimidating, many users do not fully understand the ramifications of the decisions made during the measurement stages as well as later in the modal parameter estimation process. Ideally, by consolidating the conceptual approach and unifying the theoretical development of modal identification algorithms, increased understanding, with respect to general advantages and disadvantages of different algorithms, can be achieved. This sort of overview of modal parameter estimation can be used simply as a guide toward further study and understanding of the details of the individual modal identification algorithms.

Immediate future trends in modal identification will respond to those situations that cannot be adequately solved today. First of all, specific attention will be given to methodology needed to estimate modal parameters for heavily damped systems, particularly systems with significant modal density. Second, since the measured data used for most modal identification algorithms yields a highly overdetermined solution, increased attention will be given to estimating the statistical information concerning the uncertainty associated with each modal parameter estimate. Finally, to address needs of traditional modal identification and needs of control-structure interaction, modal identifications algorithms need to be developed that can incorporate known or fixed modal parameters into a solution for remaining unknown modal parameters.

6.8 References

- [1] Ewins, D., **Modal Testing: Theory and Practice** John Wiley and Sons, Inc., New York, 1984, 269 pp.
- [2] Strang, G., **Linear Algebra and Its Applications, Third Edition**, Harcourt Brace Jovanovich Publishers, San Diego, 1988, 505 pp.
- [3] Lawson, C.L., Hanson, R.J., **Solving Least Squares Problems**, Prentice-Hall, Inc., Englewood Cliffs, New Jersey, 1974, 340 pp.

- [4] Jolliffe, I.T., **Principal Component Analysis** Springer-Verlag New York, Inc., 1986, 271 pp.
- [5] Ljung, Lennart, **System Identification: Theory for the User**, Prentice-Hall, Inc., Englewood Cliffs, New Jersey, 1987, 519 pp.
- [6] Allemang, R.J., Brown, D.L., Fladung, W., "Modal Parameter Estimation: A Unified Matrix Polynomial Approach", Proceedings, International Modal Analysis Conference, pp. 501-514, 1994.
- [7] Allemang, R.J., Brown, D.L., "Modal Parameter Estimation" Experimental Modal Analysis and Dynamic Component Synthesis, USAF Technical Report, Contract No. F33615-83-C-3218, AFWAL-TR-87-3069, Vol. 3, 1987, 130 pp.
- [8] Spitznogle, F.R., et al, "Representation and Analysis of Sonar Signals, Volume 1: Improvements in the Complex Exponential Signal Analysis Computational Algorithm", Texas Instruments, Inc. Report Number U1-829401-5, Office of Naval Research Contract Number N00014-69-C-0315, 1971, 37 pp.
- [9] Brown, D.L., Allemang, R.J., Zimmerman, R.D., Mergeay, M. "Parameter Estimation Techniques for Modal Analysis", SAE Paper No. 790221, SAE Transactions, Vol. 88, pp. 828-846, 1979.
- [10] Vold, H., Kundrat, J., Rocklin, T., Russell, R., "A Multi-Input Modal Estimation Algorithm for Mini-Computers," SAE Transactions, Vol. 91, No. 1, January 1982, pp. 815-821.
- [11] Vold, H., Rocklin, T. "The Numerical Implementation of a Multi-Input Modal Estimation Algorithm for Mini-Computers," Proceedings, International Modal Analysis Conference, pp. 542-548, 1982.
- [12] Leuridan, J.M., Brown, D.L., Allemang, R.J., "Time Domain Parameter Identification Methods for Linear Modal Analysis: A Unifying Approach," ASME Paper Number 85-DET-90, 1985.
- [13] Ibrahim, S. R., Mikulcik, E. C. "A Method for the Direct Identification of Vibration Parameters from the Free Response," Shock and Vibration Bulletin, Vol. 47, Part 4 1977, pp. 183-198.
- [14] Ibrahim, S. R. "Modal Confidence Factor in Vibration Testing," Shock and Vibration Bulletin, Volume 48, Part 1 1978, pp. 65-75.
- [15] Pappa, R.S. "Some Statistical Performance Characteristics of the ITD Modal Identification Algorithm," AIAA Paper Number 82-0768, 1982, 19 pp.
- [16] Fukuzono, K., "Investigation of Multiple-Reference Ibrahim Time Domain Modal Parameter Estimation Technique," M. S. Thesis, Dept. of Mechanical and Industrial Engineering, University of Cincinnati, 1986, 220 pp.
- [17] Juang, J.N., "Mathematical Correlation of Modal Parameter Identification Methods Via System Realization Theory", Journal of Analytical and Experimental Modal Analysis, Vol. 2, No. 1, 1987, pp. 1-18.
- [18] Juang, Jer-Nan, Pappa, Richard S., "An Eigensystem Realization Algorithm for Modal Parameter Identification and Model Reduction", AIAA Journal of Guidance, Control, and Dynamics, Vol. 8, No. 4, 1985, pp. 620-627.
- [19] Pappa, Richard S., Juang, Jer-Nan, "Galileo Spacecraft Modal Identification Using An Eigensystem Realization Algorithm" AIAA Paper Number 84-1070, 1984.
- [20] Longman, Richard W., Juang, Jer-Nan, "Recursive Form of the Eigensystem Realization Algorithm for System Identification", AIAA, Journal of Guidance, Control, and Dynamics, Vol. 12, No. 5, 1989, pp. 647-652.

- [21] Lembregts, F., Leuridan, J., Zhang, L., Kanda, H., "Multiple Input Modal Analysis of Frequency Response Functions based on Direct Parameter Identification," Proceedings, International Modal Analysis Conference, 1986.
- [22] Zhang, L., Kanda, H., Brown, D.L., Allemang, R.J. "A Polyreference Frequency Domain Method for Modal Parameter Identification," ASME Paper No. 85-DET-106 1985, 8 pp.
- [23] Lembregts, F., "Frequency Domain Identification Techniques for Experimental Multiple Input Modal Analysis", Doctoral Dissertation, Katholieke University of Leuven, Belgium, 1988, 213 pp.
- [24] Lembregts, F., Leuridan, J.L., Van Brussel, H., "Frequency Domain Direct Parameter Identification for Modal Analysis: State Space Formulation", Mechanical Systems and Signal Processing, Vol. 4, No. 1, 1989, pp. 65-76.
- [25] Coppolino, R.N., "A Simultaneous Frequency Domain Technique for Estimation of Modal Parameters from Measured Data," SAE Paper No. 811046, 1981, 12 pp.
- [26] Craig, R.R., Kurdila, A.J., Kim, H.M., "State-Space Formulation of Multi-Shaker Modal Analysis", Journal of Analytical and Experimental Modal Analysis, Vol. 5, No. 3, 1990, pp. 169-183.
- [27] Richardson, M., Formenti, D.L., "Parameter Estimation from Frequency Response Measurements Using Rational Fraction Polynomials," Proceedings, International Modal Analysis Conference, 1982, pp. 167-182.
- [28] Adcock, J., Potter, R., "A Frequency Domain Curve Fitting Algorithm with Improved Accuracy," Proceedings, International Modal Analysis Conference 1985, 8 pp.
- [29] Shih, C.Y., "Investigation of Numerical Conditioning in the Frequency Domain Modal Parameter Estimation Methods", Doctoral Dissertation, University of Cincinnati, 1989, 127 pp.
- [30] Vold, H., "Orthogonal Polynomials in the Polyreference Method," Proceedings, Eleventh International Seminar on Modal Analysis, Katholieke University of Leuven, Belgium, 1986.
- [31] Van der Auweraer, H., Leuridan, J., "Multiple Input Orthogonal Polynomial Parameter Estimation", Mechanical Systems and Signal Processing, Vol. 1, No. 3, 1987, pp. 259-272.
- [32] Shih, C.Y., Tsuei, Y.G., Allemang, R.J., Brown, D.L., "A Frequency Domain Global Parameter Estimation Method for Multiple Reference Frequency Response Measurements", Mechanical System and Signal Processing, Vol. 2, No. 4, pp. 349-365, 1988.
- [33] Van der Auweraer, H., Snoeys, R., Leuridan, J.M., "A Global Frequency Domain Modal Parameter Estimation Technique for Mini-computers," ASME Journal of Vibration, Acoustics, Stress, and Reliability in Design, 1986, 10 pp.
- [34] Van der Auweraer, H., Leuridan, J., "Multiple Input Orthogonal Polynomial Parameter Estimation", Mechanical Systems and Signal Processing, Vol. 1, No. 3, 1987, pp. 259-272.
- [35] Shih, C.Y., Tsuei, Y.G., Allemang, R.J., Brown, D.L., "Complex Mode Indication Function and Its Application to Spatial Domain Parameter Estimation", Mechanical System and Signal Processing, Vol. 2, No. 4, pp. 367-377, 1988.
- [36] Rost, R.W., "Investigation of Multiple Input Frequency Response Function Estimation Techniques for Modal Analysis," Doctoral Dissertation, University of Cincinnati, 1985, 219 pp.

- [37] Dipperry, K. D., Phillips, A. W., Allemang, R. J., "An SVD Condensation of the Spatial Domain in Modal Parameter Estimation", Proceedings, International Modal Analysis Conference, 1994, 7 pp.
- [38] Dipperry, K. D., Phillips, A. W., Allemang, R. J., Spectral Decimation in Low Order Frequency Domain Modal Parameter Estimation", Proceedings, International Modal Analysis Conference, 1994, 6 pp.
- [39] Williams, R., Crowley, J., Vold, H., "The Multivariable Mode Indicator Function in Modal Analysis", Proceedings, International Modal Analysis Conference, 1985, pp. 66-70.
- [40] Kennedy, C.C., Pancu, C.D.P., "Use of Vectors in Vibration Measurement and Analysis," Journal of Aeronautical Sciences, Volume 14, Number 11, 1947, pp. 603-625.
- [41] Hollkamp, J.J., Batill, S.M., "A Recursive Algorithm for Discrete Time Domain Parameter Identification", AIAA Paper No. AIAA-90-1221, 1990, 10 pp.
- [42] Kabe, A.M., "Mode Shape Identification and Orthogonalization", USAF Space Division Report SD-TR-88-93, 1988, 25 pp.
- [43] Ebersbach, P., Irretier, H., "On the Application of Modal Parameter Estimation Using Frequency Domain Algorithms", Journal of Analytical and Experimental Modal Analysis, Vol. 4, No. 4, 1989, pp. 109-116.
- [44] Leonard, F., "ZMODAL: A New Modal Identification Technique", Journal of Analytical and Experimental Modal Analysis, Vol. 3, No. 2, 1988, pp. 69-76.
- [45] Leuridan, J. "Some Direct Parameter Model Identification Methods Applicable for Multiple Input Modal Analysis," Doctoral Dissertation, University of Cincinnati, 1984, 384 pp.
- [46] Link, M., Volland, A. "Identification of Structural System Parameters from Dynamic Response Data," Zeitschrift Fur Flugwissenschaften, Vol. 2, No. 3 1978, pp. 165-174.
- [47] Natke, H.G., "Updating Computational Models in the Frequency Domain Based on Measured Data: A Survey", Probabilistic Engineering Mechanics, Vol. 3, No. 1, 1988, pp. 28-35.
- [48] Yam, Y., Bayard, D.S., Hadaegh, F.Y., Mettler, E., Milman, M.H., Scheid, R.E., "Autonomous Frequency Domain Identification: Theory and Experiment", NASA/JPL Publication 89-8, 1989, 204 pp.

7. MODAL DATA PRESENTATION/VALIDATION

Once the modal parameters are determined, several procedures exist that allow for the modal data (model) to be validated. Some of the procedures that are used are:

- Measurement Synthesis
- Visual Verification (Animation)
- Finite Element Analysis
- Modal Vector Orthogonality
- Modal Vector Consistency (Modal Assurance Criterion)
- Modal Modification Prediction
- Modal Complexity
- Modal Phase Colinearity and Mean Phase Deviation

All of these methods depend upon the evaluation of an assumption concerning the modal model. Unfortunately, the success of the validation method only defines the validity of the assumption; the failure of the modal validation does not generally define what the cause of the problem is.

7.1 Measurement Synthesis

The simplest validation procedure is to compare the data synthesized from the modal model with the measured data. This is particularly effective if the measured data was not part of the data used to estimate the modal parameters. This serves as an independent check of the modal parameter estimation process.

The visual match can be given a numerical value if a correlation coefficient, similar to coherence, is estimated. The basic assumption is that the measured frequency response function and the synthesized frequency response function should be linearly related (unity) at all frequencies. Any two estimates of the same frequency response function can be compared with this approach. The correlation coefficient is referred to as the *synthesis correlation coefficient* or *FRF correlation coefficient*.

Synthesis Correlation Coefficient

$$COR_{pq} = \Gamma_{pq}^2 = \frac{\left| \sum_{\omega=\omega_1}^{\omega_2} H_{pq}(\omega) \hat{H}_{pq}^*(\omega) \right|^2}{\sum_{\omega=\omega_1}^{\omega_2} H_{pq}(\omega) H_{pq}^*(\omega) \sum_{\omega=\omega_1}^{\omega_2} \hat{H}_{pq}(\omega) \hat{H}_{pq}^*(\omega)} \quad (7.1)$$

where:

- $H_{pq}(\omega)$ = Measurement
- $\hat{H}_{pq}(\omega)$ = Synthesis

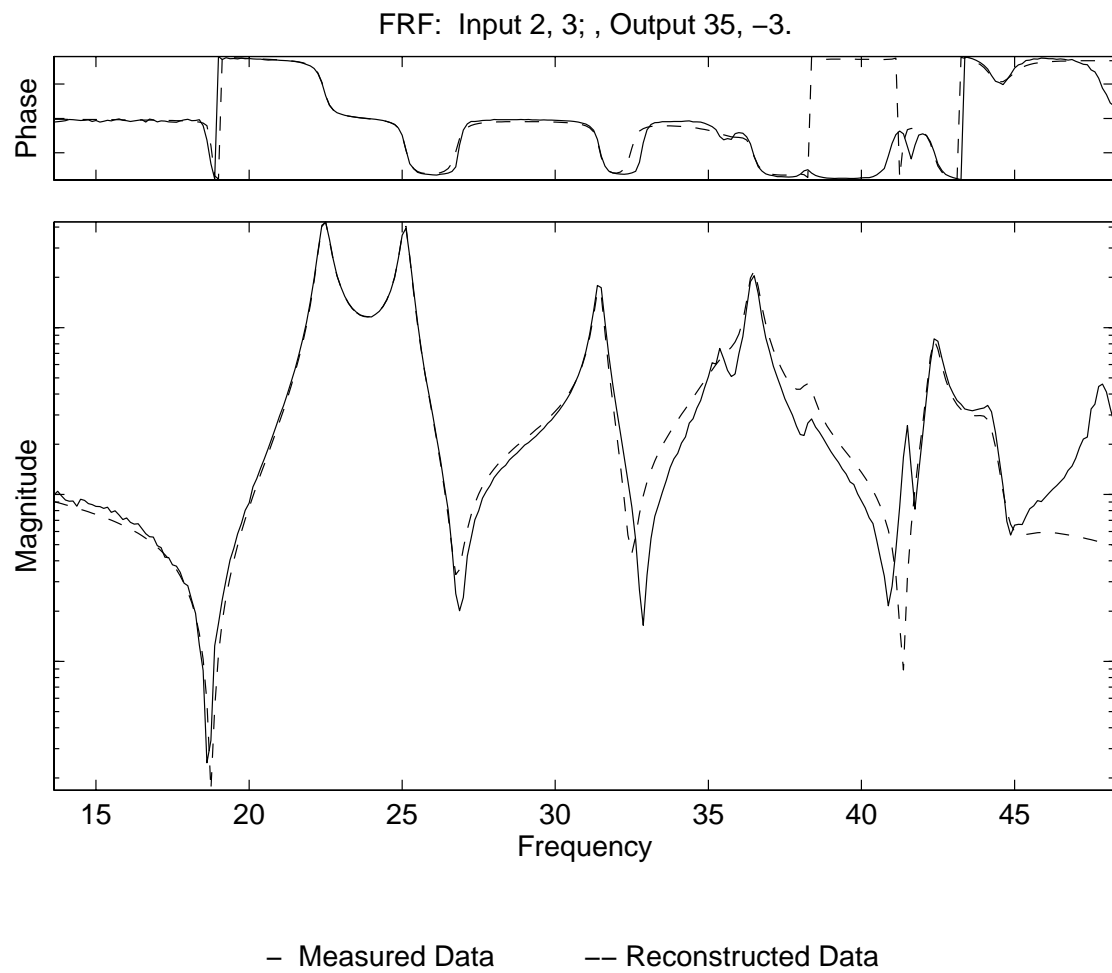


Figure 7-1. Typical FRF Synthesis

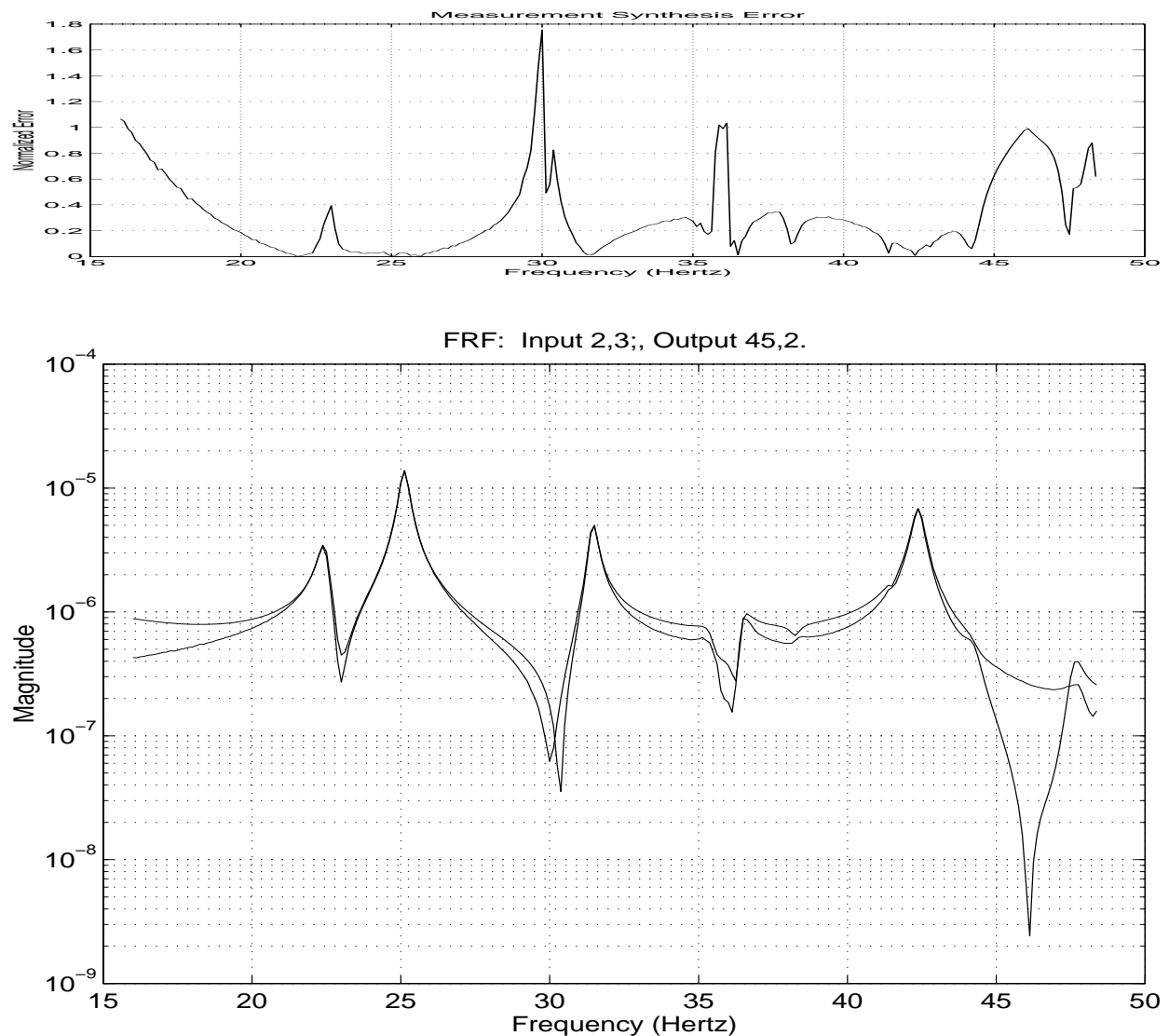


Figure 7-2. Normalized Error - FRF Synthesis

7.2 Visual Verification

Another relatively simple method of modal model validation is to evaluate the modal vectors visually. While this can be accomplished from plotted modal vectors superimposed upon the undeformed geometry, the modal vectors are normally animated (superimposed upon the undeformed geometry) in order to quickly assess the modal vector. Particularly, modal vectors are evaluated for physically realizable characteristics such as discontinuous motion or out-of-

phase problems. Often, rigid body modes of vibration are evaluated to determine scaling (calibration) errors or invalid measurement degree-of-freedom assignment or orientation. Naturally, if the system under test is believed to be proportionally damped, the modal vectors should be normal modes and this characteristic can be quickly observed by viewing an animation of the modal vector.

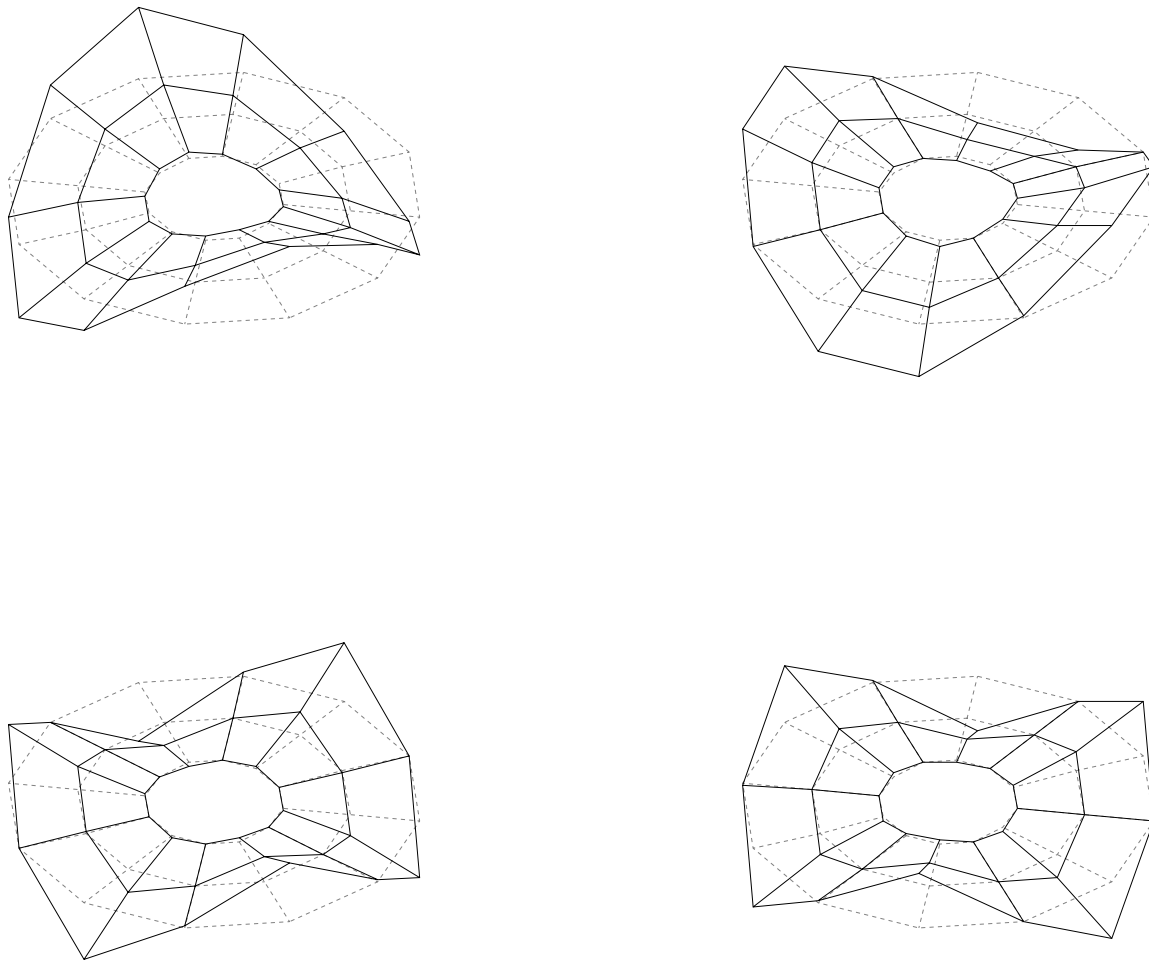


Figure 7-3. Visual Verification of Modal Vectors

7.3 Finite Element Analysis

The results of a finite element analysis of the system under test can provide another method of validating the modal model. While the problem of matching the number of analytical degrees-of-freedom N_a to the number of experimental degrees-of-freedom N_e causes some difficulty, the modal frequencies and modal vectors can be compared visually or through orthogonality or consistency checks. Unfortunately, when the comparison is not sufficiently acceptable, the question of error in the experimental model versus error in the analytical model cannot be easily resolved. Generally, assuming minimal errors and sufficient analysis and test experience, reasonable agreement can be found in the first ten deformable modal vectors but agreement for higher modal vectors will be more difficult.

7.4 Modal Vector Orthogonality

Another method that has historically been used to validate an experimental modal model is the weighted orthogonality check. In this case, the experimental modal vectors are used together with a mass matrix normally derived from a finite element model to evaluate orthogonality. The experimental modal vectors are scaled so that the diagonal terms of the modal mass matrix are unity. With this form of scaling, the off-diagonal values in the modal mass matrix are expected to be less than 0.1 (10 percent of the diagonal terms).

Theoretically, for the case of proportional damping, each modal vector of a system will be orthogonal to all other modal vectors of that system when weighted by the mass, stiffness, or damping matrix. In practice, these matrices are made available by way of a finite element analysis and normally the mass matrix is considered to be the most accurate. For this reason, any further discussion of orthogonality will be made with respect to mass matrix weighting. As a result, the orthogonality relations can be stated as follows:

Orthogonality of Modal Vectors

For $r \neq s$:

$$\{\psi_r\} [M] \{\psi_s\} = 0 \quad (7.2)$$

For $r = s$:

$$\{\psi_r\}[M]\{\psi_s\} = M_r \quad (7.3)$$

Experimentally, the result of zero for the cross orthogonality (Equation (7.2)) can rarely be achieved but values up to one tenth of the magnitude of the generalized mass of each mode are considered to be acceptable. It is a common procedure to form the modal vectors into a normalized set of mode shape vectors with respect to the mass matrix weighting. The accepted criterion in the aerospace industry, where this confidence check is made most often, is for all of the generalized mass terms to be unity and all cross orthogonality terms to be less than 0.1. Often, even under this criteria, an attempt is made to adjust the modal vectors so that the cross orthogonality conditions are satisfied ^[4-6].

In Equations (7.2) and (7.3) the mass matrix must be an $N_o \times N_o$ matrix corresponding to the measurement locations on the structure. This means that the finite element mass matrix must be modified from whatever size and distribution of grid locations required in the finite element analysis to the $N_o \times N_o$ square matrix corresponding to the measurement locations. This normally involves some sort of reduction algorithm as well as interpolation of grid locations to match the measurement situation ^[7-10].

When Equation (7.2) is not sufficiently satisfied, one (or more) of three situations may exist. First, the modal vectors can be invalid. This can be due to measurement error or problems with the modal parameter estimation algorithms. This is a very common assumption and many times contributes to the problem. Second, the mass matrix can be invalid. Since the mass matrix is not easily related to the physical properties of the system, this probably contributes significantly to the problem. Third, the reduction of the mass matrix can be invalid ^[6-11]. This can certainly be a realistic problem and cause severe errors. The most obvious example of this situation would be when a relatively large amount of mass is reduced to a measurement location that is highly flexible, such as the center of an unsupported panel. In such a situation the measurement location is weighted very heavily in the orthogonality calculation of Equation (7.2) but may represent only incidental motion of the overall modal vector.

In all probability, all three situations contribute to the failure of cross orthogonality criteria on occasion. When the orthogonality conditions are not satisfied, this result does not indicate where

the problem originates. From an experimental point of view, it is important to try to develop methods that indicate confidence that the modal vector is or is not part of the problem.

Causes of Poor Orthogonality

- The modal vectors can be invalid.
This can be due to measurement error or problems with the modal parameter estimation algorithms.
- The mass matrix
can be invalid. Since the mass matrix is not easily related to the physical properties of the system, this probably contributes significantly to the problem.
- The reduction of the mass matrix can be invalid. This can certainly be a realistic problem and cause severe errors. The most obvious example of this situation would be when a relatively large amount of mass is reduced to a measurement location that is highly flexible, such as the center of an unsupported panel.

7.5 Modal Vector Consistency

Since the residue matrix contains redundant information with respect to a modal vector, the consistency of the estimate of the modal vector under varying conditions such as excitation location or modal parameter estimation algorithms can be a valuable confidence factor to be utilized in the process of evaluation of the experimental modal vectors.

The common approach to estimation of modal vectors from the frequency response function method is to measure a complete row or column of the frequency response function matrix. This will give reasonable definition to those modal vectors that have a non-zero modal coefficient at the excitation location and can be completely uncoupled with the forced normal mode excitation method. When the modal coefficient at the excitation location of a modal vector is zero (very small with respect to the dynamic range of the modal vector) or when the modal vectors cannot

be uncoupled, the estimation of the modal vector will contain potential bias and variance errors. In such cases additional rows and/or columns of the frequency response function matrix are measured to detect such potential problems.

In these cases, information in the residue matrix corresponding to each pole of the system is evaluated to determine separate estimates of the same modal vector. This evaluation consists of the calculation of a complex modal scale factor (relating two modal vectors) and a scalar modal assurance criterion (measuring the consistency between two modal vectors). The function of the **modal scale factor (MSF)** is to provide a means of normalizing all estimates of the same modal vector. When two modal vectors are scaled similarly, elements of each vector can be averaged (with or without weighting), differenced, or sorted to provide a best estimate of the modal vector or to provide an indication of the type of error vector superimposed on the modal vector. In terms of modern, multiple reference modal parameter estimation algorithms, the modal scale factor is a normalized estimate of the modal participation factor between two references for a specific mode of vibration. The function of the **modal assurance criterion (MAC)** is to provide a measure of consistency between estimates of a modal vector. This provides an additional confidence factor in the evaluation of a modal vector from different excitation locations. The modal assurance criterion also provides a method of determining the degree of causality between estimates of different modal vectors from the same system [11-12].

The modal scale factor and the modal assurance criterion also provide a method of easily comparing estimates of modal vectors originating from different sources. The modal vectors from a finite element analysis can be compared and contrasted with those determined experimentally as well as modal vectors determined by way of different experimental or modal parameter estimation methods. In this approach, methods can be compared and contrasted in order to evaluate the mutual consistency of different procedures rather than estimating the modal vectors specifically.

The **modal scale factor** is defined, according to this approach, as follows:

$$MSF_{cdr} = \frac{\{\psi_{cr}\}^H \{\psi_{dr}\}}{\{\psi_{dr}\}^H \{\psi_{dr}\}} \quad (7.4)$$

Equation (7.4) implies that the modal vector d is the reference to which the modal vector c is

compared. In the general case, modal vector c can be considered to be made of two parts. The first part is the part correlated with modal vector d . The second part is the part that is not correlated with modal vector d and is made up of contamination from other modal vectors and of any random contribution. This error vector is considered to be noise. The **modal assurance criterion** is defined as a scalar constant relating the portion of the auto moment of the modal vector that is linearly related to the reference modal vector as follows:

$$MAC_{cdr} = \frac{\left| \{\psi_{cr}\}^H \{\psi_{dr}\} \right|^2}{\{\psi_{cr}\}^H \{\psi_{cr}\} \{\psi_{dr}\}^H \{\psi_{dr}\}} = \frac{\left(\{\psi_{cr}\}^H \{\psi_{dr}\} \right) \left(\{\psi_{dr}\}^H \{\psi_{cr}\} \right)}{\{\psi_{cr}\}^H \{\psi_{cr}\} \{\psi_{dr}\}^H \{\psi_{dr}\}} \quad (7.5)$$

The modal assurance criterion is a scalar constant relating the causal relationship between two modal vectors. The constant takes on values from zero, representing no consistent correspondence, to one, representing a consistent correspondence. In this manner, if the modal vectors under consideration truly exhibit a consistent relationship, the modal assurance criterion should approach unity and the value of the modal scale factor can be considered to be reasonable.

The modal assurance criterion can only indicate consistency, not validity. If the same errors, random or bias, exist in all modal vector estimates, this is not delineated by the modal assurance criterion. Invalid assumptions are normally the cause of this sort of potential error. Even though the modal assurance criterion is unity, the assumptions involving the system or the modal parameter estimation techniques are not necessarily correct. The assumptions may cause consistent errors in all modal vectors under all test conditions verified by the modal assurance criterion.

Modal Assurance Criterion (MAC) Zero

If the modal assurance criterion has a value near zero, this is an indication that the modal vectors are not consistent. This can be due to any of the following reasons:

- The system is non-stationary. This can occur whenever the system is undergoing a change in mass or stiffness during the testing period.

- The system is nonlinear. System nonlinearities will appear differently in frequency response functions generated from different exciter positions or excitation signals. The modal parameter estimation algorithms will also not handle the different nonlinear characteristics in a consistent manner.
- There is noise on the reference modal vector. This case is the same as noise on the input of a frequency response function measurement. No amount of signal processing can remove this type of error.
- The modal parameter estimation is invalid. The frequency response functions measurements may contain no errors but the modal parameter estimation may not be consistent with the data.
- The modal vectors are from linearly unrelated mode shape vectors. Hopefully, since the different modal vector estimates are from different excitation positions this measure of inconsistency will imply that the modal vectors are orthogonal.

Obviously, if the first four reasons can be eliminated, the modal assurance criterion can be interpreted in a similar way as an orthogonality calculation.

Modal Assurance Criterion (MAC) Unity

If the modal assurance criterion has a value near unity, this is an indication that the modal vectors are consistent. This does not necessarily mean that they are correct. The modal vectors can be consistent for any of the following reasons:

- The modal vectors have been incompletely measured. This situation can occur whenever too few response stations have been included in the experimental determination of the modal vector.
- The modal vectors are the result of a forced excitation other than the desired input. This would be the situation if, during the measurement of the frequency response function, a rotating piece of equipment with an unbalance is present in the system being tested.
- The modal vectors are primarily coherent noise. Since the reference modal vector may be arbitrarily chosen, this modal vector may not be one of the true modal vectors of the system. It could simply be a random noise vector or a vector reflecting the bias in the

modal parameter estimation algorithm. In any case, the modal assurance criterion will only reflect a causal relationship to the reference modal vector.

- The modal vectors represent the same modal vector with different arbitrary scaling. If the two modal vectors being compared have the same expected value when normalized, the two modal vectors should differ only by the complex valued scale factor which is a function of the common modal coefficients between the rows or columns.

Therefore, if the first three reasons can be eliminated, the modal assurance criterion indicates that the modal scale factor is the complex constant relating the modal vectors and that the modal scale factor can be used to average, difference, or sort the modal vectors.

Under the constraints mentioned previously, the modal assurance criterion can be applied in many different ways. The modal assurance criterion can be used to verify or correlate an experimental modal vector with respect to a theoretical modal vector (eigenvector). This can be done by computing the modal assurance criterion between N_e modal vectors estimated from experimental data and N_a modal vectors estimated from a finite element analysis evaluated at common stations. This process results in a $N_e \times N_a$ rectangular modal assurance criterion matrix with values that approach unity whenever an experimental modal vector and an analytical modal vector are consistently related.

Experimental modal vectors can be averaged, differenced, or sorted to determine the best single estimate or the potential source of contamination. Since the modal scale factor is a complex scalar that allows two vectors to be phased the same and to the same mean value, these vectors can be subtracted to evaluate whether the error is random or biased and, if the error appears to be random and the modal assurance criterion is high, the modal vectors can be averaged, using the modal scale factor, to improve the estimate of a modal vector. If the error appears to be biased or skewed, the error pattern often gives an indication that the error originates due to the location of the excitation or due to an inadequate modal parameter estimation process. Based upon partial but overlapping measurement of two columns of the frequency response function matrix, modal vectors can be sorted, assuming the modal assurance function indicates consistency, into a complete estimate of each modal vector at all measurement stations.

The modal assurance criterion can be used to evaluate modal parameter estimation methods if a set of analytical frequency response functions with realistic levels of random and bias errors is

generated and used in common to a variety modal parameter estimation methods. In this way, agreement between existing methods can be established and new modal parameter estimation methods can be checked for characteristics that are consistent with accepted procedures. Additionally, this approach can be used to evaluate the characteristics of each modal parameter estimation method in the presence of varying levels of random and bias error.

The concept of consistency in the estimate of modal vectors from separate testing constraints is important considering the potential of multiple estimates of the same modal vector from numerous input configurations and modal parameter estimation algorithms. The computation of modal scale factor and modal assurance criterion results in a complex scalar and a correlation coefficient which does not depend on weighting information outside the testing environment. Since the modal scale factor and modal assurance criterion are computed analogous to the frequency response function and coherence function, both the advantages and limitations of the computation procedure are well understood. These characteristics, as well as others, provide a useful tool in the processing of experimental modal vectors.

Coordinate Modal Assurance Criterion (COMAC)

An extension of the modal assurance criterion is the ***coordinate modal assurance criterion*** (COMAC) ^[13]. The COMAC attempts to identify which measurement degrees of freedom contribute negatively to a low value of MAC. The COMAC is calculated over a set of mode pairs, analytical versus analytical, experimental versus experimental or experimental versus analytical. The two modal vectors in each mode pair represents the same modal vector but the set of mode pairs represents all modes of interest in a given frequency range. For two sets of modes that are to be compared, there will be a value of COMAC computed for each (measurement) degree of freedom.

The coordinate modal assurance criterion (COMAC) is calculated using the following approach, once the mode pairs have been identified with MAC or some other approach:

$$COMAC_p = \frac{\sum_{r=1}^L \left| \psi_{pr} \phi_{pr} \right|^2}{\sum_{r=1}^L \psi_{pr} \psi_{pr}^* \sum_{r=1}^L \phi_{pr} \phi_{pr}^*} \quad (7.6)$$

where:

- L = Number of matching pairs of modes in the two sets of modal vectors being compared.
- ψ_{pr} = Modal coefficient from (measured) degree of freedom p and modal vector pair r from one set of modal vectors.
- ϕ_{pr} = Modal coefficient from (measured) degree of freedom p and modal vector pair r from a second set of modal vectors.

Note that the above formulation assumes that there is a match for every modal vector in the two sets and the modal vectors are renumbered according so that the matching modal vectors have the same subscript. Only those modes that match between the two sets are included in the computation.

7.6 Modal Modification Prediction

The use of a modal model to predict changes in modal parameters caused by a perturbation (modification) of the system is becoming more of a reality as more measured data is acquired simultaneously. In this validation procedure, a modal model is estimated based upon a complete modal test. This modal model is used as the basis to predict a perturbation to the system that was tested, such as the addition of a mass at a particular point on the structure. Then, the mass is added to the structure and the perturbed system is retested. The predicted and measured data or modal model can be compared and contrasted as a measure of the validity of the underlying modal model.

7.7 Modal Complexity

Modal complexity is a variation of the use of sensitivity analysis in the validation of a modal model. When a mass is added to a structure, the modal frequencies should either be unaffected

or should shift to a slightly lower frequency. Modal overcomplexity is a summation of this effect over all measured degrees of freedom for each mode. Modal complexity is particularly useful for the case of complex modes in an attempt to quantify whether the mode is genuinely a complex mode, a linear combination of several modes or a computational artifact. The mode complexity is normally indicated by the ***Mode Overcomplexity Value (MOV)*** which is the percentage of response points that actually would cause the damped natural frequency to decrease when a mass is added compared to the total number of response points. A separate MOV is estimated for each mode of vibration and the ideal result should be 1.0 (100 percent) for each mode.

7.8 Modal Phase Colinearity and Mean Phase Deviation

For proportionally damped systems, each modal coefficient for a specific mode of vibration should differ by 0° or 180° . The ***modal phase colinearity (MPC)*** is an index expressing the consistency of the linear relationship between the real and imaginary parts of each modal coefficient. This concept is essentially the same as the ordinary coherence function with respect to the linear relationship of the frequency response function for different averages or the modal assurance criterion (MAC) with respect to the modal scale factor between modal vectors. The MPC should be 1.0 (100 percent) for a mode that is essentially a normal mode. A low value of MPC indicates a mode that is complex (after normalization) and is an indication of a non-proportionally damped system or errors in the measured data and/or modal parameter estimation.

Another indicator that defines whether a modal vector is essentially a normal mode is the ***mean phase deviation (MFD)***. This index is the statistical variance of the phase angles for each mode shape coefficient for a specific modal vector from the mean value of the phase angle. The MFD is an indication of the phase scatter of a modal vector and should be near 0° for a real, normal mode.

7.9 References

- [1] Ewins, D., **Modal Testing: Theory and Practice** John Wiley and Sons, Inc., New York, 1984, 269 pp.
- [2] Strang, G., **Linear Algebra and Its Applications, Third Edition**, Harcourt Brace Jovanovich Publishers, San Diego, 1988, 505 pp.

- [3] Lawson, C.L., Hanson, R.J., **Solving Least Squares Problems**, Prentice-Hall, Inc., Englewood Cliffs, New Jersey, 1974, 340 pp.
- [4] Gravitz, S. I., "An Analytical Procedure for Orthogonalization of Experimentally Measured Modes" , Journal of the Aero/Space Sciences, Volume 25 , 1958, pp. 721-722.
- [5] McGrew, J., "Orthogonalization of Measured Modes and Calculation of Influence Coefficients", AIAA Journal, Volume 7, Number 4, 1969, pp. 774-776.
- [6] Targoff, W. P., "Orthogonality Check and Correction of Measured Modes", AIAA Journal, Volume 14, Number 2, 1976, pp. 164-167.
- [7] Guyan, R.J., "Reduction of Stiffness and Mass Matrices", AIAA Journal, Volume 3, Number 2, February 1965, pp. 380,
- [8] Irons, B., "Structural Eigenvalue Problems: Elimination of Unwanted Variables", AIAA Journal, Volume 3, Number 5, May 1965, pp. 961-962.
- [9] Downs, B., "Accurate Reduction of Stiffness and Mass Matrices for Vibration Analysis and a Rationale for Selecting Master Degrees of Freedom", ASME Paper Number 79-DET-18, 1979, 5 pp.
- [10] Sowers, J.D., "Condensation of Free Body Mass Matrices Using Flexibility Coefficients", AIAA Journal, Volume 16, Number 3, March 1978, pp. 272-273.
- [11] Allemang, R.J., "Investigation of Some Multiple Input/Output Frequency Response Function Experimental Modal Analysis Techniques", Doctor of Philosophy Dissertation University of Cincinnati, Department of Mechanical Engineering, 1980, 358 pp.
- [12] Allemang, R.J., Brown, D.L., "A Correlation Coefficient for Modal Vector Analysis", Proceedings, International Modal Analysis Conference, pp.110-116, 1982.
- [13] Lieven, N.A.J., Ewins, D.J., "Spatial Correlation of Mode Shapes, The Coordinate Modal Assurance Criterion (COMAC)", Proceedings, International Modal Analysis Conference, pp. 690-695, 1988.

Vibrations III: 20-263-662**Name:** _____**Matlab Homework Assignment:****For the information given at the bottom of this page.**

- **Formulate and plot the frequency response function H_{23} using the matrix inversion approach as before.**
- **Find the corresponding impulse response function h_{23} . Use the script 'hp_ifft.m' from the web page to form the impulse response function if have not done this before. Check to be sure that the impulse response function is real valued (imaginary part equals zero at all time).**
- **Find the modal frequencies (frequency and damping) using the LSCE algorithm. Use the script 'lsce.m' from the web page to do this. This script implements the time domain example from the Vibs III notes.**

$$[M] = \begin{bmatrix} 10 & 0 & 0 \\ 0 & 14 & 0 \\ 0 & 0 & 12 \end{bmatrix} \quad [C] = \begin{bmatrix} 5 & -3 & 0 \\ -3 & 5.5 & -2.5 \\ 0 & -2.5 & 2.5 \end{bmatrix} \quad [K] = \begin{bmatrix} 5000 & -3000 & 0 \\ -3000 & 5500 & -2500 \\ 0 & -2500 & 2500 \end{bmatrix}$$

Appendix A: Least Squares Method

The process of determination of a mathematical model for a group of variables is known as the parameter estimation process. One of the more popular approaches used in parameter estimation is the *Least Squares Method*.

In its simplest form the least squares method will be illustrated in this section. Suppose that the relationship between two group of variables x and y can be best described by the equation of a straight line:

$$y = a_1 x + a_0 \quad (\text{A-1})$$

One could arbitrarily choose two sets of x and y quantities and solve for the two unknown parameters a_1 and a_0 . Yet, the line constructed by the computed a_1 and a_0 parameters might not pass through some sets of x and y , since the information associated with those points were not used in computing a_1 and a_0 .

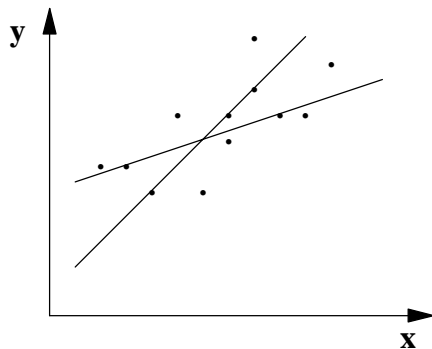


Figure A-1. Straight Lines Fitting the Data

The reasons for all the points not being located on one straight line could be:

- Errors in data set
- Inaccurate model for the data set.

The least squares criterion requires that the sum of the squares of the deviations separating the data points from the curve will be minimum. These deviations are simply the difference between the estimated values of y (hereafter denoted by \hat{y}_r) from Eq. (A-1) and the actual measured values of y (y_r). In other words, the deviations are the errors associated with the value of y predicted by the model and the actual measured data. The least squares method approach will use information associated with all of the x and y sets, to determine the "best" estimates of a_1 and a_0 .

$$E = \sum_{r=1}^N e_r^2 = \sum_{r=1}^N \left[y_r - \hat{y}_r \right]^2 = \sum_{r=1}^N \left[y_r - \left(a_1 x_r + a_0 \right) \right]^2 \quad (A-2)$$

Minimization of error, Eq. (A-2), with respect to a_1 and a_0 results in the following equations which are called the *normal equations* for the least squares problem:

$$\frac{\partial E}{\partial a_1} = \sum_{r=1}^N 2 \left[y_r - \left(a_1 x_r + a_0 \right) \right] \left[-x_r \right] = 0 \quad (A-3)$$

$$\frac{\partial E}{\partial a_0} = \sum_{r=1}^N 2 \left[y_r - \left(a_1 x_r + a_0 \right) \right] \left[-1 \right] = 0 \quad (A-4)$$

Equations (A-3) and (A-4) can be solved for the unknown parameters a_1 and a_0 .

$$a_1 = \frac{N \sum_{r=1}^N x_r y_r - \left(\sum_{r=1}^N x_r \right) \left(\sum_{r=1}^N y_r \right)}{N \sum_{r=1}^N x_r^2 - \left(\sum_{r=1}^N x_r \right)^2} \quad (A-5)$$

$$a_0 = \frac{\left(\sum_{r=1}^N y_r \right) \left(\sum_{r=1}^N x_r^2 \right) - \left(\sum_{r=1}^N x_r \right) \left(\sum_{r=1}^N x_r y_r \right)}{N \sum_{r=1}^N x_r^2 - \left(\sum_{r=1}^N x_r \right)^2} \quad (A-6)$$

The a_1 and a_0 values computed from Eqs. (A-5) and (A-6) represent the characteristics of a straight line which would "best" describe the x and y sets of values.

Similarly, one could compute a_1 and a_0 parameters with the criterion that the sum of the square of errors in the x (e_x) would be minimum. Another approach could be the minimization of the sum of the square of errors in the x and y (e_v).

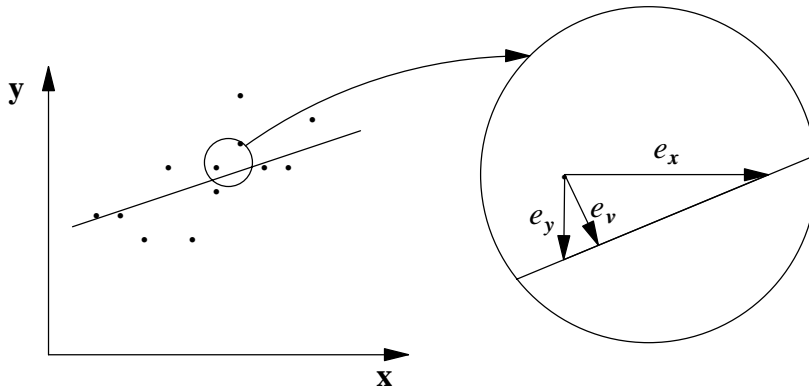


Figure A-2. Errors in Least Squares Estimation

The least squares problem can be formulated in matrix notation as:

$$\{Y\} = [X] \{A\} \quad (A-7)$$

where,

$$\{Y\} = \begin{Bmatrix} y_1 \\ y_2 \\ \cdot \\ \cdot \\ \cdot \\ y_N \end{Bmatrix} \quad [X] = \begin{bmatrix} x_1 & 1 \\ x_2 & 1 \\ \cdot & \cdot \\ \cdot & \cdot \\ \cdot & \cdot \\ x_N & 1 \end{bmatrix} \quad \{A\} = \begin{Bmatrix} a_1 \\ a_0 \end{Bmatrix}$$

The equations presented by matrix Eq. (A-7) are in general a set of inconsistent and

overdetermined equations. Inconsistent, since it is not usually possible to find $\{A\}$ that would satisfy all the individual equations of Eq. (A-7), and overdetermined, since the number of equations is larger than the number of unknowns. The least square solution of Eq. (A-7) is:

$$[X]^T \{Y\} = [X]^T [X] \{A\} \quad (\text{A-8})$$

and solving for unknown vector $\{A\}$

$$\{A\} = \left([X]^T [X] \right)^{-1} [X]^T \{Y\} \quad (\text{A-9})$$

provided that $([X]^T [X])^{-1}$ exists. In the case that the inverse of $([X]^T [X])$ does not exist, one could use numerical techniques to solve for vector $\{A\}$.

In a more general case where matrices A, X, and Y are complex valued, the transpose notation, T, must be replaced with hermitian notation, H, in Eqs. (A-8) and (A-9). Where the hermitian operator, H, is the complex conjugate transpose. Hence, the unknown vector $\{A\}$ is given by:

$$\{A\} = \left([X]^H [X] \right)^{-1} [X]^H \{Y\} \quad (\text{A-10})$$

Individual equations in matrix Eq. (A-7) could be multiplied by a weighting factor to give that equation more or less weight in the computation. The weighting factors could be presented in form of a diagonal ($N \times N$) matrix, W. The diagonal element in row i represents the weighting factor corresponding to equation i, and the off diagonal terms are all zero. Matrix W is pre-multiplied to both sides of Eq. (A-7):

$$[W] \{Y\} = [W][X] \{A\} \quad (\text{A-11})$$

where:

$$[W] = \begin{bmatrix} w_1 & 0 & \cdot & 0 \\ 0 & w_2 & \cdot & 0 \\ \cdot & \cdot & \cdot & \cdot \\ 0 & 0 & \cdot & w_N \end{bmatrix}$$

Solving for vector $\{A\}$ in Eq. (A-11):

$$\{A\} = \left([X]^H [W]^H [W] [X] \right)^{-1} [X]^H [W]^H [W] \{Y\} \quad (\text{A-12})$$

In general the relationship of Eq. (A-1) could be in the form of:

$$\mathbf{y} = \mathbf{a}_N \mathbf{x}^N + \mathbf{a}_{N-1} \mathbf{x}^{N-1} + \cdots + \mathbf{a}_1 \mathbf{x} + \mathbf{a}_0 \quad (\text{A-13})$$

A set of equations similar to the formulation above could be written and solved to obtain the least squares estimation of unknown parameters \mathbf{a}_N , \mathbf{a}_{N-1} , ..., \mathbf{a}_1 , \mathbf{a}_0 .

The least squares method stated above could easily be extended to problems involving more than one independent variable. For example, z could be expressed in terms of x and y :

$$z = \mathbf{a}_2 \mathbf{y} + \mathbf{a}_1 \mathbf{x} + \mathbf{a}_0 \quad (\text{A-14})$$

The corresponding normal equations for the least squares problem of Eq. (A-14) are:

$$\frac{\partial E}{\partial \mathbf{a}_2} = \sum_{r=1}^N 2 \left[z_r - \left(\mathbf{a}_2 \mathbf{y}_r + \mathbf{a}_1 \mathbf{x}_r + \mathbf{a}_0 \right) \right] \left[-\mathbf{y}_r \right] = 0 \quad (\text{A-15})$$

$$\frac{\partial E}{\partial \mathbf{a}_1} = \sum_{r=1}^N 2 \left[z_r - \left(\mathbf{a}_2 \mathbf{y}_r + \mathbf{a}_1 \mathbf{x}_r + \mathbf{a}_0 \right) \right] \left[-\mathbf{x}_r \right] = 0 \quad (\text{A-16})$$

$$\frac{\partial E}{\partial \mathbf{a}_0} = \sum_{r=1}^N 2 \left[z_r - \left(\mathbf{a}_2 \mathbf{y}_r + \mathbf{a}_1 \mathbf{x}_r + \mathbf{a}_0 \right) \right] \left[-1 \right] = 0 \quad (\text{A-17})$$

Equations (A-15) - (A-17) can be solved for the unknown parameters \mathbf{a}_2 , \mathbf{a}_1 , and \mathbf{a}_0 . The computed values \mathbf{a}_2 , \mathbf{a}_1 , and \mathbf{a}_0 represent the characteristics of a plane which would "best" describe the x , y , and z sets of values.

The above theory and formulation could be expanded to least squares estimation of a surface and eventually to higher order dimensions.

A.1 Correlation Coefficient

The "goodness" of the least squares estimation process is measured by the coefficient of correlation parameter which is defined in terms of **total variation** and **explained variation**. The total variation of y is defined as $\sum_{r=1}^N (y_r - \bar{y})^2$, which is the sum of the squares of the deviations of y_r from the mean value, \bar{y} . Total variation consists of two parts: (1) the explained variation, $\sum_{r=1}^N (\hat{y}_r - \bar{y})^2$; and (2) the unexplained variation, $\sum_{r=1}^N (y_r - \hat{y}_r)^2$. The terms explained variation and unexplained variation are used to denote the fact that the deviations $\hat{y}_r - \bar{y}$ have a definite pattern, while, the deviations $y_r - \hat{y}_r$ are random and unpredictable.

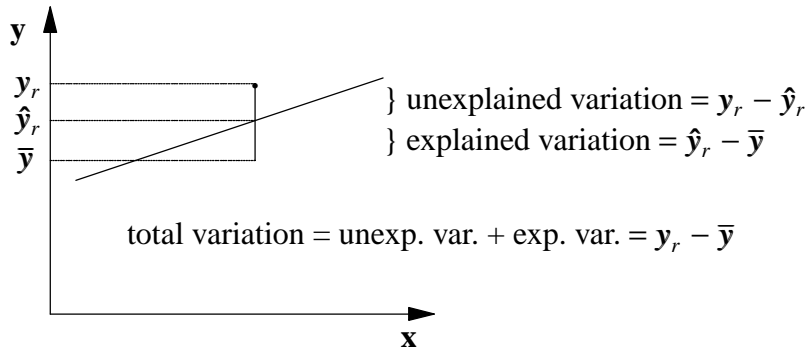


Figure A-3. Variations in Data

Therefore, the coefficient of correlation r^2 , is defined as:

$$r^2 = \frac{\sum_{r=1}^N (\hat{y}_r - \bar{y})^2}{\sum_{r=1}^N (y_r - \bar{y})^2} \quad (\text{A-18})$$

The magnitude of r^2 varies between 0 and 1. A value of 0 indicates no correlation between

dependent and independent variable(s), while a value of 1 indicates perfect correlation.

It should be pointed out that the coefficient of correlation computed for a set of data and a assumed model, only indicates the relationship of data based on the assumed model. That is, the coefficient of correlation measures the degree to which the assumed model describes the relationship for a set of data.

A.2 Examples

A.2.1 Example 1

For the data given in Table A-1 and the assumed model equation:

$$y = a_1x + a_0 \quad (\text{A-19})$$

x	65	63	67	64	68	62	70	66	68	67	69	71
y	68	66	68	65	69	66	68	65	71	67	68	70

Table A-2. x and y Values for Least Squares Fit

- Find the least squares solution of a_1 and a_0 .
- Find the coefficient of correlation.

Solution:

- The following normal equations must be solved for a_1 and a_0

$$a_0 N + a_1 \sum_{r=1}^N x_r = \sum_{r=1}^N y_r \quad (\text{A-20})$$

$$a_0 \sum_{r=1}^N x_r + a_1 \sum_{r=1}^N x_r^2 = \sum_{r=1}^N x_r y_r \quad (\text{A-21})$$

substituting the appropriate terms in Eqs. (A-20) and (A-21):

$$\begin{aligned} 12 a_0 + 800 a_1 &= 811 \\ 800 a_0 + 53418 a_1 &= 54107 \end{aligned}$$

from which we find $a_1 = 0.476$ and $a_0 = 35.82$ or

$$y = 0.476 x + 35.82 \quad (\text{A-22})$$

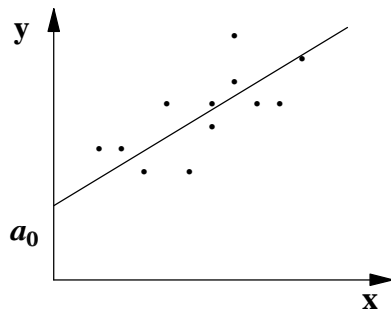


Figure A-4. Least Squares Fit of Data

$$\text{b) Explained variation} = \sum_{r=1}^N (\hat{y}_r - \bar{y})^2 = 19.22$$

$$\text{Total variation} = \sum_{r=1}^N (y_r - \bar{y})^2 = 38.92$$

$$\text{Coefficient of correlation} = r^2 = \frac{19.22}{38.92} = 0.7027$$

A.2.2 Example 2

Given the model for the sampled impulse response function between two points on a structure as,

$$h(t_k) = \sum_{r=1}^{2N} A_r e^{\lambda_r k \Delta t} \quad (\text{A-23})$$

where,

$$k = 0, 1, 2, \dots, 2N$$

$$\Delta t = \text{value of time subinterval}$$

$$t_k = k \Delta t$$

and the known pole information λ_r , formulate the least squares solution of estimating the residues, A_r .

Solution:

For simplicity and conciseness let,

$$z_r = e^{\lambda_r \Delta t}$$

and therefore Eq. (A-23) can be rewritten as,

$$h(t_k) = \sum_{r=1}^{2N} A_r z_r^k \quad (\text{A-24})$$

expanding Eq. (A-24) for time values of t_0 to t_{2N-1} will result in the following 2N equations

$$\begin{aligned} h(t_0) &= A_1 + A_2 + \dots + A_{2N} \\ h(t_1) &= A_1 z_1 + A_2 z_2 + \dots + A_{2N} z_{2N} \\ h(t_2) &= A_1 z_1^2 + A_2 z_2^2 + \dots + A_{2N} z_{2N}^2 \\ &\vdots \end{aligned} \quad (\text{A-25})$$

$$h(t_{2N-1}) = A_1 z_1^{2N-1} + A_2 z_2^{2N-1} + \cdots + A_{2N} z_{2N}^{2N-1}$$

presenting the 2N equations of Eq. (A-25) in matrix form gives,

$$\begin{bmatrix} 1 & 1 & \cdot & 1 \\ z_1 & z_2 & \cdot & z_{2N} \\ z_1^2 & z_2^2 & \cdot & z_{2N}^2 \\ \cdot & \cdot & \cdot & \cdot \\ z_1^{2N-1} & z_2^{2N-1} & \cdot & z_{2N}^{2N-1} \end{bmatrix} \begin{Bmatrix} A_1 \\ A_2 \\ \cdot \\ A_{2N} \end{Bmatrix} = \begin{Bmatrix} h(t_0) \\ h(t_1) \\ h(t_2) \\ \cdot \\ h(t_{2N-1}) \end{Bmatrix} \quad (\text{A-26})$$

or,

$$[z] \{A\} = \{h\} \quad .$$

Solving Eq. (A-26) with more than 2N rows for vector {h} and matrix [z] will result in the least squares solution of the residues. Using the $\bar{}$ notation to denote that vector {h} and matrix [z] have been expanded (more rows):

$$[\bar{z}]^H [\bar{z}] \{A\} = [\bar{z}]^H \{\bar{h}\} \quad . \quad (\text{A-27})$$

A.3 References

- [1] Ben Nobel, James W. Daniel, **Applied Linear Algebra**, Prentice-Hall, Inc., 1977.
- [2] Gibert Strang, **Introduction to Applied Mathematics**, Wellesley-Cambridge Press, 1986.
- [3] Murray R. Spiegel, **Schaum's Outline Series "Statistics"**, McGraw-Hill Book, 1961.

Appendix B: Singular Value Decomposition

The singular value decomposition will decompose a matrix into the simplest possible form, that being diagonal. This decomposition will always be possible regardless of the rank, or dimension, of the matrix ^[1].

Consider the right and left eigenvectors of the $m \times n$ matrix $[A]$, which is of rank k .

$$[A] \{v\} = \{u\} \sigma \quad (\text{B-1})$$

$$[A]^H \{u\} = \{v\} \sigma \quad (\text{B-2})$$

where:

- $\{u\} = m \times 1$ left singular vector
- $\{v\} = n \times 1$ right singular vector
- $\sigma =$ scalar singular value

By substituting Eq. (B-1) into Eq. (B-2) for $\{u\}$, the right singular vectors can be determined from:

$$[A]^H [A] \{v\} = \{v\} \sigma^2 \quad (\text{B-3})$$

$$|[A]^H [A] - \sigma^2 [I]| = 0$$

where:

- $i = 1 \rightarrow k \quad \sigma_i^2 > 0$
- $i = k + 1 \rightarrow n \quad \sigma_i^2 = 0$
- $[V] = [\{v\}_1 \{v\}_2 \{v\}_3 \cdots \{v\}_n]$ right singular unitary matrix.

By substituting Eq. (B-2) into Eq. (B-1) for $\{v\}$, the left singular vectors can be determined from:

$$[A] [A]^H \{u\} = \{u\} \sigma^2 \quad (\text{B-4})$$

$$| [A] [A]^H - \sigma^2 [I] | = 0$$

where:

- $i = 1 \rightarrow k \quad \sigma_i^2 > 0$
- $i = k + 1 \rightarrow m \quad \sigma_i^2 = 0$
- $[U] = [\{u\}_1 \ \{u\}_2 \ \{u\}_3 \ \cdots \ \{u\}_m]$ left singular unitary matrix.

If the eigenvector matrices $[U]$ and $[V]$ are unitary ($[U]^H = [U]^{-1}$ and $[V]^H = [V]^{-1}$), that is, both columns and rows form an orthonormal set, the linear transformation will preserve both angles and lengths. Interpreted geometrically, linear transformations defined by unitary matrices behave like simple rotations in space. The matrix $[A]$, can now be decomposed into diagonal form by appending the eigenvector matrices to Eq. (B-1) and premultiplying by $[U]^H$, forming the matrix product:

$$[S] = [U]^H [A] [V] = \begin{bmatrix} \{u\}_1^H \\ \vdots \\ \{u\}_k^H \\ \vdots \\ \{u\}_m^H \end{bmatrix} \begin{bmatrix} \{u\}_1 \sigma_1 & \cdots & \{u\}_k \sigma_k & \{0\}_{k+1} & \cdots & \{0\}_n \end{bmatrix} . \quad (\text{B-5})$$

Using the unitary matrix property, $[U]^H [U] = [I]$, the right hand side can be further simplified as:

$$[S] = [U]^H [A] [V] = \begin{bmatrix} \sigma_1 & 0 & 0 & \cdots & 0 & | & \\ 0 & \sigma_2 & 0 & \cdots & 0 & | & [0] \\ 0 & 0 & \sigma_3 & & 0 & | & \\ \vdots & \vdots & & & \vdots & | & \\ 0 & 0 & 0 & \cdots & \sigma_k & | & \\ - & - & - & - & - & | & - \\ & [0] & & & & | & [0] \end{bmatrix} = \begin{bmatrix} [\Sigma] & [0] \\ [0] & [0] \end{bmatrix} . \quad (\text{B-6})$$

Thus, the original matrix, $[A]$, is decomposed into the matrix $[S]$, with the singular values on the diagonal, by the unitary matrices $[U]$ and $[V]$.

Then the singular value decomposition of $[A]$ is defined by:

$$[A] = [U] [S] [V]^H \quad (\text{B-7})$$

Noting the partitioning of the matrix $[S]$ of Eq. (B-6), the unitary transformation matrices $[U]$ and $[V]$ can be partitioned in the same way to yield:

$$[A] = [U] [S] [V]^H = \begin{bmatrix} [U]_1 & [U]_2 \end{bmatrix} \begin{bmatrix} [\Sigma] & [0] \\ [0] & [0] \end{bmatrix} \begin{bmatrix} [V]_1^H \\ [V]_2^H \end{bmatrix} \quad (\text{B-8})$$

Thus, the singular value decomposition of $[A]$ can be further reduced to:

$$[A] = [U]_1 [\Sigma] [V]_1^H \quad (\text{B-9})$$

where:

- $[U]_1$ = left singular submatrix of size $m \times k$
- $[\Sigma]$ = diagonal singular value matrix of size $k \times k$
- $[V]_1^H$ = right singular submatrix of size $k \times n$.

The (Moore-Penrose) generalized inverse (pseudoinverse) ^[1-3], $[A]^+$, of $[A]$ is:

$$[A]^+ = [V] \begin{bmatrix} [\Sigma]^{-1} & [0] \\ [0] & [0] \end{bmatrix} [U]^H = [V]_1 [\Sigma]^{-1} [U]_1^H \quad .$$

where:

- $[A]^+ = n \times m$ generalized inverse of $[A]$
- $[V]_1$ = right singular submatrix of size $n \times k$.
- $[\Sigma]^{-1}$ = inverse of diagonal singular value matrix of size $k \times k$
- $[U]_1^H$ = left singular submatrix of size $k \times m$.

B.1 References

- [1] Ben Nobel, James W. Daniel, **Applied Linear Algebra**, Prentice-Hall, Inc., 1977, pp. 323-337.
- [2] Gibert Strang, **Introduction to Applied Mathematics**, Wellesley-Cambridge Press, 1986.
- [3] Gibert Strang, **Linear Algebra and Its Applications**, Academic Press, 1980.

Appendix C: Bibliography

- [1] "ASTRO-1 Integrated Payload Assembly Modal Survey Test: Test Summary and Model Correlation", Teledyne Brown Engineering, Report PMIC-RPT-5717, 1988, 53 pp.
- [2] "An Introduction to the Structural Dynamics Modification Systems", Technical Information Note #1, Structural Measurement Systems, Inc., February, 1980.
- [3] "Baseline Payload Flight Equipment Requirements for Safety-Critical Structures", Document JA-418, NASA Marshall Space Flight Center, August 1984.
- [4] "Ground/Flight Test Techniques and Correlation", Advisory Group for Aerospace Research and Development, Report AGARD-CP-339, 1983.
- [5] "Military Standard: Environmental Test Methods and Engineering Guidelines", MIL-STD-810E, July 1989.
- [6] "Military Standard: Test Requirements for Space Vehicles", MIL-STD-1540B (USAF), October 1982.
- [7] "Payload Verification Requirements: National Space Transportation System Program", Document NSTS 14046, Revision B, NASA Johnson Space Center, March 1989.
- [8] "Specifications of the Neutral File Structure Implemented in the CADA LINK Software Module", Revision 2.1, X7100-NF-021, Leuven Measurements and Systems (LMS) International, October 1990, 103 pp.
- [9] Adcock, J., Potter, R., "A Frequency Domain Curve Fitting Algorithm with Improved Accuracy," Proceedings, International Modal Analysis Conference 1985, 8 pp.
- [10] Allemang, R. J., "Investigation of Some Multiple Input/Output Frequency Response Function Experimental Modal Analysis Techniques", Doctoral Dissertation, University of Cincinnati, 1980, 358 pp.
- [11] Allemang, R.J., Brown, D.L., "Universal File Formats" *Experimental Modal Analysis and Dynamic Component Synthesis*, USAF Technical Report, Contract Number F33615-83-C-3218, AFWAL-TR-87-3069, Volume 5, 1987.
- [12] Allemang, R.J., Brown, D.L., "A Correlation Coefficient for Modal Vector Analysis", Proceedings, International Modal Analysis Conference, pp.110-116, 1982.
- [13] Allemang, R.J., Brown, D.L., "Summary of Technical Work", *Experimental Modal Analysis and Dynamic Component Synthesis*, USAF Technical Report, Contract Number F33615-83-C-3218, AFWAL-TR-87-3069, Volume 1, 1987.
- [14] Allemang, R.J., Brown, D.L., "Modal Parameter Estimation" *Experimental Modal Analysis and Dynamic Component Synthesis*, USAF Technical Report, Contract Number F33615-83-C-3218, AFWAL-TR-87-3069, Volume 3, 1987, 200 pp.
- [15] Allemang, R.J., Brown, D.L., *Experimental Modal Analysis and Dynamic Component Synthesis*, USAF Technical Report, Contract Number F33615-83-C-3218, AFWAL-TR-87-3069, Volumes 1-5, 1987.
- [16] Allemang, R.J., Brown, D.L., Rost, R.W., "Measurement Techniques for Experimental Modal Analysis", *Experimental Modal Analysis and Dynamic Component Synthesis*, USAF Technical Report, Contract Number F33615-83-C-3218, AFWAL-TR-87-3069, Volume 2, 1987.

- [17] Allemang, R.J., Brown, D.L., Rost, R.W., "Multiple Input Estimation of Frequency Response Functions for Experimental Modal Analysis", U.S. Air Force Report Number AFATL-TR-84-15, 1984, 185 pp.
- [18] Allemang, R.J., Brown, D.L., Rost, R.W., "Dual Input Estimation of Frequency Response Functions for Experimental Modal Analysis of Automotive Structures", SAE Paper Number 820193.
- [19] Allemang, R.J., Brown, D.L., Soni, M.L., "System Modeling Techniques" *Experimental Modal Analysis and Dynamic Component Synthesis*, USAF Technical Report, Contract Number F33615-83-C-3218, AFWAL-TR-87-3069, Volume 4, 1987.
- [20] Allemang, R.J., Rost, R.W., Brown, D.L., "Dual Input Estimation of Frequency Response Functions for Experimental Modal Analysis of Aircraft Structures", Proceedings, International Modal Analysis Conference, pp.333-340, 1982.
- [21] Allemang, R.J., Rost, R.W., Brown, D.L., "Multiple Input Estimation of Frequency Response Functions: Excitation Considerations", ASME Paper Number 83-DET-73, 1983, 11 pp.
- [22] Allemang, R.J., Rost, R.W., Formenti, D., "Analytical and Experimental Modal Analysis," University of Cincinnati, Modal Analysis Course Notes, 1990, 135 pp.
- [23] Asher, G. W., "A Method of Normal Mode Excitation Utilizing Admittance Measurements", Dynamics of Aeroelasticity, Proceedings, Institute of the Aeronautical Sciences, 1958, pp. 69-76.
- [24] Avitabile, P. and J. O'Callahan, "A Structural Modification Procedure Using Complex Modes", Proceedings, International Modal Analysis Conference (IMAC), 1982, pp. 418-422
- [25] Baker, M., "Component Mode Synthesis Methods for Test-Based, Rigidly Connected, Flexible Components", *AIAA Paper 84-0943*, 1984, pp. 153-163
- [26] Barrett, J.F., "Formula for Output Autocorrelation and Spectrum of a Volterra System with Stationary Gaussian Input," IEEE Proceedings, Volume 127, Part D, Number 6, November 1980, pp. 286-288.
- [27] Baruh, H., Choe, K., "Sensor Placement in Structural Control", *Journal of Guidance and Control*, Volume 13, Number 3, May-June 1990, pp. 524-533.
- [28] Benfield, W. A. and R. F. Hrudá, "Vibrational Analysis of Structures by Component Mode Substitution", *AIAA Journal*, Volume 9, Number 7, 1971, pp. 1255-1261
- [29] Bergman, Martin, Longman, Richard W., Juang, Jer-Nan, "Variance and Bias Computation for Enhanced System Identification", IEEE, 28th Conference on Decision and Control, 1989, 8 pp.
- [30] Berman, A., Flannelly, W.G. "Theory of Incomplete Models of Dynamic Structures," *AIAA Journal*, Volume 9, Number 8 1971, pp.1481-1487.
- [31] Billings, S.A., "Identification of Nonlinear Systems - A Survey," IEEE Proceedings, Volume 127, Part D, Number 6, November 1980, pp. 272-288.
- [32] Bishop, R. E. D., Gladwell, G. M. L., "An Investigation into the Theory of Resonance Testing", *Philosophical Transactions, Royal Society of London, Series A*, Volume 225, A-1055, 1963, pp. 241-280.
- [33] Brown, D.L., Carbon, G.D., Ramsey, K., "Survey of Excitation Techniques Applicable to the Testing of Automotive Structures", SAE Paper Number 770029, 1977, 16 pp.

- [34] Brown, D.L., Zimmerman, R.D., Allemang, R.J., Mergeay, M., "Parameter Estimation Techniques for Modal Analysis", SAE Paper Number 790221, *SAE Transactions*, Volume 88, 1979, pp. 828-846.
- [35] Capecchi, D., "Difference Models for Identification of Mechanical Linear Systems in Dynamics", *Mechanical Systems and Signal Processing*, Volume 3, Number 2, 1989, pp. 157-172.
- [36] Carbon, G.D., Brown, D.L., Allemang, R.J., "Application of Dual Input Excitation Techniques to the Modal Testing of Commercial Aircraft", *Proceedings, International Modal Analysis Conference*, pp.559-565, 1982.
- [37] Choi, D., Chang, J., Stearman, R.O., Powers, E.J., "Bispectral Identification of Nonlinear Mode Interactions," University of Texas at Austin, College of Engineering.
- [38] Choi, D., Chang, J., Stearman, R.O., Powers, E.J., "Bispectral Analysis of Parametric and Nonlinear Systems," University of Texas at Austin, College of Engineering.
- [39] Choi, D., Miksad, R.W., Powers, E.J., Fischer, F.J., "Application of Digital Cross bispectral Analysis Techniques to Model the Nonlinear Response of a Moored Vessel System in Random Seas," *Journal of Sound and Vibration*, 99 (3), 1985, pp. 309-326.
- [40] Cobb, R.E., Mitchell, L.D., "A Method for the Unbiased Estimate of System FRFs in the presence of Multiple-Correlated Inputs", *Journal of Analytical and Experimental Modal Analysis*, Volume 3, Number 4, 1988, pp. 123-128.
- [41] Coleman, A.D., Driskill, T.C., Anderson, J.B., Brown, D.L., "A Mass Additive Technique for Modal Testing as Applied to the Space Shuttle ASTRO-1 Payload", *Proceedings, International Modal Analysis Conference*, 1988, pp. 154-159.
- [42] Coppolino, R. N., "A Simultaneous Frequency Domain Technique for Estimation of Modal Parameters from Measured Data," SAE Paper Number 811046, 1981, 12 pp.
- [43] Corso D., Kirmman, H., Noicoud, J.D., *Microcomputer Buses and Links*, Academic Press, Inc., 1986, 384 pp.
- [44] Craig, R. Jr., *Structural Dynamics: An Introduction to Computer Methods*, John Wiley & Sons, 1981.
- [45] Craig, R. R. Jr., Su, Y. W. T., "On Multiple-Shaker Resonance Testing", *AIAA Journal*, Volume 12, Number 7, 1974, pp. 924-931.
- [46] Crowley, J. R., A. L. Klosterman, G. T. Rocklin and H. Vold, "Direct Structural Modification Using Frequency Response Functions", *Proceedings, International Modal Analysis Conference*, 1984, pp. 58-65.
- [47] De Veubeke, B.F., "A Variational Approach to Pure Mode Excitation Based on Characteristic Phase Lag Theory", AGARD, Report 39, 1956, 35 pp.
- [48] DeAngelis, Michael V., "Strain Gage Loads Measurement Techniques for Hot Structures", *Proceedings, Workshop on Correlation of Hot Structures Test Data with Analysis, Volume I*, NASA Conference Publication 3065, 1988, pp. 15-38,
- [49] DeAngelis, Michael V., "Summary of Hot Structures Workshop and Current Test Plans", *Proceedings, Workshop on Correlation of Hot Structures Test Data with Analysis, Volume II*, NASA Conference Publication 3065, 1988, pp. 345-358.
- [50] Deblauwe, F., Shih, C.Y., Rost, R., Brown, D.L., "Survey of Parameter Estimation Algorithms Applicable to Spatial Domain Sine Testing", *Proceedings, Twelfth International Seminar on Modal Analysis*, Katholieke Universiteit te Leuven, 1987, 15 pp.

- [51] Deel, J.C., Zobrist, G.J., "New Technology for Large-Scale Test Data Systems", *Sound and Vibration Magazine*, Volume 22, Number 5, May, 1988, pp. 8-14.
- [52] Delorenzo, M.L., "Sensor and Actuator Selection for Large Space Structure Control", *Journal of Guidance, Control, and Dynamics*, Volume 13, Number 2, March-April 1990, pp. 249-257.
- [53] Ebersbach, P., Irretier, H., "On the Application of Modal Parameter Estimation Using Frequency Domain Algorithms", *Journal of Analytical and Experimental Modal Analysis*, Volume 4, Number 4, 1989, pp. 109-116.
- [54] Elliott, K.B., Mitchell, L.D. "Improved Frequency Response Function Circle Fits," *Modal Testing and Model Refinement*, ASME AMD - Volume 59 1983, pp. 63-76.
- [55] Ewins, D.J., *Modal Testing: Theory and Practice*, Research Studies Press, Ltd., John Wiley and Sons, Inc., 1984, 269 pp.
- [56] Ewins, D.J., "Measurement and Application of Mechanical Impedance Data," *Journal of the Society of Environmental Engineers*, June 1976, pp. 7-17.
- [57] Ewins, D.J., Griffin, J., "A State-of-the-Art Assessment of Mobility Measurement Techniques - Results for the Mid-Range Structures", *Journal of Sound and Vibration*, Volume 78, Number 2, 1981, pp. 197-222.
- [58] Feix, M., "An Iterative Self-Organizing Method for the Determination of Structural Dynamic Characteristics", European Space Agency, ESA-TT-232 (N76-331183), 1975, pp. 36-60.
- [59] Fields, Roger A., "Hot Structures Test Techniques", *Proceedings, Workshop on Correlation of Hot Structures Test Data with Analysis, Volume I*, NASA Conference Publication 3065, 1988, pp. 133-157.
- [60] Fillod, R., Lallement, G., Piranda, J.L., "Identification Using a Variable Phase Multipoint Excitation", *Proceedings, Eleventh International Seminar on Modal Analysis*, Katholieke Universiteit te Leuven, 1986, 20 pp.
- [61] Fox, R. L. and M. P. Kapoor, "Rates of Change of Eigenvalues and Eigenvectors", *AIAA Journal*, Volume 6, December, 1968 , pp. 2426-2429
- [62] Fukuzono, K., "Investigation of Multiple-Reference Ibrahim Time Domain Modal Parameter Estimation Technique," M. S. Thesis, Dept. of Mechanical and Industrial Engineering, University of Cincinnati, 220 pp., 1986.
- [63] Garg, S., "Derivatives of Eigensolutions for a General Matrix", *AIAA Journal*, Volume 11, August, 1973, pp. 1191-1194
- [64] Gersch, W. "On the Achievable Accuracy of Structural System Parameter Estimates," *Journal of Sound and Vibration* Volume 34, Number 1 1974, pp. 63-79.
- [65] Gersch, W., Fouth, D. A. "Least Squares Estimates of Structural System Parameters Using Covariance Function Data," *IEEE Transactions on Automatic Control* Volume AC-19, Number 6 December 1974, pp. 898-903.
- [66] Gersch, W., Luo, S. "Discrete Time Series Synthesis of Randomly Excited Structural System Responses," *Journal of the Acoustical Society of America* A Volume 51, Number 1 1972, pp. 402-408.

- [67] Gersch, W., Sharpe, D. R. "Estimation of Power Spectra with Finite-Order Autoregressive Models," *IEEE Transactions on Automatic Control*, Volume AC-18, August 1973, pp. 367-369.
- [68] Ghijs, C., Helpenstein, H., Splid, A., Maanen, J., Design of Neutral Files 1 to 8, Rutherford Appleton Laboratory, CAD*I Paper RAL-012-85, 1985.
- [69] Goyder, H.G.D., "On the Measurement of Frequency Response Functions in the Presence of Nonlinearities and Noise," United Kingdom Atomic Energy Authority, Harwell, OX11 0RA, England, 26 pp.
- [70] Hale, A. L. and L. Meirovitch, "A General Substructure Synthesis Method for Dynamic Simulation of Complex Structures", *Journal of Sound and Vibration*, Volume 69, Number 2, 1980, pp. 309-326.
- [71] Hallquist, J. O. and V. W. Snyder, "Synthesis of Two Discrete Vibratory Systems Using Eigenvalue Modification", *AIAA Journal*, Volume 11, 1973.
- [72] Hallquist, J. O., "Modification and Synthesis of Large Dynamic Structural Systems", Doctoral Dissertation, Michigan Technological University, 1974.
- [73] Hasselman, T. K. and A. Kaplan, "Dynamic Analysis of Large Systems by Complex Mode Synthesis", *Journal of Dynamical Systems, Measurement and Control*, Sept. 1974, pp. 327-333.
- [74] Hawkins, F. J., "GRAMPA - An Automatic Technique for Exciting the Principal Modes of Vibration of Complex Structures", Royal Aircraft Establishment, RAE-TR-67-211, 1967.
- [75] Hawkins, F. J., "An Automatic Resonance Testing Technique for Exciting Normal Modes of Vibration of Complex Structures", Symposium IUTAM, "Progres Recents de la Mecanique des Vibrations Lineaires", 1965, pp. 37-41.
- [76] Herting, D. N. and M. J. Morgan, "A General Purpose Multi-Stage Component Modal Synthesis Method", AIAA/ASME/AHCE/AHS 20th Structural Dynamics and Materials Conference, (St. Louis, MO: 1979).
- [77] Ho, B.L., Kalman, R.E., "Effective Construction of Linear State-Variable Models from Input/Output Data", Proceedings of the Third Annual Allerton Conference on Circuit and System Theory, 1965, pp. 449-459.
- [78] Hollkamp, J.J., Batill, S.M., "Automated Parameter Identification and Order Reduction for Discrete Time Series Models", 30th AIAA/ASME/ASCE/AHS/ACS Structures, Structural Dynamics and Materials Conference, April 1989, Mobile, Alabama, 1989, 23 pp.
- [79] Hollkamp, J.J., Batill, S.M., "A Recursive Algorithm for Discrete Time Domain Parameter Identification", AIAA Paper Number AIAA-90-1221, 1990, 10 pp.
- [80] Hopton, G., "Detecting Nonlinearities Utilizing the Multiple Input Frequency Response Function Estimation Theory", Master of Science Thesis, University of Cincinnati 1987, 107 pp.
- [81] Hornung, E., Eckhardt, K., Erben, E., Hueners, E., Niedbal, N., Oery, H., Glaser, H., "Development of Experimental/Analytical Concepts for Structural Design Verification - Spacecraft Structures", European Space Agency, ESA-CR(P)-2340, 1985.
- [82] Hou, Z.Q., Cheng, Y.D., Tong, Z.F., Sun, Y.M., Lu, N.Y., "Modal Parameter Identification from Multi-Point Measured Data," 3rd International Modal Analysis Conference, 1985.
- [83] Ibanez, P., "Force Appropriation by Extended Asher's Method", SAE Paper Number 760873, 1976, 16 pp.

- [84] Ibrahim, S. R. "The Use of Random Decrement Technique for Identification of Structural Modes of Vibration," AIAA Paper Number 77-368 1977, 10 pp.
- [85] Ibrahim, S. R. "Modal Confidence Factor in Vibration Testing," Shock and Vibration Bulletin, Volume 48, Part 1 1978, pp. 65-75.
- [86] Ibrahim, S. R., Mikulcik, E. C., "A Method for the Direct Identification of Vibration Parameters from the Free Response," Shock and Vibration Bulletin, Volume 47, Part 4, 1977, pp. 183-198.
- [87] Juang, J.N., "Mathematical Correlation of Modal Parameter Identification Methods Via System Realization Theory", *Journal of Analytical and Experimental Modal Analysis*, Volume 2, Number 1, 1987, pp. 1-18.
- [88] Juang, J.N., Pappa, R.S., "Effects of Noise on ERA-Identified Modal Parameters," AAS Paper Number AAS-85-422, August, 1985 (Vail, CO.) 23 pp.
- [89] Juang, Jer-Nan, "Mathematical Correlation of Modal Parameter Identification Methods via System Realization Theory", *Journal of Analytical and Experimental Modal Analysis*, Volume 2, Number 1, 1987, pp. 1-18.
- [90] Juang, Jer-Nan, Pappa, Richard S., "An Eigensystem Realization Algorithm (ERA) for Modal Parameter Identification and Model Reduction", NASA/JPL Workshop on Identification and Control of Flexible Space Structures, 1984, 20 pp.
- [91] Juang, Jer-Nan, Pappa, Richard S., "A Comparative Overview of Modal Testing and System Identification for Control of Structures", Shock and Vibration Digest, Volume 20, Number 6, 1988, pp. 4-15.
- [92] Juang, Jer-Nan, Pappa, Richard S., "An Eigensystem Realization Algorithm for Modal Parameter Identification and Model Reduction", *AIAA, Journal of Guidance, Control, and Dynamics*, Volume 8, Number 4, 1985, pp. 620-627.
- [93] Kabe, A.M., "An Efficient Direct Measurement Mode Survey Test Procedure", USAF Space Division Report SD-TR-89-01, 1988, 34 pp.
- [94] Kabe, A.M., "Mode Shape Identification and Orthogonalization", USAF Space Division Report SD-TR-88-93, 1988, 25 pp.
- [95] Kammer, D.C., "Sensor Placement for On-Orbit Modal Identification and Correlation of Large Space Structures", Proceedings, 1990 American Control Conference, San Diego, Ca., May 23-25, 1990, pp. 2984-2990.
- [96] Kehoe, M.W., "Aircraft Ground Vibration Testing at NASA Ames-Dryden Flight Research Facility", NASA TM-88272, 1989.
- [97] Kelly, L.G., "Handbook of Numerical Methods and Applications," Addison-Wesley Publishing Company.
- [98] Kennedy, C.C., Pancu, C.D.P., "Use of Vectors in Vibration Measurement and Analysis," *Journal of Aeronautical Sciences*, Volume 14, Number 11, 1947, pp. 603-625.
- [99] Kientzy, D., Richardson, M., Blakely, K., "Using Finite Element Data to Set up Modal Tests", Sound and Vibration Magazine, Volume 23 Number 6, June, 1989, pp. 16-23.
- [100] Kim, Y.C., Powers, E.J., "Digital Bispectral Analysis and its Applications Nonlinear Wave Interactions," *IEEE Transactions on Plasma Science*, Volume PS-7, Number 2, June 1979, pp. 120-131.

- [101] Kirshenboim, J., Ewins, D.J., "A Method for Recognizing Structural Nonlinearities in Steady-State Harmonic Testing," *ASME, Journal of Vibration, Acoustics, Stress, and Reliability in Design*, Volume 106, January 1984, pp. 49 - 52.
- [102] Klosterman, A., "On the Experimental Determination and Use of Modal Representations of Dynamic Characteristics", Doctoral Dissertation, University of Cincinnati, 1971, 184 pp.
- [103] Klosterman, A., Zimmerman, R., "Modal Survey Activity via Frequency Response Functions", SAE Paper Number 751068, 1975.
- [104] Klosterman, A.L., Lemon, J.R., "Building Block Approach to Structural Dynamics", ASME Publication, VIBR-30, 1969
- [105] Kuo, Chin-Po, Wada, B.K., "Multiple Boundary Condition Test (MBCT): Identification With Mode Shapes", NASA JPL Report, NPO-17574, 1989.
- [106] Lally, M., Brown, D.L., Severyn, A.J., Vold, H., "System Support for Spatial Sine Testing", Proceedings, International Modal Analysis Conference, 1988, pp. 620-628.
- [107] Lawrence, P.J., "Estimation of the Volterra Functional Series of a Nonlinear System Using Frequency Response Data," IEE Proceedings, Volume 128, Part D, Number 5, September 1981, pp. 206-210.
- [108] Lee, G.M., Trethewey, M.W., "Application of the Least Squares Time Domain Algorithm for Efficient Modal Parameter Estimation", *Mechanical Systems and Signal Processing*, Volume 2, Number 1, 1988, pp. 21-38.
- [109] Lee, G.M., Trethewey, M.W., "Modal Parameter Separation for Oversized Finite Difference Time Domain Models", *Mechanical Systems and Signal Processing*, Volume 3, Number 4, 1989, pp. 425-436.
- [110] Lee, G.M., Trethewey, M.W., "Modal Parameter Quality Assessment from Time Domain Data", *Journal of Analytical and Experimental Modal Analysis*, Volume 3, Number 4, 1988, pp. 129-136.
- [111] Lembrechts, F., Leuridan, J., Zhang, L., Kanda, H., "Multiple Input Modal Analysis of Frequency Response Functions based on Direct Parameter Identification," Proceedings, International Modal Analysis Conference, 1986.
- [112] Lembrechts, F., Leuridan, J.L., Van Brussel, H., "Frequency Domain Direct Parameter Identification for Modal Analysis: State Space Formulation", *Mechanical Systems and Signal Processing*, Volume 4, Number 1, 1989, pp. 65-76.
- [113] Lembrechts, F., Sas, P., Van der Auweraer, H., "Integrated Stepped Sine Modal Analysis", Proceedings, Eleventh International Seminar on Modal Analysis, Katholieke Universiteit te Leuven, 1986, 12 pp.
- [114] Lembrechts, F., Snoeys, R. and Leuridan, J., "Multiple Input Modal Analysis of Frequency Response Functions Based on Direct Parameter Identification," 10th International Seminar on Modal Analysis Part IV, K.U. Leuven Belgium 1985.
- [115] Lembrechts, F., Snoeys, R., Leuridan, J., "Application and Evaluation of Multiple Input Modal Parameter Estimation", *Journal of Analytical and Experimental Modal Analysis*, Volume 2, Number 1, 1987, pp. 19-31.
- [116] Lembrechts, F., Van der Auweraer, H., Leuridan, J., "Integrated Stepped-Sine System for Modal Analysis", *Mechanical Systems and Signal Processing*, Volume 1, Number 4, 1987, pp. 415-424.

- [117] Lemcoe, M. M., Nguyen, B., "Development and Characterization of High Temperature Sensors at ADFRF", *Proceedings, Workshop on Correlation of Hot Structures Test Data with Analysis, Volume I*, NASA Conference Publication 3065, 1988, pp. 98-116.
- [118] Leonard, F., "ZMODAL: A New Modal Identification Technique", *Journal of Analytical and Experimental Modal Analysis*, Volume 3, Number 2, 1988, pp. 69-76.
- [119] Leuridan, J., "Some Direct Parameter Model Identification Methods Applicable for Multiple Input Modal Analysis," Doctoral Dissertation, University of Cincinnati, 1984, 384 pp.
- [120] Leuridan, J., Contents of the Common Database for Experimental Modal Analysis, Leuven Measurement and Systems, CAD*I Paper LMS-007-85, 1985.
- [121] Leuridan, J., Brown, D., Allemang, R., "Direct System Parameter Identification of Mechanical Structures with Application to Modal Analysis," AIAA Paper Number 82-0767 Proceedings, 23rd. Structures, Structural Dynamics and Materials Conference, Part 2, 1982, pp. 548-556.
- [122] Leuridan, J., Kundrat, J., "Advanced Matrix Methods for Experimental Modal Analysis - A Multi-Matrix Method for Direct Parameter Extraction," Proceedings, International Modal Analysis Conference 1982, pp. 192-200.
- [123] Leuridan, J.M., Brown, D.L., Allemang, R.J., "Time Domain Parameter Identification Methods for Linear Modal Analysis: A Unifying Approach," ASME Paper Number 85-DET-90.
- [124] Lewis, R.C., Wrisley, D.L., "A System for the Excitation of Pure Natural Modes of Complex Structures", *Journal of Aeronautical Sciences*, Volume 17, Number 11, 1950, pp. 705-722.
- [125] Link, M., Volland, A., "Identification of Structural System Parameters from Dynamic Response Data," *Zeitschrift Fur Flugwissenschaften*, Volume 2, Number 3 1978, pp. 165-174.
- [126] Longman, Richard W., Juang, Jer-Nan, "Recursive Form of the Eigensystem Realization Algorithm for System Identification", *AIAA, Journal of Guidance, Control, and Dynamics*, Volume 12, Number 5, 1989, pp. 647-652.
- [127] Lustig, S., "Recent Advances in U.S. Air Force Full Scale Structures Testing", Technical Cooperation Program Meeting, Ottawa, Canada, 1989, 70 pp.
- [128] Lustig, S., Carter, A., Dixon, S., "Position Paper for Hypersonic Structural Testing", Government Workshop for Structural Testing of Hypervelocity Vehicles, 1986, 25 pp.
- [129] Maghami, P.G., Joshi, S.M., "Sensor/Actuator Placement for Flexible Space Structures", Proceedings, 1990 American Control Conference, San Diego, Ca., May 23-25, 1990, pp. 1941-1948.
- [130] Malebranche, H., "Simultaneous State and Parameter Estimation and Location of Sensors for Distributed Systems" , *International Journal of Systems Science*, Volume 19, Number 8, 1988, pp. 1387-1405.
- [131] Marmarelis, V.Z., "Practicable Identification of Nonstationary Nonlinear Systems," IEE Proceedings, Volume 128, Part D, Number 5, September 1981, pp. 211-214.
- [132] Mertens, M., Van Der Auweraer, H., Vanherck, P., Snoeys, R., "Basic Rules of a Reliable Detection Method for Nonlinear Dynamic Behavior," Proceedings of the Tenth International Seminar on Modal Analysis, K.U. Leuven, Belgium, Part IV, 1985.

- [133] Mertens, M., Van Der Auweraer, H., Vanherck, P., Snoeys, R., "Detection of Nonlinear Dynamic Behavior of Mechanical Structures," *Proceedings of the Fourth International Modal Analysis Conference*, 1986, pp. 712-719.
- [134] Mertens, M., Van der Auweraer, H., Vanherck, P., Snoeys, R., "The Complex Stiffness Method to Detect and Identify Non-linear Dynamic Behaviour of SDOF Systems", *Mechanical Systems and Signal Processing*, Volume 3, Number 1, 1989, pp. 37-54.
- [135] Mirimand, N., Billaud, J. F., Leleux, F., Krenevez, J. P., "Identification of Structural Modal Parameters by Dynamic Tests at a Single Point", *Shock and Vibration Bulletin*, Volume 46, Part 5, 1976, pp. 197-212.
- [136] Mitchell, L.D. "A Perspective View of Modal Analysis" Keynote Address, Sixth International Modal Analysis Conference, *Proceedings, International Modal Analysis Conference*, 1988, 5 pp.
- [137] Mitchell, L.D., Cobb, R.E., Deel, J.C., Luk, Y.W., "An Unbiased Frequency Response Function Estimator", *Journal of Analytical and Experimental Modal Analysis*, Volume 3, Number 1, 1988, pp. 12-19.
- [138] Morosow, G., "Exciter Force Apportioning for Modal Vibration Testing Using Incomplete Excitation", Doctoral Dissertation, University of Colorado at Boulder, 1977, 132 pp.
- [139] Morosow, G., Ayre, R. S., "Force Appropriation for Modal Vibration Testing Using Excitation", *Shock and Vibration Bulletin*, Volume 48, Part 1, 1978, pp. 39-48.
- [140] Mulville, Daniel R., "Overview on High Temperature Structures" *Proceedings, Workshop on Correlation of Hot Structures Test Data with Analysis, Volume I*, NASA Conference Publication 3065, 1988, pp. 1-14.
- [141] Natke, H.G., "Updating Computational Models in the Frequency Domain Based on Measured Data: A Survey", *Probabilistic Engineering Mechanics, Volume 3, Number 1*, 1988, pp. 28-35.
- [142] Natke, H.G., "Survey on the Identification of Mechanical Systems", *Proceedings, Road-Vehicle-Systems and Related Mathematics*, 1987, pp. 69-116.
- [143] Nemeth-Johannes, J., "A Standard Instrument Programming Language Based in IEEE STD 488.2", Hewlett Packard Measurement System Operation, Loveland, Colorado, pp. 1-11.
- [144] Nesman, T.E., Reed, D.K., "SAFE/DAE: Modal Test in Space", *Shock and Vibration Bulletin*, Volume 56, Part 2, 1986, pp. 29-36.
- [145] O'Callahan, J.C., Chou, C.M., "Localization of Model Errors in Optimized Mass and Stiffness Matrices Using Modal Test Data", *Journal of Analytical and Experimental Modal Analysis*, Volume 4, Number 1, 1989, pp. 8-14.
- [146] Oloomi, H., Sawan, M.E., "Optimal Sensor Placement in Decentralized Control Systems", *International Journal of Systems Science*, Volume 20, Number 6, 1989, pp. 939-943.
- [147] Omatu, S., Seinfeld, J.H., "Optimal Sensor and Actuator Locations for Linear Distributed Parameter Systems", *Proceedings, Control of Distributed Parameter Systems, IFAC Symposium, Los Angeles, Ca., June 30 - July 2, 1986*, pp. 215-220.
- [148] Pandit, S. M., Suzuki, H. "Application of Data Dependent Systems to Diagnostic Vibration Analysis," ASME Paper Number 79-DET-7 September, 1979, 9 pp.

- [149] Pappa, R. S., Juang, J. N., "An Eigensystem Relization Algorithm (ERA) for Modal Parameter Identification," NASA-JPL Workshop, Identification and Control of Flexible Space Structures, June, 1984 (Pasadena, CA.) 20 pp.
- [150] Pappa, R. S., Juang, J. N., "Galileo Spacecraft Modal Identification Using an Eigensystem Realization Algorithm," AIAA Paper Number 84-1070-CP, 1984, 18 pp.
- [151] Pappa, R.S. "Some Statistical Performance Characteristics of the "ITD" Modal Identification Algorithm," AIAA Paper Number 82-0768, 1982, 19 pp.
- [152] Pappa, R.S., "Identification Challenges for Large Space Structures", Keynote Address, Eighth International Modal Analysis Conference, Proceedings, International Modal Analysis Conference, 1990, 9 pp.
- [153] Pappa, R.S., Ibrahim, S.R. "A Parametric Study of the "ITD" Modal Identification Algorithm", Shock and Vibration Bulletin, Volume Number 51, Part 3, 1981, pp. 43-72.
- [154] Pappa, R.S., Juang, H.N., "Studies of Modal Identification Performance Using Hybrid Data", *Journal of Analytical and Experimental Modal Analysis*, Volume 2, Number 2, 1987, pp. 99-108.
- [155] Pappa, Richard S., "The Eigensystem Realization Algorithm", Advance Modal Analysis Seminar, University of Cincinnati, 1985, 106 pp.
- [156] Pappa, Richard S., Juang, Jer-Nan, "Galileo Spacecraft Modal Identification Using An Eigensystem Realization Algorithm" AIAA Paper Number 84-1070, 1984.
- [157] Patton, M.E., Trethewey, M.W., "A Survey and Assessment of Nonintrusive Modal Testing Techniques for Ultralightweight Structures", *Journal of Analytical and Experimental Modal Analysis*, Volume 2, Number 4, 1987, pp. 163-173.
- [158] Pendered, J. W. Bishop, R. E. D., "Extraction of Data for a Sub-System From Resonance Test Results", *Journal of Mechanical Engineering Science*, Volume 5, Number 4, 1963, pp. 368-378.
- [159] Pendered, J. W., Bishop, R. E. D., "A Critical Introduction to Some Industrial Resonance Testing Techniques", *Journal of Mechanical Engineering Science*, Volume 5, Number 4, 1963, pp. 368-378.
- [160] Pendered, J. W., Bishop, R. E. D., "The Determination of Modal Shapes in Resonance Testing", *Journal of Mechanical Engineering Science*, Volume 5, Number 4, 1963, pp. 379-385.
- [161] Peterson, E. L., Klosterman, A. L., "Obtaining Good Results from an Experimental Modal Survey", Society of Environmental Engineers, Symposium, London, England, 1977, 22 pp.
- [162] Pomazal, R. J. and V. W. Snyder, "Local Modifications of Damped Linear Systems", *AIAA Journal*, Volume 9, 1971.
- [163] Pomazal, R., "The Effect of Local Modification of the Eigenvalues and Eigenvectors of Damped Linear Systems", Doctoral Dissertation, Michigan Technological University, 1969.
- [164] Potter, R. W., "A General Theory of Modal Analysis for Linear Systems", Shock and Vibration Digest, Volume 7, Number 11, 1975, 8 pp.
- [165] Pozefsky, P., Blevins, R.D., Laganelli, A.L., "Thermo-Vibro-Acoustic Loads and Fatigue of Hypersonic Flight Vehicle Structure", USAF Report AFWAL-TR-89-3014, 1989, 100 pp.

- [166] Prony, R., "Essai Experimental et Analytique sur les Loix de la Dilatabilite des Fluides Elastiques et sur Celles de la Force Expansive de la Vapeur de l'eau et de la Vapeur de l'Alcool, a Differentes Temperatures", *Journal de l'Ecole Polytechnique (Paris)*, Volume 1, Cahier 2, Floreal et Prairial, An. III, 1795, pp. 24-76.
- [167] Rades, M., "Identification of the Dynamic Characteristics of a Simple System with Quadratic Damping," *Serie de Mecanique Appliquee*, Volume 28, Number 4, 1983, pp. 439-446.
- [168] Rades, M., "Frequency Domain Experimental Modal Analysis Techniques", *Shock and Vibration Digest*, Volume 17, Number 6, 1985, 12 pp.
- [169] Rades, M., "System Identification Using Real Frequency Dependent Modal Characteristics", *Shock and Vibration Digest*, Volume 18, Number 8, 1986, 8 pp.
- [170] Rades, M., "Analysis of Measured Structural Frequency Response Data", *Shock and Vibration Digest*, Volume 14, Number 4, 1982, April, pp. 21-32.
- [171] Rafajlowicz, E., "Optimum Choice of Moving Sensor Trajectories for Distributed-Parameter System Identification", *International Journal of Control*, Volume 43, Number 5, 1986, pp. 1441-1451.
- [172] Ramsey, K., "Effective Measurements for Structural Dynamics Testing: Part II", *Sound and Vibration*, April, 1976.
- [173] Ramsey, K., "Effective Measurements for Structural Dynamics Testing: Part I", *Sound and Vibration*, November, 1975.
- [174] Reference Manual for Modal-Plus 9.0, Appendix A, SDRC Universal File Formats, SDRC GE-CAE International, 1985.
- [175] Richardson, M., "Modal Analysis Using Digital Test Systems", *Seminar on Understanding Digital Control and Analysis in Vibration Test Systems (Part 2)*, 1975, pp. 43-64.
- [176] Richardson, M., Formenti, D.L., "Parameter Estimation from Frequency Response Measurements Using Rational Fraction Polynomials," *Proceedings, International Modal Analysis Conference 1982*, 6 pp.
- [177] Richardson, M., Potter, R., "Viscous vs. Structural Damping in Modal Analysis", *46th Shock and Vibration Symposium*, 1975, 8 pp.
- [178] Richardson, M., Potter, R., "Identification of the Modal Properties of an Elastic Structure from Measured Transfer Function Data", *Instrument Society of America, ISA ASI 74250*, 1974, pp. 239-246.
- [179] Rost, R.W. "Investigation of Multiple Input Frequency Response Function Estimation Techniques for Modal Analysis," *Doctoral Dissertation, University of Cincinnati*, 1985, 219 pp.
- [180] SDRC I-deas Level 3 User's Guide, Section VI, Universal File Datasets, 1986, pp.306-470.
- [181] Salama, M.A., Rose, T.L., Garba, J.A., "Optimal Placement of Exciters and Sensors for Verification of Large Dynamical Systems", *NASA JPL Report, NPO-17293*, 1989.
- [182] Schetzen, M., "Nonlinear System Modeling Based on the Wiener Theory," *IEEE Proceedings*, Volume 69, Number 12, December 1981, pp. 1557-1573.
- [183] Schetzen, M., "A Theory of Nonlinear System Identification," *Int. J. Control*, Volume 20, Number 4, 1974, pp. 577-592.

- [184] Severyn, A.J., Lally, M., Rost, R., Brown, D.L., "Hardware Considerations for Spatial Domain Sine Testing", Proceedings, Twelfth International Seminar on Modal Analysis, Katholieke Universiteit te Leuven, 1987, 8 pp.
- [185] Shih, C.Y., "Investigation of Numerical Conditioning in the Frequency Domain Modal Parameter Estimation Methods", Doctoral Dissertation, University of Cincinnati, 1989, 127 pp.
- [186] Shih, C.Y., Tsuei, Y.G., Allemang, R.J., Brown, D.L. "Extension of a Parameter Estimation Method to Multiple Reference Frequency Response Measurements," Eleventh International Seminar on Modal Analysis, University of Leuven, Belgium 1986, 11 pp.
- [187] Simon, M., Tomlinson, G.R., "Modal Analysis of Linear and Nonlinear Structures Employing the Hilbert Transform," Proceeding of the Second International Conference on Recent Advances in Structural Dynamics, Volume II, pp. 495-510.
- [188] Simpson, A. and B. Taborrok, "On Kron's Eigenvalue Procedure and Related Methods of Frequency Analysis", *Journal of Mechanics and Applied Mathematics*, Volume XXI, 1968, pp. 1-39.
- [189] Sloane, E., McKeever, B., "Modal Survey Techniques and Theory", SAE Paper Number 751067, 1975, 27 pp.
- [190] Spitznogle, F.R., et al, "Representation and Analysis of Sonar Signals, Volume 1: Improvements in the Complex Exponential Signal Analysis Computational Algorithm", Texas Instruments, Inc. Report Number U1-829401-5, Office of Naval Research Contract Number N00014-69-C-0315, 1971, 37 pp.
- [191] Stahle, C. V., "Modal Test Methods and Applications ", *Journal of Environmental Sciences*, Jan/Feb, 1978, 4 pp.
- [192] Stahle, C. V., Forlifer, W. R., "Ground Vibration Testing of Complex Structures", Flight Flutter Testing Symposium, NASA-SP-385, 1958, pp. 83-90.
- [193] Stahle, C. V., Jr., "Phase Separation Technique for Ground Vibration Testing", *Aerospace Engineering*, July 1962, 1962, 8 pp.
- [194] Taylor, G. A., Gaukroger, D. R., Skingle, C. W., "MAMA - A semi-Automatic Technique for Exciting the Principal Modes of Vibration of Complex Structures", Aeronautical Research Council, ARC-R/M-3590, 1967, 20 pp.
- [195] Thomas, D., Maanen, J.V., Mead M., "Specifications for Exchange of Product Analysis Data, Version 3", ESPRIT Project 322, CAD*I, CAD Interfaces, October, 1988, 244 pp.
- [196] Tomlinson, G.R., "Detection, Identification, and Quantification of Nonlinearity in Modal Analysis - A Review," Proceedings, International Modal Analysis Conference, 1986, pp. 837-843.
- [197] Tomlinson, G.R., Ahmed, I., "Frequency and Damping Estimates from a Non-linear Structure - Causalisation and Random Excitation," Proceedings of the Tenth International Seminar on Modal Analysis, K.U. Leuven, Belgium, Part IV, 1985.
- [198] Tomlinson, G.R., Hilbert, J.H., "Identification of the Dynamic Characteristics of a Structure with Coulomb Friction," *Journal of Sound and Vibration*, Volume 64, Number 2, 1979, pp. 233-242.

- [199] Tomlinson, G.R., Kirk, N.E., "Modal Analysis and Identification of Structural Nonlinearity," Simon Engineering Laboratories, University of Manchester, England, 21 pp.
- [200] Tomlinson, G.R., Kirk, N.E., "On the Identification of Nonlinearities in Modal Testing Employing the Hilbert Transform," Simon Engineering Laboratories, University of Manchester - Manchester, England, 32 pp.
- [201] Trail-Nash, R.W., "On the Excitation of Pure Natural Modes in Aircraft Resonance Testing", *Journal of Aeronautical Sciences*, Volume 25, Number 12, 1958, pp. 775-778.
- [202] VXI Consortium, "VMEbus Extensions for Instrumentation System Specification", Section A, Revision 1.2, June 1988.
- [203] Van Belle, H., "The Method of Construction and the Theory of Conjugated Structures ", Doctoral Dissertation, Katholieke University of Leuven, Belgium, 1974, pp. 142-151.
- [204] Van Karsen, C., "A Survey of Excitation Techniques for Frequency Response Function Measurement", Master of Science Thesis, University of Cincinnati, 1987, 81 pp.
- [205] Van Loon, Patrick, "Modal Parameters of Mechanical Structures," Doctoral Dissertation, Katholieke University of Lueven, Belgium, 1974, 183 pp.
- [206] Van der Auweraer, H., Leuridan, J., "Multiple Input Orthogonal Polynomial Parameter Estimation", *Mechanical Systems and Signal Processing*, Volume 1, Number 3, 1987, pp. 259-272.
- [207] Van der Auweraer, H., Leuridan, J.M., "Multiple Input Orthogonal Polynomial Parameter Estimation," Proceedings, Eleventh International Seminar on Modal Analysis, Belgium, 1986.
- [208] Van der Auweraer, H., Snoeys, R., Leuridan, J.M., "A Global Frequency Domain Modal Parameter Estimation Technique for Mini-computers," *ASME, Journal of Vibration, Acoustics, Stress, and Reliability in Design*, 1986, 10 pp.
- [209] Van der Auweraer, H., Vanherck, P., Sas, P., Snoeys, R., "Accurate Modal Analysis Measurements with Programmed Sine Wave Excitation", *Mechanical Systems and Signal Processing*, Volume 1, Number 3, 1987, pp. 293-300.
- [210] VanHonacker, P., "The Use of Modal Parameters of Mechanical Structures in Sensitivity Analysis, System Synthesis and System Identification Methods", Doctoral Dissertation, Katholieke University of Leuven, Belgium, 1980.
- [211] VanHonacker, P., "Sensitivity Analysis of Mechanical Structures, Based on Experimentally Determined Modal Parameters", Proceedings, International Modal Analysis Conference, 1982, pp. 534-541
- [212] Vinh, T., Haoui, A., Chevalier, Y., "Extension of Modal Analysis to Nonlinear Structures by Using the Hilbert Transform," Proceedings of the Second International Modal Analysis Conference, 1984, pp. 852-857.
- [213] Vold, H., "Insight, Not Numbers", Keynote Address, Seventh International Modal Analysis Conference, Proceedings, International Modal Analysis Conference, 1989, 4 pp.
- [214] Vold, H., "Orthogonal Polynomials in the Polyreference Method," Proceedings, Eleventh International Seminar on Modal Analysis, Belgium, 1986.

- [215] Vold, H., Crowley, J., Rocklin, G. "A Comparison of H_{11} , H_{12} , H_{1v} , Frequency Response Functions," Proceedings, International Modal Analysis Conference, 1985, pp.272-278.
- [216] Vold, H., Kundrat, J., Rocklin, T., Russell, R., "A Multi-Input Modal Estimation Algorithm for Mini-Computers," SAE Paper Number 820194, 1982, 10 pp.
- [217] Vold, H., Rocklin, T. "The Numerical Implementation of a Multi-Input Modal Estimation Algorithm for Mini-Computers," Proceedings, International Modal Analysis Conference, pp. 542-548, 1982.
- [218] Wada, B. K., "Modal Test - Measurement and Analysis Requirements", SAE Paper Number 751066, 1975, 17 pp.
- [219] Weissenberger, J.T., "The Effect of Local Modifications on the Eigenvalues and Eigenvectors of Linear Systems", Doctoral Dissertation, Washington University, 1966.
- [220] Williams, R., Crowley, J., Vold, H., "The Multivariate Mode Indicator Function in Modal Analysis," 3rd International Modal Analysis Conference, 1985.
- [221] Williams, R., Vold, H., "The Multi-Phase Step-Sine Method for Experimental Modal Analysis", *Journal of Analytical and Experimental Modal Analysis*, Volume 1, Number 2, 1986, pp.25-34.
- [222] Yam, Y., Bayard, D.S., Hadaegh, F.Y., Mettler, E., Milman, M.H., Scheid, R.E., "Autonomous Frequency Domain Identification: Theory and Experiment", NASA JPL Report JPL Publication 89-8, 1989, 204 pp.
- [223] Zak, M., "Characteristic-Wave approach Complements Modal Analysis", NASA Tech Brief, Volume 14, Number 5, 1990, 4 pp.
- [224] Zak, M., "Dynamical Response to Pulse Excitations in Large Space Structures", *Monograph, Large Space Structures: Dynamics and Control*, S.N. Atluri and A.K. Amos, Editors, 1987.
- [225] Zhang, L., Kanda, H., Brown, D.L., Allemang, R.J. "A Polyreference Frequency Domain Method for Modal Parameter Identification," ASME Paper Number 85-DET-106 1985, 8 pp.
- [226] Zhang, Q., Allemang, R.J., Brown, D. L., "Modal Filter: Concept and Applications", Proceedings, International Modal Analysis Conference, 1990, pp. 487-496.
- [227] Zhang, Q., Shelley, S., Allemang, R.J., *Optimal Sensor Placement to Minimize Control Spillover*, Technical Report, Structural Dynamics Research Laboratory, University of Cincinnati, 1989.
- [228] Zimmerman, R.D., Brown, D.L., Allemang, R.J., "Improved Parameter Estimation Techniques for Experimental Modal Analysis", Final Report: NASA Grant NSG-1486, NASA-Langley Research Center, 23 pp., 1982.